

INFORMATION TO USERS

This manuscript has been reproduced from the microfilm master. UMI films the text directly from the original or copy submitted. Thus, some thesis and dissertation copies are in typewriter face, while others may be from any type of computer printer.

The quality of this reproduction is dependent upon the quality of the copy submitted. Broken or indistinct print, colored or poor quality illustrations and photographs, print bleedthrough, substandard margins, and improper alignment can adversely affect reproduction.

In the unlikely event that the author did not send UMI a complete manuscript and there are missing pages, these will be noted. Also, if unauthorized copyright material had to be removed, a note will indicate the deletion.

Oversize materials (e.g., maps, drawings, charts) are reproduced by sectioning the original, beginning at the upper left-hand corner and continuing from left to right in equal sections with small overlaps.

Photographs included in the original manuscript have been reproduced xerographically in this copy. Higher quality 6" x 9" black and white photographic prints are available for any photographs or illustrations appearing in this copy for an additional charge. Contact UMI directly to order.

ProQuest Information and Learning
300 North Zeeb Road, Ann Arbor, MI 48106-1346 USA
800-521-0600

UMI[®]

DISSERTATION

**NUMERICAL AND PHYSICAL MODELING OF BLUFF BODY FLOW AND
DISPERSION IN URBAN STREET CANYONS**

Submitted by

Cheng-Hsin Chang

Department of Civil Engineering

In partial fulfillment of the requirements
for the Degree of Doctor of Philosophy
Colorado State University
Fort Collins, Colorado
Spring, 2001

UMI Number: 3013831

UMI[®]

UMI Microform 3013831

Copyright 2001 by Bell & Howell Information and Learning Company.

All rights reserved. This microform edition is protected against
unauthorized copying under Title 17, United States Code.

Bell & Howell Information and Learning Company
300 North Zeeb Road
P.O. Box 1346
Ann Arbor, MI 48106-1346

Copyright by Cheng-Hsin Chang 2001


All Rights Reserved


COLORADO STATE UNIVERSITY

March 29, 2001

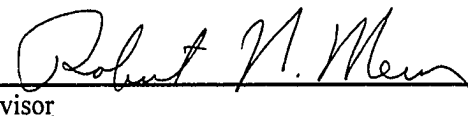
WE HEREBY RECOMMEND THAT THE DISSERTATION PREPARED UNDER OUR SUPERVISION BY **CHENG-HSIN CHANG** ENTITLED **NUMERICAL AND PHYSICAL MODELING OF BLUFF BODY FLOW AND DISPERSION IN URBAN STREET CANYONS** BE ACCEPTED AS FULFILLING IN PART REQUIREMENTS FOR THE DEGREE OF DOCTOR OF PHILOSOPHY.

Committee on Graduate Work

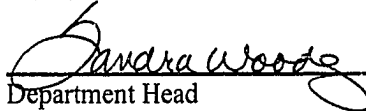








Advisor



Department Head

ABSTRACT OF DISSERTATION

NUMERICAL AND PHYSICAL MODELING OF BLUFF BODY FLOW AND DISPERSION IN URBAN STREET CANYONS

This investigation is focused on bluff body flow, wind loads and transport of pollutants or chemical and biological (CB) agents in urban environments, which require accurate measurements of the basic flow fields for carefully controlled, well known conditions. The research consists of two components: physical urban street canyon modeling in a boundary layer wind tunnel and numerical urban street canyon modeling using finite-volume numerical methods.

Fluid modeling in an industrial wind tunnel provides an opportunity to produce accurate simulations of the bluff body flow and transport of urban pollution or simulations of CB agents associated with urban terrorism incidents. A basic building shape, the Wind Engineering Research Field Laboratory building (WERFL) at Texas Tech University, is used for this study. Many studies have been performed on pressure fields, flow and dispersion patterns based on the isolated WERFL building during the past ten-year Colorado State University/Texas Tech University Cooperative Program in Wind Engineering. An urban street canyon matrix was built by using the 1:50 scale WERFL model and surrounding it by models of similar dimensions. These buildings were arranged in various symmetric configurations with different separation distances

and different numbers of buildings upwind, laterally and downwind. A series of measurements were made over the generic urban street canyon arrangements using flow visualization, anemometry, pressure transducers and gas chromatography. Experimental data include visualization, video sequences, velocity and turbulence intensity profiles, surface pressure on the building and dispersion of tracer gas. Results were examined for the influence of surroundings on the pressure and concentration distributions. Results were also compared to three-dimensional numerical models of the same configuration using the commercial code, Fluent 5.4 and the Large Eddy Simulation (LES) code Fire Dynamics Simulator (FDS). The effects of grid resolution, boundary conditions, source placement and selection of turbulence model (kappa-epsilon, RNG kappa-epsilon, Reynolds stress, LES, etc.) were examined in a series of sensitivity calculations.

Cheng-Hsin Chang
Department of Civil Engineering
Colorado State University
Fort Collins, Colorado 80523
Spring, 2001

ACKNOWLEDGEMENTS

I would like to deeply thank my advisor, Prof. Robert Meroney, who is the most patient and caring advisor that I have ever met, for his continuous support and invaluable guidance throughout this study.

I would like to thank the members of my research committee, Dr. Jack Cermak, Dr. T.G. Sanders and Dr. J.W. Thomas for their helpful comments and review of this dissertation.

I am grateful to Dr. David Neff and Prof. Virgil Sandborn for their extensive help in the laboratory.

I would also like to acknowledge the support, encouragement from my parents.

I am particularly grateful to my wife, Jessica, for her patience, understanding and help during the course of this research.

TABLE OF CONTENTS

ABSTRACT OF DISSERTATION.....	iii
ACKNOWLEDGEMENTS.....	v
TABLE OF CONTENTS.....	vi
LIST OF FIGURES.....	ix
LIST OF SYMBOLS.....	xviii
1. INTRODUCTION.....	1
1.1 Fluid Modeling.....	4
1.2 Numerical Modeling.....	5
2. ANALYTICAL AND NUMERICAL MODELS.....	8
2.1 Urban Climates and Urban Climate Modeling.....	8
2.1.1 Urban Boundary Layer Flow at High Velocities.....	9
2.1.2 Urban Boundary Layer at Low Velocity Flows.....	14
2.2 Wind Effects on Low-Rise Building in the Boundary Layers.....	16
2.2.1 Windward Wall.....	18
2.2.2 Side and Leeward Walls.....	19
2.2.3 Roof.....	20
2.3 Physical Modeling of Flow and Dispersion in Urban Street Canyons.....	23
2.3.1 The Equations of Conservation of Mass, Momentum and Energy.....	23
2.3.2 Satisfying the Similarity Criteria.....	25
2.4 Numerical Simulation Model.....	29
2.4.1 Numerical Simulation Solution Techniques.....	29
2.4.2 CFD Applications in Wind Engineering.....	31
3. ARRANGEMENT OF THE EXPERIMENTS, DATA ACQUISITION AND ANALYSIS TECHNIQUES.....	33
3.1 Wind Tunnel Facility and Physical Arrangement of the Experiment.....	33

3.1.1	Boundary Layer Wind Tunnel.....	33
3.1.2	Approach Flow Characteristics.....	36
3.1.3	Basic Building Model and Arrangement of Urban Street Canyon Model.....	39
3.2	Wind Tunnel Measurements.....	43
3.2.1	Flow Visualization on Street Canyon Area.....	43
3.2.2	Wind Profile and Turbulence Characteristics Measurements.....	45
3.2.3	Pressure Measurements.....	48
3.2.4	Concentration Measurements.....	55
4.	NUMERICAL SIMULATION PROCEDURE.....	64
4.1	Introduction of Fluent.....	64
4.1.1	Turbulence Models.....	66
4.1.2	The CFD Process.....	66
4.1.3	Inlet Conditions to the Numerical Domain.....	68
4.1.4	Numerical Domain and Meshes.....	71
4.2	Introduction of FDS.....	73
4.2.1	Inlet Conditions and Numerical Domain.....	73
5.	EXPERIMENTAL DATA.....	77
5.1	Flow Visualization.....	77
5.2	Velocity and Turbulence Intensity Profile.....	77
5.3	Pressure Coefficient.....	78
5.4	Concentration.....	78
6.	WIND TUNNEL RESULT ANALYSIS AND COMPARISION.....	80
6.1	The Effects of Surroundings on Flow Around the Low-Rise Buildings... ..	80
6.1.1	Flow Visualization of Wind Tunnel Result.....	81
6.1.2	Wind Velocity and Turbulence Intensity Profiles of Wind Tunnel Result.....	85
6.1.3	Comparison of Wind Tunnel Results and Numerical Simulation.....	95
6.2	The Effects of Surroundings on Surface Pressure on Low-Rise Buildings.....	115
6.2.1	The Effects of Surroundings.....	115
6.2.2	Comparison of Pressure Coefficients of Wind Tunnel Results and Numerical Simulations.....	141

6.3	Modeling of Pollutant Dispersion in Urban Street Canyons.....	151
6.3.1	Wind Tunnel Results and Interpretation.....	151
6.3.2	Comparison of Concentrations of Wind Tunnel Results and Numerical Simulations.....	155
7.	SUMMARY AND CONCLUSIONS.....	169
7.1	Wind Tunnel Experimental Results.....	169
7.2	Numerical Simulation Results.....	171
	REFERENCES.....	175
APPENDIX A	Flow Visualization Images.....	182
APPENDIX B	Velocity and Turbulence Intensity Profiles.....	189
APPENDIX C	Pressure Coefficients.....	195
APPENDIX D	Concentrations.....	220

LIST OF FIGURES

Figure 2.1	The urban boundary layer for neutrally stratified flow (Plate, 1995).....	9
Figure 2.2	Coordinate system showing Gaussian distributions in horizontal and vertical (Turenr, 1970).....	15
Figure 2.3	Model of flow near a sharp-edged building normal to deep boundary layer wind (from Hosker, 1984, based on Peterka, 1977).....	17
Figure 2.4	Flow pattern on windward wall (Beranek, 1980).....	18
Figure 2.5	Separation at sidewall (Cook, 1985).....	19
Figure 2.6	Wake circulations behind slab block (Cook, 1985).....	20
Figure 2.7	Separation and reattachment on the roof of low-rise building (Banks, 1999).....	21
Figure 2.8	Sketch of primary and secondary vortices (Sun, 1993).....	22
Figure 2.9	Reynolds-number independence for surface drag coefficient C_d (Cermak, 1975).....	28
Figure 3.1	Wind engineering and fluid laboratory layouts.....	34
Figure 3.2	Schematic of Industrial Wind Tunnel.....	35
Figure 3.3	Approach flow velocity profile.....	37
Figure 3.4	Approach flow turbulence intensity profile.....	38
Figure 3.5a	Picture of WERFL at TTU.....	40
Figure 3.5b	1:50 scale WERFL with 95 pressure ports.....	40
Figure 3.5c	1:50 scale WERFL with 44 concentration ports.....	41
Figure 3.5d	Industrial wind tunnel (IWT) and models.....	41
Figure 3.6	Schematic of urban street canyon model arrangement.....	42

Figure 3.7 Schematic of visualization setup.....	44
Figure 3.8 Velocity calibration and measurement system.....	46
Figure 3.9 Single-hot-film calibrations.....	47
Figure 3.10 Detail position of velocity profiles measurements.....	49
Figure 3.11 Pressure and concentration tap locations on 1:50 TTU WERFL building...50	
Figure 3.12 Pressure tap location on 1:50 TTU WERFL building at roof (face 1).....	51
Figure 3.13 Pressure tap location on 1:50 TTU WERFL building at face 2 and face3.....	52
Figure 3.14 Pressure tap location on 1:50 TTU WERFL building at face 4.....	53
Figure 3.15 Concentration sampling and measurement system schematic.....	56
Figure 3.16 Concentration tap locations on 1:50 TTU building at face 2 and face 6.....	59
Figure 3.17 Concentration tap locations on 1:50 TTU building at face 1.....	60
Figure 3.18 Concentration tap locations on 1:50 TTU building at face 4.....	61
Figure 4.1 Flow chart for numerical solution method.....	67
Figure 4.2 Numerical inlet velocity profile compared to CSU-B2.....	69
Figure 4.3 Numerical inlet kinetic energy profile compared to CSU-B2.....	69
Figure 4.4 Numerical inlet kinetic dissipation profile compared to CSU-B2.....	70
Figure 4.5 The numerical domain of 9 buildings and B/H=1 case.....	70
Figure 4.6 Typical unstructured boundary mesh used for tetrahedral mesh generation on 9 buildings and B/H=1 case.....	72
Figure 4.7 The adaption grid on 9 buildings and B/H=1 case.....	72
Figure 4.8 Numerical domain at X=100m, Y=90m, and Z=40m.....	75
Figure 4.9 The structured computational grid at x-z and y-z planes at high resolution at 192*144*64 grid cells.....	75

Figure 4.10 Approaching wind velocity profile for different ground boundary conditions.....	76
Figure 6.1 Skimming Flow, $B/H=1$	82
Figure 6.2 Interference Flow, $B/H=4$	84
Figure 6.3 Isolated Roughness Flow, $B/H=6$	85
Figure 6.4a Mean velocity magnitude profile measured at point 1, $N=1$	86
Figure 6.4b Turbulence intensity profile measured at point 1, $N=1$	86
Figure 6.5a Mean velocity magnitude profile measured at point 2, $N=1$	88
Figure 6.5b Turbulence intensity profile measured at point 2, $N=1$	88
Figure 6.6a Mean velocity magnitude profile measured at point 3, $N=1$	89
Figure 6.6b Turbulence intensity profile measured at point 3, $N=1$	89
Figure 6.7a Mean velocity magnitude profile measured at point 4, $N=1$	90
Figure 6.7b Turbulence intensity profile measured at point 4, $N=1$	90
Figure 6.8a Mean velocity magnitude profile measured at point 5, $N=1$	91
Figure 6.8b Turbulence intensity profile measured at point 5, $N=1$	91
Figure 6.9a Mean velocity magnitude profile measured at point 6, $N=1$	92
Figure 6.9b Turbulence intensity profile measured at point 6, $N=1$	92
Figure 6.10a Mean velocity magnitude profile measured at point 7, $N=1$	93
Figure 6.10b Turbulence intensity profile measured at point 7, $N=1$	93
Figure 6.11 Mean velocity magnitude profile measured at point 2, $N=8$	94
Figure 6.12 Mean velocity magnitude profile measured at point 3, $N=8$	94
Figure 6.13a Flow visualization result of case, $B/H=1$	96

Figure 6.13b	Numerical velocity vector result of case, B/H=1 from Fluent 5.4.....	96
Figure 6.13c	Numerical velocity vector result of case, B/H=1 from FDS.....	96
Figure 6.14a	Flow visualization result of case, B/H=2.....	98
Figure 6.14b	Numerical velocity vector result of case, B/H=4 from Fluent.....	98
Figure 6.15a	Flow visualization result of case, B/H=6.....	99
Figure 6.15b	Numerical velocity vector result of case, B/H=6 from Fluent.....	99
Figure 6.16a	Velocity magnitude profile at point1 for case B/H=1, N=1.....	103
Figure 6.16b	Turbulence intensity profile at point1 for case B/H=1, N=1.....	103
Figure 6.17a	Velocity magnitude profile at point 3 for case B/H=1, N=1.....	104
Figure 6.17b	Turbulence intensity profile at point 3 for case B/H=1, N=1.....	104
Figure 6.18a	Velocity magnitude profile at point 5 for case B/H=1, N=1.....	105
Figure 6.18b	Turbulence intensity profile at point 5 for case B/H=1, N=1.....	105
Figure 6.19a	Velocity magnitude profile at point 1, N=1 using κ - ϵ model.....	106
Figure 6.19b	Turbulence intensity profile at point 1, N=1 using κ - ϵ model.....	106
Figure 6.20a	Velocity magnitude profile at point 1, B/H=1 using κ - ϵ model.....	107
Figure 6.20b	Turbulence intensity profiles at point 1, B/H=1 using κ - ϵ model.....	107
Figure 6.21a	Mean velocity and turbulence profile at point 1 using FDS with different grid resolution.....	110
Figure 6.21b	Mean velocity profile at point 3 and point 5 using FDS with different grid resolution.....	111
Figure 6.22a	Velocity profile at point 1, B/H=1, N=1 using FDS.....	112
Figure 6.22b	Turbulence intensity profiles at point 1, B/H=1, N=1 using FDS.....	112
Figure 6.23a	Velocity profile at point 3, B/H=1, N=1 using FDS.....	113

Figure 6.23b	Turbulence intensity profiles at point 3, $B/H=1$, $N=1$ using FDS.....	112
Figure 6.24a	Velocity profile at point 5, $B/H=1$, $N=1$ using FDS.....	114
Figure 6.24b	Turbulence intensity profiles at point 5, $B/H=1$, $N=1$ using FDS.....	114
Figure 6.25	Pressure coefficients (-peak, mean, and RMS) on the centerline of roof for cases, $B/H=0.5$, with different N	118
Figure 6.26	Pressure coefficients (-peak, mean, and RMS) on the front edge of roof for cases, $B/H=0.5$, with different N	119
Figure 6.27	Pressure coefficients (-peak, mean, and RMS) on the centerline of downwind wall of street canyon for cases, $B/H=0.5$, with different	120
Figure 6.28	Pressure coefficients (-peak, mean, and RMS) on the centerline of roof for cases, $B/H=1$, with different N	121
Figure 6.29	Pressure coefficients (-peak, mean, and RMS) on the front edge of roof for cases, $B/H=1$, with different N	122
Figure 6.30	Pressure coefficients (-peak, mean, and RMS) on the centerline of downwind wall of street canyon for cases, $B/H=1$, with different N	123
Figure 6.31	Pressure coefficients (-peak, mean, and RMS) on the centerline of roof for cases, $B/H=2$, with different N	124
Figure 6.32	Pressure coefficients (-peak, mean, and RMS) on the front edge of roof for cases, $B/H=2$, with different N	125
Figure 6.33	Pressure coefficients (-peak, mean, and RMS) on the centerline of downwind wall of street canyon for cases, $B/H=2$, with different.....	126
Figure 6.34	Pressure coefficients (-peak, mean, and RMS) on the centerline of roof for cases, $B/H=4$, with different N	127
Figure 6.35	Pressure coefficients (-peak, mean, and RMS) on the front edge of roof for cases, $B/H=4$, with different N	128
Figure 6.36	Pressure coefficients (-peak, mean, and RMS) on the centerline of downwind wall of street canyon for cases, $B/H=4$, with different N	129
Figure 6.37	Pressure coefficients (-peak, mean, and RMS) on the centerline of roof for cases, $B/H=6$, with different N	130

Figure 6.38	Pressure coefficients (-peak, mean, and RMS) on the front edge of roof for cases, $B/H=6$, with different N	131
Figure 6.39	Pressure coefficients (-peak, mean, and RMS) on the centerline of downwind wall of street canyon for cases, $B/H=6$, with different N	132
Figure 6.40	Pressure coefficients (-peak, mean, and RMS) on the centerline of roof for cases, $N=1$ with different values of B/H	133
Figure 6.41	Pressure coefficients (-peak, mean, and RMS) on the front edge of roof for cases, $N=1$ with different values of B/H	134
Figure 6.42	Pressure coefficients (-peak, mean, and RMS) on the centerline of downwind wall of street canyon for cases, $N=1$ with different B/H	135
Figure 6.43	Pressure coefficients (-peak, mean, and RMS) on the centerline of roof for cases, $N=8$ with different B/H	136
Figure 6.44	Pressure coefficients (-peak, mean, and RMS) on the front edge of roof for cases, $N=8$ with different B/H	137
Figure 6.45	Pressure coefficients (-peak, mean, and RMS) on the centerline of downwind wall of street canyon for cases, $N=8$ with different B/H	138
Figure 6.46	The schematic of pressure coefficient measurement in different approaching angles.....	139
Figure 6.47	-Peak pressure coefficient measurement for a roof corner point for the wind azimuths ranging from 0 to 90 degrees.....	139
Figure 6.48	Mean pressure coefficient measurement for a roof corner point for the wind azimuths ranging from 0 to 90 degrees.....	140
Figure 6.49	RMS pressure coefficient measurement for a roof corner point for the wind azimuths ranging from 0 to 90 degrees.....	140
Figure 6.50a	Comparisons of mean pressure coefficients on the centerline of the roof for case $N=1$: experiments and numerical simulation using Fluent κ - ϵ model.....	145
Figure 6.50b	Comparisons of mean C_p on the centerline of the downwind wall of street canyon for case $N=1$: experiments and numerical simulation using Fluent κ - ϵ model.....	145

Figure 6.51a	RMS vs. mean pressure coefficients form roof trappings, (B/H=6, N=1)	146
Figure 6.51b	Comparison of RMS Cp for case B/H=6, N=1: experiments and predictions by Paterson –Selvam formulas.....	146
Figure 6.52a	Comparison of distributions of mean Cp for case N=1, B/H=1 between measured and calculated (Fluent) at wind direction 30 degrees.....	147
Figure 6.52b	Comparison of distributions of mean Cp for case N=1, B/H=1 between measured and calculated (Fluent) at wind direction 60 degrees.....	148
Figure 6.53a	Comparisons of mean pressure coefficients on the centerline of the roof for case N=1: experiments and numerical simulation using FDS LES model.....	149
Figure 6.53b	Comparisons of RMS pressure coefficients on the centerline of the roof for case N=1: experiments and numerical simulation using FDS LES model.....	149
Figure 6.54a	Comparisons of mean pressure coefficients on the front edge of the roof for case N=1: experiments and numerical simulation using FDS LES model.....	150
Figure 6.54b	Comparisons of RMS pressure coefficients on the front edge of the roof for case N=1: experiments and numerical simulation using FDS LES model.....	150
Figure 6.55a	Concentrations on the upwind and downwind walls of the street canyon for case B/H=0.5.....	154
Figure 6.55b	Concentrations on the upwind and downwind walls of the street canyon for case B/H=1.....	154
Figure 6.56	Concentrations on the upwind and downwind walls of the street canyon for case B/H=2.....	158
Figure 6.57	Concentrations on the upwind and downwind walls of the street canyon for case B/H=4.....	158
Figure 6.58	Concentrations on the upwind and downwind walls of the street canyon for open country roughness case N=1.....	159
Figure 6.59	Concentrations on the centerline of the roof for open country roughness case N=1.....	159

Figure 6.60	Comparisons between wind tunnel and numerical model (Fluent κ - ϵ model) concentrations for the open country roughness case $N=1$	160
Figure 6.61	Comparisons between wind tunnel and numerical model (Fluent κ - ϵ model) concentrations for the open country roughness case $N=1$	160
Figure 6.62	Comparisons between wind tunnel and numerical model (Fluent κ - ϵ model) concentrations on the centerline of the roof for open country cases $N=1$	161
Figure 6.63	Comparisons between wind tunnel and numerical model (Fluent κ - ϵ model) concentrations for different numbers of upwind buildings before master building for case $B/H=1$	161
Figure 6.64	Experimental vs. Fluent calculated normalized concentration on the centerline of the roof and upwind and downwind walls of canyon tappings.....	162
Figure 6.65	Comparisons between wind tunnel and numerical model (Fluent k - ϵ model, FDS) concentrations for the open country roughness case $N=1$ and $B/H=1$	162
Figure 6.66	Comparisons between wind tunnel and numerical model (Fluent κ - ϵ model, FDS) concentrations on the centerline of the roof $N=1$ and $B/H=1$	163
Figure 6.67	Experimental vs. calculated (Fluent and FDS) normalized concentration, K , on the centerline of the roof and upwind and downwind walls of canyon tappings ($B/H=1$, $N=1$).....	164
Figure 6.68a	Predictions of tracer-gas concentration on the master building roof for the wind azimuths with zero an 15 degrees, $N=1$, $B/H=1$	165
Figure 6.68b	Predictions of tracer-gas concentration on the master building roof for the wind azimuths with 30 an 45 degrees, $N=1$, $B/H=1$	166
Figure 6.68c	Predictions of tracer-gas concentration on the master building roof for the wind azimuths with 60 an 75 degrees, $N=1$, $B/H=1$	167

Figure 6.68d Predictions of Tracer-gas concentration on the master building
roof for the wind azimuths with 90 degrees, $N=1$, $B/H=1$168

LIST OF SYMBOLS

A, B, c	calibration constants
C	steady-state concentration at point (x, y, z)
C_{bg}	background concentration
C_m	source normalized model concentration
C_{mea}	sampled concentration
C_p	Pressure coefficient
C_p'	RMS pressure coefficient
C_{source}	source gas concentration
d_0	zero-plane displacement
E	anemometer output voltage
Ec	Eckert Number
g_c	gravitational conversion constant
H	effective stack height
K_s	equivalent sand roughness
K	normalized concentration
k	turbulent kinetic energy
κ	von Karman constant
L	length
P	pressure
Pr	Prandtl number
P_{static}	static pressure
Q	emission rate
Ro	Rosby Number
Re	Reynolds Number
Ri	Richardson Number
T	temperature
U	flow velocity

$U(z)$	mean wind velocity at elevation z
u	average wind speed at stack height
u^*	friction velocity
u_{ref}	mean velocity at reference height
$u(z)$	mean wind speed
V	mean velocity at reference point
ν	kinematic viscosity
y	horizontal distant from plume centerline
z	vertical distance from ground level
z_0	roughness length
z_{ref}	the reference height
α	power law exponent (function of roughness)
ε	kinetic dissipation
ρ	air density
σ_y, σ_z	horizontal and vertical spread parameters
λ_{ar}	Σ of areas covered by buildings / total urban area
λ_{fa}	Σ of average building areas normal to the wind /total urban area
Ω	angular velocity of earth

Abbreviations

ABL	Atmospheric boundary layer
ASL	Atmospheric surface layer
CAD	Computer aided design
CB	Chemical and Biological
CFD	Computational fluid dynamics
CSU-B2	Medium turbulence (TTU nominal turbulence) surface layer
CWE	Computational Wind Engineering

DNS	Direct Numerical Simulation
FDS	Fire Dynamics Simulator
GC	Gas Chromatograph
IWT	Industrial Wind Tunnel
LES	Large Eddy Simulation
NIST	National Institute of Standards and Technology
PSI	Pressure System Inc.
TSI	Thermo System Inc.
TTU	Texas Tech University
WERFL	Wind Engineering Research Field Laboratory
WEFL	Wind Engineering Fluid Laboratory

CHAPTER 1

INTRODUCTION

The flow patterns that develop around individual buildings govern the wind forces on the building, the distribution of pressure about the building, and scalar dispersion about the building and in its wake. The superposition and interaction of flow patterns associated with adjacent buildings govern the final distribution of facade pressures and the movement of pollutants in urban and industrial complexes. Street canyon depth and width, intersection locations, canyon orientation to dominate wind directions, and building geometries determine peak pollution incidents (Oke, 1988; Theurer, 1995).

Many studies have shown that the worst mean and peak suction on flat building roofs occur for cornering or oblique wind angles. At such angles, conical or delta wing vortices form along the roof edges, which induce higher suction pressures, associated with the strongly curved separation streamlines (Banks et al., 1999a and 1999b). Yet the presence of nearby buildings is expected to deflect streamlines, modify local circulation patterns and induce modified patterns of suction and stagnation pressure, as well as different convection patterns for pollutants. Many studies have previously examined physical models of urban street canyons. Plate et al. (1992) studied models of the development of the atmospheric boundary above urban areas by measuring flows over different arrangements of buildings. Plate (1995) considered the effects of urban climates and urban climate modeling. Surry (1994) examined the effect of both surroundings and roof corner geometric modifications on the roof pressures on a low-rise building. Hertig

et al. (1995) also performed wind tunnel tests to determine the influence of nearby buildings on mean and peak pressure coefficients. Kiefer and Plate (1998) provided modeling of mean and fluctuation wind loads in different types of built-up areas. Cermak (1995) introduced the physical modeling of flow and dispersion over larger urban areas and proposed similarity criteria required to uniquely determine flow and dispersion. Gerdes et al. (1999) measured and analyzed pollutant dispersion in an urban street canyon. Most recently, Macdonald (2000) modeled the mean velocity profiles in an urban canopy layer and examined the effect of a reduction of turbulence length scale with increasing obstacle-packing density.

Advanced technology makes computers faster and more powerful, which allows computational fluid dynamics (CFD) procedures to be applied to many experimental flow problems. Today, increasing applications of CFD to wind engineering problems include wind load of building and pollutant dispersion phenomena. Several previous studies have compared measurements made during physical modeling with numerical predictions. He and Song (1997) simulated the wind flow around the Texas Tech University (TTU) building and roof corner vortex by using a Large Eddy Simulation (LES) code. They claim that the three-dimensional roof corner vortex pattern was successfully simulated and that mean values of pressure predicted were in good agreement with wind tunnel and field test measurements. Murakami et al (1997) generated velocity fluctuations for an inflow boundary condition for LES with prescribed spatial correlation distributions and turbulence intensity levels. To generate velocity fluctuations for an inflow boundary condition for LES is one of the most important unresolved problems in CFD research.

Lee et al. (1997) solved the LES of wind effects on bluff bodies using the finite element method, and they compared simulated results with numerical and experimental studies reported by other researchers. Selvam (1997) used LES to compute the pressures around the TTU building using different inflow turbulence conditions, and he compared them with available field mean and peak pressure coefficients. Rehm et al. (1997) compared mean surface pressure on a single building by using an LES algorithm with uniform and shear inflows. Cheatham et al (2000) also simulated the flow and dispersion around a surface-mounted cube, and they examined the effect of resolution, boundary conditions, and the form of the inflow velocity profiles. Carpenter and Locke (1999) investigated wind speeds over multiple two-dimensional hills and compared results with numerical solutions. Meroney et al. (1995 and 1996) examined the behavior of line-source diffusion within two-dimensional arrays of simple rectangular model buildings. Leidl and Meroney (1997) compared traffic exhaust dispersion in street canyons as measured by Rafailidis et al. (1995) with numerical simulations including the effects of pitched roofs and finite length cross wise streets. Leidl et al. (1997) considered the numerical simulation of concentration and flow distributions in the vicinity of U-shaped building structures. They compared their calculations against detailed wind tunnel measurements produced by Klein et al. (1994).

The goal of this dissertation is to investigate the bluff body flow, wind load and transport of pollutants, or chemical and biological (CB) agents in an idealized urban environment. The experiments associated with this dissertation provide accurate measurements of the basic flow fields for carefully controlled, well known conditions.

The research consists of two components: physical urban street canyon fluid modeling in a boundary layer wind tunnel and numerical urban street canyon modeling using finite-volume numerical method.

1.1 Fluid Modeling

This study used a basic building shape, the Wind Engineering Research Field Laboratory building (WERFL), Texas Tech University, Lubbock, which is a metal building of simple rectangular prism shape (9.2 m x 13.8 m x 4.0 m tall) to build an urban street canyon model. Pressure fields, flow and dispersion patterns about this isolated building were extensively measured both at full scale and over various model scales immersed in an equivalent turbulent shear layer (Cochran, 1992; Birdsall, 1993; Bienkiewicz, 1995; Ham, 1998; Banks, 2000).

A plastic model of the WERFL structure was constructed to a 1:50 scale and instrumented with multiple pressure ports. A large number of “dummy” models of similar dimensions were constructed of plastic foam and wood to represent surrounding buildings. These buildings were arranged in various symmetric configurations with different separation distances; then they were placed in the Industrial Wind Tunnel of the Wind Engineering and Fluid Laboratory, Colorado State University. Typical building patterns are noted in Figure 3.6, and the associated arrangement patterns are listed in Table 3.1.

Wind velocity measurements were made with a single hot-film probe and anemometry equipment manufactured by Thermo-Systems, Inc. (TSI). Flow

visualization was accomplished with a laser light sheet produced by 5-watt Coherent Innova 7005 Argon ion water-cooled laser. Images were recorded by using a Panasonic Omni vision II camera/recorder system. Pressure taps on the 1:50 scale building model were connected to a 48-channel Pressure System Inc. (PSI) “ESP48” transducer unit mounted inside the model. Concentrations of tracer gases (C_2H_6) released from point and line source regions are measured using a Hewlett Packard 5710A Flame-ionization Gas Chromatography. An automated sampling system designed and built at CSU using 50 syringes captured samples simultaneously for sequential processing through the gas chromatography. Transducer voltages are integrated and recorded automatically by a National Instrument Inc. LabVIEW based data acquisition system.

1.2 Numerical Modeling

Flow and dispersion over various building pattern arrangements were also simulated with the Fluent 5.4 and Fire Dynamics Simulator (FDS) computational fluid dynamics software.

The Fluent CFD software was based on a finite volume discretization of the equations of motion, an unstructured grid volume made of either rectangular prisms or tetrahedral cells, various matrix inverting routines, and, in this case, either kappa-epsilon (κ - ϵ) or renormalized group theory kappa-epsilon (RNG- κ - ϵ) turbulence models. Steady state solutions were sought for several flow configurations, and the data generated were displayed on various isopleth contour plots of velocity, turbulence and concentration. The effects of grid resolution, boundary conditions, source placement and selection of

turbulence model (kappa-epsilon, RNG kappa-epsilon, Reynolds stress, etc.) were examined in a series of sensitivity calculations. Particle trajectories were also generated to elucidate the effect of building spacing and street configuration (Fluent 5, User's Guide, 1998).

Fire Dynamics Simulator (FDS) is a public domain computational fluid dynamics (CFD) model of fire-driven fluid flow created by the Building and Fire Research Laboratory at the National Institute of Standards and Technology (NIST) (<http://fire.nist.gov>). FDS consists of two programs, fds and smokeview. Fds solves a form of the Navier-Stokes equations appropriate for low-speed, thermally-driven flows of smoke and hot gases generated in a fire. Smokeview visualizes fds computed data by animating time dependent particle flow, 2D slice contours, and surface boundary contours. Data at a particular time may also be visualized using 2D or 3D contour plots or vector plots. FDS uses the Large Eddy Simulation (LES) methodology, and it was developed and used for the description of gas phase combustion and convection processes in fires where buoyancy is fundamental. However, since wind speeds are so high in most wind engineering applications, mechanical turbulence dominates thermal effects and buoyancy effects are relatively small. Thus, in the calculations induced here, the incoming flow is assumed to be turbulence-free. The signature turbulence effects are accounted only to the size of the grid.

Chapter 2 presents the background of analytical and numerical models considered. The arrangement of the experiments, data acquisition and analysis techniques is summarized in Chapter 3. In Chapter 4, a number of simulation procedures

using Fluent 5.4 and FDS are described. Chapter 5 presents experimental data of flow visualization, velocity and turbulence intensity profiles, pressure coefficients, and concentrations. Chapter 6 discusses the wind tunnel results and compares the experimental data with the numerical data, and Chapter 7 summarizes conclusions of this study.

CHAPTER 2

ANALYTICAL AND NUMERICAL MODELS

Characteristics of bluff body flow and transport of pollutants in urban street canyons and the theoretical background for various analytical and numerical models are discussed in this chapter. There are four topics involved: urban climates and urban climate modeling, wind effects on low-rise buildings in the turbulent boundary layers, physical modeling of flow and dispersion in urban street canyons, and numerical simulation of flow over such geometries.

2.1 Urban Climates and Urban Climate Modeling

There are two different types of boundary layer flows typical for different applications and meteorological situations during urban street canyon wind studies (Plate, 1995). One is a high velocity boundary layer flow characteristic of wind loading situations. This high speed flow is neutrally stratified and can be modeled in a conventional boundary layer wind tunnel. The other is a low velocity flow, typical for situations of significant air pollution which may require thermal stratification facilities. The low velocity flow may also be neutrally stratified, but the most extreme pollution cases occur for stratified flows with a surface level mixed layer and an elevated inversion.

2.1.1 Urban Boundary Layer Flow at High Velocities

Urban boundary layer flow at high velocities is a very typical flow condition of broad applicability for the rough surface of urban areas. From the standpoint of aerodynamics, the wind field of an urban street canyon area is a boundary layer flow along a rough surface, as shown in Figure 2.1.

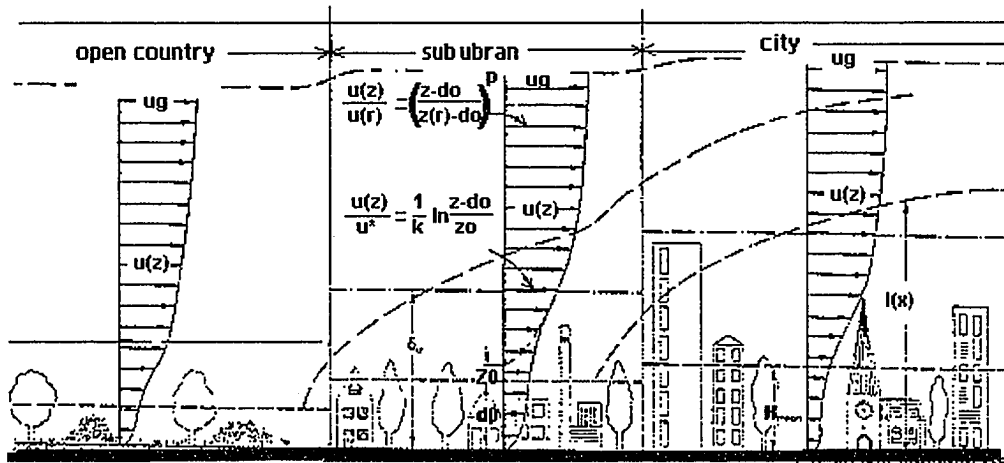


Figure 2.1 The urban boundary layer for neutrally stratified flow (Plate, 1995)

To define mean wind speed height, the logarithmic distribution for the urban boundary layer for neutrally stratified flow is usually applied.

$$\frac{u(z)}{u_*} = \frac{1}{\kappa} * \ln \frac{z - d_0}{z_0} \quad (2.1)$$

Where, z = height above the surface, [L],
 z_0 = roughness length, [L],
 d_0 = zero-plane displacement, [L],

$u(z)$ = mean wind speed, [L/T],

u_* = friction velocity, [L/T], and

κ = von Karman constant.

The application of this equation to a particular situation requires that the coefficients u_* , z_0 and d_0 are properly defined. This can be accomplished through measurements of the urban boundary layer. Table 2.1 (Wieringa, 1993) shows eight classes of different surface roughness in terms of a z_0 -value, ranging from a super smooth “sea”-surface to a super rough “chaotic”-surface characteristic of a big city center. This work represents the latest effort to classify the steadily expanding body of experimental knowledge.

Classification	z_0 (m)	Landscape description
1: “Sea”	0.0002	Open sea or lake.
2: “Smooth”	0.005	Featureless land surface.
3: “Open”	0.03	Level country with low vegetation.
4: “Roughly open”	0.10	Cultivated area with regular cover of low crop.
5: “Rough”	0.25	Recently-developed “young” landscape.
6: “Very rough”	0.5	“Old” cultivated landscape
7: “Closed”	1.0	Landscape totally and quite regularly covered.
8: “Chaotic”	≥ 2	Center of large cities.

Table 2.1: Davenport roughness classification (from Wieringa, 1993)

An alternate functional description of the flow in this part of the urban boundary is by means of the power law, as

$$\frac{u(z)}{u_{ref}} = \left(\frac{z - d_0}{z_{ref}} \right)^\alpha \quad (2.2)$$

Where, z_{ref} = the reference height, [L],
 u_{ref} is mean velocity at reference height, [L/T], and
 α = power law exponent (function of roughness).

A very comprehensive study of urban boundary layer flow was made by Theurer (1993) to summarize what is known about these parameters and to correlate them with building dimensions. These parameters can be predicted by using building parameters without performing any measurement. Theurer uses two parameters to describe the distribution of roughness elements. He suggests,

$$\lambda_{ar} = \sum \text{of areas covered by buildings} / \text{total urban area, and} \quad (2.3)$$

$$\lambda_{fa} = \sum \text{of average building areas normal to the wind} / \text{total urban area.} \quad (2.4)$$

These two parameter, λ_{ar} and λ_{fa} , are not precise enough to uniquely classify the roughness of an urban area. However, the precise roughness can be classified by using

these two parameters combined with a pictorial description of the roughness pattern. The results are shown in Table 2.2.


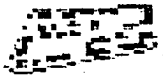



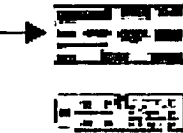

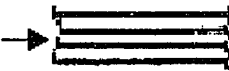
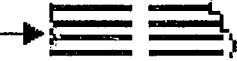
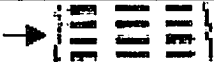
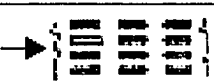
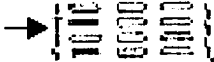
Structure	Description	H (m)	λ_{ar}	λ_{fa}	d_0	z_0
	One family building 1-2 stories	8-10 (9)	0.1-0.2	0.12	2	1.3
	Dense urban development one and more family building, 1-3 stories	8-12	0.2-0.3	0.15	4	1.4
	Building row 3-5 stories	12-20	0.2-0.3	0.1	7	1.5
	Block edge buildings 3-5 stores	15-20	0.25- 0.35	0.15	9	2.1
	City centers	>20	<0.5	0.15	10	2.4
	Industrial areas (chemical industry) with a. rows of buildings b. refinery type	15-25	0.3-0.4	0.12	12	1.6
	Suburban business center	5-15	0.25- 0.35	0.07	5	0.6
	Row like buildings (windtunnel: Theurer 1993)	20	0.44	-	15 (10)	0.1
	Interrupted rows (windtunnel: Theurer 1993)	20	0.36	0.044	12 (10)	0.6 (0.4)
	Interrupted rows (windtunnel: Theurer 1993)	20	0.3	0.093	10 (9)	1.5 (0.8)
	(windtunnel: Theurer 1993) Rows with varying heights	22.2	0.3	0.103	11 (10)	1.8 (1.8)
	Rows with varying heights (windtunnel: Theurer 1993)	19	0.3	0.088	10 (10)	1.3 (1.3)

Table 2.2 Relationship of aerodynamic parameter with building pattern (Theuer, 1993)

2.1.2 Urban Boundary Layer at Low Velocity Flows

Pollutant gases usually are diluted by the wind. The stronger the wind, the greater the dilution. But with low velocity flow inside the urban area, vertical motions induced by the thermal turbulence become more significant. In this situation, local heating of a building, either from outside by the sun or inside through room heating, may determine the flows in the urban areas. Thus, the structure of a diurnal thermal cycle of heating and cooling will be more important for the flows of contaminant gases in the urban canopy layer.

Analytical pollution studies at low wind speeds inside the urban areas are possible only in very simplified conditions. The case of a point source that exists within the outer part of the urban boundary layer is well known; it has been studied extensively both in the field and in laboratories. Semi-empirical models have been established that permit one to calculate the spreading of pollutants from an elevated point source. The empirical models are based on the “Gaussian Plume” model. A Gaussian or normal distribution often results from random processes. Such behavior has been shown by Pasquill (1961) to be well modeled by a double Gaussian equation. This equation is given below in a form that predicts the steady-state concentration at point (x, y, z) located downwind from the source:

$$C(x, y, z) = \frac{Q}{2\pi u \sigma_y \sigma_z} \exp\left(-\frac{1}{2} \frac{y^2}{\sigma_y^2}\right) \left\{ \exp\left(-\frac{1}{2} \frac{(z-H)^2}{\sigma_z^2}\right) + \exp\left(-\frac{1}{2} \frac{(z+H)^2}{\sigma_z^2}\right) \right\} \quad (2.5)$$

Where,

- C = steady-state concentration at point (x, y, z) , $[M/L^3]$,
- Q = emission rate, $[M/T]$,
- σ_y, σ_z = horizontal and vertical spread parameters, $[L]$,
- u = average wind speed at stack height, $[L]$,
- y = horizontal distant from plume centerline, $[L]$,
- z = vertical distance from ground level, $[L]$, and
- H = effective stack height, $[L]$.

A view of the double Gaussian distribution in the plume, portrayed by Equation 2.5 is presented in Figure 2.2.

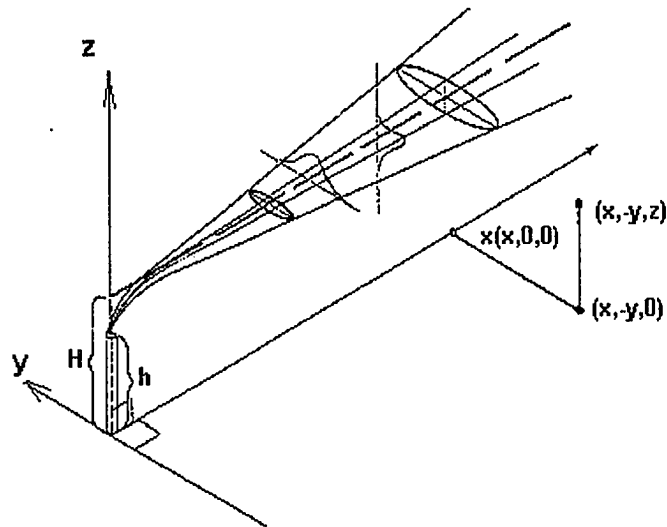


Figure 2.2 Coordinate system showing Gaussian distributions in horizontal and vertical (Turner, 1970)

Gaussian distribution plume models, which have the initial parameters reflecting urban area conditions, have been evaluated for many different studies both in the field and laboratory, and semi-empirical models have been established that permit to calculate, with some accuracy, the spreading of pollutants from an elevated point source. These semi-empirical models are not accurate enough to describe local street canyon behavior. Mathematical models are needed to connect them to meteorological mesoscale models.

2.2 Wind Effects on Low-Rise Building in the Turbulent Boundary Layers

From the viewpoint of aerodynamics, most buildings are called bluff or blunt bodies, in contrast to streamlined bodies such as aircraft wings. Most buildings are located within the Atmospheric Surface Layer (ASL), where the wind flow is more turbulent than in the upper part of Atmospheric Boundary Layer (ABL). The interaction between the building and the approaching wind leads to building-induced turbulence generated near the building surfaces. The wind-induced pressure fluctuation on the surfaces of a building varies in time and space. It is influenced by many factors: wind speed and direction, level of turbulence in the approaching wind, surrounding terrain, and geometry of the building. Airflow around bluff bodies results in distortion, deceleration, acceleration, separation and reattachment of flow. Turbulent boundary layer flows, such as the presence of a wind velocity profile and shear stress, as they are typical for natural wind, complicate the flow around bluff bodies drastically. A single rectangular-shaped bluff building in ABL flow represents an idealized case, which is illustrated in Figure 2.3.

The remainder of this section is devoted to the discussion of these characteristics on the walls and the roof of a simple building.

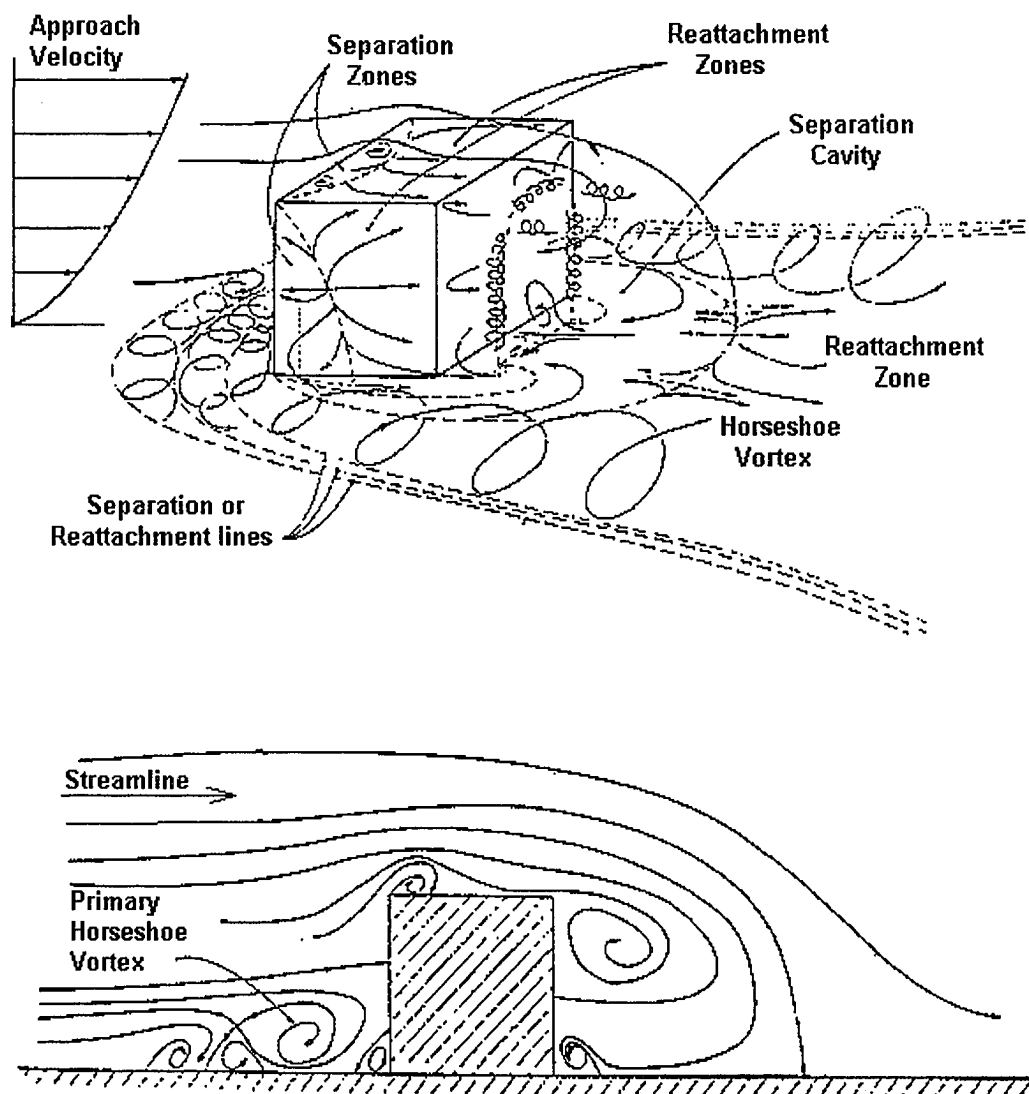


Figure 2.3 Model of flow near a sharp-edged building normal to deep boundary layer wind (from Hosker, 1984, based on Peterka, 1977)

2.2.1 Windward Wall

The flow pattern near the windward wall is shown on Figure 2.4. The wind flow comes to rest to form the front stagnation point, S1, at about two-thirds of the height of the building. The flow goes down until it reaches the ground, where it has more kinetic energy than the incident wind at this level. It moves forward against the wind and loses energy until it comes to rest at a separation point on the ground, marked S2. As Figure 2.4 shows, beyond the point, S2, the flow rolls up and forms a horseshoe vortex on the ground in front of the windward face. Near the ground, the vortex extends along the sidewalls of the building. This vortex has a significant effect on the distribution of wind pressure on the windward surface.

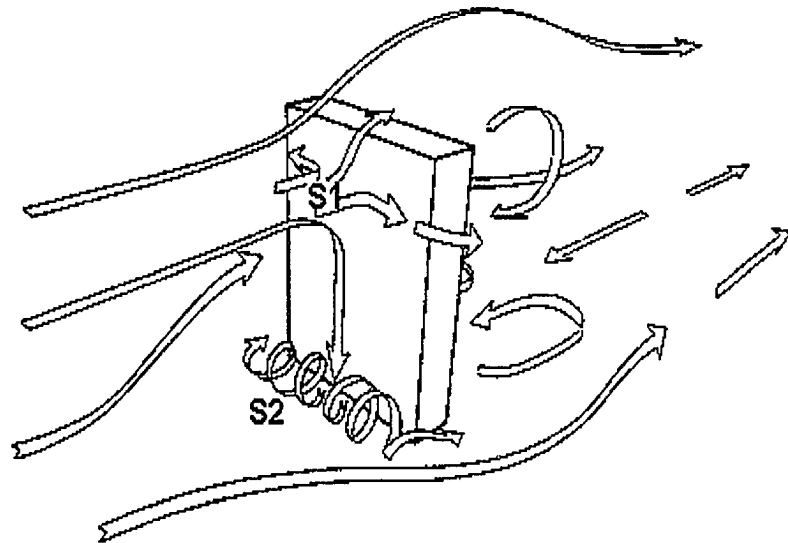


Figure 2.4 Flow pattern on windward wall (Beranek, 1980)

2.2.2 Side and Leeward Walls

In Figure 2.5, due to the flow separation along the edge of the windward surface, the two sidewalls are under the action of negative pressures (suctions). Flow around the top one-thirds of the building height is marked A. The flow at low elevations, marked B, is associated with the horseshoe vortex. It is significantly faster than the incident wind at that level. The pressure distribution is found to be nearly uniform along the upstream edge of the sidewall.

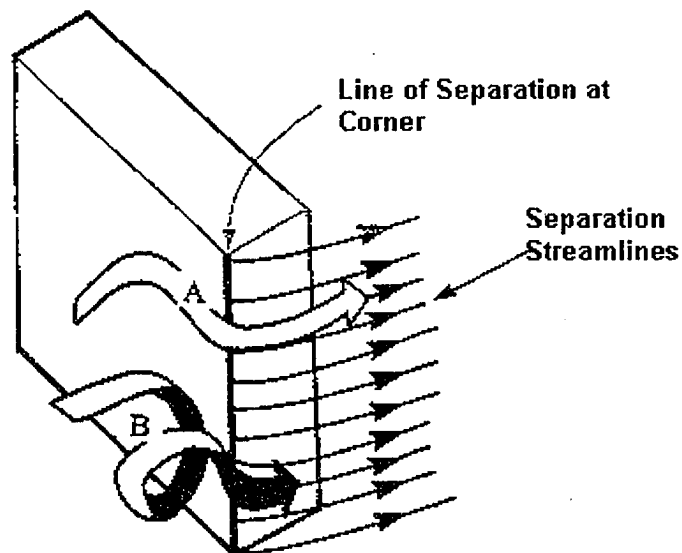


Figure 2.5 Separation at sidewall (Cook, 1985)

The flow trailing the building is called the wake. Figure 2.6 shows the flow pattern in the wake immediately behind a slab block. Two flows, marked A, indicate a pair of vertical vortices driven by a flow from the horseshoe vortex through the shear

layers on each side of the slab. The flow marked B indicates a circulation driven through the shear layer over the roof, which interacts with the flow in the vortices. A relatively uniform pressure distribution is found in the region close to the vertical sides of the leeward face (Cook, 1985).

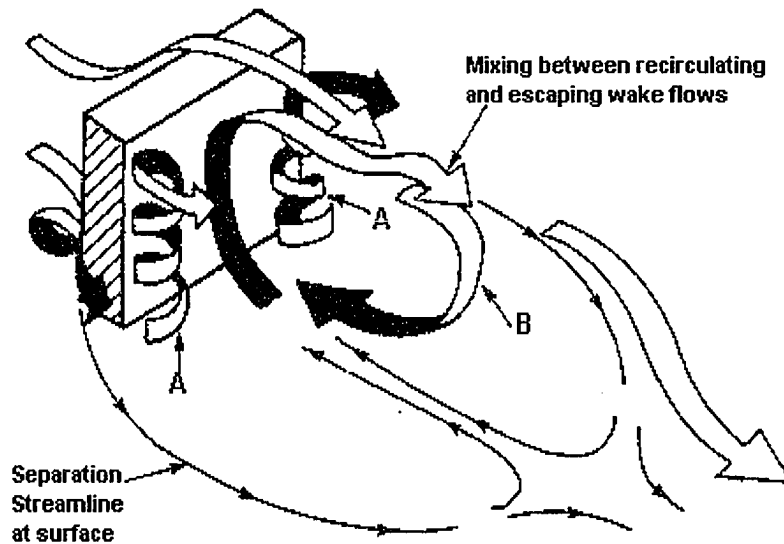


Figure 2.6 Wake circulations behind slab block (Cook, 1985)

2.2.3 Roof

The pressure on the roof surface of the building shows high suction near the roof corner and edges. Despite extensive wind-tunnel experiments, the agreement between laboratory simulation and full scale model measurements of the negative peak and rms point pressure continues to be less than satisfactory, especially at some locations near the roof corner (Ham and Bienkiewicz, 1997).

Consider a wind with a flow approaching normal to the windward face of a building. A uniform separation bubble is formed along the upstream edge of the roof. Figure 2.7 shows a streamline pattern associated with the condition described above. The flow above the stagnation point on the windward wall goes up and separates along the roof edge; then it reattaches to the roof. The joint effect of the wind profile, vorticity in the shear layer along the separation boundary, and Reynolds stress within the ABL is to lower the separated streamline and to promote earlier reattachment of the separated flow to the building roof (Banks, 1999). Higher suctions are encountered near the roof edge.

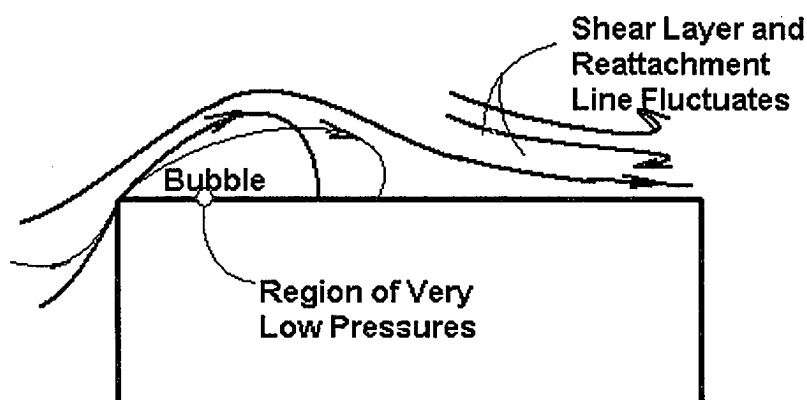


Figure 2.7 Separation and reattachment on the roof of low-rise building (Banks, 1999)

At an angle other than normal to a face, the flow separating from the upwind edge of the roof will have a component of velocity along the line of separation. Figure 2.8 illustrates the general pattern of the resulting deltawing vortices. Both of these primary

and secondary vortices roll up to form a pair of trailing vortices. The highest magnitude of the mean (negative) roof pressure occurs in the secondary vortex region. The highest pressure gradient occurs in the reattachment region, located between the reattachment line and the secondary separation line. The highest negative peak pressure and the highest pressure fluctuations occur in the separated region of the primary flow (Sun, 1993).

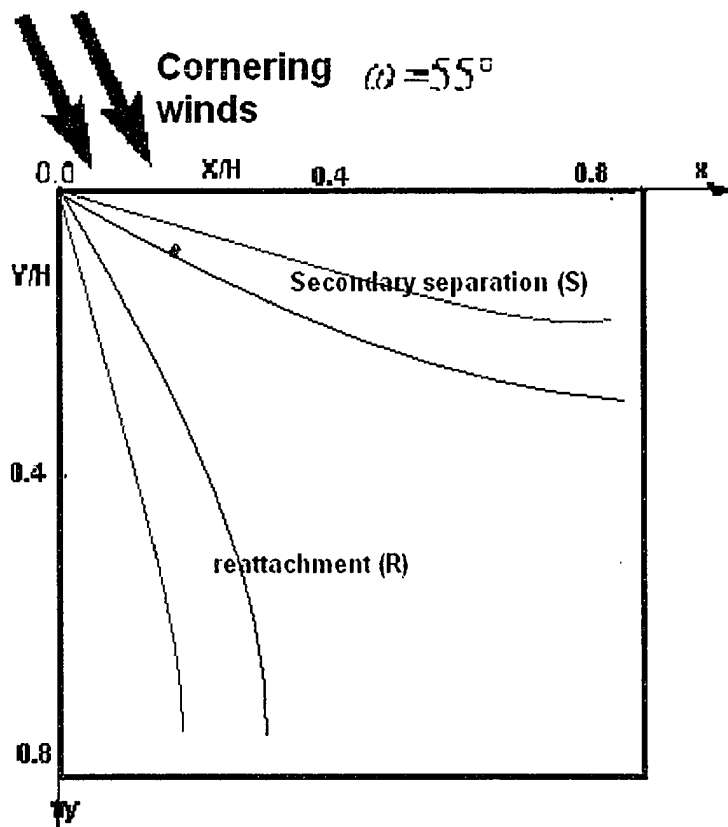


Figure 2.8 Sketch of primary and secondary vortices (Sun, 1993)

2.3 Physical Modeling of Flow and Dispersion in Urban Street Canyons

The characteristics of flow and dispersion over an urban area are determined by interaction of the approaching flow with a change in surface boundary conditions created by the urban development. Roughness and temperature of an urban area usually are higher than for the surroundings. When modeling the flow of air in the atmospheric boundary layer, certain similarity conditions must be satisfied. Similarity criteria are presented for modeling of thermally stratified, boundary layer approach flows and similarity of the urban area roughness and thermal characteristics. These requirements of similarity of the ABL and the wind tunnel boundary can be obtained from nondimensional groups found in the normalized equations of conservation of mass, momentum and energy. Cermak (1981) has summarized these requirements for wind tunnel boundary layers.

It is very difficult to obtain exact simulation of all requirements for similarity. However, there are relaxations that can be made in some situations for these requirements because of the limited effect on the flow characteristics.

2.3.1 The Equations of Conservation of Mass, Momentum and Energy

Inspectional analysis (Ruark, 1935) of the fundamental conservation equations for mass, momentum and energy and the equation of state yields non-dimensional parameters that serve as similarity criteria (Cermak, 1975). The equation of motion for a fluid in a turbulent boundary layer can be expressed in a nondimensional form by using the scaling factors:

$$U_i^* = \frac{U_i}{U_0}, \quad u_i^* = \frac{u_i}{U_0}, \quad (u_i^*)^* = \frac{u_i^*}{U_0}, \quad (\theta^*)^* = \frac{\theta^*}{T_0}, \quad x_i^* = \frac{x_i}{L_0}, \quad t^* = \frac{tU_0}{L_0},$$

$$\rho^* = \frac{\rho}{\rho_0}, \quad \Omega_j^* = \frac{\Omega_j}{\Omega_0}, \quad P^* = \frac{P}{(\rho_0 U_0^2)}, \quad T^* = \frac{T}{T_0}, \quad \Delta T^* = \frac{\Delta T}{\Delta T_0}, \quad \text{and} \quad g^* = \frac{g}{g_0}.$$

The equations which result are

$$\frac{\partial \rho^*}{\partial t^*} + \frac{\partial (\rho^* u_i^*)}{\partial x_i^*} = 0 \quad (2.6)$$

$$\begin{aligned} \frac{\partial U_i^*}{\partial t^*} + U_j^* \frac{\partial U_i^*}{\partial x_j^*} + \left[\frac{L_0 \Omega_0}{U_0} \right] 2\varepsilon_{ijk} \Omega_j^* U_k^* = \\ - \frac{\partial P^*}{\partial x_i^*} - \left[\frac{\Delta T_0}{T_0} \frac{L_0 g_0}{U_0^2} \right] \Delta T^* g^* \delta_{i3} + \left[\frac{\nu_0}{L_0 U_0} \right] \frac{\partial^2 U_i^*}{\partial x_k^* \partial x_k^*} + \frac{\partial \overline{(-u_i^* u_j^*)}}{\partial x_j^*}, \end{aligned} \quad (2.7)$$

$$\frac{\partial T^*}{\partial t^*} + U_i^* \frac{\partial T^*}{\partial x_i^*} = \left[\frac{k_0}{\rho_0 C_{p0} \nu_0} \right] \left[\frac{\nu_0}{L_0 U_0} \right] \frac{\partial^2 T^*}{\partial x_k^* \partial x_k^*} + \frac{\partial \overline{(-\theta^* u_i^*)}}{\partial x_i^*} + \left[\frac{\nu_0}{U_0 L_0} \right] \left[\frac{U_0^2}{C_{p0} T_0} \right] \phi^* \quad (2.8)$$

the dimensionless continuity, momentum and energy equations respectively (Equations (2.6), (2.7) and (2.8)).

The above equations are time averaged instantaneous equations of motion in a fixed frame of reference. These equations contain the non-dimensional groups that form the basis for the simulation of atmospheric flow in a wind tunnel.

Synoptically, the parameters that must reproduced in the wind tunnel for exact similarity between the model and prototype are:

1. Geometric scaling.
2. Rossby Number Ro , $U_0/L_0\Omega_0$.
3. Richardson Number Ri , $(\Delta T_0/T_0)(L_0g_0/U_0^2)$.
4. Prandtl number Pr , $\nu_0\rho_0C_{p0}/k_0$.
5. Eckert Number Ec , $U_0^2/(C_{p0} T_0)$.
6. Reynolds Number Re , $U_0 L_0/\nu_0$.
7. The approach flow characteristics.
8. Longitudinal pressure gradient.

2.3.2 Satisfying the Similarity Criteria

Geometric Similarity

Geometric similarity of the model and the prototype automatically require one to scale all lengths equally in 3 dimensions. The continuity equation, shown at Equation 2.6, contributes no additional dimensionless groups. Hence a correctly scaled model will automatically simulate the mass flow and satisfy the conservation of mass.

Rosby Number Similarity

The Rossby number found within the momentum equation, Equation 2.7, is a representation of the ratio of inertial forces to Coriolis forces. To exactly simulate the Rossby number, the effects of the Earth's rotation should be simulated by rotating the model sufficiently to equal that of the Earth after compensating for the length and/or velocity scaling. Relaxation of this criterion is allowed because the effects of the Earth's rotation are negligible in the prototype for the short traced distances and velocities considered in this experiment.

Richardson Number Similarity

The Richardson number represents the relative significance of buoyant forces and inertial forces. The density stratification for both the model and the prototype for proper simulation of buoyant forces must be the same. Since neutral stratification is used in this experiment, the Richardson number is zero for the model and prototype atmospheres.

Prandtl Number Similarity and Eckert Number Similarity

Both the Prandtl number and the Eckert number are dimensionless groups found in Equation 2.8, the energy equation. The Prandtl number is expressed as the ratio of molecular viscosity to thermal diffusivity, which involves only the properties of the fluid. Prandtl number equality is automatically achieved in this experiment, because the working fluid in both the model and the prototype is air.

The Eckert number is a difficult parameter to model in a wind tunnel. It represents the ratio of heat generated by friction to heat compression. The Eckert numbers of the two flows cannot be made similar, if the Richardson number equality exists. However, the range of velocities considered in these experiments produce a Mach number that is much smaller than the speed of sound. Because of these low velocities, there is little compression and little heat is generated by friction. Therefore, the Eckert number criteria may be relaxed.

Reynolds Number Similarity

The Reynolds Number is defined as the ratio of convective inertial forces to viscous forces. The equality of the Reynolds number, Re , cannot be realized; therefore, the significance of this difficulty must be assessed. Fortunately, as shown by Figure 2.9 (Cermak, 1975), local flow characteristics over a plane surface become independent of Re at values that depend upon the relative roughness K_s/L , where K_s = equivalent sand roughness. This means the approach flow can be adequately simulated, when values of Re_m are in the Reynolds number independence range, even though Re_m does not equal Re_p .

The Approach Flow Characteristics and Longitudinal Pressure Gradient

To achieve similarity in the approach flow, the boundary layer structured by the upwind fetch is characterized by a power-law velocity profile similar to those found in an

urban atmosphere. The turbulence intensity levels must also be similar to the atmosphere found in a city.

The longitudinal pressure gradient over the model is set to be zero by adjusting the wind tunnel roof height to make the flow as non-accelerating as it is in the atmosphere.

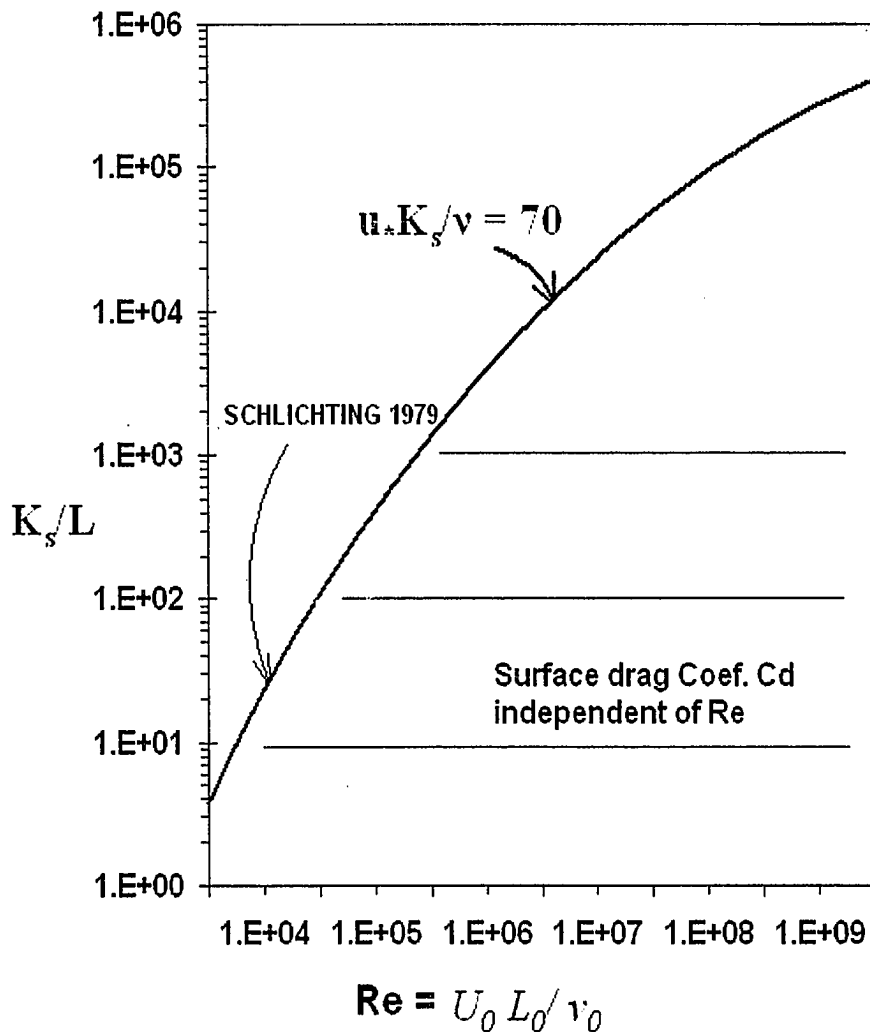


Figure 2.9 Reynolds-number independence for surface drag coefficient C_d (Cermak, 1975)

2.4 Numerical Simulation Model

Advanced technology has produced faster and more powerful desktop computers, which allows computational fluid dynamics (CFD) procedures to be applied to urban flow problems. Numerical simulation is especially useful for providing detailed flow visualization that is difficult for physical simulation to perform.

The field of CFD is a young field of research in a constant state of evolution, and the developments occur rapidly. Analysis of flow fields around bluff bodies by CFD is a very difficult task. There are two main reasons: first, flow obstacles are always inside the surface boundary layer. Second, these flow obstacles and bluff bodies have sharp edges at their corners, which require very fine grid discretization to analyze such flow fields with high precision. Some in the physical modeling community may question the precision of the numerical approaches. However, comparative exercises like those provided here provide validation efforts to assess the accuracy of the numerical approaches.

2.4.1 Numerical Simulation Solution Techniques

Three general solution approaches exist for numerical simulation of turbulent flow fields. The methodologies become increasingly powerful with each level of complexity. The approaches described here are direct numerical simulation, large eddy simulation and statistical turbulence model simulation (Murakami and Rodi, 1993).

Direct Numerical Simulation

The most fundamental, most powerful and most demanding technique used presently is direct numerical simulation (DNS). This requires direct solution of the unsteady conservation of mass and momentum equations. With proper boundary conditions and a sufficiently fine grid mesh, this approach can solve problems for all scales of turbulent motion. Needless to say, this requires immense storage and computation times and is far beyond the scope of this investigation.

Large Eddy Simulation

Large eddy simulation (LES) uses a more coarse-grid distribution to resolve only large-scale turbulent motion. Sub-grid scale turbulence and its dissipation are atmospheric dynamic simulations, which are recently being applied to building aerodynamic studies (Kato et al. 1991, Nicholls et al. 1992).

Statistical Turbulence Models

Most commercial computational fluid dynamics codes use statistical turbulence models. These solve the Reynolds averaged forms of the conservation equations while applying a numerical model to account for all scales of turbulent dissipation. The model simulates all stochastic turbulent fluctuations and turbulent stresses in the averaged equations. The κ - ϵ model is an example of a statistical code and algebraic stress models are typically more refined versions of this approach. The κ - ϵ approach assumes that turbulent stresses are strictly proportional to velocity gradients and that the eddy viscosity

is isotropic. An algebraic stress and approach solves each of the stress tensor terms and is not restricted by an isotropic eddy viscosity assumption (Rodi, 1993).

2.4.2 CFD Applications in Wind Engineering

The application of CFD in wind engineering is developing steadily (Computation Wind Engineering (CWE) 1992, 1996, and 2000). CFD has become very familiar as an analytical tool for engineers and researchers in wing engineering fields. Recent applications of CFD to wind engineering problems cover topics such as wind force, oscillation, dispersion, ventilation, atmospheric boundary layer, and regional climate (Overview of CWE 2000, Murakami). Among the most popular topics are analysis of fluid structure interaction problems in the field of structural engineering, and analysis of contaminant dispersion phenomena in the field of engineering. These two topics are often solved by CFD and are regarded as the most important and difficult research problems for each field.

There have been many CFD studies done on the analysis of velocity and pressure fields around a bluff body (See papers of Fourth International Colloquium on Bluff Body Aerodynamics & Application, Sep. 11-14, 2000). The κ - ϵ model was among the first turbulence models to be used, but the predicted values of velocity or pressure around a bluff body are significantly different from the experiment results, due to the fundamental shortcomings of EVM (Eddy Viscosity Modeling) in the κ - ϵ model. Many attempts have been made to revise the κ - ϵ model, and several new models have also been proposed. The prediction accuracy of these new models has significantly improved. The

predictions of air pollution dispersion around buildings or in city areas are very important subjects in environmental engineering. It is often arduous and time consuming to measure air pollution concentrations in a wind tunnel or in the field. CFD prediction of such dispersion phenomenon promises to eventually provide a convenient and flexible solution approach. Alternatively, CFD can help design and set up wind tunnel or field experiments, and, hence, reduce the time required to optimize a physical model and reduce expensive runs in a wind tunnel or in the field.

CHAPTER 3

ARRANGEMENT OF THE EXPERIMENTS, DATA ACQUISITION AND ANALYSIS TECHNIQUES

3.1 Wind Tunnel Facility and Physical Arrangement of the Experiment

The wind tunnel facility and the geometric arrangement of the experiments are discussed in this section. Topics include descriptions of the boundary layer wind tunnel, characteristics of the approach flow, the basic building model (TTU Building), and array arrangements of the urban street canyon model.

3.1.1 Boundary Layer Wind Tunnel

All data reported in this study are obtained in the Industrial Aerodynamics Wind Tunnel (IWT) in the Wind Engineering and Fluids Laboratory (WEFL) at Colorado State University. The layout of the WEFL and a schematic of IWT are shown on Figures 3.1 and 3.2. The IWT is a closed-circuit wind tunnel, which has a test section of 6 ft. (1.83 m) wide by 60 ft. (18.29 m) long with a ceiling height adjustable from 5 ft. (1.52 m) to 7 ft. (2.13 m). The wind speed can be continuously varied from 0 fps up to approximately 80 fps depending on blockage inside the tunnel. The ceiling of the wind tunnel is adjustable to control pressure gradient in the mean flow direction. The inlet boundary as

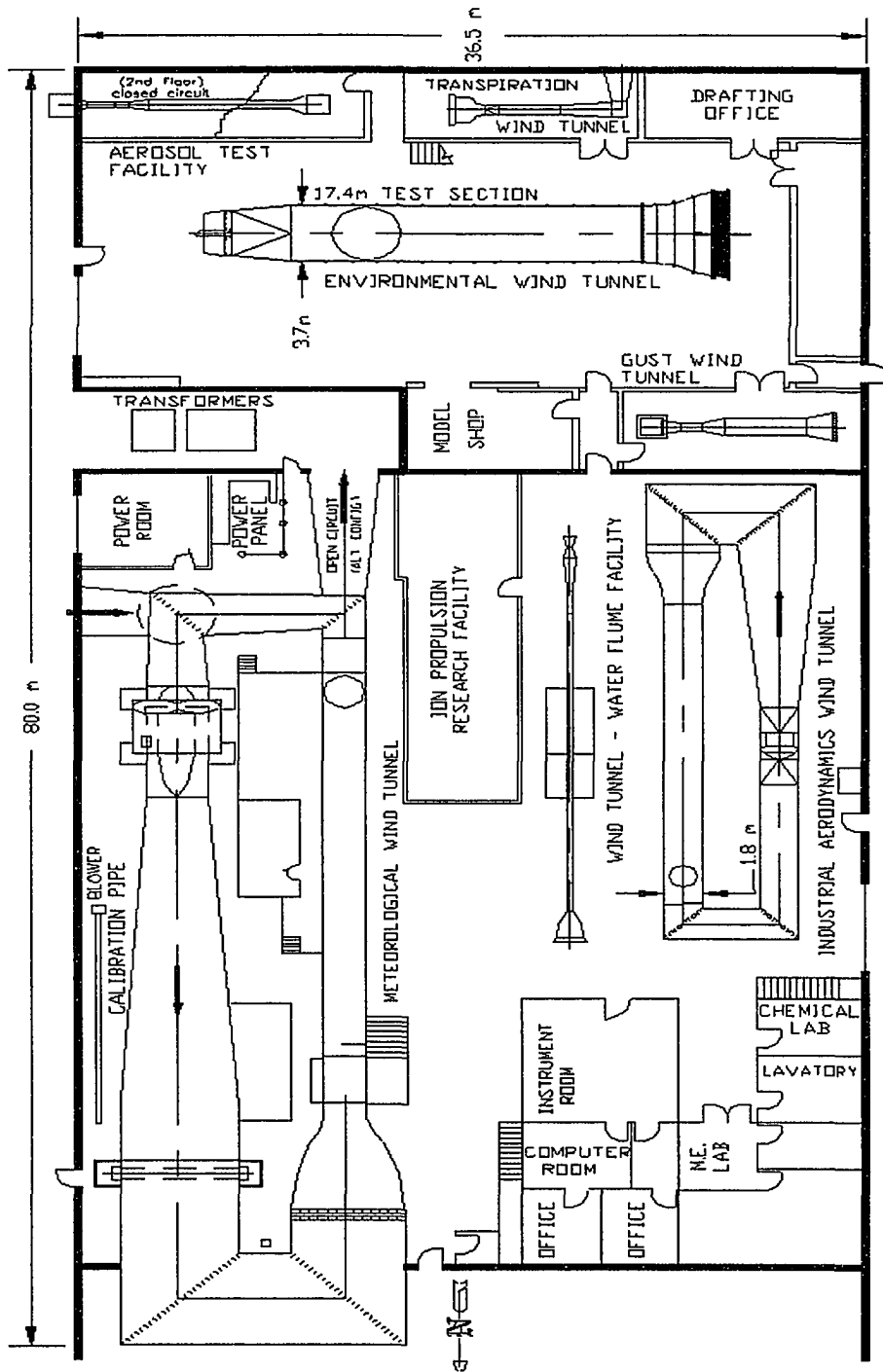


Figure 3.1 Wind engineering and fluid laboratory layouts

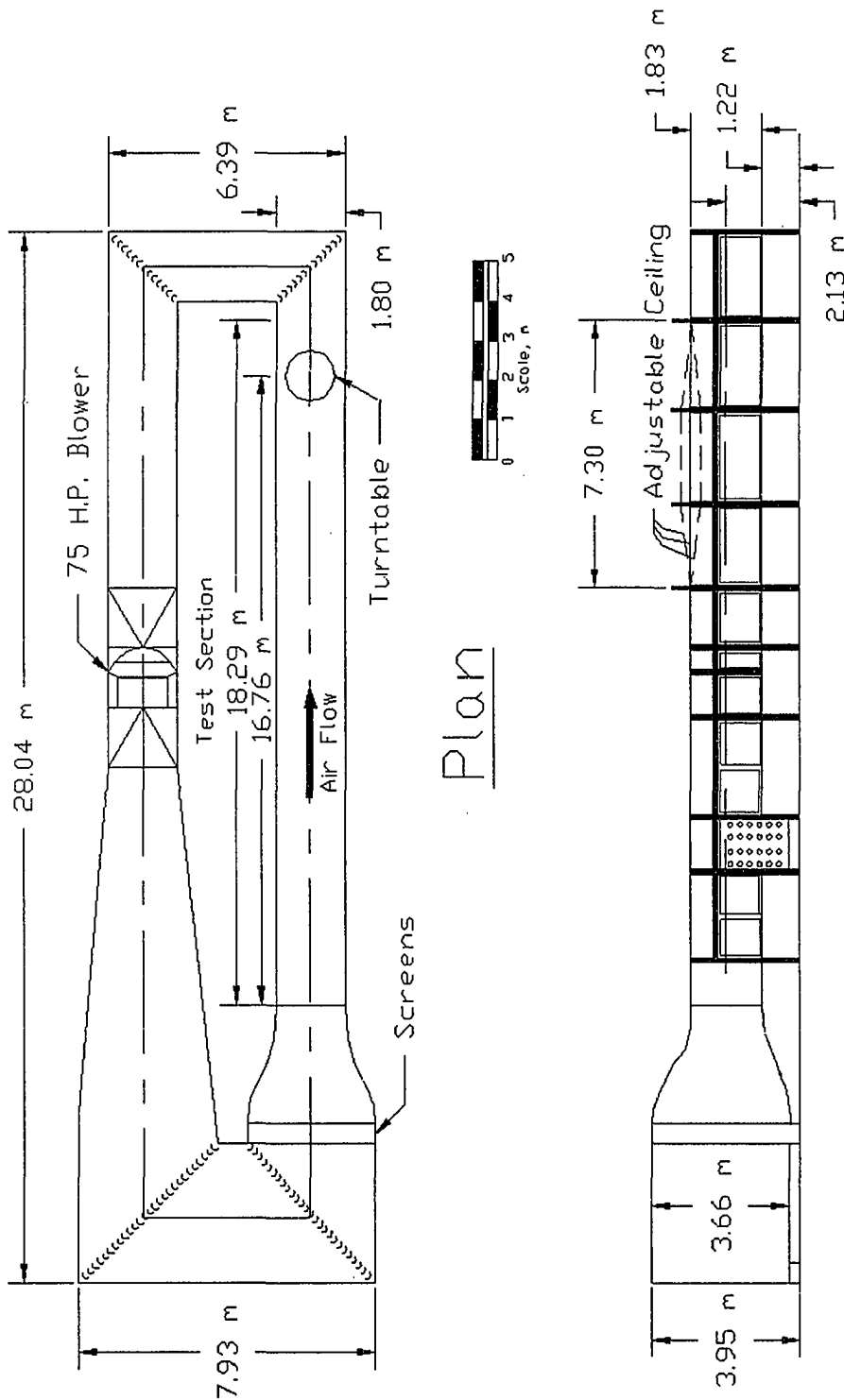


Figure 3.2 Schematic of Industrial Wind Tunnel

defined by wind velocity and turbulence intensity profiles in front of the second row of the upstream building is similar to the CSU-B2 case prepared by Ham (1998).

3.1.2 Approach Flow Characteristics

Approach flow velocity measurements were surveyed at the front of the second row of the upstream buildings. Figure 3.3 shows the approach flow velocity profile. The approach flow velocity and turbulent statistics profiles are obtained from film measurement described in section 3.2.2. The approach flow velocity profile data were regressed to find the best logarithmic law (Simiu and Scanlan, 1996) and power law fit. The logarithmic regression found a best fit roughness length $z_0 = 1.1$ cm and $u^* = 0.6$ m/sec, such that

$$u(z) = \frac{1}{k} u_* \ln \frac{z}{z_0}, k \approx 0.4 \quad (3.1)$$

The power law regression found an exponent, $p = 0.14$ (see Equation (3.2)).

$$u(z_1) = u(z_2) \left(\frac{z_1}{z_2} \right)^p \quad (3.2)$$

The local turbulence intensity profile is plotted in Figure 3.4. The longitudinal turbulence intensity is defined as

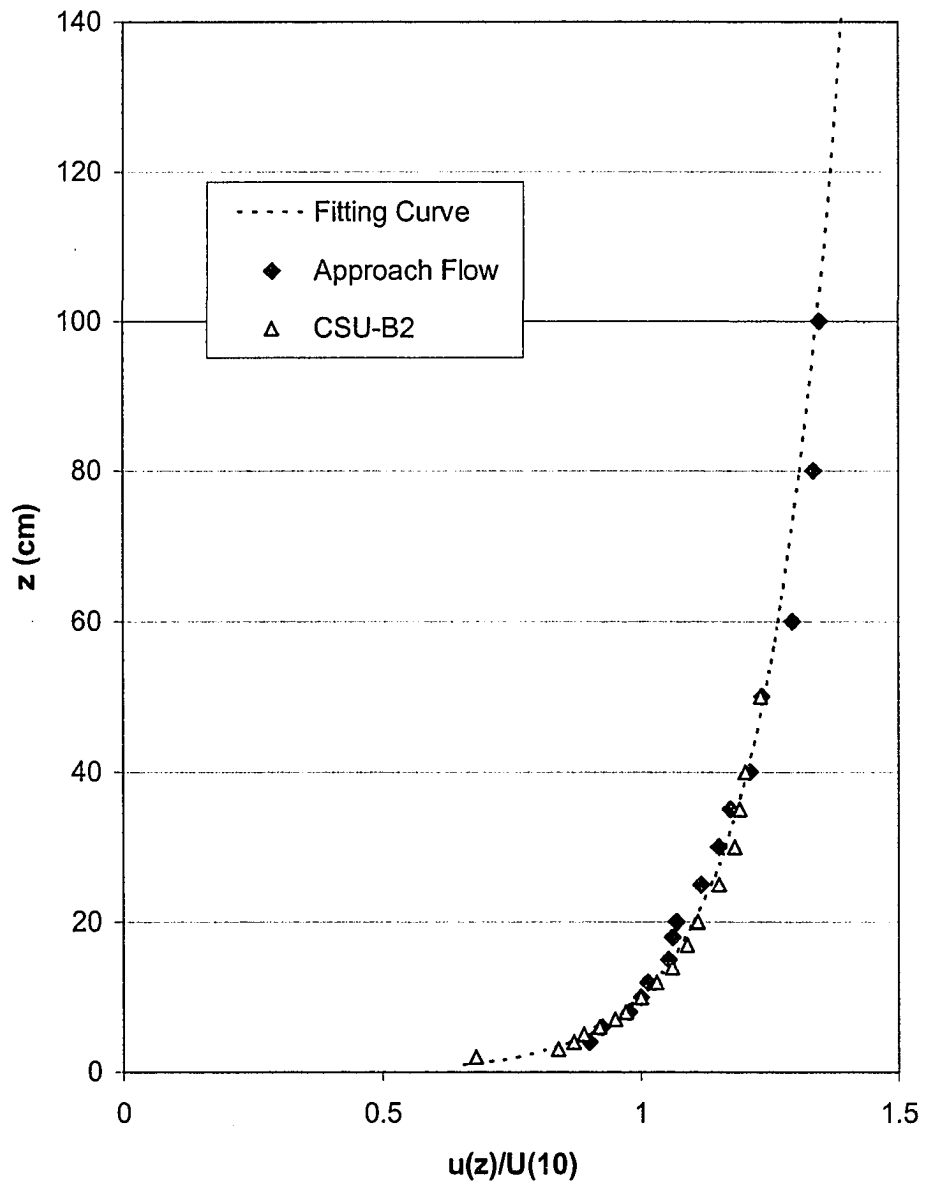


Figure 3.3 Approach flow velocity profile

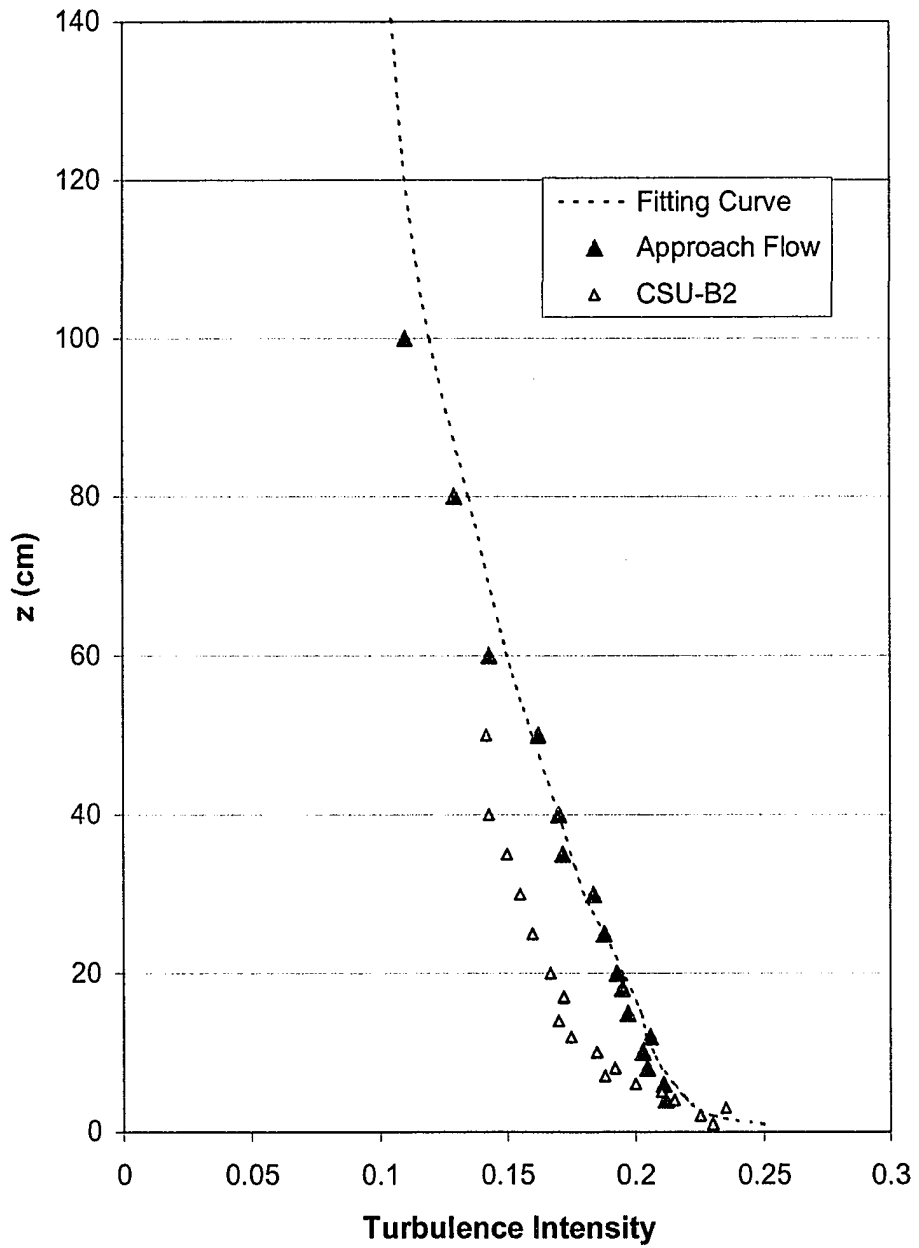


Figure 3.4 Approach flow turbulence intensity profile

$$I(z) = \frac{\sqrt{u^2(z)}}{U(z)} \quad (3.3)$$

Where $U(z)$ = mean wind velocity at elevation z and $\sqrt{u^2}$ root mean square value of u , the local perturbation velocity.

3.1.3 Basic Building Model and Arrangement of Urban Street Canyon Model

The basic shape of the Wind Engineering Research Field Laboratory building (WERFL) at Texas Tech University, Lubbock, which is a metal building of simple rectangular prism shape (9.2 m * 13.8 m * 4.0 m tall). It is used to perform the wind tunnel simulation. Figure 3.5a shows the picture of WERFL at TTU. Two plastic models of the WERFL structure are constructed to a 1:50 scale for pressure and concentration measurements. One is instrumented with 95 pressure-sampling ports, and the other is instrumented with 44 concentration-sampling ports (Figure 3.5b and 3.5c). A large number of “dummy” models of similar dimensions, constructed of plastic foam and wood, represent the surrounding buildings. These buildings are arranged in various symmetric configurations with different separation distances and placed in the Industrial Wind Tunnel of the Wind Engineering and Fluid Laboratory, Colorado State University. Typical building patterns are noted in Figure 3.6, and the associated arrangement patterns are listed in Table 3.1. Figure 3.5d shows the models inside the industrial wind tunnel.

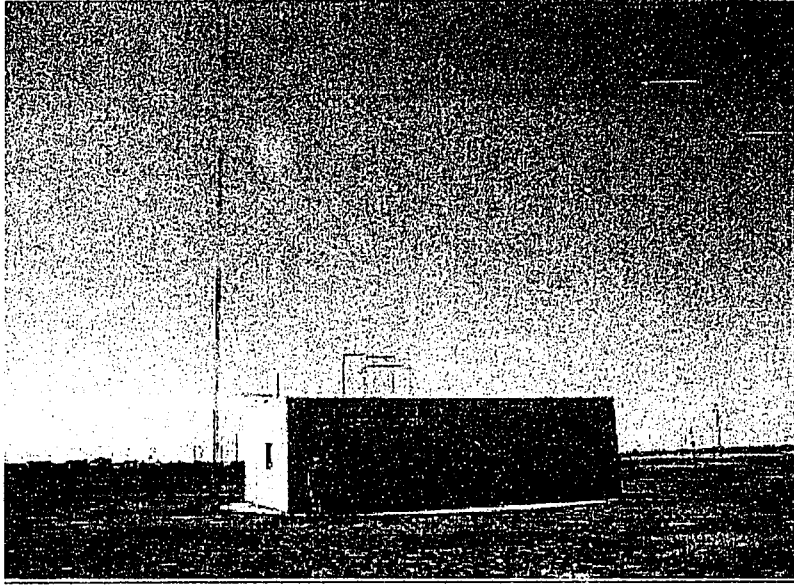


Figure 3.5a Picture of WERFL at TTU

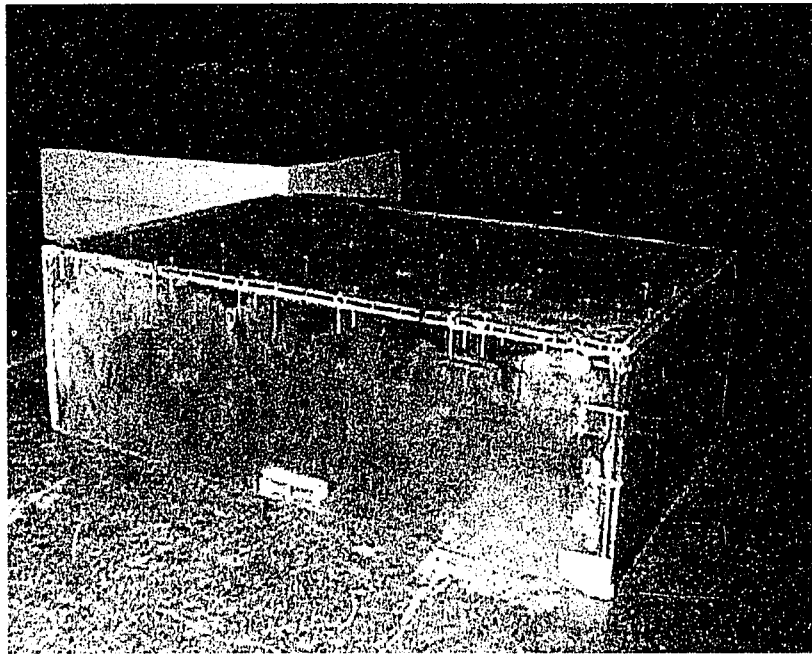


Figure 3.5b 1:50 scale WERFL with 95 pressure ports

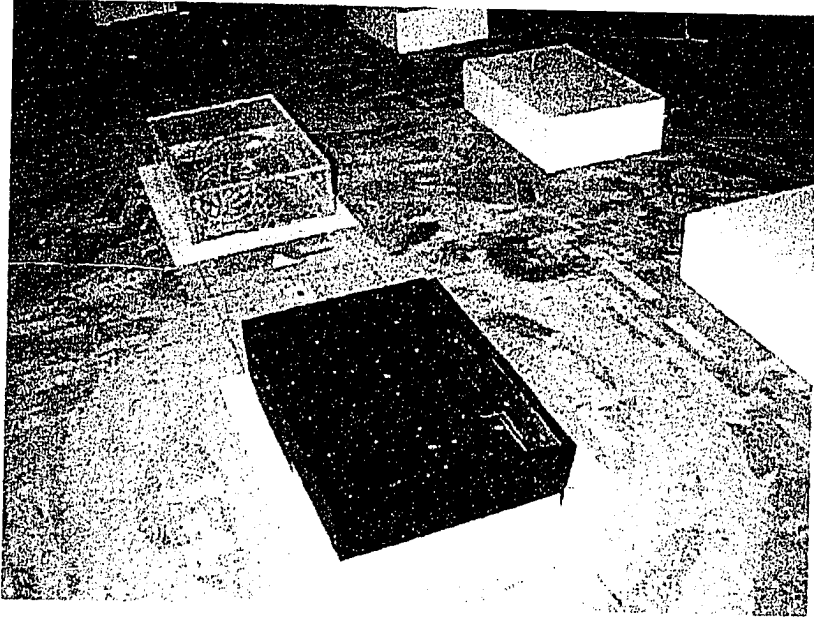


Figure 3.5c 1:50 scale WERFL with 44 concentration ports

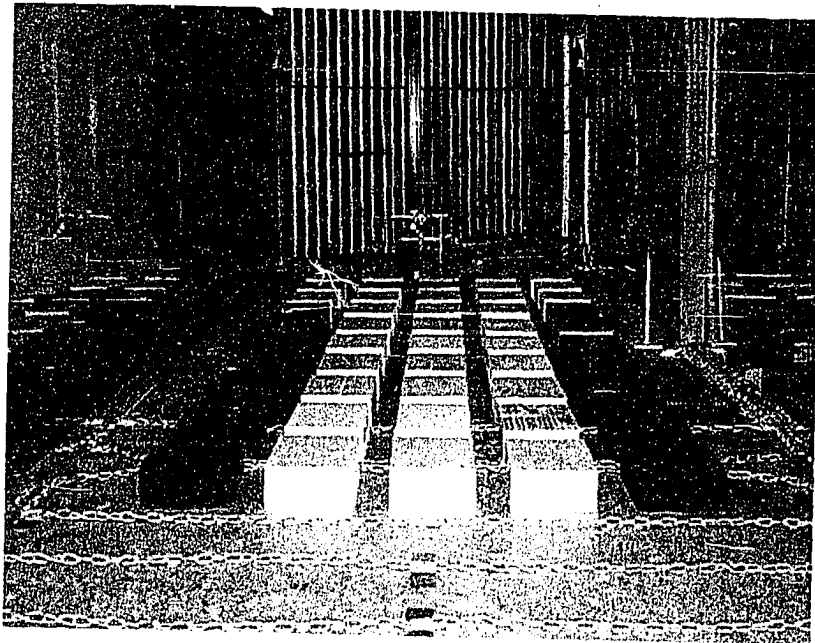


Figure 3.5d Industrial wind tunnel (IWT) and models

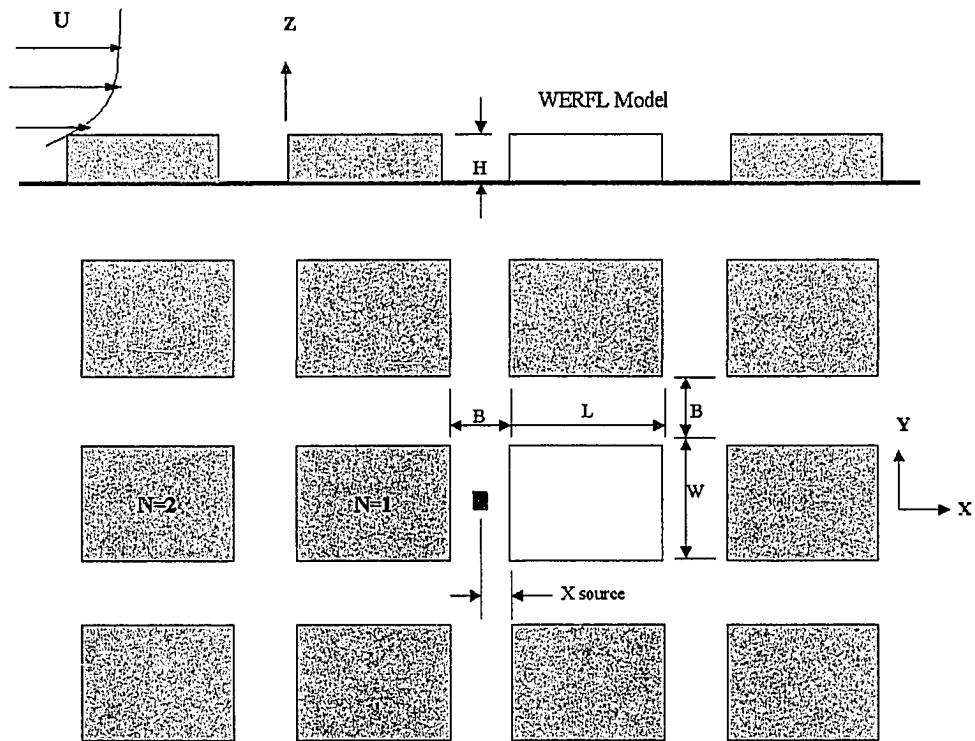


Figure 3.6 Schematic of Urban Street-canyon Model Arrangement

B/H	λ_{ar}	λ_{fa}	N rows	Structure	Flow
0.5	.72	.21	1,2,3,&8	City center	Skimming flow
1.0	.54	.16	1,2,3,&8	City center	Skimming flow
2.0	.34	.10	1,2,3,&8	Suburban	Wake interference
4.0	.17	.05	1,2,3,&8	Urban 1-2 stories	Wake interference
6.0	.10	.03	1,2,3,&8	One story houses	Isolated

$$\lambda_{ar} = \sum \text{of areas covered by buildings} / \text{total urban area}$$

$$\lambda_{fa} = \sum \text{of average building areas normal to the wind} / \text{total urban area}$$

Table 3.1 Array of model structures studied, $X_{source} = B/2$

3.2 Wind Tunnel Measurements

A series of measurements were made over a generic urban street canyon arrangement using flow visualization, anemometry and gas chromatography in the Industrial Wind Tunnel. The detailed descriptions of each measurement technique will be discussed in the following subsections.

3.2.1 Flow Visualization on Street Canyon Area

A visible plume is produced by passing the metered stimulant gas through a Rosco Model 1600 Fog/Smoke Machine located outside the wind tunnel, and then the smoke is released upstream of the model inside the wind tunnel. A laser light sheet is used to illuminate a plane within the canyon and flow separation region. Figure 3.7 shows a schematic of the flow visualization setup. The laser is a Coherent Innova 70-5 Argon ion water-cooled laser, which is operated in a multi-line mode. It has a nominal maximum output of 5 Watts, but is generally run at or below 1 Watt for these tests. Seventy percent of the laser beam light is carried into the tunnel using a fiber optic cable with a 50 micro diameter core. The fibers replace a mirror assembly that transferred 100% of the light, and require regular re-alignment. An assortment of lenses mounted at the fiber optic cable's exit is used to focus the light to a point 1 mm to 2 mm in diameter on the center of the canyon between two buildings. Various cylindrical lenses can spread this spot of light into a sheet from a few centimeters to over one meter in length. The visualizations for each test were recorded on VHS videocassettes with a Panasonic Omni

vision II camera/recorder system. The visible behavior of the smoke line is also recorded by a high-resolution television camera system on a VCR tape. The analog images may be transformed into digital arrays and saved into personal computer by Digital Photo & Video Maker (P/N DM-5000 V.3, Dazzle Multimedia), and the images can then be enhanced and manipulated by a personal computer system.

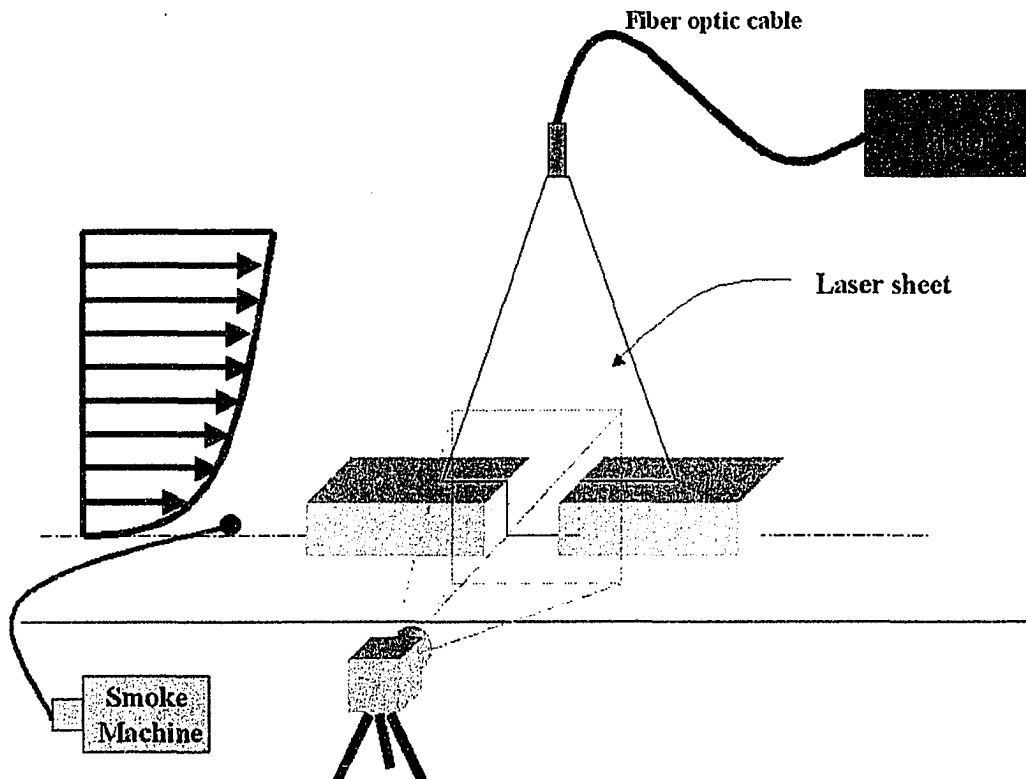


Figure 3.7 Schematic of visualization setup

3.2.2 Wind Profile and Turbulence Characteristics Measurements

Velocity measurements were made with single hot-film probes (TSI1220 Sensor) and constant-temperature anemometer model TSI 1051-2D manufactured by Thermo-System, Inc. Figure 3.8 shows a schematic chart of the velocity calibration system, velocity measurement system, and the positioning system within the wind tunnel.

Velocity Standards

TSI 1125 Velocity Calibrator System and Pitot-static Probes are used for velocity calibration. The TSI Model 1125 Velocity Calibrator System is designed to calibrate hot wire sensors. The calibration range is from about 0.1 m/s to 305 m/s in air. The accuracy of this system depends on the accuracy of the pressure measurement. The accuracy is ± 2 percent when flow velocity is above 3 m/s. Pitot-static probes are used as velocity standards during the calibration of the different hot film systems to provide the reference upwind velocity measurement. The principles of operation of pitot-static probes can be explained in terms of Bernoulli's equation. The operational relationship for these probes is $U = (2g_c\Delta P/\rho)^{1/2}$, where U = velocity, g_c = gravitational conversion constant, ΔP = difference between static and stagnation pressures, and ρ is the air density. ρ is calculated from the ideal gas law, and ΔP is measured by using a Datametrics Electronic Manometer. The pitot-static probe measurements are accurate to be within ± 2 percent of the actual velocity.

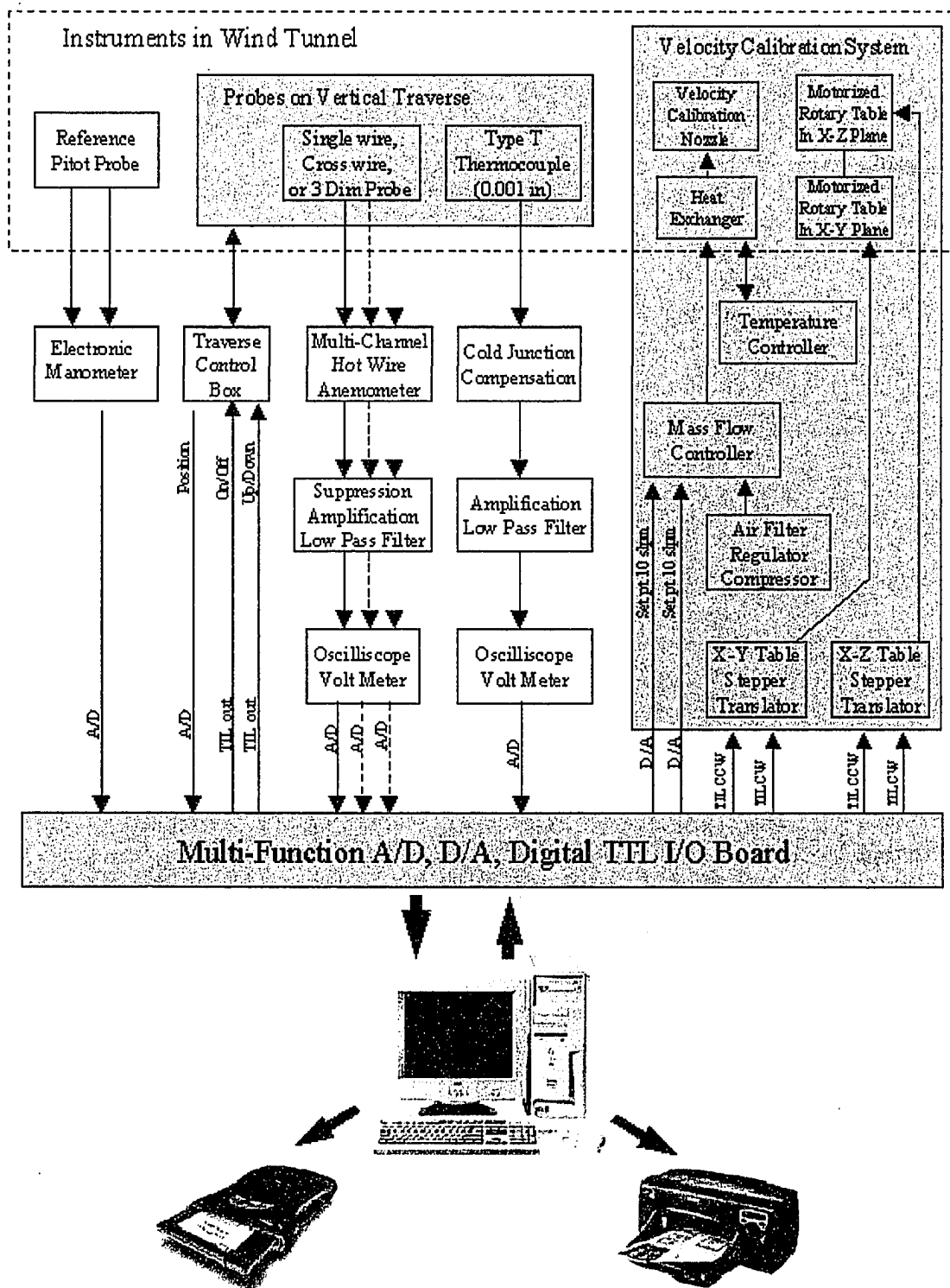


Fig.3.8 Velocity calibration and Measurement system

Single-Hot-film Probe Measurements

Single-hot-film (TSI 1220 Sensor) measurements are used to document the longitudinal turbulence level for the approach flow conditions. The probe voltages are recorded at several velocities covering the interest range during wind tunnel simulation calibration. The single-hot-film voltages are converted to velocities using King's Law (King, 1914):

$$E^2 = A + BU^c \quad (3.4)$$

Where E is the anemometer output voltage, U is the flow velocity, and A , B , and c are calibration constants. The values of A , B , and c can be obtained by the least-squares method. Figure 3.9 shows typical calibration data and the fitting curve.

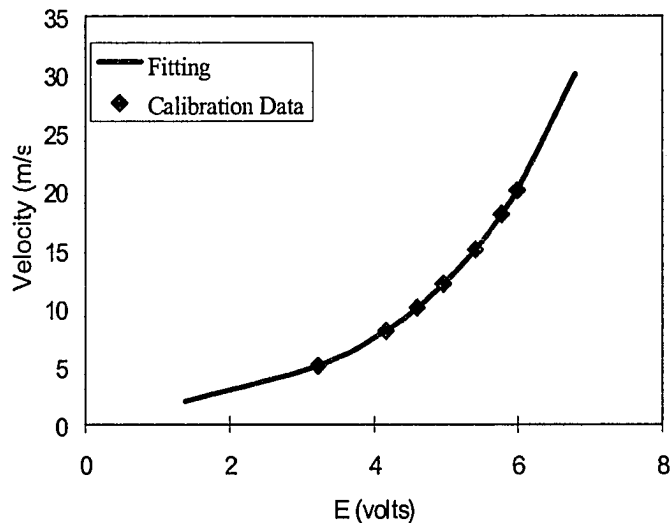


Figure 3.9 Single-hot-film calibrations

The hot-film-probe is mounted on a vertical traverse and positioned over the measurement location inside the wind tunnel. The anemometer's output voltage is digitized and stored within a PC by a LabVIEW based data acquisition system. This voltage time series is converted to a velocity time series using the inverse of the calibration equation. The computer system moves the hot-film-probe to a vertical position, acquires the data, and then moves on to the next vertical position. The entire vertical velocity profile can be obtained automatically by repeating the above steps.

Velocity measurements obtained in this study were summarized and presented through plots of vertical profiles of mean velocity and longitudinal turbulence. For velocity profile measurements inside the urban street canyon, there were seven points measured. Point 1 is located in the middle of the street in front of the central building model. Points 2, 3 and 4 are on the roof of the central building model along the building center. Points 5, 6 and 7 are located in the street beside the central building model. Figure 3.10 shows the location of each measuring point.

3.2.3 Pressure Measurements

The 0.5 mm diameter taps on the plastic 1:50 WERFL building model are connected to two 48-channel PSI transducer units (Model ESP48) and mounted inside the model. Two units may be used simultaneously. The number 1 channel of the first unit is connected to measure reference pressure, and there are a total of 95 pressure taps available for surface measurement. The building geometry pressure tap locations are shown on Figure 3.11 through Figure 3.14.

Seven velocity profiles measured:

Point 1 $(13.8+B/2, 0, 0) \rightarrow (13.8+B/2, 120, 0)$ cm

Point 2 $(13.3, 7.8, 0) \rightarrow (13.3, 120, 0)$ cm

Point 3 $(0, 7.8, 0) \rightarrow (0, 120, 0)$ cm

Point 4 $(-13.3, 7.8, 0) \rightarrow (-13.3, 120, 0)$ cm

Point 5 $(13.8+B/2, 0, 9.2+B/2) \rightarrow (13.8+B/2, 120, 92+B/2)$ cm

Point 6 $(0, 0, 9.2+B/2) \rightarrow (0, 120, 92+B/2)$ cm

Point 7 $(-13.3, 0, 9.2+B/2) \rightarrow (-13.3, 120, 92+B/2)$ cm

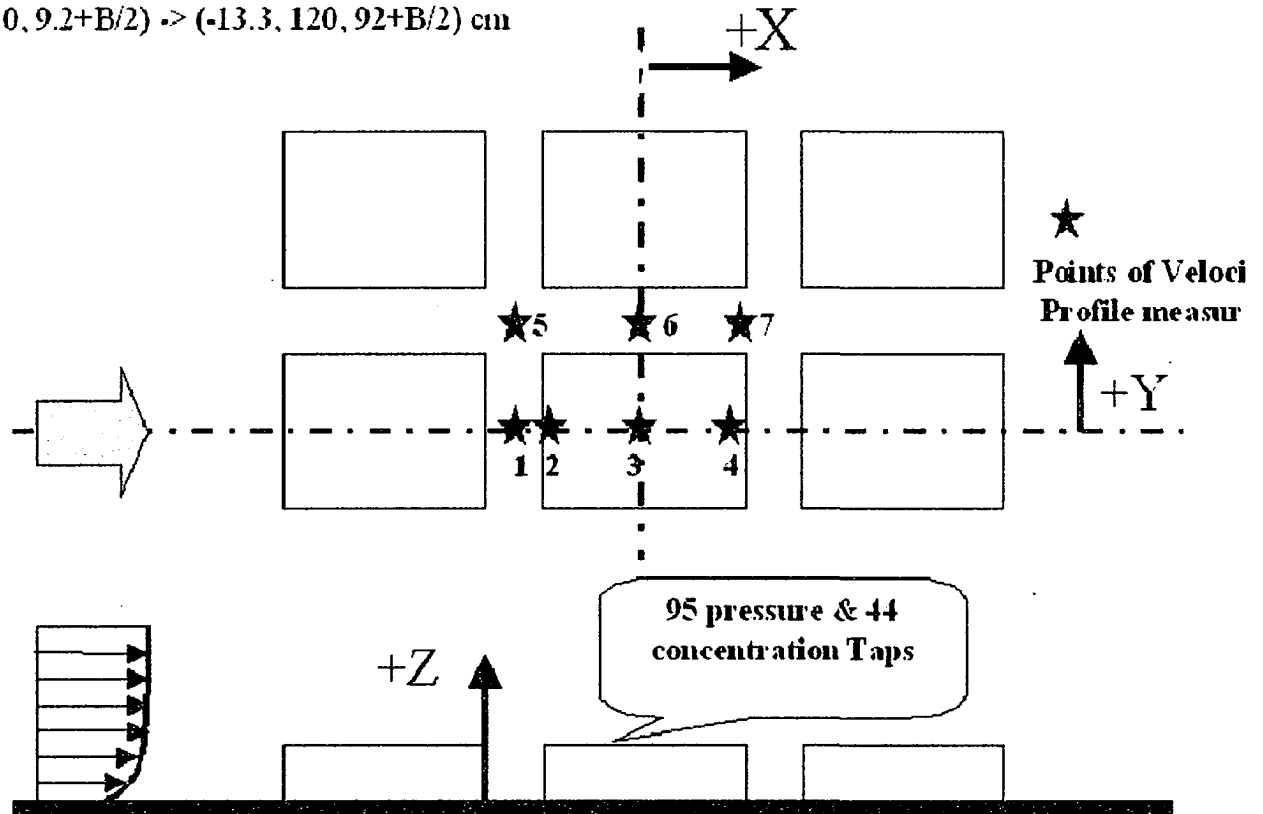
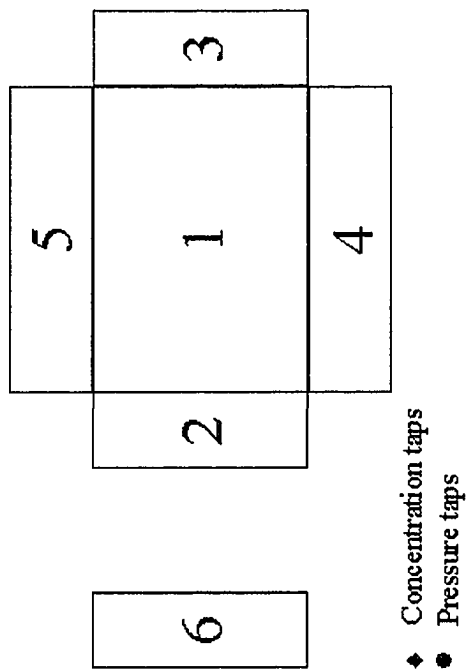


Figure 3.10 Detail position of velocity profiles measurements



Reference pressure location at $X = 260$ mm, $Y = 156$ mm, $Z = 210$ mm

47 concentration taps on the face 1 to face 6, and 95 pressure taps on the face 1 to 5.

- ◆ Concentration taps
- Pressure taps

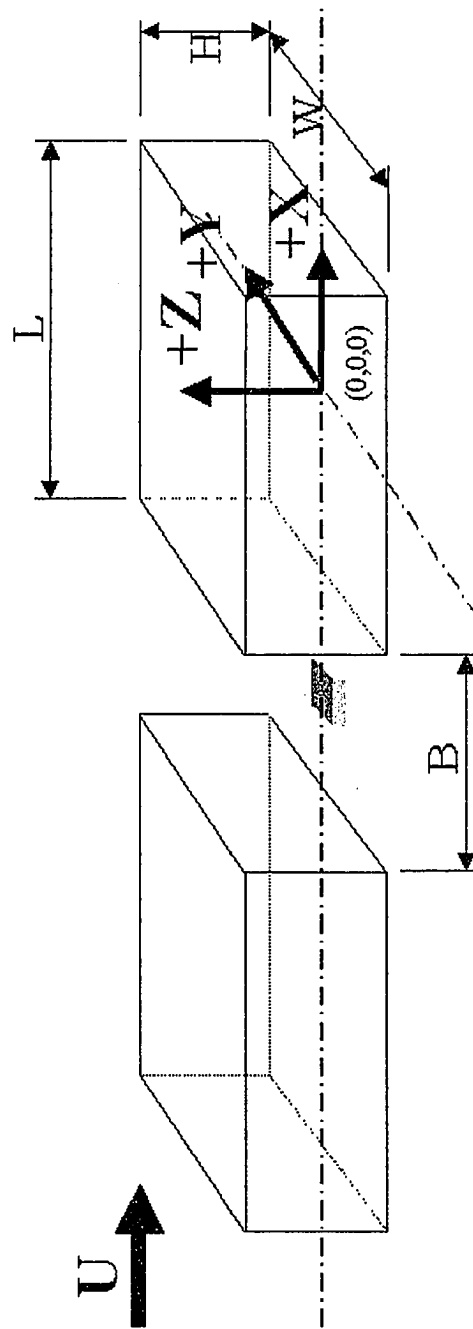


Figure 3.11 Pressure and concentration tap locations on 1:50 TTU WERFL building

tab #	X (mm)	Z (mm)	Y (mm)
1	-130	78	-84
2	-130	78	-73.5
3	-130	78	-63
4	-130	78	-38.5
5	-130	78	0
6	-130	78	38.5
7	-130	78	84
8	-118	78	-84
9	-118	78	-73.5
10	-118	78	-38.5
11	-118	78	0
12	-118	78	38.5
13	-118	78	84
14	-106	78	-81.5
15	-106	78	-73.5
16	-106	78	-38.5
17	-82	78	-81.3
18	-82	78	-63
19	-82	78	-38.5
20	-71.5	78	-84
21	-71.5	78	-76.5
22	-71.5	78	-38.5
23	-71.5	78	0
24	-71.5	78	38.5
25	-71.5	78	84
26	-24	78	-84
27	-24	78	-76.5
28	-24	78	-38.5
29	-24	78	0
30	-24	78	38.5
31	-24	78	84
32	23	78	-84
33	23	78	-76.5
34	23	78	-38.5
35	23	78	0
36	23	78	38.5
37	23	78	84
38	70	78	-84
39	70	78	-76.5
40	70	78	-38.5
41	70	78	0
42	70	78	38.5
43	70	78	84
44	130	78	-84
45	130	78	-76.5
46	130	78	-38.5
47	130	78	0
48	130	78	38.5
49	130	78	84

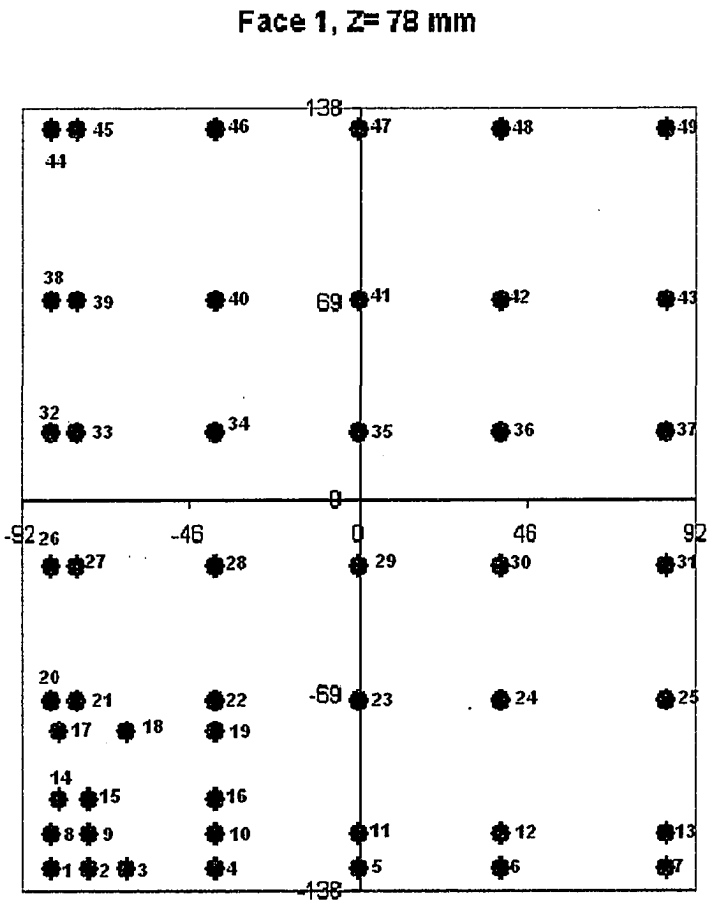
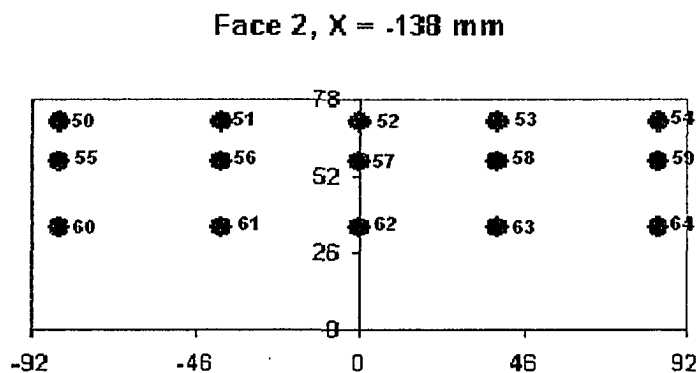


Figure 3.12 Pressure tap location on 1:50 TTU WERFL building at roof (face 1)

Tab#	X (mm)	Y (mm)	Z (mm)
50	-138	-84	70.5
51	-138	-38.5	70.5
52	-138	0	70.5
53	-138	38.5	70.5
54	-138	84	70.5
55	-138	-84	57
56	-138	-38.5	57
57	-138	0	57
58	-138	38.5	57
59	-138	84	57
60	-138	-84	35
61	-138	-38.5	35
62	-138	0	35
63	-138	38.5	35
64	-138	84	35



Tab#	X (mm)	Y (mm)	Z (mm)
65	138	-74	70.5
66	138	-26	70.5
67	138	26	70.5
68	138	74	70.5
69	138	-74	52
70	138	-26	52
71	138	26	52
72	138	74	52
73	138	-74	31
74	138	-26	31
75	138	26	31
76	138	74	31

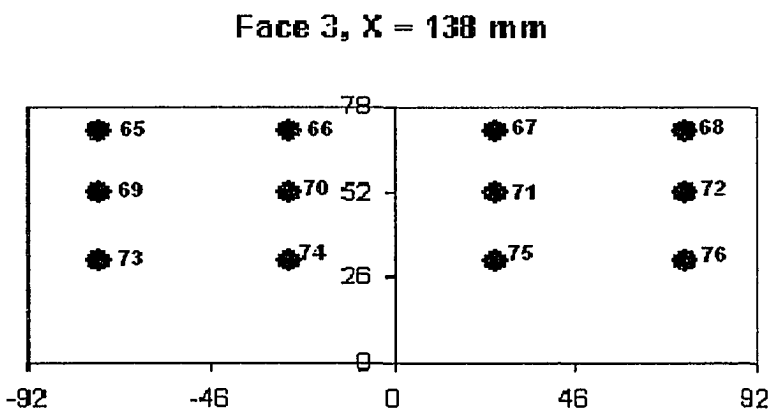


Figure 3.13 Pressure tap location on 1:50 TTU WERFL building at face 2 and face3

Tab#	X (mm)	Z (mm)	Y (mm)
77	70.5	-130	92
78	70.5	-118	92
79	70.5	-71.5	92
80	70.5	4	92
81	70.5	70	92
82	70.5	130	92
83	57	-130	92
84	57	-118	92
85	57	-71.5	92
86	57	-25	92
87	57	23	92
88	57	70	92
89	57	130	92
90	43	-130	92
91	43	-118	92
92	43	-71.5	92
93	43	4	92
94	43	70	92
95	43	130	92

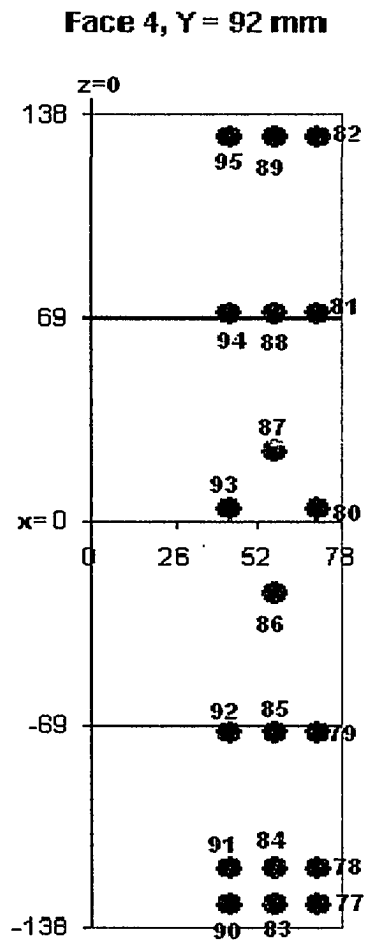


Figure 3.14 Pressure tap location on 1:50 TTU WERFL building at face 4

The restrictor tubes used with the PSI transducers provide a linear phase shift and a gain of 1.0 +/- 0.1 out to 200 Hz. A restrictor cutoff at 200 Hz is chosen in this case, since the pressure cannot be recorded much faster than 480 Hz per tap for the PSI system due to the transducer settling time. There is no possibility of low-pass filtering the signals electronically, since all 48 signals exit the transducer on the same line. The tunnels are run at its highest speed (16m/s at roof height). This provides an adequate pressure to collect data with the PSI system. The building pressure is non-dimensionalized to obtain the pressure coefficient, C_p ,

$$C_p = \frac{P - P_{static}}{\frac{1}{2} \rho \bar{U}^2} \quad (3.5)$$

where ρ is air density and \bar{U} is the mean velocity at reference point. The data records are taken at a sampling rate of 1,000 sample/sec. Typically, 10 segments with 18,000 sampling point/segment are acquired. The mean, RMS, positive peak, and negative peak of the segment are computed and converted into pressure coefficients as follows:

$$C_p (mean) = \frac{\overline{p - p_{static}}}{\frac{1}{2} \rho \bar{U}^2} \quad (3.6)$$

and

$$C_p (RMS) = \frac{\sqrt{\{(p - p_{static}) - \overline{(p - p_{static})}\}^2}}{\frac{1}{2} \rho \overline{U}^2} \quad (3.7)$$

for 10 segments,

$$C_p (+peak) = \frac{[P - P_{static}]}{\frac{1}{2} \rho \overline{U}^2} \quad (3.8)$$

maximum in a segment

$$C_p (+peak) = \frac{[P - P_{static}]}{\frac{1}{2} \rho \overline{U}^2} \quad (3.9)$$

minimum in a segment

Hence, for ten segments of the pressure data, average mean and RMS are obtained and positive and negative are determined for each of the 10 segments of the pressure data.

3.2.4 Concentration Measurements

The experimental measurements of concentration are performed by using a Hewlett Packard gas-chromatograph and a sampling system designed by Wind Engineering and Fluids Laboratory staff. Figure 3.15 shows the schematic of the source-gas release, gas sample, and concentration measurement.

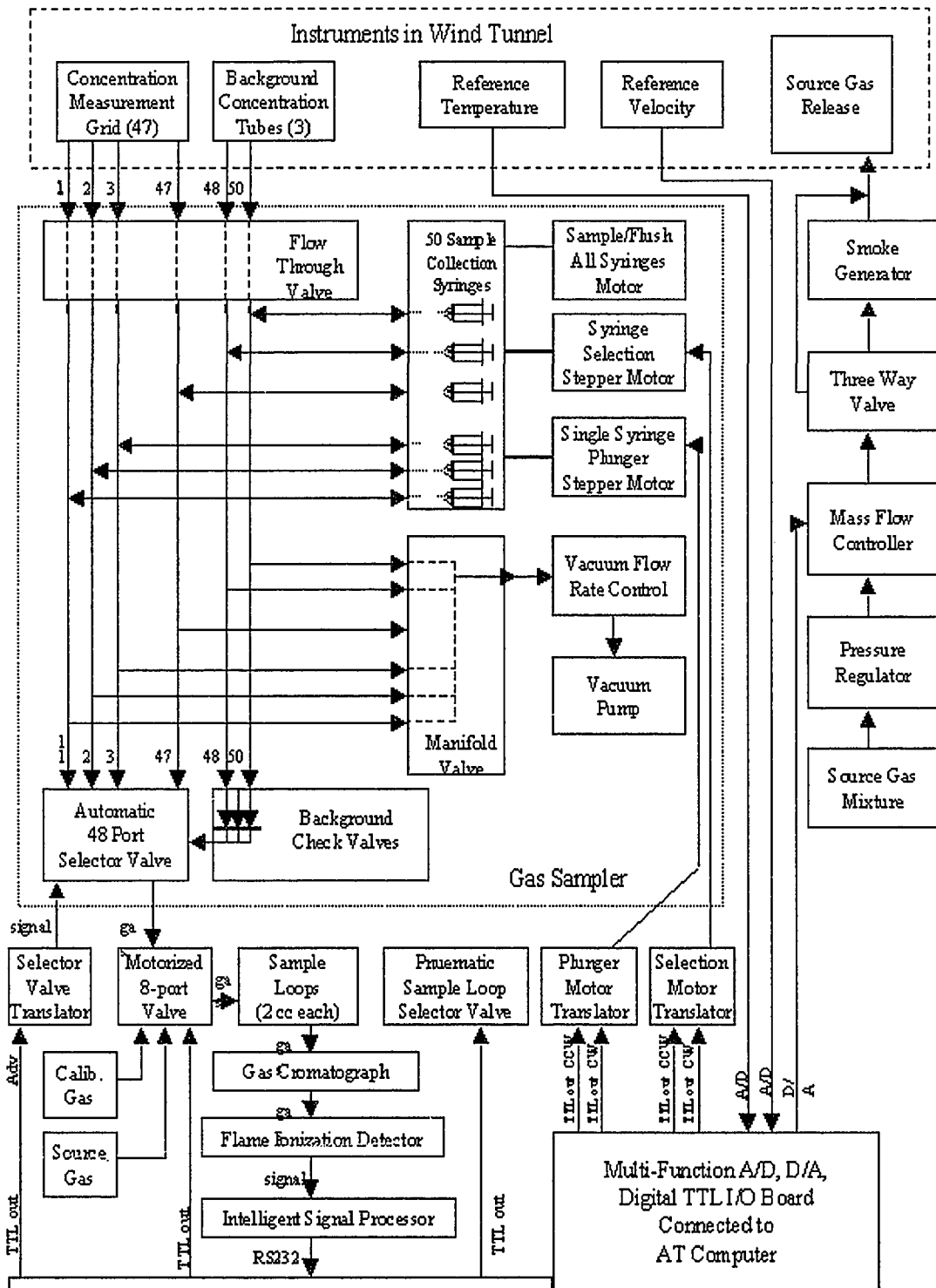


Fig. 3.15 Concentration sampling and measurement system schematic

Gas Chromatograph

A gas chromatograph (Hewlett-Packard Model 5710A) (GC) with flame ionization detector (FID) operates on the principle that the electrical conductivity of a gas is directly proportional to the concentration of charged particles within the gas. The burning mixture of hydrogen and the sample gas in the FID in this case forms the ions. The ions and electrons formed pass an electrode gap and decrease the gap resistance. The resulting voltage drop is amplified by an electrometer and passed to a Hewlett-Packard Model 3390A integrator. When no effluent gas is flowing, a carrier gas (nitrogen) flows through the FID. Due to certain impurities in the carrier, some ions and electrons are formed creating a background voltage or zero shift. When the effluent gas enters the FID, the voltage increase above this zero shift is proportional to the degree of ionization or correspondingly the amount of tracer gas present. Since the chromatograph used in this study features a temperature control on the flame and electrometer, there is very low drift of the zero shift. Given any zero drift, the HP 3390A, which integrates the effluent peak, subtracts out the zero drift.

The lower limit of measurement is imposed by the instrument sensitivity and the background concentration of tracer within the air in the wind tunnel. Background concentrations are measured and subtracted from all data.

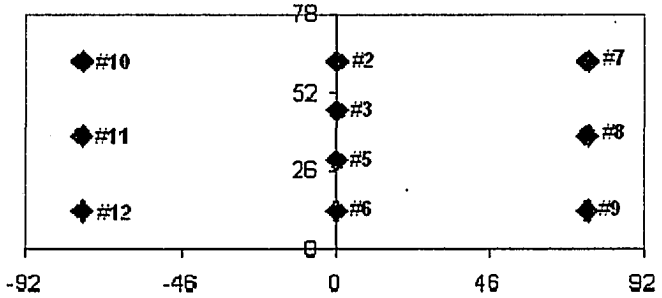
Sampling System

The tracer gas sampling system consists of a series of fifty 30 cc syringes mounted between two circular aluminum plates. A variable speed motor raises a third plate, which lifts the plunger on all 50 syringes, simultaneously. The concentration tap locations are shown on Figure 3.11, 3.16, 3.17 and 3.18. Computer controlled valves and tubing are connected so that airflow from each tunnel sampling point passes over the top of each designated syringe. When the syringe plunger is raised, a sample from the tunnel is drawn into the syringe container. The sampling procedure consists of flushing (taking and expending a ampule) the syringe three times after, which the test sample is retained. The draw rate is variable and generally set to be approximately 6 cc/min.

The sampling system is periodically calibrated to insure proper function of each of the valves and tubing assemblies. To calibrate the sampler, each intake is connected to a manifold. The manifold, in turn, is connected to a gas cylinder having a known concentration of tracer gas. The gas is turned on, and a valve on the manifold is opened to release the pressure produced in the manifold. The manifold is allowed to flush for about one minute. Normal sampling procedures are carried out during calibration to insure exactly the same procedure is reproduced as when taking a sample from the tunnel. Each sample is then analyzed for tracer gas concentration. Percent error is calculated, and "bad" syringe/tube systems (error>2 percent) are not used or repaired.

Tab#	X (mm)	Z (mm)	Y (mm)
2	-(138+B)	62.5	0
3	-(138+B)	46	0
4	-(138+B)		
5	-(138+B)	30	0
6	-(138+B)	12.5	0
7	-(138+B)	62.5	75
8	-(138+B)	37.5	75
9	-(138+B)	12.5	75
10	-(138+B)	62.5	-75
11	-(138+B)	37.5	-75
12	-(138+B)	12.5	-75

Face 6, X=-(138+B) mm



B = street width

Tab#	X (mm)	Z (mm)	Y (mm)
13	-138	62.5	0
14	-138	46	0
15	-138	30	0
16	-138	12.5	0
17	-138	62.5	37.5
18	-138	37.5	37.5
19	-138	12.5	37.5
20	-138	62.5	75
21	-138	37.5	75
22	-138	12.5	75

Face 6, X=-138 mm

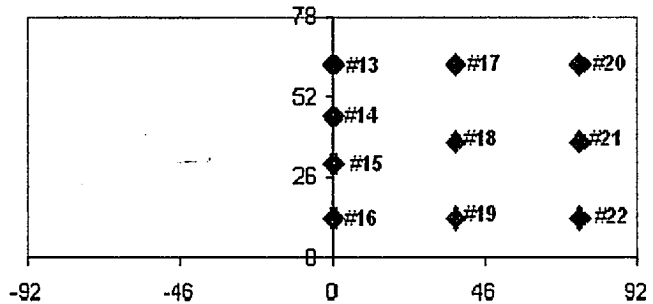


Figure 3.16 Concentration tap locations on 1:50 TTU building at face 2 and face 6

Face 1, Z = 78 mm

Tab#	X (mm)	Z (mm)	Y (mm)
23	-125.5	78	0
24	-75.5	78	0
25	-22.5	78	0
26	22.5	78	0
27	75.5	78	0
28	125.5	78	0
29	-125.5	78	37.5
30	-75.5	78	37.5
31	-22.5	78	37.5
32	-125.5	78	75
33	-75.5	78	75
34	-22.5	78	75
35	22.5	78	75
36	75.5	78	75
37	125.5	78	75
38	-125.5	78	-75
39	-75.5	78	-75

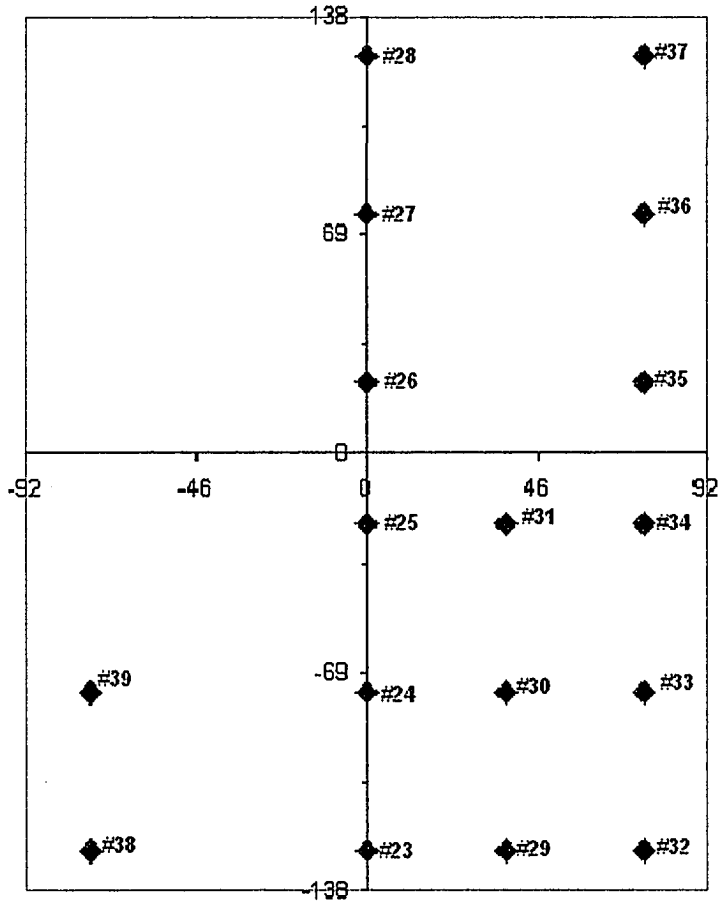


Figure 3.17 Concentration tap locations on 1:50 TTU building at face 1

Face 4, Y = 92 mm

Tab#	X (mm)	Z (mm)	Y (mm)
40	-125.5	62.5	92
41	-75.5	62.5	92
42	-22.5	62.5	92
43	-125.5	37.5	92
44	-75.5	37.5	92
45	-22.5	37.5	92
46	-125.5	12.5	92
47	-75.5	12.5	92

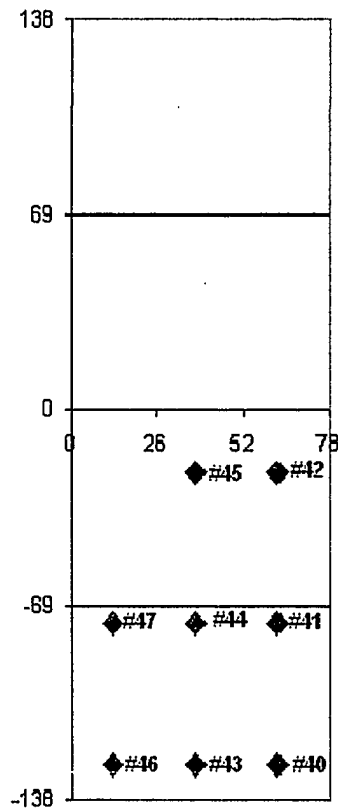


Figure 3.18 Concentration tap locations on 1:50 TTU building at face 4

Test Procedure

The test procedure consists of 4 steps:

1. Setting the proper tunnel wind speed,
2. Releasing the metered mixtures of source gas from the plant stack,
3. Withdrawing samples of air from the tunnel designated locations, and
4. Analyzing the samples with an FID.

The samples are drawn into each syringe over an ~200 second (adjustable) time period, and then consecutively injected into the GC.

The procedure for analyzing the samples from the tunnel follows:

1. User introduces the sample into the GC which separates the ethane tracer gas from other hydrocarbons,
2. The voltage output from the chromatograph FID electrometer goes to the HP 3390A Integrator,
3. The HP 3390A communicates the measured concentration in ppm to an Personal Computer for storage, and
4. These values, C_{mea} , along with the response levels for the background C_{bg} and source C_{source} are converted into source normalized model mean concentration by the equation:

$$C_m = (C_{mea} - C_{bg}) / (C_{source} - C_{bg}) \quad (3.6)$$

5. Field equivalent mean concentration values are related to model values by the

$$C_p = \frac{C_m}{C_m + (1 - C_m)[V(T_a / T_s)]_m / [V(T_a / T_s)]_p} \quad (3.7)$$

equation:

Where $V = Q/\bar{U}_h L^2$,

and L is the characteristic length scale. When there is no distortion in the model-field volume flux ratio, V, and the plumes are isothermal this equation reduces to

$$C_p = C_m.$$

Error Statement

Background concentrations, C_{bg} , (the result of previous tests within the laboratory), are measured to an accuracy of 20 percent. The larger measured concentrations, C_{mea} , are accurate to two percent. The source gas concentration, C_{source} , is known to within ten percent. Thus the source normalized concentration for $C_{mea} \gg C_{bg}$ is accurate to approximately three percent. For low concentration values, $C_{mea} > C_{bg}$, the errors are larger.

CHAPTER 4

NUMERICAL SIMULATION PROCEDURE

Two types of numerical simulation software, Fluent 5.4 and Fire Dynamics Simulator (FDS), are used to perform the numerical experiments with the same configurations as the physical experiments. Both of CFD codes, Fluent and FDS, provide numerical simulation of the mean flow within the street canyon setup and the concentration distribution for a three-dimensional street canyon of the same configuration. Four separate turbulence models, the standard κ - ϵ , the RNG κ - ϵ , the Reynolds-stress and LES, are used in Fluent to examine each flow field case. For FDS, large eddy simulations (LES) methodology is used to examine flow field cases. In LES the fluctuating motions of turbulence can be computed exactly except for eddies that are smaller than the grid size. The smaller eddies are modeled using eddy viscosity models. Because of this, LES can compute fluctuating pressures on buildings due to turbulence. This suggests that LES will be used more and more as computing hardware and software technology improve.

4.1 Introduction of Fluent

Fluent is a computer program for modeling fluid flow and heat transfer in complex geometries. It is written in the C computer language. All functions required to

compute a solution and display the results are accessed through Fluent's menu-driven interface. The user interface is written in a language called Scheme, a dialect of LISP. Fluent provides complete mesh flexibility, solving flow problems with unstructured meshes that can be generated about complex geometries with relative ease. The mesh types include 2D triangular/quadrilateral, 3D tetrahedral/hexahedral/pyramid/wedge, and mixed (hybrid) meshes. It allows the user to refine or coarsen the grid based on the flow solution.

Fluent has a solution-adaptive grid capability that provides accurate prediction on flow fields in regions with large gradients, such as free shear layers and boundary layers. This feature reduces the time required to generate a good grid. Solution-adaptive refinement makes it easier to perform grid refinement studies and reduces the computational effort required to achieve a desired level of accuracy, since mesh refinement is limited to those regions where greater mesh resolution is needed.

The Fluent CFD package consists of several tools for defining a discrete flow problem, setting boundary and initial conditions, and solving the set of complex equations for conservations of momentum, mass, energy, and chemical species. The governing equations are discretized on a curvilinear grid to permit computations over irregular geometries and are solved using a control volume based finite difference method. Discrete velocities and pressures are stored in a non-staggered grid, and interpolation is realized by using a first-order, second-order, power-law scheme or optionally by higher-order upwind scheme. The basic solver in Fluent is the

SIMPLEC/SIMPLE algorithm with iterative line-by-line matrix solver and multigrid acceleration.

4.1.1 Turbulence Models

Turbulent flows are characterized by fluctuating velocity fields. These fluctuations transport quantities, such as momentum, energy, and species concentration, cause the transported quantities to fluctuate as well. Because these fluctuations are in small scales and high frequencies, they are too computationally expensive to simulate directly in practical engineering calculations. Instead the instantaneous governing equations can be time-averaged, ensemble-averaged, or otherwise manipulated to remove the small scales, resulting in a modified set of equations that are computationally less expensive to solve. However, the modified equations contain additional unknown variables that need the turbulence models to determine these variables in terms of known quantities. The commercial CFD software, Fluent, provides six different turbulence models (details can be obtained in Fluent User's guide, Volume 2). In this research, only four turbulence models, the standard κ - ϵ , the RNG κ - ϵ , the Reynolds-stress and LES are tested in numerical simulations.

4.1.2 The CFD Process

The CFD process contains three steps: preprocessing, calculating, and postprocessing. Preprocessing is the first step in building and analyzing a flow model. It

includes building the model (or importing it from a CAD package), discretizing the geometry, applying a mesh, and entering the initial boundary data. A separate software unit Gambit 1.20 is used in this case.

After preprocessing, the CFD solver calculates a solution (solution of the conservation equations for mass, momentum, energy, and chemical species). Before solving the problem, the flow condition, fluid properties, and turbulence models have to be defined and selected. Fluent 5.4 Solver is selected for calculation for this research.

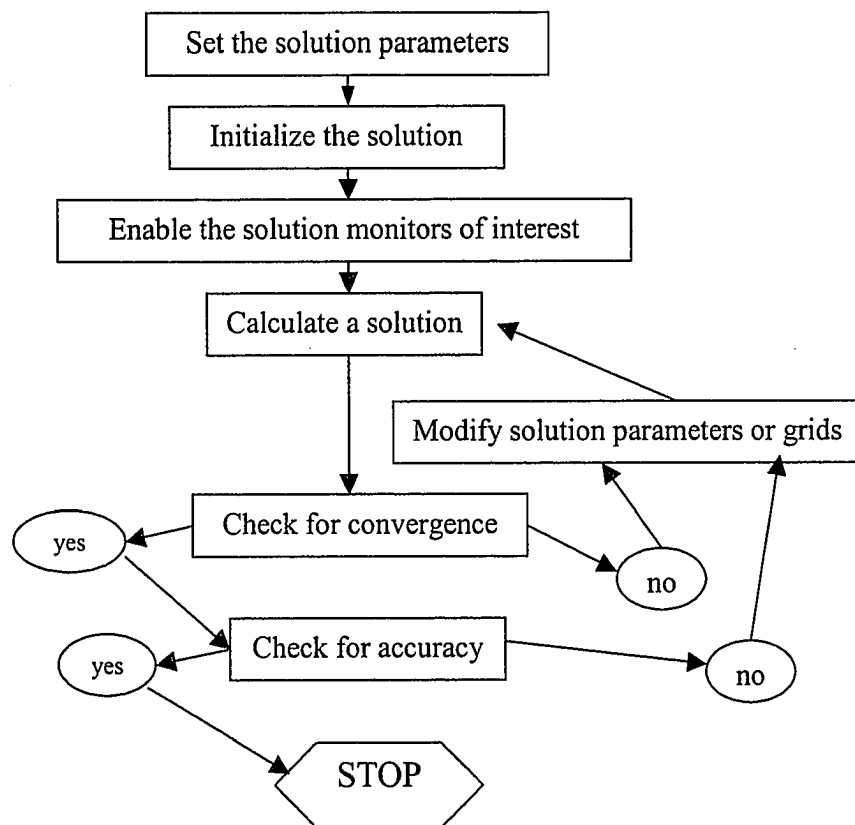


Figure 4.1 Flow chart for numerical solution method

Postprocessing is the final step in CFD analysis. It involves organization and interpretation of the data and images. The flow chart of the numerical solution method is illustrated in Figure 4.1.

4.1.3 Inlet Conditions to the Numerical Domain

The wind tunnel profiles of velocity and turbulence intensity (CSU-B2) can be used for calculating inlet boundary conditions. The wind tunnel data and input profiles of velocity, turbulent kinetic energy, and dissipation used for the numerical simulation are shown on Figure 4.2 to Figure 4.4. The inlet values of kinetic energy, k , and dissipation ratio, ϵ , are calculated from measured velocity profiles and turbulence intensities with a given friction velocity ratio, u^*/u_{ref} for the wind tunnel setup, according to Equation (4.1) and Equation (4.2).

$$\epsilon = \frac{u_*^3}{\kappa y} \quad (4.1)$$

$$k = \frac{3}{2} \sqrt{u'^2} \quad (4.2)$$

Where, y is distance from the wall, κ is the von Karman constant.

All velocity profiles are collinear, and the numerical and wind tunnel kinetic energy and dissipation ratio are very similar as well.

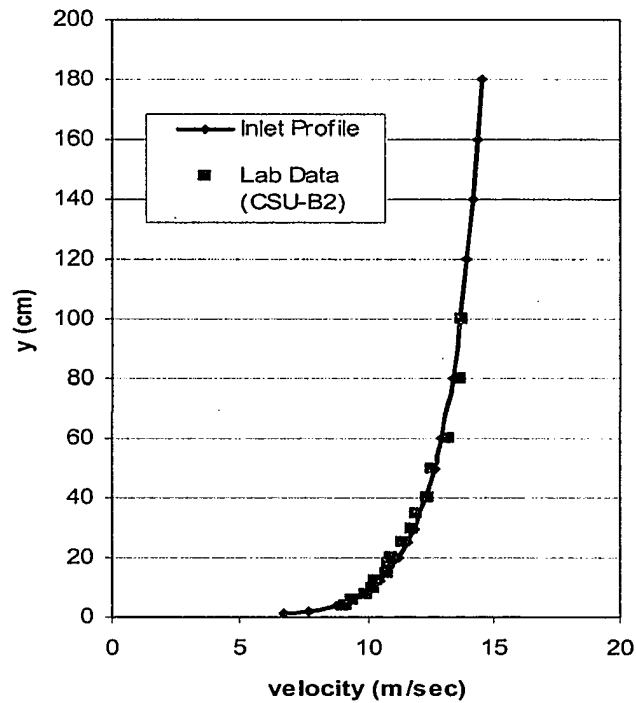


Figure 4.2 Numerical inlet velocity profile compared to Approach velocity profile.

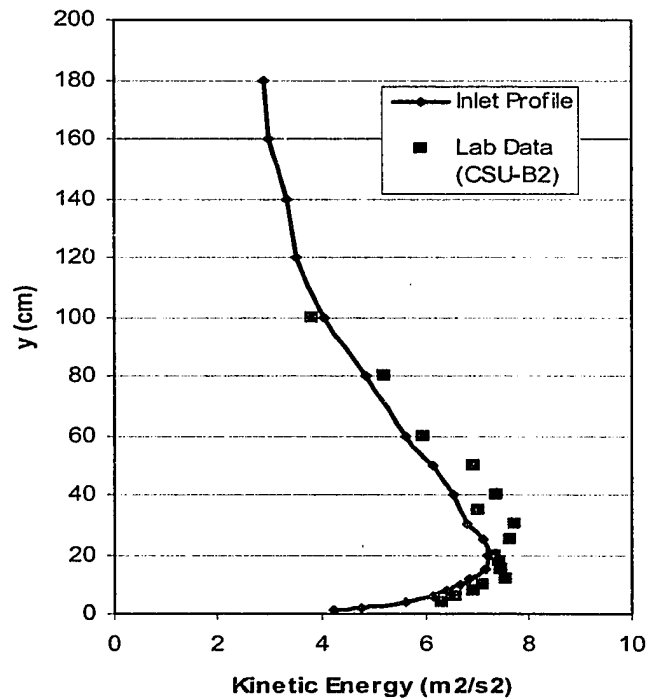


Figure 4.3 Numerical inlet kinetic energy profile compared to approach velocity profile

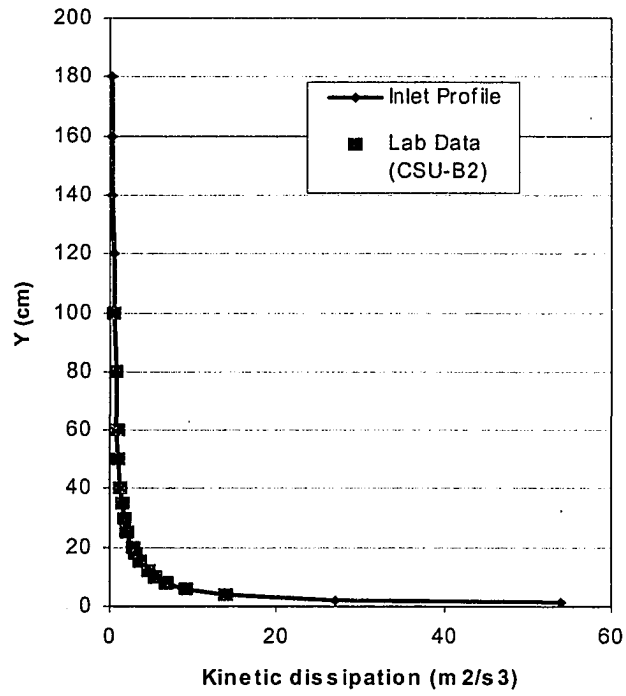


Figure 4.4 Numerical inlet kinetic dissipation profile compared to CSU-B2

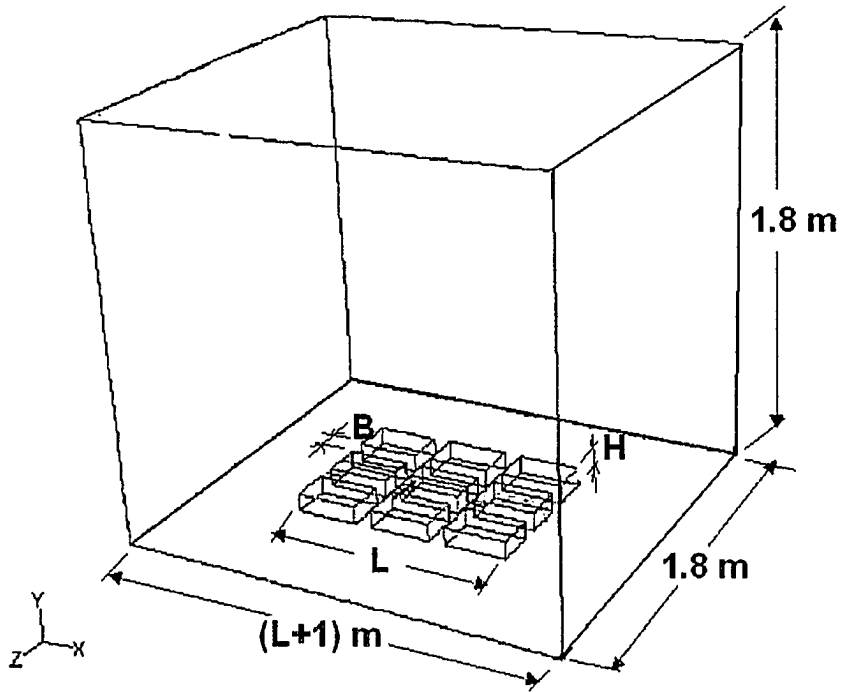


Figure 4.5 The numerical domain of 9 buildings and $B/H=1$ case

4.1.4 Numerical Domain and Meshes

Various calculation domains are chosen depending on the number of the buildings and different separation distances. The typical numerical domain represents a 1.8 m wide wind tunnel with 1.8 m flow depth and $(L+1)$ m test section length, where L is the length of the urban street canyon areas. The example of 9 buildings and $B/H=1$ case configuration is shown on Figure 4.5. Figure 4.6 shows the typical unstructured boundary mesh used for tetrahedral mesh generation for the case of 9 buildings and $B/H=1$. Figure 4.6 contains 24,731 cells; 52,471 faces; and 5,762 nodes distributed over 51 face zones. Figure 4.7 shows the grids after using solution-adaptive refinement in the same case as Figure 4.6. These grids contain 159,015 cells; 353,007 faces; and 44,390 nodes distributed over 51 face zones. By using solution-adaptive refinement, it is easy to add cells where they are needed in the mesh, thus enabling the features of the flow field to be better resolved. When adaption is used properly, the resulting mesh is optimal for the flow solution because the solution is used to determine where more cells are added. In other words, computational resources are not wasted by the inclusion of unnecessary cells, as typically occurs in the structured grid approach. Furthermore, the effect of mesh refinement on the solution can be studied without completely regenerating the mesh.

Outlet and velocity inlet or symmetry boundaries are specified at the sides and top of the grid volume, when appropriate surface roughness is specified at the ground. As noted in Section 4.4, the inflow boundary conditions are chosen to match the velocity and turbulence profiles measured during the wind tunnel experiments. Outflow boundary

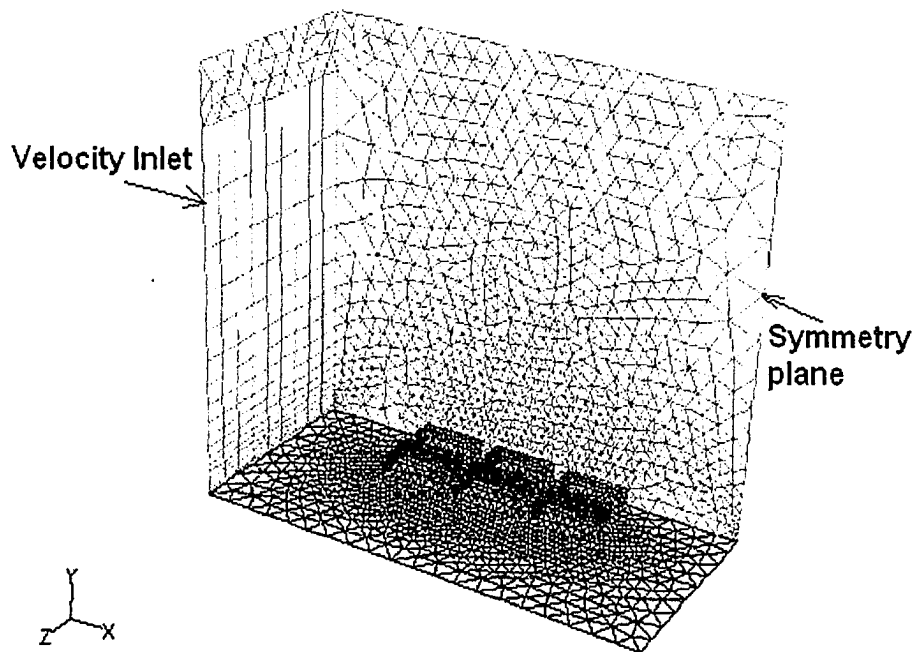


Figure 4.6 Typical unstructured boundary mesh used for tetrahedral mesh generation on 9 buildings and $B/H=1$ case

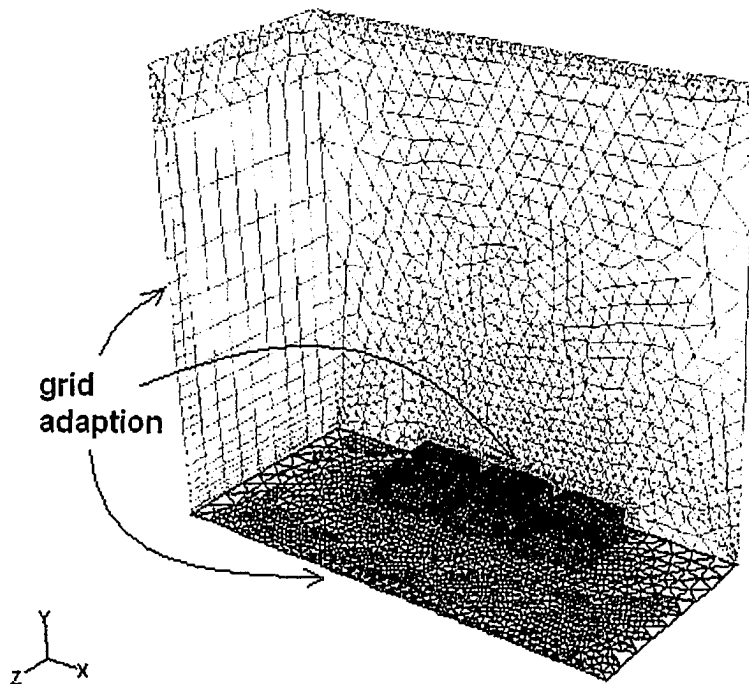


Figure 4.7 The adaption grid on 9 buildings and $B/H=1$ case

conditions are chosen to maintain constant longitudinal rate of change of all dependent variables such as constant slope.

4.2 Introduction of FDS

Fire Dynamics Simulator (FDS) is a computational fluid dynamics (CFD) model for fire-driven fluid flow (FDS-User's Manual). FDS consists of two programs, `fds` and `smokeview`. The Fire Dynamics Simulator predicts smoke and/or air flow movement caused by fire, wind, and ventilation systems. `Fds` solves a form of the Navier-Stokes equations appropriate for low-speed, thermally-driven flows of smoke and hot gases generated in a fire. `Smokeview` visualizes `fds` computed data by animating time dependent particle flow, 2D slice contours and surface boundary contours. Data at a particular time may also be visualized using 2D or 3D contour plots or vector plots. Currently, the only obstacle to the methodology is the memory capacity and computational speed of the hardware.

4.2.1 Inlet Conditions and Numerical Domain

FDS has been used only for the $B/H=1$, $N=1$ case for numerical simulations. For this computation, a numerical domain of 100 m long by 90 m wide by 40 m high is employed. Figure 4.8 shows the 9-building urban street canyon case inside numerical domain. The mesh is uniform in each direction with 192 cells in the windward, 144 cells in the cross-wind directions and 64 cells in vertical directions for a total of 1,769,472 grid cells. Each computational cell is 0.52 m long by 0.625 m wide by 0.33 m high, so that

the master building is described by about 27 nodes in the windward direction by 15 cells in the cross-wind direction by 12 nodes vertically. Some lower grid resolution cases also are run for examining the sensitivity of the calculations to grid resolution. Figure 4.9 exhibits the structured grid at x-y and x-z planes at highest grid resolution case.

The inflow boundary conditions are chosen to match the velocity profiles measured during the wind tunnel experiments. There is no turbulence intensity inflow boundary condition, since FDS does not offer the function of setting up the value of inlet turbulence intensity. Outflow boundary conditions are chosen open to the atmosphere. The top of the numerical domain is set as a mirror (symmetric) plane, and two sidewalls of numerical domain are set as a wall boundary condition with free-slip. The ground is chosen as a wall boundary condition with three different levels of slip, free-slip, half-slip and no-slip. Since the ground has three different boundary conditions, the approaching flows appear to be different near the ground for each boundary condition. Figure 4.10 shows the approaching profile for different ground boundary conditions.

The calculation speed of FDS is very slow because it uses time-dependent LES turbulence model. It requires about ten times calculation time of Fluent. It takes about 5 or 6 days continuously to finish running a case. Therefore, only one case is examined in this study due to time constraints.

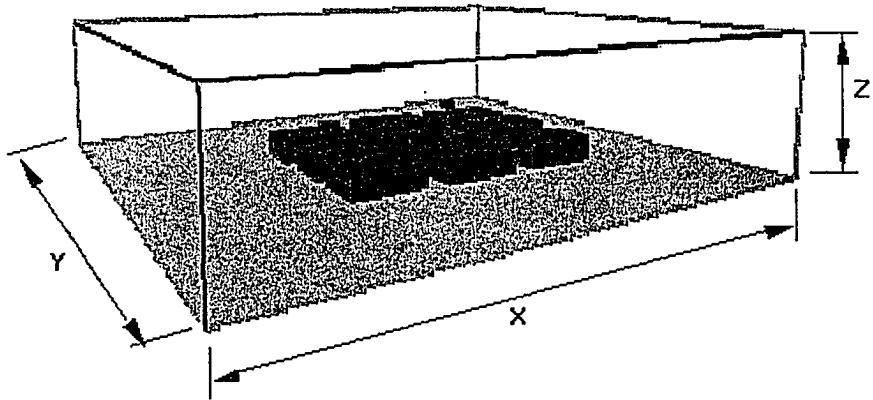


Figure 4.8 Numerical domain at $X=100\text{m}$, $Y=90\text{m}$, and $Z=40\text{m}$

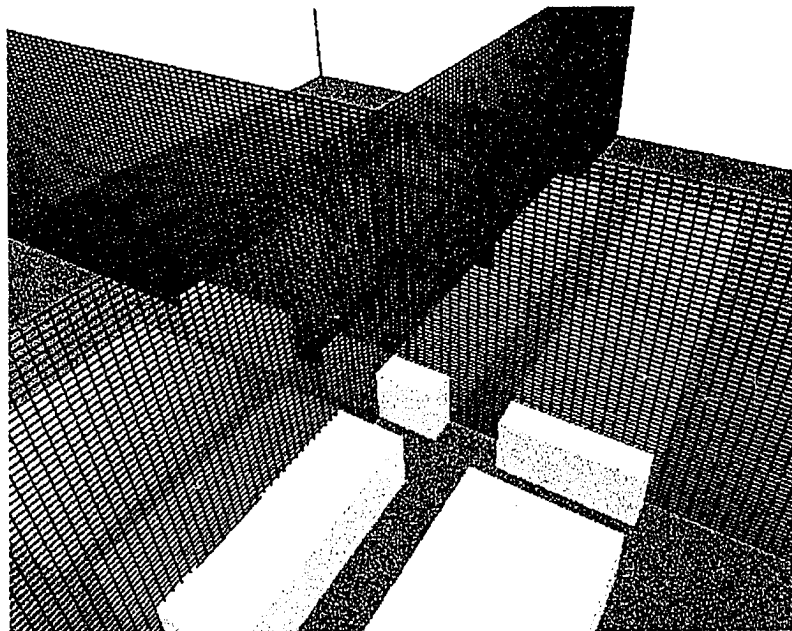


Figure 4.9 The structured computational grid at x-z and y-z planes at high resolution at $192*144*64$ grid cells

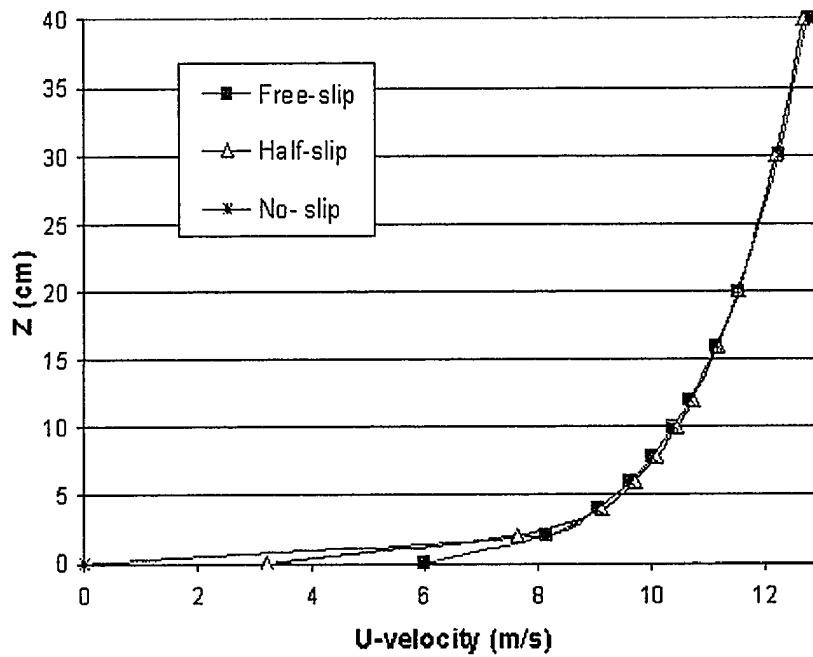


Figure 4.10 Approaching wind velocity profile for different ground boundary conditions

CHAPTER 5

EXPERIMENTAL DATA

This chapter presents all the data obtained from various physical experiments performed at the industrial wind tunnel. These physical experiments, which are discussed in the Chapter 3, consist of flow visualization, velocity and turbulence intensity profile measurements, pressure coefficient measurements, and concentration measurements. The object of this chapter is to provide original data sets as references for future research.

5.1 Flow Visualization

Flow visualization was accomplished with a laser light sheet produced by 5-watt Coherent Innova 7005 Argon ion water-cooled laser. Images were recorded by using the Panasonic Omni vision II camera/recorder system. Appendix A shows some visualization images in sequences, which are digitized from videotapes.

5.2 Velocity and Turbulence Intensity Profile

The velocity and turbulence intensity was measured by using a single hot-film. (The details of the measurement procedures are discussed in Section 3.2.2.) Twenty cases of measurements were performed, which consist of 5 different street widths to building height ratio (B/H) and 4 different rows of surrounding buildings in the upstream direction. Each case measures 7 locations around the target building. (The detailed

measuring points are shown at Figure 3.10.) The 20 sets of data results are summarized in Appendix B.

5.3 Pressure Coefficient

Two 48-channels PSI transducer units mounted inside the target building were used to measure pressure coefficient. (The details of the measuring procedures can be viewed at Section 3.2.3, and the different locations of the pressure taps are shown at Figures 3.11, 3.12, 3.13, and 3.14.) Similar to the velocity and turbulence intensity measurement, twenty cases of different B/H ratios and different rows of surrounding buildings were measured with 0 degree approaching wind. Three of these 20 cases, the different combinations of N=1, B/H=0.5, 1,2, are measured with different approaching winds from 0 degree to 90 degrees. The results of each case are interpreted for minimum value, mean, maximum value, RMS, - peak, and + peak pressure coefficients, and these values are presented in Appendix C.

5.4 Concentration

The concentration was measured by using a gas chromatograph and a sampling system. (Section 3.2.4 describes the detail procedures used during the experiment. The locations of concentration taps are shown on Figure 3.16, 3.17, and 3.18.) The 20 cases described previously were measured with 0 degree approaching wind for their concentration dispersion. One case of N=1 and B/H=1 was measured with different

approaching winds from 0 degree to 90 degrees. Appendix D presents the concentration mean values for each case.

CHAPTER 6

WIND TUNNEL RESULT ANALYSIS AND COMPARISON

This chapter presents the analysis and comparison of all the data collected from the various wind tunnel experiments. The influences surrounding buildings on the bluff body flow in an urban street canyon, the effect of the surrounding buildings on surface pressure of a low-rise building, and the dispersion of gases released in an urban street canyon are discussed in the following sections. All the physical data will also be compared to numerical data to examine the limitations of numerical modeling.

6.1 The Effects of Surroundings on Flow Around the Low-Rise Buildings

The turbulent flow of air over a surface covered with large numbers of discrete bluff obstacles occurs in many engineering applications. The flow over urban surfaces is a particular example of this type of very rough surface, boundary-layer flow. Because of the effects of the surrounding buildings there is considerable spatial non-uniformity of the flow field in the lower part of the boundary layer, which is called the roughness sub-layer. For most locations, this layer is characterized by inhomogeneous regions of reduced mean velocity and enhanced levels of turbulence intensity. Above the immediate influence of the surrounding buildings, the flow in the boundary layer becomes more homogeneous. Modeling details for the urban roughness sub-layer are not well

established. With traditional anemometry it is difficult and time-consuming to measure velocity data in the highly turbulent, recirculating flow field in the roughness sub-layer. Three flow regimes occur in practice: the skimming flow regime, wake interference flow regime and isolated roughness flow regime (Oke, 1992). The flow within the urban street canyon is extremely difficult to parameterize since it is shaped by the detailed arrangement of streets and building density. The following sections will present the results of flow visualization and flow field measurements for different configuration arrangement of an idealized urban street complex.

6.1.1 Flow Visualization of Wind Tunnel Result

As noted previously, multiple building configurations are considered (See Figure 3.6 and Table 3.1). Depending on the street width to building height ratio (B/H), the flow in the street canyons can be classified as skimming flow ($B/H=0-1.2$), wake interference flow ($B/H=1.2-5.0$), or an isolated roughness flow ($B/H>5.0$) as originally proposed by Oke (1998). Through the observation of flow visualization of wind tunnel tests performed for this dissertation, the results match the observations made by Oke.

Skimming Flow

After observing the videotapes of flow visualization tests, cases $B/H=0.5$ and $B/H=1$ are referred as skimming flow cases. Figure 6.1 exhibits the skimming flow image of case $B/H=1$. As the image indicates, the two gray blocks represent the

buildings, and the arrows represent the wind flow direction. As the wind blow normally from left to right to the buildings, a vortex-flow develops between them. The circulation as shown on the graph is a form of a cavity zone lee eddy where the downward pull of the suction is re-enforced by deflection down the windward face of the next building downstream. The winds in the street canyon zone are more turbulent than in the open at the same height because of such separation and recirculation effects. In skimming flow, the winds tend to skim over the rooftops.

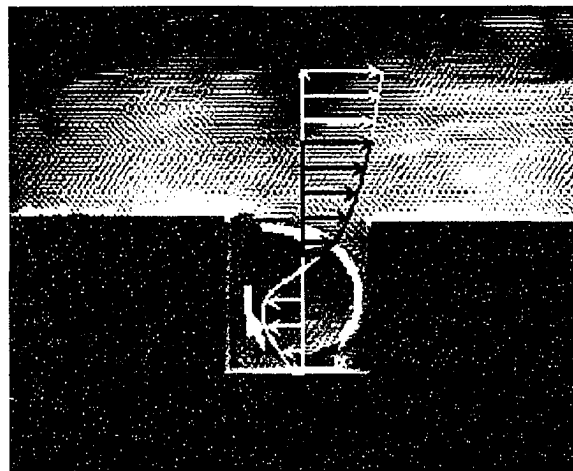


Figure 6.1 Skimming Flow, $B/H=1$

Interference Flow

Cases $B/H=2$ and $B/H=4$ are identified as interference flows. Figure 6.2 is an example of interference flow case ($B/H=4$ case). After the winds cross the left building (the gray block), the room available for expansion suddenly increases. However, the fluid cannot immediately react to fill it. The flow therefore separates from the building's

surface, and its organization breaks down into a much more turbulent condition in the low pressure or wake zone (Region A) which extends downwind from the left building. Immediately behind the left building, the pressure is low and thus tends to “suck” air into a semi-stationary lee eddy or vortex. This part of the wake is known as the cavity zone. The large lee eddy structure is dissipated into the smaller turbulent eddies of the wake zone, before finally settling down and reassuming conditions similar to those of the upwind flow. Before the flow reaches the right building, it begins to react because of the pressure build-up ahead. The bulk of the flow is forcibly displaced up and over the building. Immediately above the building, the streamlines are forced to converge as the same mass of air attempts to “squeeze” over, causing an acceleration or jet. The separation and reattachment occur on the roof of the right building. The flow in Region C can be called as displacement zone. Since the distance between the two buildings is not long enough, interference between these flows occurs at Region B. This is because a displacement flow has developed at Region C before the eddy has settled down in the wake zone (Region A).

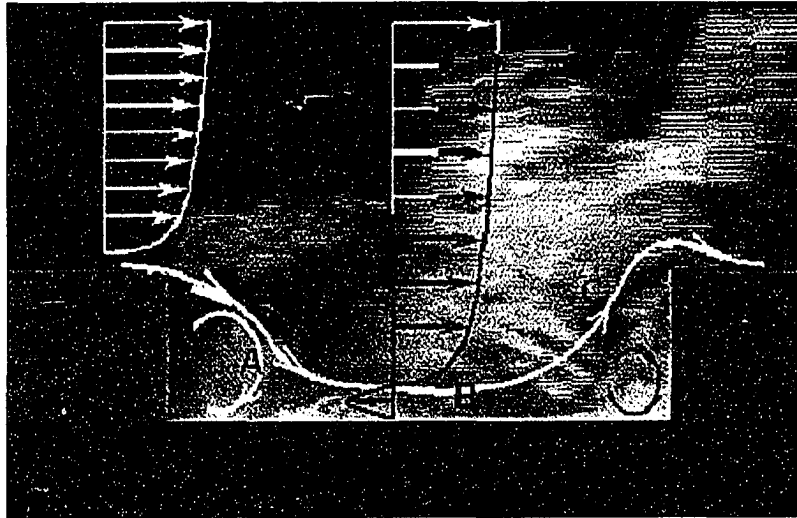


Figure 6.2 Interference Flow, $B/H=4$

Isolated Roughness Flow

In the case $B/H=6$, isolated roughness flow is observed. Figure 6.3 is an example of isolated roughness flow (Case $B/H=6$). In this case, the development of wake zone (Region A) and displacement zone (Region C) is the same as the previous case, the interference flow case. However, Region B in this case does not have any interference between the wake zone and the displacement zone, because the distance between the two buildings is large enough to provide horizontal motions parallel to the ground. Since the distance between the two buildings is large, the right building is referred to as an isolated building and the left building is referred to as a roughness.

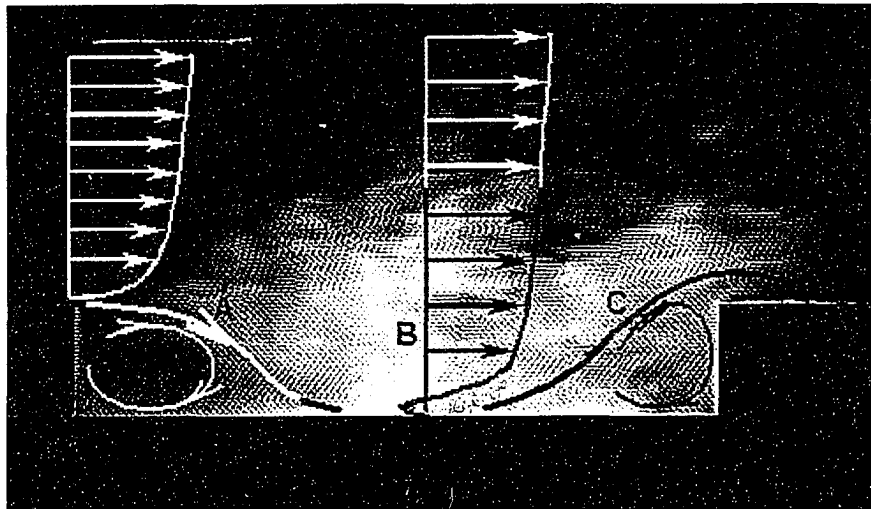


Figure 6.3 Isolated Roughness Flow, $B/H=6$

6.1.2 Wind Velocity and Turbulence Intensity Profiles of Wind Tunnel Result

Profiles of the velocity and turbulence intensity around the master building from Point 1 to Point 7 (see Figure 3.10 for detailed locations) for case N=1 open country are presented in Figures 6.4a to 6.10b. In Figure 6.4a, the X-axis represents mean velocity (u/U_{ref}), where u = measured velocity magnitude and U_{ref} = reference velocity at building roof height, and Y-axis represents heights. As the graphs indicate, the isolated roughness case ($B/H=6$) has the highest magnitude of velocity at any height among all cases, whereas the interference flow cases ($B/H=2$ and $B/H=4$) and the skimming flow cases ($B/H=0.5$ and $B/H=1$) have lower values for velocity profiles. However, at the areas above the roof height, the results of the velocity values for each case approach one another. Figure 6.4b shows the turbulence intensity profiles relative to heights for each

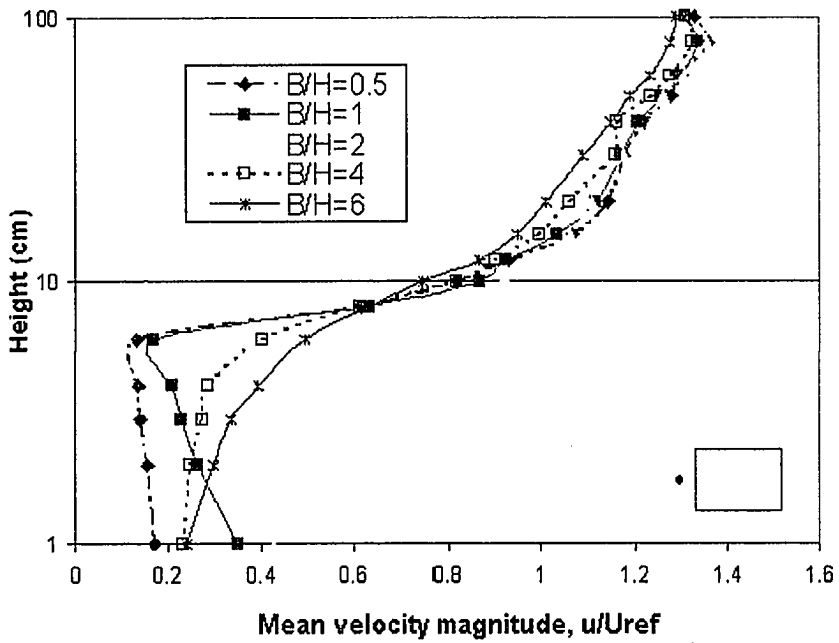


Figure 6.4a Mean velocity magnitude profile measured at point 1, N=1

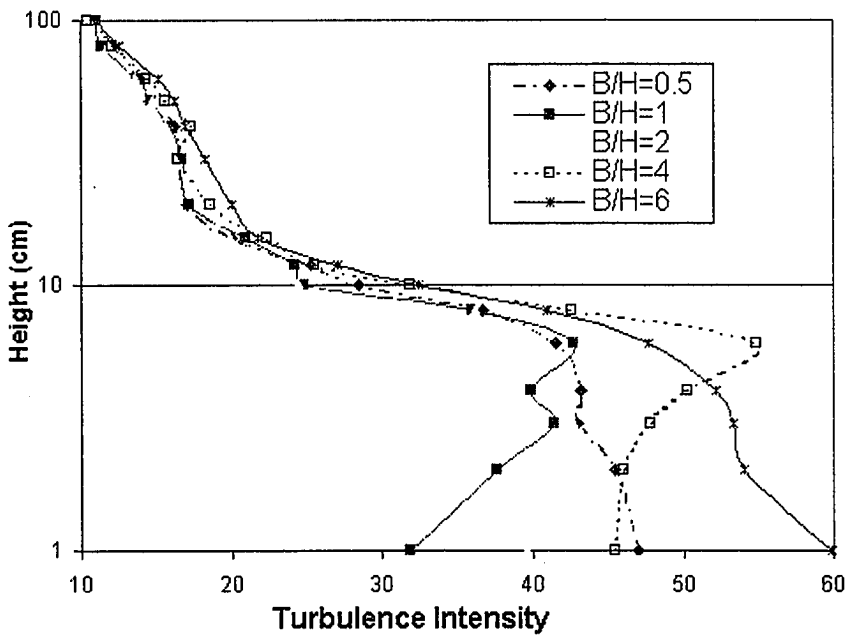


Figure 6.4b Turbulence intensity profile measured at point 1, N=1

case. At the point 1 of the street canyon area, the isolated roughness case ($B/H=6$) has the highest turbulence intensity, whereas the interference flow cases ($B/H=2$ and $B/H=4$) and the skimming flow cases ($B/H=0.5$ and $B/H=1$) have lower turbulence intensity.

Figures 6.5a and 6.5b show the velocity and turbulence intensity profiles at point 2. In the region close to the roof, when the value of B/H increases, the value of velocity increases because separation behavior occurs in this region for both interference and isolated roughness cases. Figure 6.6b shows the turbulence intensity profile over the center point of the master building (point 3). The turbulence intensity of isolated roughness cases is highest compared to the other cases in the region close to roof height, whereas the interference flow cases have the second highest turbulence intensity and the skimming flow cases have the lowest.

The velocity and turbulence intensity profiles of points 5, 6, and 7 are presented in Figures 6.8a to 6.10b. These three points are along the same line from upwind to downwind, so they have the same velocity and turbulence intensity behavior. The isolated roughness flow case has the highest velocity and lowest turbulence intensity in the region near the ground. The skimming flow cases have the lowest velocity and the highest turbulence intensity, and the interference flow cases have velocity and turbulence intensity values in between the isolated roughness cases and the skimming flow cases. Figure 6.11 and 6.12 show velocity profiles of point 2 and point 3 for urban roughness case ($N=8$). Comparing the velocity at the region of just above roof for two figures, there are higher speeds for point 2 since separation occurs at the edge of roof.

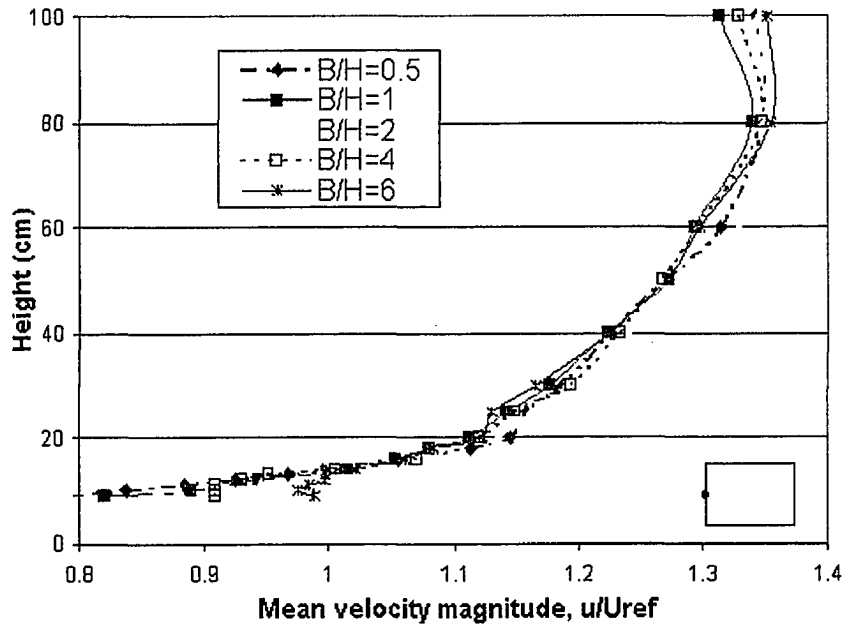


Figure 6.5a Mean velocity magnitude profile measured at point 2, N=1

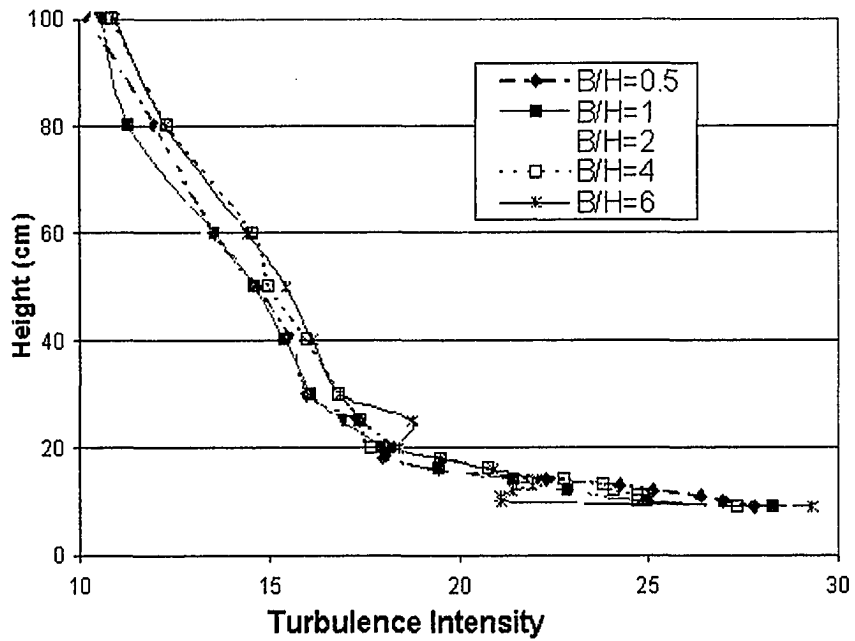


Figure 6.5b Turbulence intensity profile measured at point 2, N=1

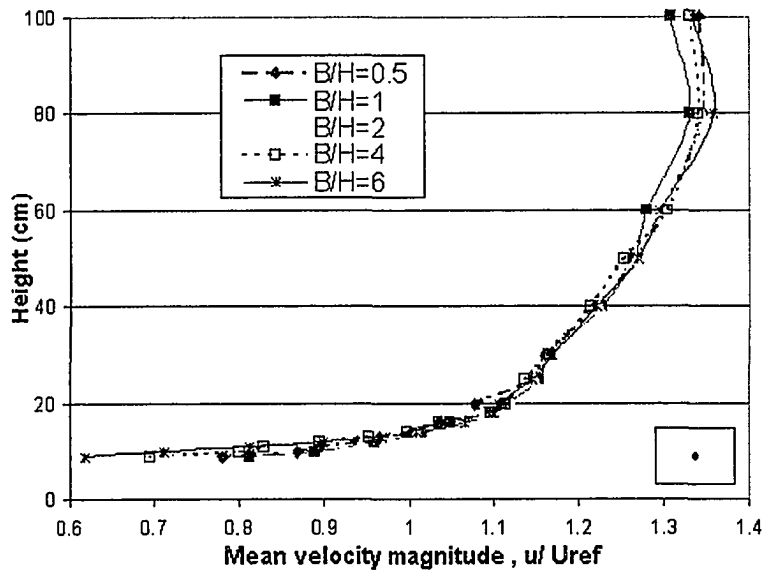


Figure 6.6a Mean velocity magnitude profile measured at point 3, N=1

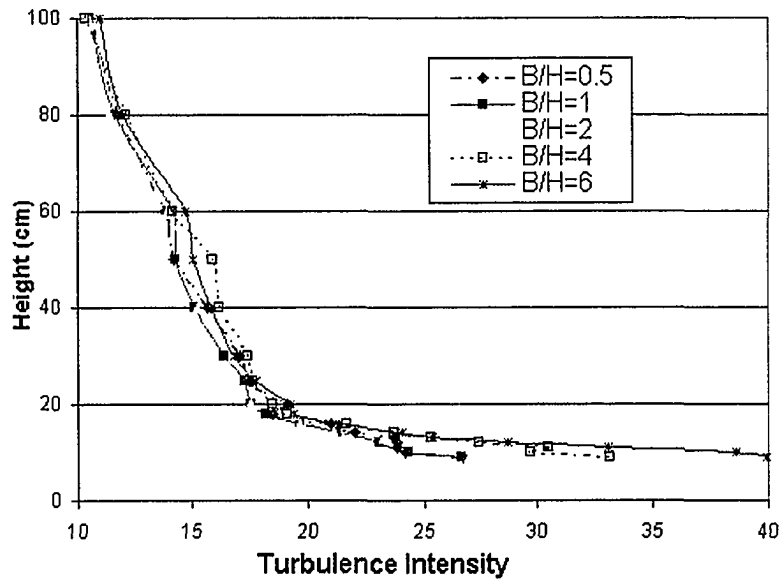


Figure 6.6b Turbulence intensity profile measured at point 3, N=1

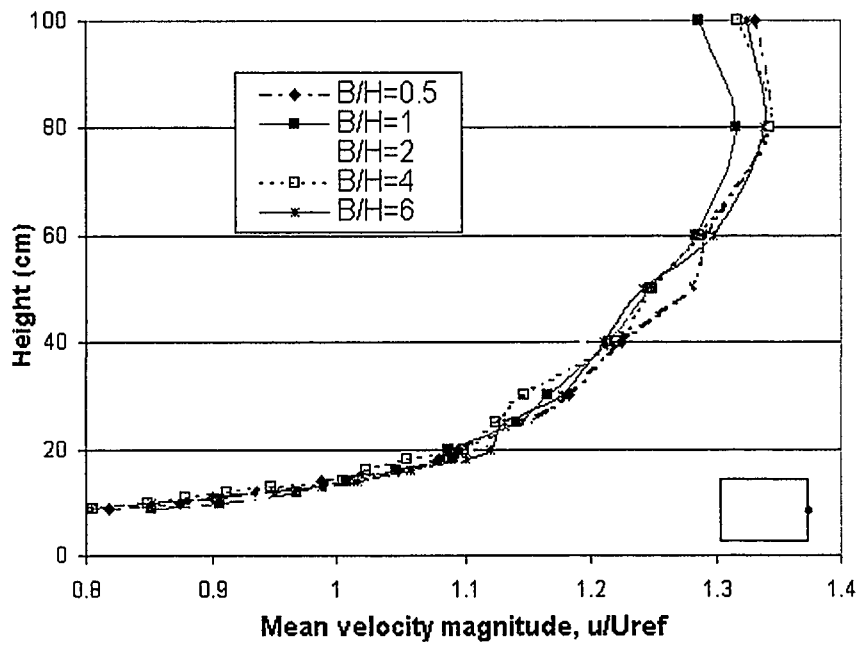


Figure 6.7a Mean velocity magnitude profile measured at point 4, N=1

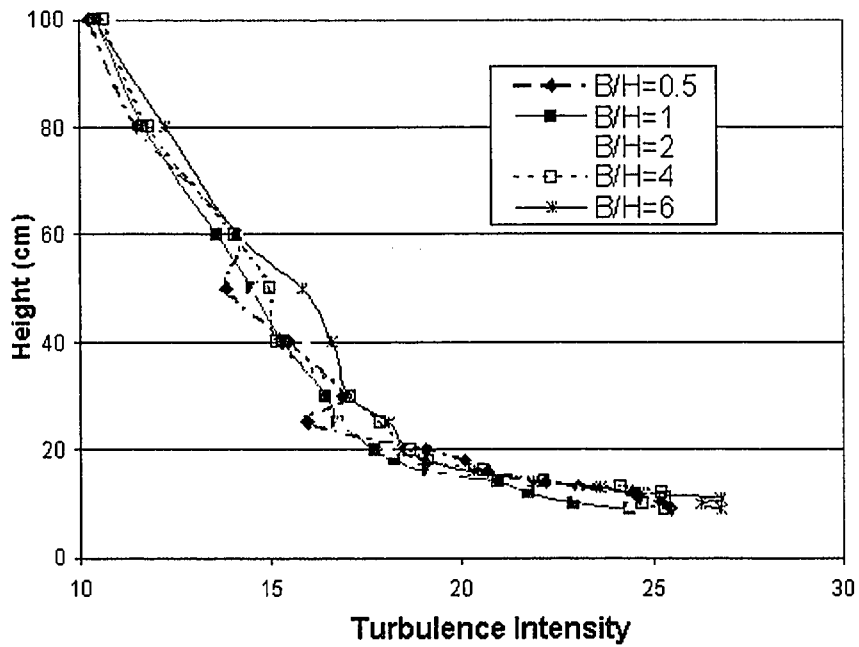


Figure 6.7b Turbulence intensity profile measured at point 4, N=1

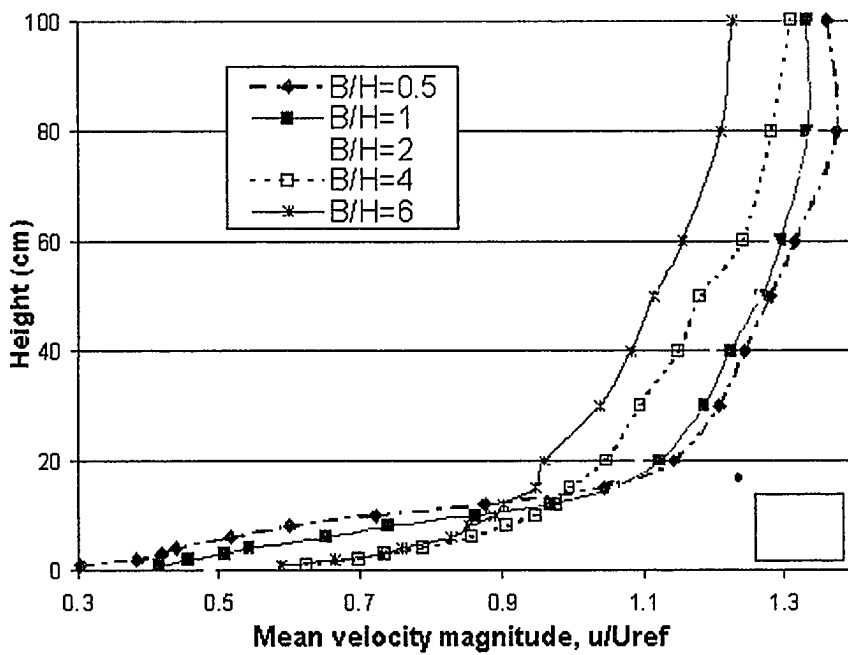


Figure 6.8a Mean velocity magnitude profile measured at point 5, N=1

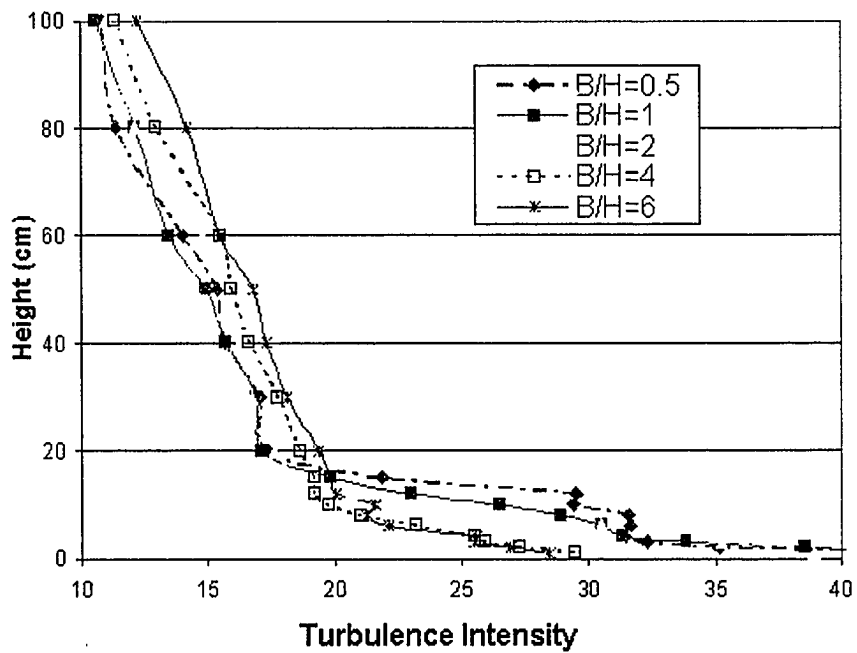


Figure 6.8b Turbulence intensity profile measured at point 5, N=1

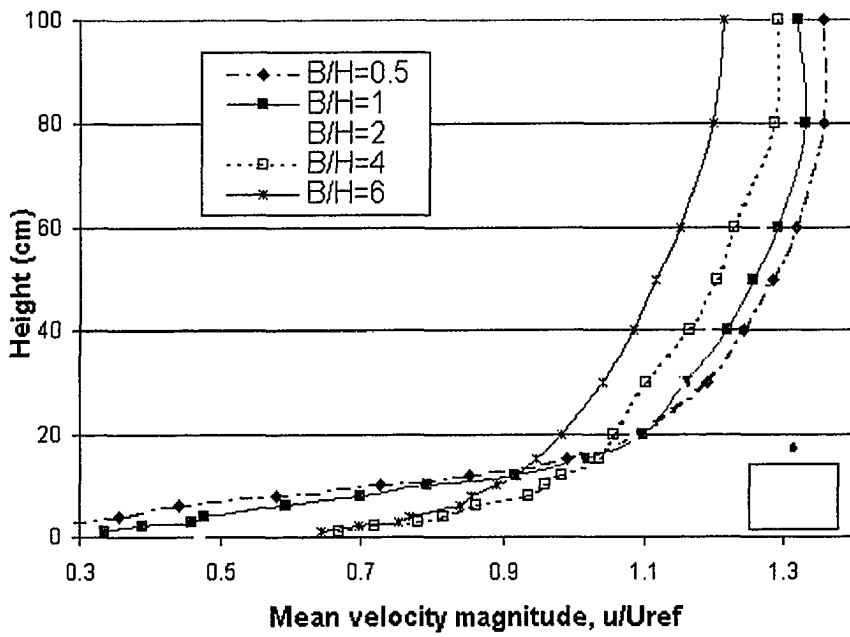


Figure 6.9a Mean velocity magnitude profile measured at point 6, N=1

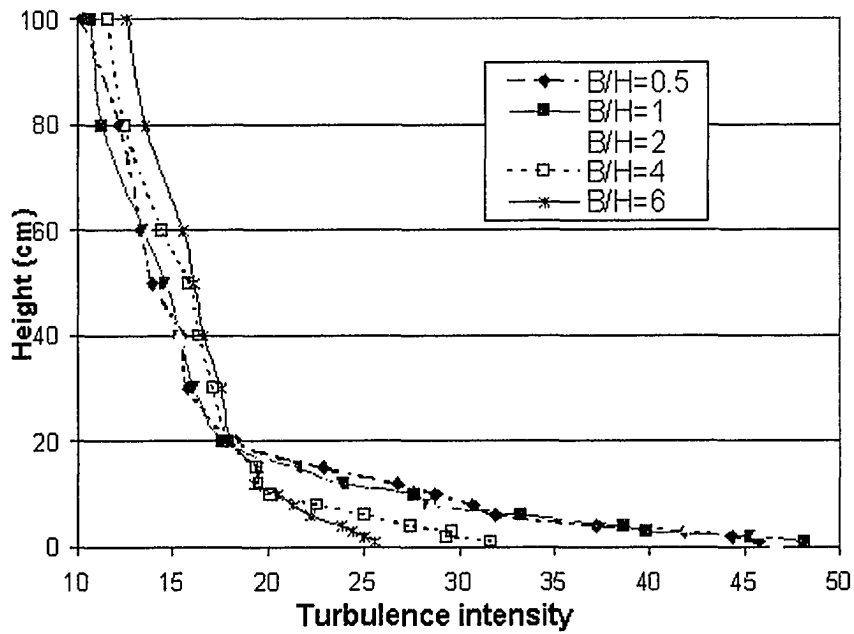


Figure 6.9b Turbulence intensity profile measured at point 6, N=1

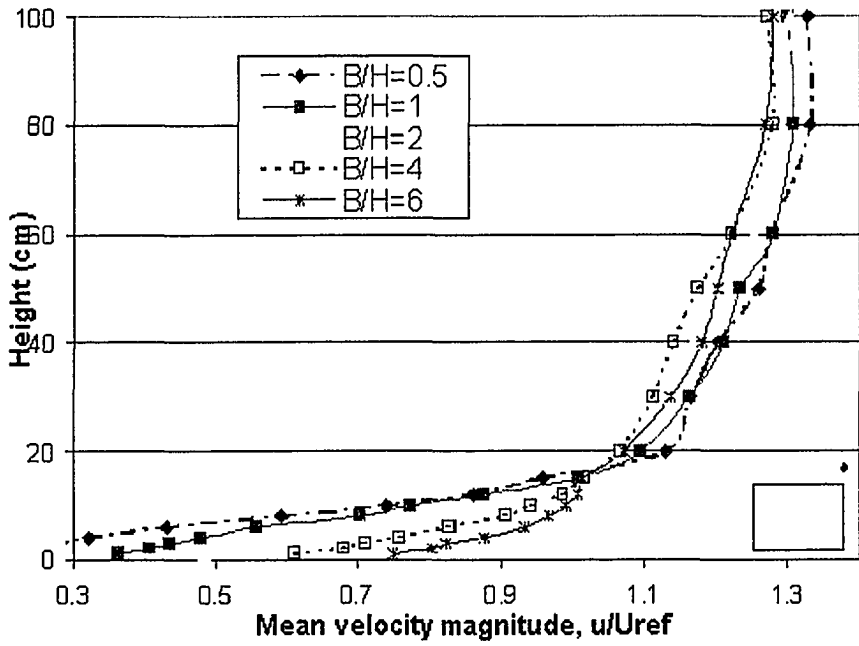


Figure 6.10a Mean velocity magnitude profile measured at point 7, N=1

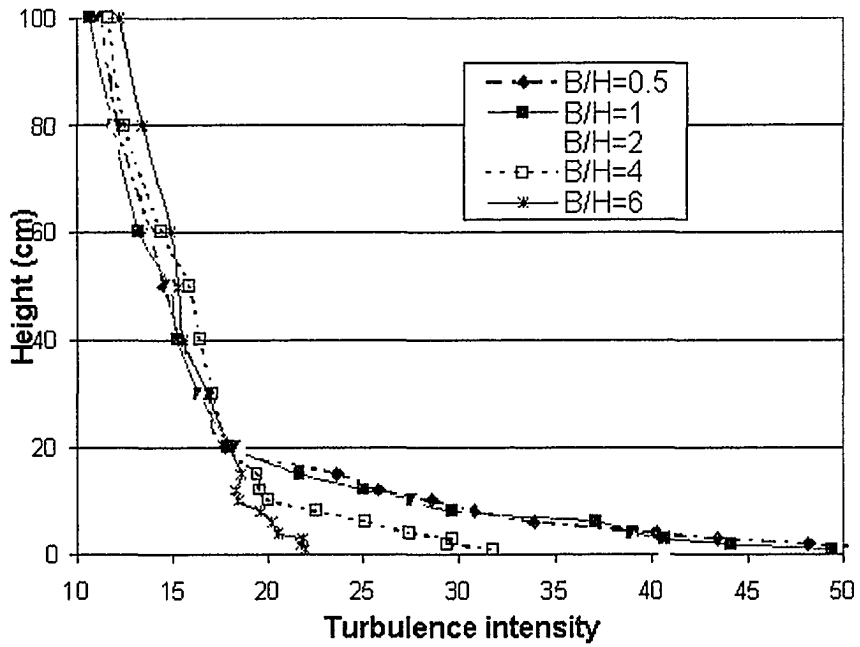


Figure 6.10b Turbulence intensity profile measured at point 7, N=1

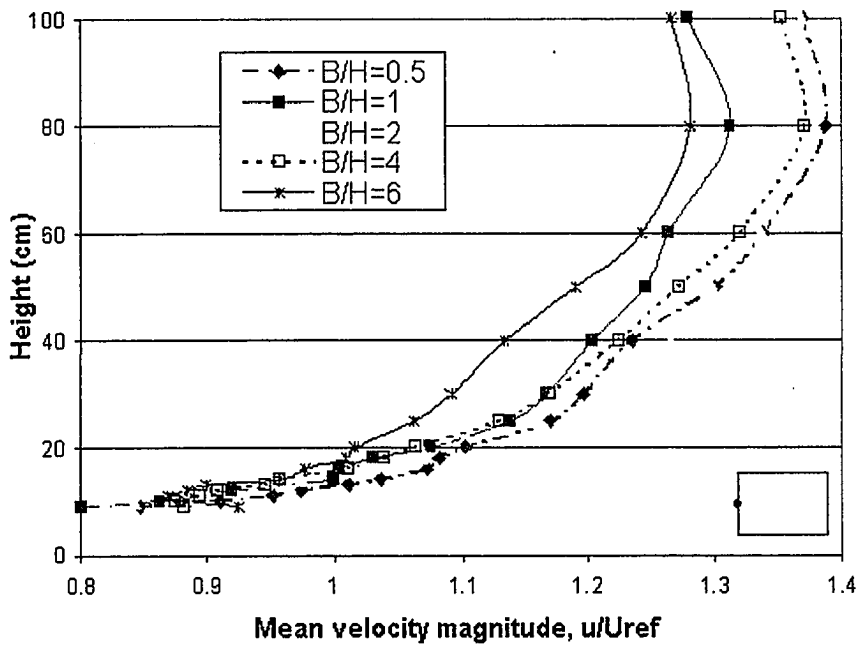


Figure 6.11 Mean velocity magnitude profile measured at point 2, N=8

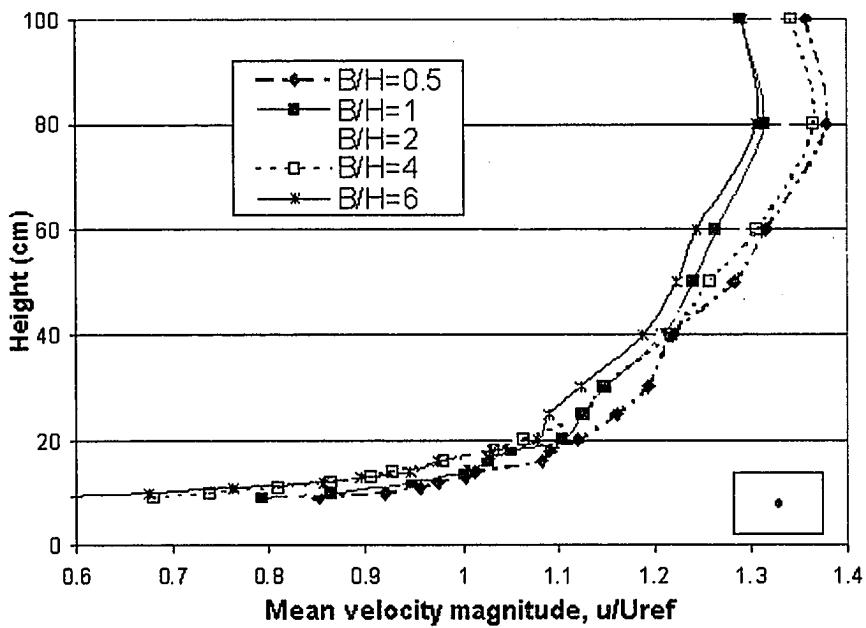


Figure 6.12 Mean velocity magnitude profile measured at point 3, N=8

6.1.3 Comparison of Wind Tunnel Results and Numerical Simulation

Two computational fluid dynamics (CFD) programs, Fluent 5.4 and Fire Dynamics Simulator (FDS), as described in Chapter 4 are used to model the wind flow over the different configurations of an urban street canyon. In this section, the comparison between wind tunnel data and numerical data for both flow visualization and velocity and turbulence profiles is presented.

Flow Visualization

Figure 6.13a shows the actual image of skimming flow visualization for case $B/H=1$ taken from the wind tunnel experiment. In the image, the clockwise circulation of flow can be seen in the street canyon as the winds blow normally from left to right. The results of the calculated velocity vector in the street canyon from both Fluent and FDS simulations within the same region display the same patterns of flow movement. Figures 6.13b and 6.13c show the numerical velocity vector results of case $B/H=1$ from Fluent and FDS simulations. The conclusion can be made that numerical simulations predict the flow pattern of skimming flow quite well.

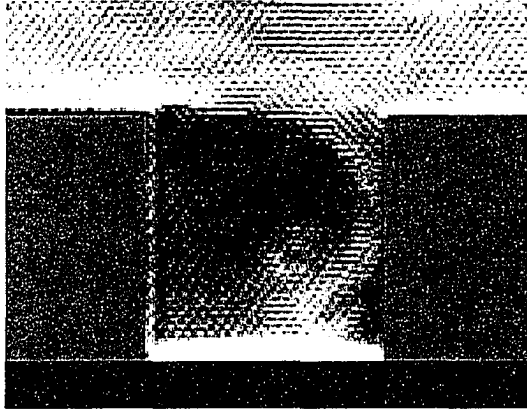


Figure 6.13a Flow visualization result of case, $B/H=1$

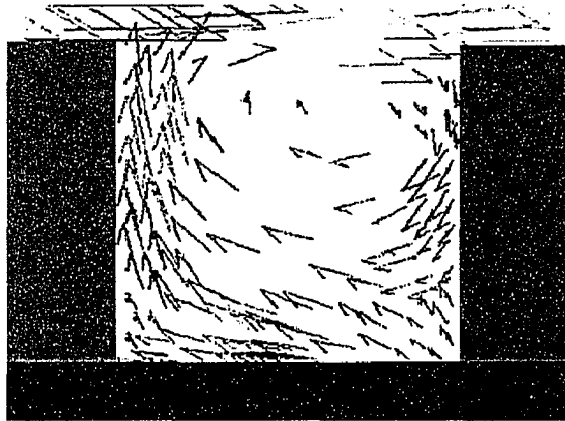


Figure 6.13b Numerical velocity vector result of case, $B/H=1$ from Fluent 5.4

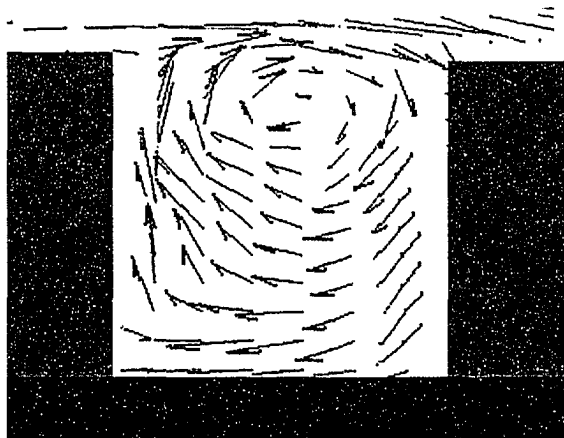


Figure 6.13c Numerical velocity vector result of case, $B/H=1$ from FDS

Figure 6.14a is an image of interference flow visualization for case $B/H=4$. In this case, the numerical experiment is performed using Fluent. Figure 6.14b shows the result of the numerical experiment. As the wind blows from left to right, a wake zone is generated right behind the left building and a displacement zone is formed before the right building in the street canyon area. In the center region of the canyon, the interference flow, a mix of part wake zone and part displacement zone, occurs. The numerical data reflect exactly the pattern of the physical experiment observed in the wind tunnel.

Figure 6.15a shows the actual image of isolated roughness flow for case $B/H=6$. Figure 6.15b presents the result of the numerical experiment for this case using Fluent. As indicated on the graph, the isolated roughness flow case has both a wake zone and a displacement zone in the street canyon region; however, the wider distance of the street canyon separates these two zones far enough so the buildings only have the isolated effect to the wind flow. The numerical data again predicts the results of the physical experiment.

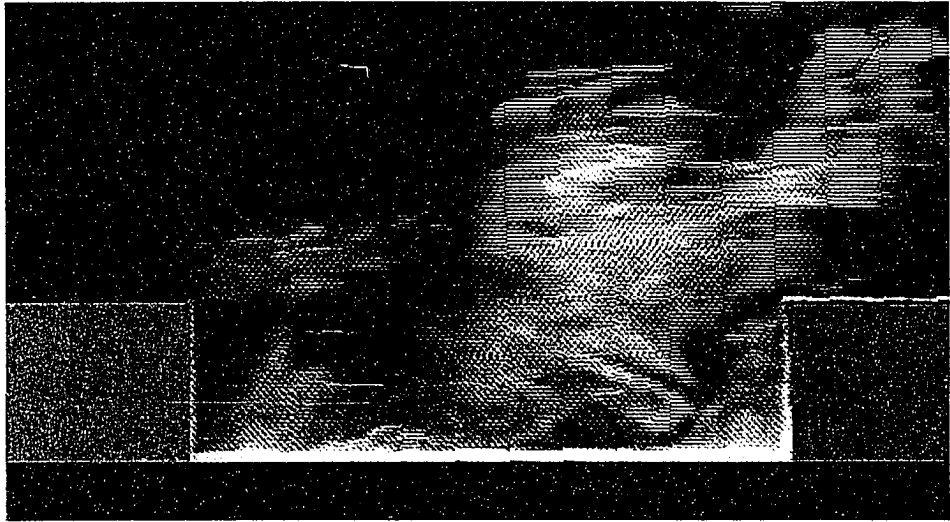


Figure 6.14a Flow visualization result of case, $B/H=2$

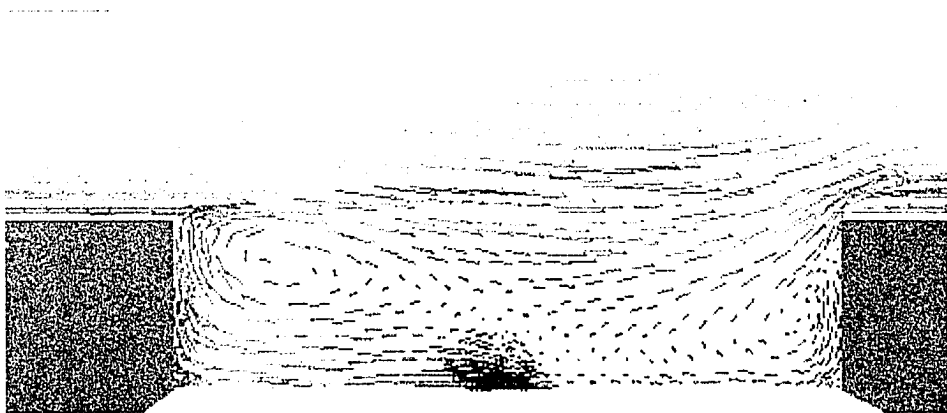


Figure 6.14b Numerical velocity vector result of case, $B/H=4$ from Fluent

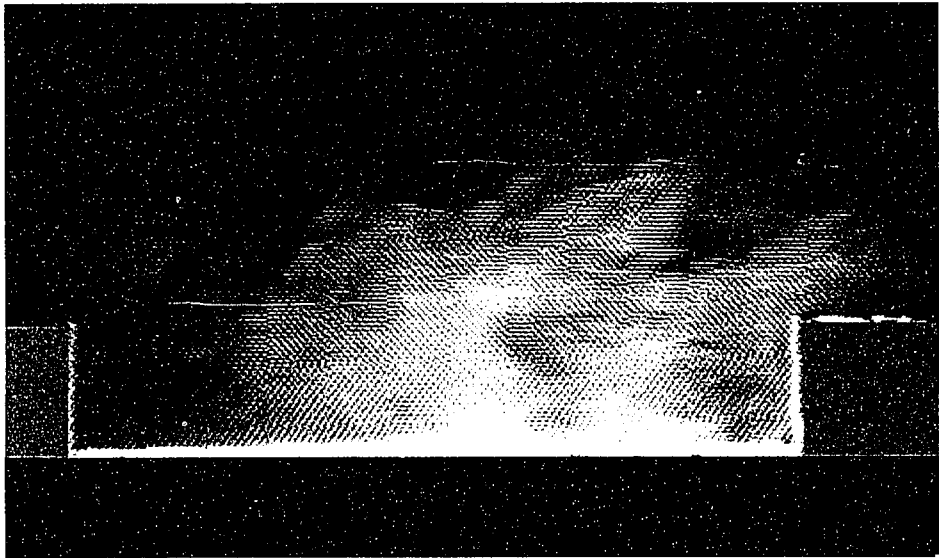


Figure 6.15a Flow visualization result of case, $B/H=6$

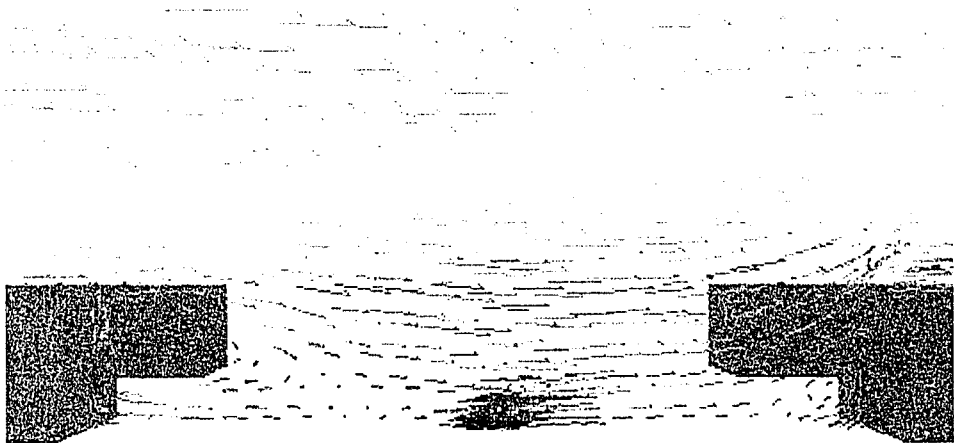


Figure 6.15b Numerical velocity vector result of case, $B/H=6$ from Fluent

Velocity and Turbulence Intensity Profiles

Fluent:

Four separate turbulence models, the standard κ - ϵ , the RNG κ - ϵ , the Reynolds-stress and the LES, are used to model wind flow over the different configurations of an urban street canyon using Fluent. By examining the results for each turbulence model, it appears that the standard κ - ϵ and the RNG κ - ϵ models give almost the same predictions for velocity magnitude profiles; however, the standard κ - ϵ provides the best simulations of the flow field in the urban street canyon.

Figures 6.16a, 6.17a, and 6.18a show the velocity magnitude profiles at points 1, 3 and 5, respectively, for case $B/H=1$, $N=1$ using four turbulence models. The graphs indicate clearly that both the standard κ - ϵ and RNG κ - ϵ models predict the measured velocity profiles. On the other hand, the Reynolds-stress and LES models underpredict the velocity profile in the region around the building roof height. Figures 6.16b, 6.17b, and 6.18b show the turbulence intensity profiles at point 1, 3, and 5, respectively, for case $B/H=1$, $N=1$ using different turbulence models. All four turbulence models produce similar turbulence intensity profiles. By comparing the predictions of turbulence intensity profiles to the physical experimental results, the prediction values are reasonable. The very large value of turbulence intensity at $z = 8 - 9$ cm are an artifact due to $U \approx 0$ at this height.

Since the κ - ϵ turbulence model outperformed the other turbulence models for the cases considered above, additional comparisons of velocity and turbulence intensity

profiles will be limited to those using the κ - ϵ model. Figure 6.19a shows the velocity magnitude and profile at point 1 for case N=1 with different values of B/H by using Fluent with the κ - ϵ turbulence model. Figure 6.19b is a graph of the comparison results of turbulence intensity profiles at point 1 for case N=1 with different values of B/H using κ - ϵ model. Both the graphs indicate that the Fluent κ - ϵ turbulence model successfully predicts dominated flow patterns for the velocity magnitude and turbulence intensity profiles for each case.

A comparison of velocity magnitude profiles over point 1 for the case B/H=1, but different values of N is shown at Figure 6.20a. The graph shows that the Fluent κ - ϵ model predicts the flow patterns for open-country roughness cases (N=1, N=2) quite well. However, the Fluent κ - ϵ model over predicts the area above the building roof height for the urban-roughness cases (N=3, N=8). Figure 6.20b presents turbulence intensity profiles at point 1 for case B/H=1 but different values of N by using κ - ϵ model. The Fluent κ - ϵ model predicts the flow patterns of open-country roughness cases (N=1, N=2), but underpredicts the flow patterns for the area around the building roof height for the urban-roughness cases (N=3, N=8).

In Figure 6.16b, the turbulence intensity values predicted by Fluent were bigger than the values collected from wind tunnel experiments. Considering the equation that was discussed in Chapter 3:

$$I(z) = \frac{\sqrt{u^2(z)}}{U(z)}$$

The turbulence intensity is equal to root mean square value of velocity at elevation z divided by mean velocity at elevation z . In some area of the canyon, mean velocity is close to zero. Since U is close to zero, the turbulence intensity, $I(z)$, becomes very large. Figures 6.19b and 6.20b show similar results of predicted turbulence intensity at point 1 of the canyon area.

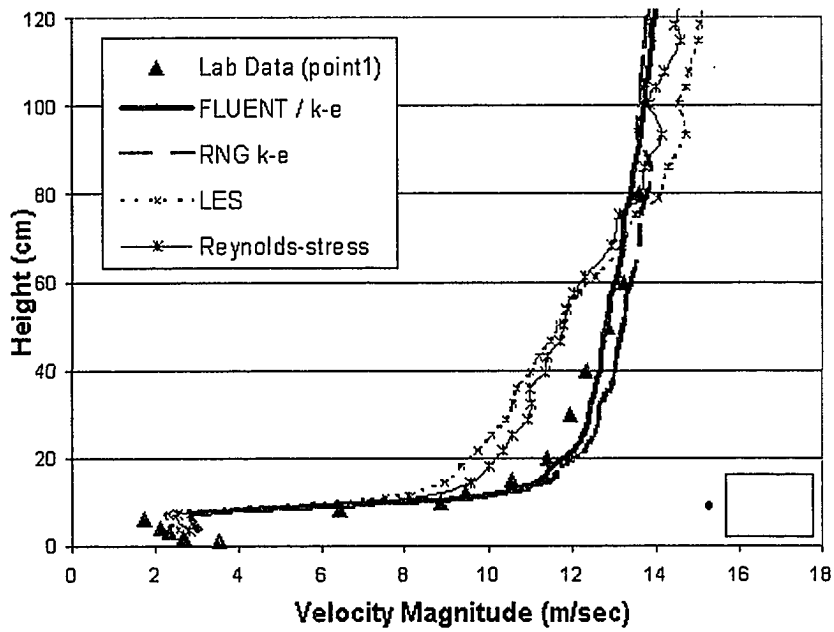


Figure 6.16a Velocity magnitude profile at point1 for case B/H=1, N=1

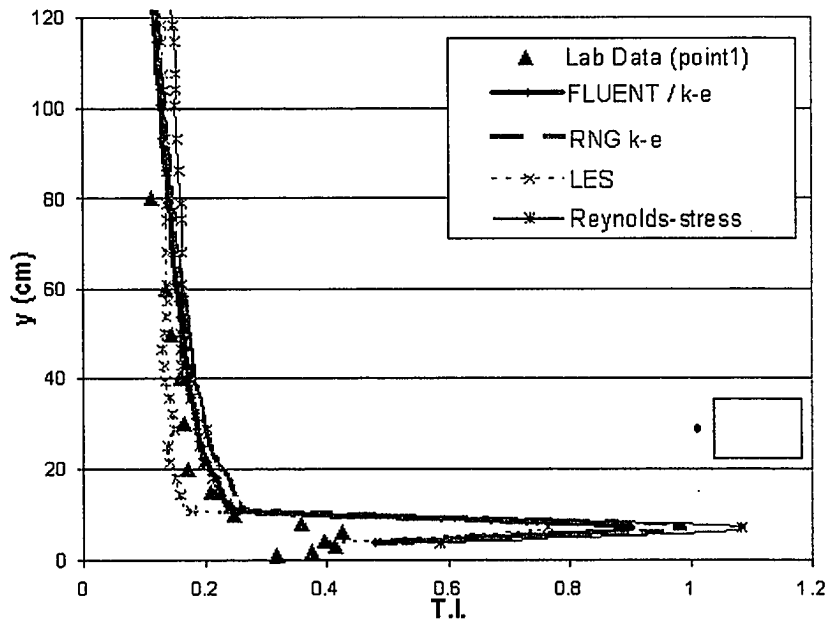


Figure 6.16b Turbulence intensity profile at point1 for case B/H=1, N=1

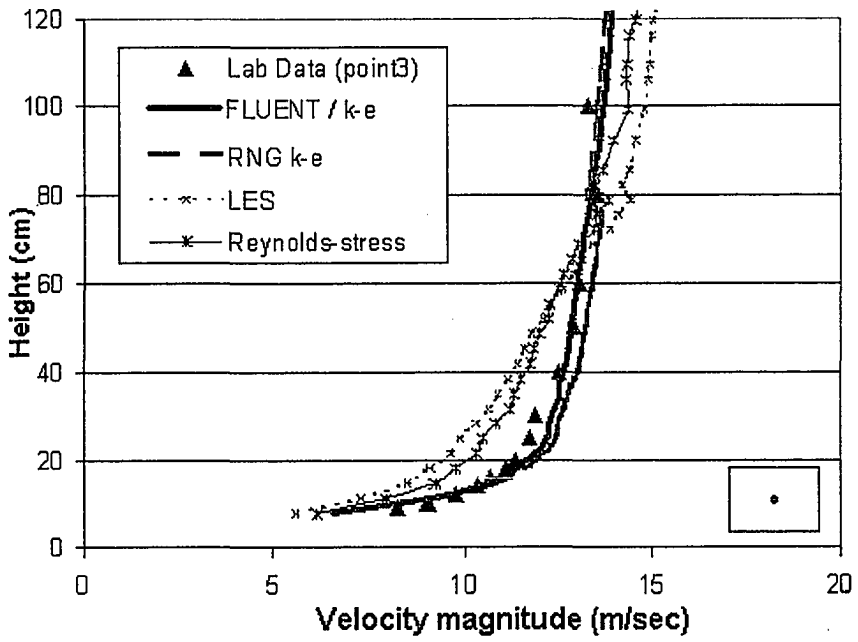


Figure 6.17a Velocity magnitude profile at point 3 for case B/H=1, N=1

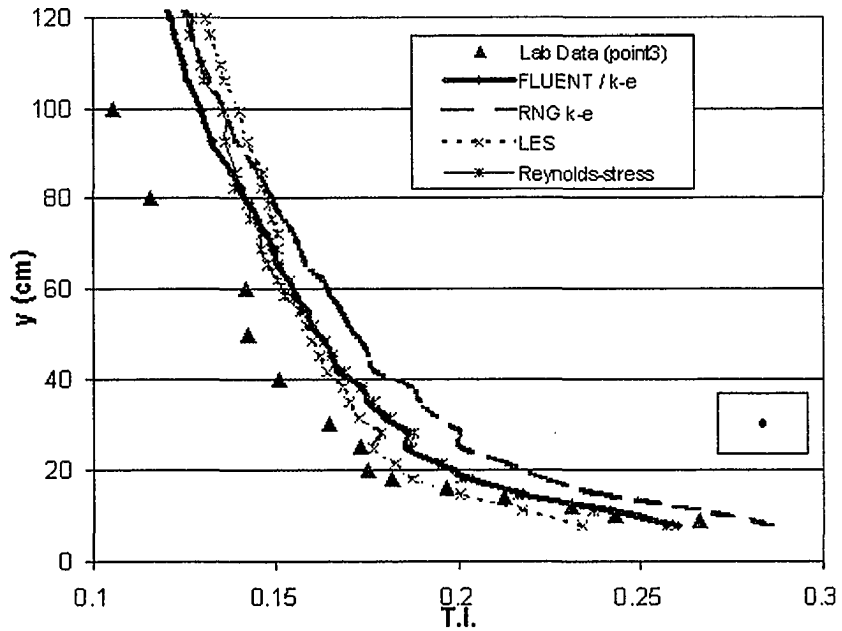


Figure 6.17b Turbulence intensity profile at point 3 for case B/H=1, N=1

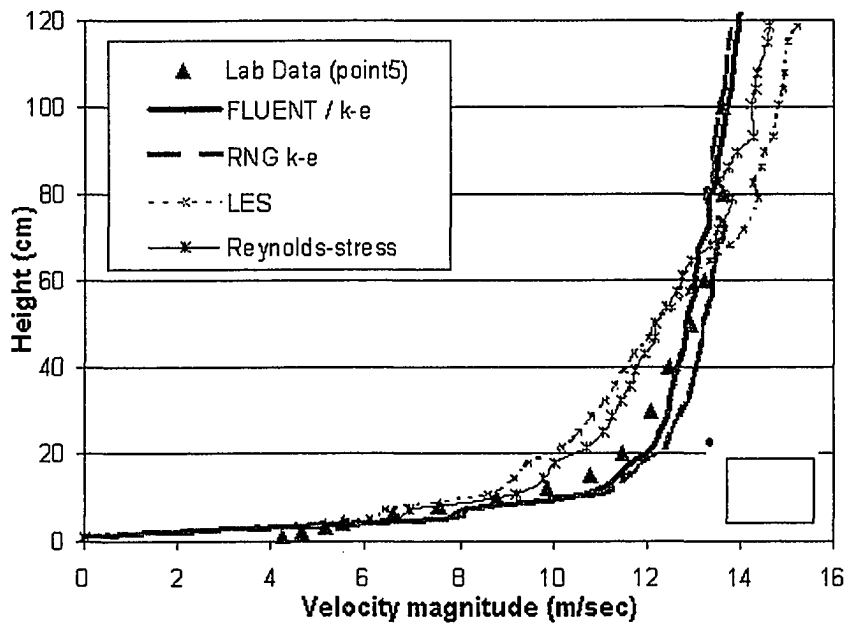


Figure 6.18a Velocity magnitude profile at point 5 for case B/H=1, N=1

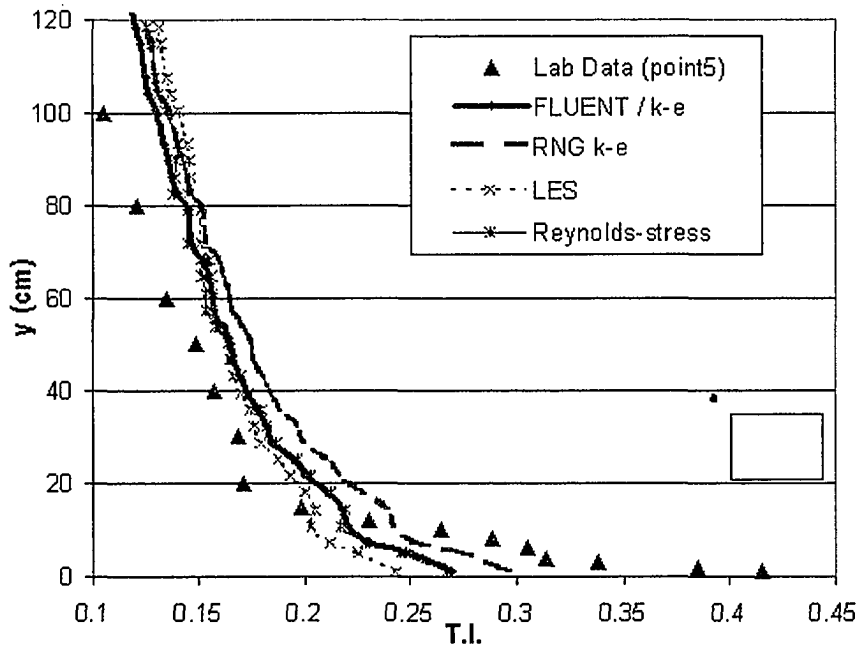


Figure 6.18b Turbulence intensity profile at point 5 for case B/H=1, N=1

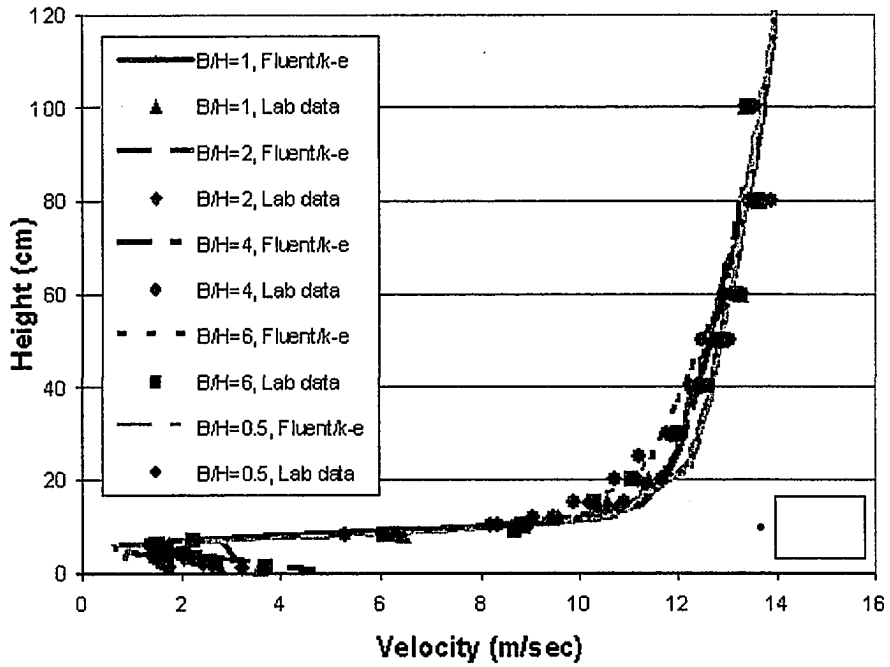


Figure 6.19a Velocity magnitude profile at point 1, N=1 using k-ε model

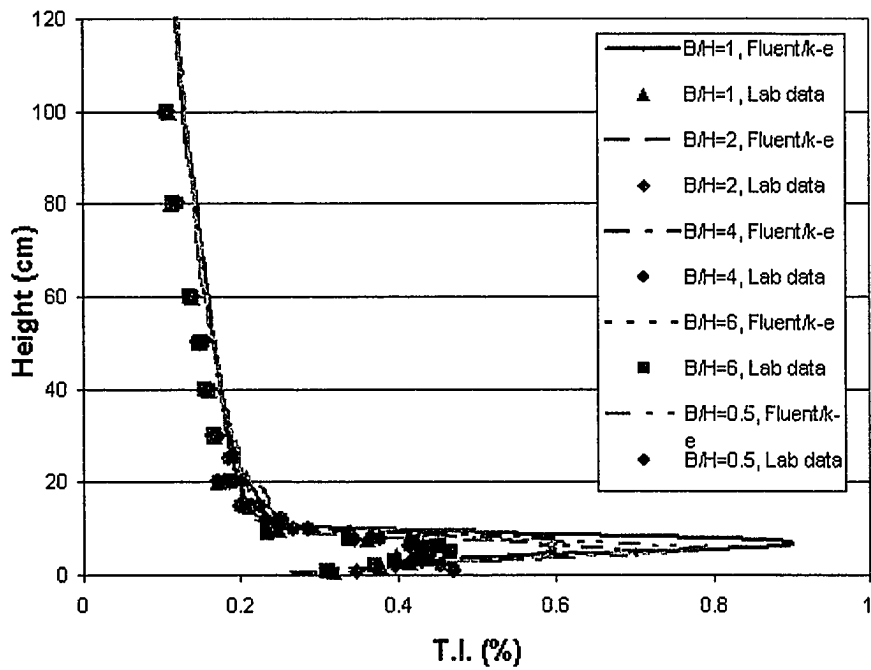


Figure 6.19b Turbulence intensity profile at point 1, N=1 using k-ε model

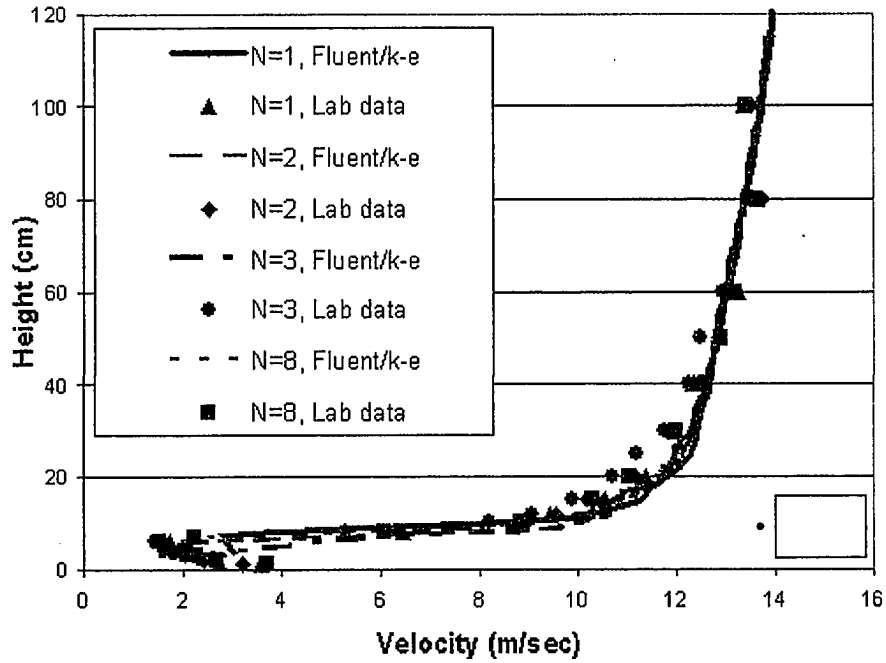


Figure 6.20a Velocity magnitude profile at point 1, $B/H=1$ using $k-\epsilon$ model

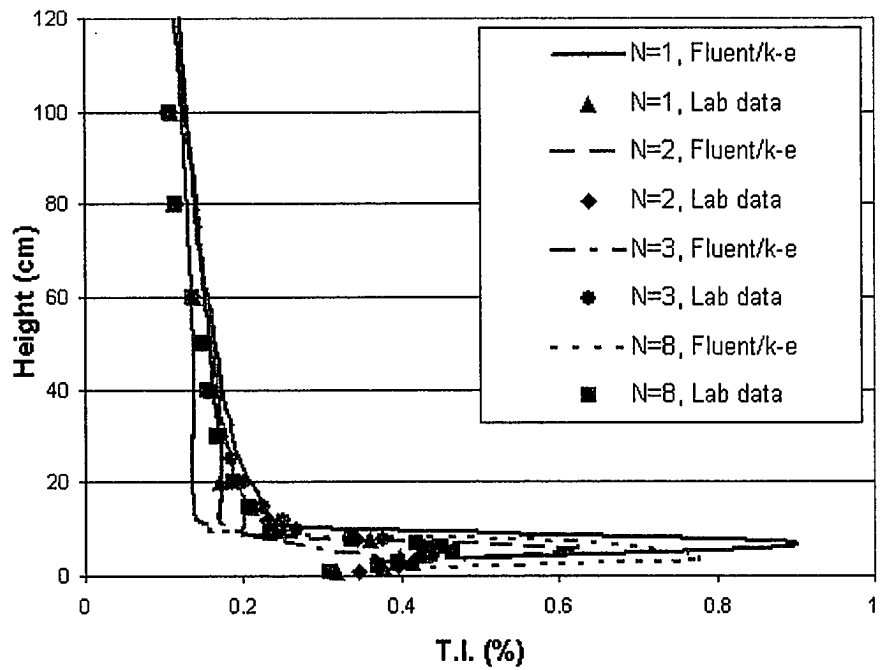


Figure 6.20b Turbulence intensity profiles at point 1, $B/H=1$ using $k-\epsilon$ model

FDS:

The effect of grid resolution on the features of the flow field is considered to determine the grid size needed to accurately resolve the flow. Four different grid resolutions, and canyon heights of 12 cells, 9 cells, 7 cells and 5 cells are examined here. Typical resolution study results are shown in Figures 6.21a and 6.21b. The graph of the velocity profile at point 1 shows that higher grid resolution cases are closer to the wind tunnel data. The graph of velocity profiles of point 3 shows that the cases of canyon heights of 5, 7 and 9 give the velocity near the roof of master building. These are much lower than the case for a height of 12 cells. From these comparisons of different calculation grid resolutions, it is obvious that a higher grid resolution better predicts the flow field in this urban street canyon simulation.

FDS is used to run the case of $B/H=1$, $N=1$ with three different ground boundary conditions, no-slip, half-slip and free-slip. The tangential velocity boundary condition can be no-slip, free-slip or something in between (a simple law of the wall). For no-slip, set VBC to -1 . For free-slip, set VBC to 1 . Numbers in between -1 and 1 can represent partial slip conditions, which may be appropriate for simulations involving large grid cells. The grid resolution is based on a canyon height of 12 cells here. Figure 6.22a shows the comparison of FDS and lab data for a velocity profile above point 1. The graph indicates that the no-slip profile provides poor agreement with wind tunnel results. The other two profiles appear to be acceptable. In contrary, the turbulence intensity profiles at point 1 have opposite results. In Figure 6.22b, the no-slip profile appears to

match best with the lab profile, but apparently the other profiles do not. Similar results can be seen for the cases of point 3 and 5 (see Figures 6.23a, 6.23b, 6.24a and 6.24b).

The previous cases discussed above reflect the questionable reliability of FDS as a CFD tool for predicting the flow fields of an urban street canyon. The problem might be a restriction of the software itself, or it may be due to lack of enough understanding and research on operating the software. For example, turbulence cannot be introduced at the inlet flow during the computational process because the software lacks that option. Another restriction is that the calculation domain had to be small because the personal computer used lacks the hardware capacity to perform a calculation with larger domain.

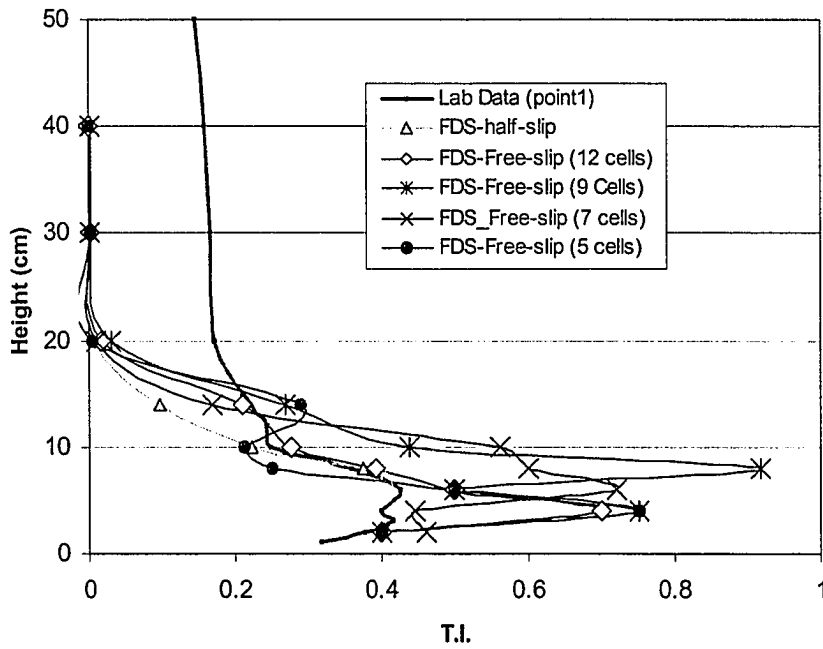
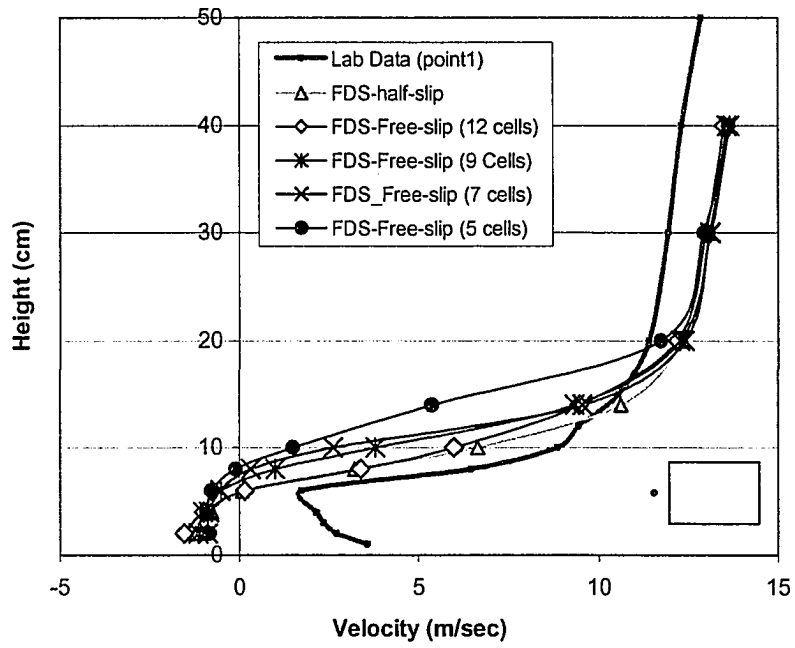


Figure 6.21a Mean velocity and turbulence profile at point 1 using FDS with different grid resolution

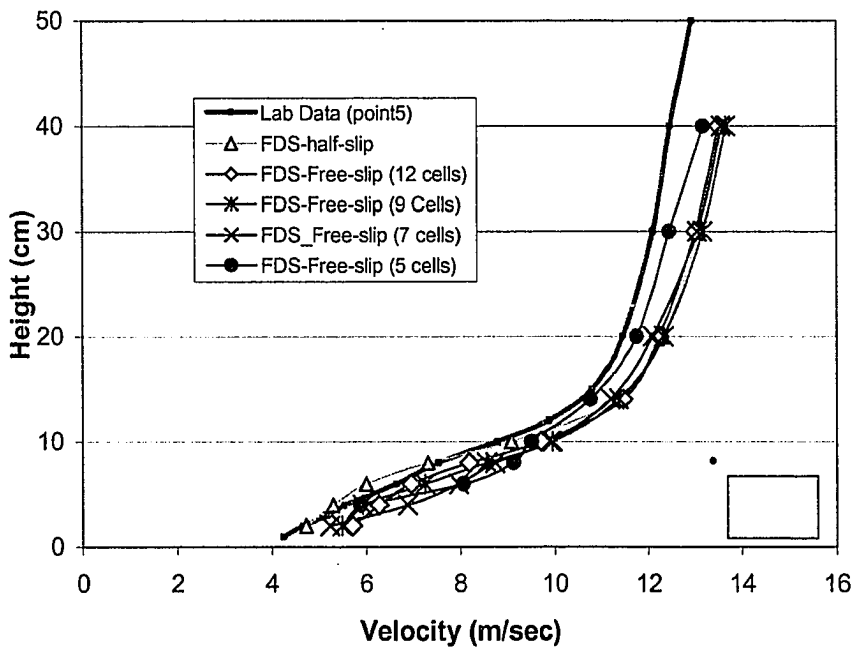
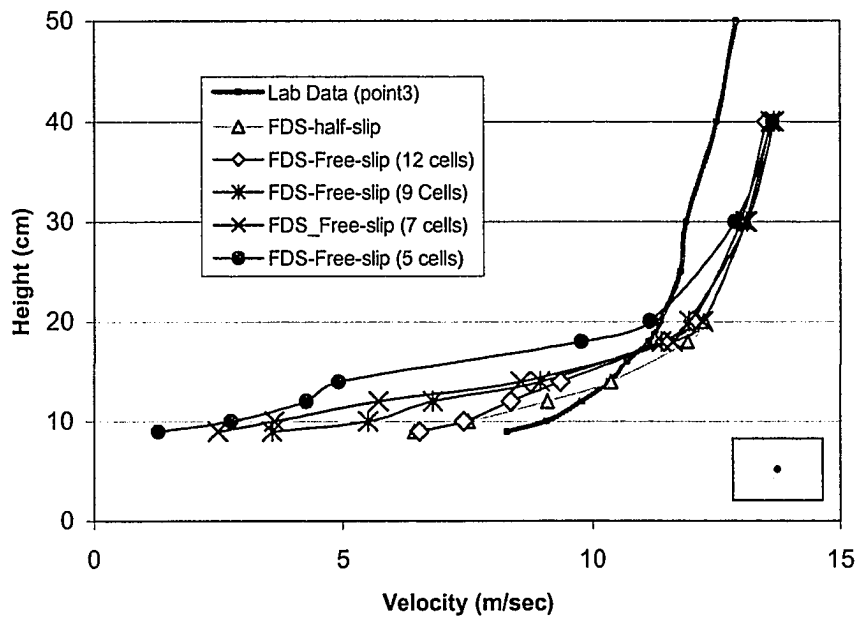


Figure 6.21b Mean velocity profile at point 3 and point 5 using FDS with different grid resolution

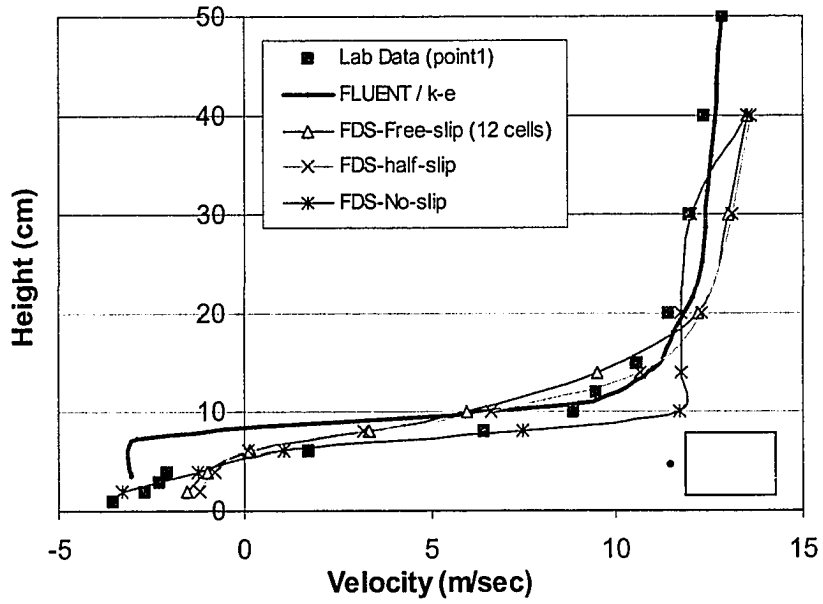


Figure 6.22a Velocity profile at point 1, $B/H=1$, $N=1$ using FDS

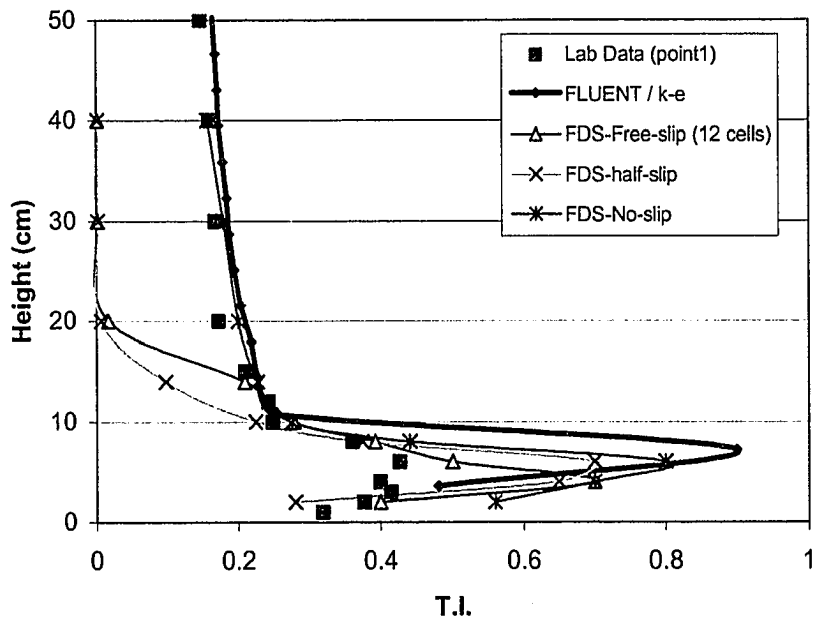


Figure 6.22b Turbulence intensity profiles at point 1, $B/H=1$, $N=1$ using FDS

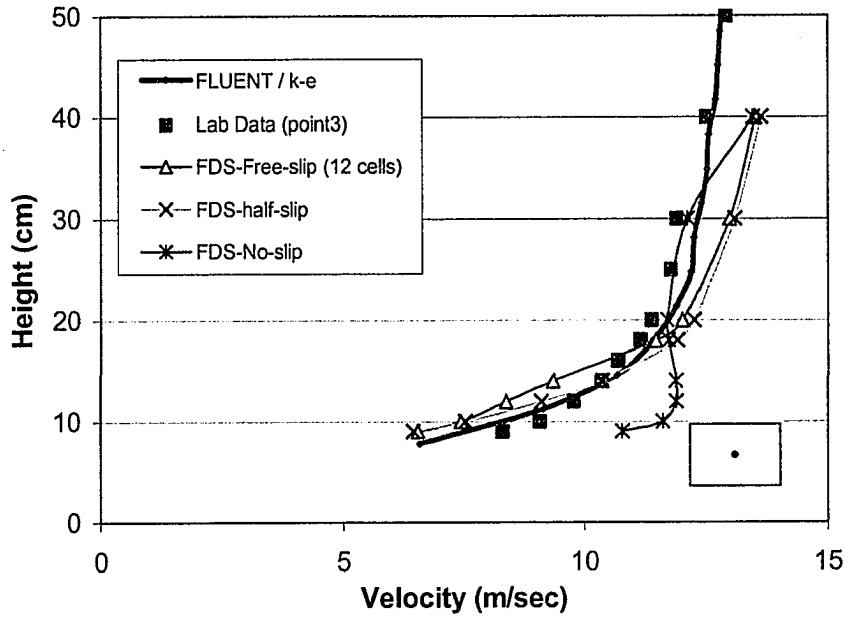


Figure 6.23a Velocity profile at point 3, B/H=1, N=1 using FDS

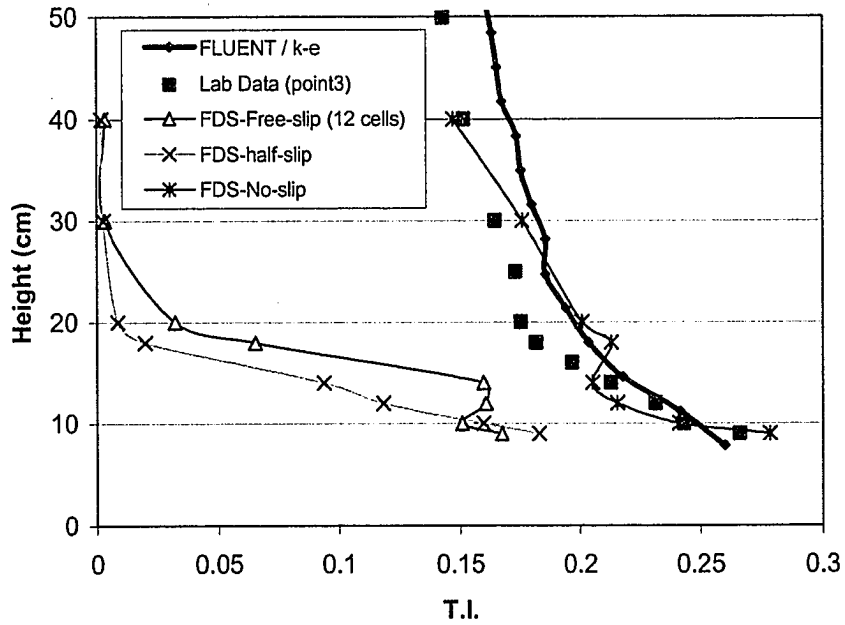


Figure 6.23b Turbulence intensity profiles at point 3, B/H=1, N=1 using FDS

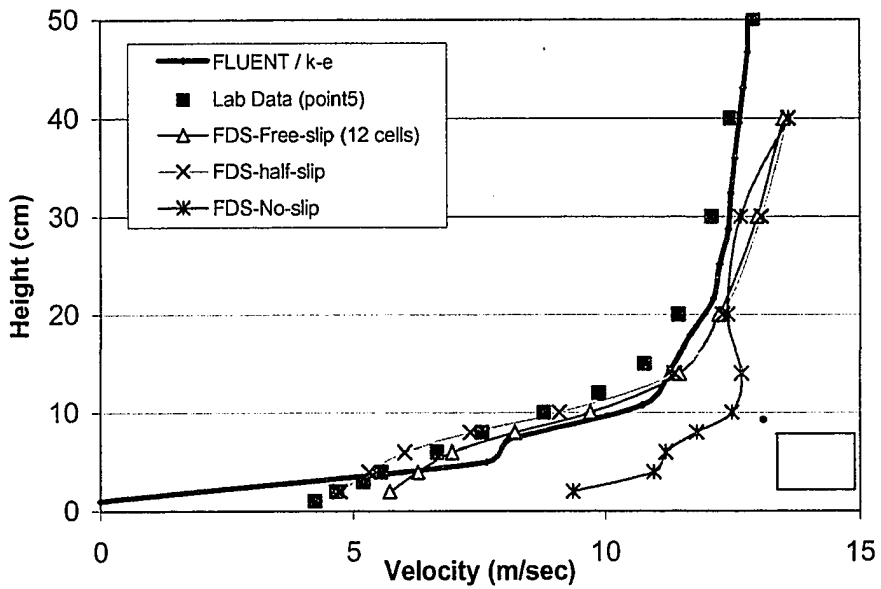


Figure 6.24a Velocity profile at point 5, B/H=1, N=1 using FDS

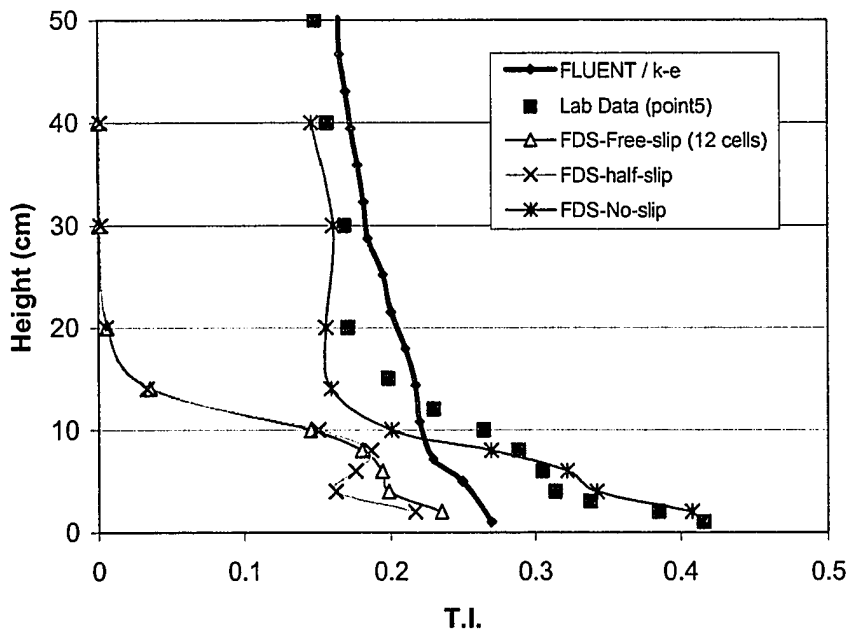


Figure 6.24b Turbulence intensity profiles at point 5, B/H=1, N=1 using FDS

6.2 The Effects of Surroundings on Surface Pressure on Low-Rise Buildings

Very large vortex-induced roof suctions on low-rise buildings have been revealed for isolated buildings in both full scale experiments and wind tunnel tests by many investigators. This section investigates the sensitivity of these high suctions to the presence of multiple surrounding building configurations. The wind tunnel experimental results are presented and are briefly compared with numerical data calculated using CFD.

6.2.1 The Effects of Surroundings

High suction pressures over the building surface are significantly reduced for a building surrounded by other buildings compared to the isolated building in the same approach flow, in terms of the peak, mean or RMS C_p . All three statistical interpretations of pressure variation are significantly reduced by the presence of surrounding buildings. See Figures 6.25 to 6.39 for detailed C_p comparisons on a single building and all surrounding cases.

It was expected that shielding effects depend on the width of the street canyon (ratio of B/H) and the number of the buildings located upstream of the master building. When examining the open-country cases ($N=1$) for different values of B/H and wind perpendicular to the building wall, the results show that as the value of B/H increases, the shielding effect on the roof C_p 's decrease. For example, the -mean, -peak and RMS C_p 's for the case of $B/H=0.5$ are all smaller than the case of $B/H=6$. Compare the open-country cases ($N=1$) for different values of B/H with the single building case, the -mean,

-peak and RMS C_p 's reduce in all cases. However, in the upwind region of the roof or of the centerline of the master building, RMS and -peak C_p 's are larger than those of the single building case due to the flow separation occurring at the forward corner. The upwind wall cases have similar results to the roof cases. The shielding effects become larger in the cases of lower B/H. (See Figures 6.40 to 6.42).

For urban roughness cases (N=8), the shielding effects have similar trends to the open-country cases mentioned above. However, the shielding effects on the urban roughness cases are better than the open-country cases, because the number of buildings located upstream of the master building is greater. (See Figures 6.43 to 6.45).

Mean, RMS and -peak pressure coefficients measured in the wind tunnel for a corner roof point (Tap #1) for the wind azimuths range from 0 degree to 90 degrees are shown at Figures 6.47, 6.48 and 6.49. Pressure tap #1 corresponds to the tap 50101 as absented in the TTU/WERFL building (see Fig 4.3, Ham's diddertation) Figure 6.46 shows a schematic for pressure coefficient measurement at different approaching angles. For mean pressure coefficient, the results show that the maximum value of -1.8 occurs at the wind angle of 10 degrees for the single building case. For other cases, the maximum mean C_p 's reduce to -0.3, -0.7 and -0.5 for cases of B/H=0.5, B/H=1 and B/H=2, respectively. For RMS pressure coefficient, the result of the single building case shows that the maximum RMS C_p is 0.8 at the wind angle of 20 degrees. The values of RMS reduce to 0.1, 0.3 and 0.35 for cases of B/H=0.5, B/H=1 and B/H=2, respectively. For -peak pressure coefficient, the maximum value of the single building case is -4.1 at the wind angle of 10 degrees. The maximum values of -peak reduce to -0.8, -1.6 and -1.5

for cases of $B/H=0.5$, $B/H=1$ and $B/H=2$, respectively. The case of $B/H=0.5$ has the maximum reduction rate for each pressure coefficient. The surroundings lead to a reduction in magnitude of 83% for the mean C_p , 87% for the RMS C_p and 80% for the – peak C_p . High suction at the roof corner is significantly reduced when surrounding buildings are presented for all cases of wind flow angle varying from 0 to 90 degrees.

The effects of surroundings significantly reduce the pressure coefficients, especially when the width of the street canyon is smaller (value of B/H is lower). In the case with the same street canyon width, urban roughness cases tend to have greater shielding effects than the open-country cases.

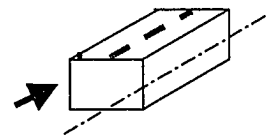
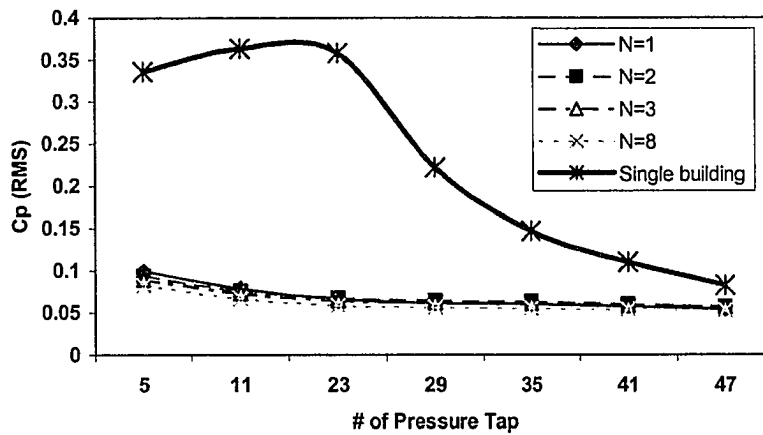
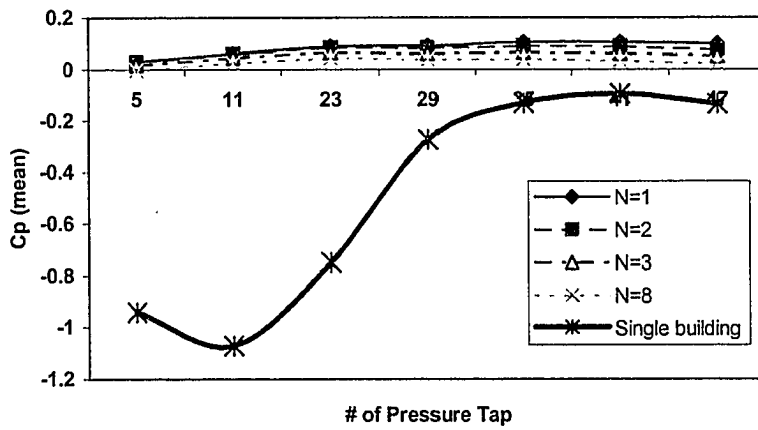
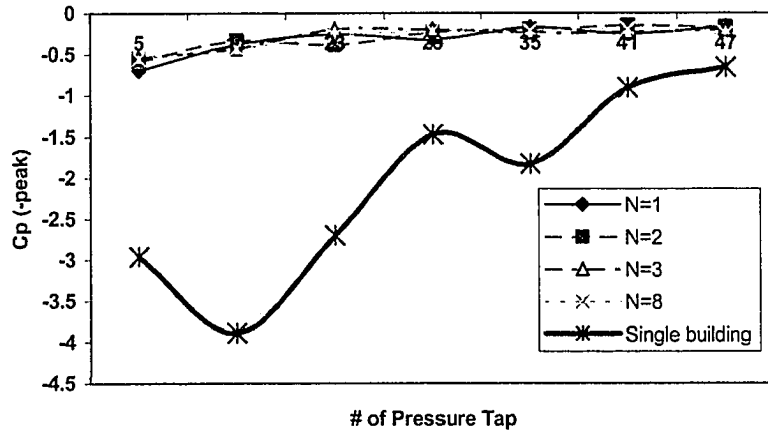


Figure 6.25 Pressure coefficients (-peak, mean, and RMS) on the centerline of roof for cases, $B/H=0.5$, with different N

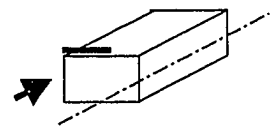
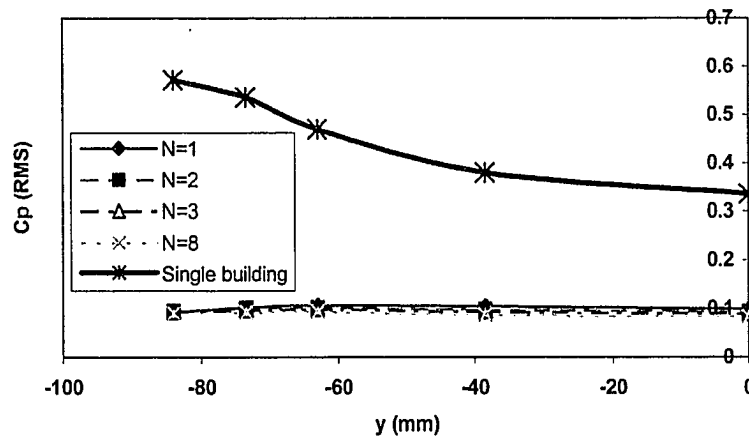
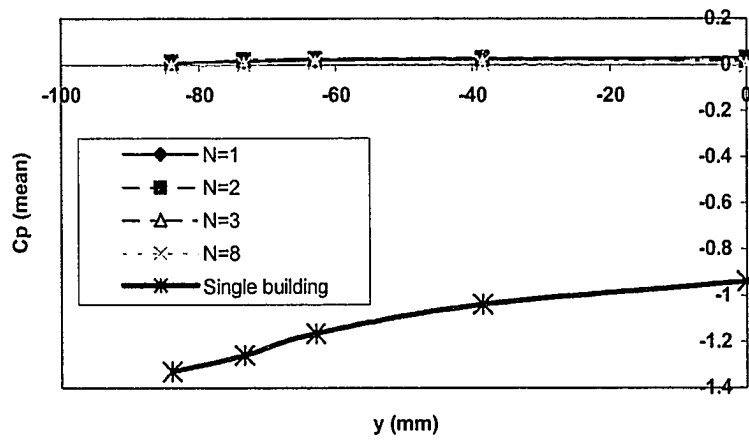
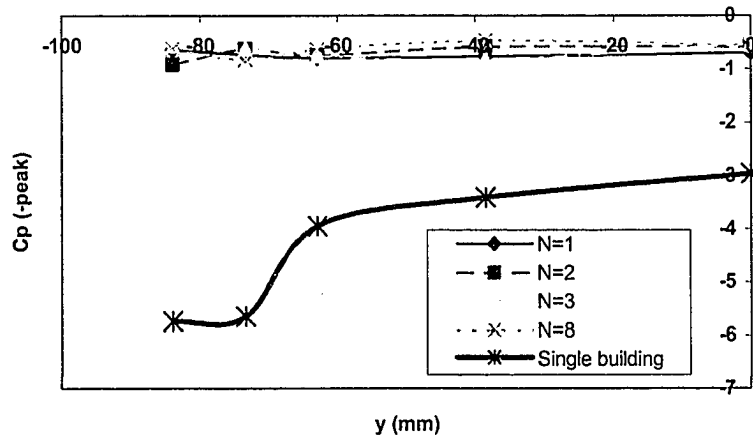


Figure 6.26 Pressure coefficients (-peak, mean, and RMS) on the front edge of roof for cases, $B/H=0.5$, with different N

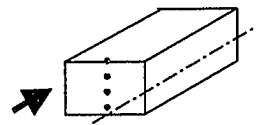
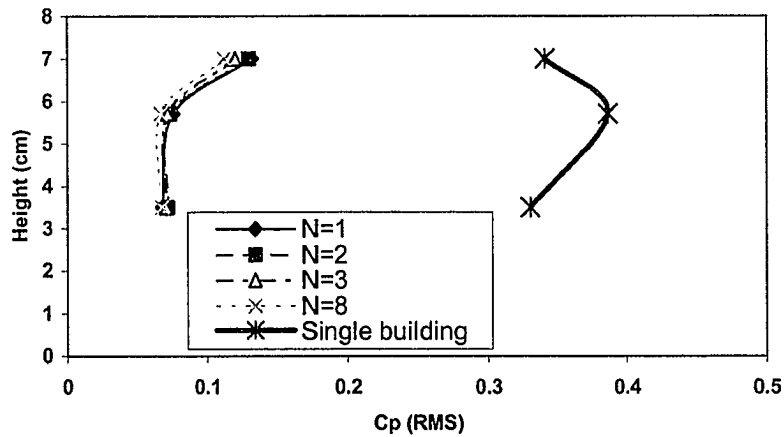
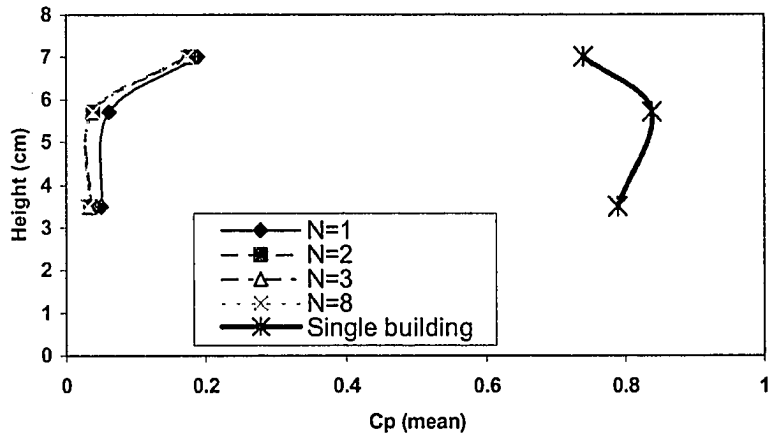
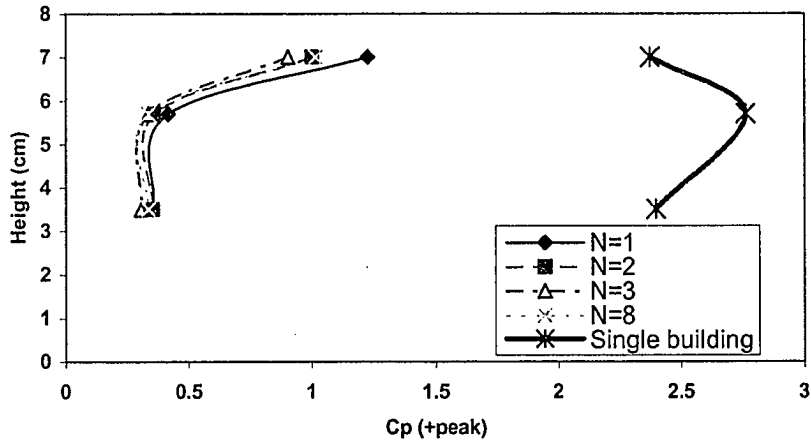


Figure 6.27 Pressure coefficients (-peak, mean, and RMS) on the centerline of downwind wall of street canyon for cases, $B/H=0.5$, with different N

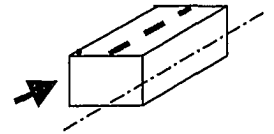
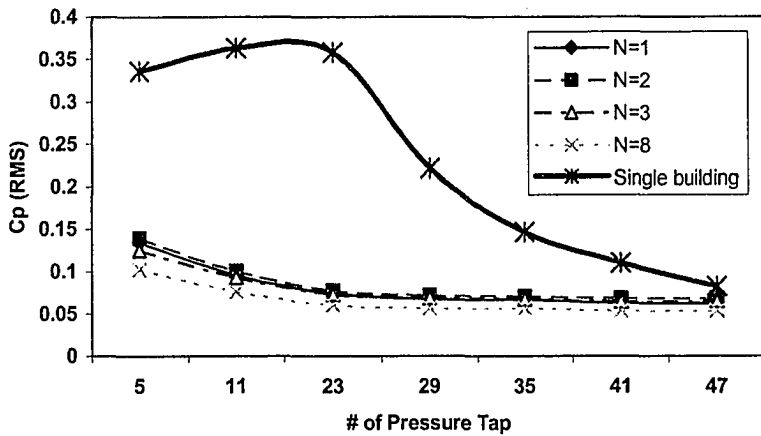
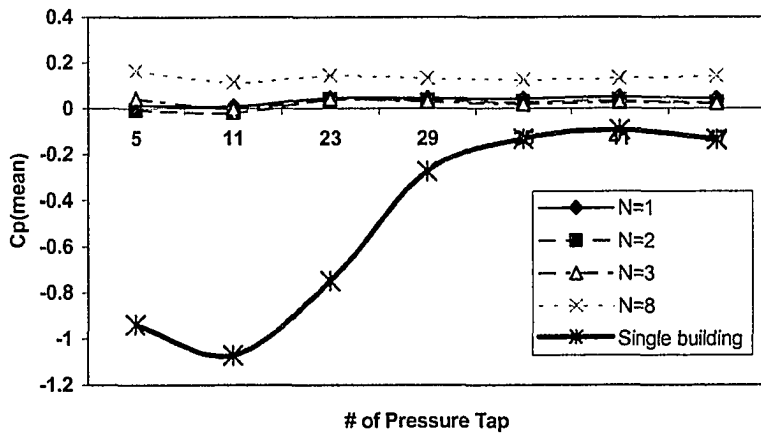
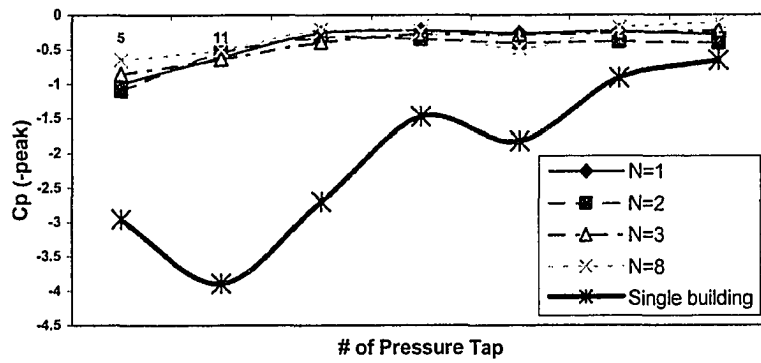


Figure 6.28 Pressure coefficients (-peak, mean, and RMS) on the centerline of roof for cases, $B/H=1$, with different N

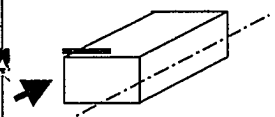
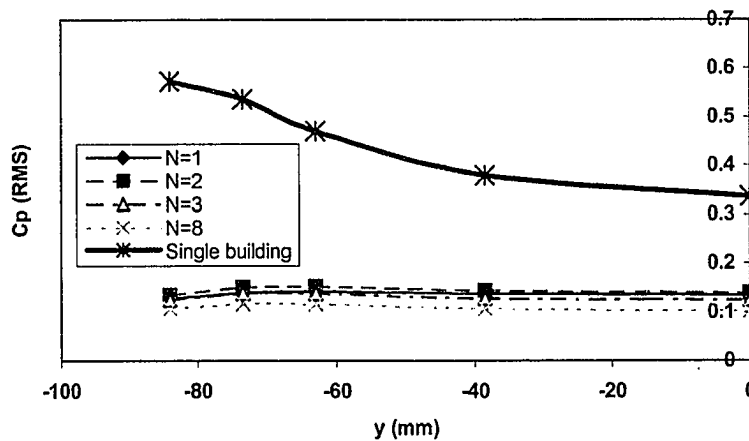
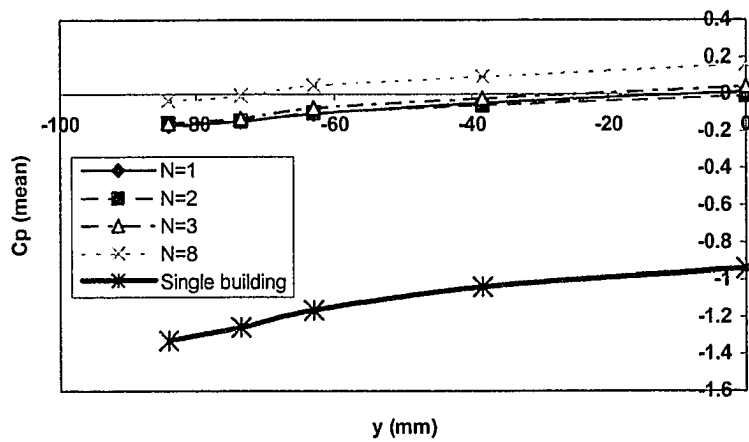
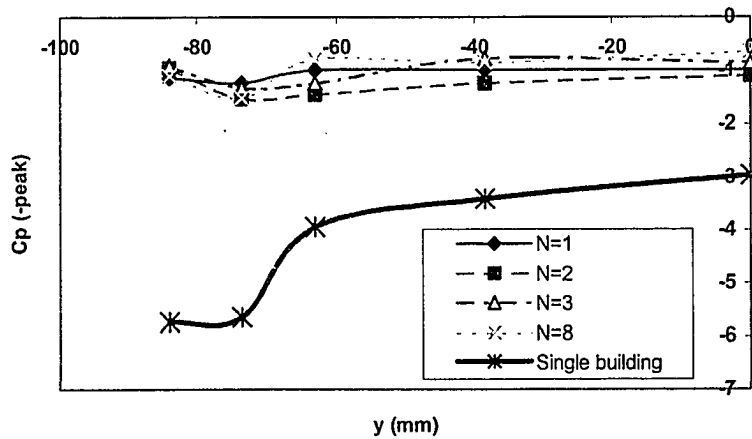


Figure 6.29 Pressure coefficients (-peak, mean, and RMS) on the front edge of roof for cases, $B/H=1$, with different N

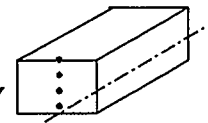
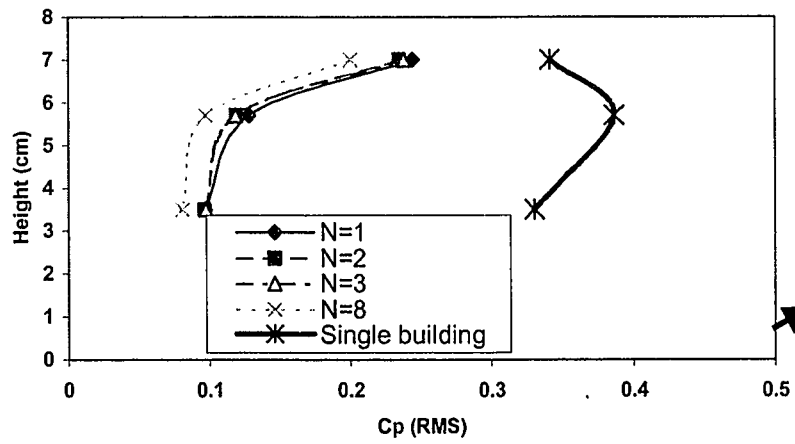
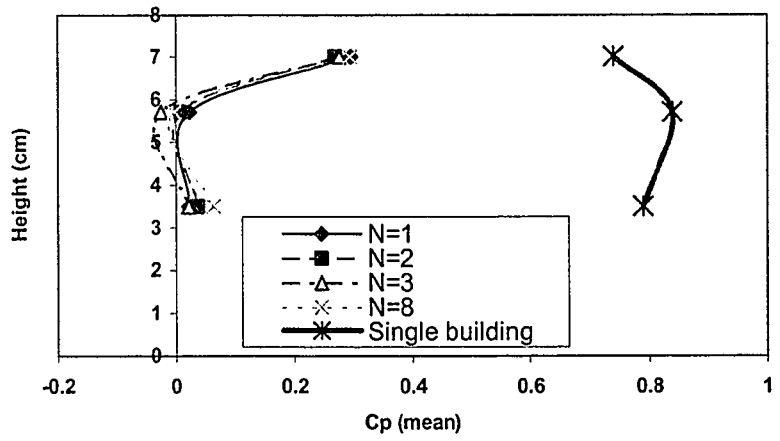
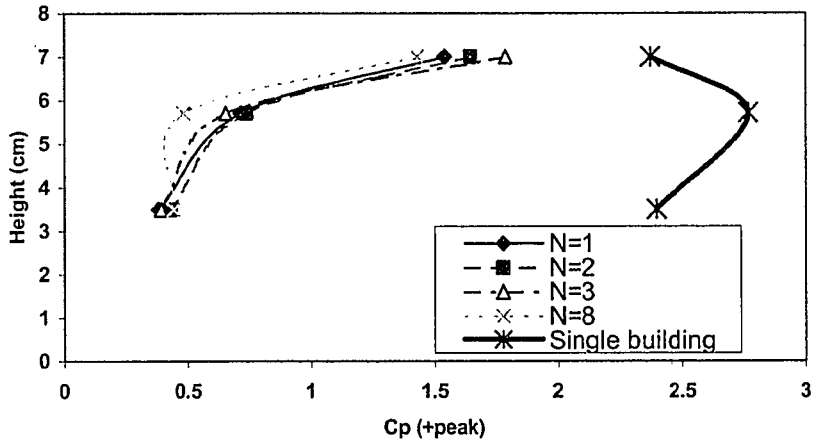


Figure 6.30 Pressure coefficients (-peak, mean, and RMS) on the centerline of downwind wall of street canyon for cases, $B/H=1$, with different N

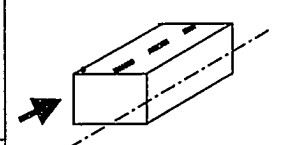
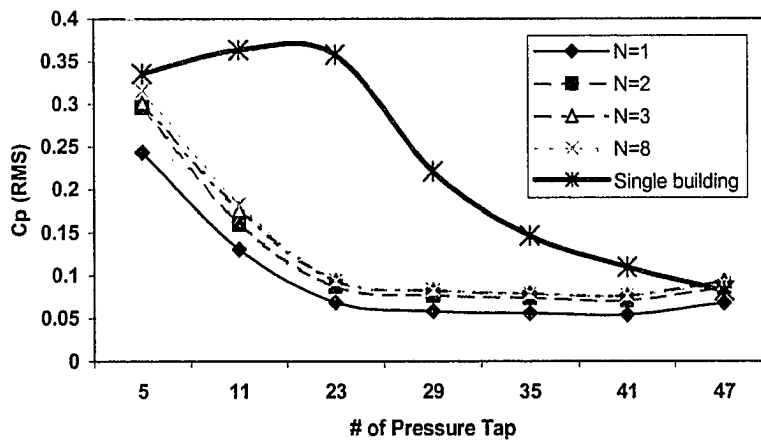
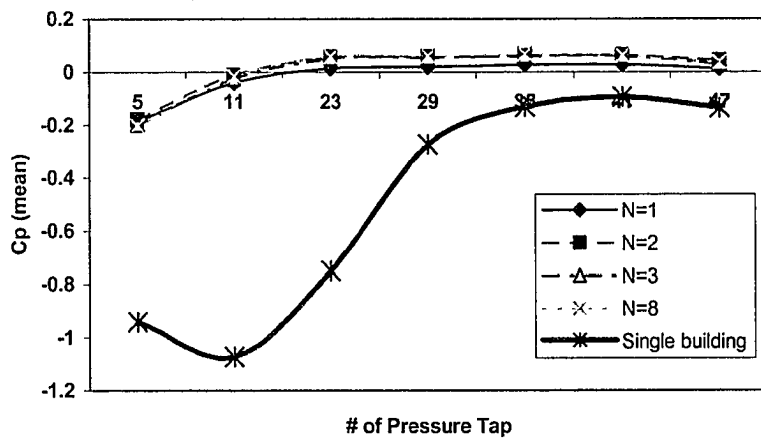
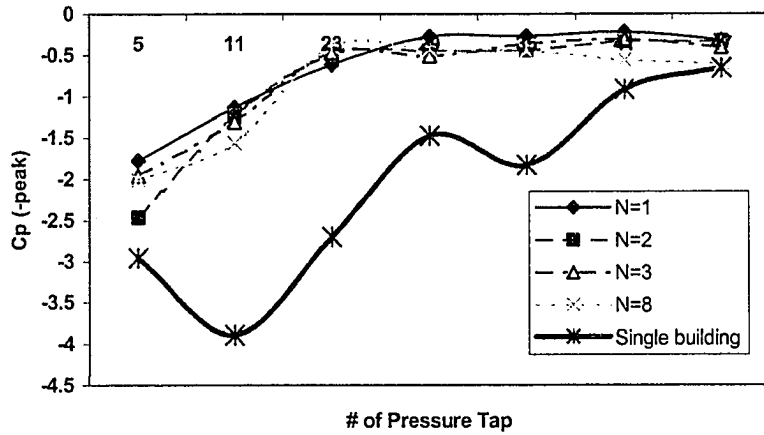


Figure 6.31 Pressure coefficients (-peak, mean, and RMS) on the centerline of roof for cases, $B/H=2$, with different N

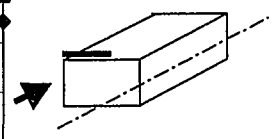
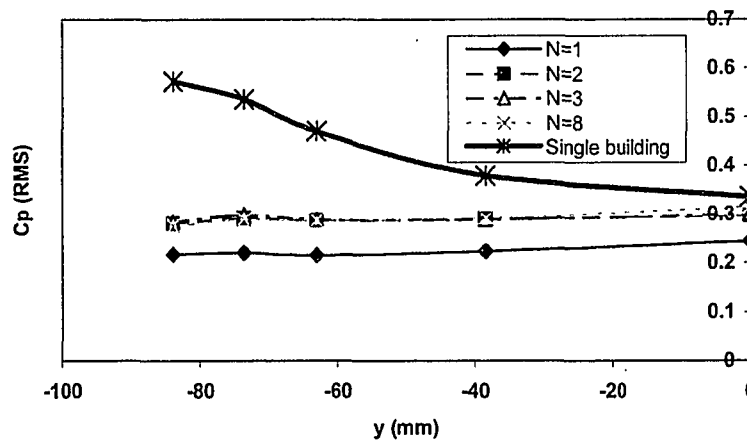
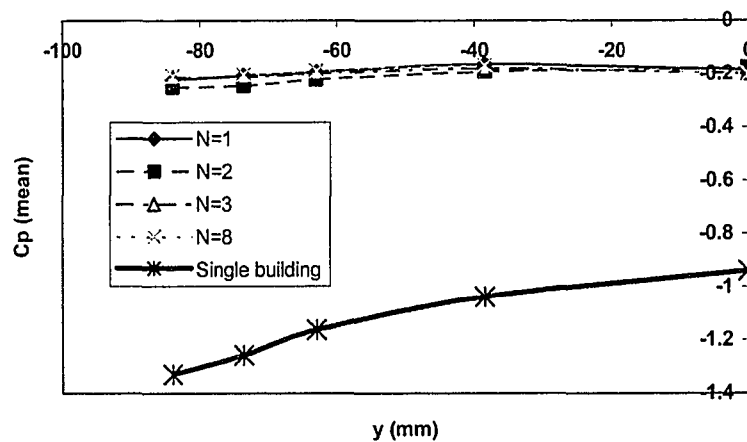
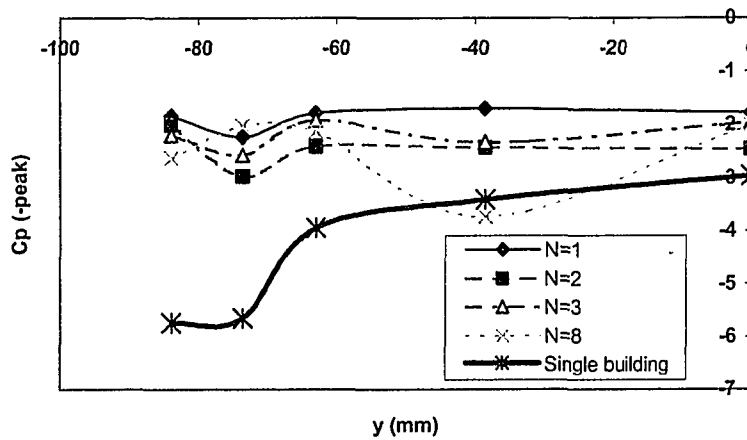


Figure 6.32 Pressure coefficients (-peak, mean, and RMS) on the front edge of roof for cases, $B/H=2$, with different N

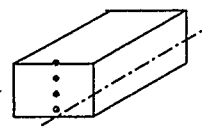
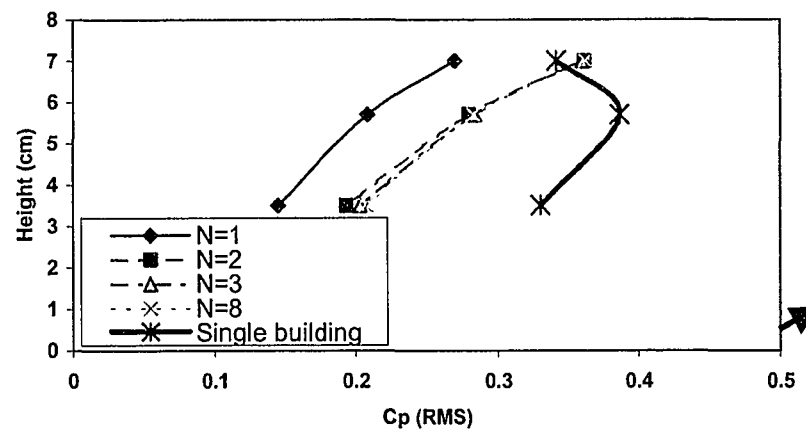
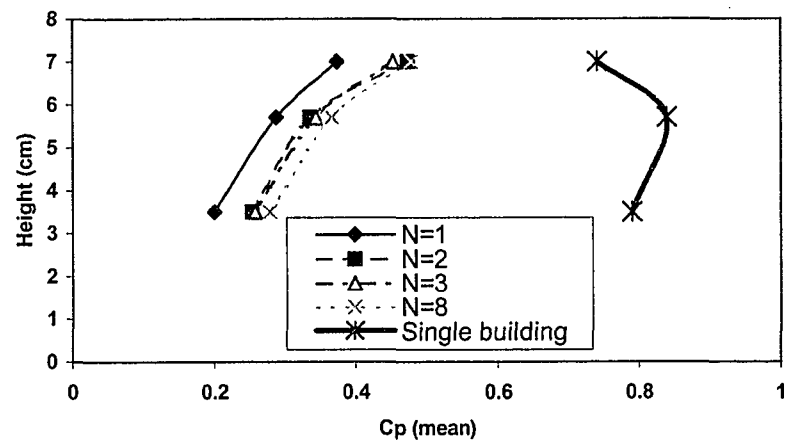
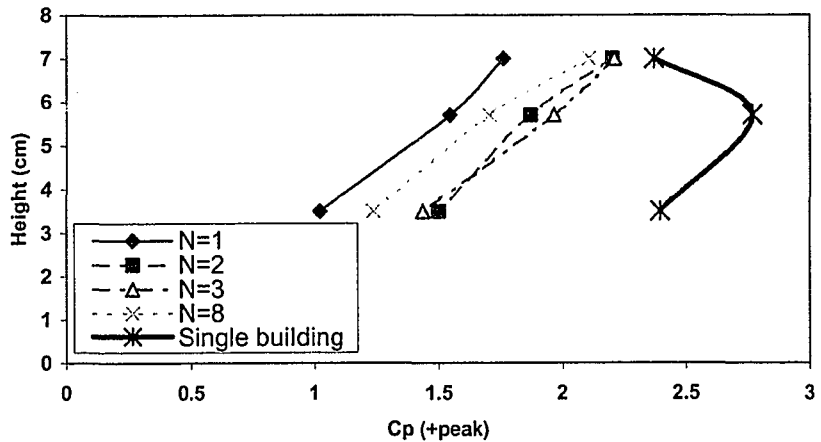


Figure 6.33 Pressure coefficients (-peak, mean, and RMS) on the centerline of downwind wall of street canyon for cases, $B/H=2$, with different N

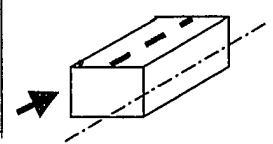
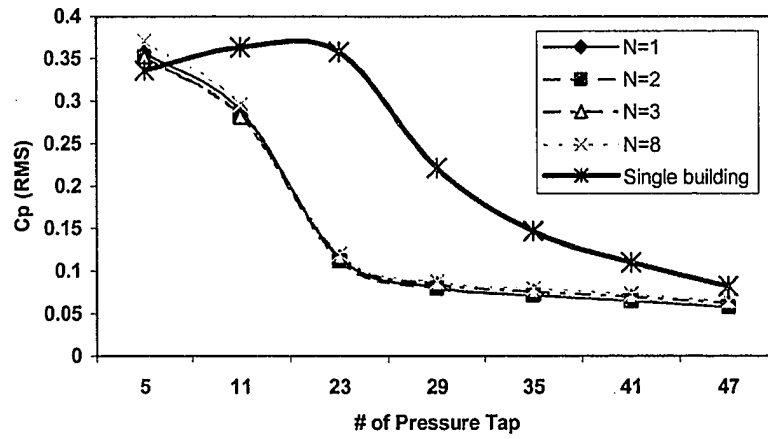
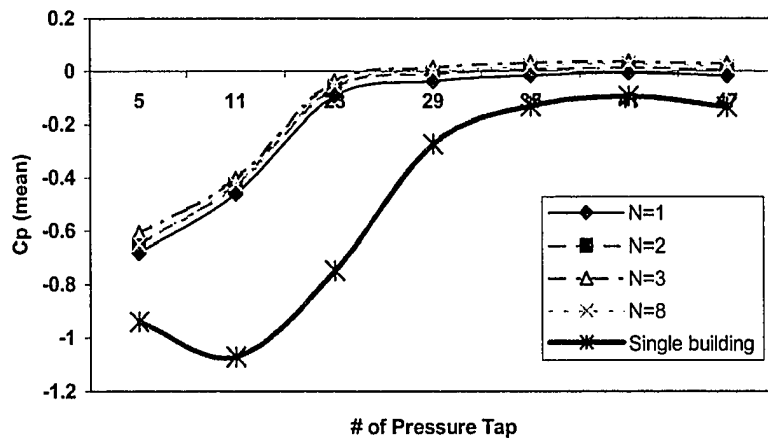
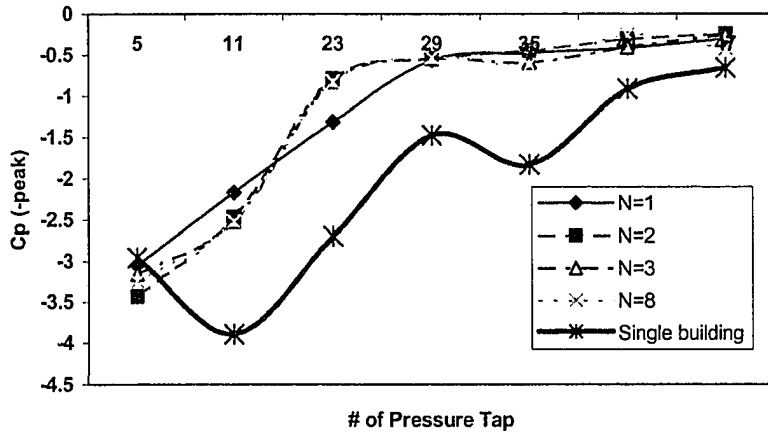


Figure 6.34 Pressure coefficients (-peak, mean, and RMS) on the centerline of roof for cases, $B/H=4$, with different N

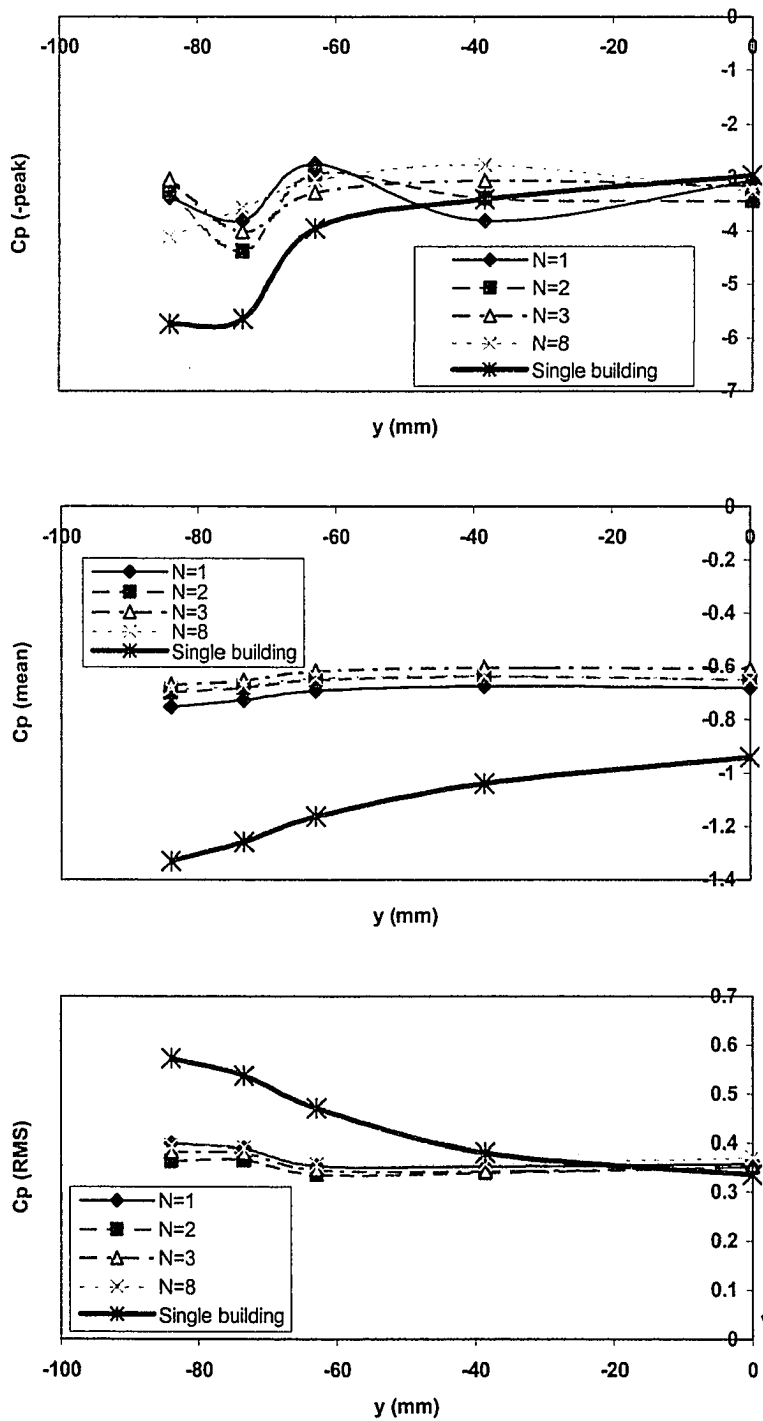


Figure 6.35 Pressure coefficients (-peak, mean, and RMS) on the front edge of roof for cases, $B/H=4$, with different N

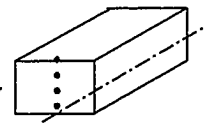
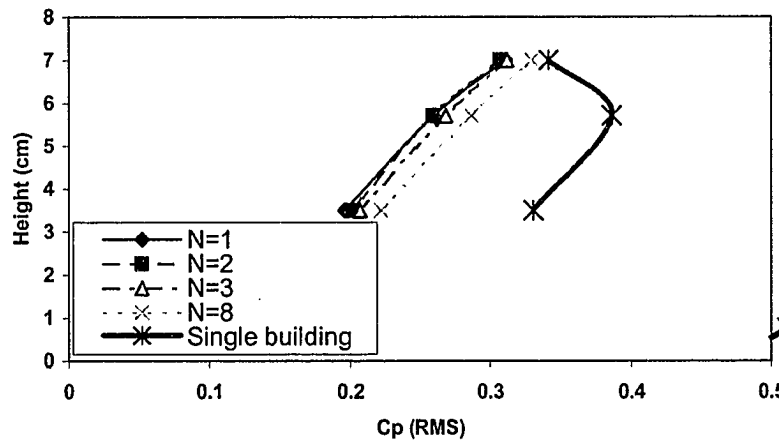
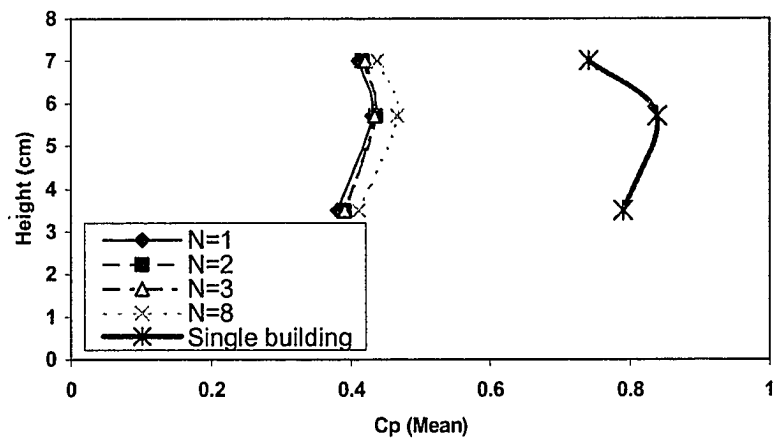
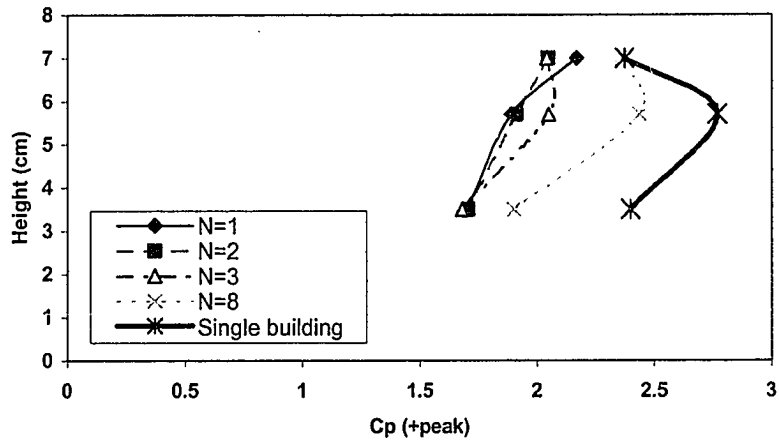


Figure 6.36 Pressure coefficients (-peak, mean, and RMS) on the centerline of downwind wall of street canyon for cases, $B/H=4$, with different N

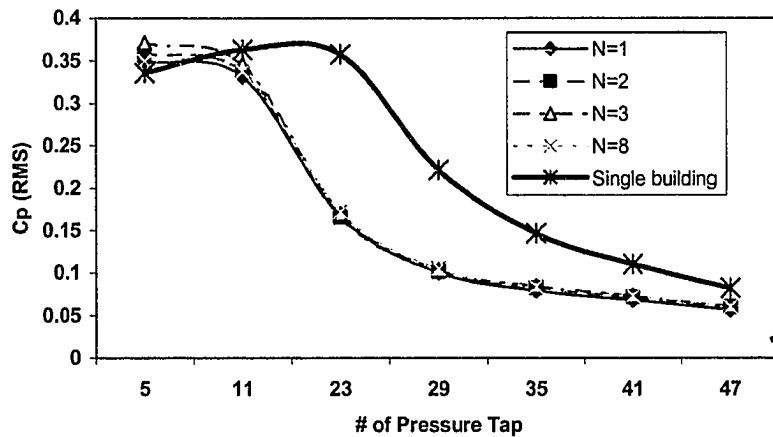
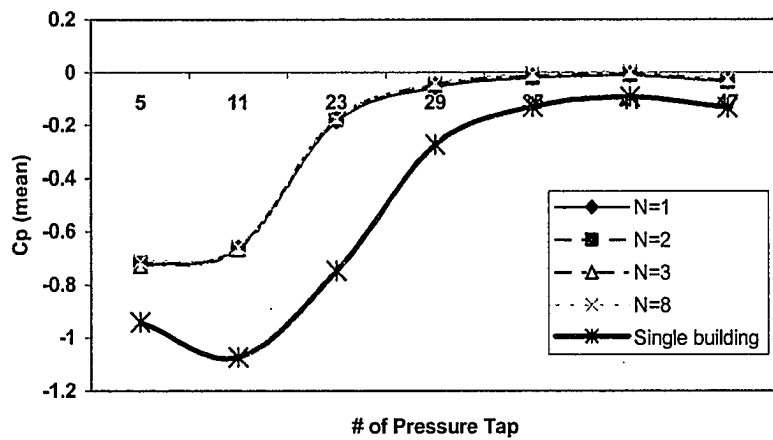
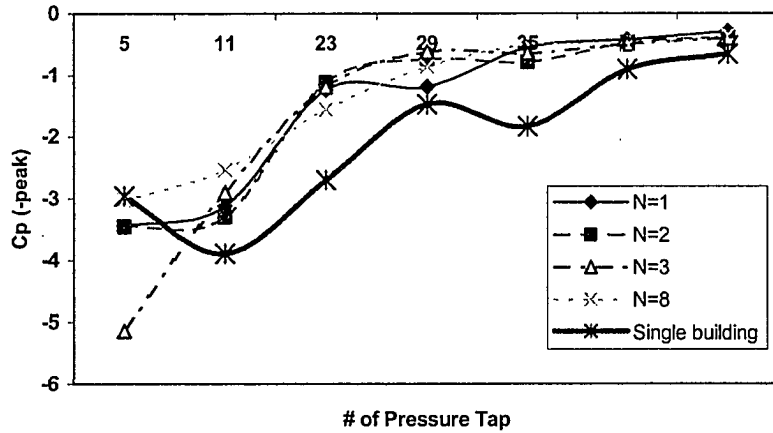


Figure 6.37 Pressure coefficients (-peak, mean, and RMS) on the centerline of roof for cases, $B/H=6$, with different N

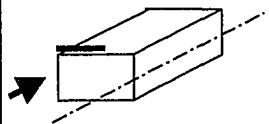
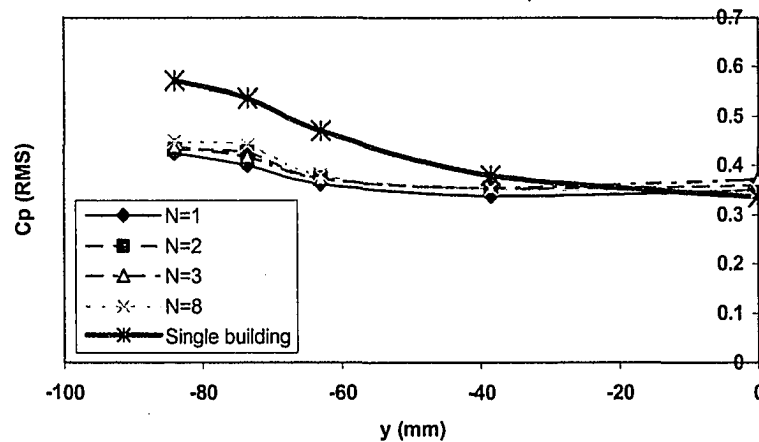
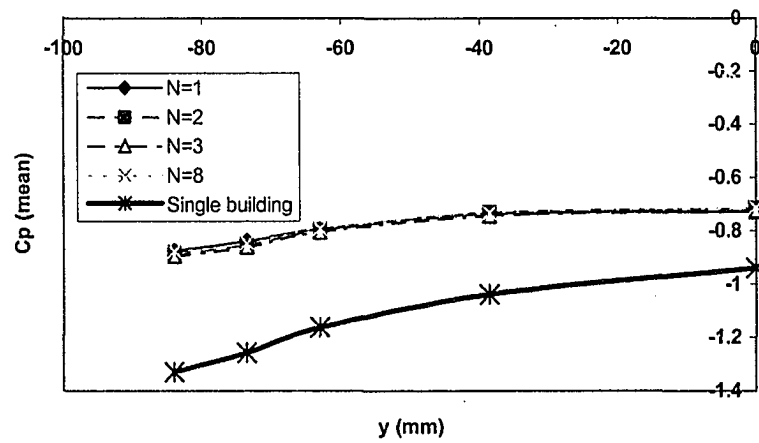
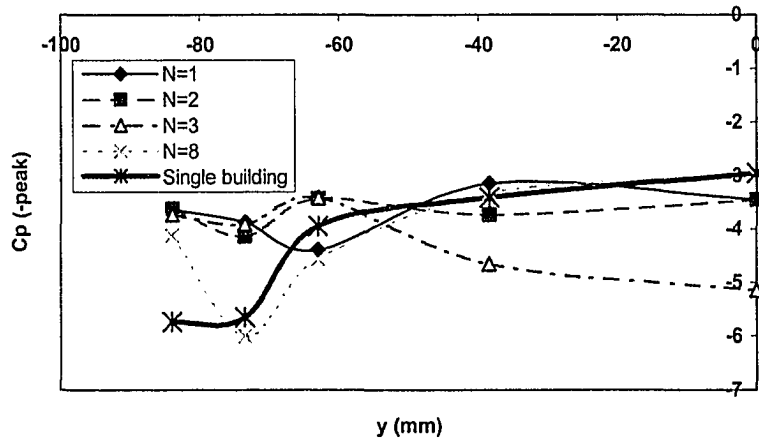


Figure 6.38 Pressure coefficients (-peak, mean, and RMS) on the front edge of roof for cases, $B/H=6$, with different N

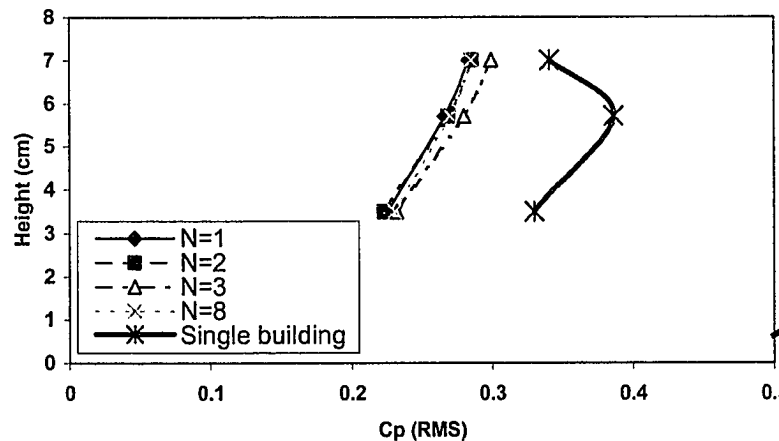
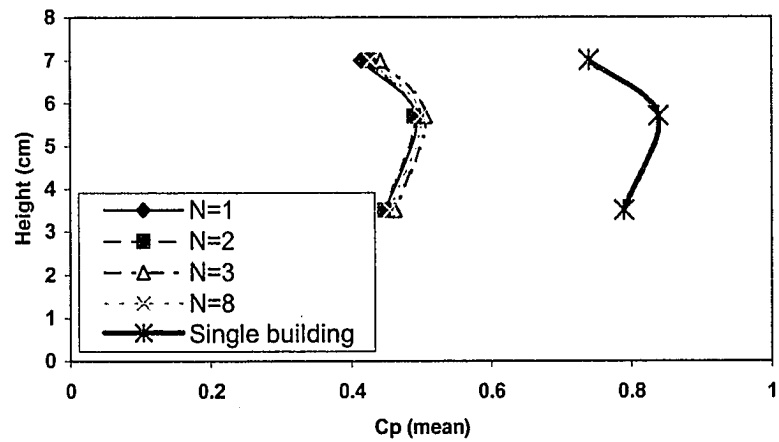
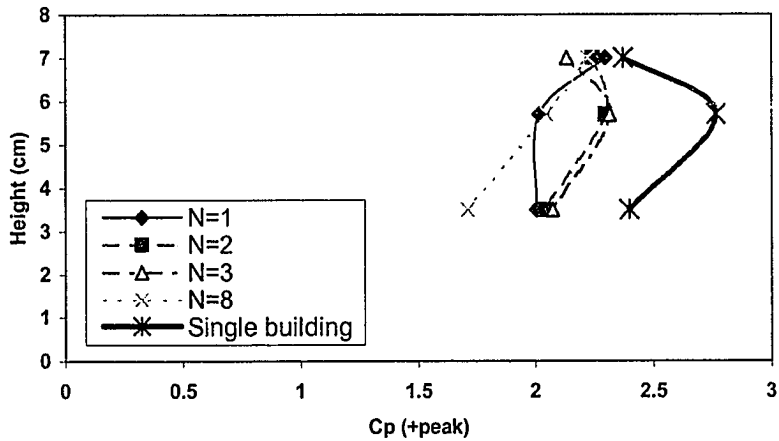


Figure 6.39 Pressure coefficients (-peak, mean, and RMS) on the centerline of downwind wall of street canyon for cases, $B/H=6$, with different N

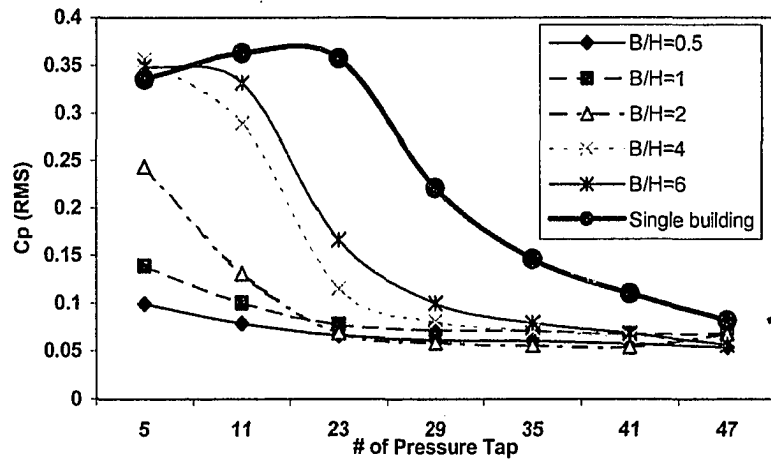
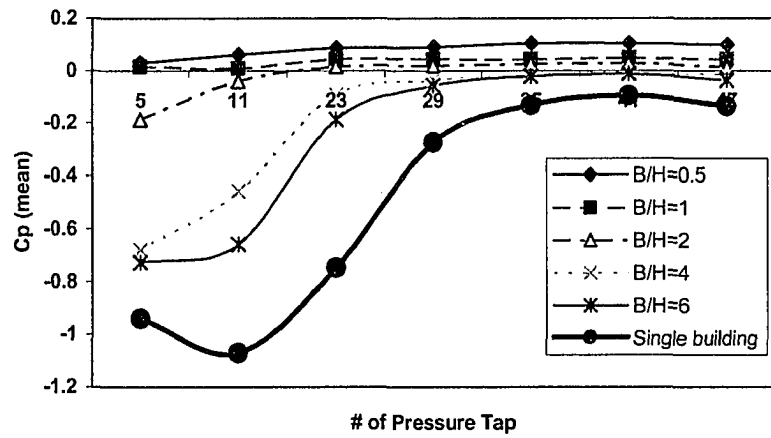
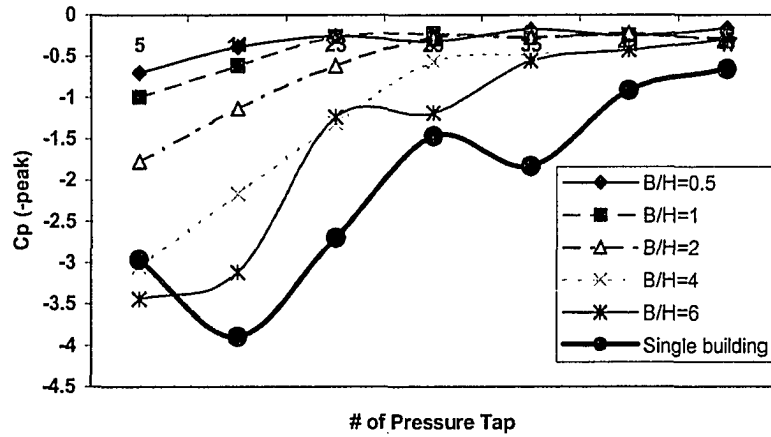


Figure 6.40 Pressure coefficients (-peak, mean, and RMS) on the centerline of roof for cases, $N=1$ with different values of B/H

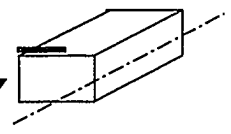
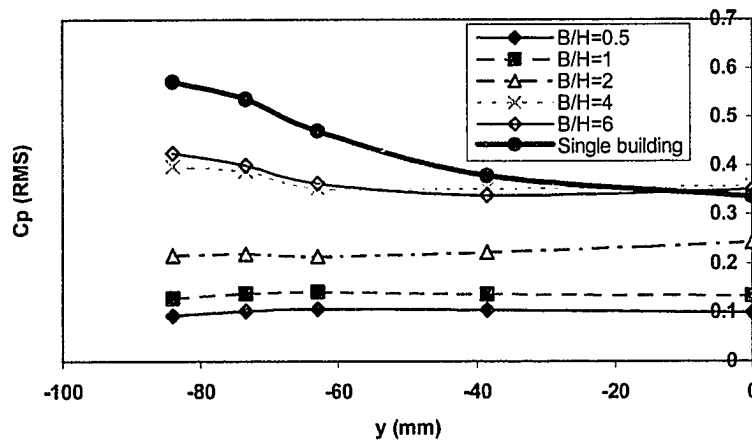
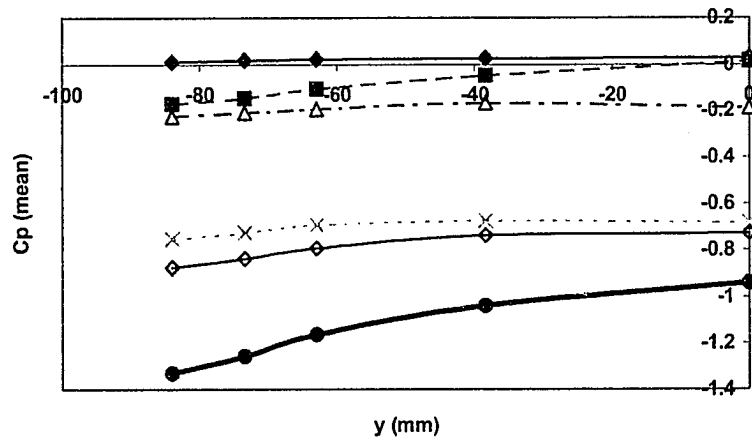
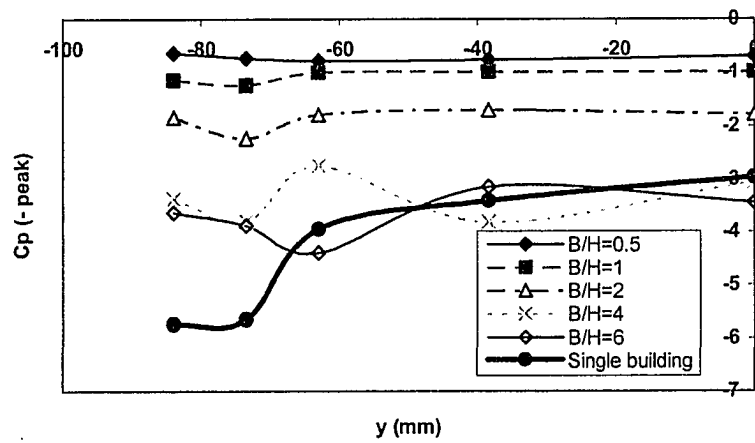


Figure 6.41 Pressure coefficients (-peak, mean, and RMS) on the front edge of roof for cases, $N=1$ with different values of B/H

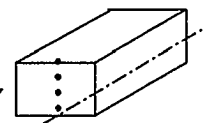
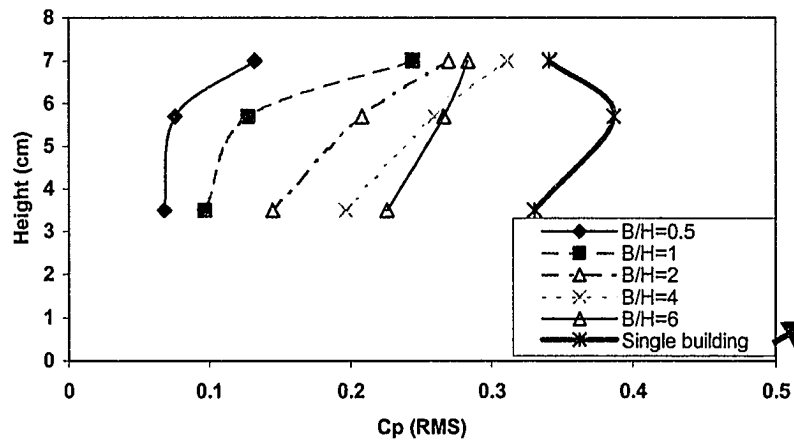
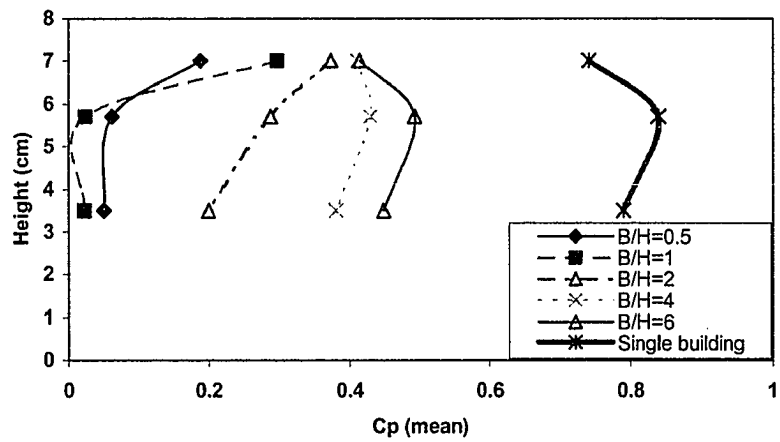
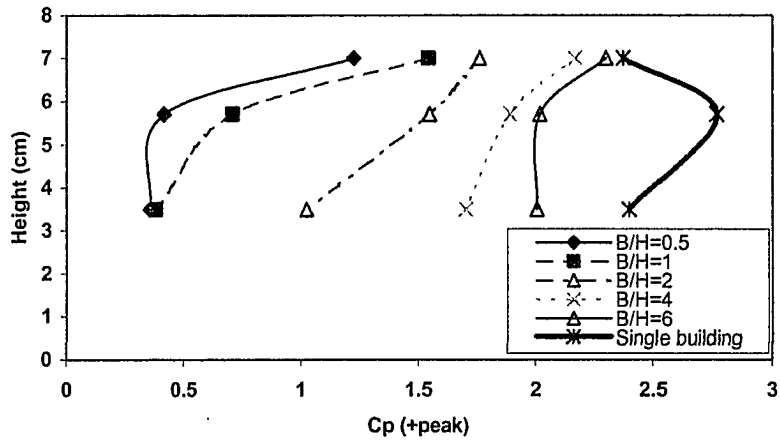


Figure 6.42 Pressure coefficients (-peak, mean, and RMS) on the centerline of downwind wall of street canyon for cases, $N=1$ with different B/H

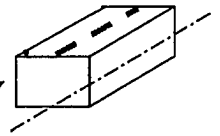
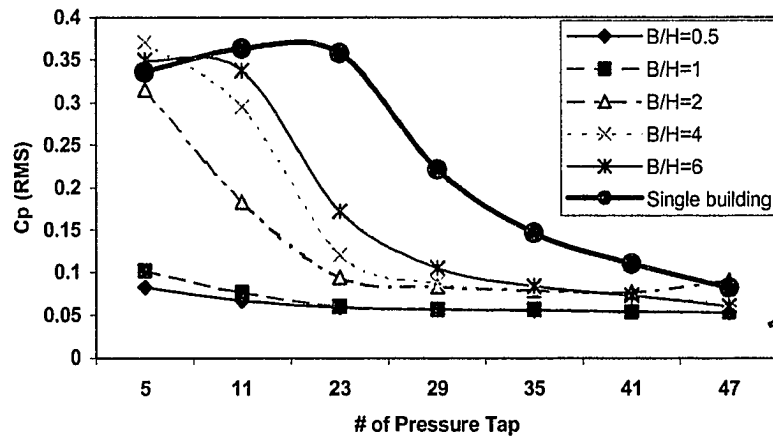
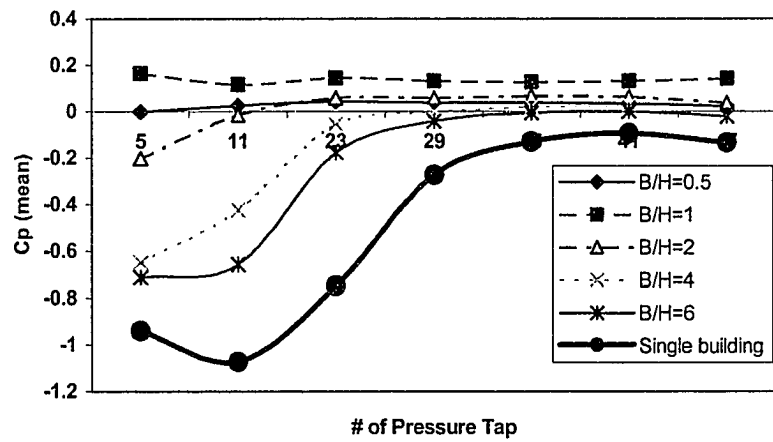
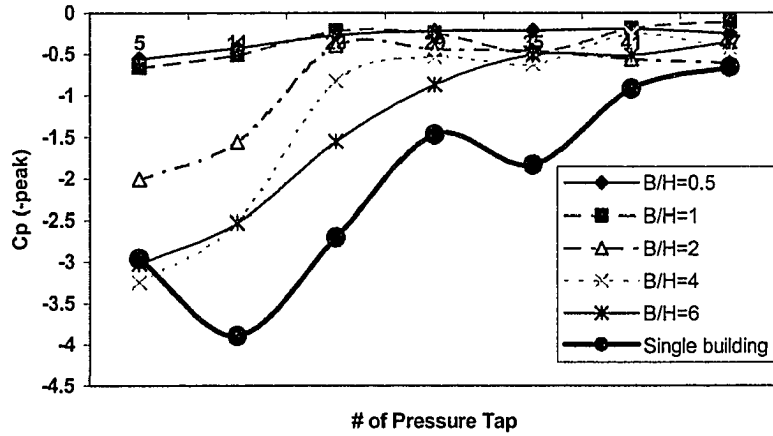


Figure 6.43 Pressure coefficients (-peak, mean, and RMS) on the centerline of roof for cases, $N=8$ with different B/H

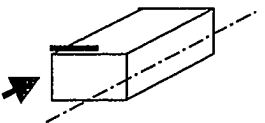
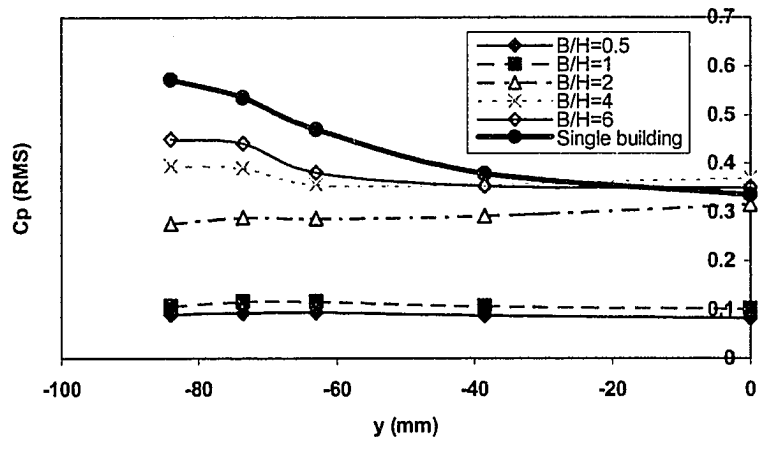
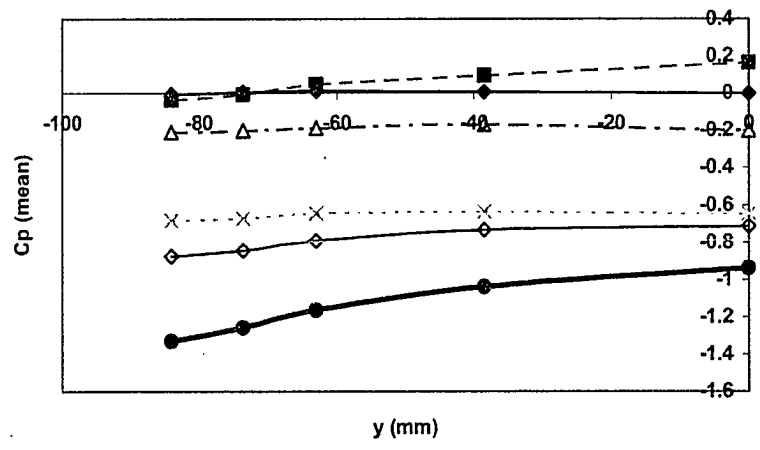
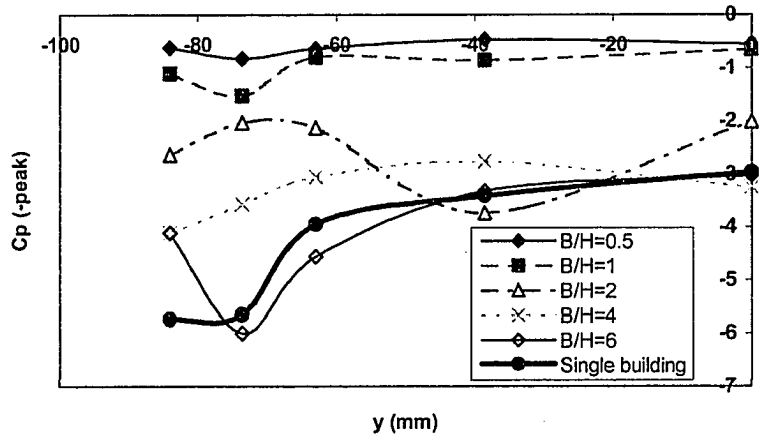


Figure 6.44 Pressure coefficients (-peak, mean, and RMS) on the front edge of roof for cases, $N=8$ with different B/H

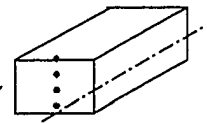
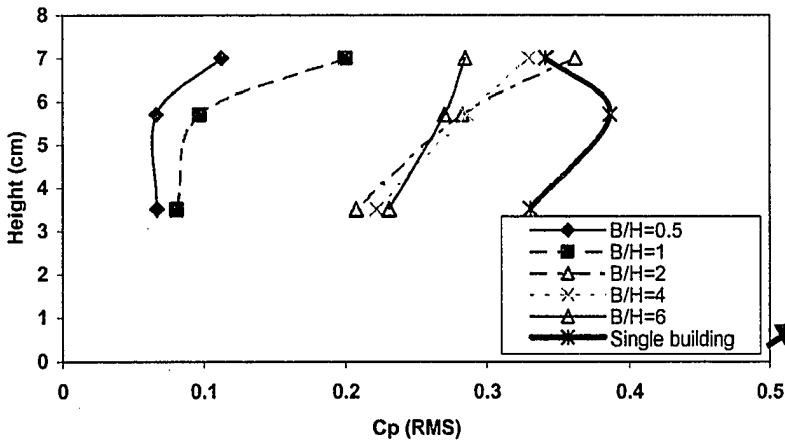
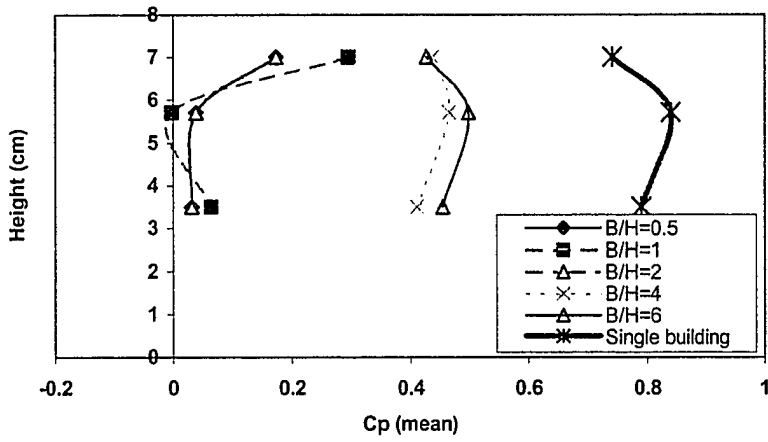
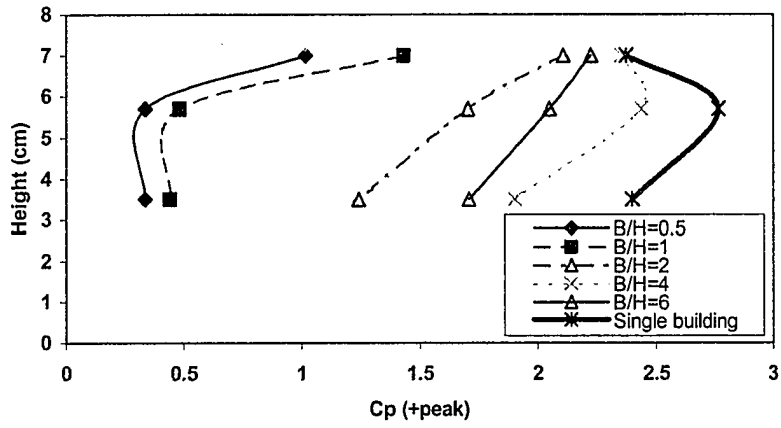


Figure 6.45 Pressure coefficients (-peak, mean, and RMS) on the centerline of downwind wall of street canyon for cases, $N=8$ with different B/H

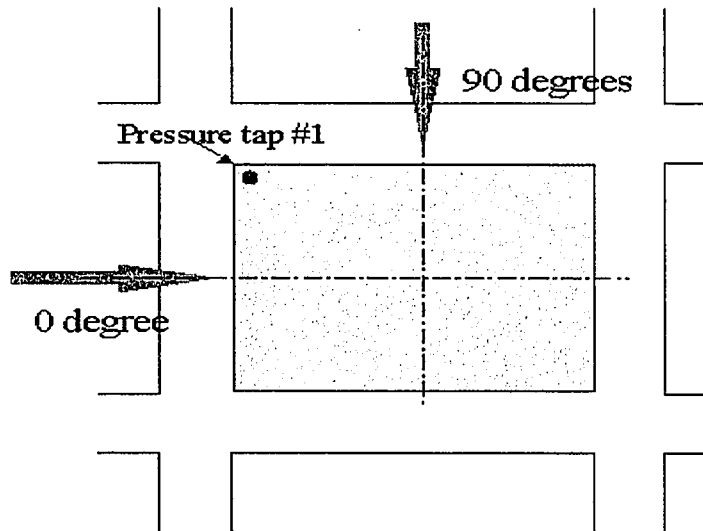


Figure 6.46 The schematic of pressure coefficient measurement in different approaching angles

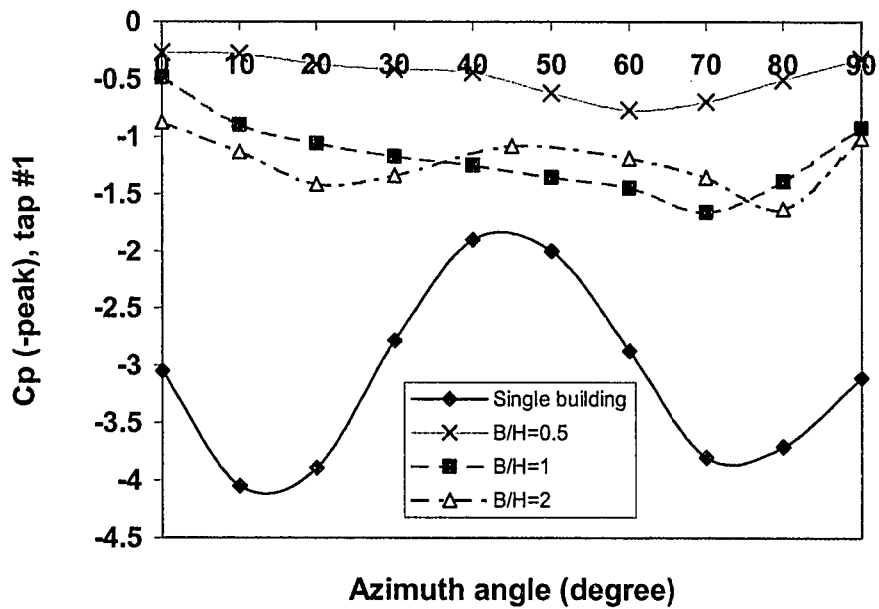


Figure 6.47 -Peak pressure coefficient measurement for a roof corner point for the wind azimuths ranging from 0 to 90 degrees

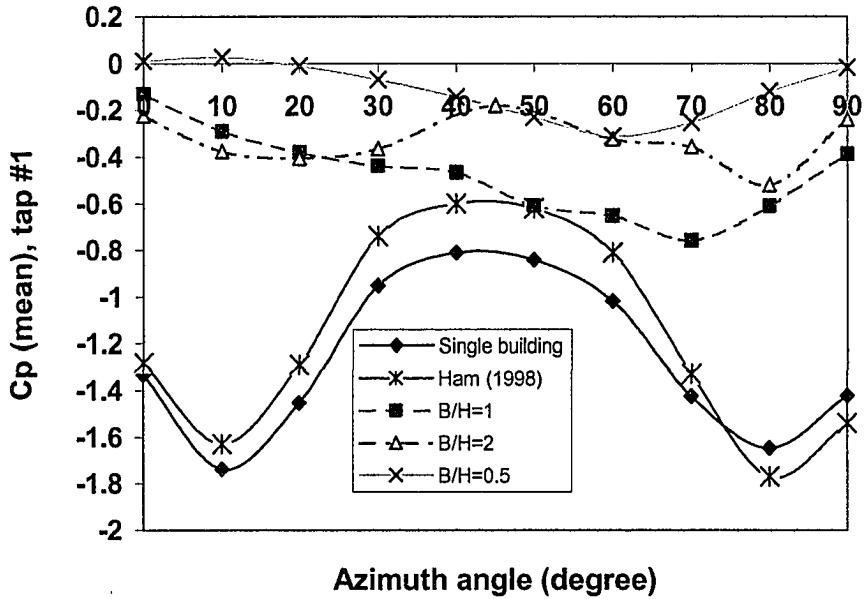


Figure 6.48 Mean pressure coefficient measurement for a roof corner point for the wind azimuths ranging from 0 to 90 degrees

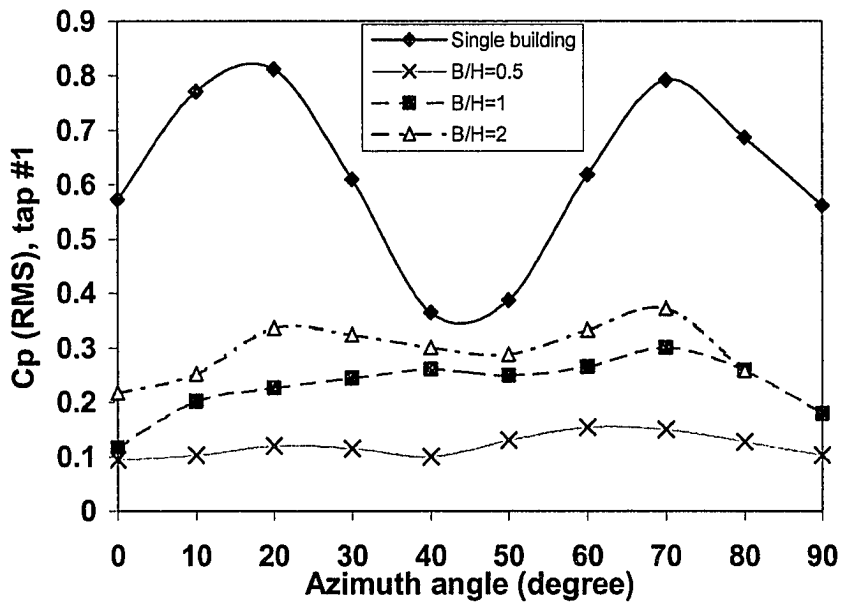


Figure 6.49 RMS pressure coefficient measurement for a roof corner point for the wind azimuths ranging from 0 to 90 degrees

6.2.2 Comparison of Pressure Coefficients of Wind Tunnel Results and Numerical Simulations

Fluent Simulation

The pressure coefficients calculated by Fluent using κ - ϵ are shown in this section. Since Fluent is a steady-state computer program, only the mean C_p can be determined. Figure 6.50a compares mean wind pressure coefficients on the centerline of the roof of the master building with relevant results from numerical simulations carried out by using the Fluent κ - ϵ model. The graph shows both numerical data and experimental data of cases for different values of B/H for comparison. The colored dots indicate the experimental data and the different style lines indicate the numerical data. The overall results appear similar to that of the experimental data with the exception of the front edge of the centerline region at flow separation in which the numerical results indicate higher suction. Figure 6.50b shows the comparisons of the mean C_p 's along the centerline of the downwind wall of the street canyon. The numerical results are similar to that of the experimental results, except that CFD predicts higher suction on the upper part of the centerline of downwind wall of the street canyon.

There is no root mean square (RMS) pressure coefficient provided from the output of Fluent, since Fluent is a steady-state Reynolds averaged model computer program. However, RMS pressure coefficients can be estimated from calculated mean pressure coefficients, mean velocities and RMS velocities using the equation 6.1 and 6.2 proposed by Paterson (1989).

$$C_p' = 2[k_1/3 + 0.816|\bar{C}_p|\bar{U}_0\sqrt{k_0}]/\bar{V}^2 \quad 6.1$$

$$C_p'^2 = 8k_0^2/\bar{U}_0^4 + 8\bar{C}_p^2\bar{U}_0^2k_0/(\bar{U}_0^2 + 2k_0 - 2k_1)^2 \quad 6.2$$

Where, C_p' is the RMS pressure coefficient,
 \bar{C}_p is the mean pressure coefficient,
 \bar{V} is a mean reference velocity,
 \bar{U} is the mean velocity, and
 k is the turbulent kinetic energy.

Subscripts 0 and 1 represent upwind and local values at similar measurement heights to the pressure part respectively. Figure 6.51a shows RMS pressure coefficients plotted against mean pressure coefficients for roof pressure tap from wind tunnel results as predicted results by Equations 6.1 and 6.2. Since the predictions of RMS pressure by both equations at the near zero mean pressure coefficients are poor, the isolated roughness flow case (B/H=6) with highest magnitude of the mean pressure coefficient are chosen here. There is a near relationship between $C_p(\text{RMS})$ and $C_p(\text{mean})$ in figure 6.51 for each set of data. The slope of the line of best fit is about -0.4 for wind tunnel results, -0.21 for equation 6.1, and -0.43 for equation 6.2, respectively.

Two numerical models are presented to compare with wind tunnel results from flow over the urban street area (isolated roughness flow case). Both equations correctly

predict an increase in RMS pressure coefficients with an increase in the magnitude of the mean pressure coefficient. The RMS pressure coefficients calculated from equation 6.2 are in much better agreement with the wind tunnel than those from equation 6.1. The comparison of the RMS C_p on the centerline of the roof between experiments and predictions by using Paterson-Selvam are shown in Figure 6.51b. Figure 6.52a and 6.52b show the comparisons of distributions of mean C_p on the roof for case $N=1$, $B/H=1$ between measured and calculated (Fluent) at wind direction 30 and 60 degrees. Both of the graphs show good results with different angles of the approaching winds. The measured values of mean C_p matched the calculated values.

FDS Simulation

FDS uses a time-dependent flow phenomena large eddy simulation (LES) algorithm to simulate field flows. LES can compute fluctuating pressures on buildings due to turbulence. Both mean and RMS C_p 's generated from FDS will be compared with the experimental data.

After running the cases of $B/H=1$, $N=1$ with three different ground boundary conditions, no-slip, half-slip and free-slip, with the grid resolution of canyon height of 12 cells, the mean C_p 's collected from the free-slip and half-slip conditions are found to be close to the experimental data. However, the mean C_p of no-slip condition is found to be significantly different from experimental data. Figures 6.53a, 6.53b, 6.54a and 6.54b show the comparisons of mean and RMS C_p 's with different grid resolutions for free-slip boundary condition cases. For mean C_p , the cases show that as the grid resolutions

become larger, the mean C_p collected from FDS becomes closer to the lab data. However, for RMS C_p , predictions of finer grid resolution are not necessarily closer to the lab results. For example, in Figures 6.52b and 6.53b, the results for grid sizes of 9 cells appear to be closer to the lab data. In general, the numerical results of RMS C_p under predict the experimental results. This is most likely due to under prediction of free stream turbulence due to inappropriate inlet turbulence conditions.

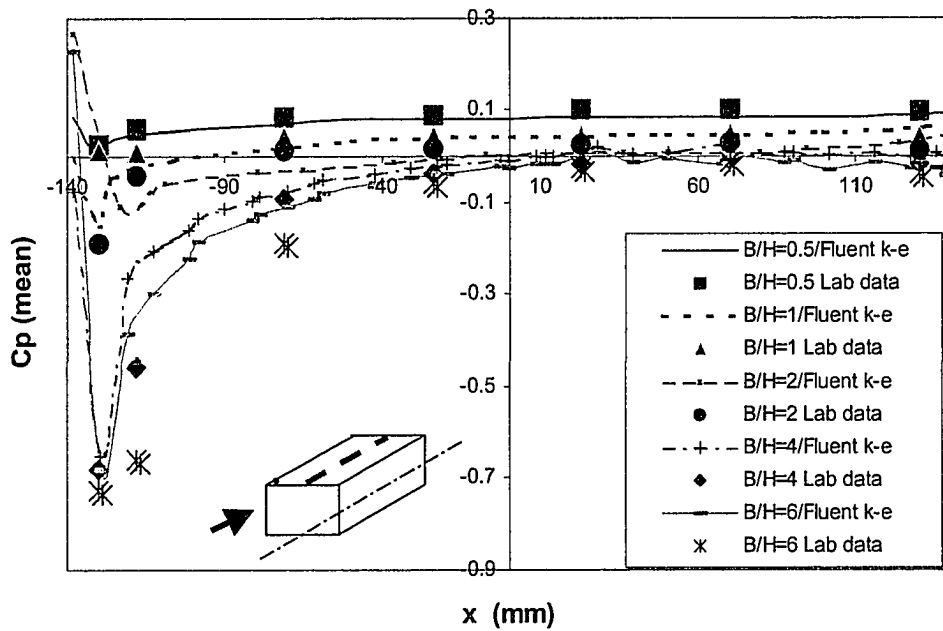


Figure 6.50a Comparisons of mean pressure coefficients on the centerline of the roof for case $N=1$: experiments and numerical simulation using Fluent κ - ϵ model

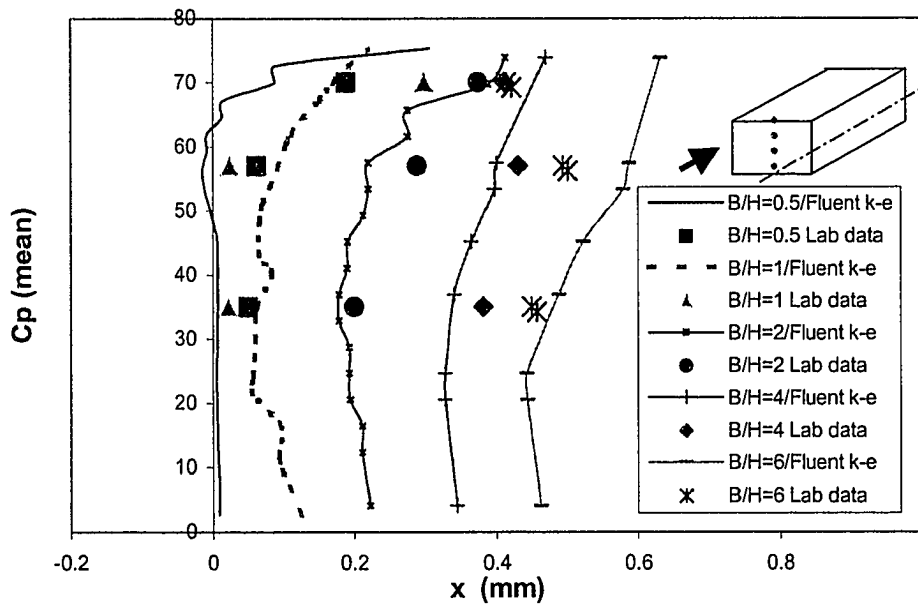


Figure 6.50b Comparisons of mean C_p on the centerline of the downwind wall of street canyon for case $N=1$: experiments and numerical simulation using Fluent κ - ϵ model

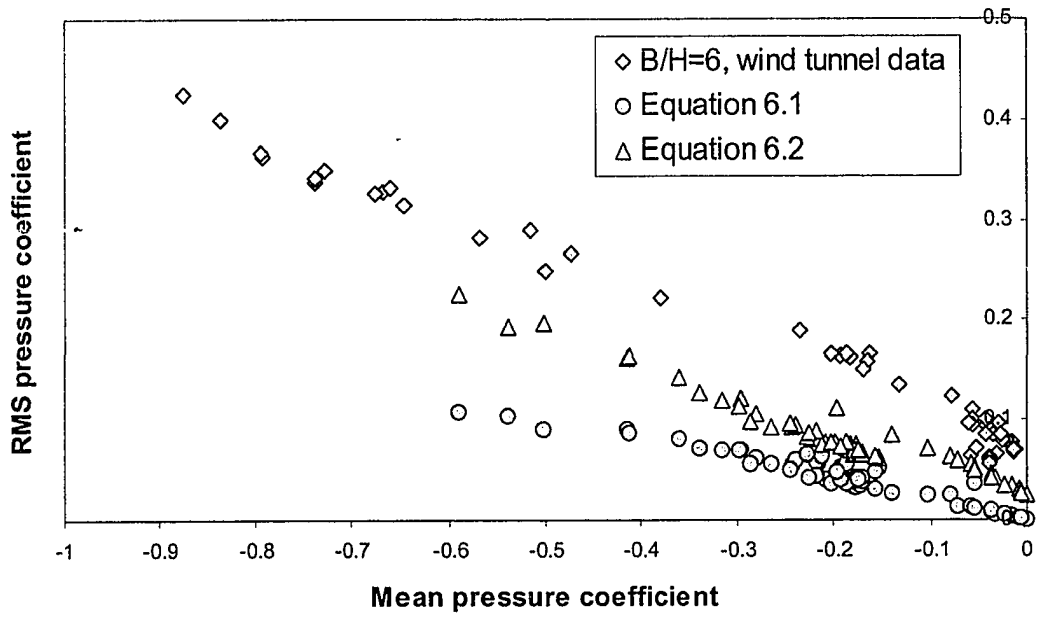


Figure 6.51a RMS vs. mean pressure coefficients form roof wind tunnel data, ($B/H=6$, $N=1$)

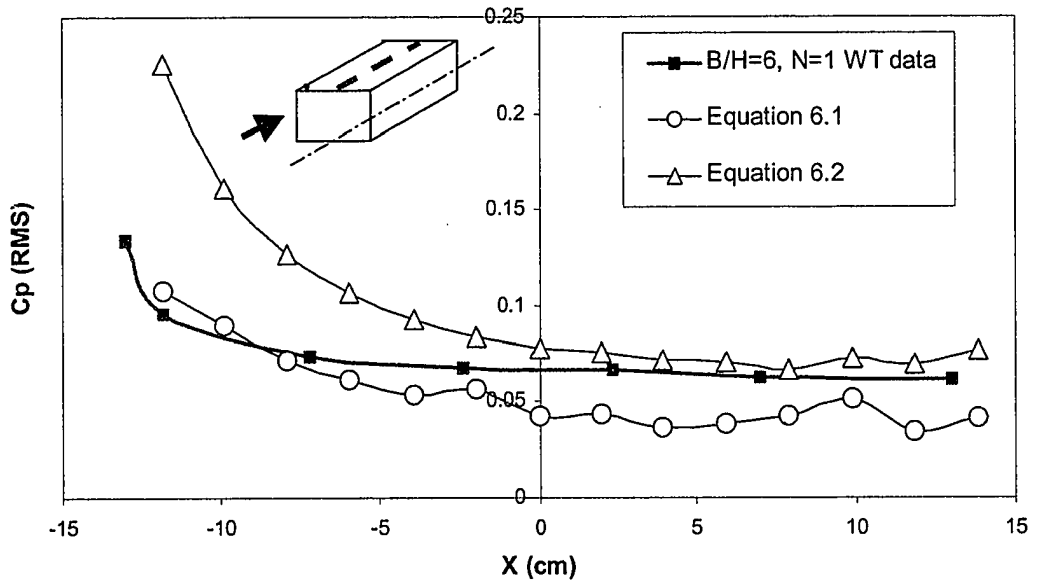


Figure 6.51b Comparison of RMS Cp for case $B/H=6$, $N=1$: experiments and predictions by Paterson –Selvam formulas

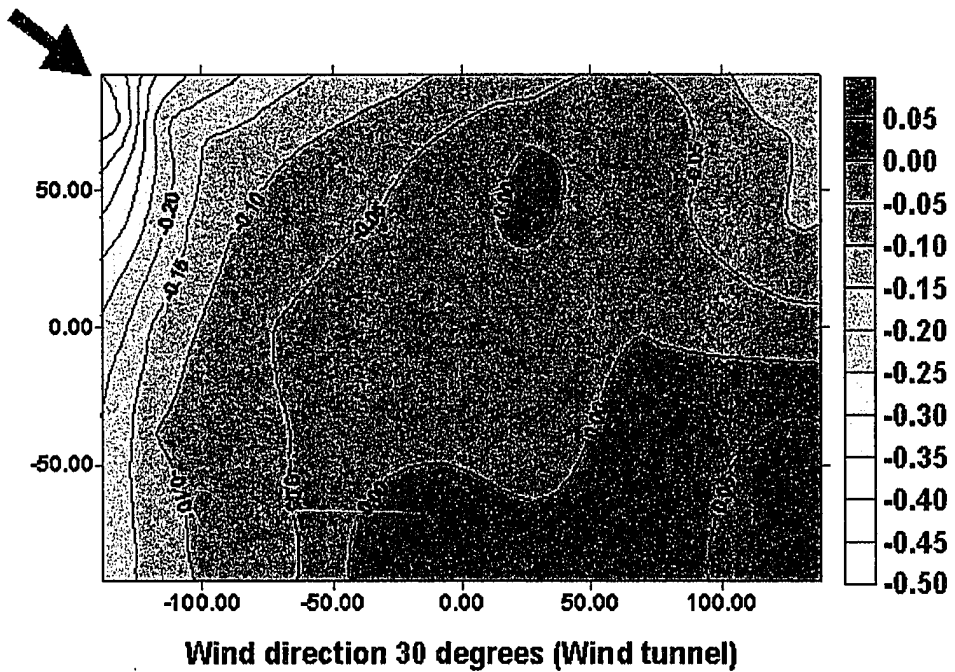
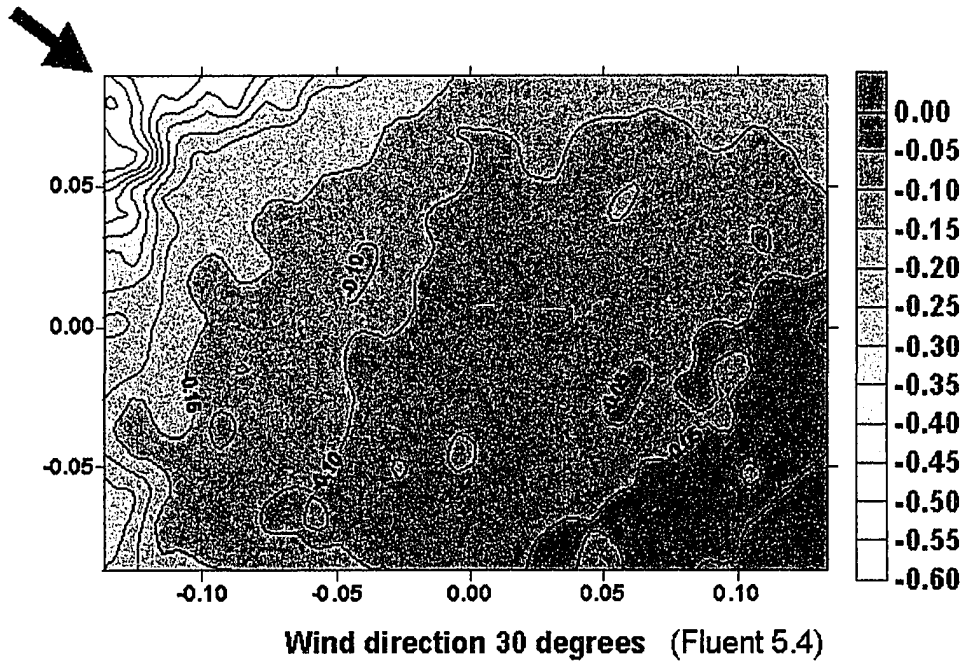


Figure 6.52a Comparison of distributions of mean C_p for case $N=1$, $B/H=1$ between measured and calculated (Fluent) at wind direction 30 degrees

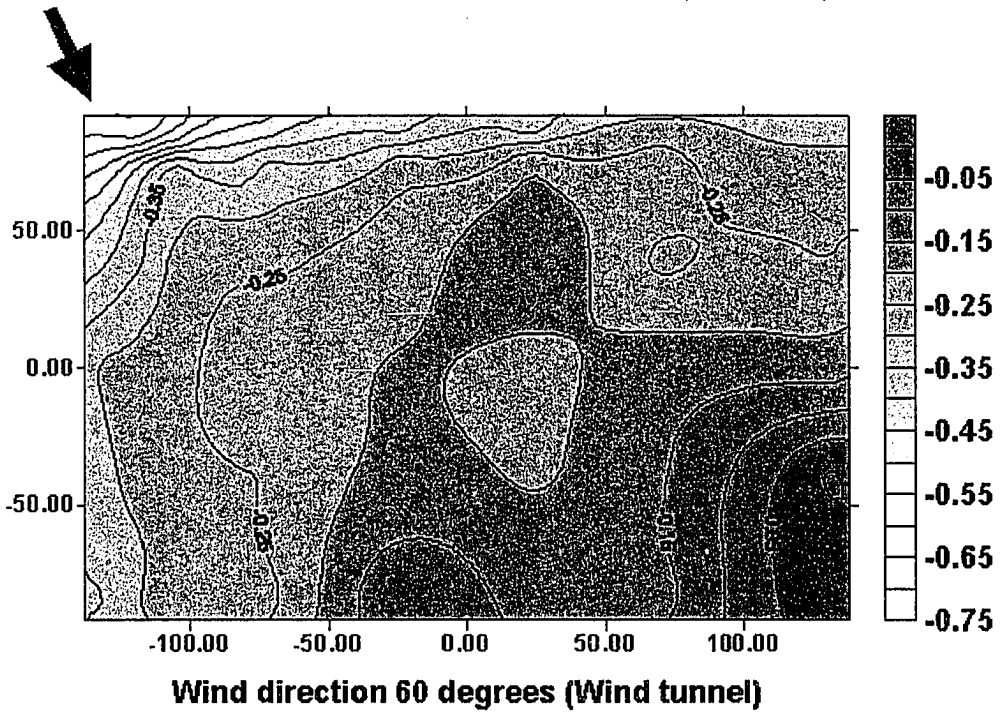
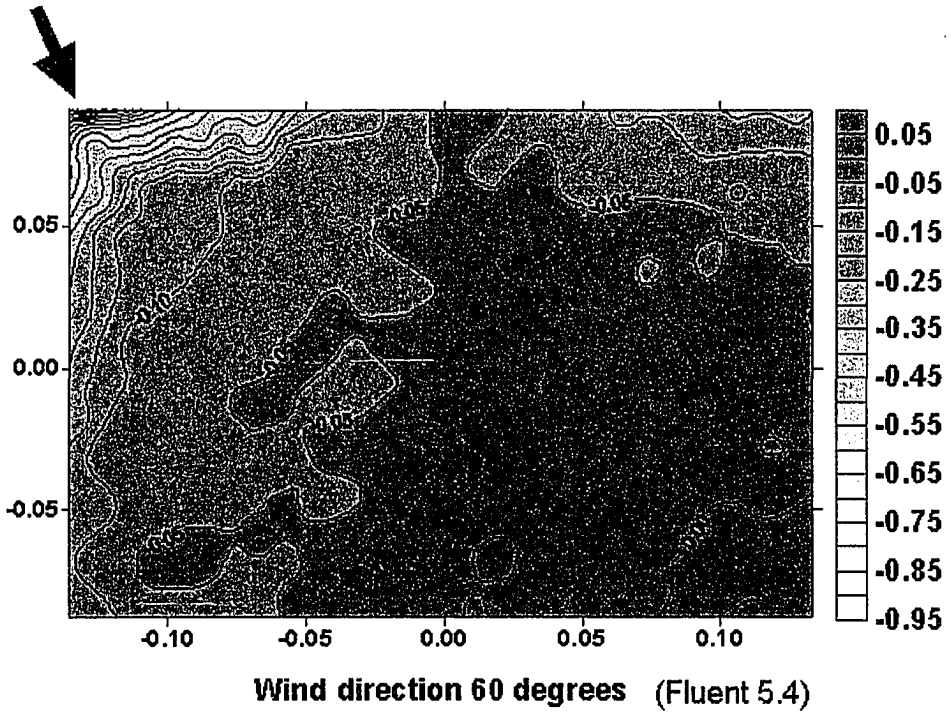


Figure 6.52b Comparison of distributions of mean C_p for case $N=1$, $B/H=1$ between measured and calculated (Fluent) at wind direction 60 degrees

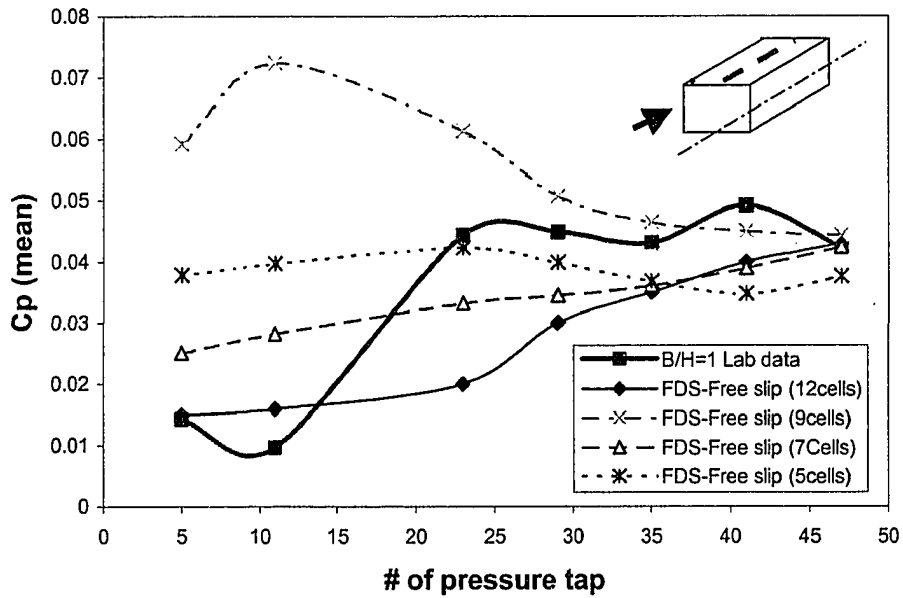


Figure 6.53a Comparisons of mean pressure coefficients on the centerline of the roof for case N=1: experiments and numerical simulation using FDS LES model

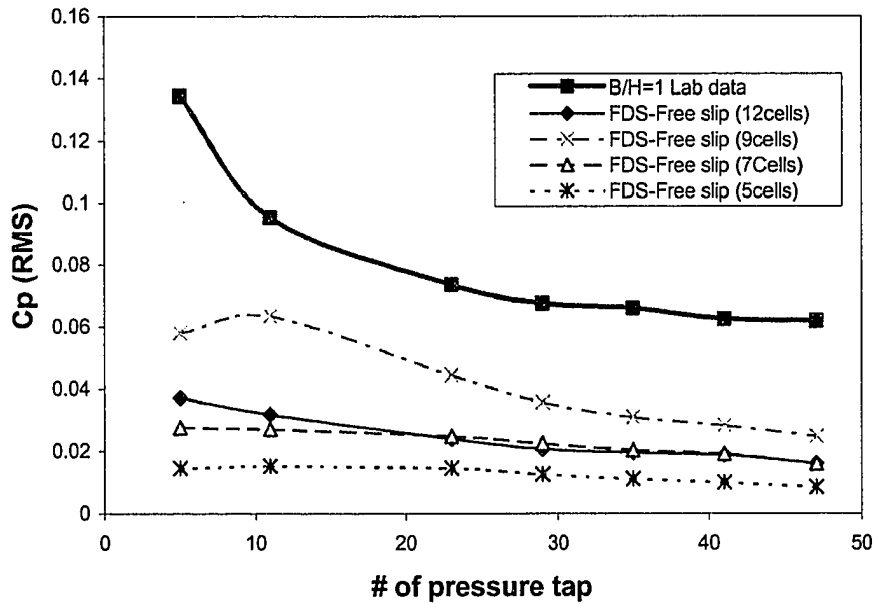


Figure 6.53b Comparisons of RMS pressure coefficients on the centerline of the roof for case N=1: experiments and numerical simulation using FDS LES model

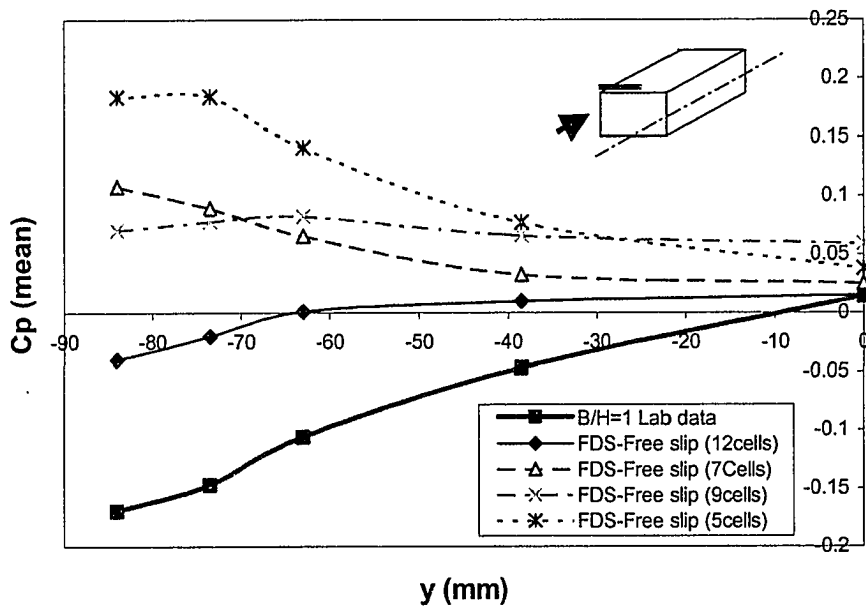


Figure 6.54a Comparisons of mean pressure coefficients on the front edge of the roof for case N=1: experiments and numerical simulation using FDS LES model

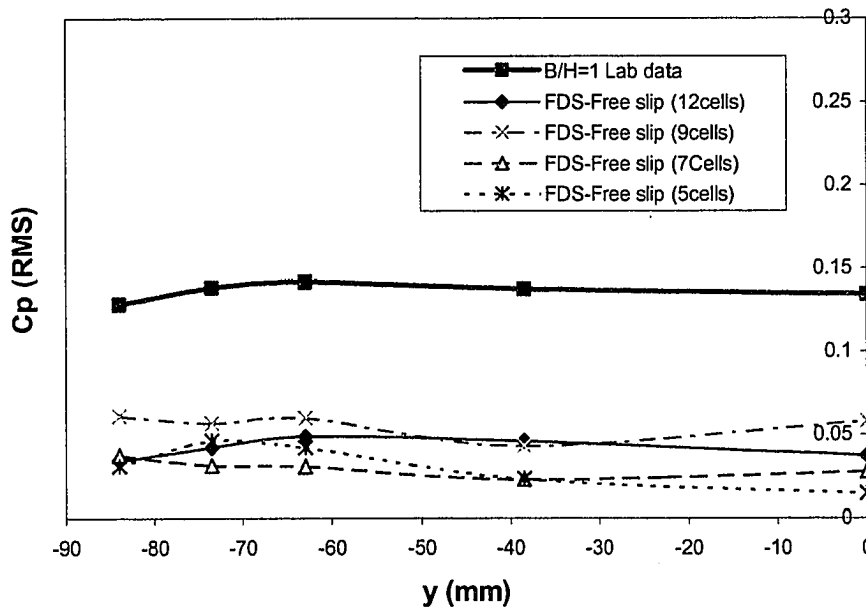


Figure 6.54b Comparisons of RMS pressure coefficients on the front edge of the roof for case N=1: experiments and numerical simulation using FDS LES model

6.3 Modeling of Pollutant Dispersion in Urban Street Canyons

Air pollution in urban street canyons resulting from exhaust emissions is a major urban problem. Often traffic pollution excess controls air pollution management decisions. There are a number of elaborate predictive models of pollutant dispersion and diffusion that address the effects of variable shapes of city buildings on pollutant concentrations, but few are fully validated. This section presents ventilation behavior in different street canyon configurations. To evaluate dispersion in a model urban street canyon, a series of tests with various street canyon aspect ratios (B/H) are presented. Both open-country roughness and urban roughness cases are considered.

6.3.1 Wind Tunnel Results and Interpretation

A point source was located at the center point of a cross street canyon in front of our base building model (see Figure 3.6 for details). The dimensionless concentration coefficient used in the presentation of the data is $K = C \cdot U \cdot H^2 / Q$, where C is the dimensional tracer species density, U is the upwind free stream velocity at roof height, H is the building height and Q is the source flow rate. It is known that the horizontal wind velocity at street level is typically of the order of 10 % the free stream velocity. For reference velocities achievable in our wind tunnel, this results in horizontal velocities at street level of a few cm/s. Simple calculations show that the tracer gas discharge velocities from the point source are the same order of magnitude, so they may influence the recirculating flow patterns in the canyon.

Figure 6.55a shows the normalized concentrations on the centerline of the upwind and downwind walls of street canyons for $B/H=0.5$ and different values of N . The normalized concentrations are the highest for the $B/H=0.5$ case, especially in the street level corners of the canyons. The upwind wall areas have higher concentrations than the downwind wall areas, because there are two circulation flows inside the street canyon: the upper circulation flow is clockwise and the lower circulation flow is counter clockwise. The circulation flows carry the emission gas to the upwind wall of the street canyon, resulting in higher concentrations on the upwind wall. The lower circulation flow (CCW) carries some emission to the downwind wall of the street canyon, so the ground corner of the downwind wall also has high concentrations. The results also show that the open-country roughness cases ($N=1, N=2$) have higher concentrations at street level than the urban roughness cases ($N=3, N=8$).

Similarly, Figure 6.55b shows normalized concentrations for $B/H=1$ with different N . Since there is only one circulation eddy (CW) in the street canyon, the clockwise flow impinges on the upwind wall areas. Therefore, the upwind wall areas have higher concentrations than the downwind wall areas. Contrary to the cases of $B/H=0.5$, the higher concentrations are in the street canyons of the urban roughness cases ($N=3, N=8$) instead of the open-country roughness cases ($N=1, N=2$). It is likely that with fewer upwind buildings (i.e. $N \leq 2$), the flow field is more unstable and intermittent ventilation of the entire canyon occurs more often resulting in lower street level concentrations.

Figures 6.56 and 6.57 both show interference flow effects on the concentrations for the cases $B/H=2$ and $B/H=4$, respectively. Similar to the cases of $B/H=0.5$ and $B/H=1$, both $B/H=2$ and $B/H=4$ show that the upwind wall areas have higher concentrations. Wake zone eddies occurring against the upwind wall areas and the resulting re-circulation keep the gas against upwind wall areas. However, with the greater width of the street canyons, the downwind wall areas have very low concentrations, because the circulation downwind of the upwind eddy carries the emissions out of the canyons. The concentrations are higher for $B/H=2$ than for $B/H=4$ because the dilution effects the cavity zone are higher for $B/H=4$.

For the isolated roughness cases ($B/H=6$), the concentrations are almost zero at the upwind wall areas of the street canyon, because the emissions are transported out of the canyon. The downwind wall areas, on the other hand, have higher concentrations because the concentrations convect to downwind wall areas more easily. Figure 6.58 presents comparisons of concentration levels for $N=1$ but different B/H . The results show that the lower the ratio of B/H , the higher the concentrations in the street canyons.

Figure 6.59 presents the concentration levels on the centerline of the roof area for $N=1$ and different B/H values. The results of each case show that the concentrations become lower on the line of the roof as the roof distances become larger.

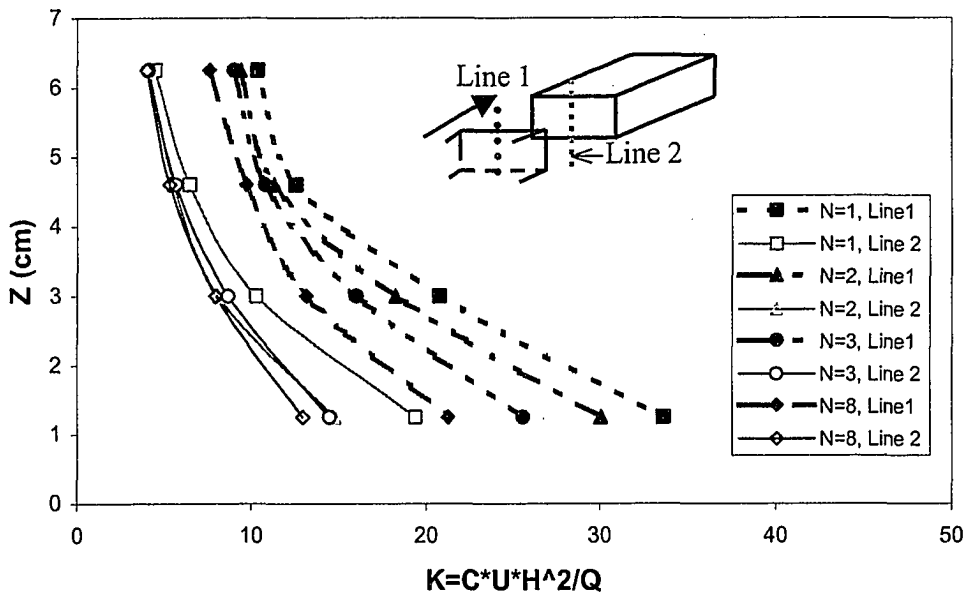


Figure 6.55a Concentrations on the upwind and downwind walls of the street canyon for case $B/H=0.5$

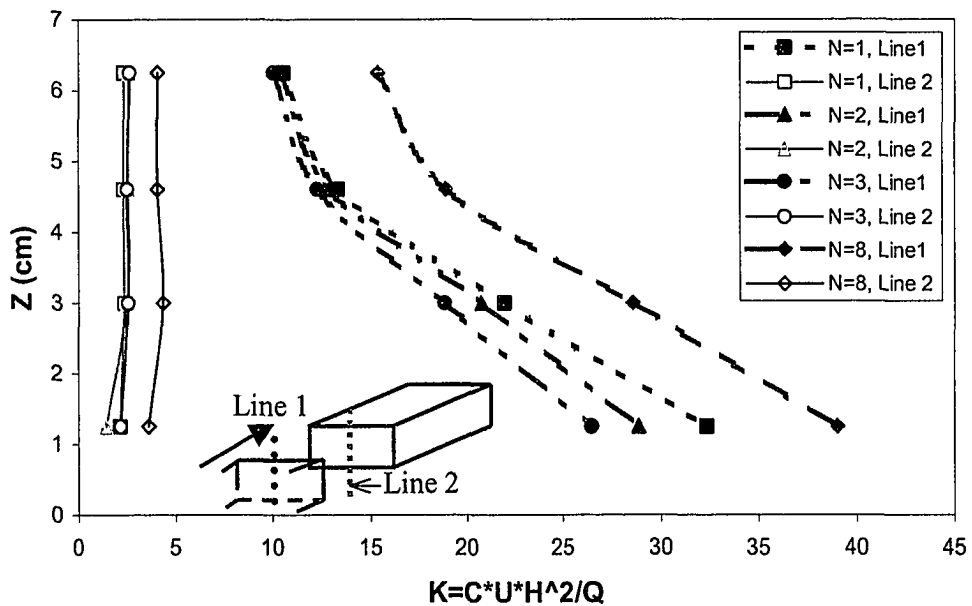


Figure 6.55b Concentrations on the upwind and downwind walls of the street canyon for case $B/H=1$

6.3.2 Comparison of Concentrations of Wind Tunnel Results and Numerical Simulations

FLUENT and FDS were used for numerical simulations. The point source inlet was modeled as a 1.3*1.3 cm vent emitting at a constant velocity and no turbulence. The inlet velocity of $w_{\text{source}} = 0.05$ m/sec was set to be equivalent to the source emission rate used in the wind tunnel simulation. A tracer mass fraction of 1 was applied to the point source inlet during the calculation. In presenting the results from the calculation, tracer species density was normalized to facilitate comparison with experiments and other numerical results.

A comparison of each set of data from wind tunnel experiments with the numerical simulation, reveals that the CFD software, Fluent 5.4, can predict the actual wind tunnel results by choosing optimum boundary condition, grid resolution and turbulence model. Figures 6.60 and 6.61 show a direct comparison between measured and calculated concentrations on the centerline of the upwind and downwind walls for a street canyon where point source inlet located mid canyon for all cases and $N = 1$. The results show that Fluent predicts the right order of mean concentration for each case. However, Fluent gives higher concentration predictions in some zones, for example, the ground level corners of the upwind walls of $B/H=1$ cases and the ground corners of both upwind and downwind walls of the $B/H=0.5$ cases.

Figure 6.62 shows a comparison of measured and numerically predicted concentrations on the centerline of the roof for open-country cases, $N=1$. The calculated concentrations (Standard κ - ϵ) for the roof surface agree reasonably well with the data

collected from the wind tunnel; however, the exceptions are the areas around the front edges of the roof for case $B/H=0.5$. The numerical simulation predicts significantly higher values than measured in the wind tunnel. This is due to that the wind flow was considered more stable in the numerical modeling than that of the physical modeling. The unstable wind flow caused the concentration value in the canyon of the physical modeling to be lower, because there was more ventilation inside the canyon, and more of the concentration was washed out of the canyon.

A comparison of measured and calculated concentrations for $B/H=1$ with different number rows of shelter models is given in Figure 6.63. Two concentration taps are chosen. One is on the downwind wall and the other is on the roof surface. Both measured and calculated results show increased concentrations with a greater sheltering effect of more upwind model structures. Figure 6.64 shows the calculated normalized concentrations using Fluent code are plotted against the experimental normalized concentrations on the centerline of rooftop and upwind and downwind walls of canyon tappings.

For FDS simulations, two ground boundary conditions are chosen to compare results with the wind tunnel measurements. Figure 6.65 presents comparisons between wind tunnel and numerical concentrations for the centerline of the upwind and downwind walls of the open-country roughness case, $N=1$ and $B/H=1$. The result shows that with the half-slip ground boundary condition, the FDS predicts the measurements of the wind tunnel experiments. For the concentrations at centerline of roof of $N=1$, $B/H=1$ cases, both Fluent and FDS numerical results predict the measurements of the wind tunnel

experiments (see Figure 6.66). The calculated normalized concentrations from both Fluent and FDS are plotted against the experimental normalized concentrations in Figure 6.67. There is a near linear relationship between the experimental data and the numerical data. The slope of the line of best fit is 2.85 for Fluent and 1.15 for FDS. The results from FDS simulation agree much better with the experimental results than those from Fluent.

The numerical simulation results conclude that wind approaching angle is a significant effect to the concentration dispersion on the roof of the master building. Figures 6.58a, 6.58b, 6.58c and 6.58d show the concentration dispersion on the master building with different angles of approaching winds. In the case of approaching wind of zero degree, the concentration distributed to the whole roof surface. The maximum normalized concentration ($K = 4$) was measured near the center of the roof front edge, and the minimum normalized concentration ($K = 0.2$) was measured around two sides of the roof rear edge. The concentration in the case of approaching wind of 15 degrees was found only at the lower corner of the front roof edge with the maximum normalized concentration of $K = 2.5$. The other areas of the roof were found no concentration at all. In the cases of approaching wind angles of both 75 degrees and 90 degrees, there was almost zero concentration found on the roof with the maximum values of $K = 0.04$ and $K = 0.003$, respectively.

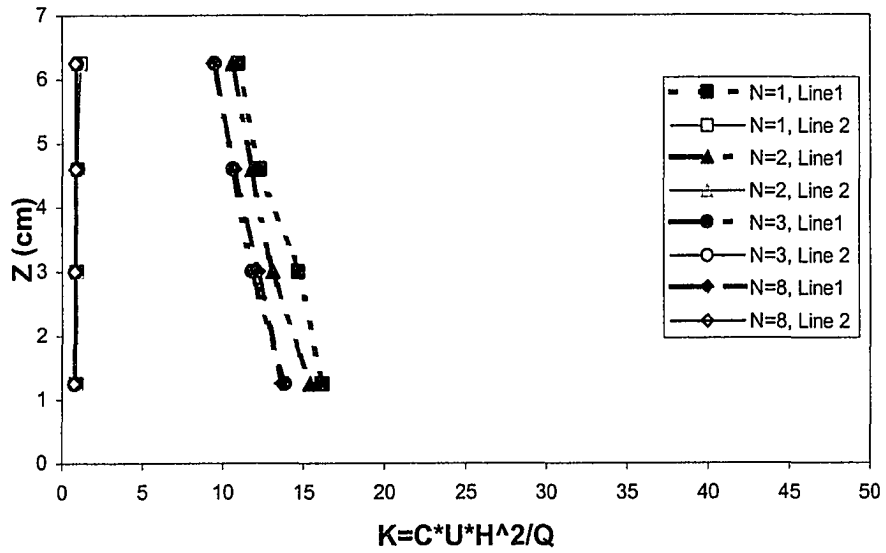


Figure 6.56 Concentrations on the upwind and downwind walls of the street canyon for case B/H=2

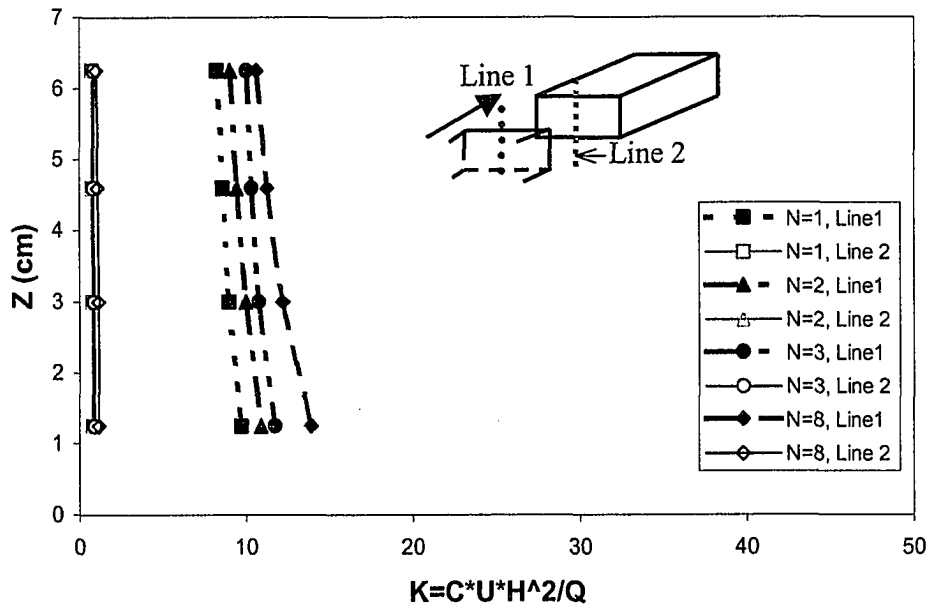


Figure 6.57 Concentrations on the upwind and downwind walls of the street canyon for case B/H=4

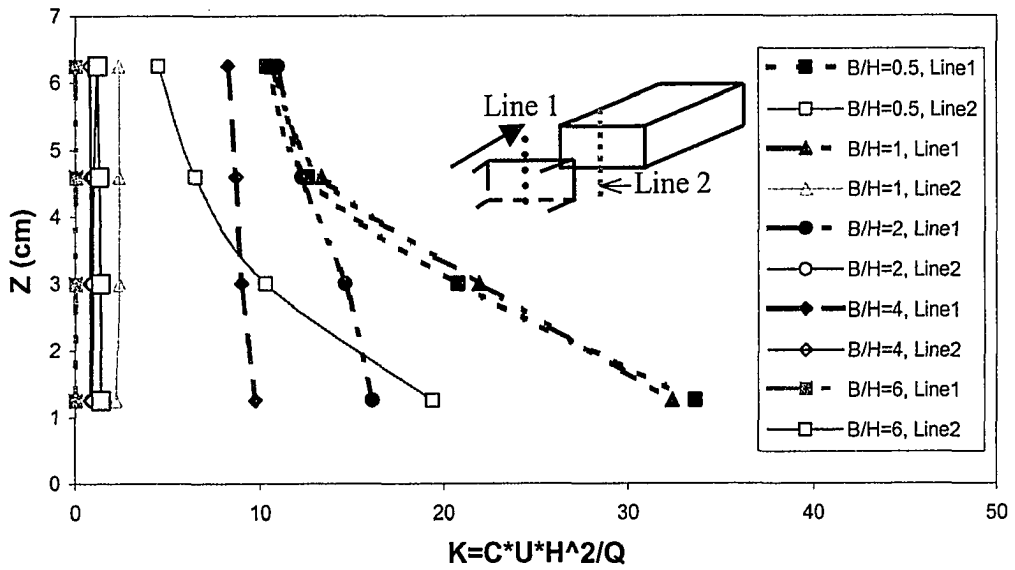


Figure 6.58 Concentrations on the upwind and downwind walls of the street canyon for open country roughness case $N=1$

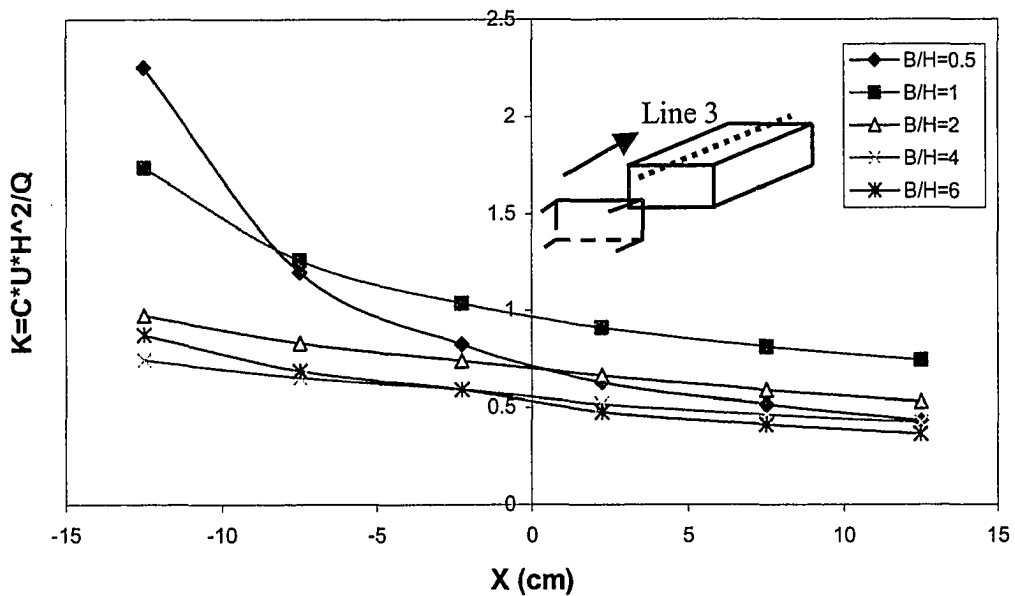


Figure 6.59 Concentrations on the centerline of the roof for open country roughness case $N=1$

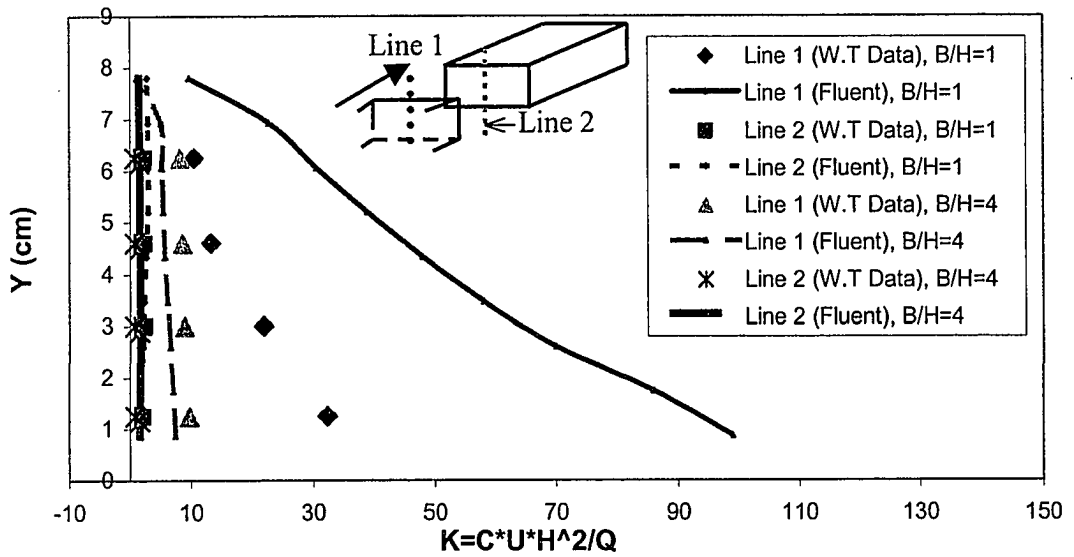


Figure 6.60 Comparisons between wind tunnel and numerical model (Fluent $\kappa\text{-}\epsilon$ model) concentrations for the open country roughness case $N=1$

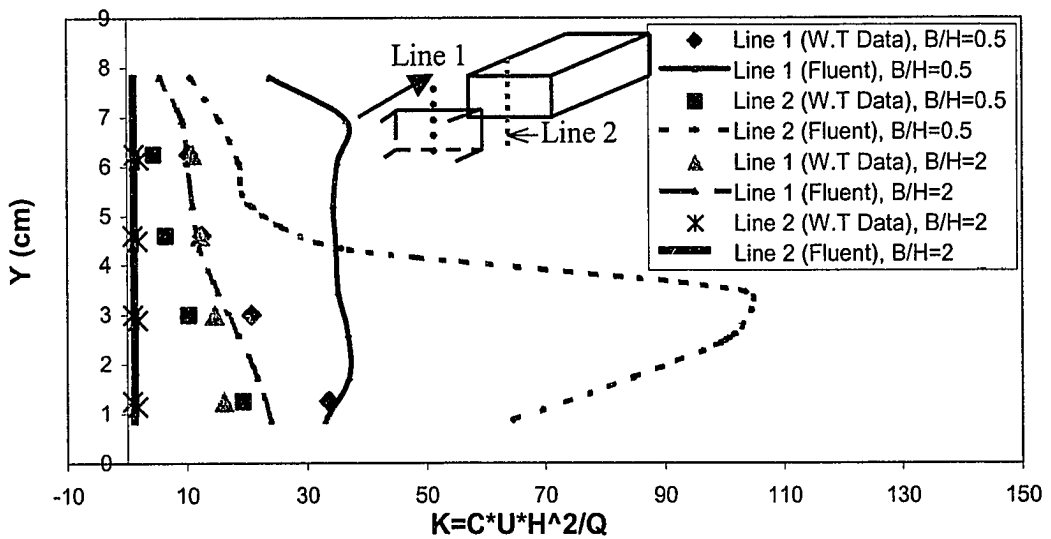


Figure 6.61 Comparisons between wind tunnel and numerical model (Fluent $\kappa\text{-}\epsilon$ model) concentrations for the open country roughness case $N=1$

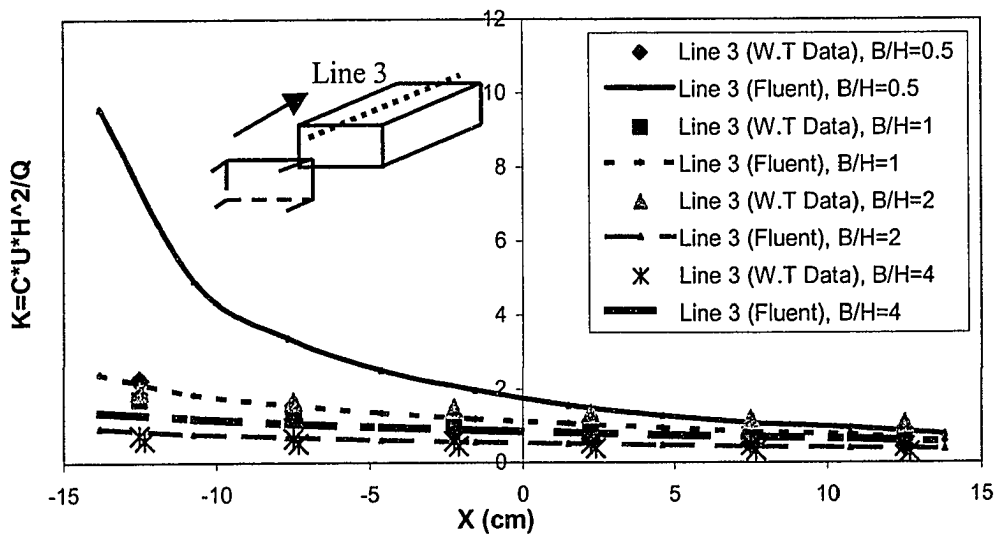


Figure 6.62 Comparisons between wind tunnel and numerical model (Fluent κ - ϵ model) concentrations on the centerline of the roof for open country cases $N=1$

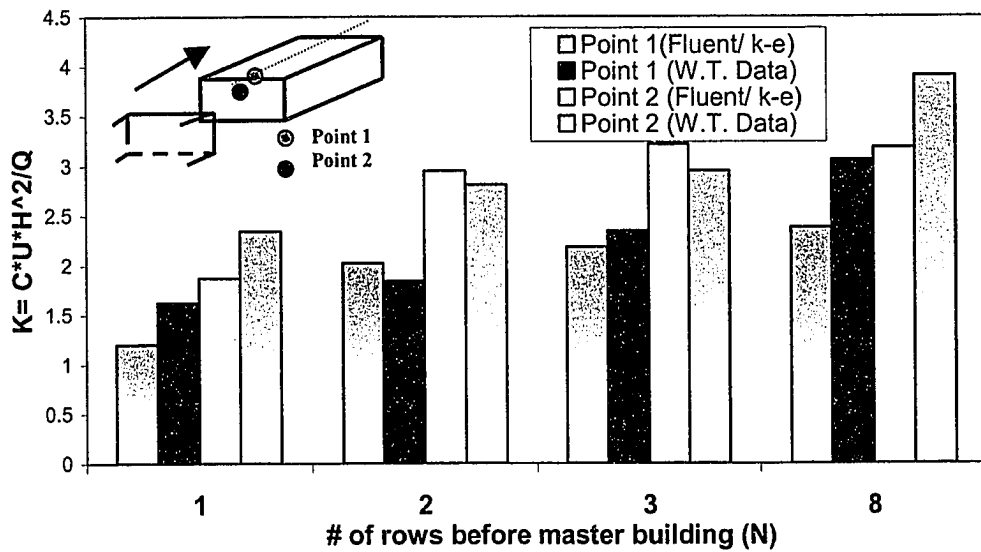


Figure 6.63 Comparisons between wind tunnel and numerical model (Fluent κ - ϵ model) concentrations for different numbers of upwind buildings before master building for case $B/H=1$

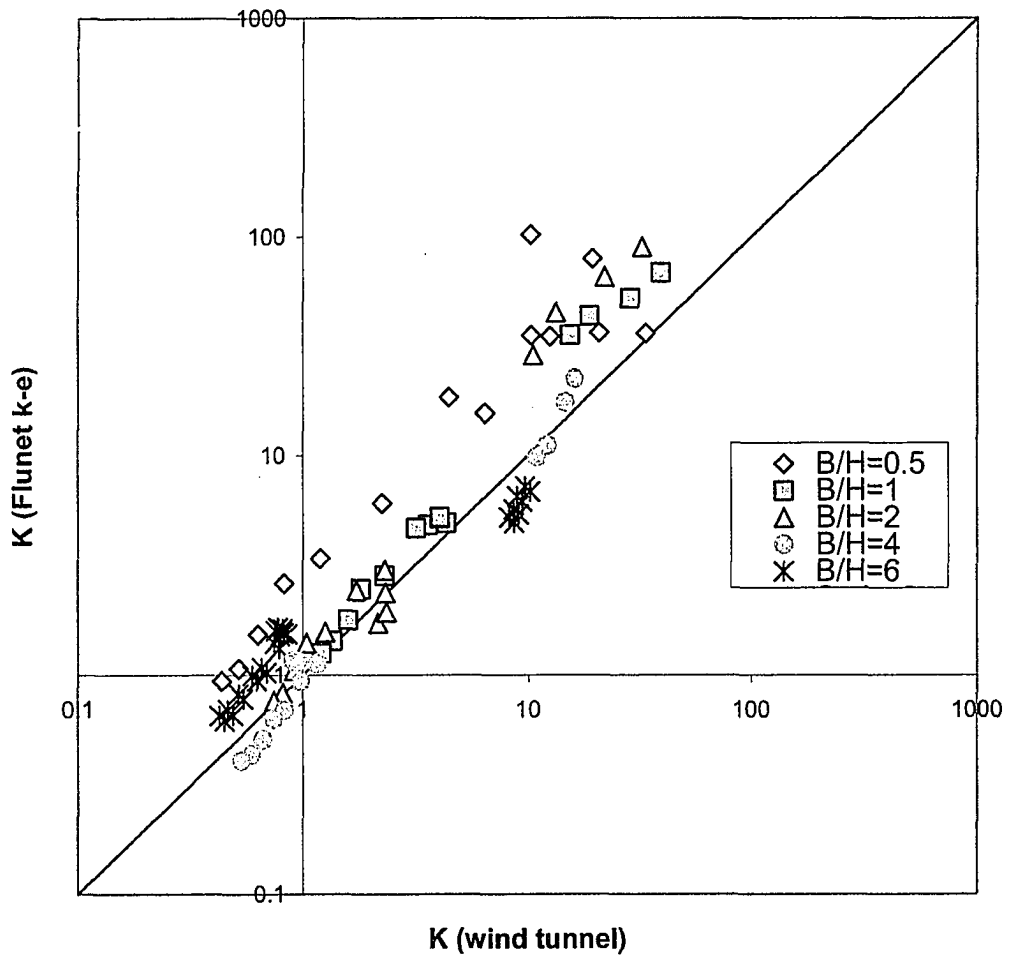


Figure 6.64 Experimental vs. Fluent calculated normalized concentration on the centerline of the roof and upwind and downwind walls of canyon tappings

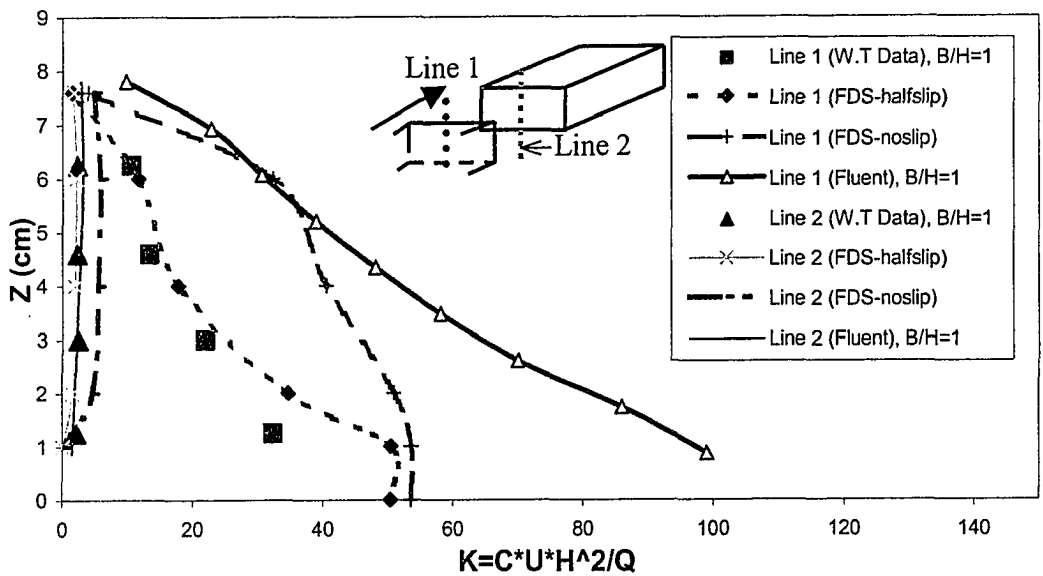


Figure 6.65 Comparisons between wind tunnel and numerical model (Fluent κ - ϵ model, FDS) concentrations for the open country roughness case $N=1$ and $B/H=1$

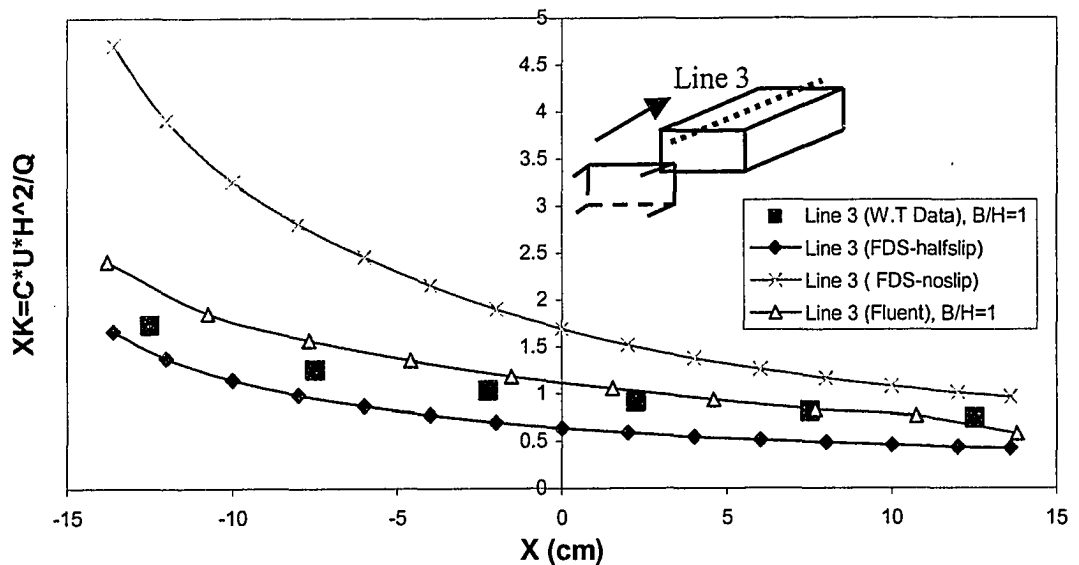


Figure 6.66 Comparisons between wind tunnel and numerical model (Fluent κ - ϵ model, FDS) concentrations on the centerline of the roof $N=1$ and $B/H=1$

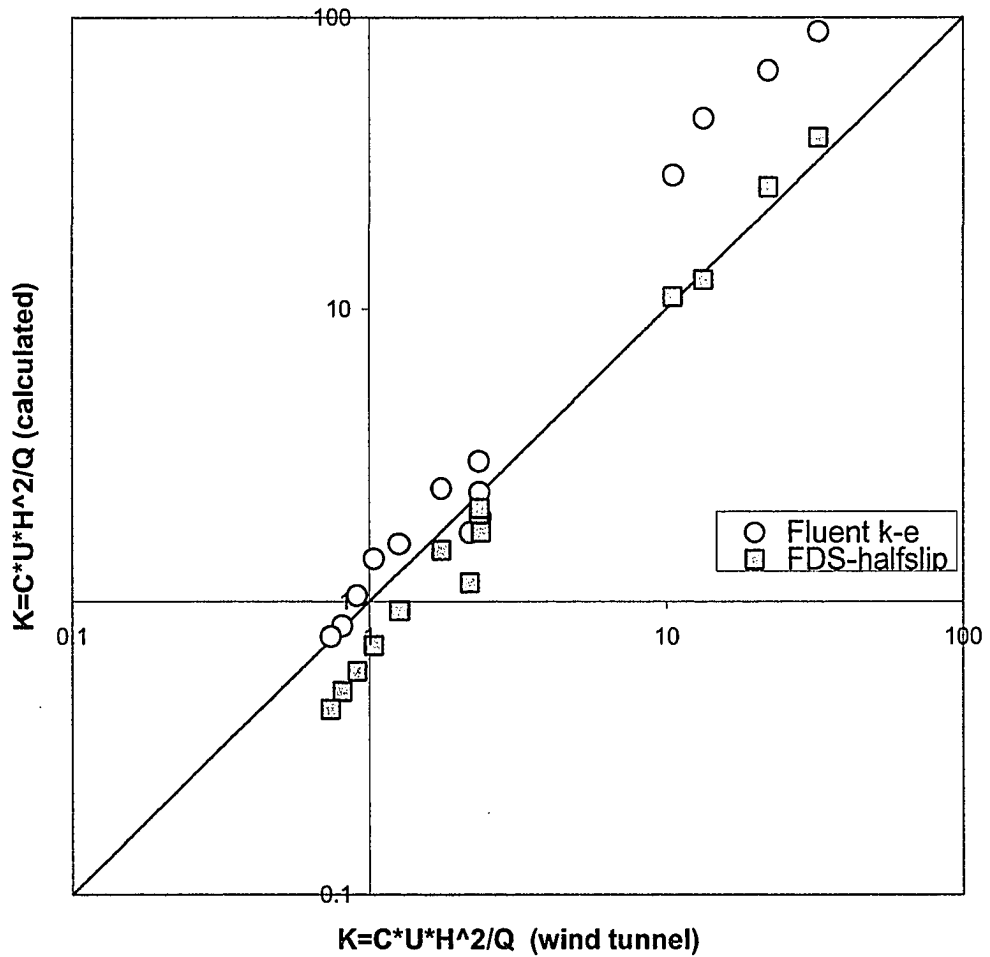


Figure 6.67 Experimental vs. calculated (Fluent and FDS) normalized concentration, K , on the centerline of the roof and upwind and downwind walls of canyon tappings ($B/H=1$, $N=1$)

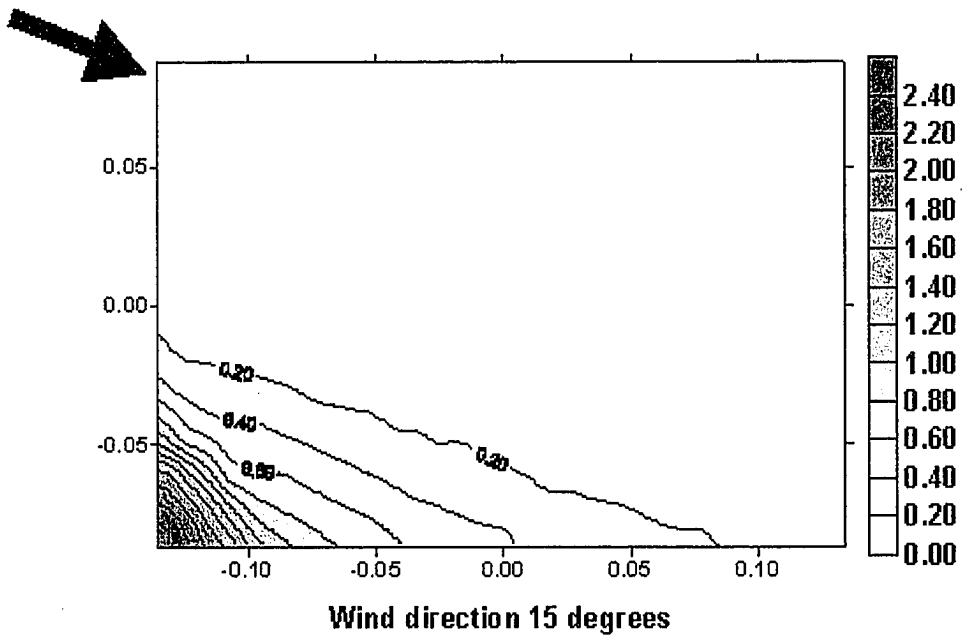
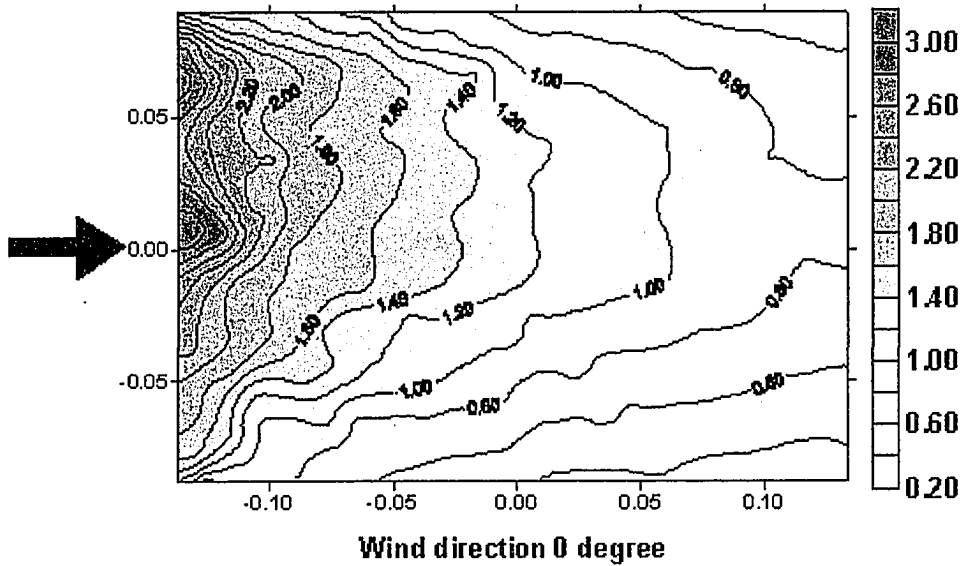


Figure 6.68a Predictions of tracer gas concentration on the master building roof for the wind azimuths with zero and 15 degrees, $N=1$, $B/H=1$

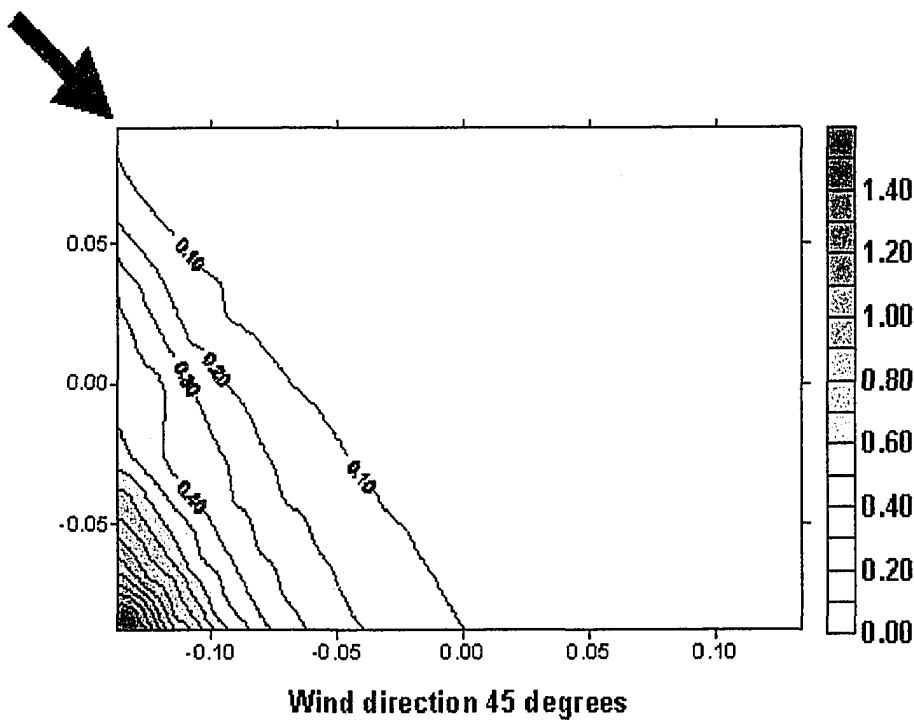
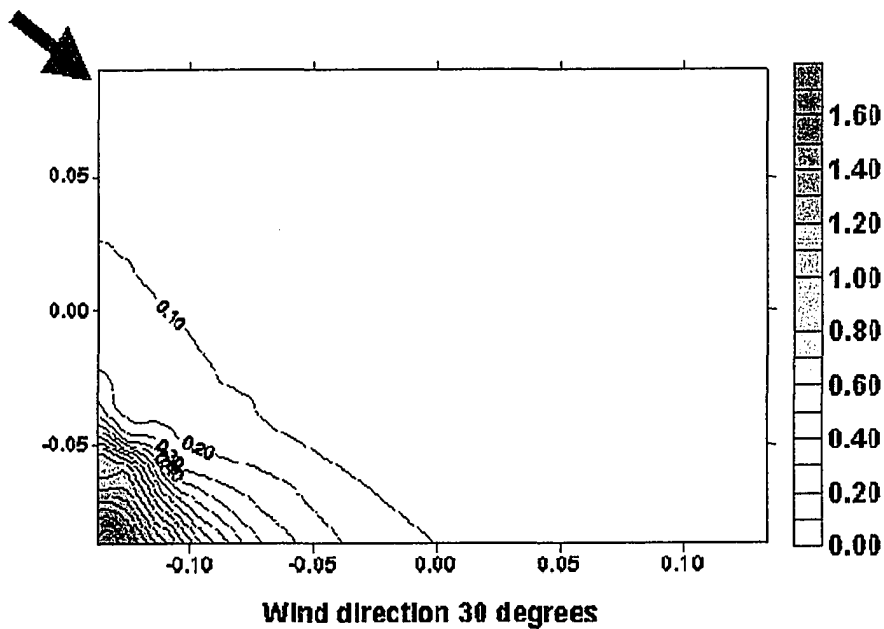


Figure 6.68b Predictions of tracer gas concentration on the master building roof for the wind azimuths with 30 and 45 degrees, $N=1$, $B/H=1$

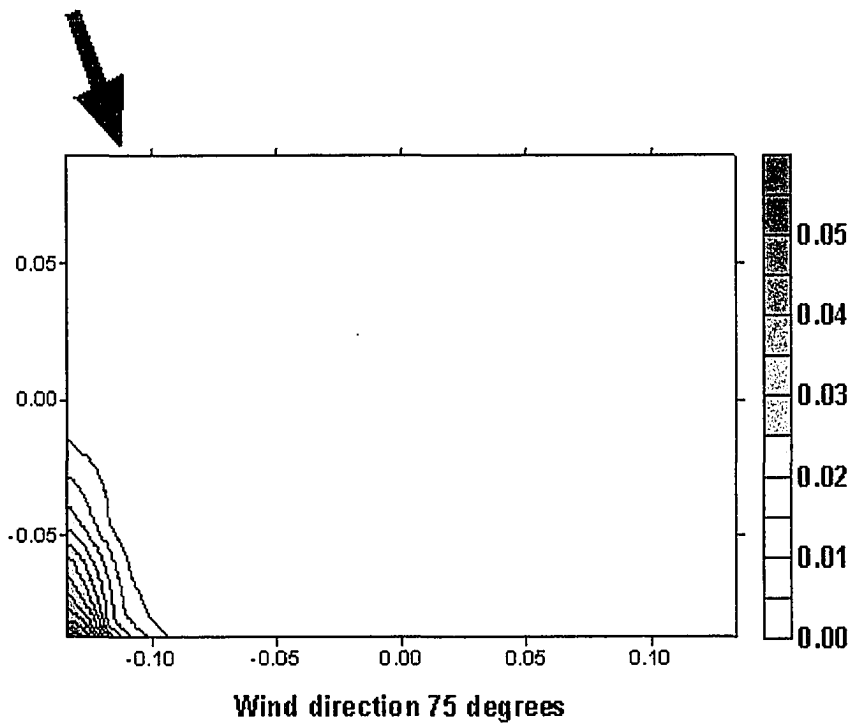
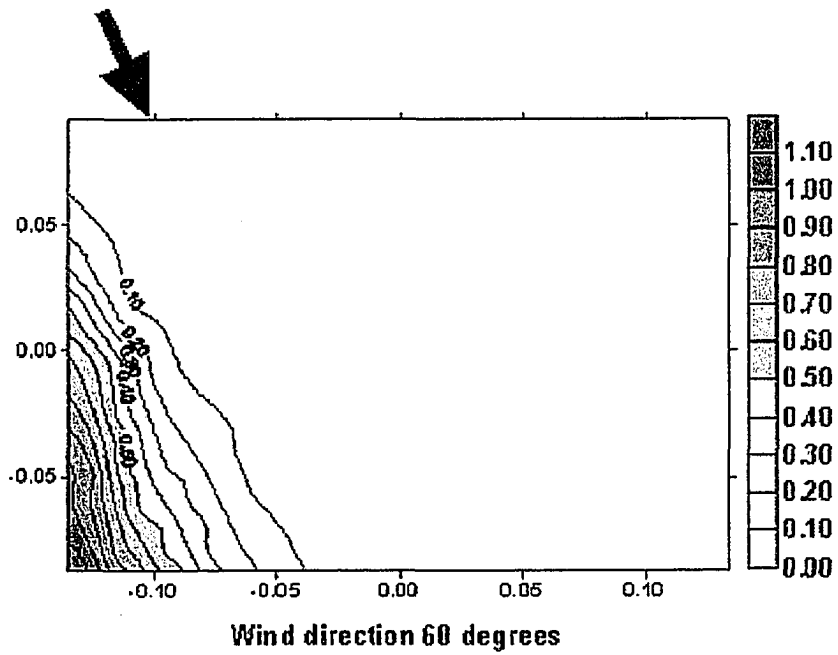


Figure 6.68c Predictions of tracer gas concentration on the master building roof for the wind azimuths with 60 and 75 degrees, $N=1$, $B/H=1$

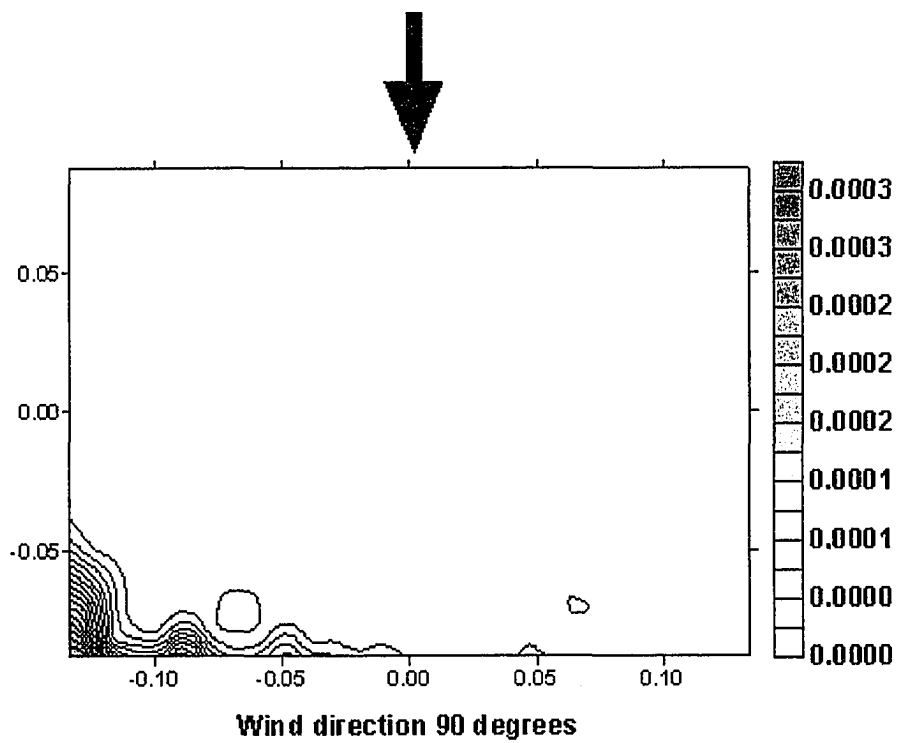


Figure 6.68d Predictions of tracer gas concentration on the master building roof for the wind azimuths with 90 degrees, $N=1$, $B/H=1$

CHAPTER 7

SUMMARY AND CONCLUSIONS

In order to better understand the bluff body flow and dispersion in urban street canyons, this study has performed wind tunnel experiments and numerical simulations. Wind tunnel experiments record flow images, velocity flow fields, multiple surface pressures, and multiple surface concentrations around urban street canyons. Numerical modeling used two computational fluid dynamics software suites, Fluent 5.4 and Fire Dynamics Simulator (FDS), to examine the simulations of urban street canyons with the same configurations as the wind tunnel experiments. The results can be summarized into four main conclusions: First, the shielding effects from the surrounding buildings are significantly larger than expected; Second, high concentrations were measured on the upwind walls of urban street canyon except the isolated roughness case; Third, the overall performance of Fluent including predictions of flow fields, surface pressure coefficients and mean concentrations is acceptable. Finally, the performance of FDS is acceptable only in predictions of mean concentrations.

7.1 Wind Tunnel Experimental Results

The results of the wind tunnel experiments suggest that depending on the street width to building height ratio (B/H), the flow in the street canyons can be classified as skimming flow ($B/H=0-1.2$), wake interference flow ($B/H=1.2-5.0$), or an isolated

roughness flow ($B/H > 5.0$) as originally proposed by Oke (1988). Results differ substantially depending upon whether the master building is surrounded by only a few or many buildings. If the surrounding depth of buildings about the central structure is only one or two circuits deep, the approach flow is characterized by an open-country roughness surrounding the complex. But if multiple building circuits exist, then an equilibrium urban roughness situation develops.

In open country cases, the characteristics of flow, pressure and concentration distributions were examined. The experimental results are:

- Visualization using smoke and vertical light sheets reveals that clean air is drawn into the canyon by intermittent eddies circulating down into the canyons or along the upwind street canyon intersections.
- Stagnation pressure occurred on the upwind face of the test building, but their magnitudes are reduced by the sheltering effect of upwind model structures. The maximum value of mean C_p on the centerline of the upwind face of the test building for single building case is 0.85. With the sheltering effect, the maximum value of mean C_p is reduced to 0.2, 0.3, 0.45, 0.47 and 0.5 for cases of $B/H=0.5$, $B/H=1$, $B/H=2$, $B/H=4$ and $B/H=6$, respectively.
- The suction on the roof can be significantly reduced by the presence of surrounding buildings. Compared to a single building case, building arrangements with $B/H=0.5$ can reduce the magnitude values of mean, RMS and $-peak C_p$'s over 80%.
- Significant pollution concentrations are measured on upwind walls of urban street canyons and along the rooftops.

- Building orientations oblique to the street canyons result in higher street level wind speed, the development of corner vortices over the roof of the test building, and lower concentrations on the building faces upwind of the ground level sources.

In urban roughness cases, experiments were also performed on the dispersion within extended urban roughness associated with additional upstream dummy buildings. The overall characteristics discussed for the open country case are also identified in canyons amidst large urban roughness, but some significant differences are observed:

- For closely spaced multiple street canyons, skimming flow dominates, advection in and out of the canyons appears intermittent, and transport over the street-canyon top streamline appears to primarily by turbulent mixing.
- As the street widths widen with respect to building height, wake-interference flows dominate the advection and dispersion of pollutant plumes.
- Once the street width to building height exceeds about 5, the flow field even for a multiple building arrangement, appears to be perturbed by individual isolated buildings.

7.2 Numerical Simulation Results

As noted by Meroney et al. (1998), it is not difficult to achieve a correct looking presentation of pressures and concentrations over a bluff body. However, it is not a given that quantitative equivalence between experimental and numerical data will occur unless careful attention is paid to inlet profiles, grid adaptation and the turbulent model chosen.

In the calculation produced to replicate some of the test cases studied above, it was found necessary to take utmost care in adapting the turbulent grids to assure that intense concentration gradients, separation locations and re-attachment locations were reproduced.

Wind-tunnel flow, pressure and diffusion tests performed about an idealized building arrangement replicate many of the features of the urban environment previously noted at full scale and in earlier laboratory simulations. Numerical simulations using Fluent and FDS reproduce these patterns, but only with care taken to provide adequate grid resolution, accurate inlet flow profiles, and improved turbulence models.

Conclusions for comparisons of the experiment with the Fluent model suite can be summarized as follows:

- Fluent 5.4 can simulate the velocity profiles in urban street canyons very well using the standard κ - ϵ model.
- The standard κ - ϵ model and the RNG κ - ϵ model give almost the same results for the calculated flow fields in urban street canyon cases.
- Fluent predicts concentration levels in urban street canyons reasonably well; however, it systematically predicts higher predictions in high concentration zones.
- Concentration magnitudes are generally under-predicted by numerical predictions for cases with $N > 2$ rows of shelter buildings.
- Improved grid resolution also results in faster numerical convergence.
- Adapted grids provide a convenient way to reproduce flow details of separation, reattachment, and high concentration regions without excessive calculation cells.

Conclusions for comparisons of the FDS simulations are summarized as follows:

- FDS can well simulate the mean velocity flow profiles in urban street canyons using free-slip and half-slip ground boundary conditions.
- Free-slip and half-slip ground boundary conditions give almost the same results for the calculated flow fields in urban street canyon cases.
- The time-dependent flow phenomena large eddy simulation (LES) has the capability to compute fluctuating pressures and concentrations on building surfaces due to the turbulence. However, results may improve with finer grid resolution and more accurate inlet turbulence specification.

REFERENCES

- Bachlin, W., Theurer, W. and Plate, E. J. (1992). Dispersion of Gases Released near the Ground in Built Up Areas: Experimental Results Compared to Simple Numerical Modelling, *Journal of Wind Engineering and Industrial Aerodynamics*, Vol. 41-44, 2721-2732.
- Bachlin, W., Theurer, W. and Plate, E. J. (1991). Wind Field and Dispersion in Built-up Area- A Comparison between Field Measurements and Wind Tunnel Data, *Atmospheric Environment*, Vol. 7, 1135-1142.
- Bachlin, W. and Plate, E. J. (1988). The Dispersion of Accidentally Released Gases in a Built-up Area, *Energy and Building*, Vol. 11, 163-169.
- Banks, D. (2000). The Suction Induced by Conical Vortices on Low-Rise Buildings with Flat Roofs. Ph.D. Thesis, Department of Civil Engineering, Colorado State University.
- Banks, D., Meroney, R. N., Sarkar, P. P. and Wu, F. (2000). The mitigation of vortex induced rooftop suction, *Volume of Abstracts for 4th Int. Colloquium on Bluff Aerodynamics & Applications*, Ruhr-Universitat Bochum, Germany, September 11-14, 2000, Vol. 4, 165-167.
- Banks, D., Meroney, R. N., Sarkar, P. P., Zhao, Z. and Wu, F. (1999). Flow visualization of conical vortices on flat roofs with simultaneous surface pressure measurement, *Journal of Wind Engineering & Industrial Aerodynamics*, 27.
- Banks, D. and Meroney, R. N., (1999). A model of roof-top surface pressure dependence upon local flow parameters, *Wind Engineering into the 21st century* (ed. Larsen, Larose & Livesey), Rotterdam: Balkema Press, 1097-1104.
- Bienkiewicz, B. (1995). First Five Years of NSF's Collaborative Program in Wind Engineering: Results and Future Activities, *27th Joint UJNR Meeting of the U.S.-Japan Panel on Wind and Seismic Effects*, 16-19 May, 1995, Tsukuba, Japan, 23.
- Birdsall, J. B. (1993). Physical Simulation of Wind-forced Natural Ventilation. Master Thesis, Department of Civil Engineering, Colorado State University.
- Borri, C. and Facchini, L. (2000). Wind tunnel tests and numerical simulation of non gaussian pressure fields on a sharp edged monumental roof structure, *Volume of Abstracts for 4th Int. Colloquium on Bluff Aerodynamics & Applications*, Ruhr-Universitat Bochum, Germany, September 11-14, 2000, Vol. 4, 405-410.

- Brown, M. J. and Williams, M. D. (1998). An Urban Canopy Parameterization for Mesoscale Meteorological Models, (Submitted to) *AMS 2nd Urban Environment Conf.*, Albuquerque, NM, Nov. 1998.
- Carpenter, P. and Locke, N. (1999). Investigation of wind speeds over multiple two-dimensional hills, *Journal of Wind Engineering and Industrial Aerodynamics*, Vol. 83, 109-120.
- Castillo, L. and George, W. K. (2001). Similarity Analysis for Turbulence Boundary Layer with Pressure Gradient: Outer Flow, *AIAA Journal*, January 2001, Vol. 39 (1), 41-47.
- Cermak, J. E., Davenport, A. G., Plate, E. J. and Viegas, D. X. (1995). *Wind Climate in Cities*. Dordrecht, The Netherlands: Kluwer Academic Publishers.
- Cermak, J. E. (1995) Physical Modeling of Flow and Dispersion over Urban Areas, *Wind Climate in Cities*, 383-403.
- Cermak J. E. (1984) Physical Modeling of Flow and Dispersion Over Complex Terrain, *Boundary-Layer Met.* 30 261-292.
- Cermak, J. E. (1981) Wind-tunnel Design for Physical modeling of Atmospheric Boundary Layers. *ASCE J. of Engineering Mechanics* 107, 623-642
- Cermak J. E. (1975) Applications of Fluid Mechanics to Wind Engineering- A Freeman Scholar Lecture. *Transactions of the ASME, J. of Fluids Engineering*, Ser. 1, 97, 9-38.
- Cheatham, S. A., Cybyk, B. Z. and Boris, J. P. Simulation of Flow and Dispersion around a Surface-mounted Cube, Naval Research Laboratory, Washington, DC.
- Cochrane, L. S. (1992). Wind-tunnel Modeling of Low-rise Structures. Ph.D. Dissertation, Department of Civil Engineering, Colorado State University, 348.
- Cooper, C. D. and Alley, F.C. (1994). *Air Pollution Control: A Design Approach* (2nd ed.). Prospect Heights, Illinois: Waveland Press Inc..
- Cowan, I. R., Castro, I. P. and Robins, A. G. (1997). Numerical considerations for simulations of flow and dispersion around buildings, *J. of Wind Engineering and Industrial Aerodynamics*, Vol. 67&68, 535-545.
- Davenport, A. G., Grimmond, C. S. B., Ore, T. R. and Wieringa, J. (2000). Estimating the Roughness of Cities and Sheltered Country, (Preprint) *12th Am. Weteor. Soc. Conf. On Applied Climatology*, Asheville, NC, May 2000.

- Fluent 5: User's Guide, July 1998. Fluent Incorporated. Website: <http://www.fluent.com>.
- Fothergill, C. E., Roberts, P. T. and Packwood, A. R. (2000). Flow and dispersion around storage tanks; comparison between wind tunnel studies and CFD simulations, *Abstracts of papers at 3rd Int. Symposium on Computational Wind Engineering*, University of Birmingham, UK, September 4-7, 2000, 55-58.
- Gayev, Y. A. and Savory, E. (1999). Influence of street obstructions on flow processes within urban canyons, *Journal of Wind Engineering and Industrial Aerodynamics*, Vol. 82, 89-103.
- Ham, H. J. (1998). Turbulence Effects on Wind-induced Building Pressures, Ph.D. Dissertation, Department of Civil Engineering, Colorado State University, 275.
- He, J. and Song, C. C. S., A numerical study of wind flow around the TTU building and the roof corner vortex, *Journal of Wind Engineering and Industrial Aerodynamics*, Vol. 67&68, 547-558.
- Hibi, K., Ueda, H., Wakahara, T. and Shimada, K. (1992). Use of large eddy simulation to measure fluctuating pressure fields around buildings with wall openings, *J. of Wind Engineering*, Vol. 52, 291-296.
- Kataoka, H. and Mizuno, M. (2000). Numerical flow computation around aeroelastic 3D square cylinder using inflow turbulence, *Abstracts of papers at 3rd Int. Symposium on Computational Wind Engineering*, University of Birmingham, UK, September 4-7, 2000, 141-144.
- Kiefer, H. and Plate, E. J. (2000). Local peak wind loads in built-up areas, *Volume of Abstracts for 4th Int. Colloquium on Bluff Aerodynamics & Applications*, Ruhr-Universitat Bochum, Germany, September 11-14, 2000, Vol. 4, 19-22.
- Kiefer, H. and Plate, E. J. (1998). Modeling of mean and fluctuating wind loads in built-up areas, *Journal of Wind Engineering and Industrial Aerodynamics*, Vol. 74-76, 619-629.
- Klein, Rau, M., Rockle, R. and Plate, E. J. (1994). Concentration estimation around point sources located in the vicinity of U-shaped buildings and in a built-up area, *2nd Int. Conf. Air Pollution*, Barcelona, Spain, 27-29 September 1994.
- Kondo, K., Murakami, S. and Mochida, A. (1997). Generation of velocity fluctuations for inflow boundary condition of LES, *Journal of Wind Engineering and Industrial Aerodynamics*, Vol. 67&68, 51-64.

- Kondo, K., Mochia, A., Murakami, S. and Tsuchiya, M. (2000). Generation of Inflow Turbulent Boundary Layer for LES Computation, *Abstracts of papers at 3rd Int. Symposium on Computational Wind Engineering*, University of Birmingham, UK, September 4-7, 2000, 83-86.
- Lee, S. and Benkiewicz, B. (1997). Large-eddy simulation of wind effects on bluff bodies using the finite element method, *Journal of Wind Engineering and Industrial Aerodynamics*, Vol. 67&68, 601-609.
- Leitl, B. Kastner-Klein, P., Rau, M., and Meroney, R. N. (1997). Concentration and flow distributions in the vicinity of U-shaped buildings: Wind-tunnel and computational data, *Journal of Wind Engineering & Industrial Aerodynamics*, Vol. 67 & 68, 745k-755k.
- Leitl, B. and Meroney, R. N. (1997). Car exhaust dispersion in a street canyon: Numerical critique of a wind-tunnel experiment, *Journal of Wind Engineering & Industrial Aerodynamics*, Vol. 67 & 68, 293-304.
- Lee, S. (1997). Unsteady aerodynamic force prediction on a square cylinder using k- ϵ turbulence models, *J. of Wind Engineering and Industrial Aerodynamics*, Vol. 67&68, 79-90.
- Letchford, C. W. and Sarkar, P. P. (2000). Wind loads on smooth and rough domes, *Volume of Abstracts for 4th Int. Colloquium on Bluff Aerodynamics & Applications*, Ruhr-Universitat Bochum, Germany, September 11-14, 2000, Vol. 4, 313-316.
- Li, Q. S. and Melbourne, W. H. (1999). Turbulence effects on surface pressures of rectangular cylinder, *Wind and Structures*, Vol. 2 (4), 253-266.
- Li, W. W. and Meroney, R. N. (1982). Gas Dispersion Near a Cubical Model Building: Part 1: Mean Concentration Measurements.
- Lombardi, D. J. (1978). Steady State Pollutant Concentrations in an Urban Area. Master Thesis. Department of Civil Engineering, Colorado State University.
- Lubcke, H., Thiele, F., Schmidt, S. and Rung, T. (2000). Comparison of LES and RANS for Bluff-Body flows, *Volume of Abstracts for 4th Int. Colloquium on Bluff Aerodynamics & Applications*, Ruhr-Universitat Bochum, Germany, September 11-14, 2000, Vol. 4, 475-478.
- MacDonald, R. W. (2000). Modelling the Mean Velocity Profile in the Urban Canopy Layer, *Boundary-Layer Meteorology*, Vol. 97, 25-45.

- Maruyama, T. and Maruyama, Y. (2000). Large eddy simulations around a rectangular prism using artificially generated turbulent flows, *Abstracts of papers at 3rd Int. Symposium on Computational Wind Engineering*, University of Birmingham, UK, September 4-7, 2000, 11-14.
- Masson, V. (2000). A Physically-based Scheme for the Urban Energy Budget in Atmospheric Models, *Boundary-Layer Meteorology*, Vol. 94, 357-397.
- McGrattan, K. B. and Forney, G. P. (2000). Fire Dynamics Simulator- User's manual. NISTIR 6469. Building and Fire Research Laboratory, NIST, Gaithersburg, MD, January 2000. Website: <http://fire.nist.gov>.
- Meroney, R. N. and Bienkiewicz, B. (1997). Computational Wind Engineering 2, *2nd International Symposium on Computational Wind Engineering*, Fort Collins, CO, August 4-8, 1996. Amsterdam, Netherlands: Elsevier Science B.V..
- Meroney, R. N. and Chang, C.-H. (2000). Numerical and physical modeling of bluff body flow and dispersion in urban street canyons, *Volume of Abstracts for 4th Int. Colloquium on Bluff Aerodynamics & Applications*, Ruhr-Universitat Bochum, Germany, September 11-14, 2000, Vol. 4, 489-492.
- Meroney, R. N., Leitl, B. M., Rafailidis, S., and Schatzmann, M. (1998). Wind-tunnel and numerical modeling of flow and dispersion about several building shapes, *Journal of Wind Engineering & Industrial Aerodynamics*, Vol. 81, 333-345.
- Meroney, R. N., Neff, D. E., and Birdsall, B. (1995). Wind-tunnel simulation of infiltration across permeable building envelopes: Energy and air pollution exchange rates, *7th Int. Symp. On Measurement and Modeling of Environmental Flows, Int. Mech. Eng. Conf.*, San Francisco, 12-17 November 1995, 8.
- Meroney, R. N., Letchford, C. W. and Sarkar, P. P. Comparison of Numerical and Wind Tunnel Simulation of Wind Loads on Smooth, Rough and Dual Domes Immersed in a Boundary Layer.
- Meroney, R. N., Rafailidis, S. and Pavageau, M. (1996). Dispersion in Idealized Urban Street Canyons, *Air Pollution Modeling and Its Application, XI* (ed. Gryning & Schiermeir), New York: Plenum Press, 451-458.
- Meroney, R. N., Pavageau, M., Rafailidis, S., and Schatzmann, M. (1996). Study of line source characteristics for 2-D physical modeling of pollutant dispersion in street canyons, *Journal of Wind Engineering & Industrial Aerodynamics*, Vol. 62, 37-56.
- Mehta, K. C., Smith, D. A. and Jokhu, U. (2000). Understanding of roof corner pressures through field measurement, *Volume of Abstracts for 4th Int. Colloquium on Bluff*

Aerodynamics & Applications, Ruhr-Universität Bochum, Germany, September 11-14, 2000, Vol. 4, 365-368.

Mochida, A., Murakami, S., Shoji, M. and Ishida, Y. (1992). Numerical Simulation of Flowfield around Texas Tech Building by Large Eddy Simulation, *J. of Wind Engineering*, Vol. 52, 42-47.

Murakami, S., Mochida, A., Kim, S., Ooka, R. Yoshida, S., Kondo, H., Genchi, Y. and Shimada, A. (2000). Software platform for the total analysis of wind climate and urban heat island- integration of CWE simulation from human scale to urban scale, *Abstracts of papers at 3rd Int. Symposium on Computational Wind Engineering*, University of Birmingham, UK, September 4-7, 2000, 23-26.

Murakami, S. (1996). Current status and future trends in computational wind engineering, *J. of Wind Engineering and Industrial Aerodynamics*, 67&68, 3-34.

Murakami, S., Mochida, A., and Hibi, K. (1987). Three dimensional numerical simulation of air flow around a cubic model by large eddy simulation, *J. of Wind Engineering and Industrial Aerodynamics*, 25, 291-305.

Oke, T. R. (1998). Street design and urban canopy layer climate, *Energy and Buildings* 11, 103-113.

Oke, T. R. (1978). *Boundary Layer Climates*. New York, NY: Halsted Press.

Oke, T. R. and East, C. (1970). The Urban Boundary Layer in Montreal, *Boundary-Layer Meteorology*. Dordrecht, Holland: D. Reidel Publishing Company.

Paterson, D. A. (1992). Predicting r.m.s. pressures from computed velocity and mean pressures, *Journal of Wind Engineering and Industrial Aerodynamics*, Vol. 46-47, 431-437.

Plate, E. (2000). Wind loads and diffusion in urban areas, *Volume of Abstracts for 4th Int. Colloquium on Bluff Aerodynamics & Applications*, Ruhr-Universität Bochum, Germany, September 11-14, 2000, Vol. 4, 3-7.

Qasim, A., Maxwell, T. T. and Parameswaran, S. (1992). Computational Predictions of Flow Over a 2-D Building, *Journal of Wind Engineering and Industrial Aerodynamics*, Vol. 41-44, 2839-2840.

Rehm, R. G., McGrattan, K. B., Baum, H. R. and Simiu, E. An Efficient Large Eddy Simulation Algorithm for Computational Wind Engineering: Application to Surface Pressure Computations on a Single Building, *NISTIR 6371*, Building and Fire Research Laboratory, NIST, Gaithersburg, MD. Website: <http://fire.nist.gov>.

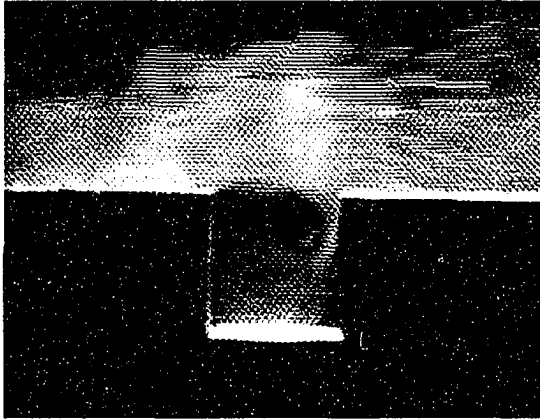
- Rehm, R. G., McGrattan, K. B., Baum, H. R. and Simiu, E. (2000). Large Eddy Simulation of flow over a building complex, *Abstracts of papers at 3rd Int. Symposium on Computational Wind Engineering*, University of Birmingham, UK, September 4-7, 2000, 125-128.
- Rafailidis, R. and Schatzmann, M. (1995). Physical modeling of car exhaust dispersion in urban street canyons, *Proc. 21st Int. Meeting on Air Pollution Modeling and Its Applications*, Baltimore, Nov. 6-10, 1995.
- Ruark, A. E. (1935) Inspectional Analysis: A Method Which Supplements Dimensional Analysis, *Journal Elisha Mitchell Science Society*, Vol. 51, 127-133.
- Selvam, R. P. (1997). Computation of pressures on Texas Tech University building using large eddy simulation, *Journal of Wind Engineering and Industrial Aerodynamics*, Vol. 67&68, 647-657.
- Selvam, R. P. (1992). Computation of Pressures on Texas Tech Building, *Journal of Wind Engineering and Industrial Aerodynamics*, Vol. 41-44, 1619-1627.
- Shankar, P. N. and Deshpande, M. D. (2000). Fluid Mechanics in the Driven Cavity, *Annu. Rev. Fluid Mech.*, Vol. 32, 93-136.
- Simiu, E., Scanlan, R. H. (1996). Wind Effects on Structures: Fundamentals and Applications to Design (3rd ed.). New York, NY: Wiley-Interscience Publication.
- Song, C. C. S., He, J. (1992). Computation of wind flow around a tall building with large eddy simulation, *J. of Wind Engineering*, Vol. 52, 285-290.
- Surry, D. and Lin, J. X. (1993). The Effect of Surroundings and Roof Corner Geometric Modifications on Roof Pressures on Low-Rise Buildings, University of Western Ontario, Ontario, Canada, December 1993.
- Theurer, W. (1995). Point Sources in Urban Areas: Modeling of Neutral Gas Clouds with Semi-empirical Models, *Wind Climate in Cities*, Kluwer Academic Publishers, (Cermak et al., eds.) 485-502.
- Theurer, W., Bachlin, W. and Plate, E. J. (1992). A Model for the Calculation of Immisions by Accidentally Released Gas Plumes within Built-up Areas, *7th Int. Symposium on Loss Prevention and Safety Promotion in the Process Industries*, Taormina, Italy, May 4-8, 1992.

- Theurer, W., Baechlin, W. and Plate, E. J. (1992). Model Study of the Development of Boundary Layers Above Urban Areas, *Journal of Wind Engineering and Industrial Aerodynamics*, Vol. 41-44, 437-448.
- Wedding, J. B., Lombardi, D. J. and Cermak, J. E. (1977). A Wind Tunnel Study of Gaseous Pollutants in City Street Canyons, *APCA Journal*, Vol. 27 (6), 557-566.
- Wu, G. (1992). Wind Tunnel Simulation of Turbulence Structure and Dispersion Processes for Air Flow Over a Step Change of Surface Roughness. Ph.D. Thesis. Department of Civil Engineering, Colorado State University.
- Yang, B. T. and Meroney, R. N. (1972). Technical Report on Diffusion from an Instantaneous Point Source in a Neutrally Stratified Turbulent Boundary Layer with a Laser Light Scattering Probe, October, 1972, Project Thesis, College of Engineering, Colorado State University.
- Zhang, Y. Q., Huber, A. H., Arya, S. P. S. and Snyder, W. H. (1992). Numerical simulation to determine the effects of incident wind shear and turbulence level on the flow around a building, *J. of Wind Engineering*, Vol. 52, 261-266.

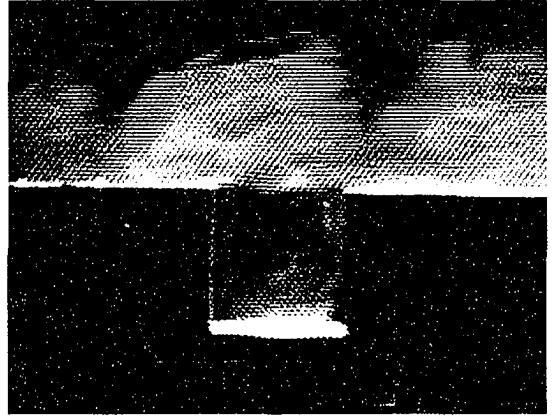
Appendix A

Flow Visualization Images

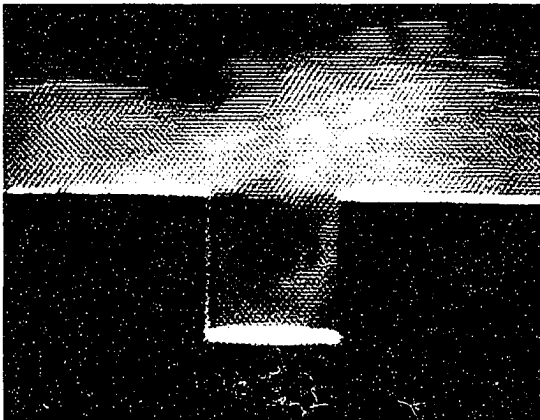
B/H=1



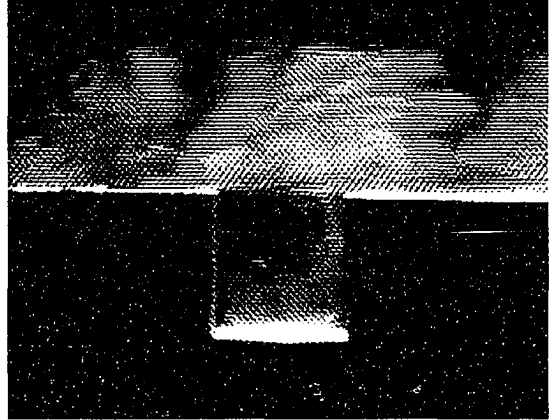
(1)



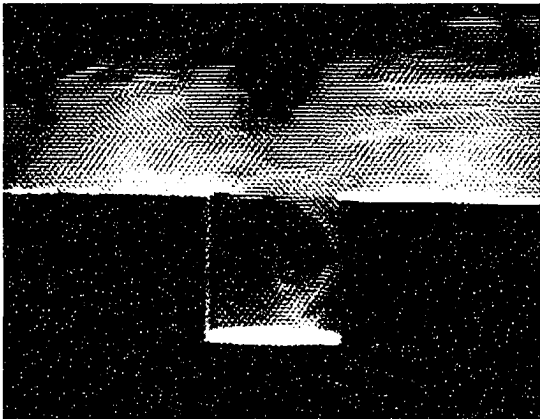
(4)



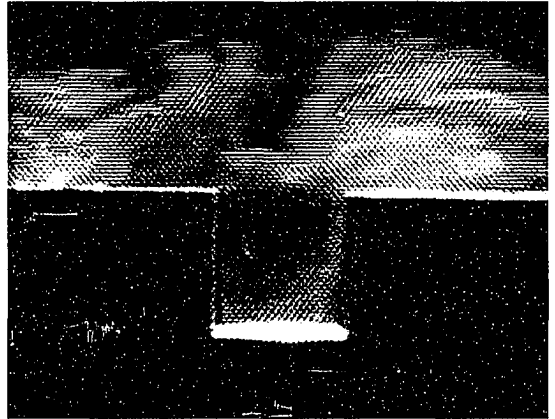
(2)



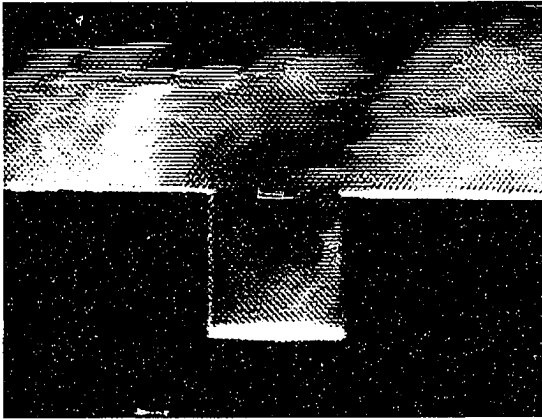
(5)



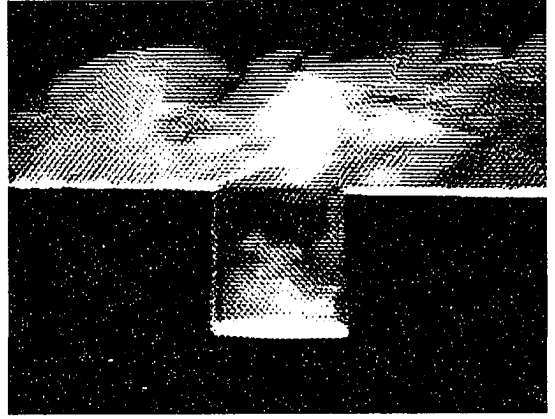
(3)



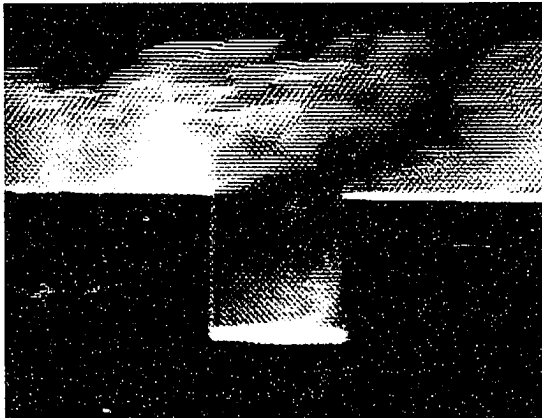
(6)



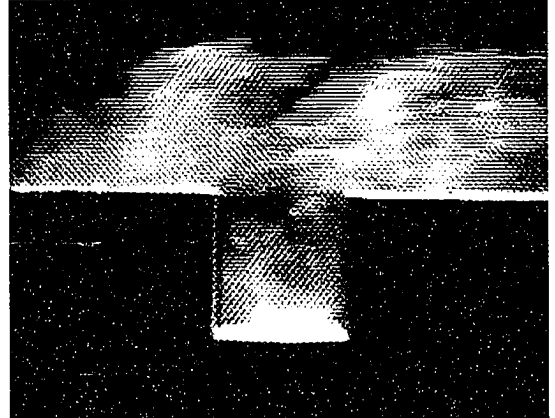
(7)



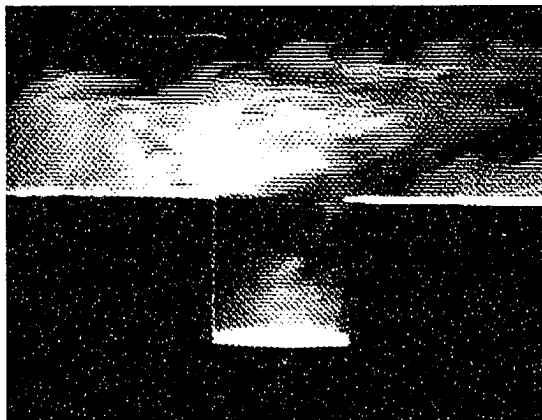
(10)



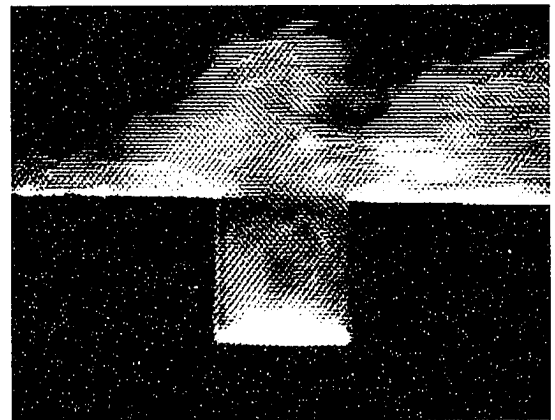
(8)



(11)

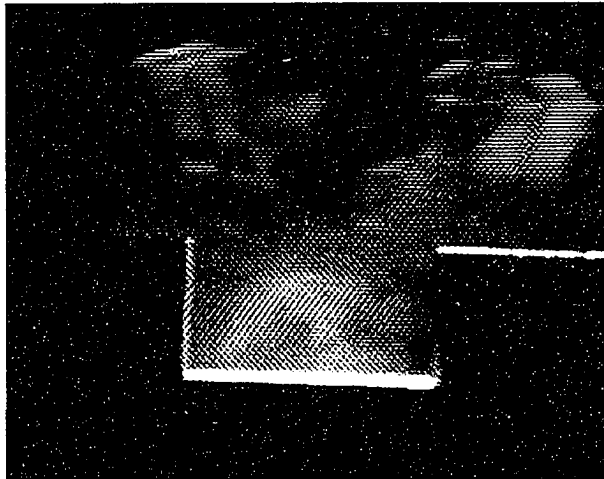


(9)

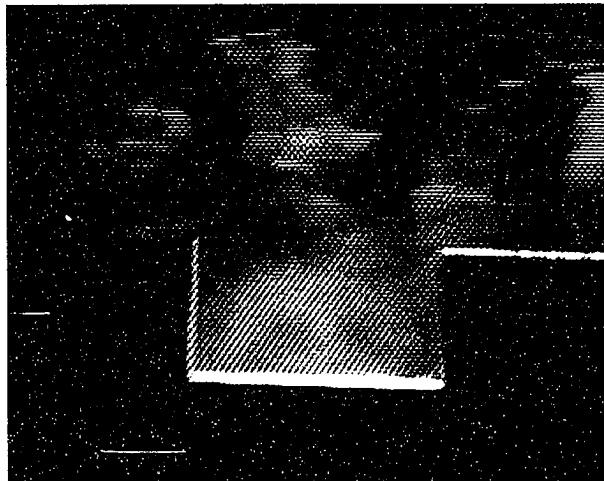


(12)

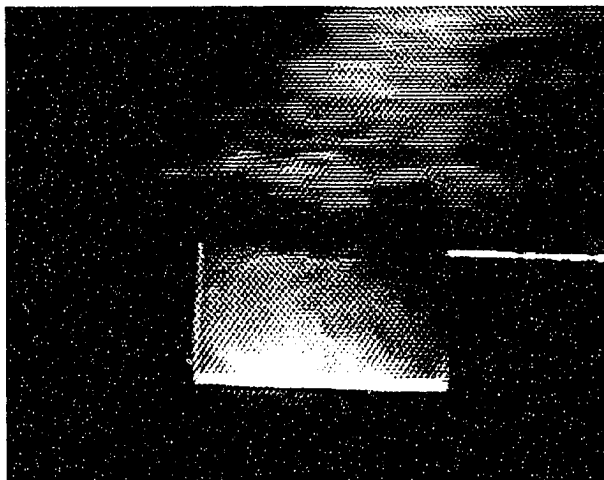
$B/H=2$



(1)

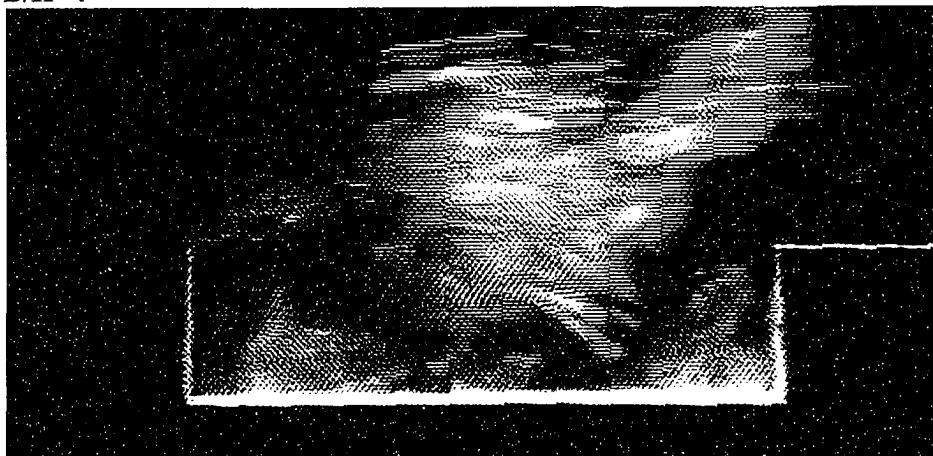


(2)

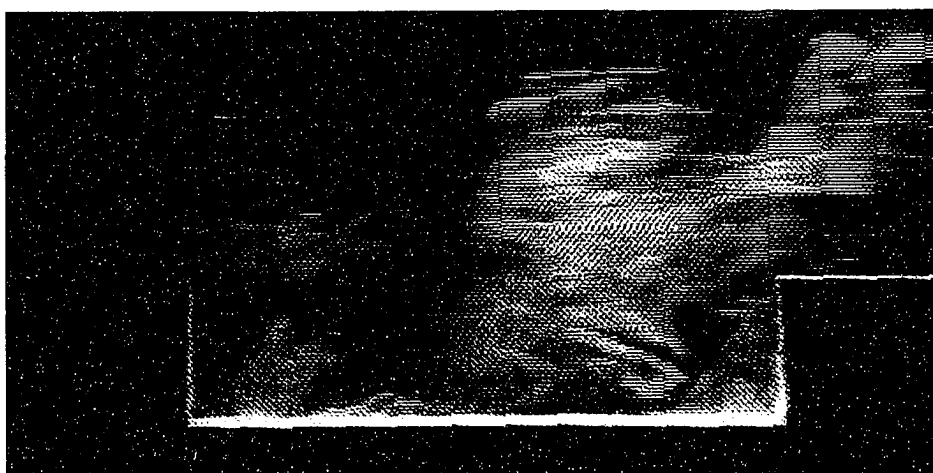


(3)

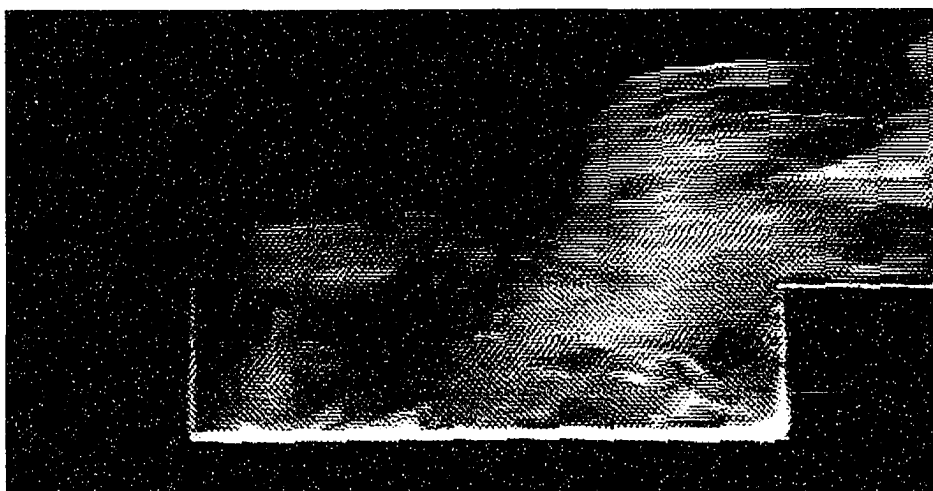
B/H=4



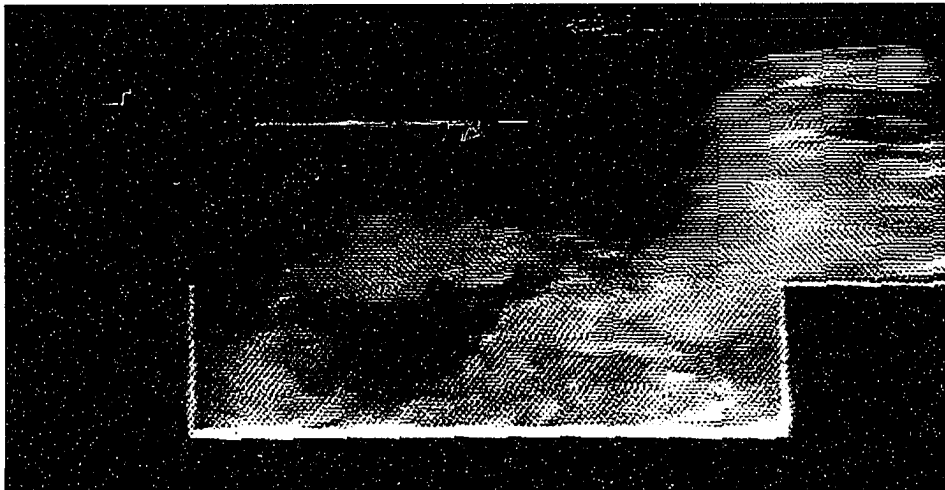
(1)



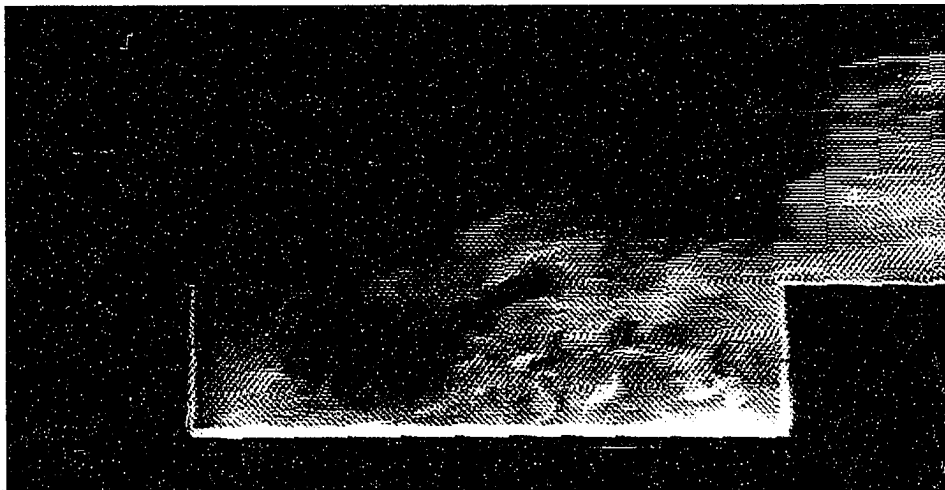
(2)



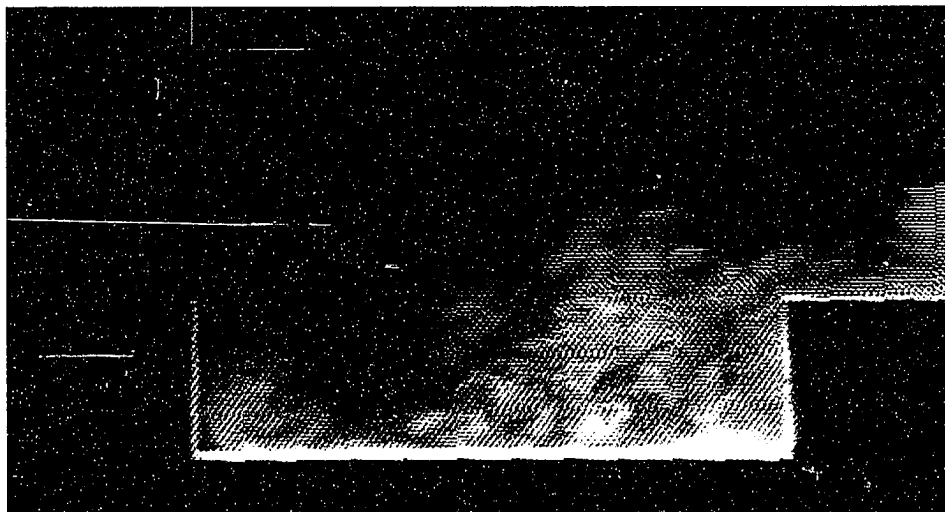
(3)



(4)

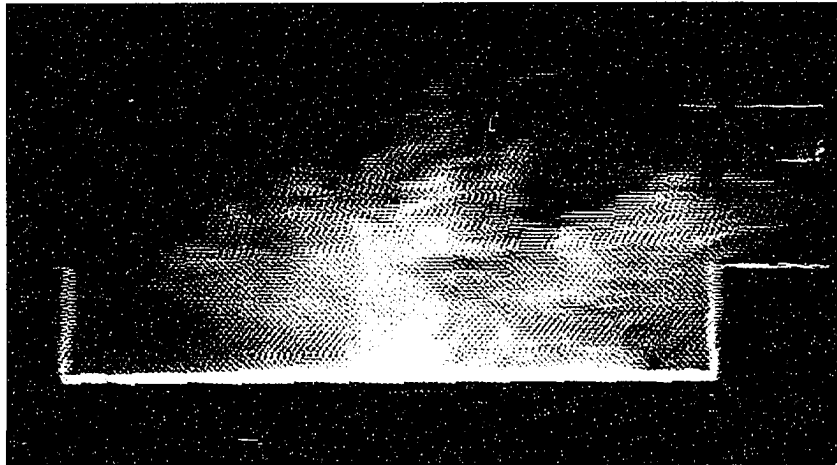


(5)

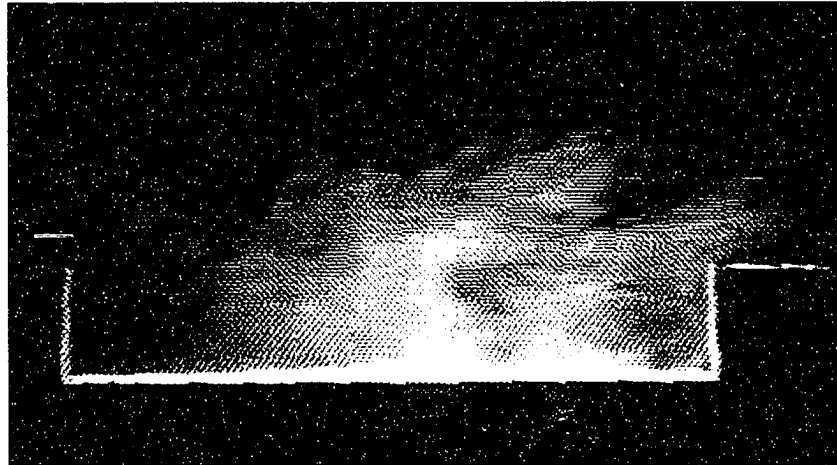


(6)

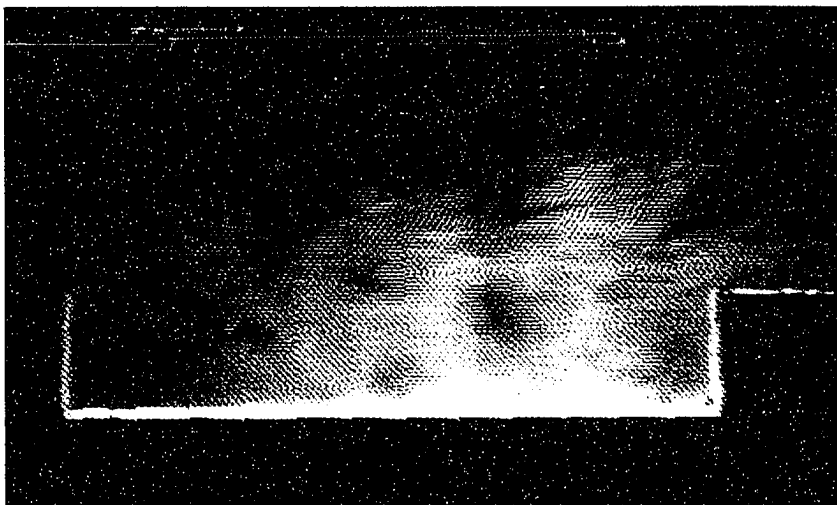
B/H=6



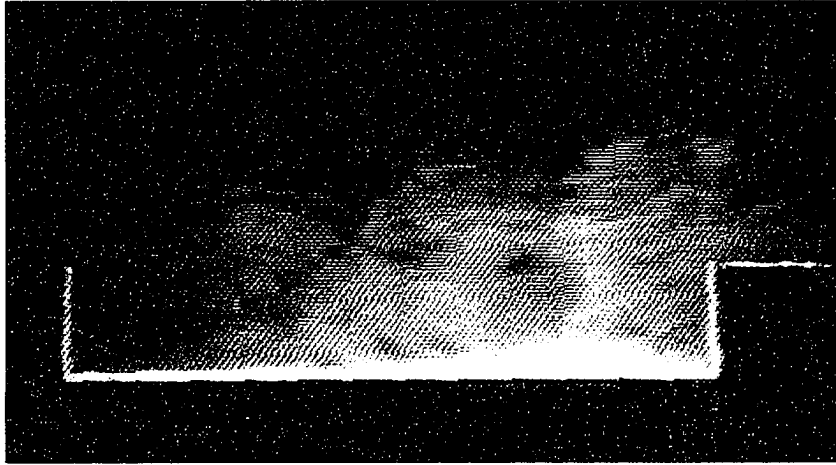
(1)



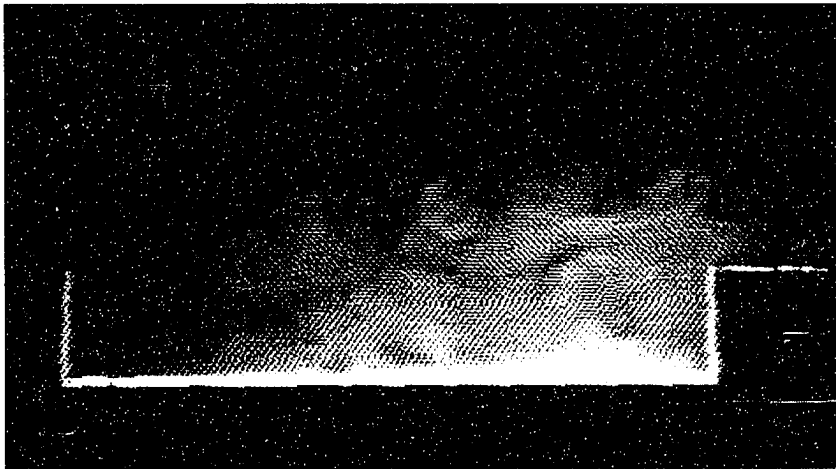
(2)



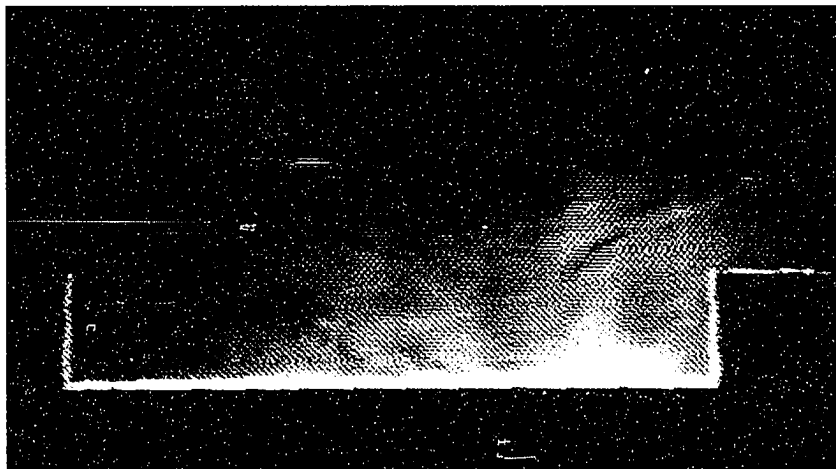
(3)



(4)



(5)



(6)

Appendix B

Velocity and Turbulence Intensity Profiles

This appendix includes five pages of data. Each data shows seven different velocity and turbulence intensity profile data with different rows of upwind buildings.

B/H=0.5 N=1			U(m/sec)				Height (cm)					
Point 1	Point 2		Point 3	Point 4	Point 5	Point 6	Point 7					
Height	U mean	u T.I.%	Height	U mean	u T.I.%	Height	U mean	u T.I.%	Height	U mean	u T.I.%	
1	1.7489	46.9921	9	8.07	27.8051	7.9808	26.7013	8.3448	25.4701	1	3.1028	44.6376
2	1.599	45.4378	10	8.5424	26.9915	8.8641	24.2176	8.9203	25.2115	2	3.9153	35.1703
3	1.4513	42.9929	11	9.0212	26.394	9.1357	23.8408	9.1879	24.6319	3	4.2745	32.2646
4	1.413	43.1804	12	9.436	25.1393	9.5836	23.8273	9.5532	24.4283	4	4.4817	31.4381
6	1.3687	41.5541	13	9.8708	24.238	9.8566	23.6799	10.1077	23.0646	6	5.2666	31.628
8	6.2837	36.7262	14	10.1619	22.3172	10.228	22.0949	10.0805	22.1909	8	6.1253	31.5748
10	8.3605	28.4887	16	10.7683	19.4375	10.5526	21.0081	10.704	20.6809	10	7.3742	29.3859
12	9.4855	25.327	18	11.3479	17.9976	11.1407	18.5018	11.0233	20.0981	12	8.9245	29.5017
15	10.8834	20.0191	20	11.6747	18.254	11.0014	19.0859	11.1668	19.0883	15	10.6524	21.8638
20	11.6437	17.0168	25	11.8105	17.3589	11.6846	17.513	11.7214	15.9669	20	11.6596	17.3304
30	12.0197	16.4654	30	12.1065	15.9854	11.8426	17.087	12.0703	16.8821	30	12.3104	17.0142
40	12.4695	16.2285	40	12.4986	15.5446	12.4548	15.7096	12.4893	15.4742	40	12.6748	15.667
50	13.0365	14.5458	50	12.9562	14.6594	12.9225	14.2668	13.0532	13.8048	50	13.0634	15.3511
60	13.2773	13.9695	60	13.4058	13.5321	13.2609	13.7775	13.176	14.074	60	13.4295	14.0409
80	13.8753	12.1815	80	13.7566	11.9721	13.7265	11.7552	13.6929	11.4852	80	14.035	11.3843
100	13.5553	10.818	100	13.6952	10.2525	13.6834	10.5618	13.5903	10.1958	100	13.8899	10.7974

B/H=0.5 N=2			U(m/sec)				Height (cm)					
Point 1	Point 2		Point 3	Point 4	Point 5	Point 6	Point 7					
Height	U mean	u T.I.%	Height	U mean	u T.I.%	Height	U mean	u T.I.%	Height	U mean	u T.I.%	
1	1.756	49.352	9	8.2764	26.4051	7.9602	26.2633	8.1951	25.3986	1	1.7403	49.1623
2	1.6299	45.9832	10	8.6617	26.1659	8.4926	25.2911	8.4951	24.0317	2	2.3655	46.6519
3	1.4519	42.8714	11	8.9556	25.7939	8.7376	25.0949	9.0237	23.9144	3	2.7557	41.6759
4	1.388	40.819	12	9.2968	24.9747	9.2466	24.5622	9.0076	24.0848	4	3.0236	41.8908
6	1.3599	41.5877	13	9.8218	22.9407	9.5096	24.0472	9.3944	23.4719	6	3.7395	40.864
8	6.1071	35.2153	14	9.9689	22.117	9.8026	24.7889	9.8742	23.2249	8	5.4812	35.7518
10	8.4223	26.3764	16	10.5059	21.7435	10.2432	21.9395	10.3291	21.4666	10	7.3247	29.0053
12	9.3437	25.1018	18	11.2401	19.5123	10.747	21.3679	10.7287	21.1971	12	8.3031	27.7299
15	10.2861	21.8669	20	11.3825	18.7119	11.3323	18.8323	11.0806	19.4818	15	9.9401	24.7884
20	11.2838	19.2851	25	11.6835	18.2767	11.7085	17.6168	11.5667	18.3626	20	11.0666	19.903
30	12.1028	16.8181	30	12.1173	16.8461	11.8912	17.2747	11.7605	17.1828	30	12.0232	16.9282
40	12.6507	15.6017	40	12.7441	16.5851	12.3023	16.4094	12.3554	15.9917	40	12.5807	15.9207
50	13.1549	14.6928	50	13.1228	14.4031	12.9976	14.8548	12.8288	14.829	50	12.9804	15.3906
60	13.4231	13.9771	60	13.4568	13.8078	13.289	13.7811	13.3026	13.3016	60	13.5541	13.6833
80	14.046	11.3859	80	13.9934	11.6195	13.8541	11.9424	13.5897	12.1208	80	13.9672	11.6826
100	13.8273	10.5899	100	13.7991	10.7564	13.649	10.3439	13.4941	10.4723	100	13.9827	11.1579

B/H=0.5 N=3			U(m/sec)				Height (cm)					
Point 1	Point 2		Point 3	Point 4	Point 5	Point 6	Point 7					
Height	U mean	u T.I.%	Height	U mean	u T.I.%	Height	U mean	u T.I.%	Height	U mean	u T.I.%	
1	1.732	46.3818	9	8.3	24.9465	7.9912	25.6985	8.3698	24.1642	1	2.0612	51.418
2	1.6133	44.1095	10	8.6445	24.713	8.6699	23.979	9.0071	21.6575	2	2.7125	42.7005
3	1.4984	41.7119	11	8.9609	24.6621	8.9114	23.7062	9.1864	22.3292	3	3.244	40.7851
4	1.4334	41.5166	12	9.2587	24.1944	9.4907	22.7659	9.5486	21.5948	4	3.4866	40.8719
6	1.3979	40.7771	13	9.4809	23.89	9.7233	22.4379	10.0122	21.0874	6	4.24	38.974
8	6.397	32.0886	14	10.0473	22.587	10.1692	22.017	10.1389	21.8985	8	6.1686	33.4
10	8.4872	25.7935	16	10.5303	21.1462	10.4988	21.5089	10.6837	21.0099	10	8.0048	26.8549
12	9.2745	24.673	18	10.5986	22.1436	10.7102	21.1674	11.0714	19.8261	12	8.8759	25.2613
15	10.2995	22.9572	20	11.1641	19.3868	11.4391	18.8036	11.2106	18.746	15	10.1042	22.6909
20	11.08	21.0367	25	11.7941	17.2395	11.7068	17.5543	11.9575	17.7581	20	11.4223	19.8784
30	12.1343	16.7147	30	12.0491	17.677	11.8701	18.0932	11.9771	17.4159	30	12.1812	16.698
40	12.6517	16.9041	40	12.5259	16.2386	12.3654	16.0499	12.7891	15.031	40	12.7256	15.303
50	13.0334	15.3125	50	13.0933	14.76	12.9708	15.5389	13.0057	14.6697	50	13.1214	14.7124
60	13.6173	13.4464	60	13.5941	13.4928	13.481	13.7741	13.4459	13.7239	60	13.5062	13.5326
80	14.0753	11.7562	80	14.0024	12.2223	13.9272	12.1884	13.8367	12.1281	80	14.0549	11.6063
100	13.859	10.8008	100	13.88	10.9904	13.7921	10.7531	13.6853	10.3596	100	13.9966	10.8915

B/H=0.5 N=8			U(m/sec)				Height (cm)					
Point 1	Point 2		Point 3	Point 4	Point 5	Point 6	Point 7					
Height	U mean	u T.I.%	Height	U mean	u T.I.%	Height	U mean	u T.I.%	Height	U mean	u T.I.%	
1	1.74	46.6559	9	8.6385	22.2586	8.687	21.7103	8.9584	21.9336	1	2.3488	49.2466
2	1.6282	42.6086	10	9.2831	20.8396	9.3895	20.9737	9.4564	20.4154	2	3.4194	38.1641
3	1.4653	41.162	11	9.7172	20.264	9.7557	20.9482	9.6992	19.8947	3	3.8357	35.6553
4	1.4207	42.2611	12	9.9376	21.0032	9.9489	20.2352	9.9317	19.8096	4	4.5029	33.3339
6	1.3725	40.5847	13	10.3141	19.2165	10.2176	20.2553	10.4766	18.6235	6	5.1219	32.5865
8	6.9786	27.6569	14	10.576	19.2636	10.3231	20.4147	10.411	18.4813	8	6.7559	27.8624
10	9.1695	21.7295	16	10.9464	19.0887	11.0438	19.0662	10.8692	19.0334	10	8.6407	22.9658
12	9.8914	20.6342	18	11.0448	19.2354	11.1295	17.812	11.1621	18.0582	12	9.7578	21.344
15	10.7267	19.1274	20	11.2406	18.4188	11.4325	18.1885	11.3799	18.5065	15	10.7647	19.5854
20	11.0842	19.3125	25	11.9423	17.7881	11.8422	17.2032	11.9744	16.7555	20	11.2031	18.822
30	12.0771	16.494	30	12.2101	16.3039	12.1743	16.4338	12.1641	17.0614	30	11.8763	17.2842
40	12.8447	15.2822	40	12.5952	16.2556	12.4489	16.1798	12.5037	16.5941	40	12.4439	16.8793
50	13.1101	14.8997	50	13.2654	14.713	13.0892	14.7009	12.8169	15.5253	50	13.1425	14.1599
60	13.5358	13.743	60	13.6527	13.6297	13.4238	14.1965	13.4577	13.5386	60	13.5083	14.2157
80	14.0773	11.8927	80	14.1528	11.6136	14.0604	11.6903	13.783	11.7493	80	14.0469	12.0023
100	13.9342	10.5439	100	13.9741	10.2567	13.8403	10.7835	13.5943	10.8964	100	14.1532	10.6754

B/H=1		N=1		Point 1		Point 2		Point 3		Point 4		Point 5		Point 6		Point 7		
Height	U mean	u t.I.%	Height	U mean	u t.I.%	U mean	u t.I.%	U mean	u t.I.%	U mean	u t.I.%	Height	U mean	u t.I.%	U mean	u t.I.%	U mean	u t.I.%
1	3.5607	31.8593	9	8.3611	28.2943	8.2891	26.6271	8.6989	24.3735	1	4.2488	41.5671	3.4305	48.188	3.6984	49.3537		
2	2.7056	37.6862	10	9.0685	24.9885	9.0713	24.323	9.2381	22.9216	2	4.6666	38.5661	3.9838	45.3751	4.1429	44.1348		
3	2.338	41.4485	12	9.6239	22.8689	9.7885	23.1179	9.8865	21.7698	3	5.1896	33.8346	4.6807	39.9013	4.4468	40.6909		
4	2.1378	39.9047	14	10.3682	21.4354	10.3556	21.2782	10.2898	20.9794	4	5.542	31.377	4.8694	38.6321	4.8892	39.0436		
6	1.7351	42.6822	16	10.7483	19.4712	10.6878	19.6736	10.693	19.1376	6	6.6508	30.4908	6.0563	33.2423	5.687	37.107		
8	6.4502	35.9922	18	11.02	18.1552	11.1483	18.1762	11.1421	18.2301	8	7.5526	28.8712	7.1242	28.559	7.171	29.6383		
10	8.8517	24.8487	20	11.3393	17.9681	11.3774	17.5322	11.0956	17.7147	10	8.7826	26.4826	8.1076	27.6615	7.9211	27.632		
12	9.4374	24.2499	25	11.639	16.904	11.7756	17.3054	11.6444	16.7578	12	9.8708	23.0239	9.3442	23.9846	8.9316	25.0564		
15	10.5552	20.964	30	12.0017	16.1011	11.8999	16.44	11.8901	16.433	15	10.7842	19.8502	10.3534	21.4737	10.2787	21.669		
20	11.3968	17.2099	40	12.4784	15.3733	12.524	15.1397	12.3815	15.3084	20	11.4491	17.1143	11.2156	17.6411	11.1723	18.3313		
30	11.9455	16.6797	50	12.9857	14.6052	12.9173	14.2828	12.7144	14.4882	30	12.0967	16.889	11.8363	16.1507	11.8709	16.4259		
40	12.3246	15.9363	60	13.1906	13.549	13.0548	14.1983	13.0927	13.555	40	12.466	15.7142	12.4474	15.4062	12.3511	15.239		
50	12.8615	14.6661	80	13.6623	11.2682	13.5691	11.6106	13.4307	11.6715	50	12.9234	14.9217	12.7959	14.6358	12.5824	14.8515		
60	13.2531	13.7683	100	13.3964	10.5753	13.3353	10.5639	13.1175	10.4292	60	13.2129	13.468	13.1806	13.4953	13.0464	13.2383		
80	13.637	11.357								80	13.6144	12.1412	13.5821	11.3073	13.3291	11.8839		
100	13.3617	11.0257								100	13.5981	10.5497	13.4642	10.7766	13.257	10.7006		

B/H=1		N=2		Point 1		Point 2		Point 3		Point 4		Point 5		Point 6		Point 7		
Height	U mean	u t.I.%	Height	U mean	u t.I.%	U mean	u t.I.%	U mean	u t.I.%	U mean	u t.I.%	Height	U mean	u t.I.%	U mean	u t.I.%	U mean	u t.I.%
1	3.1943	34.5641	9	8.0073	27.782	8.2481	26.0759	8.1365	25.2778	1	3.3115	47.218	3.3807	49.543	3.4663	51.6283		
2	2.4115	39.6445	10	8.7284	24.2781	8.6358	25.2655	8.4947	26.0264	2	3.5947	46.4237	3.6256	47.22	4.0241	43.5826		
3	2.0266	41.4758	12	9.6146	22.8626	9.4223	23.1023	9.2925	23.3691	3	4.1335	41.992	3.9908	42.9714	4.6945	40.1568		
4	1.7519	42.1143	14	9.6742	23.2113	9.8907	22.7661	9.889	22.361	4	4.8752	37.3325	4.7246	38.5974	4.6682	40.9378		
6	1.53	43.0181	16	10.4553	21.6874	10.7253	20.6201	10.4251	22.1386	6	5.3199	34.0951	5.2609	35.75	5.5949	36.4469		
8	6.3714	34.3885	18	10.8535	19.8846	10.8711	19.9243	10.6843	19.983	8	6.4282	30.5611	6.5528	32.0983	6.5443	33.2443		
10	8.9374	24.6417	20	11.0428	19.2264	11.1545	19.3847	11.077	19.0782	10	7.3438	29.6527	7.5779	28.0602	8.0282	27.1078		
12	9.5544	23.0633	25	11.7632	16.7645	11.6048	17.4559	11.7263	17.0066	12	8.5535	26.3781	8.5297	25.2674	8.6077	24.7881		
15	10.2089	21.4855	30	11.8642	16.2226	11.9888	16.4976	11.8981	16.6919	15	9.6636	23.3134	9.7819	21.8819	9.6357	22.4797		
20	11.1714	18.5186	40	12.587	15.7327	12.4807	15.7153	12.4784	15.2736	20	11.0227	19.5654	10.9145	18.9346	10.974	19.3263		
30	11.8578	17.0436	50	13.0247	13.841	12.766	14.4947	12.731	14.5291	30	11.7282	17.0157	11.9004	16.3816	11.7361	16.5767		
40	12.3707	15.6524	60	13.2378	13.347	13.0161	14.0814	13.1907	13.1301	40	12.1349	16.4006	12.0956	15.8009	12.1113	15.5979		
50	12.8579	14.8416	80	13.5908	12.3214	13.67	11.3299	13.487	11.3573	50	12.6756	14.9085	12.7315	14.1345	12.5793	14.4617		
60	13.2271	13.5882	100	13.3966	10.8435	13.3378	10.3821	13.2419	10.6552	60	13.0924	13.4842	13.0443	13.3191	12.8104	13.3082		
80	13.7485	11.8102								80	13.5033	11.1761	13.3292	11.5811	13.2438	11.798		
100	13.5208	10.4193								100	13.4173	10.8006	13.3418	10.6168	13.23	10.7498		

B/H=1		N=3		Point 1		Point 2		Point 3		Point 4		Point 5		Point 6		Point 7		
Height	U mean	u t.I.%	Height	U mean	u t.I.%	U mean	u t.I.%	U mean	u t.I.%	U mean	u t.I.%	Height	U mean	u t.I.%	U mean	u t.I.%	U mean	u t.I.%
4	1.8373	44.1087	9	7.8502	27.9297	7.688	26.8118	8.1296	25.0859	1	3.4725	46.0271	3.4489	49.8204	4.2134	41.6744		
6	1.4574	44.2273	10	8.2218	26.3717	8.4753	25.8929	8.9234	22.7438	2	3.9269	42.9448	3.919	44.355	4.522	41.5262		
8	5.2956	37.7044	12	9.3342	23.3126	9.1453	24.0382	9.3261	22.3951	3	4.2264	42.5452	4.1786	42.1157	4.8745	39.8191		
10	8.2155	26.7177	14	9.6939	22.6292	9.6219	23.5265	9.7181	21.9303	4	4.4329	39.5975	4.6897	38.058	5.2142	36.9519		
12	9.0853	24.9677	16	10.0511	22.1749	10.2734	20.9958	10.5617	19.581	6	5.2218	36.1271	5.5071	33.5208	5.7635	35.8509		
15	9.8909	22.3846	18	10.8012	20.0875	10.5175	21.4442	10.482	20.8173	8	6.1605	33.8174	6.41	31.2267	7.0286	29.9536		
20	10.7185	20.2135	20	10.7849	20.3843	10.7355	20.1114	10.8963	19.3153	10	7.1748	29.7921	7.6299	26.8935	8.2499	24.6881		
25	11.191	18.4364	25	11.2096	18.392	11.538	18.4815	11.4167	17.9074	12	8.2976	26.5234	8.5834	25.373	8.657	24.2512		
30	11.7483	16.9549	30	11.778	17.8779	11.6951	16.9587	11.7278	16.8915	15	9.2685	23.1187	9.5864	22.1413	9.5987	22.2258		
40	12.2562	16.168	40	12.4385	15.3773	12.138	16.2165	12.1112	15.7882	20	10.6054	20.5608	10.6599	19.3577	10.6047	19.9534		
50	12.4802	15.4428	50	12.6233	15.0432	12.5257	14.6807	12.3922	15.2312	30	11.8141	17.4257	11.6339	17.4185	11.5225	17.9087		
60	12.9298	13.8549	60	12.9265	14.4094	12.9569	13.7069	12.8738	13.871	40	12.2841	15.3439	12.1836	15.2277	11.9993	15.7107		
80	13.4488	11.3913	80	13.5705	11.4097	13.3961	11.3321	13.3244	12.0709	50	12.5967	15.1331	12.6578	13.8731	12.2337	14.834		
100	13.3771	11.0637	100	13.338	10.9227	13.108	10.8268	12.9953	10.9256	60	12.9572	13.6707	12.8529	13.6812	12.6485	13.5191		
										80	13.374	11.7093	13.1623	11.7627	13.083	11.7809		
										100	13.2555	10.8067	13.1379	10.7245	13.0235	10.3717		

B/H=1		N=8		Point 1		Point 2		Point 3		Point 4		Point 5		Point 6		Point 7		
Height	U mean	u t.I.%	Height	U mean	u t.I.%	U mean	u t.I.%	U mean	u t.I.%	U mean	u t.I.%	Height	U mean	u t.I.%	U mean	u t.I.%	U mean	u t.I.%
1	3.6707	31.0033	9	8.1685	25.6816	8.0941	24.0764	8.8891	23.0861	1	4.0537	44.2291	4.1111	45.7349	5.0279	38.9074		
2	2.6921	37.0512	10	8.8014	22.2119	8.8146	23.0246	9.2321	21.7213	2	4.5069	43.8988	4.5968	41.9317	5.3936	35.838		
3	2.2771	39.538	12	9.381	21.3763	9.6784	20.8321	9.7973	20.6486	3	5.0627	39.1357	4.938	38.2469	5.8747	33.2826		
4	2.0207	43.1905	14	10.2037	19.0815	10.2065	20.4695	10.4848	19.6359	4	5.2222	36.4614	5.2339	35.2322	6.0686	30.995		
5	1.6264	46.647	16	10.2388	20.3315	10.4688	19.0566	10.7328	19.272	6	6.0255	30.2487	6.2292	31.0276	6.4775	31.5633		
6	1.5234	45.295	18	10.519	19.2689	10.7121	19.0054	10.944	18.5609	8	6.673	29.8473	7.1722	29.0174	7.5326	27.3122		
7	2.2106	41.8383	20	10.9711	17.5479	11.2588	17.6401	11.2683	18.0539	10	7.9576	26.1435	8.2632	24.2064	8.1353	24.8538		
8	6.0643	33.642	25	11.5989	16.8248	11.4729	17.4473	11.5191	16.9703	12	8.9267	22.3876	9.1198	22.4595	9.1446	22.216		
9	8.7137	23.498	30	11.9045	16.129	11.7273	16.7789	12.1093	16.0085	15	9.6497	21.0821	9.796	21.3509	9.9967	20.5611		
10	8.8361	23.8498	40	12.2809	15.4399	12.3422	15.5473	12.5168	14.6384	20	10.4683	18.8339	10.758	18.8653	10.651	19.5799		
15	10.3008	20.6243	50	12.7053	14.0241	12.6584	14.4964	12.7716	14.8018	30	11.5459	16.8583	11.7652	15.8818	11.406	17.1797		
20	11.0655	18.7856	60	12.8946	13.537	12.8963	13.7517	13.0827	13.3059	40	11.9437	16.0148	12.0804	15.5339	11.8761	16.4337		
30	11.9967	16.679	80	13.3904	11.9796	13.3996	11.3335	13.4389	11.8936	50	12.5087							

B/H=2			N=1			Point 3			Point 4			Point 5			Point 6			Point 7		
Point 1	Point 2		Point 3	Point 4	Point 5	Point 6	Point 7													
Height	U mean	u t.1.%	Height	U mean	u t.1.%	U mean	u t.1.%	U mean	u t.1.%	U mean	u t.1.%	U mean	u t.1.%	U mean	u t.1.%	U mean	u t.1.%	U mean	u t.1.%	
1	4.3633	39.593	9	8.7708	28.7384	8.1018	27.0318	8.4906	25.1528	1	4.9726	38.9265	4.7941	46.6563	4.9279	40.6706				
2	3.3737	40.01	10	8.9668	26.6934	8.764	27.3084	9.0567	24.4115	2	5.548	37.9881	5.3479	43.8228	5.4138	39.8084				
3	3.055	42.6678	11	9.6478	23.313	9.4094	25.3919	9.4957	24.8163	3	6.1153	35.2521	5.4038	45.7003	5.9136	39.1221				
4	2.9787	50.7155	12	9.9438	23.1125	9.633	24.943	9.5858	23.0669	4	6.7423	35.2477	6.1923	42.0541	6.306	36.6586				
6	3.9504	55.1937	13	10.1316	21.8636	9.9978	23.3174	10.1505	22.3592	6	7.8526	30.4965	7.2255	35.7342	7.2202	32.1485				
8	7.3648	36.2242	14	10.533	20.6926	10.2815	21.1439	10.4891	21.608	8	9.1809	25.0075	8.4792	28.6075	8.0702	30.3514				
10	9.3845	24.5054	16	10.949	19.8139	11.0885	19.6942	10.9421	19.2163	10	9.5541	22.3342	9.2576	25.3131	8.705	27.8312				
12	9.9398	23.0872	18	11.0774	18.2658	11.0893	19.3455	11.1951	18.766	12	10.2009	20.625	9.8267	23.52	9.7866	24.0759				
15	10.8388	19.9187	20	11.5621	18.4413	11.4479	17.5855	11.2762	18.1191	15	10.7945	18.6396	10.2616	21.203	10.3901	20.4928				
20	11.3032	18.2098	25	11.8449	16.7337	11.7123	16.7634	11.7351	16.7712	20	11.1591	17.5941	11.0719	18.1402	10.8556	18.5977				
30	12.0045	16.2372	30	12.1407	16.8152	12.2484	15.8336	12.3053	16.0072	30	11.9212	16.7196	11.7871	16.4201	11.4486	16.5485				
40	12.616	15.6282	40	12.6409	15.6682	12.4829	15.2948	12.1792	15.9218	40	12.209	16.2086	12.1902	15.3825	11.8915	16.0521				
50	12.8655	14.7882	50	12.9	15.2107	12.9382	14.6786	13.0426	14.58	50	12.8806	14.4612	12.531	14.9107	12.3332	14.9193				
60	13.3295	13.6765	60	13.5571	13.2375	13.2599	13.984	13.2211	14.1792	60	13.0914	14.808	12.9779	13.7448	12.7678	13.8091				
80	13.8438	11.8615	80	13.7596	12.1165	13.7216	11.4068	13.6962	11.9817	80	13.703	12.1277	13.3552	12.5507	13.1771	11.8759				
100	13.8059	10.5472	100	13.7127	10.3503	13.5466	10.5174	13.467	10.8095	100	13.7466	10.9775	13.3163	11.5454	13.2937	11.4516				

B/H=2			N=2			Point 3			Point 4			Point 5			Point 6			Point 7		
Point 1	Point 2		Point 3	Point 4	Point 5	Point 6	Point 7													
Height	U mean	u t.1.%	Height	U mean	u t.1.%	U mean	u t.1.%	U mean	u t.1.%	U mean	u t.1.%	U mean	u t.1.%	U mean	u t.1.%	U mean	u t.1.%	U mean	u t.1.%	
1	4.216	41.3835	9	8.3689	30.271	7.7821	30.7837	8.2391	27.7368	1	4.4283	45.7824	4.4577	53.1957	4.8474	43.9406				
2	3.2125	42.3965	10	8.6652	27.4723	8.4755	28.6342	8.9953	25.5117	2	4.8976	42.8386	5.1388	49.6527	5.3825	41.5822				
3	2.8975	43.6337	11	8.9964	25.4308	8.8989	27.0737	8.8293	27.0549	3	5.2115	41.9088	5.4318	48.8767	5.5873	39.9608				
4	2.7959	47.7886	12	9.3604	24.0445	9.3296	25.4743	9.5681	23.7302	4	5.7122	40.687	5.7219	44.1299	5.9287	39.922				
6	3.5759	57.1057	13	9.726	23.5771	9.8028	24.2553	9.6456	23.6633	6	6.8288	34.5232	6.6976	39.2942	6.8865	35.7572				
8	6.959	38.877	14	10.1529	22.6429	10.1539	22.4635	10.0519	23.1589	8	7.8061	28.856	7.6713	32.0307	7.7921	30.5782				
10	8.6787	27.8991	16	10.5501	20.7333	10.3856	21.9379	10.7597	20.4855	10	8.3115	28.6479	8.2348	29.2526	8.8031	26.9443				
12	9.5325	24.2656	18	10.8525	19.7679	10.9105	19.833	10.7924	20.7787	12	9.0639	26.8179	9.1647	26.0591	9.5081	23.895				
15	10.4257	21.884	20	11.1441	19.3779	11.201	19.5221	11.155	19.8376	15	10.2156	21.1302	10.178	22.437	10.2066	23.3149				
20	11.2993	18.6037	25	11.6346	17.4905	11.67	17.6535	11.6899	17.7579	20	10.9453	19.3313	10.9324	19.3749	10.6392	20.3513				
30	12.3544	16.1612	30	11.6481	17.9954	11.9764	17.5886	11.91	16.5057	30	11.6581	16.6517	11.8195	17.0393	11.8961	17.3815				
40	12.5771	15.661	40	12.3106	16.2966	12.4762	15.9101	12.4564	16.0474	40	12.1228	15.6751	12.0583	16.1761	12.2475	15.4814				
50	12.834	15.2836	50	13.0457	14.6773	12.9912	14.9141	12.7969	15.2284	50	12.699	15.014	12.5972	15.596	12.6149	15.0738				
60	13.3557	14.2411	60	13.3561	14.1062	13.4461	13.2529	13.3543	13.4576	60	13.1675	13.8644	13.0426	13.6715	13.085	13.8231				
80	13.9039	11.8014	80	13.955	12.0766	13.8452	11.7947	13.6253	11.9283	80	13.6052	12.3593	13.4973	12.6354	13.3905	12.5093				
100	13.7531	10.3857	100	13.6255	10.6891	13.632	10.4267	13.3929	10.7445	100	13.7299	11.1613	13.6028	10.6302	13.4587	11.2215				

B/H=2			N=3			Point 3			Point 4			Point 5			Point 6			Point 7		
Point 1	Point 2		Point 3	Point 4	Point 5	Point 6	Point 7													
Height	U mean	u t.1.%	Height	U mean	u t.1.%	U mean	u t.1.%	U mean	u t.1.%	U mean	u t.1.%	U mean	u t.1.%	U mean	u t.1.%	U mean	u t.1.%	U mean	u t.1.%	
1	4.0998	43.32	9	8.4685	31.01	7.0282	33.062	8.3005	27.1065	1	4.318	45.8444	4.4	51.15	5.2035	43.2607				
2	3.1647	44.367	10	8.5081	29.5199	8.2099	29.4378	9.0192	25.055	2	4.8293	44.3415	4.7347	53.0547	5.3769	41.116				
3	2.793	43.4282	11	8.8975	27.2618	8.7878	29.0454	8.8407	25.9483	3	5.2072	42.647	5.3492	48.4269	5.545	44.1128				
4	2.5884	49.124	12	9.1189	25.805	8.9942	26.6274	9.5152	24.86	4	5.4137	42.1738	6.2974	43.9154	5.9782	39.3394				
6	3.3573	57.1824	13	9.4465	24.6776	9.5777	24.3617	9.7445	24.116	6	6.5197	33.6888	6.9752	38.607	6.9233	36.3172				
8	6.7831	39.3202	14	9.5742	23.8337	9.8641	24.845	9.9953	23.2913	8	7.4141	29.6015	7.4174	32.4379	7.8195	31.4173				
10	8.9588	26.4541	16	10.1881	22.0727	10.1626	23.3283	10.5074	21.5438	10	8.2183	29.1968	8.2878	29.2662	8.4212	29.6702				
12	9.4046	25.0047	18	10.4598	21.5999	10.7983	20.1341	10.7095	20.7099	12	8.9457	27.7284	9.3204	25.8455	9.1285	26.921				
15	10.1938	22.7693	20	10.8713	19.6068	10.9949	20.8206	11.1854	19.3348	15	9.9095	23.3803	10.0171	22.19	10.129	23.7465				
20	11.1502	19.5882	25	11.4939	18.1219	11.5746	18.5776	11.763	17.6525	20	11.0197	19.3684	10.8812	20.7458	10.7381	21.4411				
30	11.9397	17.9532	30	12.014	16.6876	12.1593	16.0301	11.9848	16.5455	30	11.6986	16.8028	12.1667	17.2987	11.8295	17.1166				
40	12.2191	16.281	40	12.4853	16.4463	12.6615	15.1798	12.5414	16.3392	40	12.1538	16.4124	12.4985	15.138	12.2707	15.8314				
50	12.8235	15.3431	50	12.982	14.9781	12.9601	14.4955	12.8401	14.7049	50	12.9114	14.9006	12.6969	14.7272	12.8024	14.6182				
60	13.2206	13.8812	60	13.4253	13.501	13.228	13.8278	13.1043	14.4989	60	13.3175	13.6836	13.2956	13.5791	12.9058	13.9797				
80	13.862	12.0316	80	13.6742	11.5131	13.7692	11.5226	13.5546	12.0222	80	13.8178	12.2705	13.518	12.4653	13.4206	12.2783				
100	13.689	10.6309	100	13.537	10.801	13.5861	10.5119	13.4985	10.5322	100	13.8892	10.6842	13.7357	10.7002	13.5001	10.8906				

B/H=2			N=8			Point 3			Point 4			Point 5			Point 6			Point 7		
Point 1	Point 2		Point 3	Point 4	Point 5	Point 6	Point 7													
Height	U mean	u t.1.%	Height	U mean	u t.1.%	U mean	u t.1.%	U mean	u t.1.%	U mean	u t.1.%	U mean	u t.1.%	U mean	u t.1.%	U mean	u t.1.%	U mean	u t.1.%	
1	4.14	41.8319	9	8.3308	31.277	7.5143	28.7001	7.924	28.0955	1	5.395	38.1724	5.4366	42.549	5.7359	40.7602				
2	3.1791	40.6853	10	8.5905	28.708	8.418	26.8788	8.5106	27.4482	2	5.5159	40.5552	5.5522	44.9731	5.6501	41.9701				
3	2.8481	45.2728	11	9.0014	25.0943	8.6342	27.1525	8.9644	24.6722	3	5.8325	41.1336	6.1679	39.9598	6.4581	36.5811				
4	2.5709	46.7591	12	9.1649	26.2561	9.0129	26.6164	9.0762	25.5792	4	6.3238	38.3315	6.1589	42.7199	7.0707	31.8339				
6	3.6203	57.2176	13	9.809	23.5897	9.4856	24.0686	9.5937	23.1215	6	6.7187	35.1577	7.2527	35.6306	7.2592	32.1414				

B/H=4 N=1																					
Point 1			Point 2			Point 3			Point 4			Point 5			Point 6			Point 7			
Height	U mean	u t.1.1%	Height	U mean	u t.1.1%	U mean	u t.1.1%	U mean	u t.1.1%	U mean	u t.1.1%	Height	U mean	u t.1.1%	U mean	u t.1.1%	U mean	u t.1.1%	U mean	u t.1.1%	
1	2.3991	45.421	9	9.2753	27.3752	7.0926	33.1483	8.2135	25.3064	6.1369	29.4378	6.8184	27.0375	6.2478	31.7252	6.9433	29.3845	6.2478	31.7252	6.9433	29.3845
2	2.5408	46.0268	10	9.2684	24.758	8.1803	29.6856	8.6615	24.7135	7.4428	27.2521	7.3305	25.8524	6.9433	29.3845	7.2585	29.63	7.2585	29.63	7.2585	29.63
3	2.7901	47.8091	11	9.2698	24.7488	8.4548	30.4473	8.9642	25.3004	7.4957	25.9644	7.9654	24.8495	7.2585	29.63	7.2585	29.63	7.2585	29.63	7.2585	29.63
4	2.9218	50.2753	12	9.4848	24.0763	9.1392	27.4115	9.2992	25.2393	8.0634	25.5173	8.3293	24.2582	7.7583	27.4598	7.7583	27.4598	7.7583	27.4598	7.7583	27.4598
6	4.1147	54.8328	13	9.7087	23.8014	9.7305	25.3442	9.6609	24.1615	8.7258	23.2369	8.7947	22.4514	8.4478	25.1073	8.4478	25.1073	8.4478	25.1073	8.4478	25.1073
8	6.2628	42.6166	14	10.2595	22.7993	10.1725	23.6675	10.2553	22.1516	9.2396	21.0528	9.5615	20.5269	9.2347	22.5438	9.2347	22.5438	9.2347	22.5438	9.2347	22.5438
10	8.3637	31.9054	16	10.9218	20.7934	10.5461	21.7352	10.4451	20.605	9.6697	19.781	9.7803	20.3042	9.6048	20.0958	9.6048	20.0958	9.6048	20.0958	9.6048	20.0958
12	9.2073	25.5711	18	11.0319	19.5225	11.1976	19.1278	10.7857	19.1616	9.9549	19.2156	10.0258	19.724	10.0637	19.5342	10.0637	19.5342	10.0637	19.5342	10.0637	19.5342
15	10.1421	22.3738	20	11.4291	17.6688	11.3727	18.472	11.2156	18.6417	10.1435	19.1927	10.57	18.6493	10.3707	19.4469	10.3707	19.4469	10.3707	19.4469	10.3707	19.4469
20	10.7999	18.53	25	11.7075	17.4139	11.588	17.6118	11.4717	17.8669	10.6764	18.6401	10.7869	18.4232	10.8748	17.9395	10.8748	17.9395	10.8748	17.9395	10.8748	17.9395
30	11.8069	16.525	30	12.1675	16.8529	11.8752	17.4101	11.6995	17.0967	11.1706	17.7723	11.2605	17.3345	11.3403	17.1275	11.3403	17.1275	11.3403	17.1275	11.3403	17.1275
40	11.8761	17.3094	40	12.571	15.974	12.3813	16.218	12.4485	15.1811	10.4451	15.1811	11.8781	16.9901	11.6278	16.4397	11.6278	16.4397	11.6278	16.4397	11.6278	16.4397
50	12.6024	15.666	50	12.9272	14.9821	12.7813	15.9007	12.7349	14.9666	10.2364	15.937	12.2801	15.25	11.993	15.8906	11.993	15.8906	11.993	15.8906	11.993	15.8906
60	13.0295	14.3541	60	13.2152	14.5702	13.3105	14.1933	13.1162	14.0132	10.2657	15.5297	12.5416	14.4722	12.4627	14.4586	12.4627	14.4586	12.4627	14.4586	12.4627	14.4586
80	13.522	12.0685	80	13.7348	12.3059	13.6764	12.1467	13.6944	11.7944	10.3793	13.003	13.1199	12.2814	13.0392	12.5182	13.0392	12.5182	13.0392	12.5182	13.0392	12.5182
100	13.3764	10.4501	100	13.5525	10.8644	13.5732	10.3188	13.448	10.5947	10.3701	11.3612	13.1774	11.1866	12.9816	11.6373	12.9816	11.6373	12.9816	11.6373	12.9816	11.6373

B/H=4 N=2																							
Point 1			Point 2			Point 3			Point 4			Point 5			Point 6			Point 7					
Height	U mean	u t.1.1%	Height	U mean	u t.1.1%	U mean	u t.1.1%	U mean	u t.1.1%	U mean	u t.1.1%	Height	U mean	u t.1.1%	U mean	u t.1.1%	U mean	u t.1.1%	U mean	u t.1.1%	U mean	u t.1.1%	
1	2.4604	42.9578	9	9.4271	24.2084	7.1175	32.4712	8.0614	25.2003	6.5698	31.6494	6.4459	26.8798	5.9044	31.7975	6.3658	31.3216	6.3658	31.3216	6.3658	31.3216	6.3658	31.3216
2	2.4884	44.2387	10	8.9377	24.4984	7.7325	32.6892	8.4799	25.5622	6.3366	31.6625	6.8703	26.6847	6.6358	31.3216	6.6358	31.3216	6.6358	31.3216	6.6358	31.3216	6.6358	31.3216
3	2.7175	46.7238	11	9.1823	24.7588	8.5161	30.0546	9.081	26.1441	6.7041	29.5248	7.2169	27.688	7.1388	30.4984	7.1388	30.4984	7.1388	30.4984	7.1388	30.4984	7.1388	30.4984
4	2.9741	50.5362	12	9.495	25.0504	9.0703	26.716	9.349	24.7094	6.72389	28.8495	7.6327	24.9633	7.4958	28.981	7.4958	28.981	7.4958	28.981	7.4958	28.981	7.4958	28.981
6	4.0665	52.0619	13	9.6638	24.5092	9.5231	25.9962	9.6951	24.0256	6.80396	27.1033	6.3544	23.3625	6.1637	26.338	6.1637	26.338	6.1637	26.338	6.1637	26.338	6.1637	26.338
8	6.2419	42.5112	14	10.2028	22.2774	10.136	23.8368	9.748	24.2529	6.8589	24.7353	6.9876	22.0137	6.6967	24.6753	6.6967	24.6753	6.6967	24.6753	6.6967	24.6753	6.6967	24.6753
10	8.121	30.9021	16	10.5367	21.1829	10.446	21.407	10.4342	22.7235	9.1239	21.9251	9.381	20.7487	9.4166	22.6038	9.4166	22.6038	9.4166	22.6038	9.4166	22.6038	9.4166	22.6038
12	8.9678	25.8193	18	10.7226	20.6412	10.8186	21.2195	10.6612	20.7271	9.4978	22.2846	9.6734	21.3535	9.7374	21.7307	9.7374	21.7307	9.7374	21.7307	9.7374	21.7307	9.7374	21.7307
15	10.0068	21.6484	20	11.1545	18.8363	11.2707	19.4824	11.1228	19.6587	10.0618	20.8915	10.1262	20.2555	10.1923	20.6298	10.1923	20.6298	10.1923	20.6298	10.1923	20.6298	10.1923	20.6298
20	10.7585	19.8259	25	11.4058	18.3902	11.5988	18.2408	11.4324	18.3566	10.6472	19.6992	10.8155	18.7954	10.7196	19.6208	10.7196	19.6208	10.7196	19.6208	10.7196	19.6208	10.7196	19.6208
30	11.8451	17.1417	30	11.8695	16.7471	12.0267	17.7035	11.7866	17.249	10.3673	17.1866	11.2533	17.8639	11.5663	16.8784	11.5663	16.8784	11.5663	16.8784	11.5663	16.8784	11.5663	16.8784
40	12.2921	16.8914	40	12.3166	16.4706	12.4018	16.8537	12.3433	16.2109	10.19168	17.0941	11.9507	16.9578	12.0671	16.1438	12.0671	16.1438	12.0671	16.1438	12.0671	16.1438	12.0671	16.1438
50	12.8235	15.5787	50	13.0784	14.7998	13.0464	14.6945	12.8633	14.8792	10.12409	15.6941	12.306	15.7323	12.542	15.5041	12.542	15.5041	12.542	15.5041	12.542	15.5041	12.542	15.5041
60	13.1013	15.5914	60	13.1946	14.2795	13.2645	14.2176	13.0971	14.0754	10.12856	14.9286	12.6728	14.8364	12.8838	14.6056	12.8838	14.6056	12.8838	14.6056	12.8838	14.6056	12.8838	14.6056
80	13.7318	11.8878	80	13.8389	12.2673	13.7953	12.1488	13.7781	11.6992	10.13506	12.9098	13.2126	12.9486	13.3234	13.1946	13.3234	13.1946	13.3234	13.1946	13.3234	13.1946	13.3234	13.1946
100	13.6502	10.598	100	13.6391	10.8905	13.6743	10.344	13.5107	10.6674	10.135174	11.5871	13.3505	11.9125	13.3629	11.92	13.3629	11.92	13.3629	11.92	13.3629	11.92	13.3629	11.92

B/H=4 N=3																									
Point 1			Point 2			Point 3			Point 4			Point 5			Point 6			Point 7							
Height	U mean	u t.1.1%	Height	U mean	u t.1.1%	U mean	u t.1.1%	U mean	u t.1.1%	U mean	u t.1.1%	Height	U mean	u t.1.1%	U mean	u t.1.1%	U mean	u t.1.1%	U mean	u t.1.1%	U mean	u t.1.1%	U mean	u t.1.1%	
1	2.2871	44.0909	9	9.2647	26.0852	6.7782	33.3382	7.931	26.5328	5.7237	33.3198	6.6843	27.3785	5.9893	32.4501	6.6299	31.117	6.6299	31.117	6.6299	31.117	6.6299	31.117	6.6299	31.117
2	2.5354	45.4207	10	8.7323	24.8945	7.7171	32.8891	8.5581	25.9446	6.3792	31.0019	7.0063	27.172	6.6299	31.117	7.0417	30.192	7.0417	30.192	7.0417	30.192	7.0417	30.192	7.0417	30.192
3	2.7848	48.5445	11	8.9784	25.0934	8.3899	31.0558	8.9768	25.4474	6.8304	28.8428	7.5541	26.713	7.5047	30.192	7.5047	30.192	7.5047	30.192	7.5047	30.192	7.5047	30.192	7.5047	30.192
4	3.1367	51.2752	12	9.3029	25.1135	8.7728	27.8452	9.2094	25.7322	7.1823	29.0693	7.7809	26.5464	7.407	28.9598	7.407	28.9598	7.407	28.9598	7.407	28.9598	7.407	28.9598	7.407	28.9598
6	4.4426	50.9173	13	9.7407	23.1245	9.1235	26.3155	9.5492	23.9468	7.8864	27.2353	8.3851	24.2953	8.0655	26.75	8.0655	26.75	8.0655	26.75	8.0655	26.75	8.0655	26.75	8.0655	26.75
8	6.2679	42.4382	14	9.6924	23.6987	9.6833	26.0734	9.7203	23.8438	8.8498	24.5441	8.8682	23.9756	8.5435	24.9745	8.5435	24.9745	8.5435	24.9745	8.5435	24.9745	8.5435	24.9745	8.5435	24.9745
10	8.4106	30.1861	16	10.3006	21.6326	10.1527	22.0589	10.323	22.8653	10.2256	23.6003	9.3347	23.4885	9.227	23.3847	9.227	23.3847	9.227	23.3847	9.227	23.3847	9.227	23.3847	9.227	23.3847
12	9.0848	26.6388	18	10.8656	20.0352	10.7594	21.0871	10.8665	20.556	9.5413	22.4583	9.905	22.0373	9.6048	22.4821	9.6048	22.4821	9.6048	22.4821	9.6048	22.4821	9.6048	22.4821	9.6048	22.4821
15	10.1534	22.9034	20	10.8749	19.5279	10.9322	19.7402	11.1463	18.9387	10.2697	21.3854	10.5732	19.9632	10.2088	21.0712	10.2088	21.0712	10.2088	21.0712	10.2088	21.0712	10.2088	21.0712	10.2088	21.0712
20	11.0174	19.7797	25	11.5208	17.7	11.3946	18.3729	11.5542	18.3816	10.9897	19.484	11.0678	20.1533	10.971	18.8149	10.971									

B/H=6		N=1																					
Point 1		Point 2			Point 3			Point 4			Point 5			Point 6			Point 7						
Height	U mean	u	t.1.%	Height	U mean	u	t.1.%	U mean	u	t.1.%	U mean	u	t.1.%	U mean	u	t.1.%	U mean	u	t.1.%				
1	2.4473		59.8697	9	10.083		29.3225	6.3099		39.8955	8.2001		26.7927	1	5.9955		28.4698	6.5555		25.5836	7.6529		21.9201
2	3.0367		53.9626	10	9.9498		21.0972	7.2608		38.5753	8.6948		26.2542	2	6.7861		26.9058	7.1055		25.0399	8.2208		21.709
3	3.4301		53.3342	11	10.0401		21.0698	8.2981		33.0634	9.2469		26.7791	3	7.4736		25.4711	7.6904		24.4555	8.4153		21.8014
4	4.0343		52.0688	12	10.1733		21.3998	9.1755		28.6767	9.6925		24.6266	4	7.7445		25.5955	7.8436		23.8957	8.9275		20.5454
6	5.0456		47.6546	13	10.1723		21.9105	9.8747		25.3646	10.0898		23.6105	6	8.4625		22.098	8.5625		22.192	9.5092		20.2055
8	5.4827		40.9476	14	10.4253		22.0457	10.2873		24.0524	10.3693		21.8593	8	8.6767		21.2659	8.7188		21.3191	9.8558		19.5824
10	7.6555		32.4995	16	10.8241		20.8765	10.8709		21.3463	10.8141		20.3061	10	9.0608		21.575	9.0866		20.4861	10.1035		18.4519
12	8.8457		27.0954	18	11.0586		19.4849	11.2289		19.3831	11.2219		18.9948	12	9.1935		20.0452	9.3539		19.3086	10.2694		18.3098
15	9.6603		21.7758	20	11.4395		18.4023	11.2855		19.2422	11.4274		18.4431	15	9.6445		19.8679	9.6514		19.4729	10.3611		18.577
20	10.3092		19.9898	25	11.5237		18.7711	11.6941		17.749	11.5396		18.0795	20	9.7816		19.3736	10.0208		18.0407	10.9241		17.9423
30	11.1108		18.1888	30	11.8792		16.8647	11.9231		16.8579	12.0043		17.0423	30	10.584		18.1239	10.6208		17.5468	11.6001		16.853
40	11.7191		16.9286	40	12.492		16.1265	12.4542		15.8712	12.3465		16.5982	40	11.033		17.2995	11.0676		16.605	12.0414		15.56
50	12.1471		16.1655	50	12.9568		15.4148	12.9551		15.0974	12.6542		15.8246	50	11.3615		16.7697	11.3991		16.1095	12.26		15.2079
60	12.5778		15.1683	60	13.2384		14.4182	13.2207		14.6945	13.2391		14.1083	60	11.7793		15.4629	11.7451		15.5579	12.4616		14.9104
80	13.0227		12.554	80	13.8124		12.2471	13.8567		11.9449	13.6524		12.2166	80	12.333		14.1914	12.2401		13.5695	12.9418		13.4379
100	13.1581		11.078	100	13.7773		10.9	13.6159		10.9783	13.5203		10.3756	100	12.5016		12.2201	12.3858		12.6374	13.0409		12.2501

B/H=6		N=2																					
Point 1		Point 2			Point 3			Point 4			Point 5			Point 6			Point 7						
Height	U mean	u	t.1.%	Height	U mean	u	t.1.%	U mean	u	t.1.%	U mean	u	t.1.%	U mean	u	t.1.%	U mean	u	t.1.%				
1	2.5387		57.4762	9	10.033		23.7117	6.1317		41.4359	8.1432		26.8167	1	6.5389		28.1966	7.3118		23.0118	7.2784		24.013
2	3.0895		53.6576	10	9.7428		21.3155	7.5304		36.1345	8.5252		27.0181	2	7.1682		26.7464	7.869		22.6527	7.9111		23.5812
3	3.6151		52.6924	11	9.6204		21.7532	8.2582		34.5394	9.0178		26.7557	3	7.6056		26.3687	8.3677		21.732	8.2544		21.2038
4	3.9828		51.2007	12	9.7944		21.6941	8.9449		29.1242	9.6573		24.775	4	7.8555		25.5031	8.6923		21.8395	8.5531		22.3206
6	5.1354		47.2715	13	9.7201		23.0623	9.5759		25.8529	9.9445		23.8544	6	8.2509		23.5994	9.1487		21.7047	8.9728		21.7215
8	6.6367		38.6151	14	9.9595		23.0645	9.9464		23.5595	10.1837		22.9448	8	8.9517		22.8849	9.3996		21.5803	9.2456		21.2269
10	7.8165		32.3147	16	10.5014		20.2857	10.7383		21.8733	10.5168		21.5245	10	9.4103		20.4474	9.5974		21.7167	9.803		20.8947
12	8.8339		27.3124	18	10.6365		19.8851	11.0648		19.8404	10.8167		21.1854	12	9.5384		20.7674	10.0759		20.214	10.2674		20.1776
15	9.5951		24.4466	20	11.0019		18.4293	10.9456		19.6215	11.1904		18.2384	15	9.7303		20.5525	10.3934		18.1164	10.3621		20.1634
20	10.4633		20.7471	25	11.4432		17.8262	11.22		18.7864	11.4659		18.0182	20	10.3581		19.0844	10.4933		19.4543	11.0389		17.8563
30	11.4614		18.5385	30	11.3843		18.0056	11.715		16.9931	11.9641		16.9194	30	10.8895		17.8835	11.3488		17.0117	11.603		16.9136
40	12.1301		16.5468	40	12.1027		16.3228	12.1652		16.6894	12.2497		15.8425	40	11.448		16.8937	11.732		17.1018	11.9706		16.4017
50	12.625		15.5754	50	12.6143		15.2887	12.5013		15.4598	12.3261		16.4558	50	11.9435		15.9863	12.1909		16.0913	12.4014		15.3513
60	13.0701		14.8899	60	13.0789		14.0236	13.0055		14.2992	13.0002		14.293	60	12.2345		15.1322	12.6472		14.4449	12.833		14.4289
80	13.5511		12.6736	80	13.6848		12.0169	13.409		12.4618	13.4823		11.4646	80	12.9142		13.3058	12.9955		13.4136	13.2704		13.6454
100	13.5053		11.3332	100	13.4889		10.517	13.3694		10.9063	13.2736		10.8378	100	13.0232		12.4698	13.077		12.2284	13.3425		12.0691

B/H=6		N=3																					
Point 1		Point 2			Point 3			Point 4			Point 5			Point 6			Point 7						
Height	U mean	u	t.1.%	Height	U mean	u	t.1.%	U mean	u	t.1.%	U mean	u	t.1.%	U mean	u	t.1.%	U mean	u	t.1.%				
1	2.594		55.3707	9	10.0248		24.621	6.0347		40.4939	8.2575		26.5262	1	5.9955		29.2911	7.1552		22.8101	7.602		23.4768
2	3.1408		52.1201	10	9.5795		21.6567	6.7797		39.562	8.5164		26.4894	2	6.8754		27.3984	7.5913		22.7426	7.9283		23.0659
3	3.5138		51.6141	11	9.2865		23.1776	8.062		33.6368	9.0075		26.3052	3	7.4557		26.0204	8.0078		22.4693	8.2197		23.2677
4	3.9294		50.5166	12	9.6384		21.9127	8.9609		29.0959	9.4064		25.3149	4	7.6743		26.1682	8.5122		21.9394	8.4867		23.1747
6	5.3085		45.4066	13	9.9019		21.4804	9.4619		24.9023	9.647		23.9885	6	8.3757		24.3656	8.7769		22.6625	8.9582		22.6529
8	6.5924		39.8248	14	10.0128		22.705	9.7397		24.2374	10.0372		22.7843	8	8.645		23.5709	9.087		22.148	9.3611		20.8297
10	7.9227		32.8176	16	10.1802		22.9262	10.184		22.3582	10.5308		21.3832	10	9.0589		22.4532	9.582		20.0071	9.7897		19.842
12	8.755		27.0107	18	10.6565		20.786	10.8427		20.8044	10.6906		20.4455	12	9.3262		21.5446	9.9233		20.432	9.9873		19.1949
15	9.6724		22.8048	20	10.9735		19.7662	11.1339		19.1115	10.9636		20.4441	15	9.7123		21.6974	10.3559		19.3318	10.3267		19.5789
20	10.5299		20.4523	25	11.5216		17.8094	11.466		18.7043	11.2716		18.7157	20	10.2536		19.9964	10.7961		18.6209	10.6454		19.2624
30	11.362		18.913	30	11.6689		17.8977	11.6664		17.5781	11.7502		17.2368	30	10.1125		17.122	11.3221		17.736	11.4095		17.4353
40	12.0782		16.9926	40	12.1509		16.6029	12.2643		16.5027	12.0599		16.8353	40	11.4509		17.4271	11.9404		16.6822	11.7751		16.5296
50	12.6476		16.0517	50	12.5363		15.7791	12.6026		15.6332	12.61		14.8428	50	12.0473		15.871	12.3057		15.1636	12.2647		15.3059
60	13.2452		13.6478	60	13.1107		14.3058	13.0643		14.0147	13.0498		14.197	60	12.3753		15.7729	12.7135		14.622	12.383		15.2599
80	13.5906		12.3221	80	13.6302		12.1878	13.5505		12.4313	13.4962		11.8616	80	12.8922		13.6968	13.1042		13.4736	12.898		13.9139
100	13.5481		10.7465	100	13.4021		10.8998	13.4723		10.7631	13.3896		10.4122	100	13.0814		12.3486	13.239		12.1065	13.1734		11.8957

B/H=6		N=8																					
Point 1		Point 2			Point 3			Point 4			Point 5			Point 6			Point 7						
Height	U mean	u	t.1.%	Height	U mean	u	t.1.%	U mean	u	t.1.%	U mean	u	t.1.%	U mean	u	t.1.%	U mean	u	t.1.%				
1.01	2.7692		49.1741	9	9.4355		21.511	5.7237		42.6249	8.2664		27.1114	1	6.017		29.8594	7.0281		23.3132	7.1804		24.2856
2	3.1844		45.8874	10	9.0092		21.8507	6.8924		38.9147	8.7472		26.9227	2	6.6167		28.2767	7.6118		22.7923	7.7565		24.2121
3	3.5675		47.1777	11	8.8633		22.1272	7.7787		34.8246	9.0039		25.8178	3	7.1281		27.5584	7.9611		22.			

Appendix C

Pressure Coefficients

This appendix presents the values of minimum, mean, maximum, RMS, -peak and +peak pressure coefficients for 95 pressure taps on the surface of testing building.

B/H=0.5 N=1 0 degree						
# of tap	Min	Mean	max	STDV	- peak	+ peak
1	0.5799	1.266	2.1343	0.2613	0.4822	2.0498
2	-0.6391	0.0094	0.392	0.0935	-0.2709	0.2898
3	-0.7342	0.0159	0.4245	0.1021	-0.2904	0.3221
4	-0.7922	0.0207	0.4692	0.1067	-0.2993	0.3407
5	-0.7683	0.0252	0.4475	0.1049	-0.2895	0.3399
6	-0.6999	0.0284	0.4242	0.0892	-0.269	0.3259
7	-1.0242	0.0398	0.4722	0.0989	-0.2599	0.3365
8	-0.6759	-0.011	0.4686	0.0936	-0.2018	0.2998
9	-0.5079	0.0443	0.3936	0.0776	-0.1888	0.2772
10	-0.4651	0.0472	0.4063	0.0793	-0.1908	0.2853
11	-0.4412	0.0599	0.4545	0.0826	-0.188	0.3078
12	-0.385	0.0597	0.4316	0.0788	-0.1762	0.2956
13	-0.3774	0.0843	0.456	0.0787	-0.172	0.3005
14	-0.8574	0.0431	0.3448	0.0789	-0.1875	0.2737
15	-0.4219	0.0573	0.3723	0.0738	-0.1841	0.2787
16	-0.3054	0.0832	0.4135	0.074	-0.1599	0.2852
17	-0.3107	0.0669	0.3942	0.0743	-0.1561	0.2898
18	-0.4143	0.0666	0.4165	0.0709	-0.1481	0.2792
19	-0.3014	0.0754	0.4324	0.0702	-0.1352	0.286
20	-0.4137	0.0805	0.3908	0.0696	-0.1282	0.2891
21	-0.5206	0.0659	0.4033	0.0712	-0.1477	0.2795
22	-0.2433	0.0725	0.3871	0.0691	-0.1348	0.2797
23	-0.2912	0.0838	0.3846	0.0681	-0.1204	0.288
24	-0.2573	0.0887	0.3808	0.0661	-0.1118	0.2851
25	-0.3479	0.0811	0.3918	0.0655	-0.1153	0.2778
26	-0.7038	0.0568	0.3324	0.07	-0.1533	0.267
27	-0.5541	0.0772	0.3769	0.0692	-0.1305	0.2849
28	-0.3159	0.0832	0.4132	0.0675	-0.1193	0.2857
29	-0.245	0.0914	0.4179	0.0639	-0.1004	0.2832
30	-0.3187	0.0903	0.3798	0.0615	-0.0944	0.2749
31	-0.2649	0.0896	0.3848	0.0619	-0.0962	0.2754
32	-0.5541	0.0772	0.3769	0.0692	-0.1305	0.2849
33	-0.3291	0.088	0.4094	0.0683	-0.1168	0.2929
34	-0.2354	0.0943	0.3939	0.0655	-0.1022	0.2909
35	-0.2327	0.103	0.3841	0.0617	-0.0822	0.2882
36	-0.1744	0.1028	0.4098	0.0602	-0.0778	0.2835
37	-0.2239	0.0997	0.376	0.0602	-0.081	0.2804
38	-0.528	0.0883	0.415	0.0642	-0.1043	0.2809
39	-0.2979	0.093	0.4139	0.0666	-0.1069	0.2929
40	-0.355	0.0992	0.4139	0.063	-0.0897	0.288
41	-0.1863	0.1048	0.4124	0.0588	-0.0718	0.2813
42	-0.2497	0.1035	0.3841	0.0574	-0.0688	0.2758
43	-0.1761	0.1019	0.3455	0.0579	-0.072	0.2756
44	-0.4902	0.0883	0.358	0.0619	-0.0973	0.2738
45	-0.3005	0.1041	0.3846	0.0607	-0.0778	0.2862
46	-0.2027	0.1032	0.348	0.0568	-0.0673	0.2736
47	-0.1386	0.1013	0.3275	0.0534	-0.0588	0.2814
48	-0.161	0.0976	0.312	0.0538	-0.0638	0.259
49	-0.259	0.0906	0.2897	0.0552	-0.1149	0.2161
50	-0.392	0.0356	0.3413	0.0609	-0.1489	0.2182
51	-0.2563	0.1414	0.8667	0.1167	-0.2087	0.4915
52	-0.2754	0.1597	0.8234	0.1189	-0.191	0.5104
53	-0.2556	0.1889	1.2257	0.1322	-0.2078	0.5855
54	-0.7032	0.2195	1.07	0.1529	-0.2392	0.6783
55	-0.2393	0.2307	1.1741	0.1559	-0.237	0.6983
56	-0.176	0.0935	0.5814	0.0808	-0.1489	0.3359
57	-0.3077	0.0818	0.3766	0.0731	-0.1575	0.2811
58	-0.3727	0.0616	0.4184	0.0756	-0.1654	0.2885
59	-0.2731	0.0571	0.3855	0.0755	-0.1693	0.2836
60	-0.2453	0.1635	0.8131	0.1095	-0.1851	0.4921
61	-0.5735	0.0719	0.4307	0.0898	-0.1389	0.2807
62	-0.2605	0.0533	0.3468	0.0654	-0.1428	0.2494
63	-0.2148	0.0499	0.3546	0.0676	-0.153	0.2528
64	-0.2907	0.055	0.3577	0.0701	-0.1552	0.2651
65	-0.5519	0.1082	0.7358	0.0894	-0.1599	0.3763
66	-0.1724	0.0648	0.2911	0.0542	-0.0979	0.2275
67	-0.221	0.0572	0.2443	0.0536	-0.1035	0.218
68	-0.3421	0.0384	0.2888	0.0591	-0.139	0.2158
69	-0.3701	-0.0033	0.249	0.0656	-0.2002	0.1936
70	-0.1682	0.0684	0.2808	0.0536	-0.0948	0.2273
71	-0.2816	0.0576	0.2409	0.0555	-0.109	0.2243
72	-0.2394	0.0475	0.2782	0.0571	-0.1237	0.2187
73	-0.4783	-0.0142	0.2311	0.0671	-0.2156	0.1872
74	-0.1842	0.0811	0.2725	0.0533	-0.0989	0.221
75	-0.2309	0.053	0.2775	0.056	-0.1151	0.2211
76	-0.181	0.0551	0.3259	0.0538	-0.1063	0.2184
77	-0.3779	-0.0093	0.2306	0.0656	-0.2059	0.1874
78	-0.7071	-0.0089	0.3961	0.0878	-0.3034	0.2836
79	-0.3976	0.0356	0.3889	0.0858	-0.1812	0.2323
80	-0.3437	0.051	0.3929	0.0629	-0.1378	0.2398
81	-0.3513	0.0582	0.4188	0.0648	-0.1361	0.2525
82	-0.5022	0.063	0.3828	0.0659	-0.1347	0.2607
83	-0.3897	0.0415	0.3163	0.0607	-0.1407	0.2236
84	-0.5625	0.0177	0.332	0.0746	-0.2082	0.2418
85	-0.2889	0.0374	0.3378	0.0613	-0.1468	0.2215
86	-0.29	0.0493	0.3517	0.0602	-0.1314	0.2289
87	-0.3491	0.06	0.3544	0.0612	-0.1235	0.2438
88	-0.3859	0.0685	0.3581	0.082	-0.1195	0.2528
89	-0.2883	0.064	0.3308	0.0616	-0.1209	0.2489
90	-0.2855	0.0432	0.276	0.0557	-0.1238	0.2102
91	-0.4569	0.0424	0.3883	0.0658	-0.1549	0.2397
92	-0.2486	0.0415	0.3026	0.0597	-0.1347	0.2177
93	-0.2347	0.0471	0.3571	0.0577	-0.1259	0.2201
94	-0.2884	0.0441	0.333	0.0588	-0.1118	0.2399
95	-0.2342	0.0726	0.3184	0.0571	-0.0886	0.2438
96	-0.1855	0.0545	0.2939	0.0514	-0.0896	0.2085

B/H=0.5 N=1 10 degree						
# of tap	Min	Mean	max	STDV	- peak	+ peak
1	0.5384	1.2689	2.1033	0.2516	0.515	2.0244
2	-0.6345	0.026	0.5107	0.1021	-0.2802	0.3322
3	-0.8984	0.0379	0.5092	0.1091	-0.2893	0.3652
4	-0.6136	0.0585	0.5684	0.1047	-0.2559	0.3727
5	-0.8206	0.078	0.5995	0.0992	-0.2196	0.3756
6	-0.7388	0.086	0.5482	0.0952	-0.2187	0.3517
7	-0.6587	0.0527	0.4792	0.095	-0.2324	0.3378
8	-0.7463	0.0243	0.457	0.0858	-0.237	0.2816
9	-0.7417	0.058	0.4733	0.0916	-0.217	0.3329
10	-0.4806	0.0735	0.4473	0.0783	-0.1612	0.3084
11	-0.3578	0.0952	0.5023	0.0804	-0.1458	0.3363
12	-0.335	0.092	0.5804	0.0784	-0.1371	0.321
13	-0.393	0.0981	0.4381	0.0763	-0.1407	0.3169
14	-0.3614	0.0721	0.4083	0.0703	-0.1388	0.283
15	-0.6191	0.0588	0.4864	0.0846	-0.185	0.3226
16	-0.3683	0.0882	0.46	0.0721	-0.128	0.3044
17	-0.3507	0.0967	0.4501	0.0722	-0.1198	0.3132
18	-0.5571	0.0765	0.4659	0.0777	-0.1546	0.3116
19	-0.3176	0.0963	0.4566	0.0884	-0.1088	0.3074
20	-0.3307	0.1047	0.4449	0.0673	-0.0973	0.3066
21	-0.6891	0.0748	0.4506	0.0803	-0.1682	0.3158
22	-0.4859	0.0886	0.4382	0.0713	-0.1253	0.3024
23	-0.3225	0.106	0.4424	0.0658	-0.0914	0.3035
24	-0.2355	0.1135	0.4045	0.0647	-0.0807	0.3077
25	-0.1857	0.1108	0.4076	0.064	-0.0811	0.3028
26	-0.3677	0.0967	0.4267	0.064	-0.0954	0.2888
27	-0.5525	0.0938	0.4885	0.0728	-0.1245	0.3121
28	-0.3735	0.1017	0.5206	0.0673	-0.1002	0.3036
29	-0.3066	0.1138	0.4249	0.0625	-0.0737	0.3012
30	-0.2113	0.1164	0.4607	0.0605	-0.0652	0.2979
31	-0.2473	0.1202	0.4089	0.0608	-0.0616	0.3021
32	0.10357	0.1761	0.3303	0.0337	0.0782	0.2801
33	-0.6789	0.1102	0.4585	0.07	-0.0897	0.3201
34	-0.4307	0.1181	0.4288	0.0642	-0.0765	0.3088
35	-0.2408	0.1258	0.427	0.0604	-0.0597	0.3065
36	-0.5525	0.1278	0.4177	0.0699	-0.0618	0.3074
37	-0.1975	0.1292	0.4027	0.0597	-0.0469	0.3083
38	-0.1962	0.1249	0.4053	0.0615	-0.0597	0.3096
39	-0.5956	0.1161	0.4692	0.0675	-0.0864	0.3187
40	-0.3202	0.1214	0.4211	0.0613	-0.0626	0.3054
41	-0.1858	0.1253	0.386	0.0577	-0.0478	0.2884
42	-0.1929	0.1297	0.4229	0.0568	-0.0408	0.3003
43	-0.2003	0.1338	0.4022	0.0571	-0.0374	0.305
44	-0.2852	0.1262	0.373	0.0599	-0.0535	0.3058
45	-0.2426	0.1029	0.3753	0.0583	-0.0719	0.2777
46	-0.2868	0.0991	0.3639	0.0549	-0.0656	0.2638
47	-0.1638	0.1084	0.3603	0.0528	-0.05	0.2688
48	-0.3292	0.123	0.3195	0.0517	-0.032	0.278
49	-0.1969	0.098	0.3731	0.0516	-0.0569	0.2529
50	-0.3987	0.1007	0.3849	0.0592	-0.0769	0.2783
51	-0.381	0.2044	0.0728	0.1248	-0.117	0.5788
52	-0.1765	0.2025	0.9456	0.128	-0.1816	0.5867
53	-0.2002	0.2226	1.0761	0.1369	-0.1881	0.6334
54	-0.2084	0.2081	1.0669	0.1269	-0.1604	0.5767
55	-0.1763	0.2037	1.1977	0.1294	-0.1843	0.5918
56	-0.3562	0.1632	0.7308	0.0924	-0.1141	0.4404
57	-0.3248	0.0775	0.4114	0.0738	-0.1437	0.2988
58	-0.308	0.0901	0.4713	0.0727	-0.1282	0.3083
59	-0.2723	0.0987	0.43	0.0716	-0.1152	0.3147
60	-0.2446	0.1307	0.7483	0.0915	-0.1139	0.3754
61	-0.3037	0.133	0.7872	0.0901	-0.107	

B/H=0.5 N=1 20 degree						
# of tap	Min	Mean	max	STDV	- peak	+ peak
1	0.5176	1.2425	2.0723	0.2779	0.409	2.0761
2	-0.8177	-0.012	0.4761	0.1192	-0.3697	0.3457
3	-1.1548	-0.105	0.5115	0.1346	-0.4144	0.3934
4	-0.7729	0.0303	0.5979	0.1232	-0.3393	0.3999
5	-0.5905	0.0751	0.5517	0.1067	-0.2451	0.3953
6	-0.7217	0.081	0.5175	0.0965	-0.2084	0.3705
7	-0.5454	0.0511	0.5324	0.0912	-0.2224	0.3245
8	-0.7815	0.0014	0.4248	0.082	-0.2446	0.2473
9	-0.9322	0.018	0.4671	0.1168	-0.3324	0.3683
10	-0.6811	0.0513	0.4556	0.0874	-0.2109	0.3135
11	-0.4411	0.0855	0.5133	0.0861	-0.1727	0.3437
12	-0.3508	0.0914	0.4397	0.0769	-0.1391	0.322
13	-0.4526	0.0816	0.4476	0.0734	-0.1387	0.3019
14	-0.4532	0.0497	0.4099	0.0681	-0.1556	0.2531
15	-0.7594	0.0356	0.4214	0.1025	-0.2719	0.3432
16	-0.3845	0.0793	0.4619	0.0774	-0.1528	0.3115
17	-0.3249	0.089	0.485	0.0754	-0.1394	0.3143
18	-0.526	0.0545	0.4502	0.088	-0.2096	0.3186
19	-0.3507	0.0874	0.4753	0.0724	-0.1298	0.3045
20	-0.2711	0.0964	0.4712	0.0589	-0.1104	0.3031
21	-1.0886	0.0514	0.4852	0.0944	-0.2317	0.3345
22	-0.445	0.0757	0.4457	0.0764	-0.1536	0.3049
23	-0.2278	0.0991	0.4435	0.0677	-0.104	0.3021
24	-0.2199	0.1078	0.4133	0.0645	-0.0856	0.3012
25	-0.3025	0.1016	0.3819	0.0629	-0.0869	0.2902
26	-0.3432	0.0849	0.3792	0.062	-0.1011	0.2708
27	-0.6164	0.0894	0.4185	0.0795	-0.1492	0.329
28	-0.3134	0.0996	0.4295	0.0704	-0.1116	0.3108
29	-0.2693	0.1112	0.4342	0.0639	-0.0805	0.3029
30	-0.1489	0.1108	0.4708	0.0606	-0.0709	0.2924
31	-0.1638	0.1131	0.4092	0.0598	-0.0694	0.2925
32	0.0365	0.1798	0.3548	0.0349	0.0751	0.2845
33	-0.4978	0.1144	0.5542	0.0749	-0.1103	0.3392
34	-0.3622	0.1219	0.5318	0.0667	-0.0783	0.3219
35	-0.1832	0.1248	0.4722	0.0618	-0.0606	0.3101
36	-0.1312	0.1202	0.4361	0.0601	-0.0502	0.3005
37	-0.1318	0.1208	0.4553	0.0592	-0.0567	0.2983
38	-0.4601	0.1212	0.4055	0.0597	-0.0581	0.3004
39	-0.5179	0.1212	0.5371	0.0722	-0.0652	0.3377
40	-0.2411	0.1235	0.4991	0.063	-0.0656	0.3127
41	-0.121	0.1165	0.4374	0.0578	-0.0569	0.2898
42	-0.1399	0.1229	0.3832	0.0568	-0.0475	0.2932
43	-0.1118	0.1264	0.3773	0.0583	-0.0427	0.2954
44	-0.2523	0.1233	0.3976	0.0579	-0.0505	0.2971
45	-0.3977	0.0719	0.4582	0.08	-0.108	0.2519
46	-0.2325	0.0841	0.4322	0.0545	-0.0695	0.2277
47	-0.1585	0.074	0.4285	0.0545	-0.0895	0.2375
48	-0.1555	0.1024	0.3953	0.0528	-0.0561	0.2609
49	-0.1205	0.1058	0.3454	0.0525	-0.0515	0.2632
50	-0.3902	0.1193	0.4024	0.057	-0.0517	0.2903
51	-0.3552	0.258	1.3264	0.1494	-0.19	0.7081
52	-0.2715	0.2227	1.0571	0.1407	-0.1993	0.6448
53	-0.1873	0.2333	1.0437	0.1364	-0.178	0.6426
54	-0.1943	0.2135	0.9042	0.118	-0.1405	0.5874
55	-0.2346	0.1904	1.104	0.117	-0.1605	0.5414
56	-0.2519	0.2148	0.9103	0.106	-0.1032	0.5328
57	-0.2493	0.092	0.4387	0.0798	-0.1475	0.3314
58	-0.3127	0.0836	0.4529	0.0742	-0.139	0.3063
59	-0.213	0.11	0.4581	0.0719	-0.1057	0.3255
60	-0.223	0.1217	0.5503	0.0746	-0.102	0.3454
61	-0.2099	0.1944	0.7597	0.0958	-0.093	0.4818
62	-0.3217	0.1045	0.599	0.0726	-0.1132	0.3222
63	-0.253	0.103	0.4381	0.0705	-0.1087	0.3146
64	-0.3329	0.0922	0.3644	0.0696	-0.1168	0.301
65	-0.2582	0.0872	0.5181	0.0705	-0.1242	0.2988
66	-0.4844	-0.0144	0.3228	0.0662	-0.2131	0.1843
67	-0.3042	0.035	0.3629	0.063	-0.1541	0.2241
68	-0.1487	0.0815	0.3255	0.0537	-0.0795	0.2425
69	-0.1299	0.1018	0.3267	0.0534	-0.0584	0.282
70	-0.495	-0.0167	0.304	0.0572	-0.2182	0.1848
71	-0.4388	0.0545	0.3701	0.0677	-0.1486	0.2577
72	-0.2075	0.0724	0.3289	0.059	-0.1044	0.2493
73	-0.1439	0.088	0.3167	0.0545	-0.0753	0.2514
74	-0.4339	-0.0141	0.2959	0.0656	-0.211	0.1827
75	-0.1549	0.0985	0.4256	0.0632	-0.091	0.288
76	-0.3089	0.0819	0.332	0.059	-0.0951	0.2589
77	-0.2188	0.0905	0.3277	0.0588	-0.0708	0.2888
78	-0.9779	-0.0849	0.2929	0.0922	-0.3415	0.2118
79	-0.7896	-0.0042	0.3347	0.0802	-0.2447	0.2384
80	-0.2484	0.0628	0.3446	0.0672	-0.1387	0.2843
81	-0.3215	0.0898	0.3719	0.0608	-0.0926	0.2721
82	-0.2608	0.1004	0.3714	0.0609	-0.0823	0.2831
83	-0.3961	0.1116	0.3499	0.0588	-0.0641	0.2872
84	-0.7161	-0.0459	0.3025	0.0843	-0.2969	0.207
85	-0.501	0.0044	0.3352	0.0733	-0.2155	0.2244
86	-0.2688	0.0718	0.3673	0.0631	-0.1176	0.2812
87	-0.3278	0.0931	0.3798	0.0605	-0.0883	0.2745
88	-0.2441	0.0995	0.3904	0.0598	-0.0798	0.2789
89	-0.2073	0.1026	0.3888	0.0593	-0.0753	0.2805
90	-0.1349	0.1128	0.3445	0.055	-0.0523	0.2775
91	-0.3929	-0.0005	0.3142	0.0703	-0.2114	0.2104
92	-0.3244	0.0209	0.3512	0.0658	-0.179	0.2209
93	-0.1558	0.0739	0.3731	0.0584	-0.1012	0.249
94	-0.2314	0.1056	0.3928	0.059	-0.0715	0.2827
95	-0.2294	0.1141	0.3614	0.059	-0.0629	0.281
96	-0.0875	0.1321	0.3639	0.0556	-0.0347	0.2989

B/H=0.5 N=1 30 degree						
# of tap	Min	Mean	max	STDV	- peak	+ peak
1	0.528	1.2421	2.124	0.2579	0.4685	2.0156
2	-0.8005	-0.0696	0.3821	0.1144	-0.4127	0.2735
3	-0.8698	-0.0908	0.5205	0.1473	-0.5326	0.351
4	-0.8504	-0.0349	0.4697	0.1347	-0.4389	0.3691
5	-0.6169	0.0392	0.4388	0.1144	-0.304	0.3824
6	-0.7049	0.0767	0.4835	0.095	-0.2082	0.3616
7	-0.9665	0.0421	0.4045	0.0894	-0.2261	0.3104
8	-0.7227	-0.0313	0.2801	0.0785	-0.2607	0.198
9	-0.7333	-0.0549	0.3764	0.1256	-0.4316	0.3218
10	-0.4482	0.0078	0.4741	0.0852	-0.2477	0.2633
11	-0.4161	0.0549	0.388	0.0862	-0.2037	0.3136
12	-0.3508	0.0745	0.4399	0.0757	-0.1525	0.3015
13	-0.6231	0.0631	0.3715	0.0704	-0.1482	0.2744
14	-0.5206	0.0074	0.2593	0.0623	-0.1795	0.1942
15	-0.6498	-0.0297	0.3542	0.1093	-0.3576	0.2982
16	-0.3846	0.0456	0.3971	0.0742	-0.177	0.2882
17	-0.6516	0.0804	0.3851	0.0728	-0.1579	0.2787
18	-0.4742	0.0056	0.3555	0.0698	-0.2637	0.275
19	-0.3995	0.0584	0.3712	0.0694	-0.1518	0.2647
20	-0.2462	0.0723	0.3714	0.0656	-0.1244	0.2689
21	-0.6217	0.0052	0.4194	0.0867	-0.285	0.2853
22	-0.4109	0.0375	0.3432	0.0758	-0.1899	0.265
23	-0.2279	0.0755	0.3834	0.0642	-0.117	0.268
24	-0.2116	0.085	0.3882	0.0617	-0.1002	0.2702
25	-0.2158	0.0747	0.3907	0.059	-0.1023	0.2517
26	-0.3598	0.0428	0.3063	0.0574	-0.1292	0.2149
27	-0.4699	0.0884	0.3641	0.0817	-0.1787	0.3115
28	-0.305	0.0754	0.3784	0.0709	-0.1372	0.288
29	-0.2311	0.0885	0.3842	0.0613	-0.0953	0.2724
30	-0.216	0.0875	0.3871	0.0576	-0.0854	0.2605
31	-0.2442	0.0867	0.3922	0.0562	-0.0819	0.2554
32	0.0279	0.1541	0.3549	0.0322	0.0576	0.2507
33	-0.894	0.0908	0.4516	0.078	-0.1372	0.3188
34	-0.3537	0.0996	0.4537	0.0666	-0.1002	0.2994
35	-0.2102	0.1023	0.3825	0.0582	-0.0751	0.2798
36	-0.2056	0.0844	0.3525	0.0589	-0.0783	0.2651
37	-0.1632	0.0941	0.3502	0.0557	-0.0729	0.2612
38	-0.3391	0.0933	0.3537	0.0545	-0.0702	0.2568
39	-0.3944	0.089	0.4384	0.0751	-0.1363	0.3144
40	-0.2584	0.0927	0.4132	0.0638	-0.0988	0.2842
41	-0.2157	0.0857	0.3603	0.056	-0.0623	0.2536
42	-0.189	0.0969	0.3425	0.0542	-0.0656	0.2594
43	-0.2893	0.1003	0.369	0.0535	-0.0802	0.2607
44	-0.3925	0.0863	0.3813	0.0532	-0.0833	0.2559
45	-0.4561	0.07	0.308	0.0533	-0.1789	0.2128
46	-0.3191	0.0153	0.2944	0.0559	-0.1524	0.1831
47	-0.1759	0.0323	0.2992	0.0546	-0.1316	0.1861
48	-0.2762	0.0727	0.3438	0.053	-0.0863	0.2317
49	-0.1654	0.0884	0.3545	0.0518	-0.067	0.2438
50	-0.2901	0.1029	0.3843	0.0538	-0.0586	0.2643
51	-0.1501	0.2531	1.4293	0.1453	-0.183	0.6891
52	-0.3992	0.2328	1.2485	0.154	-0.2294	0.6848
53	-0.2233	0.237	1.1	0.1414	-0.1872	0.6611
54	-0.1851	0.1988	0.8674	0.1147	-0.1444	0.5439
55	-0.1782	0.1571	0.7353	0.0949	-0.1274	0.4417
56	-0.1249	0.2191	0.9015	0.1032	-0.0905	0.5287
57	-0.2953	0.0921	0.4481	0.0828	-0.1564	0.3405
58	-0.3128	0.0625	0.3861	0.0765	-0.1669	0.2919
59	-0.269	0.0631	0.4489	0.0715	-0.1315	0.2977
60	-0.2321	0.0937	0.3888	0.071	-0.1104	0.3089
61	-0.21	0.2102	0.7856	0.0999	-0.0895	

B/H=0.5 N=1 40 degree

# of tap	Min	Mean	max	STDV	- peak	+ peak
1	0.6006	1.2406	2.1136	0.2533	0.4808	2.0003
2	-0.9158	-0.1441	0.2688	0.0999	-0.4439	0.1557
3	-1.1301	-0.1884	0.3276	0.1394	-0.6065	0.2289
4	-0.903	-0.1312	0.4017	0.1276	-0.5139	0.2514
5	-0.6284	-0.034	0.3957	0.1095	-0.3627	0.2947
6	-0.8543	0.0385	0.3902	0.0916	-0.2363	0.3134
7	-0.8085	0.0231	0.328	0.0810	-0.2225	0.2887
8	-0.8504	-0.0832	0.1976	0.0717	-0.2782	0.1518
9	-1.1685	-0.1459	0.3024	0.1246	-0.5198	0.2279
10	-0.486	-0.0543	0.2767	0.0747	-0.2785	0.1699
11	-0.4418	-0.0041	0.3466	0.0785	-0.2398	0.2313
12	-0.4179	0.0348	0.3155	0.0707	-0.1773	0.2460
13	-0.3511	0.0353	0.2785	0.0659	-0.162	0.2327
14	-0.5044	-0.0368	0.2261	0.0569	-0.2075	0.1339
15	-0.788	-0.1085	0.304	0.1089	-0.4333	0.2202
16	-0.3524	-0.0049	0.2917	0.0675	-0.2073	0.1978
17	-0.3171	0.0137	0.302	0.0657	-0.1835	0.2108
18	-0.6049	-0.0436	0.3473	0.0955	-0.3301	0.2428
19	-0.4908	0.0107	0.3021	0.0682	-0.194	0.2154
20	-0.2988	0.0319	0.3051	0.0622	-0.1547	0.2185
21	-0.6307	-0.0354	0.3821	0.1074	-0.3578	0.2869
22	-0.3858	-0.0063	0.3007	0.0806	-0.2481	0.2356
23	-0.3058	0.0381	0.3063	0.0824	-0.1512	0.2234
24	-0.2795	0.0491	0.3128	0.0588	-0.1265	0.2248
25	-0.2858	0.038	0.2524	0.058	-0.13	0.206
26	-0.2481	-0.0012	0.2498	0.0531	-0.1605	0.158
27	-0.7211	0.0305	0.3846	0.0941	-0.2518	0.3128
28	-0.6045	0.038	0.3361	0.0801	-0.2021	0.2782
29	-0.4003	0.0503	0.276	0.0635	-0.1402	0.2409
30	-0.2685	0.0517	0.2788	0.0573	-0.1203	0.2238
31	-0.2617	0.0512	0.3151	0.0545	-0.1122	0.2148
32	0.0021	0.1223	0.2692	0.0301	0.032	0.2128
33	-0.7547	0.0374	0.375	0.0895	-0.2311	0.3058
34	-0.8403	0.0509	0.3324	0.0762	-0.1778	0.2798
35	-0.8754	0.0818	0.329	0.064	-0.1304	0.2537
36	-0.4685	0.0544	0.2784	0.0584	-0.1208	0.2285
37	-0.2723	0.0584	0.3156	0.055	-0.1087	0.2216
38	-0.2788	0.0588	0.2587	0.0518	-0.0988	0.2123
39	-0.7334	0.0181	0.4059	0.0829	-0.2605	0.2967
40	-0.6039	0.0322	0.319	0.0732	-0.1873	0.2517
41	-0.8729	0.0345	0.3091	0.06	-0.1455	0.2145
42	-0.2384	0.057	0.2938	0.0583	-0.1119	0.2259
43	-0.3405	0.0631	0.2935	0.0539	-0.0986	0.2248
44	-0.2857	0.0595	0.283	0.0508	-0.093	0.2121
45	-0.6735	-0.0571	0.2594	0.0781	-0.2855	0.1713
46	-0.3888	-0.0407	0.2429	0.0606	-0.2226	0.1412
47	-0.306	-0.0128	0.2478	0.0562	-0.1814	0.1588
48	-0.2075	0.0371	0.2753	0.0539	-0.1246	0.1989
49	-0.1836	0.0682	0.3011	0.053	-0.0929	0.2252
50	-0.2539	0.0785	0.3118	0.0522	-0.078	0.2349
51	-0.2445	0.0444	1.0467	0.1142	-0.1381	0.547
52	-0.4088	0.1894	0.9131	0.1381	-0.2249	0.6038
53	-0.2515	0.2292	0.924	0.1364	-0.18	0.8384
54	-0.2508	0.1888	0.8125	0.1175	-0.1858	0.539
55	-0.2535	0.1213	0.8948	0.0928	-0.1571	0.3997
56	-0.225	0.1879	0.8935	0.0932	-0.0917	0.4674
57	-0.2884	0.0786	0.4211	0.0778	-0.1549	0.3122
58	-0.2853	0.0546	0.4345	0.0775	-0.178	0.2872
59	-0.288	0.06	0.3854	0.07	-0.1501	0.2701
60	-0.2323	0.0517	0.3713	0.0715	-0.1629	0.2683
61	-0.3383	0.1838	0.7233	0.1012	-0.1198	0.4874
62	-0.2848	0.0485	0.354	0.0658	-0.149	0.246
63	-0.3389	0.0837	0.379	0.0723	-0.1333	0.3007
64	-0.3242	0.0654	0.365	0.0768	-0.1643	0.2851
65	-0.3482	0.0207	0.3404	0.069	-0.1863	0.2277
66	-0.6581	-0.1152	0.1832	0.0755	-0.3417	0.1112
67	-0.2859	-0.03	0.2493	0.067	-0.2311	0.1712
68	-0.1989	0.0408	0.276	0.0555	-0.126	0.2071
69	-0.1851	0.0885	0.3089	0.0522	-0.0902	0.2232
70	-0.5318	-0.1168	0.1899	0.0723	-0.3336	0.1003
71	-0.3975	0.0009	0.3124	0.0678	-0.202	0.2038
72	-0.2281	0.0363	0.3112	0.0608	-0.1461	0.2188
73	-0.1984	0.0535	0.281	0.0531	-0.1058	0.2128
74	-0.4346	-0.1047	0.1593	0.0678	-0.308	0.0986
75	-0.2178	0.0211	0.4084	0.0849	-0.1738	0.2159
76	-0.2292	0.053	0.3325	0.057	-0.118	0.224
77	-0.1819	0.0676	0.2725	0.0538	-0.0933	0.2289
78	-0.10255	-0.122	0.1548	0.0778	-0.3554	0.1114
79	-0.8597	-0.1169	0.1832	0.0799	-0.3569	0.1227
80	-0.4435	-0.0453	0.2182	0.0729	-0.284	0.1734
81	-0.3494	0.0404	0.2538	0.0547	-0.1238	0.2045
82	-0.3078	0.0575	0.2895	0.0527	-0.1006	0.2158
83	-0.2954	0.079	0.3043	0.0523	-0.0781	0.236
84	-0.753	-0.1209	0.1508	0.0753	-0.3467	0.105
85	-0.8097	-0.1209	0.2388	0.0778	-0.3541	0.1129
86	-0.4215	-0.0184	0.2422	0.0719	-0.2343	0.1974
87	-0.319	0.0278	0.2497	0.06	-0.1524	0.2078
88	-0.2721	0.0399	0.262	0.0558	-0.1275	0.2073
89	-0.2789	0.0532	0.2598	0.0531	-0.1083	0.2128
90	-0.1804	0.0785	0.327	0.0515	-0.076	0.2331
91	-0.8578	-0.0897	0.1805	0.0672	-0.2912	0.1119
92	-0.5447	-0.1011	0.1873	0.0709	-0.3139	0.1118
93	-0.2303	0.0184	0.253	0.0601	-0.164	0.1969
94	-0.2498	0.0518	0.2882	0.0601	-0.1284	0.2319
95	-0.239	0.0598	0.2787	0.0547	-0.1042	0.2239
96	-0.1818	0.0947	0.3481	0.0509	-0.0581	0.2474

B/H=0.5 N=1 50 degree

# of tap	Min	Mean	max	STDV	- peak	+ peak
1	0.5072	1.1586	2.0929	0.2414	0.4345	1.8827
2	-1.3943	-0.2298	0.2783	0.1301	-0.6202	0.1607
3	-1.3904	-0.2671	0.247	0.1541	-0.7293	0.1951
4	-1.4458	-0.2105	0.3476	0.1359	-0.6181	0.1972
5	-0.9052	-0.1093	0.377	0.1184	-0.4846	0.2481
6	-0.8859	-0.0169	0.4381	0.0993	-0.3147	0.2861
7	-0.7046	-0.0174	0.3696	0.0874	-0.2794	0.2447
8	-0.8118	-0.0988	0.2025	0.0767	-0.3288	0.1311
9	-1.2758	-0.236	0.2794	0.1531	-0.6952	0.2232
10	-0.7653	-0.122	0.2501	0.0925	-0.3995	0.1554
11	-0.5563	-0.073	0.3532	0.0881	-0.3373	0.1913
12	-0.5011	-0.0228	0.3825	0.0793	-0.2506	0.215
13	-0.5037	-0.0098	0.2527	0.0714	-0.2241	0.2046
14	-0.4951	-0.0799	0.1882	0.0621	-0.266	0.1084
15	-0.3414	-0.1748	0.2804	0.1293	-0.5826	0.2131
16	-0.4998	-0.0638	0.2687	0.0836	-0.3147	0.1871
17	-0.4741	-0.0453	0.2518	0.0781	-0.2798	0.1819
18	-0.8521	-0.1015	0.3184	0.113	-0.4404	0.2374
19	-0.8808	-0.0552	0.3807	0.0856	-0.3119	0.2015
20	-0.5955	-0.0277	0.2999	0.0761	-0.2581	0.2008
21	-0.6931	-0.0903	0.3905	0.122	-0.4562	0.2757
22	-0.6153	-0.0689	0.3037	0.0974	-0.3591	0.2253
23	-0.4476	-0.0282	0.3096	0.0784	-0.2553	0.203
24	-0.4352	-0.0003	0.2894	0.0697	-0.2121	0.2061
25	-0.4545	-0.0139	0.3167	0.0842	-0.2065	0.179
26	-0.3942	-0.0454	0.2068	0.0688	-0.2217	0.1308
27	-1.0591	-0.0621	0.3471	0.1116	-0.3969	0.2726
28	-0.6747	-0.0463	0.3232	0.0824	-0.3235	0.231
29	-0.4198	-0.0192	0.3135	0.0752	-0.2447	0.2062
30	-0.4469	-0.0062	0.2803	0.068	-0.2104	0.1979
31	-0.6781	-0.0003	0.2821	0.0843	-0.1925	0.1931
32	-0.09	0.0799	0.2513	0.0334	-0.0204	0.1803
33	-1	-0.0772	0.328	0.1104	-0.4083	0.2539
34	-0.8206	-0.0404	0.3	0.0882	-0.2899	0.2182
35	-0.4756	-0.0076	0.3042	0.0716	-0.2224	0.2072
36	-0.4895	-0.0118	0.3081	0.0688	-0.2119	0.1887
37	-0.3478	-0.0016	0.3191	0.0637	-0.1829	0.1896
38	-0.5213	0.0096	0.277	0.0577	-0.1636	0.1827
39	-0.8384	-0.0816	0.3109	0.0816	-0.4075	0.2443
40	-0.5727	-0.0491	0.2677	0.0819	-0.294	0.1957
41	-0.5285	-0.039	0.2298	0.0873	-0.2408	0.1828
42	-0.3606	-0.0023	0.2708	0.0653	-0.1914	0.1888
43	-0.3102	0.0106	0.3053	0.0818	-0.1743	0.1854
44	-0.3059	0.0105	0.2589	0.0583	-0.1583	0.1794
45	-0.8482	-0.1269	0.2867	0.0918	-0.4022	0.1485
46	-0.5092	-0.0947	0.2878	0.0739	-0.3163	0.127
47	-0.5874	-0.0558	0.219	0.0682	-0.2543	0.1427
48	-0.5827	-0.0059	0.2856	0.0622	-0.1924	0.1806
49	-0.408	0.0381	0.2744	0.0601	-0.1423	0.2188
50	-0.3109	0.0442	0.2856	0.0583	-0.1307	0.2191
51	-0.4084	0.1414	0.8561	0.113	-0.1978	0.4804
52	-0.5452	0.1189	0.8899	0.1186	-0.2373	0.4745
53	-0.3891	0.1778	0.8194	0.1253	-0.198	0.5537
54	-0.3384	0.148	0.8401	0.1128	-0.1918	0.4937
55	-0.2615	0.0798	0.7588	0.0937	-0.2015	0.3807
56	-0.3675	0.1277	0.5769	0.0974	-0.1646	0.4199
57	-0.4445	0.0455	0.3722	0.0765	-0.184	0.275
58	-0.4888	0.0307	0.3318	0.0788	-0.2057	0.2672
59	-0.4483	0.0414	0.3713	0.0725	-0.1759	0.2588
60	-0.2874	0.015	0.3398	0.0727	-0.2031	0.2331
61	-0.3133	0.117	0.7058	0.0995	-0.1814	0.4154
62	-0.324					

B/H=0. N=1 60 degree

# of lap	Min	Mean	max	STDV	- peak	+ peak
1	0.4761	1.1629	1.9895	0.264	0.371	1.9548
1	-1.7269	-0.312	0.324	0.1534	-0.7723	0.1482
2	-1.6315	-0.3198	0.2049	0.1687	-0.8258	0.1892
3	-1.4772	-0.2658	0.2731	0.1434	-0.6958	0.1647
4	-1.0515	-0.1728	0.2547	0.1205	-0.5342	0.189
5	-0.7986	-0.0635	0.2685	0.1048	-0.398	0.231
6	-0.9772	-0.0741	0.2952	0.0975	-0.3665	0.2184
7	-0.6548	-0.1255	0.2108	0.0822	-0.372	0.121
8	-1.5197	-0.3062	0.3137	0.1671	-0.8076	0.1651
9	-1.1248	-0.1812	0.2491	0.1014	-0.4854	0.123
10	-0.5968	-0.1343	0.2447	0.091	-0.4075	0.1388
11	-0.6418	-0.0862	0.2557	0.0844	-0.3395	0.1671
12	-0.8839	-0.0549	0.2427	0.0789	-0.3015	0.1717
13	-0.4933	-0.1097	0.2054	0.0667	-0.3095	0.0903
14	-1.4174	-0.2267	0.3333	0.1402	-0.6472	0.1939
15	-0.742	-0.1209	0.259	0.0887	-0.387	0.1452
16	-0.6691	-0.1034	0.2410	0.0817	-0.3485	0.1416
17	-0.8953	-0.1519	0.3337	0.1171	-0.5031	0.1994
18	-0.7471	-0.1161	0.2944	0.0895	-0.3847	0.1524
19	-0.504	-0.0891	0.3077	0.0792	-0.3268	0.1484
20	-0.9825	-0.1401	0.4039	0.1254	-0.5163	0.238
21	-0.7964	-0.1231	0.3391	0.1007	-0.4253	0.1791
22	-0.6577	-0.0983	0.3084	0.079	-0.3253	0.1487
23	-0.4158	-0.0598	0.3515	0.0731	-0.279	0.1594
24	-0.5455	-0.0677	0.26	0.0887	-0.274	0.1385
25	-0.3841	-0.0817	0.2058	0.0613	-0.2657	0.1022
26	-0.9168	-0.1354	0.3182	0.1134	-0.4759	0.2049
27	-0.7087	-0.1093	0.3129	0.0922	-0.3859	0.1672
28	-0.5338	-0.0763	0.2858	0.0758	-0.3031	0.1505
29	-0.3917	-0.0602	0.2793	0.0692	-0.2677	0.1473
30	-0.6828	-0.0509	0.3362	0.0885	-0.2504	0.1488
31	-0.0897	0.0435	0.2136	0.0339	-0.0583	0.1452
32	-0.9235	-0.1489	0.2828	0.1153	-0.4928	0.199
33	-0.6553	-0.096	0.2525	0.0879	-0.3595	0.1676
34	-0.5122	-0.0551	0.2455	0.0726	-0.2729	0.1627
35	-0.6763	-0.0621	0.2274	0.0686	-0.2679	0.1437
36	-0.5057	-0.0504	0.2523	0.065	-0.2454	0.1445
37	-0.4547	-0.0353	0.2298	0.0579	-0.2088	0.1393
38	-1.0203	-0.1279	0.4242	0.1192	-0.4855	0.2297
39	-0.543	-0.0925	0.2943	0.0888	-0.3588	0.1739
40	-0.6168	-0.0833	0.2196	0.0706	-0.2952	0.1289
41	-0.4206	-0.0428	0.2262	0.0558	-0.2401	0.1545
42	-0.4987	-0.0305	0.2231	0.0631	-0.2197	0.1587
43	-0.3224	-0.0327	0.2053	0.0563	-0.2016	0.1362
44	-0.6788	-0.1721	0.2413	0.0995	-0.4705	0.1953
45	-0.7202	-0.1353	0.2315	0.0812	-0.3789	0.1081
46	-0.465	-0.0906	0.2459	0.0701	-0.3009	0.1198
47	-0.3687	-0.0432	0.3029	0.0642	-0.2359	0.1496
48	-0.2916	0.0191	0.3892	0.0621	-0.1671	0.2054
49	-0.2708	0.0191	0.3521	0.0589	-0.1585	0.1947
50	-0.4891	0.0714	0.7065	0.1111	-0.2819	0.4048
51	-0.4945	0.0525	0.7701	0.1059	-0.2853	0.3702
52	-0.3677	0.1069	0.6969	0.116	-0.241	0.4548
53	-0.3471	0.0922	0.5487	0.1067	-0.229	0.4124
54	-0.3099	0.0456	0.5585	0.0885	-0.2201	0.3112
55	-0.4631	0.0652	0.6039	0.0977	-0.2278	0.3583
56	-0.3644	0.0069	0.4002	0.0753	-0.2191	0.2329
57	-0.5285	-0.0003	0.3306	0.0776	-0.233	0.2323
58	-0.4855	0.0233	0.3201	0.0732	-0.1982	0.2427
59	-0.3345	-0.0035	0.3097	0.0676	-0.2083	0.1892
60	-0.3511	0.0538	0.5079	0.0916	-0.2233	0.3284
61	-0.3437	-0.019	0.3175	0.0657	-0.216	0.1781
62	-0.2977	0.0266	0.3314	0.0672	-0.175	0.2282
63	-0.3459	0.011	0.3111	0.0677	-0.1921	0.2141
64	-0.2855	-0.0193	0.2393	0.0628	-0.2078	0.1692
65	-0.8051	-0.1738	0.1955	0.0920	-0.4524	0.1048
66	-0.4002	-0.0582	0.2659	0.0703	-0.2891	0.1526
67	-0.3279	-0.0065	0.2501	0.0637	-0.1978	0.1848
68	-0.54	0.012	0.2614	0.0592	-0.1854	0.1895
69	-0.5096	-0.164	0.1908	0.0798	-0.4034	0.0753
70	-0.3689	-0.0392	0.2712	0.066	-0.2372	0.1588
71	-0.2806	0.0089	0.264	0.0814	-0.1743	0.194
72	-0.2503	0.0038	0.2419	0.0564	-0.1654	0.1731
73	-0.5806	-0.1439	0.1992	0.0787	-0.374	0.0882
74	-0.3564	-0.049	0.2162	0.0644	-0.2421	0.1441
75	-0.216	0.0074	0.3187	0.0592	-0.1701	0.185
76	-0.2336	0.0204	0.2412	0.0584	-0.1489	0.1897
77	-0.6518	-0.1612	0.1159	0.083	-0.4102	0.0879
78	-0.6514	-0.1579	0.1286	0.0866	-0.4176	0.1018
79	-0.4632	-0.0812	0.1998	0.0749	-0.306	0.1436
80	-0.2559	-0.0116	0.2315	0.0569	-0.1823	0.1591
81	-0.2191	0.0021	0.218	0.0557	-0.1651	0.1692
82	-0.2464	0.0281	0.2558	0.057	-0.143	0.1991
83	-0.6315	-0.1598	0.094	0.0831	-0.409	0.0898
84	-0.6984	-0.1850	0.089	0.0889	-0.4325	0.1068
85	-0.4784	-0.0889	0.2267	0.0796	-0.3075	0.1698
86	-0.3006	-0.0244	0.2465	0.0658	-0.2216	0.1729
87	-0.2804	-0.0164	0.2304	0.0589	-0.1931	0.1602
88	-0.2399	-0.0013	0.2218	0.0536	-0.1717	0.1691
89	-0.2311	0.0289	0.2812	0.0559	-0.1388	0.1959
90	-0.5168	-0.1272	0.0939	0.072	-0.343	0.0887
91	-0.5322	-0.1454	0.1023	0.0792	-0.3829	0.0921
92	-0.2754	-0.0128	0.2798	0.0657	-0.2097	0.1846
93	-0.333	-0.0051	0.2482	0.0645	-0.1984	0.1883
94	-0.2353	0.0042	0.2382	0.0588	-0.1718	0.18
95	-0.1822	0.0485	0.2708	0.0552	-0.1172	0.2143

B/H=0. N=1 70 degree

# of lap	Min	Mean	max	STDV	- peak	+ peak
1	0.5176	1.163	1.9998	0.2419	0.4374	1.8885
1	-1.2297	-0.2525	0.3053	0.1495	-0.7011	0.1962
2	-1.0259	-0.199	0.3024	0.1478	-0.6423	0.2444
3	-0.8807	-0.164	0.3828	0.1291	-0.5514	0.2235
4	-0.8644	-0.1038	0.4407	0.1038	-0.4143	0.2071
5	-0.7711	-0.0376	0.3706	0.0925	-0.3152	0.24
6	-1.1483	-0.0354	0.359	0.0921	-0.3117	0.2409
7	-0.6997	-0.0488	0.3819	0.0822	-0.2955	0.1979
8	-1.0669	-0.2147	0.4373	0.1519	-0.6701	0.2408
9	-0.6908	-0.1164	0.3595	0.0864	-0.4057	0.173
10	-0.5699	-0.0754	0.4323	0.0863	-0.3343	0.1835
11	-0.4369	-0.0433	0.381	0.0801	-0.2835	0.1989
12	-0.8284	-0.0265	0.3877	0.0781	-0.2608	0.2079
13	-0.4753	-0.0358	0.3395	0.0698	-0.2445	0.1733
14	-0.8294	-0.1288	0.4412	0.1278	-0.5133	0.2536
15	-0.5066	-0.0618	0.4241	0.0857	-0.319	0.1954
16	-0.7496	-0.0496	0.3845	0.0795	-0.2882	0.1889
17	-0.9045	-0.0649	0.4442	0.1084	-0.3902	0.2604
18	-0.775	-0.0512	0.3501	0.0875	-0.3138	0.2174
19	-0.4146	-0.034	0.3811	0.0719	-0.2677	0.1996
20	-1.0001	-0.0495	0.4215	0.1152	-0.3952	0.2952
21	-0.7963	-0.0476	0.3848	0.0939	-0.3293	0.2342
22	-0.4459	-0.0301	0.336	0.0785	-0.2655	0.2053
23	-0.3614	-0.0355	0.3334	0.0739	-0.227	0.2161
24	-0.3292	-0.0155	0.334	0.071	-0.2286	0.1976
25	-0.3407	-0.0189	0.2925	0.0639	-0.2107	0.1728
26	-0.7323	-0.0649	0.4442	0.1104	-0.396	0.2661
27	-0.6448	-0.0396	0.4041	0.0929	-0.3183	0.2391
28	-0.4448	-0.0112	0.339	0.0775	-0.2438	0.2214
29	-0.3469	0.0013	0.315	0.071	-0.2117	0.2143
30	-0.7928	0.0098	0.3178	0.0692	-0.198	0.2172
31	-0.0897	0.0973	0.2963	0.0393	-0.0206	0.2152
32	-1.0236	-0.0837	0.5555	0.1238	-0.4551	0.2877
33	-0.7292	-0.0312	0.4474	0.0972	-0.3227	0.2893
34	-0.5409	0.0115	0.3606	0.0796	-0.2273	0.2503
35	-0.3586	0.0013	0.3864	0.0728	-0.217	0.2195
36	-0.4963	0.0103	0.3834	0.0688	-0.1962	0.2168
37	-0.2512	0.0211	0.313	0.0607	-0.1611	0.2033
38	-0.9145	-0.0773	0.5386	0.1304	-0.4683	0.3138
39	-0.7179	-0.0415	0.4413	0.1027	-0.3496	0.2695
40	-0.5706	-0.0319	0.293	0.0808	-0.2743	0.2105
41	-0.3418	0.0149	0.3858	0.0732	-0.2048	0.2345
42	-0.3361	0.0284	0.3671	0.0692	-0.1793	0.2362
43	-0.2871	0.0184	0.3195	0.0601	-0.1608	0.1997
44	-0.8698	-0.1201	0.4364	0.1044	-0.4332	0.193
45	-0.5906	-0.0763	0.3329	0.0899	-0.3459	0.1832
46	-0.6221	-0.0354	0.2919	0.079	-0.2725	0.2016
47	-0.4884	0.0058	0.3488	0.0741	-0.2163	0.228
48	-0.4258	0.0597	0.3691	0.0698	-0.1498	0.2692
49	-0.4559	0.053	0.3327	0.0642	-0.1395	0.2455
50	-0.5348	0.0578	0.6244	0.0947	-0.2284	0.3419
51	-0.3485	0.0489	0.6728	0.0857	-0.2102	0.304
52	-0.5268	0.0868	0.7367	0.0942	-0.1957	0.3593
53	-0.357	0.0793	0.5785	0.0824	-0.198	0.3697
54	-0.2704	0.0577	0.4993	0.0812	-0.1859	0.3011
55	-0.3661	0.0587	0.5747	0.086	-0.1993	0.3166
56	-0.2271	0.0278	0.3904	0.0699	-0.1819	0.2376
57	-0.3443	0.0237	0.3817	0.0711	-0.1808	0.2371
58	-0.3471	0.0331	0.3998	0.0698	-0.1458	0.2717
59	-0.2767	0.0444	0.3001	0.0628	-0.1439	0.2326
60	-0.					

B/H=0.5 N=1 80 degree							
# of lap	Min	Mean	max	STDV	peak	+ peak	
1	0.5591	1.2345	2.1964	0.2572	0.4327	2.0362	
1	-1.0084	-0.121	0.3404	0.1275	-0.5034	0.2614	
2	-0.7974	-0.0486	0.3469	0.1059	-0.3663	0.2691	
3	-0.16397	-0.024	0.3176	0.102	-0.3302	0.2821	
4	-0.5328	0.005	0.3451	0.0848	-0.2495	0.2555	
5	-0.3991	0.0537	0.435	0.0782	-0.1809	0.2883	
6	-0.4886	0.05	0.3554	0.0766	-0.1797	0.2798	
7	-0.4128	0.0554	0.3852	0.0709	-0.1573	0.2682	
8	-0.7211	-0.07	0.3953	0.1248	-0.4444	0.3043	
9	-0.4598	-0.0145	0.3474	0.0853	-0.2705	0.2415	
10	-0.3427	0.0163	0.3399	0.0775	-0.2161	0.2486	
11	-0.3513	0.0404	0.3422	0.0743	-0.1826	0.2634	
12	-0.3015	0.0534	0.3311	0.073	-0.1657	0.2725	
13	-0.2198	0.0621	0.3872	0.0687	-0.1381	0.2823	
14	-0.5262	-0.005	0.4326	0.1067	-0.3251	0.315	
15	-0.346	0.0286	0.424	0.0809	-0.2137	0.2714	
16	-0.3607	0.0357	0.3707	0.0744	-0.1875	0.2588	
17	-0.5643	0.0379	0.4792	0.0983	-0.2527	0.3328	
18	-0.6774	0.0402	0.4259	0.084	-0.212	0.2923	
19	-0.3402	0.0515	0.4911	0.0758	-0.176	0.279	
20	-0.6088	0.0493	0.5713	0.1085	-0.2761	0.3747	
21	-0.5515	0.0459	0.4917	0.0907	-0.2261	0.3176	
22	-0.2726	0.0553	0.3771	0.0776	-0.1774	0.288	
23	-0.2979	0.0797	0.3821	0.0728	-0.1386	0.298	
24	-0.287	0.0683	0.3756	0.0696	-0.1405	0.2771	
25	-0.46	0.069	0.3735	0.064	-0.1229	0.2609	
26	-0.7941	0.0077	0.4906	0.1158	-0.3396	0.3551	
27	-0.5817	0.0336	0.4581	0.0989	-0.2659	0.3331	
28	-0.3771	0.0563	0.4538	0.0824	-0.1809	0.3135	
29	-0.4869	0.0912	0.4064	0.0757	-0.146	0.3083	
30	-0.3235	0.0914	0.3946	0.0711	-0.1219	0.3046	
31	-0.0066	0.1643	0.3398	0.0432	-0.0346	0.2939	
32	-0.8957	-0.0216	0.5578	0.1262	-0.4002	0.357	
33	-0.6957	0.0319	0.5285	0.105	-0.2832	0.347	
34	-0.4915	0.0798	0.7014	0.0879	-0.1838	0.3435	
35	-0.3285	0.0728	0.5889	0.0789	-0.1638	0.3095	
36	-0.397	0.0831	0.4759	0.0742	-0.1395	0.3056	
37	-0.4196	0.0985	0.3733	0.065	-0.0965	0.2934	
38	-0.9196	-0.003	0.6494	0.1294	-0.3912	0.3792	
39	-0.7457	0.0254	0.5458	0.1051	-0.2899	0.3406	
40	-0.6155	0.0317	0.4661	0.0875	-0.2309	0.2944	
41	-0.5033	0.0801	0.4432	0.0798	-0.1592	0.3195	
42	-0.2696	0.0953	0.4648	0.0747	-0.1277	0.3203	
43	-0.3285	0.0895	0.3754	0.0542	-0.1032	0.2822	
44	-0.702	-0.0421	0.5364	0.1007	-0.3441	0.26	
45	-0.4517	0.0044	0.435	0.0809	-0.2622	0.2709	
46	-0.5948	0.0391	0.3879	0.0814	-0.206	0.2823	
47	-0.3126	0.0718	0.4411	0.0767	-0.1587	0.3018	
48	-0.3288	0.1163	0.528	0.0738	-0.105	0.3376	
49	-0.4295	0.1041	0.4508	0.0675	-0.0983	0.3066	
50	-0.4522	0.0887	0.6589	0.0831	-0.1604	0.3379	
51	-0.1999	0.0906	0.4507	0.0699	-0.1192	0.3004	
52	-0.2246	0.1204	0.5085	0.0706	-0.0915	0.3322	
53	-0.2813	0.1087	0.6011	0.0716	-0.106	0.3234	
54	-0.2919	0.1002	0.5447	0.0674	-0.102	0.3023	
55	-0.2261	0.0896	0.5983	0.0774	-0.1424	0.3217	
56	-0.2047	0.0878	0.4047	0.0656	-0.1088	0.2845	
57	-0.257	0.0808	0.427	0.0642	-0.1117	0.2733	
58	-0.1582	0.1252	0.4329	0.0634	-0.0649	0.3154	
59	-0.161	0.1167	0.3822	0.0604	-0.0644	0.2976	
60	-0.2112	0.0897	0.4969	0.0747	-0.1344	0.3138	
61	-0.1728	0.0818	0.3934	0.0623	-0.054	0.2888	
62	-0.143	0.1097	0.4066	0.06	-0.0703	0.2897	
63	-0.1502	0.0907	0.4037	0.0594	-0.0677	0.269	
64	-0.134	0.1028	0.3511	0.0564	-0.0664	0.272	
65	-0.5468	0.0025	0.3889	0.0894	-0.2566	0.2617	
66	-0.315	0.0783	0.3917	0.0702	-0.1324	0.289	
67	-0.3257	0.0998	0.4198	0.0687	-0.1065	0.306	
68	-0.3611	0.1037	0.3838	0.0671	-0.0976	0.305	
69	-0.4801	0.0085	0.3891	0.0804	-0.2327	0.2497	
70	-0.1682	0.0818	0.4227	0.0651	-0.1138	0.2772	
71	-0.2089	0.1219	0.4317	0.0634	-0.0693	0.312	
72	-0.2358	0.1013	0.3641	0.0601	-0.0791	0.2817	
73	-0.2899	0.026	0.4355	0.0767	-0.204	0.256	
74	-0.1739	0.0704	0.3475	0.0648	-0.1242	0.2649	
75	-0.1229	0.1137	0.4418	0.0809	-0.069	0.2964	
76	-0.1362	0.1162	0.3764	0.0583	-0.0589	0.2912	
77	-0.2526	0.0596	0.3319	0.0687	-0.1407	0.2598	
78	-0.2734	0.0688	0.3369	0.0678	-0.1349	0.272	
79	-0.2221	0.0866	0.3856	0.0645	-0.0969	0.29	
80	-0.1034	0.1166	0.3488	0.0598	-0.0623	0.2855	
81	-0.1034	0.1122	0.4019	0.0596	-0.0667	0.291	
82	-0.1488	0.1147	0.3801	0.0621	-0.0716	0.3009	
83	-0.2622	0.0632	0.3585	0.0659	-0.1344	0.2609	
84	-0.2872	0.0677	0.3649	0.0688	-0.1388	0.2742	
85	-0.2523	0.0952	0.3606	0.0648	-0.0988	0.289	
86	-0.124	0.1258	0.3635	0.0619	-0.06	0.3115	
87	-0.1161	0.1142	0.3559	0.0593	-0.0636	0.292	
88	-0.0855	0.1154	0.374	0.06	-0.0646	0.2955	
89	-0.1449	0.1152	0.3832	0.0597	-0.0639	0.2841	
90	-0.2875	0.0719	0.3527	0.0626	-0.1157	0.2586	
91	-0.2621	0.069	0.326	0.0646	-0.1247	0.2627	
92	-0.1473	0.1071	0.3848	0.0601	-0.0732	0.2874	
93	-0.1162	0.1345	0.3774	0.0597	-0.0446	0.3136	
94	-0.073	0.1278	0.373	0.0582	-0.0471	0.3023	
95	-0.1159	0.1385	0.4033	0.0572	-0.035	0.308	

B/H=0.5 N=1 90 degree							
# of lap	Min	Mean	max	STDV	peak	+ peak	
1	0.6006	1.3049	2.2058	0.2625	0.5175	2.0924	
1	-0.6784	-0.0194	0.3803	0.102	-0.3255	0.2868	
2	-0.5273	0.0301	0.4202	0.0837	-0.2211	0.2813	
3	-0.4174	0.0583	0.4552	0.0839	-0.1834	0.3099	
4	-0.4374	0.0767	0.459	0.078	-0.1574	0.3107	
5	-0.3124	0.1129	0.4928	0.073	-0.1061	0.3319	
6	-0.4295	0.0521	0.4291	0.0722	-0.1114	0.3216	
7	-0.3262	0.1232	0.5249	0.0678	-0.0803	0.3267	
8	-0.3666	0.0201	0.5077	0.1039	-0.2913	0.3314	
9	-0.4584	0.042	0.5007	0.0844	-0.2113	0.2952	
10	-0.3003	0.0685	0.4728	0.0761	-0.1598	0.2969	
11	-0.3022	0.0922	0.4583	0.072	-0.1237	0.3082	
12	-0.35	0.1034	0.515	0.0708	-0.1091	0.3159	
13	-0.2398	0.1276	0.5176	0.0657	-0.0695	0.3245	
14	-0.6345	0.0529	0.5454	0.0885	-0.2427	0.3486	
15	-0.4127	0.0753	0.5094	0.0826	-0.1726	0.3292	
16	-0.4368	0.0825	0.4935	0.0757	-0.1445	0.3095	
17	-0.7896	0.0641	0.6091	0.101	-0.2388	0.3671	
18	-0.533	0.0748	0.5104	0.088	-0.1891	0.3387	
19	-0.465	0.0911	0.5042	0.0798	-0.1476	0.3299	
20	-1.0964	0.0634	0.6345	0.1115	-0.2711	0.3978	
21	-0.5054	0.0733	0.514	0.0947	-0.2106	0.3573	
22	-0.4384	0.0914	0.5123	0.0815	-0.153	0.3357	
23	-0.2657	0.12	0.498	0.0747	-0.104	0.344	
24	-0.2715	0.1107	0.4378	0.0712	-0.1028	0.3242	
25	-0.1567	0.1193	0.446	0.0629	-0.0694	0.3079	
26	-1.0472	0.0266	0.8086	0.1629	-0.3307	0.384	
27	-0.6153	0.0575	0.6123	0.1036	-0.2532	0.3682	
28	-0.436	0.0955	0.5326	0.0855	-0.1611	0.3522	
29	-0.357	0.1146	0.4802	0.0765	-0.1149	0.344	
30	-0.4123	0.1288	0.5209	0.0716	-0.0879	0.3415	
31	0.0593	0.1828	0.387	0.0404	0.0715	0.3142	
32	-1.4309	0.0181	0.6256	0.1237	-0.355	0.3873	
33	-0.6065	0.0688	0.5808	0.1022	-0.2382	0.3753	
34	-0.4223	0.1149	0.5437	0.0857	-0.142	0.3719	
35	-0.6734	0.1063	0.4153	0.0775	-0.1261	0.3388	
36	-0.7339	0.1145	0.4669	0.073	-0.1043	0.3334	
37	-0.2074	0.1299	0.4273	0.0619	-0.059	0.3157	
38	-0.8072	0.0495	0.582	0.1209	-0.3131	0.4121	
39	-0.5987	0.0735	0.5326	0.0971	-0.2178	0.3648	
40	-0.5659	0.0699	0.4481	0.0742	-0.1678	0.3075	
41	-0.3592	0.1161	0.4115	0.0797	-0.108	0.3402	
42	-0.5733	0.1287	0.4315	0.0713	-0.0851	0.3425	
43	-0.1696	0.1144	0.363	0.0607	-0.0678	0.2966	
44	-0.6641	0.0052	0.4521	0.0946	-0.2786	0.289	
45	-0.6748	0.049	0.4525	0.0841	-0.2032	0.3011	
46	-0.4309	0.0674	0.3916	0.078	-0.1667	0.3016	
47	-0.4188	0.098	0.4009	0.0742	-0.1247	0.3207	
48	-0.35	0.1365	0.4589	0.0721	-0.099	0.3528	
49	-0.5453	0.1077	0.4091	0.0638	-0.0837	0.2991	
50	-0.5092	0.0942	0.4589	0.0824	-0.1529	0.3413	
51	-0.1111	0.128	0.4697	0.0651	-0.0673	0.3233	
52	-0.3809	0.1538	0.5678	0.068	-0.0441	0.3518	
53	-0.2649						

B/H=0.5 N=1 0 degree						
# of tap	Min	Mean	max	STOV	- peak	+ peak
1	0.5799	1.266	2.1343	0.2613	0.4822	2.0498
2	-0.6391	0.0094	0.392	0.0935	-0.2709	0.2893
3	-0.7342	0.0159	0.4245	0.1021	-0.2904	0.3221
4	-0.7922	0.0207	0.4692	0.1087	-0.2993	0.3407
5	-0.7683	0.0252	0.4475	0.1049	-0.2895	0.3399
6	-0.6999	0.0284	0.4242	0.0992	-0.289	0.3259
7	-1.0242	0.0398	0.4722	0.0989	-0.2569	0.3365
8	-0.6759	-0.011	0.4666	0.0936	-0.2918	0.2998
9	-0.5079	0.0443	0.3936	0.0776	-0.1886	0.2772
10	-0.4651	0.0472	0.4063	0.0793	-0.1908	0.2853
11	-0.4412	0.0599	0.4545	0.0826	-0.188	0.3078
12	-0.385	0.0597	0.4316	0.0786	-0.1782	0.2956
13	-0.3774	0.0643	0.458	0.0787	-0.172	0.3005
14	-0.6674	0.0431	0.3448	0.0769	-0.1875	0.2747
15	-0.4219	0.0573	0.3723	0.0798	-0.1641	0.2787
16	-0.3054	0.0632	0.4135	0.074	-0.1589	0.2652
17	-0.3107	0.0669	0.3942	0.0743	-0.1561	0.2698
18	-0.4143	0.0666	0.4165	0.0709	-0.1461	0.2792
19	-0.3014	0.0754	0.4324	0.0702	-0.1352	0.286
20	-0.4137	0.0805	0.3808	0.0696	-0.1282	0.2891
21	-0.5206	0.0659	0.4033	0.0712	-0.1477	0.2795
22	-0.2433	0.0725	0.3871	0.0691	-0.1348	0.2797
23	-0.2912	0.0838	0.3846	0.0881	-0.1204	0.286
24	-0.2573	0.0887	0.3808	0.0861	-0.1118	0.2851
25	-0.3479	0.0811	0.3918	0.0855	-0.1153	0.2776
26	-0.7038	0.0588	0.3324	0.07	-0.1533	0.2677
27	-0.5541	0.0772	0.3769	0.0692	-0.1305	0.2849
28	-0.3159	0.0832	0.4132	0.0675	-0.1193	0.2857
29	-0.245	0.0914	0.4179	0.0639	-0.1004	0.2832
30	-0.3187	0.0903	0.3798	0.0615	-0.0944	0.2749
31	-0.2849	0.0896	0.3848	0.0619	-0.0962	0.2754
32	-0.5541	0.0772	0.3769	0.0692	-0.1305	0.2849
33	-0.3291	0.088	0.4094	0.0683	-0.1169	0.2929
34	-0.2364	0.0943	0.3939	0.0655	-0.1022	0.2899
35	-0.2327	0.103	0.3641	0.0617	-0.0822	0.2882
36	-0.1744	0.1028	0.4089	0.0602	-0.0778	0.2835
37	-0.2239	0.0997	0.378	0.0602	-0.081	0.2804
38	-0.528	0.0883	0.415	0.0642	-0.1043	0.2809
39	-0.2979	0.093	0.4139	0.0660	-0.1069	0.2929
40	-0.355	0.0992	0.4139	0.063	-0.0897	0.288
41	-0.1883	0.1048	0.4124	0.0588	-0.0718	0.2813
42	-0.2497	0.1035	0.3841	0.0574	-0.0685	0.2758
43	-0.1761	0.1018	0.3455	0.0579	-0.072	0.2758
44	-0.4902	0.0883	0.359	0.0619	-0.0973	0.2739
45	-0.3005	0.1041	0.3846	0.0607	-0.078	0.2862
46	-0.2027	0.1032	0.348	0.0588	-0.0673	0.2736
47	-0.1386	0.1013	0.3275	0.0534	-0.0589	0.2614
48	-0.161	0.0978	0.312	0.0538	-0.0638	0.259
49	-0.259	0.0506	0.2887	0.0552	-0.1149	0.2181
50	-0.392	0.0356	0.3413	0.0609	-0.1489	0.2182
51	-0.2583	0.1414	0.8887	0.1167	-0.2087	0.4915
52	-0.2754	0.1597	0.8234	0.1189	-0.191	0.5104
53	-0.2558	0.1889	1.2257	0.1322	-0.2078	0.5855
54	-0.7032	0.2195	1.07	0.1529	-0.2382	0.6783
55	-0.2393	0.2307	1.1741	0.1589	-0.237	0.6983
56	-0.176	0.0935	0.5814	0.0808	-0.1489	0.3359
57	-0.3077	0.0618	0.3766	0.0731	-0.1575	0.2611
58	-0.3727	0.0616	0.4164	0.0758	-0.1654	0.2885
59	-0.2731	0.0571	0.3855	0.0755	-0.1693	0.2836
60	-0.2453	0.1635	0.8131	0.1085	-0.1651	0.4921
61	-0.5735	0.0719	0.4307	0.0808	-0.1389	0.2807
62	-0.2805	0.0533	0.3468	0.0554	-0.1428	0.2494
63	-0.2148	0.0499	0.3546	0.0676	-0.153	0.2528
64	-0.2907	0.065	0.3577	0.0701	-0.1552	0.2651
65	-0.5519	0.1082	0.7358	0.0894	-0.1599	0.3783
66	-0.1724	0.0648	0.2911	0.0542	-0.0979	0.2275
67	-0.221	0.0572	0.2443	0.0538	-0.1035	0.218
68	-0.3421	0.0394	0.2868	0.0591	-0.139	0.2158
69	-0.3701	-0.0033	0.246	0.0659	-0.2002	0.1936
70	-0.1882	0.0684	0.2808	0.0538	-0.0948	0.2273
71	-0.2819	0.0578	0.2409	0.0555	-0.109	0.2243
72	-0.2394	0.0475	0.2762	0.0571	-0.1237	0.2187
73	-0.4783	-0.0142	0.2311	0.0671	-0.2156	0.1872
74	-0.1842	0.0611	0.2725	0.0533	-0.0989	0.221
75	-0.2309	0.063	0.2775	0.056	-0.1151	0.2211
76	-0.181	0.0551	0.3259	0.0538	-0.1083	0.2164
77	-0.3779	-0.0093	0.2306	0.0658	-0.2051	0.1874
78	-0.7071	-0.0099	0.3981	0.0978	-0.3034	0.2836
79	-0.3878	0.0358	0.3899	0.0858	-0.1612	0.2923
80	-0.3437	0.051	0.3929	0.0829	-0.1378	0.2999
81	-0.3513	0.0582	0.4188	0.0848	-0.1391	0.2925
82	-0.5022	0.063	0.3828	0.0659	-0.1347	0.2607
83	-0.3887	0.0415	0.3183	0.0607	-0.1407	0.2236
84	-0.5825	0.0177	0.332	0.0749	-0.2062	0.2416
85	-0.2889	0.0374	0.3378	0.0613	-0.1488	0.2215
86	-0.29	0.0493	0.3517	0.0602	-0.1314	0.2289
87	-0.3491	0.06	0.3544	0.0612	-0.1235	0.2436
88	-0.3858	0.0685	0.3581	0.062	-0.1195	0.2528
89	-0.2883	0.064	0.3309	0.0618	-0.1208	0.2489
90	-0.2655	0.0432	0.276	0.0557	-0.1238	0.2102
91	-0.4569	0.0424	0.3863	0.0656	-0.1549	0.2397
92	-0.2466	0.0415	0.3826	0.0587	-0.1347	0.2177
93	-0.2347	0.0471	0.3571	0.0577	-0.1259	0.2201
94	-0.2884	0.0441	0.333	0.0588	-0.1118	0.2399
95	-0.2342	0.0728	0.3184	0.0571	-0.0988	0.2438
96	-0.1855	0.0545	0.2939	0.0514	-0.0998	0.2085

B/H=0.5 N=2 0 degree						
# of tap	Min	Mean	max	STOV	- peak	+ peak
1	0.4613	1.1082	1.9629	0.2574	0.3341	1.8784
2	-0.6123	0.0113	0.4588	0.095	-0.2739	0.2964
3	-0.6277	0.0199	0.4105	0.1008	-0.2825	0.322
4	-0.7506	0.0246	0.4171	0.1024	-0.2826	0.3319
5	-0.5871	0.0297	0.401	0.098	-0.2644	0.3238
6	-0.5866	0.0284	0.4099	0.094	-0.2536	0.3105
7	-0.5366	0.0324	0.5216	0.0966	-0.2574	0.3222
8	-0.6696	0.0331	0.4552	0.0942	-0.2795	0.2857
9	-0.7008	0.0406	0.5048	0.0798	-0.1989	0.28
10	-0.4331	0.0495	0.5231	0.08	-0.1906	0.2896
11	-0.3225	0.0571	0.3829	0.0789	-0.1793	0.2935
12	-0.3381	0.0565	0.4042	0.0786	-0.1715	0.2846
13	-0.4189	0.0567	0.4619	0.0788	-0.1798	0.2931
14	-1.0386	0.0397	0.3989	0.0839	-0.2119	0.2913
15	-0.5154	0.0573	0.4674	0.0788	-0.1731	0.2877
16	-0.3893	0.0643	0.4851	0.0743	-0.1587	0.2872
17	-0.3133	0.0679	0.3944	0.0726	-0.15	0.2858
18	-0.3429	0.0656	0.4294	0.0733	-0.1543	0.2854
19	-0.2534	0.0746	0.4234	0.0707	-0.1376	0.2867
20	-0.3351	0.0783	0.4003	0.0694	-0.1299	0.2864
21	-0.3769	0.0646	0.4148	0.0738	-0.157	0.2861
22	-0.2571	0.0717	0.4575	0.0705	-0.1397	0.2832
23	-0.33	0.0799	0.3979	0.0684	-0.1254	0.2853
24	-0.3808	0.0807	0.3721	0.0673	-0.1212	0.2825
25	-0.2462	0.0756	0.3786	0.0677	-0.1278	0.2789
26	-0.4683	0.0516	0.3565	0.0745	-0.1718	0.2751
27	-0.2697	0.0727	0.4397	0.0713	-0.1412	0.2866
28	-0.2629	0.0778	0.4359	0.0687	-0.1285	0.284
29	-0.2972	0.0842	0.4034	0.0654	-0.1119	0.2803
30	-0.2348	0.0809	0.3862	0.0644	-0.1123	0.2741
31	-0.2413	0.0806	0.3932	0.0649	-0.1141	0.2752
32	-0.0994	0.1246	0.314	0.0644	-0.0214	0.2789
33	-0.3543	0.0792	0.4172	0.0696	-0.1297	0.2881
34	-0.4554	0.084	0.3856	0.0671	-0.1174	0.2854
35	-0.3028	0.0911	0.3804	0.0641	-0.1012	0.2834
36	-0.2032	0.0893	0.3671	0.0628	-0.0991	0.2777
37	-0.2915	0.0856	0.402	0.0629	-0.1032	0.2744
38	-0.2518	0.0757	0.367	0.0679	-0.128	0.2795
39	-0.3844	0.0807	0.4705	0.0677	-0.1223	0.2838
40	-0.2429	0.0859	0.4298	0.0644	-0.1073	0.2792
41	-0.1943	0.0897	0.3917	0.0614	-0.0944	0.2739
42	-0.1537	0.0877	0.37	0.0602	-0.0929	0.2683
43	-0.2998	0.0858	0.3905	0.0604	-0.0954	0.267
44	-0.3798	0.0743	0.382	0.0645	-0.1191	0.2677
45	-0.3487	0.0646	0.3762	0.062	-0.1013	0.2705
46	-0.2531	0.0793	0.3375	0.059	-0.0977	0.2564
47	-0.187	0.0781	0.334	0.0565	-0.0913	0.2475
48	-0.3844	0.0747	0.4705	0.0677	-0.1223	0.2838
49	-0.2598	0.0623	0.3108	0.0603	-0.1547	0.2073
50	-0.3496	0.0164	0.373	0.0647	-0.1776	0.2105
51	-0.378	0.1345	1.0845	0.1223	-0.2326	0.5015
52	-0.3108	0.149	0.8587	0.1105	-0.1824	0.4803
53	-0.2345	0.1782	1.0019	0.1303	-0.2128	0.5591
54	-0.4474	0.1916	1.1226	0.1419	-0.2342	0.6173
55	-0.2717	0.2029	1.3282	0.1553	-0.263	0.6688
56	-0.3845	0.0629	0.5777	0.0651	-0.1925	0.3182
57	-0.4302	0.0405	0.3284	0.0725	-0.1771	0.2582
58	-0.282	0.0387	0.3591	0.0732	-0.1808	0.2583
59	-0.3234	0.0384	0.3696	0.0743	-0.1843	0.2612
60	-0.3246	0.1143	0.8161	0.1073	-0.2075	0.4382
61	-0.3883	0.0444	0.4823	0.0728	-	

B/H=0.5 N=3 0 degree						
# of lap	Min	Mean	max	STDV	- peak	+ peak
1	0.4462	1.1185	1.9325	0.2468	0.378	1.8589
2	-0.5602	0.0101	0.5372	0.0932	-0.2695	0.2897
3	-0.6188	0.0198	0.5035	0.0969	-0.2709	0.3106
4	-0.761	0.0246	0.5155	0.0991	-0.2728	0.3219
5	-0.82	0.0281	0.4839	0.0938	-0.2548	0.3069
6	-0.5381	0.0181	0.4002	0.0897	-0.2511	0.2873
7	-0.5814	0.0227	0.464	0.0914	-0.2517	0.297
8	-0.6002	-0.0081	0.3978	0.0902	-0.2788	0.2625
9	-0.3649	0.0368	0.4585	0.0759	-0.1912	0.2643
10	-0.3784	0.0441	0.46	0.0763	-0.1849	0.2732
11	-0.4186	0.0505	0.4978	0.0757	-0.1767	0.2777
12	-0.4266	0.0455	0.4003	0.0728	-0.1724	0.2634
13	-0.2908	0.0476	0.3538	0.0732	-0.1719	0.2671
14	-0.4243	0.0311	0.3317	0.075	-0.1938	0.2581
15	-0.4292	0.0501	0.4251	0.0721	-0.1863	0.2685
16	-0.4027	0.0548	0.4134	0.0703	-0.1562	0.2658
17	-0.4144	0.0538	0.4894	0.0693	-0.1541	0.2618
18	-0.2789	0.0547	0.4243	0.069	-0.1522	0.2616
19	-0.3179	0.0609	0.388	0.0671	-0.1404	0.2622
20	-0.275	0.0639	0.3477	0.0662	-0.1346	0.2623
21	-0.3554	0.0547	0.4176	0.0695	-0.1537	0.2632
22	-0.2532	0.0593	0.3852	0.0687	-0.1416	0.2583
23	-0.2451	0.0653	0.3966	0.0653	-0.1305	0.2611
24	-0.1982	0.0652	0.3672	0.0644	-0.128	0.2583
25	-0.2825	0.0602	0.3451	0.0638	-0.1313	0.2517
26	-0.2803	0.0391	0.3521	0.0688	-0.1674	0.2456
27	-0.2838	0.0583	0.4159	0.0676	-0.1446	0.2613
28	-0.2291	0.0626	0.4149	0.0649	-0.1322	0.2575
29	-0.2366	0.0669	0.389	0.0627	-0.1217	0.2549
30	-0.2037	0.0623	0.3718	0.0617	-0.1229	0.2475
31	-0.2676	0.0609	0.349	0.0612	-0.1228	0.2445
32	-0.2838	0.0583	0.4159	0.0678	-0.1446	0.2613
33	-0.306	0.0602	0.3542	0.0681	-0.1381	0.2585
34	-0.29	0.0631	0.3598	0.0638	-0.1278	0.2538
35	-0.2407	0.0659	0.3341	0.0614	-0.1182	0.2501
36	-0.232	0.0645	0.3225	0.0605	-0.1169	0.2459
37	-0.202	0.0628	0.3284	0.0605	-0.1188	0.2442
38	-0.4252	0.0534	0.3697	0.065	-0.1417	0.2485
39	-0.3478	0.0566	0.375	0.0636	-0.1342	0.2474
40	-0.2456	0.0592	0.3574	0.0613	-0.1246	0.243
41	-0.1802	0.061	0.337	0.0594	-0.1173	0.2394
42	-0.2311	0.0608	0.3423	0.068	-0.1133	0.2348
43	-0.188	0.0597	0.3303	0.0588	-0.1188	0.2381
44	-0.3285	0.0496	0.3764	0.0626	-0.139	0.2373
45	-0.2857	0.0595	0.309	0.0603	-0.1214	0.2405
46	-0.2288	0.0528	0.2949	0.0582	-0.1219	0.227
47	-0.2077	0.0525	0.2581	0.0558	-0.1149	0.2189
48	-0.1927	0.0517	0.301	0.0568	-0.1181	0.2215
49	-0.2545	0.0101	0.3181	0.0596	-0.1688	0.1891
50	-0.4478	0.0001	0.3097	0.0639	-0.1916	0.1917
51	-0.2113	0.1571	1.1489	0.1323	-0.2388	0.554
52	-0.2288	0.152	0.8437	0.1066	-0.1878	0.4719
53	-0.1383	0.1715	0.9658	0.1205	-0.1889	0.5331
54	-0.1937	0.1883	1.0961	0.1352	-0.2074	0.604
55	-0.2564	0.2271	1.5743	0.1871	-0.2741	0.7282
56	-0.2719	0.0759	0.7551	0.0897	-0.1931	0.3449
57	-0.2936	0.0388	0.3223	0.0709	-0.1729	0.2525
58	-0.4458	0.0378	0.3362	0.0716	-0.1769	0.2525
59	-0.2855	0.0388	0.3389	0.0713	-0.1754	0.2525
60	-0.2584	0.1236	1.0729	0.1137	-0.2176	0.4648
61	-0.5846	0.0517	0.4547	0.0761	-0.1785	0.2801
62	-0.388	0.033	0.3471	0.0693	-0.1749	0.2409
63	-0.3721	0.0331	0.3044	0.0704	-0.1781	0.2443
64	-0.274	0.0388	0.3305	0.0705	-0.1716	0.2511
65	-0.3421	0.0835	0.6553	0.0886	-0.1822	0.3493
66	-0.2594	0.0203	0.2598	0.0604	-0.1608	0.2014
67	-0.2974	0.0159	0.2235	0.0577	-0.1573	0.189
68	-0.4109	-0.0012	0.2404	0.0659	-0.1888	0.1984
69	-0.5053	-0.036	0.2814	0.0737	-0.2573	0.1852
70	-0.2252	0.0236	0.2582	0.0609	-0.159	0.2082
71	-0.3073	0.0206	0.2334	0.0589	-0.1593	0.2004
72	-0.377	0.0138	0.3145	0.0642	-0.1789	0.2085
73	-0.5342	-0.0475	0.2537	0.0753	-0.2733	0.1783
74	-0.2728	0.0167	0.2597	0.0614	-0.1675	0.2009
75	-0.3836	0.0168	0.2724	0.0606	-0.1651	0.1986
76	-0.2306	0.0194	0.363	0.0613	-0.1645	0.2033
77	-0.4692	-0.0384	0.2604	0.072	-0.2545	0.1776
78	-0.4975	-0.0282	0.456	0.1225	-0.3868	0.3392
79	-0.6892	0.0194	0.4053	0.0812	-0.2241	0.2829
80	-0.3785	0.0297	0.4085	0.0747	-0.1943	0.2537
81	-0.3953	0.0287	0.4384	0.075	-0.1883	0.2519
82	-0.3187	0.0283	0.3656	0.0737	-0.1828	0.2495
83	-0.3714	0.0045	0.3576	0.069	-0.1864	0.2055
84	-0.8773	-0.0085	0.3285	0.089	-0.2755	0.2586
85	-0.4065	0.0147	0.355	0.0696	-0.1939	0.2234
86	-0.3091	0.0244	0.3631	0.0695	-0.1842	0.2329
87	-0.4296	0.0289	0.3413	0.0707	-0.1832	0.241
88	-0.3419	0.0337	0.3782	0.0707	-0.1785	0.2459
89	-0.2985	0.0283	0.3144	0.0698	-0.1825	0.2352
90	-0.3201	0.0227	0.301	0.0823	-0.1842	0.1888
91	-0.2902	0.0208	0.4049	0.0687	-0.1653	0.2269
92	-0.2307	0.0188	0.3824	0.0641	-0.1724	0.212
93	-0.2832	0.0222	0.3685	0.0661	-0.1762	0.2206
94	-0.2602	0.0321	0.3882	0.0685	-0.1733	0.2375
95	-0.2651	0.0387	0.3238	0.0684	-0.1605	0.2378
96	-0.2849	0.0213	0.2958	0.0587	-0.1548	0.1974

B/H=0.5 N=8 0 degree						
# of lap	Min	Mean	max	STDV	- peak	+ peak
1	0.5083	1.1113	1.8584	0.243	0.3822	1.8404
2	-0.6213	-0.0077	0.4764	0.0902	-0.2783	0.2628
3	-0.8228	0.0029	0.4745	0.0928	-0.2755	0.2812
4	-0.6428	0.0108	0.44	0.0939	-0.271	0.2925
5	-0.4701	0.0058	0.4351	0.0874	-0.2564	0.2882
6	-0.5525	-0.0029	0.4385	0.0828	-0.2508	0.2448
7	-0.7198	0.0042	0.4283	0.0854	-0.252	0.2604
8	-0.5378	-0.0307	0.4332	0.0878	-0.284	0.2364
9	-0.7445	0.0182	0.3292	0.0721	-0.1981	0.2344
10	-0.4313	0.0211	0.3382	0.0716	-0.1938	0.236
11	-0.3274	0.0302	0.3814	0.0697	-0.1789	0.2393
12	-0.4247	0.0241	0.4098	0.0688	-0.1762	0.2244
13	-0.4711	0.027	0.3738	0.0683	-0.1778	0.2317
14	-0.5749	0.0095	0.3185	0.0718	-0.2057	0.2249
15	-0.6668	0.0285	0.3081	0.068	-0.1758	0.2325
16	-0.3033	0.0346	0.3131	0.0652	-0.161	0.2302
17	-0.3383	0.0334	0.3315	0.0635	-0.1571	0.2238
18	-0.4336	0.0316	0.3375	0.064	-0.1603	0.2236
19	-0.327	0.0293	0.3227	0.0616	-0.148	0.2277
20	-0.3014	0.0417	0.3297	0.0606	-0.1401	0.2234
21	-0.6457	0.0323	0.3524	0.0646	-0.1613	0.228
22	-0.422	0.0388	0.2927	0.062	-0.1491	0.2225
23	-0.2881	0.0416	0.3234	0.0598	-0.1377	0.2208
24	-0.2884	0.0427	0.3305	0.0587	-0.1333	0.2185
25	-0.3299	0.0387	0.3047	0.0591	-0.1405	0.2139
26	-0.433	0.0175	0.327	0.0658	-0.1794	0.2143
27	-0.5323	0.0346	0.3016	0.0623	-0.1525	0.2216
28	-0.4139	0.0395	0.2944	0.0604	-0.1416	0.2207
29	-0.2613	0.0431	0.3349	0.0573	-0.1289	0.215
30	-0.2178	0.0382	0.288	0.0583	-0.1307	0.207
31	-0.2348	0.0375	0.3124	0.0568	-0.133	0.208
32	-0.5323	0.0346	0.3016	0.0623	-0.1525	0.2216
33	-0.6149	0.0378	0.289	0.061	-0.1452	0.2208
34	-0.3727	0.0403	0.2835	0.0587	-0.1357	0.2164
35	-0.2154	0.0413	0.335	0.0584	-0.1278	0.2104
36	-0.2148	0.0387	0.3127	0.0554	-0.1275	0.205
37	-0.2358	0.0378	0.3211	0.0559	-0.13	0.2056
38	-0.2888	0.0277	0.311	0.0618	-0.1576	0.213
39	-0.4723	0.0289	0.3482	0.0592	-0.1478	0.2075
40	-0.329	0.0318	0.3093	0.057	-0.1392	0.2028
41	-0.282	0.0355	0.3087	0.055	-0.1295	0.2007
42	-0.1929	0.0342	0.2953	0.0538	-0.1273	0.1958
43	-0.1859	0.031	0.3202	0.0533	-0.1348	0.1988
44	-0.3088	0.0216	0.2847	0.058	-0.1577	0.2009
45	-0.284	0.0294	0.2987	0.0581	-0.1448	0.2036
46	-0.2667	0.0211	0.2827	0.0565	-0.1485	0.1908
47	-0.2839	0.021	0.3043	0.0533	-0.1388	0.1807
48	-0.2517	0.0213	0.2859	0.0528	-0.1373	0.1798
49	-0.3251	-0.003	0.2915	0.0585	-0.1728	0.1867
50	-0.3932	-0.0122	0.296	0.0622	-0.1997	0.1742
51	-0.2476	0.178	1.3844	0.1422	-0.2488	0.6048
52	-0.2287	0.1552	0.9851	0.1054	-0.181	0.4715
53	-0.1784	0.1738	1.0159	0.1124	-0.1837	0.5108
54	-0.1885	0.2085	1.0489	0.1291	-0.1809	0.5938
55	-0.197	0.238	1.3494	0.1829	-0.2526	0.7246
56	-0.2582	0.0913	0.8199	0.0948	-0.1923	0.375
57	-0.2614	0.0391	0.3153	0.0671	-0.1621	0.2404
58	-0.2988	0.0385	0.3382	0.0667	-0.1616	0.2388
59	-0.4302	0.0365	0.3555	0.0689	-0.1643	0.2372
60	-0.2596	0.1329	0.8839	0.1133	-0.2071	0.4728
61	-0.2874	0.0555	0.4738	0.078	-0.172	

B/H=1 N=1 0 degree

# of lap	Min	Mean	max	STDV	- peak	+ peak
1	-0.8837	-0.1318	0.3889	0.1164	-0.4809	0.2173
2	-1.038	-0.1089	0.5447	0.1244	-0.4822	0.2644
3	-0.9769	-0.0785	0.4978	0.1297	-0.4675	0.3104
4	-1.1413	-0.0271	0.4784	0.1269	-0.4078	0.3536
5	-0.8917	0.0212	0.5069	0.1272	-0.3604	0.4027
6	-1.2836	-0.0528	0.4341	0.1636	-0.5435	0.438
7	-1.3108	-0.1927	0.3964	0.1841	-0.745	0.3595
8	-0.6461	-0.0528	0.3594	0.0937	-0.3339	0.2282
9	-0.5517	-0.0498	0.4118	0.0948	-0.334	0.2345
10	-0.7291	-0.0669	0.4061	0.0969	-0.2976	0.2637
11	-0.6422	0.0268	0.4129	0.0915	-0.2477	0.3012
12	-0.8316	0.0129	0.3943	0.1011	-0.2904	0.3162
13	-0.7252	-0.0265	0.3559	0.102	-0.3325	0.2795
14	-0.6588	-0.0256	0.3284	0.09	-0.2955	0.2444
15	-0.594	-0.0622	0.3948	0.0975	-0.2687	0.2563
16	-0.4934	0.0098	0.3948	0.0853	-0.2461	0.2658
17	-0.4868	-0.0097	0.3739	0.085	-0.2648	0.2455
18	-0.6503	0.0057	0.3451	0.0815	-0.2388	0.2503
19	-0.4479	0.0272	0.3631	0.0783	-0.2078	0.2621
20	-0.684	-0.0022	0.3609	0.0853	-0.2581	0.2537
21	-0.53	0.0084	0.3459	0.081	-0.2347	0.2515
22	-0.5835	0.0249	0.3255	0.0764	-0.2042	0.2539
23	-0.4032	0.0449	0.3413	0.0716	-0.1699	0.2598
24	-0.3472	0.0269	0.3231	0.0717	-0.168	0.2419
25	-0.5737	0.0018	0.3717	0.0839	-0.2399	0.2535
26	-0.5388	0.0034	0.3699	0.0801	-0.2388	0.2437
27	-0.4729	0.0109	0.3501	0.0769	-0.2197	0.2415
28	-0.4922	0.0368	0.3563	0.0705	-0.1746	0.2482
29	-0.2921	0.0446	0.3545	0.0685	-0.1549	0.2441
30	-0.3225	0.0462	0.3405	0.0688	-0.1541	0.2465
31	-0.5388	0.0034	0.3699	0.0801	-0.2388	0.2437
32	-0.6526	0.0139	0.3629	0.0771	-0.2173	0.2452
33	-0.399	0.0371	0.3711	0.0733	-0.1828	0.2571
34	-0.3113	0.0601	0.3724	0.0678	-0.1428	0.2631
35	-0.285	0.0465	0.3453	0.0652	-0.149	0.242
36	-0.3745	0.0439	0.296	0.0655	-0.1528	0.2405
37	-0.9405	0.0442	0.377	0.0732	-0.1756	0.2639
38	-0.5749	0.0416	0.3614	0.0754	-0.1844	0.2677
39	-0.4249	0.04	0.3319	0.0699	-0.1697	0.2496
40	-0.3352	0.0285	0.3183	0.0643	-0.1645	0.2214
41	-0.3577	0.0543	0.3175	0.062	-0.1316	0.2403
42	-0.2612	0.063	0.3271	0.0635	-0.1275	0.2535
43	-0.6068	0.0457	0.3568	0.0722	-0.1709	0.2624
44	-0.4088	0.0077	0.3322	0.0722	-0.2088	0.2242
45	-0.3868	0.0177	0.3559	0.0699	-0.1981	0.2214
46	-0.377	0.0154	0.3359	0.065	-0.1796	0.2105
47	-0.2904	0.0545	0.3833	0.0595	-0.124	0.2331
48	-0.2497	0.0709	0.3509	0.0655	-0.1255	0.2674
49	-0.8893	0.0678	0.4244	0.079	-0.1692	0.3045
50	-0.5591	0.1205	0.3744	0.1641	-0.3719	0.6129
51	-0.5395	0.2053	0.4938	0.223	-0.4635	0.8742
52	-0.5068	0.2909	0.7824	0.2777	-0.4222	1.0041
53	-0.4243	0.3896	0.2624	0.2709	-0.4231	1.2024
54	-0.2355	0.3492	1.7741	0.2475	-0.3932	1.0916
55	-0.5794	0.0306	0.7034	0.1408	-0.3922	0.4533
56	-0.5389	0.0697	0.7865	0.13	-0.3803	0.3977
57	-0.5545	0.0346	0.6868	0.1236	-0.3363	0.4055
58	-0.3204	0.1965	1.165	0.1532	-0.2829	0.656
59	-0.2838	0.3356	1.5708	0.2131	-0.3038	0.9751
60	-0.5458	-0.0157	0.957	0.1484	-0.4609	0.4294
61	-0.5317	-0.0173	0.414	0.1053	-0.3332	0.2988
62	-0.5063	0.0286	0.5417	0.0943	-0.2543	0.3118
63	-0.4744	0.0798	0.6306	0.1026	-0.2287	0.3684
64	-0.3701	0.2692	1.3303	0.1917	-0.306	0.8443
65	-0.5771	-0.0357	0.2645	0.0921	-0.312	0.2406
66	-0.5063	0.0093	0.2917	0.0746	-0.2146	0.2332
67	-0.2778	0.0552	0.3445	0.0685	-0.1444	0.2548
68	-0.4843	0.0705	0.4178	0.0789	-0.1882	0.3073
69	-0.6591	-0.0532	0.245	0.0979	-0.3489	0.2405
70	-0.5243	-0.0177	0.2759	0.0871	-0.2731	0.2497
71	-0.3808	0.049	0.3219	0.0711	-0.1702	0.2562
72	-0.353	0.0517	0.3208	0.0758	-0.1756	0.279
73	-0.6325	-0.0485	0.3205	0.0983	-0.3433	0.2462
74	-0.3765	0.0067	0.3543	0.0715	-0.2077	0.221
75	-0.341	0.0498	0.3155	0.0661	-0.1484	0.248
76	-0.4283	0.0588	0.3457	0.0795	-0.1816	0.2953
77	-1.3129	-0.1462	0.4157	0.1778	-0.879	0.3886
78	-1.1373	-0.0029	0.3608	0.1052	-0.3186	0.3128
79	-0.5134	0.0279	0.5458	0.0786	-0.208	0.2637
80	-0.5336	0.0541	0.4327	0.073	-0.185	0.2731
81	-0.7193	0.0644	0.5153	0.0752	-0.1611	0.2899
82	-0.6709	0.0891	0.4515	0.0776	-0.1437	0.3218
83	-1.5489	-0.1292	0.3607	0.1882	-0.8878	0.4293
84	-0.8727	0.003	0.4031	0.1011	-0.3005	0.3064
85	-0.3885	0.0272	0.4021	0.0765	-0.2023	0.2567
86	-0.3812	0.0564	0.4704	0.0716	-0.1584	0.2712
87	-0.3389	0.0579	0.4325	0.0701	-0.1525	0.2883
88	-0.3328	0.0648	0.4432	0.0722	-0.1517	0.2813
89	-0.4432	0.0888	0.4161	0.0745	-0.1349	0.3122
90	-1.2102	-0.0283	0.626	0.1461	-0.826	0.4159
91	-0.5465	0.021	0.4048	0.0828	-0.2575	0.2965
92	-0.3693	0.0135	0.4459	0.0771	-0.2178	0.2448
93	-0.3091	0.0676	0.4147	0.069	-0.1393	0.2745
94	-0.304	0.0782	0.4051	0.0688	-0.1276	0.284
95	-0.4748	0.1154	0.4654	0.0788	-0.1149	0.3458

B/H=1 N=1 10 degree

# of lap	Min	Mean	max	STDV	- peak	+ peak
1	-1.7142	-0.2905	0.4141	0.2016	-0.8954	0.3144
2	-1.5442	-0.2743	0.3404	0.1932	-0.854	0.3054
3	-1.4475	-0.2315	0.411	0.1979	-0.8234	0.3605
4	-1.3577	-0.1521	0.484	0.2054	-0.7683	0.464
5	-1.197	-0.0283	0.457	0.163	-0.5173	0.4609
6	-1.172	-0.0409	0.449	0.1307	-0.433	0.3512
7	-0.956	-0.1119	0.357	0.1094	-0.4399	0.2162
8	-0.8902	-0.0879	0.3744	0.1181	-0.4421	0.2653
9	-0.7699	-0.0697	0.3157	0.1227	-0.4677	0.2683
10	-0.7684	-0.0376	0.4118	0.1234	-0.4079	0.3224
11	-0.5834	0.0083	0.3917	0.1013	-0.2858	0.3344
12	-0.5872	-0.0079	0.4094	0.0936	-0.2887	0.2729
13	-0.7555	-0.0564	0.335	0.0863	-0.3154	0.2028
14	-0.7532	-0.0507	0.353	0.1028	-0.3592	0.2578
15	-0.6243	-0.0292	0.339	0.0955	-0.3157	0.2572
16	-0.5314	-0.0127	0.4003	0.0954	-0.2989	0.2735
17	-0.6871	-0.0369	0.368	0.0806	-0.3088	0.2349
18	-0.6452	-0.0134	0.3144	0.0809	-0.2561	0.2292
19	-0.4443	0.0087	0.3245	0.0798	-0.2307	0.2481
20	-0.7739	-0.0343	0.314	0.0912	-0.308	0.2394
21	-0.645	-0.0125	0.3087	0.0815	-0.257	0.232
22	-0.5899	0.0059	0.3137	0.0762	-0.2229	0.2345
23	-0.3369	0.0299	0.3986	0.0722	-0.1866	0.2463
24	-0.4	0.0082	0.3943	0.0698	-0.2011	0.2176
25	-0.4822	-0.0206	0.3514	0.0785	-0.256	0.2188
26	-0.7191	-0.0211	0.3577	0.0831	-0.2703	0.2281
27	-0.5418	-0.0105	0.3383	0.0763	-0.2393	0.2183
28	-0.4705	0.0192	0.3092	0.0688	-0.1871	0.2254
29	-0.495	0.0296	0.3071	0.0656	-0.1671	0.2263
30	-0.3199	0.0327	0.3934	0.0659	-0.1641	0.2295
31	-0.126	0.0827	0.303	0.0351	-0.0226	0.188
32	-0.6747	-0.0084	0.351	0.0843	-0.2814	0.2446
33	-0.488	0.0212	0.3406	0.0727	-0.1968	0.2392
34	-0.3854	0.0437	0.293	0.0658	-0.1537	0.2411
35	-0.3423	0.0291	0.2929	0.064	-0.1628	0.2221
36	-0.2666	0.0306	0.303	0.0645	-0.1629	0.224
37	-0.5902	0.0345	0.4389	0.0742	-0.188	0.2571
38	-1.0032	0.0177	0.3585	0.0871	-0.2435	0.2789
39	-0.403	0.0225	0.32	0.0703	-0.1883	0.2333
40	-0.277	0.0058	0.2694	0.0628	-0.1829	0.1941
41	-0.302	0.0389	0.3238	0.0613	-0.1449	0.2227
42	-0.3047	0.0528	0.2971	0.0623	-0.1344	0.2395
43	-0.7877	0.0422	0.4246	0.0767	-0.188	0.2724
44	-1.0228	-0.0708	0.2577	0.0841	-0.323	0.1814
45	-0.6818	-0.055	0.2691	0.0692	-0.2625	0.1525
46	-0.4019	-0.0376	0.2119	0.0677	-0.2407	0.1655
47	-0.2324	0.0297	0.2874	0.0635	-0.1607	0.2201
48	-0.1612	0.0859	0.3674	0.0623	-0.1011	0.2729
49	-0.6667	0.0867	0.4504	0.0835	-0.1637	0.337
50	-0.5271	0.3558	2.0058	0.2329	-0.343	1.0647
51	-0.3398	0.4823	2.08	0.3233	-0.5075	1.4322
52	-0.4828	0.4106	1.8098	0.3013	-0.4933	1.3145
53	-0.3709	0.2425	1.4434	0.2169	-0.4081	0.8931
54	-0.3728	0.1293	1.2307	0.155	-0.3357	0.5942
55	-0.5845	0.314	1.7242	0.2215	-0.3506	0.9787
56	-0.4537	0.2559	1.0509	0.1777	-0.2771	0.7889
57	-0.5193	0.1039	0.9176	0.1481	-0.3404	0.5482
58	-0.4978	0.0417	0.5934	0.1195	-0.3168	0.4002
59	-0.5915	0.0474	0.9871	0.1205	-0.3142	0.4009
60	-0.4827	0.2214	1.6871	0.2227	-0.4468	0.8895
61	-0.4066	0.1212	0.8126	0.1065	-0.2073	0.4496
62	-0.4012	0.0492	0.436	0.0		

B/H=1		N=1 20 degree						
# of lap	Min	Mean	max	STDV	- peak	+ peak		
1	0.3445	1.1818	1.9752	0.2573	0.39	1.9338		
1	-1.6095	-0.391	0.4515	0.2263	-1.06	0.298		
2	-1.8175	-0.3758	0.4543	0.2081	-1.0003	0.2486		
3	-1.7774	-0.3206	0.4659	0.2024	-0.9277	0.2665		
4	-1.8074	-0.2518	0.4367	0.2094	-0.8801	0.3764		
5	-1.8481	-0.1173	0.5025	0.1845	-0.6708	0.4363		
6	-1.3369	-0.085	0.4579	0.1483	-0.5238	0.3538		
7	-1.0006	-0.1194	0.3295	0.1086	-0.4453	0.2065		
8	-1.2988	-0.1729	0.4186	0.1365	-0.5823	0.2364		
9	-1.0659	-0.1828	0.4082	0.133	-0.5815	0.2163		
10	-0.9119	-0.1311	0.5015	0.1342	-0.5338	0.2715		
11	-0.9813	-0.0504	0.4629	0.1112	-0.384	0.2833		
12	-0.8669	-0.0335	0.4091	0.0963	-0.3223	0.2553		
13	-0.9712	-0.0697	0.2718	0.0835	-0.32	0.1807		
14	-1.1064	-0.1264	0.4161	0.1185	-0.4819	0.2201		
15	-0.8426	-0.0915	0.4087	0.1031	-0.4008	0.2179		
16	-0.6027	-0.0775	0.4289	0.102	-0.3835	0.2286		
17	-0.7145	-0.0976	0.3889	0.1035	-0.4081	0.2128		
18	-0.8187	-0.062	0.3606	0.0869	-0.3226	0.1987		
19	-0.4709	-0.0358	0.3689	0.0821	-0.2822	0.2103		
20	-0.8443	-0.089	0.3402	0.1072	-0.4104	0.2325		
21	-0.6537	-0.0625	0.3703	0.0915	-0.3369	0.2118		
22	-0.4587	-0.0342	0.4052	0.0792	-0.2717	0.2034		
23	-0.4889	-0.0008	0.3833	0.0742	-0.2233	0.2217		
24	-0.3905	-0.0138	0.2934	0.0699	-0.2236	0.1959		
25	-0.534	-0.0361	0.4291	0.0765	-0.2659	0.1937		
26	-0.8477	-0.0579	0.3575	0.1023	-0.3647	0.2489		
27	-0.5951	-0.0423	0.3561	0.0842	-0.285	0.2103		
28	-0.3815	-0.0072	0.3002	0.0719	-0.2229	0.2085		
29	-0.5392	0.0085	0.3069	0.0671	-0.1928	0.2099		
30	-0.3562	0.0177	0.374	0.0655	-0.1787	0.2141		
31	-0.0803	0.0789	0.2575	0.0349	-0.0259	0.1837		
32	-0.8923	-0.0339	0.396	0.1044	-0.3472	0.2795		
33	-0.6074	0.0082	0.423	0.0814	-0.2361	0.2525		
34	-0.3277	0.028	0.331	0.0692	-0.1796	0.2355		
35	-0.6098	0.0088	0.2828	0.0681	-0.1894	0.207		
36	-0.3151	0.0148	0.3122	0.0649	-0.18	0.2096		
37	-0.4323	0.0307	0.3737	0.0738	-0.1908	0.2521		
38	-1.0907	0.0034	0.4201	0.1084	-0.3218	0.3287		
39	-0.4582	0.0188	0.3661	0.079	-0.2183	0.2556		
40	-0.3785	-0.0114	0.3155	0.0674	-0.2137	0.1508		
41	-0.3194	0.0251	0.3676	0.0636	-0.1855	0.2158		
42	-0.2953	0.0404	0.3516	0.0635	-0.1502	0.2309		
43	-0.8046	0.0393	0.3624	0.0741	-0.183	0.2617		
44	-0.8259	-0.097	0.2399	0.1031	-0.4062	0.2122		
45	-0.551	-0.0648	0.2409	0.0772	-0.2963	0.1667		
46	-0.578	-0.0535	0.2304	0.0771	-0.2846	0.1777		
47	-0.325	0.0107	0.3428	0.0694	-0.1974	0.2187		
48	-0.2283	0.0839	0.3479	0.065	-0.1112	0.2789		
49	-0.5585	0.0917	0.4795	0.0784	-0.1433	0.3268		
50	-0.4259	0.2889	1.8576	0.2352	-0.4168	0.9945		
51	-0.3393	0.3345	1.8315	0.2815	-0.51	1.1789		
52	-0.5821	0.4019	1.8773	0.2894	-0.4863	1.2702		
53	-0.4008	0.2951	1.5527	0.2261	-0.3833	0.9734		
54	-0.4222	0.184	1.3794	0.1874	-0.3382	0.8681		
55	-0.5085	0.2394	1.5291	0.2393	-0.4788	0.9573		
56	-0.2857	0.2258	1.1748	0.1871	-0.2157	0.7288		
57	-0.3447	0.1506	0.9765	0.1486	-0.2853	0.5865		
58	-0.5373	0.1017	0.7333	0.1239	-0.2701	0.4735		
59	-0.3975	0.0494	0.6961	0.1094	-0.2789	0.3776		
60	-0.6488	0.1119	1.4988	0.2338	-0.5895	0.8133		
61	-0.3881	0.1135	0.8520	0.1182	-0.241	0.468		
62	-0.458	0.0835	0.5831	0.0966	-0.2063	0.3733		
63	-0.5295	0.0017	0.558	0.1024	-0.3055	0.309		
64	-0.8786	-0.0383	0.6151	0.1114	-0.3728	0.295		
65	-1.2888	-0.188	0.3277	0.1445	-0.6198	0.2475		
66	-0.7471	-0.063	0.2986	0.1174	-0.4151	0.2891		
67	-0.3916	0.0498	0.3505	0.076	-0.1781	0.2776		
68	-0.2439	0.0912	0.4043	0.0693	-0.1168	0.2891		
69	-1.108	-0.2102	0.2333	0.1418	-0.635	0.2146		
70	-0.9304	-0.0888	0.3091	0.1349	-0.4934	0.3158		
71	-0.4551	0.0251	0.3577	0.0895	-0.2435	0.2897		
72	-0.2533	0.0583	0.3838	0.07	-0.1518	0.2681		
73	-1.3885	-0.1779	0.2691	0.1444	-0.8112	0.2553		
74	-0.6024	-0.0228	0.4854	0.0987	-0.3188	0.2735		
75	-0.3589	0.049	0.4182	0.0755	-0.1774	0.2754		
76	-0.2887	0.0676	0.4213	0.0712	-0.146	0.2813		
77	-1.1343	-0.1423	0.3049	0.1244	-0.5156	0.231		
78	-0.8525	-0.1048	0.3954	0.1144	-0.4478	0.2383		
79	-0.7551	-0.0509	0.3943	0.1027	-0.3589	0.2571		
80	-0.7422	0.0279	0.4096	0.0911	-0.2454	0.3012		
81	-0.7527	0.052	0.4222	0.0906	-0.2197	0.3237		
82	-0.7921	0.0962	0.4573	0.083	-0.1529	0.3453		
83	-0.8857	-0.1218	0.3828	0.113	-0.4607	0.2175		
84	-0.8227	-0.0894	0.323	0.0984	-0.3946	0.1858		
85	-0.5278	-0.0506	0.3318	0.0926	-0.3284	0.2273		
86	-0.4573	0.0157	0.4067	0.0849	-0.2389	0.2703		
87	-0.4439	0.0271	0.3112	0.0806	-0.2148	0.2688		
88	-0.4502	0.0472	0.3745	0.0779	-0.1867	0.281		
89	-0.4587	0.0891	0.4028	0.0709	-0.1235	0.3017		
90	-0.7099	-0.0917	0.3413	0.0923	-0.3889	0.1852		
91	-0.63	-0.0895	0.2931	0.0841	-0.3418	0.1829		
92	-0.4559	-0.0514	0.2924	0.0804	-0.2826	0.1897		
93	-0.3823	0.0489	0.344	0.078	-0.185	0.2827		
94	-0.4101	0.0639	0.3818	0.0746	-0.1598	0.2876		
95	-0.2327	0.1164	0.4415	0.0723	-0.1004	0.3333		

B/H=1		N=1 30 degree						
# of lap	Min	Mean	max	STDV	- peak	+ peak		
1	0.5117	1.1079	1.8393	0.2488	0.3674	1.8493		
1	-1.8082	-0.4378	0.2581	0.2451	-1.1731	0.2975		
2	-1.8853	-0.4547	0.2868	0.2331	-1.1539	0.2445		
3	-1.8061	-0.3855	0.2572	0.2109	-1.0182	0.2782		
4	-1.7181	-0.3151	0.2709	0.2096	-0.9439	0.3136		
5	-1.7455	-0.2121	0.4211	0.201	-0.8151	0.3909		
6	-1.3923	-0.1743	0.4223	0.1721	-0.6907	0.3421		
7	-1.1157	-0.175	0.2792	0.122	-0.5409	0.1909		
8	-1.3713	-0.2747	0.2803	0.1769	-0.8054	0.256		
9	-1.0303	-0.2514	0.2238	0.1469	-0.692	0.1892		
10	-1.1451	-0.2289	0.29	0.1523	-0.8869	0.2271		
11	-1.2114	-0.1422	0.4386	0.1377	-0.5554	0.2709		
12	-1.0467	-0.0999	0.3045	0.1165	-0.4493	0.2495		
13	-0.7634	-0.1172	0.2378	0.0864	-0.3764	0.1421		
14	-1.2078	-0.2218	0.3983	0.1528	-0.8802	0.2356		
15	-0.9296	-0.159	0.291	0.119	-0.516	0.1979		
16	-0.8767	-0.1551	0.2978	0.1198	-0.5138	0.2039		
17	-1.4026	-0.1755	0.3204	0.1349	-0.5803	0.2292		
18	-0.8228	-0.1286	0.31	0.1072	-0.4482	0.1951		
19	-0.7587	-0.0832	0.2748	0.0974	-0.3855	0.1891		
20	-1.5558	-0.1598	0.4029	0.145	-0.5949	0.2754		
21	-0.7625	-0.1275	0.3213	0.1167	-0.4776	0.2226		
22	-0.6646	-0.0802	0.2806	0.0935	-0.3666	0.1942		
23	-0.5043	-0.0496	0.3265	0.0862	-0.3082	0.2091		
24	-0.555	-0.0578	0.3262	0.0794	-0.296	0.1805		
25	-0.5508	-0.0749	0.2865	0.0753	-0.3005	0.1513		
26	-1.1893	-0.1038	0.3749	0.14	-0.5238	0.3163		
27	-0.6727	-0.0764	0.3545	0.0958	-0.3936	0.2408		
28	-0.5675	-0.0423	0.287	0.0839	-0.2941	0.2005		
29	-0.5	-0.0246	0.3125	0.0764	-0.2538	0.2045		
30	-0.4215	-0.0145	0.3061	0.0723	-0.2313	0.2023		
31	-0.1416	0.0501	0.2318	0.0359	-0.0576	0.1578		
32	-1.1361	-0.0705	0.4153	0.1343	-0.4734	0.3324		
33	-0.5597	-0.0074	0.3858	0.089	-0.3015	0.2866		
34	-0.5742	0.0074	0.3271	0.0793	-0.2905	0.2453		
35	-0.4315	-0.021	0.3382	0.0735	-0.2414	0.1994		
36	-0.3795	-0.017	0.3175	0.0707	-0.229	0.1949		
37	-0.4339	0.0057	0.3141	0.07	-0.2042	0.2157		
38	-1.2733	-0.0282	0.422	0.1205	-0.4168	0.3604		
39	-0.7617	-0.0003	0.3545	0.081	-0.2733	0.2728		
40	-0.3926	-0.0413	0.2823	0.0739	-0.283	0.1803		
41	-0.3903	-0.001	0.2808	0.0696	-0.2099	0.2076		
42	-0.3288	0.0137	0.3209	0.0884	-0.1914	0.2188		
43	-0.3527	0.0172	0.3522	0.0896	-0.1919	0.2259		
44	-1.5305	-0.1496	0.2419	0.123	-0.5186	0.2195		
45	-0.8413	-0.1041	0.2037	0.0845	-0.3577	0.1495		
46	-0.5283	-0.1062	0.2611	0.0793	-0.3441	0.1316		
47	-0.438	-0.0339	0.2817	0.0735	-0.2589	0.1912		
48	-0.3802	0.0658	0.4152	0.0721	-0.1504	0.2821		
49	-0.5035	0.0872	0.4104	0.0752	-0.1382	0.3127		
50	-0.8889	0.1828	0.2592	0.2358	-0.5246	0.8903		
51	-0.8326	0.1792	1.5734	0.2088	-0.4472	0.8057		
52	-0.8522	0.2786	1.5588	0.2416	-0.4462			

B/H=1		N=1 40 degree					
# of lap	Min	Mean	max	STDV	- peak	+ peak	
1	0.3758	-1.069	1.9547	0.2498	0.3203	1.8170	
2	-2.0046	-0.4671	0.3371	0.2612	-1.2508	0.3165	
3	-1.9229	-0.507	0.2352	0.2639	-1.2985	0.2845	
4	-1.7419	-0.4309	0.2765	0.2287	-1.1168	0.2551	
5	-1.8826	-0.3432	0.3317	0.2178	-0.9985	0.3103	
6	-1.9287	-0.2373	0.4763	0.2067	-0.8574	0.3829	
7	-1.4029	-0.2179	0.3777	0.1835	-0.7686	0.3327	
8	-1.1661	-0.2363	0.2992	0.1369	-0.6469	0.1743	
9	-2.3491	-0.4051	0.3679	0.2513	-1.159	0.3488	
10	-1.1997	-0.2895	0.2521	0.1593	-0.7673	0.1884	
11	-1.3433	-0.2899	0.2809	0.1611	-0.7532	0.2133	
12	-0.9542	-0.1821	0.3962	0.1479	-0.6259	0.2617	
13	-1.0251	-0.1365	0.2957	0.1265	-0.5162	0.2431	
14	-0.9858	-0.1705	0.1779	0.0938	-0.4519	0.1109	
15	-1.8238	-0.3393	0.3341	0.2094	-0.8675	0.2899	
16	-0.9443	-0.1693	0.254	0.1276	-0.5822	0.1635	
17	-0.9378	-0.1919	0.2599	0.1257	-0.5686	0.1651	
18	-1.2008	-0.2645	0.3321	0.1703	-0.7754	0.2465	
19	-0.8223	-0.1864	0.3213	0.123	-0.5553	0.1826	
20	-0.7063	-0.1329	0.3716	0.1038	-0.4442	0.1783	
21	-1.5841	-0.247	0.408	0.1802	-0.7875	0.2835	
22	-0.9398	-0.2019	0.3132	0.145	-0.638	0.2343	
23	-0.7188	-0.1301	0.2709	0.1003	-0.4311	0.1709	
24	-0.5815	-0.087	0.3775	0.0918	-0.3823	0.1894	
25	-0.6557	-0.1026	0.3281	0.0857	-0.3597	0.1544	
26	-0.552	-0.13	0.1933	0.0791	-0.3673	0.1072	
27	-1.6349	-0.1838	0.3885	0.1672	-0.6854	0.3177	
28	-0.8851	-0.1424	0.3182	0.1295	-0.5308	0.246	
29	-0.5592	-0.0884	0.2782	0.0944	-0.3716	0.1947	
30	-0.4794	-0.063	0.2859	0.0915	-0.3076	0.1816	
31	-0.4984	-0.0539	0.2875	0.0767	-0.2839	0.1781	
32	-0.1289	0.0198	0.1807	0.0369	-0.0911	0.1303	
33	-1.147	-0.1529	0.45	0.1519	-0.6085	0.3027	
34	-0.8705	-0.0724	0.4397	0.1121	-0.4087	0.2839	
35	-0.5847	-0.0356	0.3182	0.0894	-0.3038	0.2327	
36	-0.4687	-0.0621	0.3181	0.0802	-0.3027	0.1786	
37	-0.4136	-0.0559	0.2782	0.0746	-0.2797	0.1879	
38	-0.339	-0.0318	0.3155	0.0717	-0.2469	0.1834	
39	-1.3004	-0.1122	0.4586	0.1478	-0.5556	0.3311	
40	-0.8206	-0.0681	0.418	0.1012	-0.3717	0.2355	
41	-0.582	-0.0828	0.2928	0.0801	-0.333	0.1479	
42	-0.414	-0.0363	0.2842	0.0747	-0.2895	0.1879	
43	-0.4594	-0.018	0.3823	0.0728	-0.2359	0.1899	
44	-0.4231	-0.0184	0.2592	0.069	-0.2254	0.1887	
45	-1.2176	-0.2038	0.2019	0.1279	-0.5975	0.1799	
46	-0.7608	-0.1372	0.2213	0.0894	-0.4052	0.1309	
47	-0.5777	-0.12	0.2708	0.0798	-0.3596	0.1195	
48	-0.3733	-0.0553	0.2818	0.0755	-0.2817	0.1711	
49	-0.3003	0.0535	0.3885	0.0738	-0.1973	0.2743	
50	-0.3822	0.0725	0.404	0.0728	-0.1459	0.2908	
51	-0.7119	0.1114	1.4807	0.218	-0.5424	0.7853	
52	-0.7512	0.1344	1.4603	0.2065	-0.4855	0.7542	
53	-0.5568	0.2551	1.5825	0.2422	-0.4714	0.9816	
54	-0.468	0.2855	1.4367	0.227	-0.4155	0.9465	
55	-0.5235	0.1192	1.174	0.1778	-0.4143	0.6527	
56	-0.8772	0.0943	1.3988	0.2125	-0.5532	0.7218	
57	-0.4713	0.1188	0.9331	0.1442	-0.3158	0.5494	
58	-0.5417	0.123	0.9407	0.1485	-0.3225	0.5885	
59	-0.3889	0.1787	0.9387	0.1367	-0.2315	0.5888	
60	-0.4951	0.0471	1.0825	0.1346	-0.3588	0.4508	
61	-1.4187	0.0528	1.2858	0.2246	-0.6212	0.7265	
62	-0.551	0.0558	0.5995	0.1141	-0.2786	0.4078	
63	-0.3958	0.1013	0.6437	0.0989	-0.1956	0.3981	
64	-0.4381	0.0447	0.5399	0.0956	-0.242	0.3315	
65	-0.8168	-0.0361	1.2341	0.1418	-0.4816	0.3894	
66	-1.0602	-0.2119	0.3358	0.1374	-0.6241	0.2003	
67	-0.8222	-0.1035	0.3143	0.1125	-0.4409	0.234	
68	-0.4645	0.0082	0.3323	0.0859	-0.2515	0.2639	
69	-0.3078	0.0653	0.3861	0.0735	-0.1551	0.2858	
70	-1.0028	-0.2287	0.2431	0.1277	-0.6127	0.1534	
71	-0.7877	-0.1225	0.3282	0.1318	-0.5171	0.2722	
72	-0.4735	0.0017	0.3258	0.0997	-0.2892	0.2926	
73	-0.3383	0.0368	0.3543	0.0751	-0.1885	0.262	
74	-1.095	-0.1855	0.3453	0.1295	-0.5741	0.2031	
75	-0.6443	-0.0855	0.3403	0.1073	-0.4078	0.2365	
76	-0.3368	0.0359	0.391	0.0841	-0.2183	0.2881	
77	-0.2888	0.0632	0.3818	0.0751	-0.1821	0.2884	
78	-1.832	-0.2875	0.1405	0.1807	-0.8207	0.2547	
79	-1.6584	-0.2435	0.2248	0.18	-0.7234	0.2385	
80	-1.2387	-0.1532	0.228	0.1217	-0.5182	0.2118	
81	-0.4908	-0.0036	0.3297	0.0812	-0.2473	0.2401	
82	-0.4416	0.033	0.3412	0.0712	-0.1805	0.2486	
83	-0.2865	0.0906	0.3998	0.0707	-0.1215	0.3027	
84	-1.8791	-0.282	0.1984	0.1778	-0.8154	0.2515	
85	-1.3991	-0.2521	0.2158	0.1472	-0.6936	0.1895	
86	-0.8127	-0.1638	0.2382	0.1203	-0.5246	0.1971	
87	-0.5294	-0.0485	0.3019	0.0944	-0.3318	0.2348	
88	-0.4811	-0.0205	0.2849	0.0789	-0.2802	0.219	
89	-0.3382	0.0124	0.2863	0.0742	-0.2102	0.2349	
90	-0.2357	0.073	0.3746	0.0697	-0.136	0.2821	
91	-1.8851	-0.2524	0.3286	0.1675	-0.755	0.2501	
92	-1.2173	-0.2443	0.2223	0.1437	-0.6753	0.1867	
93	-0.889	-0.1345	0.3178	0.1039	-0.4461	0.1772	
94	-0.5813	0.0128	0.3323	0.0843	-0.2402	0.2858	
95	-0.4027	0.0246	0.3287	0.0804	-0.2165	0.2657	
96	-0.2205	0.1032	0.4044	0.073	-0.1159	0.3223	

B/H=1		N=1 50 degree					
# of lap	Min	Mean	max	STDV	- peak	+ peak	
1	0.2818	-1.0015	1.9811	0.2423	0.2747	1.7284	
2	-1.8998	-0.609	0.1413	0.2495	-1.3575	0.1386	
3	-2.0084	-0.6195	0.251	0.2586	-1.3894	0.1503	
4	-1.8168	-0.5369	0.1991	0.2261	-1.2153	0.1414	
5	-1.7917	-0.4371	0.3214	0.2018	-1.0425	0.1683	
6	-1.6965	-0.314	0.4019	0.1809	-0.8	0.272	
7	-1.8714	-0.318	0.2964	0.1609	-0.8607	0.2247	
8	-1.7275	-0.363	0.057	0.1475	-0.8055	0.0795	
9	-2.5796	-0.6304	0.2378	0.2848	-1.4846	0.224	
10	-1.4084	-0.4209	0.1507	0.1582	-0.8894	0.0476	
11	-1.3815	-0.3761	0.1746	0.1453	-0.812	0.0589	
12	-1.1844	-0.2852	0.2885	0.1355	-0.6917	0.1213	
13	-1.2214	-0.2491	0.2309	0.1247	-0.6233	0.125	
14	-1.1832	-0.2876	0.1168	0.0982	-0.5852	0.01	
15	-2.1155	-0.5368	0.2936	0.2282	-1.2154	0.1418	
16	-1.0079	-0.3184	0.2103	0.1271	-0.7007	0.0619	
17	-1.0739	-0.2843	0.1633	0.116	-0.6422	0.0536	
18	-1.4328	-0.44	0.2685	0.1804	-0.9813	0.1012	
19	-1.0619	-0.3355	0.1812	0.1273	-0.7174	0.0463	
20	-0.7639	-0.2514	0.1796	0.1026	-0.5593	0.0584	
21	-1.7726	-0.4157	0.2719	0.195	-1.0009	0.1694	
22	-1.4722	-0.358	0.2391	0.1517	-0.8111	0.0991	
23	-0.8314	-0.2586	0.1826	0.1007	-0.5588	0.0455	
24	-0.8521	-0.1925	0.1944	0.0911	-0.4659	0.081	
25	-0.6589	-0.2247	0.1684	0.0859	-0.482	0.0328	
26	-0.89	-0.2459	0.0987	0.0848	-0.5004	0.0088	
27	-1.6161	-0.3795	0.2444	0.1906	-0.9513	0.1823	
28	-1.2089	-0.3064	0.1611	0.1381	-0.7148	0.102	
29	-0.7101	-0.2228	0.2148	0.0989	-0.5131	0.0674	
30	-0.8773	-0.1836	0.191	0.0948	-0.4381	0.0709	
31	-0.5405	-0.1689	0.1805	0.0807	-0.411	0.0732	
32	-0.2415	-0.0899	0.0764	0.0401	-0.2102	0.0303	
33	-1.7213	-0.3573	0.2072	0.1802	-0.8979	0.1832	
34	-0.9827	-0.2242	0.1815	0.1164	-0.5734	0.125	
35	-0.9459	-0.1636	0.218	0.091	-0.4365	0.1094	
36	-0.6844	-0.2032	0.1785	0.0829	-0.4519	0.0458	
37	-0.626	-0.1896	0.1557	0.0794	-0.4277	0.0486	
38	-0.6089	-0.1505	0.197	0.0776	-0.3833	0.0824	
39	-1.8178	-0.2789	0.2824	0.1721	-0.7953	0.2375	
40	-0.8962	-0.2135	0.2096	0.1089	-0.54	0.1129	
41	-0.7178	-0.2442	0.0653	0.0821	-0.4907	0.0022	
42	-0.5746	-0.1593	0.1505	0.0778	-0.3928	0.074	
43	-0.5537	-0.1386	0.154	0.0758	-0.3658	0.0887	
44	-0.4824	-0.1421	0.1844	0.0725	-0.3596	0.0754	
45	-0.2789	-0.3344	0.122	0.134	-0.7364	0.0675	
46	-0.8982	-0.2512	0.128	0.0934	-0.5314	0.029	
47	-0.6598	-0.232	0.127	0.0812	-0.4757	0.0117	
48	-0.6027	-0.1594	0.2255	0.0773	-0.3914	0.0726	
49	-0.521	0.0222	0.3387	0.0754	-0.2094	0.2483	
50	-0.3411	0.0175	0.3745	0.0747	-0.2087	0.2416	
51	-1.2705	0.0338	1.8208	0.2059	-0.5838	0.8514	
52	-0.8884	0.0803	1.4584	0.1846	-0.4735	0.6341	
53	-0.5481	0.2088	1.4916	0.2227	-0.4594	0.8755	
54	-0.4879	0.2174	1.266	0.2223	-0.4484	0.8843	
55	-0.605	0.0806	1.1027	0.182	-0.4954	0.6567	
56	-1.3415	-0.0135	1.5041	0.1886	-0.5823	0.5552	
57	-0.6288	0.0574	0.744	0.1306	-0.3344	0.4492	
58	-0.697	0.0532	0.8969	0.1418	-0.3716	0.4779	
59	-0.3917	0.155	0.9321	0.1345	-0.2484	0.5584	
60	-0.6071	0.0598	1.032	0.1577	-0.4138	0.5328	
61	-1.9992	-0.0633	1.5994	0.2			

B/H=1		N=1 60 degree					
# of lap	Min	Mean	max	STDV	- peak	+ peak	
1	0.4176	1.0659	1.7556	0.249	0.2589	1.7523	
2	-2.3692	-0.6514	0.1298	0.2855	-1.4479	0.1452	
3	-2.186	-0.5527	0.173	0.2261	-1.2311	0.1256	
4	-1.7238	-0.4859	0.177	0.207	-1.1069	0.1352	
5	-1.587	-0.405	0.1465	0.1688	-0.9056	0.0955	
6	-1.4558	-0.2897	0.1153	0.1544	-0.7529	0.1734	
7	-1.3399	-0.1444	0.2208	0.1503	-0.7653	0.1365	
8	-1.5006	-0.351	0.1403	0.1315	-0.7454	0.0435	
9	-2.3836	-0.6767	0.1545	0.2721	-1.493	0.1395	
10	-1.5521	-0.4471	0.1179	0.1628	-0.9358	0.0413	
11	-1.2198	-0.3589	0.1114	0.1242	-0.7318	0.0139	
12	-1.3136	-0.2922	0.2043	0.1126	-0.6299	0.0455	
13	-1.0261	-0.2729	0.2404	0.1076	-0.5955	0.0498	
14	-1.1739	-0.2972	0.0851	0.0931	-0.5768	-0.0177	
15	-1.8544	-0.56	0.1564	0.2227	-1.2291	0.1081	
16	-1.1452	-0.3289	0.1285	0.1249	-0.7035	0.0457	
17	-0.9759	-0.289	0.1212	0.1041	-0.6015	0.0234	
18	-2.3307	-0.4542	0.2674	0.1964	-1.0432	0.1349	
19	-1.219	-0.3423	0.1804	0.128	-0.7203	0.0358	
20	-0.9784	-0.2809	0.22	0.0978	-0.5537	0.032	
21	-2.5575	-0.4655	0.342	0.2464	-1.2046	0.2735	
22	-1.6786	-0.3525	0.2802	0.1547	-0.8168	0.1177	
23	-0.8491	-0.2668	0.203	0.0981	-0.5551	0.0215	
24	-0.8998	-0.2076	0.1832	0.0864	-0.4669	0.0518	
25	-0.8038	-0.2479	0.1357	0.0836	-0.4989	0.003	
26	-0.677	-0.2822	0.0953	0.0828	-0.51	-0.0144	
27	-1.9837	-0.4059	0.2858	0.2125	-1.0432	0.2315	
28	-0.9722	-0.282	0.2232	0.1273	-0.664	0.1001	
29	-0.7885	-0.2232	0.1833	0.0914	-0.4973	0.051	
30	-0.7259	-0.1982	0.1901	0.0815	-0.4427	0.0462	
31	-0.7283	-0.19	0.1897	0.0783	-0.4251	0.045	
32	-0.2616	-0.0964	0.1183	0.0418	-0.2218	0.0289	
33	-1.451	-0.3631	0.2482	0.1788	-0.8989	0.1727	
34	-0.9571	-0.2115	0.2338	0.1076	-0.5345	0.1114	
35	-0.8534	-0.1638	0.206	0.0851	-0.419	0.0915	
36	-0.7502	-0.2197	0.1434	0.0791	-0.4541	0.0207	
37	-0.7314	-0.2088	0.1354	0.0763	-0.4377	0.0204	
38	-0.5835	-0.1694	0.1747	0.0735	-0.39	0.0512	
39	-1.6266	-0.2788	0.2707	0.1835	-0.7694	0.2119	
40	-0.9777	-0.2217	0.2184	0.1042	-0.5343	0.091	
41	-0.7147	-0.2631	0.1719	0.0792	-0.5008	-0.0254	
42	-0.623	-0.1716	0.16	0.0747	-0.3957	0.0525	
43	-0.6459	-0.1545	0.2165	0.0737	-0.3758	0.0687	
44	-0.6131	-0.1685	0.1938	0.0697	-0.3757	0.0427	
45	-1.2321	-0.3397	0.225	0.127	-0.7206	0.0412	
46	-0.9898	-0.2839	0.2138	0.0958	-0.5515	0.0238	
47	-1.2144	-0.2505	0.2231	0.0854	-0.5068	0.0058	
48	-1.0816	-0.1784	0.2031	0.081	-0.4228	0.0837	
49	-1.0841	0.0062	0.3574	0.0817	-0.24	0.2504	
50	-0.8825	-0.0196	0.3955	0.081	-0.2568	0.2294	
51	-1.0794	-0.0536	1.1817	0.2172	-0.7052	0.598	
52	-0.7193	0.0082	0.8169	0.1429	-0.4204	0.4367	
53	-0.5802	0.1022	1.2423	0.1883	-0.4027	0.6071	
54	-0.5697	0.0985	1.0899	0.1865	-0.4629	0.656	
55	-0.5335	0.0139	1.2592	0.1738	-0.5075	0.5352	
56	-1.7503	-0.1687	0.828	0.2048	-0.721	0.5077	
57	-0.4781	0.0029	0.8268	0.1113	-0.3312	0.3369	
58	-0.5402	-0.0173	0.6916	0.1197	-0.3784	0.3417	
59	-0.5169	0.0929	0.8238	0.1229	-0.2758	0.4615	
60	-0.5262	0.0299	0.9493	0.1381	-0.3843	0.444	
61	-1.4379	-0.1487	1.0277	0.1887	-0.7149	0.4174	
62	-0.4809	-0.0316	0.4973	0.0949	-0.3162	0.2531	
63	-0.4525	0.0178	0.5032	0.0941	-0.2644	0.2999	
64	-0.5546	-0.0433	0.38	0.0948	-0.3276	0.241	
65	-0.7237	-0.0402	1.1688	0.1529	-0.4988	0.4183	
66	-1.1051	-0.2068	0.2595	0.112	-0.5427	0.1291	
67	-0.886	-0.1049	0.2906	0.0999	-0.4046	0.1948	
68	-1.052	-0.0423	0.3222	0.0941	-0.3246	0.2401	
69	-1.1693	-0.0119	0.3424	0.0942	-0.3017	0.2637	
70	-0.9206	-0.2282	0.1695	0.0984	-0.5243	0.066	
71	-0.5282	-0.1158	0.2233	0.0879	-0.3798	0.148	
72	-0.5032	-0.1003	0.3128	0.0792	-0.2405	0.2348	
73	-0.5494	-0.0258	0.3208	0.0783	-0.2895	0.2092	
74	-0.7354	-0.1794	0.2898	0.0889	-0.478	0.1172	
75	-0.5854	-0.1079	0.2407	0.0793	-0.3457	0.1289	
76	-0.3688	-0.0044	0.3395	0.0778	-0.2379	0.2291	
77	-1.4108	-0.0067	0.3277	0.0784	-0.245	0.2317	
78	-1.5259	-0.3157	1.0422	0.1458	-0.7526	0.1212	
79	-1.6858	-0.2732	0.1515	0.1349	-0.678	0.1315	
80	-1.2709	-0.1795	0.1835	0.1084	-0.5047	0.1458	
81	-0.3647	-0.0317	0.3169	0.0772	-0.2832	0.1997	
82	-0.4465	-0.0213	0.3825	0.0708	-0.2338	0.1911	
83	-0.398	0.0294	0.4381	0.0771	-0.2019	0.2807	
84	-1.5085	-0.3135	0.1448	0.1528	-0.7714	0.1445	
85	-1.1433	-0.2819	0.1409	0.1288	-0.6683	0.1044	
86	-0.9742	-0.2259	0.1738	0.1282	-0.6104	0.1589	
87	-0.5826	-0.0838	0.2832	0.0911	-0.3569	0.1897	
88	-0.422	-0.0797	0.2575	0.0752	-0.3053	0.1459	
89	-0.4557	-0.0571	0.2934	0.0709	-0.2699	0.1557	
90	-0.351	0.0081	0.3534	0.0748	-0.2159	0.232	
91	-1.7348	-0.2888	0.1914	0.1614	-0.7829	0.1853	
92	-1.0901	-0.2838	0.2476	0.1328	-0.6815	0.1143	
93	-0.0764	-0.1826	0.3032	0.1044	-0.5058	0.1205	
94	-0.3759	-0.041	0.2757	0.0814	-0.2853	0.2033	
95	-0.4052	-0.0533	0.315	0.0755	-0.2797	0.1731	
96	-0.2573	0.0485	0.4089	0.0753	-0.1793	0.2723	

B/H=1		N=1 70 degree					
# of lap	Min	Mean	max	STDV	- peak	+ peak	
1	0.2285	0.9173	1.7452	0.2821	0.131	1.7035	
2	-2.3838	-0.7587	0.3213	0.3008	-1.861	0.1435	
3	-1.9528	-0.5165	0.262	0.196	-1.047	0.0716	
4	-2.0766	-0.4424	0.3888	0.1942	-1.0249	0.1401	
5	-1.6828	-0.3922	0.3034	0.1548	-0.8567	0.0723	
6	-1.5616	-0.2814	0.3459	0.1312	-0.6749	0.1122	
7	-1.4367	-0.3163	0.2538	0.1265	-0.8957	0.0693	
8	-1.2444	-0.3389	0.1768	0.1142	-0.6874	0.0036	
9	-2.4562	-0.7477	0.2032	0.2832	-1.5972	0.1018	
10	-1.7124	-0.4847	0.2938	0.1781	-1.019	0.0497	
11	-1.4287	-0.3515	0.259	0.1172	-0.7029	0	
12	-1.0555	-0.2999	0.2466	0.1073	-0.6218	0.0219	
13	-1.0095	-0.2931	0.2868	0.1023	-0.6001	0.0138	
14	-0.9307	-0.3086	0.1732	0.0932	-0.5882	-0.029	
15	-2.068	-0.6037	0.2059	0.2448	-1.3382	0.1307	
16	-1.0784	-0.3381	0.3182	0.1305	-0.7296	0.0634	
17	-1.0134	-0.2936	0.2909	0.1035	-0.604	0.0168	
18	-1.8828	-0.4594	0.387	0.2178	-1.1129	0.1941	
19	-1.7511	-0.3366	0.2096	0.129	-0.7237	0.0505	
20	-0.8232	-0.2672	0.1981	0.0899	-0.5869	0.0326	
21	-2.3978	-0.5123	0.4843	0.2975	-1.4048	0.3803	
22	-1.4561	-0.3266	0.3073	0.1545	-0.79	0.1369	
23	-0.7443	-0.272	0.1878	0.0994	-0.5704	0.0263	
24	-0.7349	-0.2135	0.1781	0.0897	-0.4827	0.0579	
25	-0.8932	-0.2652	0.1138	0.0871	-0.5266	-0.0039	
26	-0.6984	-0.2816	0.0608	0.0831	-0.531	-0.0321	
27	-1.788	-0.3787	0.325	0.2185	-1.0342	0.2788	
28	-1.193	-0.2838	0.1218	0.1216	-0.6286	0.101	
29	-1.1128	-0.2218	0.1449	0.0893	-0.5017	0.0582	
30	-0.7734	-0.2016	0.1409	0.0857	-0.4588	0.0555	
31	-0.7639	-0.1852	0.1387	0.082	-0.4412	0.0507	
32	-0.2753	-0.108	0.1287	0.0441	-0.2403	0.0243	
33	-1.7411	-0.3648	0.3525	0.1777	-0.8977	0.1685	
34	-1.1314	-0.2368	0.3379	0.1194	-0.595	0.1215	
35	-0.7784	-0.1768	0.2259	0.0844	-0.4599	0.1063	
36	-0.7096	-0.235	0.107	0.0862	-0.4836	0.0236	
37	-0.6717	-0.2231	0.1582	0.0818	-0.4885	0.0224	
38	-0.5124	-0.1776	0.1584	0.0752	-0.4032	0.048	
39	-1.6385	-0.3186	0.5321	0.1813	-0.8828	0.2253	
40	-1.0137	-0.2757	0.358	0.1284	-0.5549	0.1034	
41	-1.0061	-0.3101	0.1651	0.0957	-0.5974	-0.0229	
42	-0.8057	-0.1975	0.1977	0.0873	-0.4594	0.0649	
43	-0.8968	-0.1746	0.1797	0.0831	-0.424	0.0747	
44	-0.6163	-0.1811	0.1901	0.0737	-0.4123	0.03	
45	-1.5547	-0.3928	0.2808	0.1418	-0.8183	0.0327	
46	-0.9807	-0.3119	0.2107	0.1136	-0.6528	0.029	
47	-1.0666	-0.2829	0.2211	0.104	-0.6049	0.0192	
48	-0.8341	-0.2234	0.258	0.0973	-0.5153	0.0685	
49	-0.812	-0.0056	0.4163	0.0951	-0.2808	0.2797	
50	-0.8686	-0.0327	0.3717	0.0919	-0.3084	0.2429	
51	-2.1654	-0.1245	0.9706	0.2653	-0.9203	0.6713	
52	-0.8528	-0.0155	0.8215	0.1193	-0.3735	0.3424	
53	-0.4091	0.0583	1.1078	0.1276	-0.3248	0.4411	
54	-0.4821	0.0199	0.9834	0.1448	-0.4149	0.4541	
55	-0.5096	0.0456	0.8129	0.1472	-0.4871	0.3959	
56	-1.8593	-0.1582	0.8357	0.2504	-0.8085	0.5932	
57	-0.5243	-0.0077	0.5873	0.1049	-0.3225	0.3072	
58	-0.7481	-0.053	0.5835	0.1039	-0.3647	0.2586	
59	-0.415	0.0618	0.6749	0.1058	-0.2557	0.3794	
60	-0.5525	0.009	0.9062	0.1165	-0.3465	0.3524	
61	-0.7129	-0.1519	0.7293	0.2048			

B/H=1 N=1 80 degree

# of lap	Min	Mean	max	S1DV	-peak	* peak
0	0.3654	1.0147	1.9124	0.2516	-0.2598	1.7696
1	-2.6174	-0.6035	0.2689	0.2592	-1.3372	0.1682
2	-1.4173	-0.347	0.1824	0.1386	-0.7629	0.0689
3	-1.3298	-0.2678	0.2387	0.1396	-0.6866	0.1511
4	-1.1987	-0.2499	0.1775	0.1254	-0.6261	0.1262
5	-1.0647	-0.1895	0.2179	0.103	-0.4784	0.1394
6	-1.3409	-0.2081	0.1976	0.0957	-0.4952	0.079
7	-0.8244	-0.2067	0.1391	0.0863	-0.4657	0.0523
8	-2.2305	-0.581	0.3366	0.2518	-1.3164	0.1945
9	-1.6658	-0.338	0.2231	0.1431	-0.6764	0.0914
10	-0.8482	-0.2433	0.1414	0.0943	-0.5263	0.0397
11	-0.9132	-0.2002	0.1718	0.0894	-0.4683	0.0679
12	-1.237	-0.1978	0.1547	0.0864	-0.4569	0.0613
13	-0.8128	-0.1959	0.0947	0.0799	-0.4354	0.0437
14	-1.8694	-0.4142	0.2691	0.214	-1.0562	0.2278
15	-0.8646	-0.2221	0.2376	0.1082	-0.5488	0.1029
16	-0.7825	-0.2025	0.1714	0.0884	-0.4676	0.0628
17	-1.3609	-0.2805	0.2969	0.1709	-0.7932	0.2322
18	-1.0266	-0.2187	0.2001	0.1077	-0.5417	0.1043
19	-0.8365	-0.1793	0.3203	0.0891	-0.4466	0.068
20	-1.9228	-0.3236	0.3966	0.2429	-1.0522	0.405
21	-1.0322	-0.1974	0.236	0.121	-0.5603	0.1655
22	-0.8945	-0.1846	0.2538	0.0894	-0.4529	0.0837
23	-0.561	-0.1339	0.2845	0.081	-0.3768	0.109
24	-1.0516	-0.1825	0.1768	0.0768	-0.4129	0.0478
25	-0.7408	-0.1871	0.1739	0.0715	-0.4017	0.0275
26	-1.6375	-0.2835	0.4408	0.1633	-0.7535	0.2265
27	-1.1306	-0.2096	0.3249	0.1144	-0.5528	0.1337
28	-0.7415	-0.1618	0.3234	0.0906	-0.4336	0.1099
29	-0.597	-0.1365	0.2903	0.0807	-0.3786	0.1056
30	-0.7953	-0.128	0.2716	0.077	-0.3588	0.1049
31	-0.207	-0.0619	0.1277	0.041	-0.185	0.0611
32	-1.7303	-0.3186	0.3912	0.182	-0.8045	0.1673
33	-1.1812	-0.2132	0.4527	0.1202	-0.5736	0.1473
34	-0.8788	-0.1387	0.4683	0.0961	-0.4269	0.1495
35	-0.7684	-0.1831	0.2897	0.0851	-0.4385	0.0722
36	-0.7357	-0.166	0.218	0.0801	-0.4064	0.0745
37	-0.7812	-0.1159	0.2581	0.0718	-0.3312	0.0995
38	-2.0264	-0.2808	0.6026	0.1789	-0.8174	0.2558
39	-1.149	-0.2404	0.3978	0.1245	-0.6141	0.1332
40	-1.0575	-0.2645	0.1492	0.0889	-0.5811	0.0321
41	-0.6276	-0.1536	0.2595	0.0881	-0.4178	0.1108
42	-0.6923	-0.128	0.2459	0.0833	-0.378	0.122
43	-0.6887	-0.1441	0.1516	0.072	-0.36	0.0719
44	-1.4463	-0.3616	0.3359	0.1489	-0.8082	0.085
45	-1.1848	-0.2641	0.2651	0.1139	-0.6058	0.0775
46	-0.8851	-0.2333	0.3277	0.1007	-0.5354	0.0688
47	-0.9131	-0.1713	0.3713	0.0933	-0.4512	0.1087
48	-0.8439	0.0226	0.5083	0.0895	-0.2459	0.291
49	-0.817	-0.0713	0.4032	0.0843	-0.2643	0.2416
50	-1.3695	-0.1197	0.9194	0.2364	-0.8288	0.5894
51	-0.5716	0.0127	0.5409	0.0924	-0.2644	0.2897
52	-0.4268	0.064	0.9107	0.0898	-0.2053	0.3333
53	-0.5159	0.0063	1.02	0.0936	-0.2745	0.2871
54	-0.4607	-0.0413	0.5752	0.0911	-0.3144	0.2319
55	-1.8907	-0.1238	0.6301	0.2238	-0.7951	0.3475
56	-0.376	0.0273	0.4405	0.0876	-0.2356	0.2602
57	-0.3477	-0.0295	0.4659	0.0829	-0.2783	0.2193
58	-0.2722	0.0686	0.6674	0.0802	-0.172	0.3091
59	-0.3221	0.0301	0.5976	0.0798	-0.2085	0.2693
60	-1.4702	-0.0676	0.5807	0.1856	-0.5844	0.4292
61	-0.3729	0.0183	0.4467	0.0843	-0.2346	0.2712
62	-0.3329	0.0479	0.3618	0.0773	-0.1841	0.2799
63	-0.3464	-0.0327	0.3202	0.0744	-0.2558	0.1905
64	-0.376	-0.0718	0.6161	0.0789	-0.2485	0.2128
65	-1.3426	-0.1746	0.4825	0.1385	-0.59	0.2408
66	-0.7366	-0.0395	0.4927	0.1025	-0.3472	0.2681
67	-0.5816	-0.0139	0.4217	0.0944	-0.2971	0.2693
68	-0.9332	-0.0048	0.4292	0.0904	-0.276	0.2684
69	-0.8905	-0.1763	0.2781	0.1199	-0.5381	0.1836
70	-0.4624	-0.0355	0.3641	0.0913	-0.3095	0.2385
71	-0.3545	0.0399	0.3975	0.0841	-0.2124	0.2921
72	-0.4118	-0.0036	0.3401	0.0784	-0.2389	0.2319
73	-0.6732	-0.0891	0.4195	0.1077	-0.4122	0.234
74	-0.4184	-0.0535	0.3256	0.087	-0.3144	0.2074
75	-0.3005	0.0257	0.3796	0.0792	-0.2117	0.2632
76	-0.317	0.0098	0.3811	0.0739	-0.2119	0.2316
77	-0.7255	-0.091	0.2262	0.0923	-0.3682	0.1862
78	-0.7158	-0.0784	0.2583	0.0953	-0.3842	0.2074
79	-0.6841	-0.0534	0.3166	0.0802	-0.294	0.1873
80	-0.2396	0.0529	0.4137	0.0889	-0.154	0.2592
81	-0.3088	0.0167	0.3595	0.0887	-0.1893	0.2227
82	-0.3367	0.0393	0.4356	0.0784	-0.1958	0.2745
83	-0.6753	-0.075	0.2417	0.095	-0.36	0.2101
84	-0.749	-0.086	0.2712	0.1007	-0.388	0.2161
85	-0.7576	-0.0887	0.3035	0.0985	-0.3942	0.1969
86	-0.3758	0.0163	0.4088	0.0764	-0.213	0.2456
87	-0.3285	-0.0065	0.3583	0.0702	-0.2171	0.2041
88	-0.4199	-0.0137	0.2803	0.0687	-0.2198	0.1923
89	-0.3258	0.0278	0.4279	0.0766	-0.2021	0.2574
90	-0.7598	-0.0774	0.3238	0.097	-0.3684	0.2195
91	-0.8786	-0.1117	0.3018	0.1113	-0.4456	0.2223
92	-0.6019	-0.094	0.3462	0.0901	-0.3643	0.1762
93	-0.318	0.0377	0.4487	0.0751	-0.1877	0.2631
94	-0.4696	-0.0042	0.3236	0.0739	-0.2259	0.2174
95	-0.3459	0.0681	0.4261	0.0737	-0.1551	0.2873

B/H=1 N=1 90 degree

# of lap	Min	Mean	max	S1DV	-peak	* peak
0	0.3654	1.0215	1.9861	0.2571	-0.2502	1.7928
1	-2.1834	-0.3686	0.2349	0.1782	-0.9242	0.1509
2	-1.2243	-0.2509	0.1704	0.1089	-0.5777	0.0759
3	-1.1955	-0.1707	0.258	0.1064	-0.449	0.1485
4	-1.0626	-0.1441	0.3151	0.1003	-0.4448	0.1507
5	-0.7681	-0.0728	0.3105	0.0972	-0.3344	0.1889
6	-0.7456	-0.1209	0.2593	0.0917	-0.366	0.1242
7	-0.4587	-0.0924	0.3235	0.0787	-0.3286	0.1437
8	-1.6088	-0.3226	0.4255	0.1851	-0.8778	0.2327
9	-1.0648	-0.2322	0.2638	0.1134	-0.5723	0.1079
10	-0.7299	-0.1938	0.2724	0.0984	-0.449	0.0913
11	-0.6224	-0.1729	0.252	0.0818	-0.3743	0.1162
12	-0.553	-0.1234	0.2575	0.0794	-0.3615	0.1147
13	-0.4796	-0.0891	0.2784	0.0752	-0.3149	0.1366
14	-1.2068	-0.2434	0.432	0.1511	-0.6968	0.21
15	-0.7692	-0.1576	0.3793	0.1023	-0.4645	0.1492
16	-0.5937	-0.1477	0.333	0.0991	-0.4151	0.1196
17	-1.0029	-0.2153	0.3475	0.1332	-0.6147	0.1842
18	-0.7545	-0.1807	0.3045	0.1057	-0.4978	0.1383
19	-0.6879	-0.137	0.237	0.0938	-0.4178	0.1438
20	-1.7178	-0.2269	0.4571	0.1723	-0.7436	0.29
21	-1.2761	-0.1747	0.3382	0.1182	-0.5293	0.1798
22	-0.6988	-0.1512	0.2939	0.0957	-0.4385	0.136
23	-0.6394	-0.0864	0.3439	0.086	-0.3445	0.1717
24	-0.6335	-0.1287	0.2595	0.0807	-0.371	0.1135
25	-0.4986	-0.1039	0.2319	0.0738	-0.3252	0.1174
26	-2.1329	-0.2848	0.4274	0.1654	-0.784	0.2145
27	-0.9159	-0.2289	0.406	0.1279	-0.6128	0.1549
28	-0.6982	-0.1426	0.3112	0.1018	-0.4481	0.1628
29	-0.6843	-0.1	0.2985	0.0895	-0.3684	0.1684
30	-0.5923	-0.0787	0.2905	0.0818	-0.3241	0.1688
31	-0.1744	-0.0261	0.1788	0.0426	-0.1543	0.1022
32	-2.1232	-0.3054	0.4807	0.1762	-0.834	0.2232
33	-0.6796	-0.1823	0.5124	0.127	-0.5632	0.1987
34	-1.1561	-0.097	0.4198	0.1024	-0.4043	0.2102
35	-0.7049	-0.1432	0.2991	0.0994	-0.4113	0.1249
36	-0.7841	-0.1254	0.2379	0.0837	-0.3764	0.1255
37	-0.3653	-0.072	0.2584	0.073	-0.2911	0.1472
38	-2.3037	-0.2488	0.5785	0.2181	-0.993	0.4055
39	-1.0259	-0.1867	0.4269	0.1259	-0.5443	0.2109
40	-0.9034	-0.2116	0.2535	0.0956	-0.4983	0.0752
41	-0.6135	-0.1074	0.2878	0.0868	-0.3619	0.1591
42	-0.6774	-0.0813	0.3065	0.0818	-0.3262	0.1635
43	-0.473	-0.1233	0.1908	0.0889	-0.3301	0.0935
44	-1.7107	-0.3593	0.3541	0.1819	-0.905	0.1884
45	-0.9853	-0.1971	0.327	0.1162	-0.5457	0.1514
46	-1.1009	-0.1787	0.2409	0.1028	-0.4889	0.1266
47	-0.7701	-0.1193	0.3055	0.0905	-0.3909	0.1522
48	-0.5872	0.0658	0.4831	0.0844	-0.1875	0.3192
49	-0.4459	-0.0025	0.3003	0.0747	-0.2264	0.2215
50	-1.9687	-0.1032	0.738	0.1937	-0.6844	0.478
51	-0.397	0.0468	0.4261	0.0868	-0.2138	0.3073
52	-0.322	0.0993	0.5295	0.0802	-0.1415	0.34
53	-0.6149	0.0342	0.4322	0.0791	-0.203	0.2714
54	-0.3786	0.0212	0.413	0.078	-0.1162	0.2551
55	-1.8022	-0.1032	0.5287	0.1827	-0.8513	0.4448
56	-0.4484	0.0691	0.4264	0.0822	-0.1775	0.3157
57	-0.3571	0.0046	0.366	0.0768	-0.2257	0.2349
58	-0.3813	0.1088	0.4465	0.074	-0.1151	0.3287
59	-0.2069	0.1132	0.4726	0.0758	-0.114	0.3405
60	-0.9157	-0.0557	0.8326	0.1368	-0.4662	0.3549
61	-0					

B/H=1		N=1 0 degree					
# of tap	Min	Mean	max	STDV	peak	* peak	
1	-0.45	1.1375	1.962	0.2621	-0.3513	1.9238	
2	-1.1512	-0.1696	0.3095	0.1286	-0.5558	0.2163	
3	-1.2466	-0.1469	0.4726	0.1386	-0.5626	0.2688	
4	-0.6975	-0.1061	0.5875	0.1418	-0.5313	0.3192	
5	-0.6905	-0.0472	0.5858	0.1376	-0.4801	0.3657	
6	-0.6956	0.0143	0.4982	0.1344	-0.3988	0.4173	
7	-1.2818	-0.0672	0.47	0.1718	-0.5928	0.4485	
8	-1.6929	-0.2004	0.3422	0.1875	-0.7628	0.362	
9	-0.7266	-0.073	0.3397	0.1002	-0.3737	0.2276	
10	-0.7753	-0.0589	0.4318	0.1021	-0.3652	0.2473	
11	-0.6003	-0.025	0.4143	0.1018	-0.3304	0.2805	
12	-0.6138	0.0097	0.4018	0.0953	-0.2762	0.2956	
13	-0.6051	-0.0021	0.4157	0.104	-0.314	0.3099	
14	-0.6163	-0.0325	0.411	0.1045	-0.3461	0.2811	
15	-0.7051	-0.0346	0.354	0.0956	-0.3213	0.2521	
16	-0.5068	-0.0214	0.3787	0.0921	-0.2976	0.2548	
17	-0.5158	-0.0057	0.3824	0.0886	-0.2714	0.2601	
18	-0.527	-0.0211	0.3649	0.0894	-0.2894	0.2472	
19	-0.4831	-0.0052	0.3708	0.0838	-0.2565	0.2461	
20	-0.4284	0.0156	0.3497	0.0801	-0.2246	0.2558	
21	-0.7384	-0.0124	0.3648	0.0899	-0.2821	0.2573	
22	-0.4465	0.0057	0.3943	0.0836	-0.2452	0.2566	
23	-0.4149	0.0214	0.3552	0.0778	-0.212	0.2547	
24	-0.2608	0.0443	0.3922	0.0735	-0.1782	0.2648	
25	-0.3069	0.0172	0.3444	0.0741	-0.2051	0.2395	
26	-0.5763	-0.0028	0.3265	0.0845	-0.2563	0.2506	
27	-1.2514	-0.0058	0.3683	0.0837	-0.2568	0.2453	
28	-0.4982	0.0009	0.3573	0.0788	-0.2355	0.2373	
29	-0.3211	0.031	0.3643	0.0718	-0.1838	0.2458	
30	-0.2228	0.0448	0.3428	0.0676	-0.158	0.2476	
31	-0.3052	0.0466	0.3294	0.0681	-0.1578	0.2451	
32	-1.2514	-0.0058	0.3683	0.0837	-0.2568	0.2453	
33	-0.7718	-0.0014	0.3556	0.0792	-0.2389	0.2382	
34	-0.4895	0.0313	0.4192	0.075	-0.1937	0.2582	
35	-0.2449	0.0584	0.441	0.0691	-0.1408	0.2735	
36	-0.2645	0.0431	0.3239	0.0681	-0.1534	0.2415	
37	-0.3415	0.0361	0.3287	0.0685	-0.1635	0.2356	
38	-0.5712	0.04	0.3581	0.0731	-0.1794	0.2593	
39	-0.6655	0.0435	0.3933	0.0774	-0.1889	0.2758	
40	-0.3737	0.0365	0.3829	0.0711	-0.1765	0.2495	
41	-0.3701	0.0085	0.3198	0.0654	-0.1878	0.2048	
42	-0.2418	0.0491	0.361	0.0626	-0.1388	0.237	
43	-0.2587	0.0628	0.3639	0.064	-0.1293	0.255	
44	-0.7306	0.039	0.3304	0.0724	-0.1784	0.2583	
45	-0.5385	-0.0199	0.3642	0.0749	-0.2446	0.2048	
46	-0.4158	-0.0141	0.3363	0.0732	-0.2337	0.2055	
47	-0.3949	-0.0115	0.2803	0.0686	-0.2172	0.1942	
48	-0.2819	0.0423	0.2955	0.0619	-0.1435	0.2281	
49	-0.2219	0.0697	0.317	0.0644	-0.1234	0.2628	
50	-0.4651	0.0638	0.4156	0.0792	-0.1737	0.3013	
51	-0.4412	0.1366	1.2499	0.1762	-0.3919	1.6651	
52	-0.5043	0.2176	1.6654	0.2351	-0.4876	1.9233	
53	-0.4314	0.2972	1.5425	0.244	-0.4349	1.9293	
54	-0.3585	0.3801	1.8273	0.2798	-0.4596	1.2198	
55	-0.5135	0.3274	1.9515	0.2458	-0.4102	1.0649	
56	-0.6469	0.0414	1.0701	0.153	-0.4177	0.5005	
57	-0.623	0.0132	0.7803	0.1372	-0.3984	0.4249	
58	-0.5554	0.0234	0.7115	0.1277	-0.3598	0.4067	
59	-0.337	0.1977	1.0822	0.182	-0.2883	0.6837	
60	-0.3083	0.3241	1.5884	0.2134	-0.316	0.9642	
61	-0.6466	-0.012	0.8583	0.1624	-0.4993	0.4754	
62	-0.6282	-0.0143	0.426	0.096	-0.3431	0.3144	
63	-0.4903	0.022	0.3623	0.0908	-0.2686	0.3125	
64	-0.4003	0.0531	0.5581	0.1061	-0.2652	0.3715	
65	-0.4851	0.2499	1.4583	0.191	-0.3284	0.8228	
66	-0.6738	-0.0914	0.2742	0.1051	-0.4088	0.2239	
67	-0.4538	-0.0262	0.2578	0.0829	-0.2749	0.2225	
68	-0.3245	0.0455	0.3308	0.0858	-0.152	0.243	
69	-0.3949	0.0669	0.4283	0.0747	-0.1571	0.2908	
70	-0.1888	-0.1105	0.2818	0.1138	-0.4519	0.2309	
71	-0.5937	-0.059	0.2331	0.1019	-0.3647	0.2488	
72	-0.4562	0.0338	0.2975	0.0746	-0.19	0.2577	
73	-0.3519	0.0393	0.3299	0.0709	-0.1734	0.2519	
74	-0.671	-0.1017	0.3056	0.1121	-0.438	0.2345	
75	-0.5075	-0.0162	0.3187	0.0762	-0.2449	0.2125	
76	-0.2688	0.0509	0.3409	0.0672	-0.1509	0.2526	
77	-0.3295	0.0561	0.3836	0.0737	-0.1651	0.2772	
78	-1.5231	-0.1645	0.4564	0.1805	-0.706	0.377	
79	-1.1196	-0.0168	0.4172	0.195	-0.3317	0.2982	
80	-0.7283	0.0123	0.3611	0.0806	-0.2284	0.254	
81	-0.4495	0.0399	0.4332	0.0748	-0.1848	0.2645	
82	-0.4285	0.0617	0.51	0.0785	-0.1678	0.2913	
83	-0.3865	0.1013	0.4848	0.0787	-0.1346	0.3373	
84	-1.5871	-0.1403	0.4413	0.1885	-0.7057	0.4251	
85	-0.8989	-0.0034	0.4544	0.1023	-0.3102	0.3035	
86	-0.8612	0.011	0.4102	0.0791	-0.2284	0.2483	
87	-0.8823	0.059	0.4245	0.0739	-0.1627	0.2808	
88	-0.651	0.041	0.3928	0.0719	-0.1748	0.2566	
89	-0.276	0.0603	0.4328	0.0725	-0.1573	0.2779	
90	-0.3828	0.0656	0.4284	0.0755	-0.1308	0.322	
91	-1.312	-0.0287	0.4995	0.1492	-0.4764	0.419	
92	-0.5708	0.0186	0.4112	0.095	-0.2664	0.3036	
93	-0.4081	-0.0085	0.3757	0.0788	-0.245	0.228	
94	-0.3052	0.0691	0.4479	0.0701	-0.1413	0.2795	
95	-0.2817	0.0766	0.4289	0.069	-0.1305	0.2837	

B/H=1		N=2 0 degree					
# of tap	Min	Mean	max	STDV	peak	* peak	
1	0.2927	0.9893	1.8885	0.2662	0.1877	1.7848	
2	-0.9818	-0.1571	0.4013	0.1349	-0.5809	0.2487	
3	-1.5385	-0.1436	0.4442	0.1501	-0.5939	0.3087	
4	-1.4546	-0.1001	0.5359	0.1525	-0.5577	0.3575	
5	-1.2422	-0.0573	0.4982	0.1443	-0.4902	0.3755	
6	-1.0942	-0.0056	0.5421	0.1391	-0.424	0.4108	
7	-1.5653	-0.0767	0.4552	0.1526	-0.5346	0.3811	
8	-1.1738	-0.1422	0.4801	0.1534	-0.6024	0.318	
9	-0.9536	-0.051	0.3702	0.1016	-0.3556	0.2537	
10	-0.938	-0.0417	0.3883	0.1027	-0.3497	0.2663	
11	-0.5435	-0.0367	0.3501	0.0466	-0.3524	0.2751	
12	-0.5498	-0.0171	0.4001	0.1003	-0.3179	0.2838	
13	-0.6116	-0.0263	0.3605	0.1039	-0.3377	0.2851	
14	-0.6955	-0.0284	0.4847	0.1008	-0.3312	0.2723	
15	-1.0701	-0.0144	0.3547	0.0956	-0.3012	0.2424	
16	-0.4288	-0.0111	0.3955	0.0918	-0.2866	0.2644	
17	-0.5738	-0.0113	0.3777	0.09	-0.2813	0.2586	
18	-0.6845	-0.012	0.3771	0.0889	-0.2787	0.2517	
19	-0.4368	-0.0053	0.3294	0.0841	-0.2576	0.247	
20	-0.397	0.0084	0.3718	0.0819	-0.2362	0.2549	
21	-0.7263	-0.0012	0.3896	0.0899	-0.2709	0.2686	
22	-0.4344	0.0145	0.3472	0.0842	-0.2382	0.2672	
23	-0.4134	0.0139	0.3891	0.0802	-0.2257	0.2546	
24	-0.3221	0.0387	0.3876	0.0773	-0.1939	0.2699	
25	-0.3322	-0.0015	0.3537	0.0774	-0.2337	0.2307	
26	-0.5315	-0.012	0.3687	0.0857	-0.2691	0.245	
27	-0.5514	-0.0146	0.3708	0.0856	-0.2714	0.2422	
28	-0.4344	-0.0095	0.3157	0.0809	-0.2523	0.2331	
29	-0.4539	0.0219	0.3266	0.0748	-0.2025	0.2462	
30	-0.3409	0.0363	0.3743	0.072	-0.1798	0.2524	
31	-0.3412	0.0396	0.3799	0.073	-0.1795	0.2588	
32	-0.5514	-0.0146	0.3706	0.0856	-0.2714	0.2422	
33	-0.7288	-0.0213	0.3456	0.0854	-0.2773	0.2348	
34	-0.4446	0.027	0.3742	0.0753	-0.2108	0.285	
35	-0.3503	0.0578	0.4635	0.0731	-0.1515	0.2872	
36	-0.3987	0.0286	0.3034	0.0708	-0.1837	0.241	
37	-0.4491	0.018	0.3571	0.0722	-0.1987	0.2347	
38	-0.8009	0.0288	0.3802	0.0821	-0.2176	0.2752	
39	-0.5799	0.0408	0.4745	0.0849	-0.2135	0.2951	
40	-0.5509	0.0309	0.398	0.0772	-0.2008	0.2626	
41	-0.3724	-0.0193	0.2588	0.0698	-0.2288	0.1902	
42	-0.3824	0.0358	0.3334	0.068	-0.1683	0.2399	
43	-0.3091	0.0546	0.4188	0.0699	-0.1552	0.2644	
44	-0.3471	0.0208	0.4125	0.0829	-0.228	0.2698	
45	-0.5895	-0.0532	0.3175	0.0866	-0.3129	0.2065	
46	-0.4906	-0.0398	0.4977	0.0834	-0.2901	0.2105	
47	-0.3788	-0.042	0.3013	0.0778	-0.2503	0.1912	
48	-0.4016	0.0251	0.319	0.0683	-0.1799	0.2301	
49	-0.3124	0.0558	0.3656	0.0694	-0.1525	0.2642	
50	-0.5826	0.0382	0.4101	0.0886	-0.2275	0.304	
51	-0.4842	0.2088	1.5717	0.2136	-0.4318	0.8495	
52	-0.4894	0.2584	1.8516	0.2457	-0.4778	0.9965	
53	-0.3088	0.2708	1.648	0.2349	-0.434	0.9755	
54	-0.587	0.2646	1.6653	0.2694	-0.5237	1.0929	
55	-0.4386	0.2174	1.6822	0.2346	-0.4865	0.9213	
56	-0.5624	0.0791	1.2458	0.1658	-0.4183	0.5766	
57	-0.5674	0.064	0.7484	0.1338	-0.3975	0.4655	
58	-0.4706	0.0086	0.7352	0.1187	-0.3474	0.3647	
59	-0.6601	0.1307	0.9982	0.1352	-0.2749	0.5362	
60	-0.4927	0.1995	1.4878	0.1796	-0.3392	0.7382	
61	-0.6418	0.0251	0.9582	0.1567	-0.4451	0.4952	
62	-0.7127	0.0264	0.44				

B/H=1 N=3 0 degree

# of lap	Min	Mean	max	STDEV	- peak	+ peak
1	0.3346	1.0006	1.7834	0.255	0.2355	1.7657
1	-0.9262	-0.1561	0.4393	0.1248	-0.5304	0.2182
2	-1.3289	-0.1315	0.5263	0.1384	-0.5468	0.2839
3	-1.2411	-0.0755	0.625	0.1384	-0.4907	0.3397
4	-0.7766	-0.0212	0.5676	0.1279	-0.4048	0.3624
5	-0.8542	0.0438	0.513	0.1253	-0.332	0.4198
6	-0.9567	-0.0641	0.4918	0.1544	-0.5272	0.3989
7	-1.3463	-0.166	0.368	0.1723	-0.6829	0.3507
8	-0.7743	-0.0549	0.3551	0.0994	-0.353	0.2432
9	-0.7412	-0.043	0.4476	0.0984	-0.3382	0.2522
10	-0.6405	-0.0348	0.471	0.0975	-0.3272	0.2577
11	-0.6355	0.0009	0.384	0.0931	-0.2784	0.2801
12	-0.7305	-0.0071	0.4299	0.0962	-0.2958	0.2815
13	-0.6646	-0.0152	0.4253	0.0947	-0.2094	0.2689
14	-0.6327	-0.0176	0.3498	0.0938	-0.2999	0.2838
15	-0.5558	-0.0115	0.3896	0.0887	-0.2776	0.2546
16	-0.576	-0.0081	0.3723	0.0857	-0.2851	0.249
17	-0.5452	-0.0186	0.3609	0.0874	-0.2807	0.2435
18	-0.506	-0.0124	0.3139	0.0819	-0.2581	0.2333
19	-0.464	0.0058	0.3561	0.0785	-0.23	0.2417
20	-0.5924	-0.0064	0.3943	0.0894	-0.2746	0.2617
21	-0.5076	0.0092	0.3528	0.0825	-0.2383	0.2566
22	-0.3968	0.008	0.3292	0.0765	-0.2218	0.2376
23	-0.3908	0.0409	0.4355	0.0732	-0.1789	0.2604
24	-0.3704	-0.0051	0.3594	0.0724	-0.2222	0.2121
25	-0.423	-0.0108	0.3735	0.0805	-0.2523	0.2309
26	-0.7699	-0.0303	0.3546	0.084	-0.2824	0.2218
27	-0.8195	-0.0265	0.3429	0.076	-0.2605	0.2075
28	-0.3547	0.0116	0.3239	0.0717	-0.2034	0.2267
29	-0.2738	0.0309	0.3379	0.0684	-0.1743	0.236
30	-0.3151	0.0377	0.3745	0.0882	-0.1689	0.2424
31	-0.7899	-0.0303	0.3546	0.084	-0.2824	0.2218
32	-0.8137	-0.0403	0.3725	0.0819	-0.289	0.2054
33	-0.5888	0.0189	0.412	0.076	-0.2092	0.2469
34	-0.3678	0.0884	0.5794	0.0697	-0.1406	0.2773
35	-0.2777	0.0194	0.3221	0.0673	-0.1824	0.2211
36	-0.323	0.0086	0.3737	0.0689	-0.1921	0.2093
37	-0.574	0.0296	0.3532	0.0736	-0.1911	0.2504
38	-0.6127	0.0393	0.5604	0.0795	-0.1992	0.2778
39	-0.3926	0.027	0.4892	0.0734	-0.1931	0.2471
40	-0.3778	-0.0367	0.3528	0.0671	-0.2381	0.1648
41	-0.2543	0.0289	0.4104	0.0644	-0.1844	0.2222
42	-0.273	0.0515	0.3715	0.0649	-0.1428	0.2458
43	-0.8821	0.0166	0.3756	0.0735	-0.2039	0.237
44	-0.7182	-0.0517	0.4066	0.0842	-0.3044	0.201
45	-0.4285	-0.032	0.404	0.0836	-0.2827	0.2188
46	-0.3625	-0.0448	0.3186	0.076	-0.2729	0.1832
47	-0.2236	0.022	0.3574	0.065	-0.173	0.217
48	-0.2745	0.0425	0.3715	0.0689	-0.1643	0.2493
49	-0.506	0.0225	0.4488	0.0843	-0.2309	0.2755
50	-0.5656	0.185	1.8999	0.2153	-0.4609	0.8308
51	-0.6415	0.2211	1.6204	0.2388	-0.4948	0.937
52	-0.4672	0.2772	1.7889	0.2378	-0.4362	0.8905
53	-0.6287	0.3595	1.9489	0.3045	-0.5542	1.2731
54	-0.387	0.2888	1.8331	0.2738	-0.5326	1.1103
55	-0.7242	0.0328	1.9573	0.1718	-0.4827	0.5463
56	-0.7083	0.0167	0.7852	0.1361	-0.3915	0.4249
57	-0.6314	-0.025	0.6524	0.1181	-0.3794	0.3294
58	-0.4878	0.1755	1.0191	0.1832	-0.3141	0.6851
59	-0.4406	0.2805	1.6381	0.2207	-0.3815	0.9428
60	-0.6782	-0.0302	1.0229	0.1708	-0.5425	0.482
61	-0.5736	-0.0107	0.39	0.1125	-0.3482	0.3268
62	-0.8639	0.0212	0.3919	0.0973	-0.2708	0.3132
63	-0.5898	-0.0095	0.4739	0.1082	-0.3341	0.3151
64	-0.4956	0.2054	1.2532	0.2058	-0.4121	0.8228
65	-0.0603	-0.1461	0.3661	0.1282	-0.5307	0.2385
66	-0.5595	-0.066	0.2492	0.0934	-0.3463	0.2143
67	-0.3171	0.0059	0.3244	0.0717	-0.2094	0.221
68	-0.3918	0.0235	0.3597	0.0828	-0.225	0.272
69	-1.0869	-0.1829	0.2889	0.1399	-0.6025	0.2367
70	-0.8705	-0.1183	0.2753	0.1203	-0.4792	0.2428
71	-0.4982	0.0022	0.3044	0.0873	-0.2595	0.264
72	-0.4593	-0.0132	0.2852	0.0819	-0.2588	0.2324
73	-0.8442	-0.155	0.3588	0.1356	-0.5619	0.2519
74	-0.5327	-0.0616	0.3403	0.0876	-0.3249	0.2016
75	-0.3384	0.0238	0.3436	0.0741	-0.1986	0.2463
76	-0.466	0.0081	0.3221	0.089	-0.25	0.2662
77	-1.6287	-0.2074	0.3945	0.2033	-0.8174	0.4026
78	-1.6692	-0.0435	0.4304	0.1185	-0.399	0.3119
79	-1.0683	-0.0137	0.3976	0.0872	-0.2752	0.2479
80	-0.5223	0.0156	0.4587	0.0708	-0.2239	0.2551
81	-0.4871	0.028	0.5455	0.0793	-0.2119	0.264
82	-0.485	0.0775	0.4258	0.0815	-0.1671	0.3222
83	-1.6151	-0.1733	0.4131	0.2061	-0.7817	0.4452
84	-1.3286	-0.0262	0.4722	0.1093	-0.3542	0.3018
85	-0.8075	-0.0161	0.3558	0.0822	-0.2827	0.2305
86	-0.4878	0.0533	0.4248	0.0775	-0.1792	0.2859
87	-0.5462	0.0031	0.3895	0.0781	-0.2252	0.2314
88	-0.5073	0.0215	0.3799	0.0763	-0.2074	0.2504
89	-0.4125	0.0721	0.4188	0.0797	-0.1689	0.3111
90	-1.2763	-0.0456	0.5593	0.1649	-0.5482	0.4492
91	-0.6831	-0.001	0.5131	0.1038	-0.3119	0.31
92	-0.4177	-0.0416	0.3346	0.0821	-0.2879	0.2047
93	-0.4914	0.0659	0.3688	0.0744	-0.1573	0.2891
94	-0.309	0.0527	0.3701	0.073	-0.1663	0.2717
95	-0.208	0.135	0.5232	0.0845	-0.1184	0.3884

B/H=1 N=8 0 degree

# of lap	Min	Mean	max	STDEV	- peak	+ peak
1	0.5864	1.1778	1.941	0.2378	0.4043	1.8912
1	-1.1118	-0.035	0.3917	0.1069	-0.3556	0.2855
2	-1.5227	-0.0071	0.4753	0.1163	-0.3562	0.3419
3	-0.7997	0.0484	0.4488	0.1166	-0.2996	0.3964
4	-0.8546	0.065	0.5101	0.1074	-0.2272	0.4171
5	-0.6531	0.1836	0.5811	0.102	-0.1424	0.4898
6	-0.9195	0.0648	0.5267	0.132	-0.3412	0.4507
7	-1.0802	-0.0261	0.4378	0.1493	-0.4739	0.4216
8	-0.4895	0.0588	0.3986	0.0855	-0.1976	0.3152
9	-0.6297	0.058	0.4079	0.0835	-0.1826	0.3087
10	-0.5887	0.0654	0.4269	0.0819	-0.1802	0.3111
11	-0.5045	0.1157	0.4854	0.0762	-0.1131	0.3444
12	-0.467	0.1095	0.4266	0.0769	-0.1219	0.3403
13	-0.5023	0.0937	0.3791	0.075	-0.1313	0.3187
14	-0.5644	0.0846	0.3599	0.0794	-0.1534	0.3227
15	-0.5759	0.0993	0.409	0.0748	-0.125	0.3235
16	-0.4097	0.1034	0.4138	0.0712	-0.1102	0.3169
17	-0.7566	0.0901	0.3432	0.0737	-0.1309	0.3111
18	-0.485	0.0658	0.3582	0.0683	-0.109	0.3006
19	-0.3501	0.1123	0.3906	0.0649	-0.0823	0.3069
20	-0.547	0.1048	0.3785	0.0748	-0.1197	0.3289
21	-0.4674	0.1106	0.3718	0.0683	-0.0943	0.3159
22	-0.2828	0.1034	0.3522	0.0633	-0.0866	0.2934
23	-0.2163	0.1438	0.4055	0.0599	-0.0359	0.3235
24	-0.1869	0.1063	0.4145	0.0587	-0.0699	0.2825
25	-0.4708	0.0941	0.3711	0.065	-0.1008	0.289
26	-0.6984	0.0741	0.3466	0.0695	-0.1345	0.2828
27	-0.3907	0.0703	0.3451	0.0643	-0.1227	0.2632
28	-0.4238	0.112	0.3712	0.059	-0.0651	0.2892
29	-0.2414	0.1318	0.3663	0.0564	-0.0374	0.3009
30	-0.3128	0.1444	0.4082	0.0559	-0.0233	0.3121
31	-0.6894	0.0741	0.3468	0.0695	-0.1345	0.2829
32	-0.4844	0.0682	0.3615	0.0667	-0.1318	0.2682
33	-0.5459	0.127	0.4049	0.0621	-0.0594	0.3134
34	-0.4353	0.1735	0.4544	0.058	-0.0006	0.3477
35	-0.4808	0.1265	0.3913	0.0563	-0.0423	0.2953
36	-0.3688	0.1141	0.4008	0.0555	-0.0523	0.2805
37	-0.4419	0.1417	0.4559	0.0612	-0.0477	0.3252
38	-0.3983	0.1343	0.4761	0.0649	-0.0603	0.3289
39	-0.4522	0.1301	0.4521	0.0601	-0.0501	0.3103
40	-0.4843	0.0717	0.3911	0.0553	-0.0943	0.2377
41	-0.19	0.1322	0.4008	0.0533	-0.0276	0.2919
42	-0.4383	0.1513	0.4323	0.0542	-0.0114	0.314
43	-0.4258	0.1205	0.3805	0.0604	-0.0608	0.3016
44	-0.5378	0.0516	0.3454	0.0691	-0.1555	0.2588
45	-0.4936	0.0808	0.3524	0.0696	-0.1279	0.2895
46	-0.4457	0.06	0.335	0.0637	-0.1312	0.2513
47	-0.1077	0.1474	0.4042	0.0536	-0.0195	0.3022
48	-0.1764	0.0787	0.3723	0.0576	-0.094	0.2514
49	-0.4269	0.0568	0.4208	0.0721	-0.1595	0.2728
50	-0.4533	0.2012	1.7611	0.1958	-0.3862	0.7885
51	-0.487	0.2442	1.5312	0.2125	-0.3933	0.8818
52	-0.3439	0.2952	1.4299	0.1999	-0.3045	0.895
53	-0.3265	0.3571	1.7252	0.2484	-0.3881	1.1022
54	-0.226	0.2881	1.5673	0.2297	-0.4009	0.9771
55	-0.8441	0.0761	1.5175	0.16	-0.4037	0.556
56	-0.4946	0.0559	0.8025	0.1224	-0.3112	0.4231
57	-0.6888	-0.0024	0.4827	0.0971	-0.2938	0.289
58	-0.2958	0.1921	0.9655	0.1413	-0.2319	0.618
59	-0.3456	0.3095	1.4476	0.2017	-0.2957	0.9146
60	-0.5762	0.011	1.0244	0.1669	-0.4897	0.5118
61	-0.4					

B/H=2		N=1		0 degree			
# of lap	Min	Mean	max	STDV	- peak	+ peak	
1	-0.4236	1.3474	2.8119	0.4023	-0.1405	2.5543	
1	-1.8364	-0.2231	0.344	0.2169	-0.8739	0.4277	
2	-2.2405	-0.2084	0.3363	0.2204	-0.8696	0.4529	
3	-1.7865	-0.1936	0.3859	0.2145	-0.8371	0.4498	
4	-1.7011	-0.1659	0.4202	0.2234	-0.8362	0.5045	
5	-1.776	-0.1885	0.4874	0.2433	-0.9165	0.5435	
6	-1.7034	-0.2395	0.4968	0.2512	-0.9931	0.5142	
7	-1.7108	-0.2969	0.3175	0.2414	-1.0211	0.4273	
8	-0.9904	-0.0793	0.2895	0.1077	-0.4025	0.2439	
9	-0.947	-0.0738	0.3214	0.1168	-0.4302	0.2828	
10	-0.8481	-0.0396	0.3638	0.1241	-0.412	0.3329	
11	-1.132	-0.0394	0.3476	0.1309	-0.4322	0.3535	
12	-1.1934	-0.0741	0.43	0.1533	-0.5339	0.3858	
13	-1.1806	-0.0873	0.2797	0.1203	-0.4481	0.2735	
14	-1.0597	-0.0423	0.3323	0.0933	-0.3222	0.2376	
15	-0.7174	-0.03	0.3897	0.0901	-0.3002	0.2402	
16	-0.6396	-0.0158	0.3593	0.0919	-0.2913	0.2598	
17	-0.9465	-0.0213	0.2728	0.0856	-0.2782	0.2355	
18	-0.5175	-0.0048	0.2725	0.0742	-0.2275	0.218	
19	-0.4052	0.0057	0.3381	0.0742	-0.2169	0.2284	
20	-0.8472	-0.0269	0.2714	0.0925	-0.3084	0.2466	
21	-0.7975	-0.0078	0.3142	0.0758	-0.2353	0.2197	
22	-0.4215	0.0107	0.3286	0.0704	-0.2008	0.2222	
23	-0.6149	0.0145	0.2956	0.0689	-0.1922	0.2213	
24	-0.4095	0.0112	0.2956	0.0885	-0.1943	0.2168	
25	-1.0065	-0.0229	0.3243	0.0935	-0.3033	0.2576	
26	-0.7897	-0.005	0.3417	0.0781	-0.2392	0.2292	
27	-0.4938	0.0079	0.3154	0.07	-0.2021	0.2179	
28	-0.3725	0.0191	0.3325	0.081	-0.164	0.2022	
29	-0.2743	0.0197	0.3041	0.0587	-0.1565	0.166	
30	-0.3168	0.0196	0.314	0.059	-0.1574	0.1968	
31	-0.7897	-0.005	0.3417	0.0781	-0.2392	0.2292	
32	-0.6012	0.0092	0.337	0.0717	-0.2059	0.2242	
33	-0.4766	0.0138	0.3082	0.0682	-0.1851	0.2123	
34	-0.3785	0.0248	0.2781	0.0573	-0.1471	0.1967	
35	-0.2692	0.0273	0.2689	0.056	-0.1407	0.1954	
36	-0.2674	0.028	0.3021	0.0571	-0.1432	0.1893	
37	-0.8526	0.0102	0.3557	0.072	-0.2658	0.2262	
38	-0.5039	0.0124	0.3522	0.071	-0.2007	0.2255	
39	-0.4926	0.0164	0.3073	0.0658	-0.1609	0.2137	
40	-0.2564	0.0268	0.2979	0.0567	-0.1432	0.1968	
41	-0.2175	0.0286	0.3257	0.0544	-0.1348	0.1919	
42	-0.2194	0.0331	0.3193	0.057	-0.1379	0.2041	
43	-0.5805	0.0188	0.3549	0.0725	-0.1988	0.2363	
44	-0.5721	0.0077	0.3804	0.0978	-0.2858	0.3012	
45	-0.4879	-0.004	0.3811	0.1018	-0.3085	0.3015	
46	-0.4352	-0.0017	0.3154	0.0885	-0.2873	0.264	
47	-0.3185	0.0131	0.2772	0.0678	-0.1602	0.2165	
48	-0.3877	0.0632	0.4809	0.0975	-0.2293	0.3557	
49	-0.4835	0.0417	0.4346	0.1017	-0.2635	0.3469	
50	-0.687	0.226	1.5013	0.2541	-0.5363	0.9883	
51	-0.8154	0.2865	1.9881	0.2931	-0.5027	1.0758	
52	-0.533	0.3741	1.7619	0.2894	-0.4343	1.1824	
53	-0.4897	0.3802	2.071	0.2795	-0.4583	1.2187	
54	-0.8025	0.3442	1.948	0.2789	-0.4886	1.175	
55	-0.7338	0.1437	1.4534	0.2474	-0.5885	0.8859	
56	-0.7256	0.2093	1.6999	0.2115	-0.4253	0.8438	
57	-0.5004	0.2875	1.5464	0.2082	-0.3372	0.9122	
58	-0.459	0.3071	1.4922	0.2312	-0.3865	1.0007	
59	-0.6328	0.2814	1.9147	0.2603	-0.4994	1.0822	
60	-0.8168	0.0792	1.7249	0.235	-0.6257	0.7841	
61	-0.8419	0.1501	1.0882	0.1591	-0.3271	0.6272	
62	-0.3444	0.1999	1.0222	0.1448	-0.2344	0.6343	
63	-0.4695	0.2283	1.1353	0.1753	-0.2896	0.7521	
64	-0.8713	0.2077	1.876	0.2459	-0.5301	0.9455	
65	-0.8923	-0.0356	0.4243	0.1542	-0.4983	0.427	
66	-0.715	-0.0346	0.288	0.1107	-0.3968	0.2974	
67	-0.8388	-0.0031	0.3534	0.1091	-0.3303	0.3241	
68	-0.7924	0.0166	0.4263	0.1437	-0.4144	0.4475	
69	-0.9233	-0.0481	0.3025	0.1515	-0.5025	0.4063	
70	-0.9401	-0.0709	0.2504	0.133	-0.4699	0.3281	
71	-0.9557	-0.0433	0.2717	0.1291	-0.4308	0.3441	
72	-1.0829	-0.0125	0.31	0.1435	-0.443	0.418	
73	-0.9371	-0.0614	0.353	0.1593	-0.5393	0.4186	
74	-0.7797	-0.0504	0.3113	0.1114	-0.3845	0.2838	
75	-0.8162	-0.0252	0.3977	0.1103	-0.358	0.3055	
76	-0.9065	-0.0013	0.4984	0.1546	-0.4852	0.4629	
77	-2.0748	-0.2518	0.4011	0.2302	-0.9424	0.4388	
78	-1.352	-0.0907	0.3823	0.1601	-0.571	0.3895	
79	-0.7554	-0.0038	0.4247	0.0999	-0.3036	0.2961	
80	-0.8263	0.0173	0.4201	0.0761	-0.211	0.2457	
81	-0.5146	0.0416	0.4213	0.0727	-0.1784	0.2595	
82	-0.4751	0.0432	0.4375	0.0853	-0.2428	0.3289	
83	-1.8956	-0.2476	0.4723	0.2247	-0.9219	0.4268	
84	-1.3055	-0.1041	0.515	0.1703	-0.6149	0.4087	
85	-0.75	0.0143	0.4786	0.0866	-0.2545	0.2831	
86	-0.5881	0.0297	0.3819	0.0774	-0.2054	0.2588	
87	-0.4178	0.0371	0.3888	0.0718	-0.1783	0.2529	
88	-0.4698	0.0489	0.4191	0.0717	-0.1882	0.282	
89	-0.3725	0.0422	0.425	0.0978	-0.2511	0.3355	
90	-1.8084	-0.1948	0.8181	0.2298	-0.8839	0.4945	
91	-1.2012	-0.0745	0.521	0.1816	-0.5592	0.4103	
92	-0.5771	0.0177	0.4174	0.0827	-0.2304	0.2857	
93	-0.2897	0.0425	0.3757	0.0672	-0.1592	0.2442	
94	-0.2711	0.0589	0.4426	0.0878	-0.1445	0.2623	
95	-0.4951	0.061	0.8893	0.0988	-0.2385	0.3604	

B/H=2		N=1		10 degree			
# of lap	Min	Mean	max	STDV	- peak	+ peak	
1	0.4864	1.6881	2.6888	0.318	-0.7402	2.639	
1	-1.7378	-0.3765	0.2099	0.2522	-1.1332	0.3802	
2	-2.1089	-0.4018	0.1706	0.247	-1.1428	0.3392	
3	-1.8574	-0.3624	0.2638	0.2052	-0.9781	0.2533	
4	-1.4807	-0.3322	0.2667	0.2	-0.9321	0.2677	
5	-2.1397	-0.3143	0.3386	0.2297	-1.0034	0.3748	
6	-1.7595	-0.23	0.3142	0.2271	-0.9114	0.4514	
7	-0.9855	-0.1572	0.2721	0.1398	-0.5761	0.2616	
8	-1.1029	-0.1458	0.3411	0.1292	-0.5335	0.2419	
9	-1.2418	-0.1778	0.2311	0.1456	-0.8143	0.2591	
10	-1.2161	-0.1936	0.3083	0.1637	-0.6847	0.2975	
11	-1.2544	-0.139	0.3081	0.1574	-0.6112	0.3333	
12	-1.5755	-0.0751	0.3747	0.126	-0.453	0.3029	
13	-0.6817	-0.0853	0.2295	0.0829	-0.3338	0.1633	
14	-1.027	-0.0955	0.2029	0.1135	-0.4361	0.2451	
15	-1.0247	-0.0947	0.283	0.1037	-0.4058	0.2184	
16	-0.9497	-0.1084	0.3053	0.1178	-0.4618	0.2449	
17	-0.9285	-0.0719	0.2826	0.1039	-0.3837	0.2389	
18	-0.5032	-0.0352	0.269	0.0792	-0.2727	0.2024	
19	-0.478	-0.0329	0.2822	0.0764	-0.262	0.1963	
20	-0.7741	-0.0888	0.2472	0.1075	-0.4113	0.2337	
21	-0.6746	-0.0468	0.2635	0.0872	-0.3086	0.2147	
22	-0.4447	-0.0197	0.2559	0.0713	-0.2336	0.1942	
23	-0.4846	-0.0144	0.3014	0.0669	-0.2151	0.1884	
24	-0.3524	-0.0119	0.2615	0.081	-0.1849	0.1711	
25	-0.4672	-0.0468	0.2288	0.0826	-0.2345	0.1412	
26	-1.0761	-0.0538	0.3045	0.0872	-0.3156	0.2079	
27	-0.5823	-0.0349	0.2893	0.0811	-0.278	0.2083	
28	-0.4258	-0.0362	0.2287	0.0829	-0.195	0.1826	
29	-0.4221	-0.0014	0.3351	0.0548	-0.1659	0.163	
30	-0.2717	0.0016	0.2254	0.0513	-0.1522	0.1554	
31	-0.0791	0.0419	0.1665	0.0249	-0.0328	0.1166	
32	-1.0873	-0.0362	0.3935	0.0873	-0.289	0.2258	
33	-0.9957	-0.0253	0.3155	0.0792	-0.2827	0.2122	
34	-0.5319	0.0023	0.2351	0.0609	-0.1805	0.1851	
35	-0.3509	0.0095	0.2198	0.0524	-0.1475	0.1667	
36	-0.3095	0.0142	0.2219	0.0491	-0.133	0.1614	
37	-0.2989	0.007	0.2396	0.0524	-0.1502	0.1643	
38	-0.8203	-0.0341	0.3475	0.091	-0.3668	0.2388	
39	-0.9126	-0.0226	0.3274	0.0802	-0.2632	0.2179	
40	-0.8252	0.0026	0.2567	0.0599	-0.177	0.1822	
41	-0.3988	0.0143	0.272	0.0506	-0.1375	0.1661	
42	-0.2874	0.0254	0.2362	0.0478	-0.1181	0.169	
43	-0.8889	0.0255	0.3254	0.0535	-0.1349	0.1859	
44	-0.9299	-0.0526	0.2853	0.0825	-0.3002	0.195	
45	-0.6806	-0.0515	0.3106	0.0758	-0.2788	0.1758	
46	-0.4558	-0.0244	0.3155	0.0699	-0.234	0.1852	
47	-0.2804	0.0085	0.4812	0.0584	-0.1668	0.1839	
48	-0.2388	0.1054	0.3376	0.055	-0.0597	0.2705	
49	-0.581	0.0662	0.4813	0.0632	-0.1233	0.2557	
50	-0.9835	0.2729	1.439	0.2501	-0.4773	1.0231	
51	-0.4358	0.2812	1.4189	0.2185	-0.3743	0.9368	
52	-0.4597	0.349					

B/H=2		N=1 20 degree						
# of lap	Min	Mean	max	STDV	- peak	+ peak		
1	-3.0101	-0.405	0.424	0.3965	-1.4144	0.6044		
2	-3.006	-0.4804	0.3559	0.349	-1.5373	0.5564		
3	-2.4825	-0.4437	0.3512	0.2871	-1.3046	0.4175		
4	-2.0622	-0.4001	0.5839	0.2619	-1.1856	0.3855		
5	-2.3918	-0.4176	0.3773	0.2993	-1.3155	0.4802		
6	-2.8653	-0.4184	0.482	0.3261	-1.3989	0.58		
7	-1.9621	-0.291	0.4045	0.2966	-1.0007	0.4186		
8	-1.8482	-0.2421	0.3668	0.2225	-0.9096	0.4253		
9	-1.6575	-0.2273	0.401	0.2007	-0.8293	0.3747		
10	-1.7508	-0.2921	0.495	0.217	-0.9432	0.359		
11	-1.7453	-0.2554	0.3701	0.2237	-0.9264	0.4155		
12	-1.6302	-0.1775	0.4665	0.2073	-0.7994	0.4444		
13	-1.1259	-0.1454	0.4523	0.1361	-0.5546	0.2639		
14	-1.9558	-0.1656	0.4023	0.2	-0.7955	0.4043		
15	-1.1435	-0.1401	0.4252	0.151	-0.5931	0.3129		
16	-1.2567	-0.1801	0.4442	0.166	-0.6781	0.3179		
17	-1.7365	-0.1619	0.4153	0.1803	-0.7027	0.3789		
18	-0.9568	-0.0791	0.4574	0.1305	-0.4706	0.3123		
19	-1.0742	-0.0633	0.5144	0.1169	-0.4141	0.2875		
20	-1.8519	-0.1752	0.5293	0.1814	-0.7193	0.3689		
21	-1.4262	-0.1152	0.4808	0.157	-0.5862	0.3557		
22	-0.7276	-0.0433	0.5307	0.1113	-0.3772	0.2607		
23	-0.9002	-0.0347	0.4794	0.1057	-0.3518	0.2824		
24	-0.6328	-0.0208	0.3453	0.0976	-0.3137	0.2721		
25	-0.6457	-0.0605	0.3245	0.0915	-0.3351	0.2141		
26	-2.8622	-0.12	0.4762	0.1761	-0.8482	0.4083		
27	-1.7697	-0.088	0.4781	0.152	-0.5441	0.3881		
28	-0.6619	-0.0125	0.5115	0.1065	-0.3319	0.3069		
29	-0.6603	0.0057	0.4783	0.0895	-0.2628	0.2741		
30	-0.5294	0.0151	0.3808	0.0813	-0.2287	0.259		
31	-0.0891	0.0981	0.2551	0.0355	-0.0083	0.2045		
32	-3.0224	-0.0955	0.5808	0.1834	-0.8458	0.4548		
33	-2.9044	-0.0625	0.5411	0.1548	-0.527	0.4019		
34	-0.562	0.008	0.4672	0.1044	-0.3071	0.319		
35	-0.5217	0.0267	0.4562	0.0884	-0.2386	0.2821		
36	-0.4198	0.0366	0.4567	0.0788	-0.1978	0.275		
37	-0.5893	0.0403	0.398	0.0751	-0.1851	0.2658		
38	-1.9381	-0.0865	0.5879	0.1916	-0.8613	0.4884		
39	-1.4423	-0.0498	0.5212	0.1547	-0.5139	0.4142		
40	-0.568	0.0131	0.4506	0.1011	-0.2902	0.3163		
41	-0.501	0.0396	0.4161	0.0848	-0.2146	0.2939		
42	-0.4192	0.0582	0.4273	0.0765	-0.1712	0.2875		
43	-0.4879	0.0653	0.3955	0.0745	-0.1582	0.2889		
44	-1.7055	-0.0628	0.665	0.1532	-0.5224	0.3969		
45	-1.0975	-0.0393	0.5137	0.1214	-0.4037	0.325		
46	-0.7368	-0.0034	0.4375	0.0909	-0.276	0.2691		
47	-0.4782	0.0348	0.3895	0.079	-0.2021	0.2719		
48	-0.7395	0.0385	0.3997	0.0757	-0.1805	0.2694		
49	-0.4582	0.0973	0.5007	0.085	-0.1577	0.3522		
50	-1.5545	0.2016	1.8993	0.3193	-0.7564	1.1596		
51	-0.8242	0.2378	1.7755	0.2643	-0.555	1.0306		
52	-0.5848	0.3358	1.9035	0.2976	-0.5571	1.2284		
53	-0.8952	0.4533	2.1085	0.3344	-0.5499	1.4565		
54	-0.5422	0.3502	1.8647	0.2857	-0.507	1.2074		
55	-1.1458	0.2007	2.1672	0.307	-0.7203	1.1218		
56	-0.8565	0.2895	1.6664	0.2582	-0.4992	1.0382		
57	-0.6583	0.335	2.0505	0.2593	-0.443	1.113		
58	-0.3431	0.397	1.9489	0.2742	-0.4256	1.2196		
59	-0.6542	0.1775	1.4546	0.207	-0.4435	0.7984		
60	-1.8531	0.1739	1.6883	0.2878	-0.6897	1.0374		
61	-0.8242	0.2527	1.4596	0.2351	-0.4527	0.9582		
62	-0.6209	0.2839	1.3998	0.209	-0.3402	0.908		
63	-0.4988	0.2837	1.588	0.2	-0.3163	0.8837		
64	-0.6283	0.029	0.8616	0.1313	-0.365	0.423		
65	-0.7701	-0.0789	0.4113	0.1129	-0.4178	0.2598		
66	-0.8434	-0.059	0.3678	0.1059	-0.3765	0.2585		
67	-0.9639	0.0232	0.3943	0.0824	-0.2241	0.2705		
68	-0.7479	0.0822	0.4854	0.084	-0.1899	0.3341		
69	-0.6241	-0.0779	0.3424	0.1066	-0.3982	0.2425		
70	-0.6928	-0.0681	0.2737	0.1099	-0.3974	0.2813		
71	-0.6284	-0.0019	0.331	0.0887	-0.2678	0.2641		
72	-0.339	0.0537	0.4328	0.0827	-0.1944	0.3019		
73	-0.7591	-0.0805	0.3795	0.1091	-0.4049	0.244		
74	-0.6132	-0.0588	0.3551	0.0953	-0.3428	0.229		
75	-0.4227	0.0087	0.3374	0.0822	-0.238	0.2555		
76	-0.415	0.0785	0.473	0.0884	-0.1897	0.3437		
77	-1.4831	-0.3162	0.2805	0.1807	-0.8584	0.226		
78	-1.5698	-0.3061	0.242	0.1907	-0.8782	0.2661		
79	-1.536	-0.2147	0.3534	0.1739	-0.736	0.3067		
80	-0.7525	-0.0464	0.3557	0.0979	-0.3393	0.2465		
81	-0.6358	0.0257	0.3872	0.0815	-0.2189	0.2704		
82	-0.4817	0.085	0.4355	0.0815	-0.1595	0.3204		
83	-1.3736	-0.3142	0.2545	0.1744	-0.8373	0.2089		
84	-1.3123	-0.318	0.3114	0.1809	-0.8596	0.2289		
85	-1.55	-0.2348	0.2975	0.1906	-0.8068	0.337		
86	-1.0388	-0.1256	0.3032	0.1396	-0.5451	0.2935		
87	-0.7087	-0.0517	0.4538	0.1027	-0.3598	0.2563		
88	-0.4834	0.0014	0.3881	0.0841	-0.2508	0.2537		
89	-0.4898	0.0735	0.434	0.0759	-0.1539	0.3031		
90	-1.16	-0.2782	0.1886	0.1634	-0.7683	0.2118		
91	-1.286	-0.3089	0.2096	0.1817	-0.8542	0.2363		
92	-1.059	-0.1833	0.3809	0.1563	-0.8521	0.2855		
93	-0.7648	-0.0269	0.4882	0.1081	-0.3453	0.2915		
94	-0.5505	0.023	0.4188	0.086	-0.235	0.2808		
95	-0.3697	0.0893	0.4489	0.0792	-0.1483	0.3269		

B/H=2		N=1 30 degree						
# of lap	Min	Mean	max	STDV	- peak	+ peak		
1	-2.8205	-0.3641	0.6126	0.3243	-1.3371	0.6089		
2	-2.8223	-0.4928	0.4748	0.3368	-1.5033	0.5178		
3	-2.527	-0.4517	0.3956	0.2789	-1.2884	0.385		
4	-1.9572	-0.391	0.4067	0.2459	-1.1286	0.3467		
5	-2.7466	-0.3657	0.3857	0.2683	-1.1706	0.392		
6	-2.4874	-0.363	0.3904	0.2849	-1.2167	0.4091		
7	-1.9919	-0.2662	0.2908	0.2118	-0.9015	0.3691		
8	-2.2478	-0.2661	0.6229	0.2651	-1.0614	0.5293		
9	-1.5008	-0.1973	0.514	0.1969	-0.788	0.3934		
10	-1.3529	-0.2804	0.4312	0.2067	-0.8004	0.3395		
11	-1.6678	-0.2484	0.378	0.2034	-0.8585	0.3617		
12	-2.0911	-0.1887	0.4985	0.182	-0.7648	0.3874		
13	-1.2623	-0.1442	0.2356	0.1322	-0.5408	0.2523		
14	-1.9161	-0.2292	0.5732	0.2371	-0.9405	0.4862		
15	-1.0145	-0.1181	0.3813	0.1493	-0.5659	0.3297		
16	-1.0275	-0.1603	0.4551	0.1594	-0.6386	0.3181		
17	-1.5326	-0.2038	0.3697	0.2070	-0.8266	0.4191		
18	-1.1781	-0.0845	0.3995	0.1324	-0.4989	0.33		
19	-0.8783	-0.0502	0.3824	0.1125	-0.3876	0.2871		
20	-1.8659	-0.2222	0.4243	0.2083	-0.8501	0.4057		
21	-1.5589	-0.1474	0.3888	0.1779	-0.6811	0.3862		
22	-0.7182	-0.0351	0.3414	0.1076	-0.358	0.2878		
23	-0.7128	-0.026	0.3722	0.0969	-0.3257	0.2739		
24	-0.5902	-0.029	0.3812	0.091	-0.2961	0.25		
25	-0.814	-0.0589	0.3418	0.0977	-0.3221	0.2042		
26	-2.1345	-0.1746	0.5537	0.2097	-0.8037	0.4545		
27	-1.5154	-0.1288	0.4903	0.1721	-0.6431	0.3995		
28	-0.7651	-0.0107	0.4199	0.1066	-0.3355	0.304		
29	-0.4892	0.0144	0.37	0.0849	-0.2402	0.2691		
30	-0.4636	0.0235	0.3826	0.0765	-0.2058	0.2529		
31	-0.0604	0.1018	0.2488	0.0322	0.0053	0.1983		
32	-2.2037	-0.154	0.4879	0.2197	-0.813	0.505		
33	-1.8009	-0.0939	0.4745	0.1699	-0.6036	0.4157		
34	-0.585	0.0009	0.4188	0.1039	-0.3101	0.3118		
35	-0.585	0.032	0.3977	0.0949	-0.2224	0.2893		
36	-0.4813	0.0502	0.3734	0.0963	-0.1787	0.2792		
37	-0.6974	0.0623	0.4229	0.0798	-0.1584	0.2831		
38	-2.1271	-0.1459	0.4632	0.2241	-0.8181	0.5263		
39	-1.7872	-0.0777	0.455	0.1635	-0.5883	0.4129		
40	-0.5983	0.0014	0.4483	0.1006	-0.3009	0.3037		
41	-0.4042	0.0416	0.4395	0.0821	-0.2046	0.2877		
42	-0.4088	0.0704	0.4515	0.0758	-0.1569	0.2977		
43	-0.4673	0.0955	0.4235	0.0758	-0.1312	0.3118		
44	-1.5776	-0.1284	0.3834	0.1636	-0.6191	0.3823		
45	-2.2489	-0.0918	0.3691	0.1248	-0.4655	0.2923		
46	-0.638	-0.0492	0.3102	0.0942	-0.3318	0.2335		
47	-0.4842	0.0195	0.382	0.0795	-0.2189	0.258		
48	-0.2889	0.0805	0.4723	0.0779	-0.1533	0.3143		
49	-0.5977	0.1387	0.5829	0.0887	-0.1213	0.3897		
50	-1.0974	0.212	1.7551	0.2834	-0.6882	1.0623		
51	-1.0855	0.2246	1.448	0.2245	-0.4489	0.9892		
52	-0.618	0.2652	1.8272	0.2319	-0.4306	0.961		
53	-0.4188	0.3346	2.0564	0.2758	-0.4923	1.1815		
54	-0.7673	0.289	1.5013	0.2607	-0.4929	1.071		

B/H=2		N=1 45 degree						
# of lap	Min	Mean	max	STDV	- peak	+ peak		
1	0.5503	-1.2375	2.0351	0.2535	0.477	1.9981		
1	-2.5976	-0.1801	0.502	0.3009	-1.0829	0.7225		
2	-3.0111	-0.4268	0.4646	0.4502	-1.7774	0.9239		
3	-3.1802	-0.5048	0.4563	0.4142	-1.7475	0.7379		
4	-2.3644	-0.4588	0.4334	0.3144	-1.4019	0.8483		
5	-2.1014	-0.3887	0.3887	0.2586	-1.1824	0.389		
6	-2.1634	-0.3876	0.3733	0.2458	-1.1052	0.3699		
7	-1.8044	-0.3464	0.225	0.199	-0.9433	0.2505		
8	-2.0318	-0.134	0.4603	0.2538	-0.8955	0.6275		
9	-1.887	-0.0854	0.3483	0.1797	-0.8245	0.4536		
10	-1.6624	-0.1857	0.4387	0.2505	-0.9371	0.5657		
11	-1.5593	-0.2465	0.3782	0.2324	-0.9437	0.4507		
12	-1.6932	-0.2122	0.3501	0.2042	-0.8249	0.4005		
13	-1.4469	-0.2488	0.2976	0.161	-0.7319	0.2343		
14	-2.0291	-0.1268	0.4261	0.2244	-0.7099	0.5467		
15	-1.0685	-0.0472	0.3978	0.1988	-0.4685	0.372		
16	-1.3849	-0.0453	0.3889	0.1511	-0.4886	0.4081		
17	-1.3859	-0.1303	0.3876	0.1857	-0.7174	0.4567		
18	-1.2669	-0.0583	0.3669	0.145	-0.4933	0.3766		
19	-0.7813	-0.0059	0.3742	0.107	-0.331	0.3111		
20	-1.4665	-0.1548	0.4553	0.1897	-0.751	0.4413		
21	-1.1536	-0.102	0.3814	0.1735	-0.8225	0.4184		
22	-0.7897	-0.0109	0.3944	0.1062	-0.3265	0.3078		
23	-0.672	0.023	0.3557	0.0925	-0.2544	0.3004		
24	-0.8289	0.0102	0.3382	0.0871	-0.2512	0.2715		
25	-0.9195	-0.118	0.236	0.0824	-0.3853	0.1593		
26	-1.8801	-0.1498	0.4894	0.1823	-0.7266	0.427		
27	-1.4485	-0.1049	0.3944	0.1605	-0.5864	0.3767		
28	-0.7654	-0.0102	0.4266	0.105	-0.3252	0.3047		
29	-0.5208	0.0252	0.4041	0.0845	-0.2284	0.2788		
30	-0.3504	0.0367	0.3462	0.0744	-0.1866	0.2601		
31	-0.0245	0.1055	0.3128	0.0314	0.0113	0.1996		
32	-1.8311	-0.1477	0.4774	0.2063	-0.7666	0.4712		
33	-1.556	-0.0842	0.4643	0.1542	-0.5407	0.3784		
34	-0.7705	0.0041	0.4189	0.0991	-0.2933	0.3018		
35	-0.5631	0.0356	0.4541	0.0836	-0.2151	0.2863		
36	-0.3566	0.0564	0.4447	0.0782	-0.1723	0.2852		
37	-0.2911	0.0776	0.6228	0.0758	-0.1499	0.305		
38	-2.1889	-0.1477	0.4201	0.2282	-0.8323	0.5369		
39	-1.7921	-0.0683	0.4828	0.1527	-0.5244	0.3918		
40	-0.8109	0.0069	0.3868	0.0931	-0.2724	0.2891		
41	-0.4039	0.0481	0.4218	0.0806	-0.1938	0.29		
42	-0.8384	0.0783	0.5777	0.0756	-0.1488	0.3052		
43	-0.258	0.1164	0.5308	0.0766	-0.1134	0.3462		
44	-1.2334	-0.0782	0.3919	0.1571	-0.5496	0.3933		
45	-0.6892	-0.0256	0.3941	0.1072	-0.3472	0.2959		
46	-0.6593	0.0073	0.4087	0.0832	-0.2423	0.2599		
47	-0.3954	0.0565	0.5287	0.0782	-0.178	0.291		
48	-0.3711	0.1038	0.4621	0.0789	-0.1329	0.3406		
49	-0.511	0.154	0.5797	0.0847	-0.1	0.408		
50	-1.2187	0.4098	2.0885	0.3933	-0.7704	1.5895		
51	-0.575	0.3887	1.5186	0.2707	-0.4253	1.1987		
52	-1.1671	0.3855	1.3978	0.2212	-0.2882	1.0291		
53	-0.9454	0.34	1.3893	0.1894	-0.2553	0.9353		
54	-0.5548	0.1583	1.2153	0.1813	-0.3856	0.7023		
55	-1.586	0.4104	1.9946	0.3571	-0.8609	1.4816		
56	-0.4786	0.4423	1.5349	0.2564	-0.3269	1.2116		
57	-0.3755	0.3963	1.53	0.2035	-0.2152	1.0059		
58	-0.3836	0.3575	1.1736	0.1708	-0.1542	0.8692		
59	-0.7694	0.0685	0.8484	0.139	-0.3474	0.4865		
60	-1.1718	0.4147	1.8871	0.2915	-0.4589	1.2882		
61	-0.5034	0.4762	1.5815	0.224	-0.1959	1.1483		
62	-0.199	0.4063	1.267	0.1704	-0.1049	0.9176		
63	-0.2632	0.3235	1.0736	0.1406	-0.0983	0.7454		
64	-0.4469	0.0005	0.6085	0.099	-0.2066	0.2976		
65	-0.7173	-0.0589	0.3134	0.0967	-0.3489	0.231		
66	-1.0261	-0.0433	0.3245	0.1057	-0.3805	0.2739		
67	-0.9031	0.0506	0.4179	0.0946	-0.2331	0.3343		
68	-1.3528	0.1242	0.5273	0.0927	-0.1539	0.4023		
69	-0.7788	-0.0915	0.3087	0.0927	-0.3395	0.2165		
70	-0.8192	-0.057	0.2193	0.0944	-0.34	0.2261		
71	-0.4824	0.0252	0.4188	0.0834	-0.2252	0.2755		
72	-0.4418	0.0887	0.4676	0.0848	-0.1858	0.3432		
73	-0.8348	-0.0599	0.2331	0.0945	-0.3435	0.2237		
74	-0.5762	-0.0413	0.3299	0.0897	-0.3104	0.2278		
75	-0.3785	0.0418	0.3937	0.0829	-0.2081	0.2896		
76	-0.4053	0.1201	0.5728	0.0858	-0.1688	0.4069		
77	-1.3044	-0.3805	0.2029	0.1778	-0.8134	0.1523		
78	-1.4	-0.4023	0.1886	0.1809	-0.8752	0.1705		
79	-1.2816	-0.3409	0.2349	0.1674	-0.8432	0.1615		
80	-0.5175	-0.0214	0.3577	0.0876	-0.2842	0.2414		
81	-0.2811	0.0848	0.4902	0.0839	-0.1671	0.3362		
82	-0.202	0.1486	0.5541	0.0839	-0.1032	0.4004		
83	-1.4095	-0.3978	0.162	0.1853	-0.8537	0.1581		
84	-1.4508	-0.4224	0.144	0.1851	-1.0078	0.183		
85	-1.7039	-0.4687	0.1759	0.2269	-1.1473	0.2138		
86	-0.9088	-0.2679	0.1858	0.1511	-0.7211	0.1853		
87	-0.8209	-0.113	0.2295	0.1084	-0.4382	0.2121		
88	-0.444	-0.0606	0.3358	0.0918	-0.285	0.2658		
89	-0.1941	0.1054	0.4505	0.0803	-0.1356	0.3484		
90	-1.107	-0.3705	0.1435	0.1631	-0.8597	0.1188		
91	-1.3469	-0.4501	0.1171	0.2002	-1.0507	0.1505		
92	-1.573	-0.4003	0.1765	0.1865	-0.9899	0.1893		
93	-0.7478	-0.1172	0.3218	0.1156	-0.4839	0.2294		
94	-0.3674	0.0069	0.3885	0.0899	-0.2831	0.2762		
95	-0.1831	0.1319	0.5133	0.0828	-0.118	0.3797		

B/H=2		N=1 60 degree						
# of lap	Min	Mean	max	STDV	- peak	+ peak		
1	0.4457	1.1564	2.2757	0.276	0.3284	1.9844		
1	-2.7441	-0.324	0.5751	0.2887	-1.1902	0.5422		
2	-2.8904	-0.3648	0.5067	0.3048	-1.2786	0.5489		
3	-2.757	-0.3534	0.516	0.2832	-1.2031	0.4962		
4	-1.874	-0.3048	0.5111	0.248	-1.0426	0.4331		
5	-2.4057	-0.2514	0.5983	0.236	-0.9584	0.4565		
6	-2.5097	-0.2475	0.5479	0.2448	-0.9812	0.4862		
7	-1.6307	-0.2172	0.4222	0.2036	-0.8281	0.3936		
8	-2.4346	-0.3224	0.5104	0.3042	-1.2351	0.5902		
9	-1.6807	-0.2166	0.4923	0.199	-0.8137	0.3805		
10	-1.8512	-0.2153	0.5235	0.1958	-0.8111	0.3905		
11	-1.7285	-0.1968	0.6101	0.1991	-0.7909	0.3974		
12	-1.7016	-0.1805	0.5311	0.1866	-0.7209	0.4		
13	-1.1138	-0.1455	0.4251	0.1513	-0.5993	0.3083		
14	-1.7086	-0.2881	0.6452	0.2584	-1.0631	0.487		
15	-1.414	-0.1585	0.4255	0.1814	-0.6428	0.3256		
16	-0.8958	-0.1291	0.4945	0.1468	-0.5696	0.3114		
17	-1.8966	-0.2692	0.4148	0.2205	-0.9306	0.3922		
18	-1.3182	-0.1868	0.4113	0.1738	-0.7081	0.3345		
19	-0.7372	-0.0982	0.3647	0.1244	-0.4694	0.277		
20	-1.8629	-0.2803	0.4252	0.2255	-0.9568	0.3962		
21	-2.0771	-0.2384	0.3805	0.203	-0.8475	0.3706		
22	-0.9193	-0.1002	0.4128	0.1255	-0.4767	0.2783		
23	-0.7191	-0.042	0.4533	0.1105	-0.3734	0.2884		
24	-0.6461	-0.0322	0.5111	0.1086	-0.3519	0.2879		
25	-0.563	-0.0591	0.4018	0.1059	-0.3887	0.2705		
26	-2.5973	-0.3174	0.4584	0.2816	-1.162	0.5273		
27	-1.8441	-0.2401	0.4862	0.2209	-0.9029	0.4228		
28	-0.9979	-0.0979	0.4866	0.1316	-0.4927	0.2968		
29	-0.6743	-0.0368	0.4954	0.1048	-0.3511	0.2778		
30	-0.596	-0.0048	0.5177	0.0959	-0.2922	0.2825		
31	-0.0633	0.1171	0.316	0.0451	-0.0183	0.2525		
32	-0.5925	-0.3473	0.5017	0.3447	-1.4084	0.6599		
33	-1.8244	-0.2076	0.4969	0.2348	-0.9119	0.4967		
34	-1.0751	-0.0543	0.4985	0.1313	-0.4482	0.3396		
35	-0.882	-0.0221	0.428	0.1078	-0.3455	0.3013		
36	-0.6922	0.0075	0.457	0.0961	-0.2809	0.2959		
37	-0.3767	0.0399	0.4521	0.0935	-0.2107	0.2906		
38	-2.5109	-0.3687	0.4851	0.3444	-1.4019	0.6645		
39	-1.7233	-0.1505	0.5137	0.2179	-0.8041	0.503		
40	-1.879	-0.0388	0.4416	0.1199	-0.3965	0.3228		
41	-0.853	0.0086	0.4514	0.101	-0.2985	0.3097		
42	-0.8473	0.0356	0.4384	0.0936	-0.2451	0.3162		
43	-0.4183	0.068	0.4702	0.0828	-0.1824	0.3143		
44	-1.6789	-0.2216	0.4704	0.2153	-0.8674	0.4242		
45	-1.0928	-0.1216	0.3468	0.1406	-0.5442	0.301		
46	-0.7242	-0.0781	0.3623	0.1046	-0.3918	0.2587		
47	-0.4977	-0.0116	0.5005	0.093	-0.2906	0.2674		
48	-1.3927	0.0405	0.5043	0.0947	-0.2435	0.3245		
49	-0.5588	0.0928	0.5113	0.0919	-0.2001	0.3857		
50	-1.8289	0.0497	1.6435	0.2976	-0.828	0.9255		
51	-1.6154	0.1488	1.4965	0.2336	-0.5511	0.8507		
52	-0.6863	0.1916	1.6994	0.2125	-0.4458</			

B/H=2		N=1 70 degree					
# of lap	Min	Mean	max	STDV	- peak	+ peak	
1	0.3293	1.1029	1.9487	0.25	0.3529	1.8528	
1	-2.9218	-0.3568	0.5943	0.3332	-1.3563	0.6428	
2	-2.3774	-0.2378	0.5677	0.232	-0.9339	0.4583	
3	-1.9134	-0.2146	0.4671	0.2248	-0.8699	0.4599	
4	-1.5708	-0.1755	0.505	0.1985	-0.7649	0.4139	
5	-1.5129	-0.1335	0.5263	0.1927	-0.7114	0.4445	
6	-1.862	-0.1183	0.5255	0.1917	-0.6933	0.4567	
7	-1.4769	-0.1014	0.5031	0.1732	-0.6221	0.4182	
8	-2.9626	-0.4715	0.4743	0.3593	-1.5793	0.6363	
9	-1.9236	-0.2361	0.4675	0.2301	-0.9264	0.4542	
10	-1.2953	-0.1026	0.6265	0.1683	-0.6075	0.4024	
11	-1.2867	-0.0963	0.587	0.17	-0.6081	0.4136	
12	-1.2153	-0.0791	0.5344	0.1613	-0.569	0.4048	
13	-1.2734	-0.063	0.5384	0.1439	-0.4948	0.3689	
14	-2.0985	-0.404	0.6229	0.3045	-1.3176	0.5096	
15	-1.8275	-0.1529	0.4751	0.1793	-0.6908	0.3849	
16	-0.8647	-0.0536	0.487	0.1459	-0.5014	0.3742	
17	-2.5964	-0.3535	0.4304	0.2674	-1.1558	0.4487	
18	-1.4004	-0.1919	0.4578	0.1932	-0.7777	0.3818	
19	-0.9436	-0.0543	0.5093	0.1365	-0.4637	0.3551	
20	-3.0743	-0.3821	0.4163	0.29	-1.2523	0.488	
21	-2.4235	-0.2876	0.3959	0.2423	-1.0144	0.4391	
22	-0.8841	-0.0573	0.4378	0.1389	-0.468	0.3534	
23	-0.7352	0.0032	0.4581	0.1245	-0.3704	0.3767	
24	-0.8239	0.0134	0.4618	0.1185	-0.3422	0.389	
25	-0.911	0.0232	0.5564	0.1139	-0.3184	0.3647	
26	-3.4729	-0.4272	0.5813	0.3561	-1.4953	0.641	
27	-2.0458	-0.2292	0.5288	0.2587	-1.0051	0.5468	
28	-1.2616	-0.0266	0.5358	0.1233	-0.4556	0.3994	
29	-1.0146	0.0185	0.4528	0.1137	-0.3228	0.3597	
30	-0.5971	0.042	0.4426	0.1024	-0.2652	0.3492	
31	-0.0064	0.1647	0.3884	0.0433	0.0348	0.2945	
32	-2.3901	-0.3743	0.6921	0.3722	-1.4717	0.7422	
33	-2.1582	-0.1154	0.6291	0.2449	-0.6501	0.6192	
34	-0.7587	0.0343	0.5585	0.1291	-0.3531	0.4218	
35	-0.5364	0.0478	0.557	0.1073	-0.274	0.3695	
36	-0.5236	0.0607	0.4771	0.0959	-0.227	0.3484	
37	-0.4889	0.0754	0.4536	0.0828	-0.1729	0.3239	
38	-2.4669	-0.2384	0.6779	0.3478	-1.2618	0.805	
39	-1.3945	-0.0242	0.6623	0.1953	-0.6102	0.5617	
40	-0.7078	0.0357	0.4651	0.1042	-0.2768	0.3483	
41	-0.6678	0.064	0.5338	0.0935	-0.2165	0.3445	
42	-0.667	0.0809	0.5365	0.0878	-0.1826	0.3444	
43	-0.3899	0.0832	0.4581	0.0782	-0.1513	0.3177	
44	-1.4557	-0.1285	0.4793	0.1983	-0.7153	0.4623	
45	-0.8506	-0.0705	0.5285	0.1307	-0.4827	0.3217	
46	-0.6569	-0.0427	0.3195	0.1046	-0.3563	0.271	
47	-0.6923	0.0121	0.3998	0.0932	-0.2676	0.2918	
48	-1.0088	0.0383	0.509	0.092	-0.2397	0.3124	
49	-0.469	0.0739	0.5528	0.0925	-0.2041	0.3512	
50	-2.0399	-0.0906	1.3698	0.2853	-0.9466	0.7653	
51	-0.7972	0.0372	1.234	0.1579	-0.4364	0.5108	
52	-0.6434	0.0654	1.1169	0.1556	-0.4134	0.5443	
53	-0.5488	0.0817	1.1285	0.1525	-0.4057	0.5691	
54	-0.8181	0.0888	1.1658	0.1739	-0.4327	0.6104	
55	-2.1938	-0.0602	1.2193	0.2844	-0.9133	0.7929	
56	-0.7567	0.0744	1.2248	0.157	-0.3965	0.5453	
57	-0.5054	0.0856	1.1268	0.1551	-0.3797	0.551	
58	-0.7432	0.1205	1.1572	0.1538	-0.341	0.582	
59	-0.7096	0.1382	1.2299	0.197	-0.455	0.7273	
60	-1.9596	0.0195	1.5988	0.2826	-0.8283	0.6673	
61	-0.7281	0.0994	1.1466	0.1541	-0.3593	0.5718	
62	-0.4045	0.1204	0.9314	0.1417	-0.3046	0.5453	
63	-0.6726	0.1439	1.158	0.1376	-0.289	0.5598	
64	-1.0249	0.1937	1.8476	0.2302	-0.497	0.8844	
65	-1.3859	-0.2886	0.3158	0.1939	-0.8504	0.3131	
66	-1.4396	-0.2015	0.3708	0.1743	-0.7243	0.3213	
67	-1.1124	-0.0691	0.5013	0.1359	-0.477	0.3387	
68	-1.5705	0.0243	0.572	0.1302	-0.3684	0.415	
69	-1.2788	-0.2887	0.2479	0.1839	-0.818	0.2846	
70	-1.168	-0.2415	0.3767	0.1994	-0.8396	0.3567	
71	-0.8052	-0.1155	0.3745	0.1441	-0.5479	0.3189	
72	-1.0479	-0.0146	0.4974	0.1048	-0.3289	0.2997	
73	-1.2219	-0.2767	0.3228	0.1698	-0.646	0.2926	
74	-1.0115	-0.2032	0.3491	0.159	-0.6801	0.2738	
75	-0.7271	-0.0848	0.5188	0.1189	-0.4214	0.2919	
76	-0.8122	0.0157	0.4157	0.0992	-0.2818	0.3132	
77	-1.5408	-0.1814	0.8991	0.188	-0.7395	0.3767	
78	-1.8213	-0.1247	0.573	0.1749	-0.6493	0.3999	
79	-1.1915	-0.0196	0.4654	0.1333	-0.4196	0.3803	
80	-0.4478	0.0334	0.5112	0.088	-0.2306	0.2973	
81	-0.2871	0.0533	0.4088	0.0789	-0.1774	0.2841	
82	-0.3932	0.0611	0.521	0.0871	-0.2001	0.3224	
83	-1.7973	-0.2214	0.5504	0.2104	-0.8526	0.4098	
84	-1.523	-0.1388	0.4816	0.1709	-0.6494	0.3757	
85	-0.9686	-0.031	0.4356	0.1295	-0.4198	0.3576	
86	-0.6649	0.0194	0.4286	0.0984	-0.2768	0.3137	
87	-0.5332	0.0349	0.4739	0.0822	-0.2116	0.2814	
88	-0.3219	0.0482	0.3876	0.0761	-0.1821	0.2746	
89	-0.3919	0.0543	0.4632	0.0837	-0.1968	0.3054	
90	-2.0686	-0.2181	0.448	0.2372	-0.8276	0.4954	
91	-1.9325	-0.1312	0.4134	0.1834	-0.6813	0.4189	
92	-0.7957	-0.0267	0.4931	0.1193	-0.3946	0.3313	
93	-0.4334	0.0325	0.5023	0.0871	-0.2289	0.2939	
94	-0.3327	0.0522	0.4088	0.0761	-0.1762	0.2805	
95	-0.4697	0.0733	0.5557	0.0842	-0.1795	0.326	

B/H=2		N=1 80 degree					
# of lap	Min	Mean	max	STDV	- peak	+ peak	
1	0.4129	1.1219	2.3875	0.2547	0.3579	1.8859	
1	-2.6967	-0.5201	0.3875	0.3713	-1.6342	0.5939	
2	-1.4812	-0.2159	0.47	0.1907	-0.7881	0.3563	
3	-2.2715	-0.1533	0.6637	0.1902	-0.724	0.4173	
4	-1.6704	-0.1291	0.5354	0.1821	-0.6754	0.4172	
5	-2.3141	-0.0992	0.6409	0.1596	-0.578	0.3796	
6	-1.7447	-0.1009	0.5282	0.1474	-0.5431	0.3413	
7	-1.0305	-0.1326	0.5227	0.142	-0.5586	0.3634	
8	-3.0043	-0.5905	0.3833	0.3579	-1.6643	0.4833	
9	-1.6676	-0.3055	0.4212	0.2491	-1.0526	0.4418	
10	-1.1801	-0.0595	0.4604	0.1308	-0.4518	0.3328	
11	-1.4962	-0.0626	0.4665	0.1358	-0.47	0.3447	
12	-1.3745	-0.0675	1.0066	0.1308	-0.46	0.325	
13	-0.8227	-0.1126	0.436	0.136	-0.5205	0.2952	
14	-2.2896	-0.4989	0.3667	0.3104	-1.4281	0.4342	
15	-1.2978	-0.1649	0.5665	0.1801	-0.7051	0.3754	
16	-0.8035	-0.0418	0.5722	0.1179	-0.3955	0.312	
17	-2.1182	-0.4042	0.4135	0.2922	-1.2807	0.4722	
18	-1.3186	-0.1745	0.3922	0.1977	-0.7677	0.4186	
19	-0.779	-0.0383	0.4266	0.1189	-0.3951	0.3184	
20	-2.4691	-0.4693	0.3633	0.3228	-1.4378	0.4992	
21	-1.9912	-0.2692	0.4747	0.2554	-1.0355	0.497	
22	-0.8787	-0.0367	0.4685	0.1209	-0.3991	0.3257	
23	-0.6477	0.0007	0.4297	0.0997	-0.2905	0.2916	
24	-0.9115	-0.0132	0.4251	0.0911	-0.2864	0.26	
25	-0.706	-0.0607	0.4479	0.1165	-0.4101	0.2887	
26	-2.8568	-0.3483	0.5905	0.3572	-1.42	0.7233	
27	-1.6896	-0.1245	0.5104	0.2319	-0.8202	0.5712	
28	-0.7338	-0.0056	0.4808	0.1101	-0.3558	0.3245	
29	-0.5531	0.0077	0.3528	0.0875	-0.2549	0.2703	
30	-0.6154	0.0096	0.3594	0.0801	-0.2307	0.2498	
31	-0.0442	0.0968	0.3534	0.0394	-0.0215	0.2148	
32	-2.01	-0.1842	0.8117	0.3037	-1.0952	0.7288	
33	-1.5102	-0.031	0.5707	0.1678	-0.5344	0.4724	
34	-0.6379	0.0225	0.3908	0.0952	-0.2631	0.3081	
35	-0.5375	0.0182	0.4148	0.083	-0.2328	0.2653	
36	-0.679	0.0184	0.4112	0.0789	-0.2182	0.255	
37	-0.4132	0.025	0.3887	0.0819	-0.2206	0.2706	
38	-1.9494	-0.1072	0.63	0.2397	-0.8262	0.6118	
39	-1.1512	-0.0252	0.4797	0.138	-0.4391	0.3897	
40	-0.753	-0.0179	0.343	0.0933	-0.2978	0.262	
41	-0.6657	0.0124	0.3613	0.0843	-0.2405	0.2653	
42	-0.6181	0.0286	0.4149	0.0814	-0.2177	0.2708	
43	-0.4459	0.031	0.4301	0.084	-0.2211	0.2813	
44	-1.7272	-0.1428	0.4896	0.1614	-0.8271	0.3415	
45	-0.8249	-0.1025	0.4137	0.1274	-0.4847	0.2787	
46	-0.6533	-0.0743	0.4196	0.1146	-0.4181	0.2696	
47	-0.7954	-0.0366	0.4809	0.1085	-0.3622	0.289	
48	-0.723	-0.0249	0.5075	0.1082	-0.3494	0.2996	
49	-0.6425	0.0112	0.5434	0.1071	-0.3101	0.3325	
50	-2.3089	-0.2847	0.9	0.3538	-1.3461	0.7767	
51	-0.856	0	0.8578	0.1208	-0.3625	0.3624	
52	-0.9011	0.0117	0.7241	0.1185	-0.3439	0.367	

B/H=2		N=1			90 degree		
# of lap	Min	Mean	max	STDV	- peak	+ peak	
1	0.5487	1.222	2.3143	0.2589	0.4423	2.0018	
2	-2.2253	-0.2394	0.3684	0.2583	-1.0142	0.5355	
3	-1.2606	-0.068	0.4136	0.1325	-0.4654	0.3295	
4	-1.1848	-0.0202	0.4652	0.1289	-0.407	0.3656	
5	-0.9449	0.0066	0.3666	0.1204	-0.3546	0.3678	
4	-1.3217	0.0381	0.4488	0.1004	-0.2831	0.3393	
6	-0.8563	0.0376	0.4655	0.0945	-0.2459	0.3212	
7	-0.8086	0.0404	0.8172	0.1302	-0.3503	0.4311	
8	-1.9219	-0.234	0.5042	0.2652	-1.0266	0.5617	
9	-1.426	-0.081	0.4131	0.1604	-0.5621	0.4001	
10	-0.6297	0.0219	0.4142	0.0948	-0.2625	0.3063	
11	-0.7619	0.039	0.4027	0.0878	-0.2244	0.3024	
12	-0.6108	0.0482	0.5083	0.0871	-0.2132	0.3097	
13	-0.507	0.0411	0.5459	0.1333	-0.3589	0.4412	
14	-1.5918	-0.159	0.6224	0.2319	-0.8546	0.5366	
15	-0.7007	-0.0054	0.4769	0.1158	-0.3527	0.3419	
15	-0.4886	0.0326	0.3889	0.0891	-0.2348	0.2998	
17	-1.5108	-0.0785	0.5825	0.1655	-0.6651	0.508	
18	-0.784	0.0063	0.4575	0.116	-0.3476	0.3603	
19	-0.434	0.0403	0.4681	0.0888	-0.2262	0.3069	
20	-1.9793	-0.1164	0.5695	0.2422	-0.8431	0.6104	
21	-1.1542	-0.0149	0.5144	0.1464	-0.4541	0.4243	
22	-0.438	0.0438	0.4739	0.0891	-0.2238	0.3112	
23	-0.3623	0.068	0.4116	0.0774	-0.1843	0.3003	
24	-0.51	0.0612	0.4079	0.0758	-0.1563	0.2885	
25	-0.5405	0.0469	0.5435	0.1108	-0.2854	0.3791	
26	-1.4425	-0.0501	0.6561	0.2088	-0.6796	0.5793	
27	-0.9785	0.026	0.5378	0.1316	-0.3688	0.4208	
28	-0.53	0.0547	0.5089	0.0897	-0.2125	0.3219	
29	-0.3974	0.0662	0.5019	0.0757	-0.1609	0.2933	
30	-0.3128	0.0747	0.3734	0.0712	-0.1388	0.2881	
31	-0.0145	0.1279	0.2984	0.0362	0.0193	0.2366	
32	-1.5251	-0.0697	0.7452	0.2234	-0.7398	0.6003	
33	-0.9393	0.0266	0.6466	0.1322	-0.3699	0.4231	
34	-0.3857	0.068	0.4859	0.0895	-0.2026	0.3346	
35	-0.4841	0.0534	0.3806	0.0775	-0.1891	0.2958	
36	-0.2954	0.0697	0.404	0.074	-0.1524	0.2916	
37	-0.2829	0.0878	0.5757	0.0842	-0.1648	0.3404	
38	-2.0835	-0.1493	0.7369	0.2676	-0.9521	0.6534	
39	-1.2497	-0.0205	0.554	0.1551	-0.4858	0.4447	
40	-0.5512	0.0215	0.4372	0.0899	-0.2482	0.2913	
41	-0.419	0.0611	0.4817	0.0813	-0.1828	0.305	
42	-0.389	0.0742	0.5273	0.0817	-0.1709	0.3193	
43	-0.5519	0.0536	0.5538	0.118	-0.3005	0.4077	
44	-2.0959	-0.2484	0.5172	0.273	-1.0875	0.5707	
45	-1.2651	-0.0784	0.4505	0.1463	-0.5153	0.3628	
46	-0.8029	-0.0871	0.5172	0.122	-0.3728	0.3594	
47	-0.8358	0.0282	0.5542	0.1048	-0.2863	0.3426	
48	-0.9196	0.0299	0.4885	0.1015	-0.2744	0.3343	
49	-0.5433	0.0228	0.6385	0.1435	-0.4076	0.4532	
50	-2.1632	-0.2037	0.5122	0.2815	-0.8882	0.5809	
51	-1.0913	0.013	0.4895	0.1163	-0.3359	0.3618	
52	-0.685	0.0412	0.5123	0.1018	-0.2841	0.3466	
53	-0.8259	0.04	0.5522	0.1003	-0.2809	0.3409	
54	-1.1511	0.0311	0.663	0.1313	-0.3827	0.4249	
55	-1.7585	-0.1817	0.6394	0.2587	-0.8618	0.5784	
56	-0.7577	0.0287	0.562	0.1084	-0.2864	0.3537	
57	-0.7678	0.028	0.5482	0.0986	-0.2877	0.3238	
58	-0.4428	0.0589	0.5189	0.0966	-0.2308	0.3486	
59	-1.0087	0.0389	0.6491	0.1416	-0.3859	0.4637	
60	-1.8703	-0.1355	0.7559	0.2373	-0.8474	0.5764	
61	-0.5133	0.0391	0.5722	0.1031	-0.2702	0.3485	
62	-0.3584	0.0575	0.5517	0.0913	-0.2185	0.3315	
63	-0.3913	0.0467	0.4722	0.0905	-0.2249	0.3183	
64	-0.6323	0.0372	0.7044	0.1399	-0.3824	0.4588	
65	-1.4203	-0.0875	0.5708	0.1747	-0.6217	0.4287	
66	-0.6796	0.0088	0.6576	0.1216	-0.3581	0.3736	
67	-0.6036	0.0374	0.5801	0.1088	-0.2891	0.3639	
68	-1.0403	0.0435	0.5911	0.1265	-0.3359	0.4229	
69	-1.1833	-0.0586	0.6001	0.1836	-0.6474	0.4542	
70	-0.6461	0.0288	0.5685	0.1138	-0.3127	0.3703	
71	-0.4303	0.0607	0.5508	0.1053	-0.2551	0.3765	
72	-0.4565	0.0421	0.643	0.1287	-0.338	0.4223	
73	-1.2141	-0.061	0.7286	0.1717	-0.5761	0.4541	
74	-0.4672	0.0247	0.4697	0.108	-0.2882	0.3486	
75	-0.4671	0.059	0.585	0.0981	-0.2352	0.3532	
76	-0.4588	0.0582	0.6377	0.1207	-0.304	0.4205	
77	-1.4186	-0.0199	0.6889	0.2055	-0.6383	0.5964	
78	-1.4906	-0.0255	0.6522	0.2171	-0.6788	0.6257	
79	-1.066	-0.0029	0.5412	0.164	-0.4846	0.4895	
80	-0.5513	0.0604	0.5073	0.0861	-0.1879	0.3188	
81	-1.022	0	0.5936	0.1608	-0.4817	0.4817	
82	-1.089	-0.0019	0.5629	0.2032	-0.6115	0.6077	
83	-1.395	-0.0324	0.623	0.2119	-0.6682	0.6033	
84	-1.6753	-0.043	0.618	0.2182	-0.6074	0.6115	
85	-1.5833	-0.0481	0.4711	0.1884	-0.6134	0.5171	
86	-0.6094	0.0204	0.3586	0.1038	-0.2909	0.3317	
87	-0.8021	0.0106	0.3258	0.1033	-0.2993	0.3205	
88	-1.1345	-0.0418	0.4193	0.1846	-0.5857	0.5121	
89	-1.0153	-0.0151	0.5558	0.2097	-0.6443	0.614	
90	-1.0208	-0.0223	0.6444	0.2073	-0.6443	0.5997	
91	-1.4384	-0.0512	0.5597	0.2309	-0.744	0.6416	
92	-0.9457	-0.0333	0.3884	0.18	-0.5132	0.4468	
93	-0.5273	0.0222	0.4351	0.1041	-0.2898	0.3344	
94	-1.2204	-0.0143	0.4233	0.1589	-0.4936	0.465	
95	-0.8679	0.0067	0.6525	0.2061	-0.6117	0.6251	

B/H=2		N=2			0 degree		
# of lap	Min	Mean	max	STDV	- peak	+ peak	
1	0.2533	1.0627	2.0166	0.2586	0.287	1.8385	
1	-2.0125	-0.2499	0.4092	0.2807	-1.092	0.5923	
2	-2.9782	-0.2451	0.4884	0.2824	-1.1224	0.6321	
3	-2.4154	-0.2216	0.528	0.2874	-1.0838	0.6406	
4	-2.4308	-0.1928	0.594	0.29	-1.0627	0.677	
5	-2.46	-0.1781	0.6684	0.2962	-1.0597	0.7104	
6	-2.2846	-0.2294	0.5566	0.3096	-1.1583	0.6995	
7	-2.0569	-0.2703	0.4555	0.2857	-1.1574	0.6188	
8	-1.3299	-0.0528	0.5321	0.1375	-0.4653	0.3597	
9	-1.0938	-0.0626	0.441	0.1511	-0.5159	0.3908	
10	-1.2595	-0.0326	0.5409	0.1629	-0.5213	0.4561	
11	-1.2336	-0.011	0.5233	0.1601	-0.4914	0.4693	
12	-1.4559	-0.0488	0.4691	0.1885	-0.6144	0.5188	
13	-1.5429	-0.063	0.4703	0.1464	-0.5021	0.3761	
14	-1.0691	-0.0077	0.4052	0.1166	-0.3575	0.3422	
15	-0.9129	0.0086	0.5767	0.1139	-0.333	0.3502	
16	-1.0699	0.0179	0.4069	0.1145	-0.3285	0.3622	
17	-0.8081	0.0171	0.4689	0.1089	-0.3087	0.3443	
18	-0.6209	0.0328	0.4811	0.0958	-0.2546	0.3203	
19	-0.4887	0.0433	0.4507	0.0931	-0.236	0.3227	
20	-1.3058	0.0121	0.3874	0.1144	-0.331	0.3551	
21	-0.7061	0.0335	0.4674	0.0973	-0.2585	0.3255	
22	-0.4979	0.0438	0.4695	0.0889	-0.2231	0.3106	
23	-0.4869	0.0553	0.4237	0.0871	-0.2061	0.3168	
24	-0.5842	0.0419	0.3876	0.0853	-0.2141	0.2979	
25	-1.5287	0.0054	0.4305	0.1115	-0.328	0.3408	
26	-0.8219	0.0221	0.5529	0.1004	-0.2782	0.3234	
27	-0.7548	0.0327	0.5622	0.0918	-0.2427	0.3081	
28	-0.507	0.0534	0.4563	0.08	-0.1867	0.2935	
29	-0.4428	0.0555	0.36	0.0771	-0.1759	0.2889	
30	-0.4784	0.058	0.3749	0.0772	-0.1736	0.2896	
31	-0.8219	0.0221	0.5529	0.1004	-0.2792	0.3234	
32	-0.7673	0.0269	0.4695	0.0946	-0.2569	0.3107	
33	-0.7178	0.05	0.4929	0.0872	-0.2115	0.3116	
34	-0.349	0.0688	0.416	0.0788	-0.1615	0.2991	
35	-0.4357	0.059	0.3864	0.0738	-0.1623	0.2803	
36	-0.5776	0.0593	0.3844	0.0747	-0.1648	0.2834	
37	-0.9574	0.0488	0.58	0.0931	-0.328	0.3281	
38	-0.8969	0.0471	0.5079	0.0949	-0.2428	0.3263	
39	-0.5488	0.0471	0.4684	0.0884	-0.212	0.3062	
40	-0.4079	0.0484	0.3459	0.0745	-0.177	0.2699	
41	-0.3324	0.063	0.3769	0.071	-0.1499	0.2759	
42	-0.4041	0.0705	0.378	0.0729	-0.1481	0.2892	
43	-0.5633	0.0491	0.5817	0.0929	-0.2297	0.3279	
44	-0.7648	0.0129	0.618	0.1281	-0.3654	0.3913	
45	-0.8483	0.0119	0.583	0.132	-0.384	0.4079	
46	-0.5564	0.0697	0.4441	0.116	-0.3382	0.3575	
47	-0.3318	0.0409	0.3934	0.0862	-0.2177	0.2985	
48	-0.4633	0.0418	0.4056	0.1036	-0.269	0.3527	
49	-0.8216	0.0422	0.5776	0.12	-0.3179	0.4023	
50	-0.771	0.0322	2.1124	0.3427	-0.7059	1.35	
51	-0.991	0.0473	2.4549	0.3882	-0.6873	1.522	
52	-0.805	0.4732	2.2051	0.361	-0.6099	1.5563	
53	-0.8042	0.4391	2.5154	0.3662	-0.6594	1.5376	
54	-0.7558	0.3625	2.0944	0.3437	-0.6686	1.3936	
55	-0.8281	0.2288	1.9488	0.3282	-0.7517	1.2054	
56	-0.7127	0.3125	1.8031	0.2966	-0.5774	1.2024	
57	-0.6773	0.3345	1.8728	0.2793	-0.5032	1.1723	
58	-0.9527	0.3487	2.0897	0.3036	-0.6442	1.2575	
59	-0.7992	0.2804	1.8496	0.3173	-0.6615	1.2422	
60	-0.0819	0.1533	1.8718	0			

B/H=2 N=3 0 degree							
# of tap	Min	Mean	max	STDV	- peak	+ peak	
1	-0.2128	1.0129	1.7671	0.2492	0.2653	1.7605	
2	-2.1936	-0.2161	0.6333	0.2839	-1.0677	0.6355	
3	-2.5769	-0.2128	0.6692	0.2984	-1.1081	0.6825	
4	-1.9123	-0.1977	0.928	0.2891	-1.065	0.6896	
5	-2.3292	-0.1816	0.8337	0.2896	-1.0503	0.6871	
6	-1.956	-0.1892	0.5883	0.3011	-1.1025	0.7041	
7	-1.7574	-0.2477	0.6696	0.307	-1.1696	0.6732	
8	-2.4643	-0.2842	0.522	0.3055	-1.2007	0.6322	
9	-1.2131	-0.05	0.4697	0.1409	-0.4726	0.3726	
10	-1.8355	-0.0474	0.5273	0.1592	-0.5251	0.4303	
11	-1.44	-0.0273	0.5731	0.1733	-0.5473	0.4926	
12	-1.3039	-0.024	0.4955	0.1763	-0.5529	0.505	
13	-1.7233	-0.0639	0.5345	0.199	-0.6547	0.5274	
14	-1.0736	-0.062	0.4822	0.1483	-0.5068	0.3827	
15	-1.0848	-0.005	0.5208	0.1216	-0.3699	0.36	
16	-0.7984	0.0089	0.5449	0.1209	-0.3539	0.3715	
17	-0.8037	0.0137	0.512	0.1252	-0.3617	0.3932	
18	-1.0875	0.0184	0.4846	0.1143	-0.3246	0.3613	
19	-0.6084	0.0367	0.5118	0.102	-0.2693	0.3427	
20	-0.6979	0.0436	0.4834	0.1003	-0.2573	0.3446	
21	-1.1021	0.0149	0.4638	0.1178	-0.3385	0.3883	
22	-0.8186	0.0349	0.4375	0.1032	-0.2748	0.3447	
23	-0.5365	0.0476	0.4567	0.0957	-0.2394	0.3346	
24	-0.4864	0.0514	0.5302	0.0942	-0.2312	0.3341	
25	-0.5349	0.0456	0.5093	0.0931	-0.2337	0.325	
26	-0.6797	0.0084	0.4024	0.1153	-0.3366	0.3555	
27	-1.1041	0.0305	0.5031	0.1046	-0.2833	0.3442	
28	-0.9947	0.0427	0.5073	0.0963	-0.2463	0.3318	
29	-0.4769	0.0583	0.4371	0.0845	-0.1971	0.3098	
30	-0.5071	0.0533	0.4112	0.0826	-0.1946	0.3011	
31	-0.455	0.0531	0.435	0.0827	-0.1949	0.3011	
32	-1.1041	0.0305	0.5031	0.1046	-0.2833	0.3442	
33	-1.1913	0.0392	0.4817	0.0997	-0.283	0.3394	
34	-0.936	0.0504	0.4654	0.0911	-0.2229	0.3238	
35	-0.3486	0.062	0.4406	0.081	-0.1811	0.3051	
36	-0.3629	0.0597	0.4546	0.0792	-0.178	0.2974	
37	-0.3659	0.0581	0.404	0.0794	-0.1799	0.2962	
38	-0.9152	0.0388	0.4822	0.097	-0.2523	0.3298	
39	-0.9038	0.0404	0.4494	0.0996	-0.2585	0.3394	
40	-0.8413	0.0466	0.4299	0.0916	-0.228	0.3213	
41	-0.3228	0.0541	0.4174	0.0799	-0.1856	0.2939	
42	-0.3079	0.0586	0.4304	0.0765	-0.1709	0.2892	
43	-0.3221	0.0504	0.4093	0.0783	-0.1746	0.2953	
44	-0.8001	0.04	0.4599	0.0978	-0.2533	0.3333	
45	-0.8134	0.0271	0.5781	0.1294	-0.3612	0.4153	
46	-0.6329	0.0197	0.6094	0.135	-0.3655	0.4248	
47	-0.8128	0.0166	0.4644	0.1202	-0.3441	0.3772	
48	-0.4028	0.0321	0.3827	0.0931	-0.2473	0.3175	
49	-0.5319	0.0331	0.4473	0.1144	-0.3102	0.3764	
50	-0.7132	0.037	0.5771	0.1275	-0.3455	0.4195	
51	-0.9076	0.2994	2.4524	0.3388	-0.7164	1.3152	
52	-0.8339	0.4012	2.9915	0.3606	-0.6805	1.4828	
53	-0.7285	0.4524	2.2114	0.3585	-0.6254	1.5313	
54	-0.7351	0.4482	2.2256	0.3635	-0.6418	1.54	
55	-0.8457	0.3879	2.1082	0.3546	-0.6759	1.4517	
56	-0.8208	0.2022	2.139	0.3206	-0.7596	1.164	
57	-0.6084	0.2988	2.3634	0.2921	-0.5796	1.1732	
58	-1.0302	0.3431	1.9647	0.2833	-0.5089	1.193	
59	-0.6377	0.3805	1.917	0.3096	-0.5684	1.2894	
60	-0.8282	0.3149	2.028	0.334	-0.6871	1.317	
61	-0.9236	0.1436	2.313	0.3004	-0.7575	1.0447	
62	-0.504	0.2188	1.7127	0.2234	-0.4503	0.8889	
63	-0.3972	0.2575	1.4391	0.2033	-0.3523	0.8973	
64	-0.9578	0.266	1.5418	0.2435	-0.4644	0.9965	
65	-0.9900	0.2349	1.7497	0.3094	-0.6934	1.1633	
66	-1.1142	-0.0533	0.5076	0.2044	-0.6686	0.56	
67	-1.2792	-0.0473	0.4088	0.1539	-0.509	0.4144	
68	-1.0716	-0.0138	0.4712	0.1415	-0.4383	0.4108	
69	-1.487	0.0075	0.4771	0.1817	-0.5374	0.5525	
70	-1.435	-0.0714	0.4285	0.2007	-0.6734	0.5307	
71	-1.4422	-0.092	0.3439	0.1853	-0.6481	0.464	
72	-1.1988	-0.0502	0.3448	0.167	-0.5613	0.4409	
73	-1.3939	-0.0287	0.442	0.1775	-0.5592	0.5058	
74	-1.2866	-0.0766	0.6696	0.2123	-0.7136	0.5604	
75	-0.9432	-0.0884	0.4744	0.1527	-0.5264	0.3897	
76	-1.0935	-0.0423	0.4692	0.1476	-0.485	0.4004	
77	-1.2122	-0.0119	0.5771	0.1935	-0.5925	0.5686	
78	-2.4636	-0.2518	0.9082	0.2879	-1.1145	0.8111	
79	-1.5443	-0.082	0.8579	0.2027	-0.6902	0.5262	
80	-1.1222	0.0159	0.8558	0.1288	-0.3735	0.4053	
81	-1.2483	0.0333	0.7189	0.1042	-0.2782	0.3459	
82	-0.8035	0.047	0.6775	0.1011	-0.2583	0.3504	
83	-0.8696	0.0452	0.5392	0.1242	-0.3275	0.4179	
84	-1.6336	-0.2443	0.902	0.2758	-1.0717	0.5832	
85	-1.3135	-0.0982	0.8372	0.2118	-0.7335	0.537	
86	-0.8729	0.0346	0.6352	0.1186	-0.3214	0.3905	
87	-0.6502	0.0488	0.613	0.1047	-0.2672	0.3808	
88	-0.4935	0.0549	0.6484	0.0996	-0.2438	0.3537	
89	-0.5083	0.0535	0.6347	0.0992	-0.2441	0.351	
90	-0.8399	0.0466	0.5566	0.1273	-0.3354	0.4287	
91	-2.1357	-0.1982	0.8789	0.2738	-1.0377	0.6553	
92	-1.441	-0.0645	0.7838	0.109	-0.6617	0.5326	
93	-0.7553	0.0386	0.6428	0.1089	-0.288	0.3852	
94	-0.8356	0.0608	0.6898	0.0928	-0.2175	0.3391	
95	-0.4576	0.0725	0.6255	0.0942	-0.2101	0.3551	
96	-0.5939	0.072	1.1528	0.1299	-0.3178	0.4618	

B/H=2 N=8 0 degree							
# of tap	Min	Mean	max	STDV	- peak	+ peak	
1	0.2199	0.9829	1.7622	0.2488	0.2364	1.7294	
2	-2.6345	-0.2101	0.2769	0.2617	-1.0407	0.6206	
3	-2.0321	-0.2039	0.6648	0.2892	-1.0714	0.6635	
4	-2.1337	-0.1897	0.6363	0.2867	-1.0499	0.6705	
5	-3.7337	-0.1692	0.7003	0.2925	-1.0466	0.7082	
6	-2.0078	-0.2019	0.7865	0.3157	-1.1489	0.7451	
7	-2.4923	-0.2551	0.9001	0.3264	-1.2343	0.7241	
8	-2.2452	-0.2958	0.6595	0.3256	-1.2720	0.6809	
9	-1.4416	-0.0427	0.6585	0.1396	-0.4615	0.3762	
10	-1.4622	-0.0425	0.5448	0.1549	-0.5072	0.4222	
11	-1.2082	-0.0127	0.598	0.1699	-0.5224	0.4971	
12	-1.5594	-0.0153	0.6255	0.1828	-0.5636	0.5331	
13	-1.4967	-0.0597	0.6945	0.2158	-0.7072	0.5877	
14	-1.4842	-0.0604	0.5594	0.1595	-0.539	0.4181	
15	-1.1102	0.0012	0.5258	0.1215	-0.3633	0.3658	
16	-0.6849	0.0169	0.5042	0.119	-0.3401	0.374	
17	-0.6971	0.0251	0.5608	0.1238	-0.3464	0.3966	
18	-0.7019	0.0229	0.5294	0.1121	-0.3133	0.3592	
19	-0.801	0.0415	0.4768	0.1016	-0.2634	0.3464	
20	-0.6513	0.0499	0.462	0.1002	-0.2508	0.3506	
21	-1.0852	0.017	0.5617	0.1168	-0.3334	0.3674	
22	-0.8822	0.0363	0.4482	0.102	-0.2898	0.3424	
23	-0.699	0.0523	0.4587	0.0957	-0.2347	0.3393	
24	-0.3949	0.0579	0.4601	0.0938	-0.2235	0.3394	
25	-0.5116	0.055	0.4881	0.0925	-0.2215	0.3335	
26	-0.8291	0.0182	0.5173	0.1149	-0.3255	0.364	
27	-0.8054	0.0337	0.4702	0.1031	-0.2755	0.3429	
28	-0.8533	0.0458	0.4495	0.0952	-0.2398	0.3313	
29	-0.4104	0.0605	0.4914	0.0854	-0.1957	0.3166	
30	-0.4342	0.0588	0.421	0.0831	-0.1904	0.308	
31	-0.4026	0.0611	0.4945	0.0823	-0.188	0.308	
32	-0.8054	0.0337	0.4702	0.1031	-0.2755	0.3429	
33	-0.7947	0.0438	0.5234	0.0987	-0.2523	0.3399	
34	-0.8995	0.0524	0.5708	0.0903	-0.2186	0.3233	
35	-0.3521	0.0618	0.416	0.0812	-0.1819	0.3054	
36	-0.4534	0.0684	0.4789	0.0791	-0.1709	0.3036	
37	-0.3773	0.0677	0.4594	0.0794	-0.1704	0.3058	
38	-1.5991	0.0482	0.5062	0.0971	-0.243	0.3394	
39	-0.8428	0.0391	0.486	0.0969	-0.2517	0.3298	
40	-0.5687	0.0453	0.475	0.0891	-0.2219	0.3124	
41	-0.4274	0.0588	0.4207	0.0789	-0.1779	0.2852	
42	-0.5568	0.0621	0.5202	0.0767	-0.168	0.2921	
43	-0.4469	0.0675	0.3994	0.0781	-0.1688	0.3018	
44	-0.8684	0.0496	0.5054	0.0962	-0.2389	0.3381	
45	-0.7691	0.0177	0.584	0.1277	-0.3653	0.4089	
46	-0.5594	0.0662	0.5258	0.1326	-0.3917	0.404	
47	-0.4822	0.0687	0.4372	0.1164	-0.3405	0.3579	
48	-0.6029	0.0369	0.4236	0.0902	-0.2336	0.3074	
49	-0.4546	0.0458	0.5403	0.1111	-0.2875	0.3791	
50	-0.7673	0.0582	0.5918	0.1273	-0.3238	0.4402	
51	-0.914	0.3008	2.2787	0.3401	-0.7194	1.3211	
52	-0.6944	0.4075	2.4443	0.3588	-0.6689	1.4838	
53	-0.482	0.4781	2.1069	0.382	-0.6078	1.584	

B/H=4 N=1 0 degree							
# of lap	Min	Mean	max	STDEV	- peak	+ peak	
1	0.4802	1.1235	1.9781	0.2383	0.4147	1.8324	
2	-3.3727	-0.753	0.237	0.3981	-1.9472	0.4411	
3	-3.8054	-0.7267	0.2905	0.3882	-1.8913	0.438	
4	-2.7474	-0.6918	0.3215	0.3532	-1.7515	0.3879	
5	-3.8117	-0.6756	0.335	0.3522	-1.7321	0.3808	
6	-3.0507	-0.6807	0.2885	0.3569	-1.7515	0.3901	
8	-2.8338	-0.6754	0.3653	0.3479	-1.7191	0.3894	
7	-3.0558	-0.672	0.253	0.3401	-1.6922	0.3492	
8	-1.7781	-0.3758	0.2986	0.2211	-1.0388	0.2878	
9	-1.8881	-0.4586	0.3246	0.2781	-1.297	0.3777	
10	-2.2597	-0.47	0.5067	0.292	-1.3461	0.406	
11	-2.1706	-0.4586	0.3602	0.2892	-1.3271	0.408	
12	-3.0613	-0.4484	0.3851	0.2828	-1.2967	0.4	
13	-1.542	-0.3488	0.2642	0.2047	-0.9627	0.2655	
14	-1.693	-0.223	0.3244	0.1815	-0.7075	0.2816	
15	-2.1035	-0.27	0.3995	0.203	-0.879	0.3389	
16	-1.8295	-0.2644	0.4129	0.2291	-0.9726	0.3837	
17	-1.8449	-0.1228	0.3801	0.1291	-0.5101	0.2648	
18	-0.8518	-0.1125	0.4893	0.1158	-0.36	0.235	
19	-0.9976	-0.1239	0.4812	0.1311	-0.5172	0.2685	
20	-1.5668	-0.1259	0.3235	0.1527	-0.5841	0.3323	
21	-1.3824	-0.0671	0.4127	0.1044	-0.4004	0.2282	
22	-0.7614	-0.0925	0.5037	0.1139	-0.4331	0.2482	
23	-1.31	-0.0593	0.475	0.1153	-0.4388	0.2528	
24	-1.2031	-0.0988	0.3974	0.1082	-0.4235	0.2259	
25	-1.3278	-0.1417	0.3479	0.1488	-0.5819	0.2986	
26	-1.2008	-0.072	0.4483	0.1166	-0.4271	0.2727	
27	-1.358	-0.0551	0.4878	0.1038	-0.3659	0.2557	
28	-0.625	-0.0342	0.3534	0.0808	-0.2706	0.2082	
29	-0.5642	-0.0362	0.3839	0.0807	-0.2784	0.206	
30	-0.4307	-0.0358	0.3582	0.0791	-0.273	0.2013	
31	-1.2008	-0.072	0.4483	0.1166	-0.4271	0.2727	
32	-0.8854	-0.0492	0.2744	0.0949	-0.3339	0.2356	
33	-0.9295	-0.0278	0.2971	0.0934	-0.308	0.2524	
34	-0.3774	-0.0028	0.2897	0.0712	-0.2164	0.2107	
35	-0.4767	-0.016	0.2752	0.0714	-0.2303	0.1982	
36	-0.4178	-0.0185	0.3393	0.07	-0.2286	0.1917	
37	-0.8589	-0.0442	0.3101	0.0914	-0.3183	0.2289	
38	-0.9917	-0.023	0.2885	0.0835	-0.2736	0.2276	
39	-0.8208	-0.022	0.2701	0.083	-0.2711	0.2271	
40	-0.5512	-0.016	0.2926	0.066	-0.2141	0.182	
41	-0.4116	-0.0061	0.3003	0.0651	-0.2074	0.1893	
42	-0.4622	-0.0036	0.3189	0.0651	-0.2019	0.1947	
43	-0.8862	-0.0353	0.3588	0.0808	-0.2778	0.2071	
44	-0.4795	-0.0159	0.2618	0.0682	-0.2144	0.1827	
45	-0.5285	-0.0191	0.2639	0.0642	-0.2117	0.1734	
46	-0.4011	-0.0218	0.218	0.0508	-0.2043	0.1607	
47	-0.3018	-0.0171	0.2539	0.0574	-0.1893	0.155	
48	-0.3924	-0.0164	0.2455	0.0632	-0.2061	0.1732	
49	-0.74	-0.0208	0.2431	0.0889	-0.2276	0.186	
50	-0.6369	0.4114	2.1387	0.3434	-0.6188	1.4415	
51	-0.5435	0.4091	2.1372	0.3045	-0.5045	1.3226	
52	-0.4833	0.4109	2.1671	0.311	-0.5221	1.344	
53	-0.5227	0.3922	2.0209	0.3024	-0.5148	1.2993	
54	-1.0014	0.3633	2.0427	0.3271	-0.618	1.3446	
55	-0.7806	0.3723	2.0185	0.3254	-0.5039	1.3488	
56	-0.3043	0.4452	2.1318	0.2617	-0.34	1.2303	
57	-0.2562	0.4304	1.8929	0.2591	-0.3468	1.2076	
58	-0.2762	0.4291	1.9285	0.258	-0.344	1.2039	
59	-0.7191	0.3309	2.0583	0.3084	-0.5883	1.2502	
60	-0.5585	0.2685	1.9147	0.2871	-0.5927	1.1297	
61	-0.1941	0.3841	1.6094	0.2059	-0.2457	1.0139	
62	-0.2789	0.3814	1.7019	0.1963	-0.2074	0.9702	
63	-0.3063	0.3443	1.5012	0.2037	-0.2689	0.9554	
64	-0.7309	0.2682	1.7222	0.2718	-0.5088	1.021	
65	-0.4477	-0.0352	0.1881	0.0649	-0.2289	0.1594	
66	-0.3429	-0.0375	0.1891	0.0642	-0.2302	0.1592	
67	-0.5725	-0.0432	0.3002	0.068	-0.2413	0.1549	
68	-0.3671	-0.0396	0.2182	0.0682	-0.2304	0.1589	
69	-0.4263	-0.0404	0.1979	0.065	-0.2355	0.1547	
70	-0.3922	-0.0433	0.24	0.064	-0.2352	0.1487	
71	-0.3829	-0.043	0.2362	0.0682	-0.2418	0.1555	
72	-0.4113	-0.0508	0.1837	0.0683	-0.2497	0.1481	
73	-0.4558	-0.047	0.1978	0.0878	-0.2505	0.1565	
74	-0.3749	-0.0508	0.2214	0.0683	-0.2557	0.1539	
75	-0.3586	-0.0445	0.2845	0.0888	-0.254	0.165	
76	-0.4419	-0.0478	0.2065	0.0711	-0.291	0.1655	
77	-2.6709	-0.5881	0.5028	0.303	-1.4971	0.321	
78	-1.8948	-0.3808	0.4244	0.2707	-1.1929	0.4313	
79	-2.0948	-0.1559	0.3189	0.2026	-0.7638	0.4518	
80	-1.1504	-0.0568	0.3185	0.1121	-0.3931	0.2795	
81	-0.6719	-0.0248	0.3682	0.0828	-0.2725	0.2228	
82	-0.4748	-0.0085	0.2889	0.087	-0.2084	0.1923	
83	-2.3185	-0.5565	0.8188	0.2801	-1.4287	0.3137	
84	-1.9882	-0.4085	0.5243	0.2789	-1.2382	0.4222	
85	-1.6441	-0.1334	0.4381	0.1891	-0.7006	0.4337	
86	-1.1059	-0.056	0.3709	0.1373	-0.4678	0.3558	
87	-0.7759	-0.0372	0.3495	0.1046	-0.3511	0.2786	
88	-0.5494	-0.0247	0.3831	0.085	-0.2798	0.2304	
89	-0.3887	-0.0109	0.2705	0.0688	-0.2108	0.1888	
90	-2.4932	-0.4719	0.5911	0.2788	-1.3083	0.3644	
91	-1.8426	-0.3781	0.5537	0.2628	-1.1639	0.4117	
92	-1.2312	-0.1425	0.4145	0.1711	-0.8559	0.3708	
93	-0.8722	-0.0131	0.4076	0.0949	-0.2078	0.2716	
94	-0.4575	0.0013	0.3781	0.0758	-0.226	0.2286	
95	-0.3581	0.0134	0.2834	0.0686	-0.1884	0.2132	

B/H=4 N=2 0 degree							
# of lap	Min	Mean	max	STDEV	- peak	+ peak	
1	0.4177	1.0884	1.9487	0.2429	0.3599	1.8171	
2	-3.2715	-0.6971	0.1612	0.364	-1.7891	0.3849	
3	-4.3782	-0.6801	0.1859	0.3654	-1.7762	0.4159	
4	-2.9327	-0.6509	0.2939	0.336	-1.6589	0.3572	
5	-3.3854	-0.638	0.2243	0.3395	-1.6566	0.3806	
6	-3.4276	-0.6493	0.2604	0.3523	-1.7064	0.4077	
7	-4.1731	-0.6295	0.4902	0.349	-1.6764	0.4174	
8	-2.9344	-0.6338	0.4361	0.344	-1.6657	0.3981	
9	-2.5208	-0.3356	0.2681	0.211	-0.9696	0.2954	
10	-2.226	-0.4082	0.3394	0.2578	-1.1817	0.3853	
11	-2.5225	-0.4327	0.3973	0.2804	-1.2736	0.4083	
12	-2.4677	-0.4263	0.3362	0.2828	-1.2747	0.4221	
13	-2.3397	-0.4096	0.52	0.278	-1.2435	0.4243	
14	-1.8207	-0.3083	0.4085	0.2011	-0.9118	0.2951	
15	-2.2051	-0.1883	0.3543	0.1583	-0.6632	0.2868	
16	-1.8204	-0.2306	0.5201	0.1908	-0.8032	0.3419	
17	-1.9398	-0.2569	0.4063	0.2144	-0.9002	0.3884	
18	-1.5889	-0.0888	0.3803	0.1282	-0.4715	0.2979	
19	-0.8863	-0.076	0.5439	0.1742	-0.4189	0.2655	
20	-0.9081	-0.0867	0.5427	0.1266	-0.4688	0.2912	
21	-1.3392	-0.0872	0.3634	0.1383	-0.5021	0.3277	
22	-1.3477	-0.0554	0.4151	0.106	-0.3734	0.2627	
23	-0.7685	-0.059	0.4674	0.1101	-0.3892	0.2712	
24	-0.7874	-0.0611	0.4384	0.1125	-0.3988	0.2764	
25	-1.1005	-0.0607	0.3728	0.1065	-0.3904	0.2589	
26	-1.6889	-0.1071	0.3627	0.1402	-0.5276	0.3134	
27	-0.9177	-0.0415	0.3197	0.1078	-0.365	0.282	
28	-1.1507	-0.0241	0.324	0.0884	-0.3192	0.271	
29	-0.3656	-0.0062	0.3201	0.0788	-0.2458	0.2333	
30	-0.548	-0.0101	0.323	0.0804	-0.2514	0.2312	
31	-0.5904	-0.0092	0.3402	0.0798	-0.2486	0.2302	
32	-0.9177	-0.0415	0.3197	0.1078	-0.365	0.282	
33	-0.7167	-0.0192	0.3221	0.0911	-0.2925	0.2542	
34	-0.6635	-0.003	0.3487	0.0875	-0.2654	0.2565	
35	-0.3168	0.0162	0.3248	0.0717	-0.1987	0.2312	
36	-0.4458	0.0081	0.3653	0.0719	-0.2075	0.2237	
37	-0.413	0.0062	0.3919	0.0714	-0.208	0.2204	
38	-0.8384	-0.0206	0.3208	0.0912	-0.2941	0.2529	
39	-0.8554	-0.0045	0.3071	0.0813	-0.2486	0.2385	
40	-0.5863	-0.001	0.286	0.0781	-0.2353	0.2333	
41	-0.4859	0.007	0.3484	0.0668	-0.1928	0.2068	
42	-0.3041	0.014	0.3688	0.0648	-0.1805	0.2065	
43	-0.4082	0.0148	0.3248	0.0682	-0.1839	0.2135	
44	-0.8805	-0.0131	0.2852	0.0815	-0.2576	0.2314	
45	-0.7179	0.0028	0.2692	0.0666	-0.1988	0.2025	
46	-0.5545	-0.0009	0.2452	0.064	-0.193	0.1912	
47	-0.3513	-0.0025	0.2188	0.0608	-0.185	0.18	
48	-0.2474	0.0049	0.2635	0.0574	-0.1674	0.1772	
49	-0.5042	-0.019	0.2286	0.0631	-0.2084	0.1704	
50	-0.6059	-0.0192	0.2883	0.0701	-0.2296	0.1912	
51	-0.8129	0.3951	1.9784	0.3251	-0.5801	1.3703	
52	-0.7007	0.4156	2.0188	0.3003	-0.4853	1.3165	
53	-0.6007	0.4158	2.0472	0.307	-0.5052	1.3888	
54	-0.58						

B/H=4 N=3 0 degree

# of lap	Min	Mean	max	STDEV	- peak	+ peak
1	0.3971	1.0413	1.8226	0.2439	0.3097	1.7729
2	-3.0372	-0.6897	0.1927	0.3929	-1.8185	0.4791
3	-4.0098	-0.6537	0.3199	0.3797	-1.7928	0.4854
4	-3.2751	-0.6193	0.295	0.3453	-1.6553	0.4168
5	-3.0586	-0.6039	0.3771	0.3425	-1.6312	0.4236
6	-3.1516	-0.606	0.4437	0.3519	-1.6638	0.4479
7	-2.8939	-0.5951	0.31	0.3381	-1.6093	0.4191
8	-2.9371	-0.5928	0.3525	0.3398	-1.6121	0.4265
9	-1.6604	-0.3054	0.311	0.2074	-0.9276	0.3168
10	-2.0728	-0.385	0.3241	0.2801	-1.1653	0.3952
11	-2.1125	-0.4125	0.4123	0.2848	-1.2669	0.4417
12	-2.5195	-0.4031	0.4872	0.2817	-1.2482	0.4419
13	-2.2544	-0.3874	0.4327	0.2743	-1.2102	0.4354
14	-2.1605	-0.2856	0.391	0.2305	-0.8872	0.316
15	-2.0174	-0.1685	0.3256	0.1581	-0.6348	0.3018
16	-1.3511	-0.2064	0.429	0.1898	-0.7757	0.3629
17	-1.5204	-0.2371	0.5917	0.2177	-0.8901	0.4159
18	-1.7604	-0.2701	0.3764	0.1344	-0.4731	0.333
19	-0.9366	-0.053	0.4837	0.1151	-0.3984	0.2924
20	-1.1528	-0.0639	0.6638	0.1286	-0.4495	0.3218
21	-1.973	-0.0705	0.3863	0.1479	-0.5144	0.3733
22	-1.403	-0.0324	0.4122	0.1097	-0.3618	0.2967
23	-1.1391	-0.0339	0.489	0.1133	-0.3739	0.3051
24	-0.823	-0.0367	0.4729	0.1188	-0.3871	0.3137
25	-0.8182	-0.0369	0.4999	0.1081	-0.3631	0.2852
26	-1.4979	-0.0837	0.3934	0.1403	-0.5045	0.3371
27	-1.1825	-0.0255	0.3555	0.1172	-0.377	0.329
28	-1.4432	-0.0089	0.3717	0.1057	-0.3261	0.3082
29	-0.6741	0.0181	0.3993	0.0842	-0.2366	0.2687
30	-0.544	0.0131	0.3576	0.0847	-0.2411	0.2673
31	-1.018	0.0142	0.4143	0.0823	-0.2327	0.2611
32	-1.1825	-0.0255	0.3555	0.1172	-0.377	0.326
33	-0.9799	-0.0028	0.3504	0.0885	-0.3012	0.2857
34	-1.078	0.0162	0.3334	0.0652	-0.2695	0.3019
35	-0.7605	0.0405	0.3925	0.0761	-0.1878	0.2688
36	-0.5872	0.0326	0.4295	0.0757	-0.1944	0.2596
37	-0.503	0.028	0.4458	0.0745	-0.1954	0.2515
38	-0.7928	0.0031	0.3829	0.0941	-0.2791	0.2852
39	-0.9837	0.0169	0.3231	0.0888	-0.2497	0.2828
40	-0.8769	0.0205	0.315	0.085	-0.2374	0.2785
41	-0.4161	0.0265	0.3859	0.0705	-0.1849	0.2379
42	-0.4007	0.0376	0.3641	0.0898	-0.1717	0.247
43	-0.2911	0.0395	0.3453	0.0696	-0.1699	0.2489
44	-0.7229	0.0097	0.3197	0.0947	-0.2444	0.2637
45	-0.5803	0.0241	0.3132	0.0709	-0.1887	0.2369
46	-0.4984	0.0224	0.3216	0.0888	-0.1839	0.2285
47	-0.3888	0.0193	0.2932	0.0653	-0.1765	0.2151
48	-0.2539	0.0289	0.2825	0.0625	-0.1586	0.2182
49	-0.3874	-0.0108	0.2864	0.0671	-0.212	0.1904
50	-0.5581	-0.0153	0.294	0.0733	-0.2352	0.2046
51	-0.8008	0.3832	2.6039	0.3228	-0.5747	1.3811
52	-0.6045	0.4201	2.3507	0.3069	-0.5007	1.3409
53	-0.5179	0.4205	2.0404	0.3116	-0.5148	1.3558
54	-1.3997	0.3981	2.1772	0.3068	-0.5222	1.3184
55	-0.6229	0.3574	2.0537	0.3282	-0.6271	1.3419
56	-0.7665	0.3507	2.3917	0.3056	-0.5861	1.2675
57	-0.3521	0.4513	2.0043	0.2899	-0.3494	1.252
58	-0.3008	0.4335	2.0495	0.2881	-0.3707	1.2376
59	-0.4733	0.4336	2.0086	0.2842	-0.359	1.2261
60	-0.7727	0.3285	2.1198	0.3063	-0.5894	1.2483
61	-0.8629	0.2502	1.6778	0.276	-0.5777	1.0781
62	-0.3057	0.3903	1.897	0.2162	-0.2584	1.0389
63	-0.1989	0.3913	1.6602	0.2068	-0.229	1.0116
64	-0.2535	0.3574	1.7767	0.208	-0.2666	0.9815
65	-0.7058	0.2144	2.0207	0.2891	-0.593	1.0217
66	-0.4033	0.0283	0.2553	0.0688	-0.2345	0.178
67	-0.438	-0.0281	0.2241	0.069	-0.2351	0.179
68	-0.5107	-0.0313	0.228	0.0712	-0.2448	0.1822
69	-0.508	-0.0259	0.2581	0.0719	-0.2415	0.1897
70	-0.414	-0.0323	0.2762	0.07	-0.2423	0.1778
71	-0.4064	-0.0322	0.2324	0.07	-0.2421	0.1778
72	-0.5794	-0.0291	0.2276	0.0719	-0.2446	0.1865
73	-0.556	-0.0379	0.2238	0.0728	-0.2582	0.1804
74	-0.5045	-0.0385	0.2845	0.0731	-0.2579	0.1809
75	-0.3772	-0.0428	0.2427	0.0736	-0.2637	0.1781
76	-0.6395	-0.037	0.2421	0.0747	-0.2812	0.1872
77	-0.4551	-0.0376	0.2303	0.0767	-0.2875	0.1924
78	-2.4597	-0.5284	0.8823	0.3002	-1.4291	0.3723
79	-1.089	-0.3513	0.544	0.2844	-1.1444	0.4417
80	-1.5835	-0.1333	0.4026	0.1975	-0.7257	0.4592
81	-1.1955	-0.0402	0.3955	0.1132	-0.3787	0.2993
82	-0.7637	-0.0151	0.4281	0.0846	-0.269	0.2388
83	-0.417	-0.0034	0.2715	0.0705	-0.2151	0.2082
84	-2.7004	-0.5015	0.9367	0.2885	-1.3973	0.3544
85	-2.1655	-0.3807	0.7447	0.2797	-1.202	0.4405
86	-1.6101	-0.1198	0.4549	0.1863	-0.6787	0.4391
87	-1.2403	-0.0429	0.3894	0.1338	-0.4438	0.358
88	-1.1917	-0.0229	0.3891	0.108	-0.3409	0.2951
89	-0.5818	-0.0163	0.3581	0.0875	-0.2789	0.2483
90	-0.3742	-0.0057	0.2956	0.0692	-0.2132	0.2019
91	-2.6582	-0.4308	0.7089	0.2747	-1.255	0.3934
92	-2.1311	-0.3475	0.701	0.2603	-1.1283	0.4334
93	-1.3457	-0.1243	0.4266	0.1716	-0.6392	0.3906
94	-1.0758	-0.0039	0.4275	0.097	-0.2948	0.287
95	-0.5313	0.0097	0.3918	0.0777	-0.2234	0.2428
96	-0.3148	0.0182	0.3285	0.0687	-0.1879	0.2242

B/H=4 N=8 0 degree

# of lap	Min	Mean	max	STDEV	- peak	+ peak
1	0.3203	0.9787	2.072	0.2449	0.2439	1.7134
2	-4.1124	-0.6845	0.218	0.3946	-1.8683	0.4994
3	-3.5882	-0.673	0.5008	0.3904	-1.8443	0.4982
4	-3.049	-0.6436	0.4875	0.3568	-1.7141	0.4268
5	-2.7635	-0.6356	0.3564	0.357	-1.7065	0.4353
6	-3.2485	-0.6485	0.3475	0.3711	-1.7618	0.4648
7	-3.1487	-0.6299	0.5174	0.3617	-1.715	0.4552
8	-2.8481	-0.6204	0.3315	0.3512	-1.674	0.4333
9	-2.2521	-0.3313	0.4272	0.2224	-0.9984	0.3359
10	-2.43	-0.4071	0.4153	0.2767	-1.2371	0.4228
11	-2.2708	-0.4271	0.4357	0.2957	-1.3142	0.4599
12	-2.5188	-0.4239	0.4578	0.2949	-1.3086	0.4607
13	-2.0801	-0.4101	0.4307	0.2875	-1.2725	0.4524
14	-2.129	-0.3059	0.2307	0.2089	-0.9326	0.3208
15	-2.0161	-0.1879	0.4249	0.1656	-0.6846	0.3086
16	-1.8627	-0.2282	0.5376	0.2025	-0.8358	0.3794
17	-1.9983	-0.2543	0.4938	0.2262	-0.9328	0.4242
18	-1.6563	-0.0849	0.4067	0.1319	-0.4805	0.3107
19	-1.0981	-0.0719	0.4805	0.1209	-0.4346	0.2908
20	-1.2992	-0.0824	0.5064	0.135	-0.4875	0.3226
21	-1.0868	-0.0856	0.4732	0.1458	-0.5229	0.3518
22	-1.2969	-0.052	0.5118	0.1123	-0.389	0.285
23	-0.8997	-0.0512	0.4993	0.1163	-0.4	0.2977
24	-0.8246	-0.0547	0.4525	0.1199	-0.4144	0.305
25	-0.8061	-0.0503	0.5038	0.1133	-0.3902	0.2866
26	-1.4392	-0.1	0.4283	0.1458	-0.5373	0.3373
27	-0.8713	-0.032	0.4148	0.1122	-0.3665	0.3045
28	-1.0583	-0.0143	0.3951	0.102	-0.3204	0.2918
29	-0.4608	0.0016	0.3902	0.0882	-0.263	0.2662
30	-0.5322	-0.0023	0.4082	0.0877	-0.2855	0.2608
31	-0.5193	-0.0017	0.4208	0.0858	-0.2591	0.2557
32	-0.8173	-0.032	0.4148	0.1122	-0.3885	0.3045
33	-1.0608	-0.0085	0.3795	0.0985	-0.3039	0.2863
34	-0.9555	0.0025	0.3971	0.0941	-0.2797	0.2847
35	-0.3372	0.0199	0.4207	0.0794	-0.2184	0.2582
36	-0.6193	0.02	0.3781	0.0793	-0.218	0.2579
37	-0.3932	0.0196	0.4268	0.0787	-0.2164	0.2557
38	-1.0963	-0.0096	0.298	0.1006	-0.3113	0.2922
39	-1.2214	0.0022	0.3785	0.0889	-0.2644	0.2689
40	-1.5906	0.0091	0.3885	0.0971	-0.2523	0.2705
41	-0.3604	0.0274	0.3953	0.0739	-0.1943	0.2492
42	-0.2574	0.0295	0.3591	0.0728	-0.1883	0.2473
43	-0.3782	0.0272	0.3482	0.0739	-0.1946	0.249
44	-0.8242	0.0002	0.3958	0.0902	-0.2703	0.2707
45	-0.6919	0.014	0.3472	0.0747	-0.21	0.2379
46	-0.4978	0.0071	0.3089	0.0719	-0.2086	0.2227
47	-0.2334	0.0091	0.2906	0.068	-0.1948	0.213
48	-0.4217	0.0178	0.3257	0.0642	-0.1747	0.2103
49	-0.4809	-0.0023	0.2927	0.07	-0.2122	0.2077
50	-0.6782	-0.0008	0.329	0.078	-0.2349	0.2333
51	-1.177	0.3858	2.3081	0.336	-0.6121	1.4037
52	-0.6158	0.4331	2.1306	0.3186	-0.5258	1.3921
53	-0.5768	0.4375	2.353	0.3294	-0.5508	1.4257
54	-0.4276	0.4366	2.6123	0.3263	-0.5422	1.4155
55	-0.6369	0.3831	2.078	0.3342	-0.6197	1.3858
56	-0.8945	0.3631	2.3126	0.3251	-0.6122	1.3384
57	-0.3822	0.4645	1.9847	0.2815	-0.3799	1.3088
58	-0.2517	0.4665	2.4357	0.2863	-0.3923	1.3253
59	-0.2509	0.4579	2.3103	0.2842	-0.3947	1.3105
60	-0.7489	0.3408	1.8778	0.3177	-0.5944	1.2756
61	-0.7881	0.2648	1.9502	0.2896	-0.604	1.1336
62	-0.2					

B/H=6		N=1		0 degree			
# of lap	Min	Mean	max	STDV	- peak	+ peak	
1	0.1694	1.1368	1.8671	0.2393	0.419	1.6546	
1	-3.6352	-0.875	0.0816	0.4251	-2.1503	0.4002	
2	-3.9746	-0.8371	0.1124	0.4	-2.0372	0.3693	
3	-4.9929	-0.7926	0.1768	0.3823	-1.8796	0.2944	
4	-3.1525	-0.7375	0.1255	0.3381	-1.752	0.2769	
5	-3.4439	-0.7283	0.1773	0.3497	-1.7775	0.3209	
6	-3.9364	-0.7366	0.2164	0.3423	-1.7636	0.2904	
7	-3.2493	-0.794	0.1308	0.3659	-1.8917	0.3036	
8	-2.444	-0.5881	0.4125	0.2816	-1.413	0.2768	
9	-2.3537	-0.6875	0.335	0.328	-1.6516	0.3166	
10	-3.484	-0.6751	0.4132	0.3262	-1.6538	0.3035	
11	-3.1193	-0.6596	0.4264	0.3317	-1.6546	0.3355	
12	-2.8398	-0.645	0.3018	0.3153	-1.591	0.301	
13	-2.0851	-0.5006	0.1709	0.2492	-1.2492	0.2471	
14	-2.4892	-0.3789	0.4117	0.2229	-1.0484	0.2897	
15	-2.1121	-0.4733	0.4603	0.2667	-1.2735	0.3269	
16	-2.9304	-0.5148	0.5564	0.2898	-1.384	0.3546	
17	-1.7968	-0.1831	0.3762	0.1629	-0.6716	0.3055	
18	-1.3976	-0.1925	0.6188	0.1634	-0.682	0.2971	
19	-1.4292	-0.2353	0.6066	0.1892	-0.803	0.3324	
20	-1.6177	-0.163	0.3483	0.1659	-0.6608	0.3347	
21	-1.3311	-0.1329	0.5083	0.1342	-0.5355	0.2696	
22	-1.4108	-0.1657	0.5577	0.1586	-0.6415	0.3101	
23	-1.2374	-0.1865	0.4905	0.1583	-0.6854	0.3123	
24	-1.0258	-0.1685	0.4227	0.1504	-0.6189	0.2827	
25	-1.6385	-0.2021	0.3258	0.1262	-0.7007	0.2965	
26	-1.0391	-0.078	0.3649	0.1668	-0.4464	0.2905	
27	-1.2239	-0.0552	0.3388	0.1104	-0.3873	0.2748	
28	-0.6934	-0.0447	0.4681	0.0966	-0.3346	0.2451	
29	-1.1868	-0.0569	0.5134	0.0999	-0.3567	0.243	
30	-0.6291	-0.0571	0.4275	0.0952	-0.3428	0.2285	
31	-1.0391	-0.078	0.3649	0.1228	-0.4464	0.2905	
32	-0.8547	-0.0431	0.3183	0.0989	-0.3428	0.2566	
33	-0.9476	-0.0301	0.4343	0.0958	-0.3168	0.2566	
34	-0.7003	-0.0156	0.4151	0.0772	-0.2473	0.2161	
35	-0.5535	-0.0223	0.388	0.079	-0.2594	0.2148	
36	-0.495	-0.0248	0.3829	0.0795	-0.2632	0.2136	
37	-0.7551	-0.0601	0.3493	0.0974	-0.3524	0.2322	
38	-0.9391	-0.0342	0.3492	0.0851	-0.2894	0.221	
39	-0.7539	-0.0274	0.3122	0.084	-0.2793	0.2246	
40	-0.8038	-0.0126	0.3209	0.0867	-0.2167	0.1935	
41	-0.4247	-0.0129	0.3834	0.0882	-0.2177	0.1918	
42	-0.4933	-0.0145	0.3501	0.0704	-0.2257	0.1966	
43	-0.6358	-0.0435	0.3123	0.0848	-0.2981	0.2108	
44	-0.5339	-0.0319	0.26	0.0655	-0.2284	0.1646	
45	-0.3993	-0.0394	0.2287	0.0626	-0.227	0.1483	
46	-0.345	-0.0392	0.2147	0.059	-0.2162	0.1378	
47	-0.2942	-0.0385	0.2256	0.0584	-0.2078	0.1308	
48	-0.4291	-0.0581	0.2482	0.0633	-0.248	0.1318	
49	-0.582	-0.0524	0.2691	0.0711	-0.2658	0.1608	
50	-0.527	0.4181	1.9145	0.3125	-0.5189	1.3555	
51	-0.5236	0.4378	2.0725	0.2876	-0.425	1.3005	
52	-0.3415	0.4143	2.2075	0.2835	-0.4361	1.2647	
53	-0.4933	0.4095	2.3947	0.2816	-0.4353	1.2543	
54	-0.6203	0.3535	1.7376	0.3046	-0.5604	1.2673	
55	-0.8339	0.4012	2.4346	0.2981	-0.4872	1.2896	
56	-0.19	0.5207	2.0982	0.2766	-0.3091	1.3505	
57	-0.2372	0.4931	2.0172	0.2861	-0.3053	1.2915	
58	-0.2863	0.4748	2.1038	0.2639	-0.3172	1.2683	
59	-0.7519	0.3217	1.7264	0.2834	-0.5285	1.1718	
60	-0.5952	0.3017	1.7547	0.2582	-0.4727	1.0762	
61	-0.1178	0.4648	1.9892	0.2394	-0.2535	1.1827	
62	-0.2266	0.4488	2.0048	0.2258	-0.2265	1.1261	
63	-0.1961	0.4125	1.7983	0.2199	-0.2472	1.0722	
64	-0.6269	0.1963	1.4869	0.2409	-0.5263	0.9189	
65	-0.328	-0.0685	0.1882	0.063	-0.2575	0.1205	
66	-0.3744	-0.0776	0.1438	0.0501	-0.2578	0.1026	
67	-0.4597	-0.0835	0.1967	0.064	-0.2755	0.1086	
68	-0.467	-0.0738	0.2453	0.0656	-0.2703	0.1231	
69	-0.3706	-0.0693	0.1593	0.0632	-0.2589	0.1202	
70	-0.3634	-0.0803	0.1468	0.06	-0.2601	0.0986	
71	-0.4938	-0.0895	0.1801	0.0643	-0.2825	0.1034	
72	-0.3961	-0.0877	0.2278	0.0659	-0.2653	0.1099	
73	-0.3691	-0.0839	0.1486	0.0665	-0.2834	0.1157	
74	-0.3517	-0.0869	0.1365	0.0632	-0.2767	0.1028	
75	-0.3926	-0.0948	0.1789	0.0674	-0.2971	0.1074	
76	-0.4026	-0.0869	0.2237	0.0693	-0.2948	0.121	
77	-2.6713	-0.598	0.3518	0.2896	-1.4957	0.2707	
78	-2.5685	-0.5035	0.409	0.2871	-1.3647	0.3577	
79	-2.3669	-0.2588	0.408	0.2459	-0.9983	0.4789	
80	-1.6941	-0.1126	0.5233	0.1457	-0.5495	0.3244	
81	-1.023	-0.0613	0.4588	0.0996	-0.3601	0.2375	
82	-0.5587	-0.0561	0.3221	0.0738	-0.2775	0.1653	
83	-2.4021	-0.5664	0.6347	0.2716	-1.3814	0.2485	
84	-2.2398	-0.5101	0.5239	0.2851	-1.3654	0.3452	
85	-1.6801	-0.2543	0.7388	0.234	-0.9562	0.4477	
86	-1.278	-0.1325	0.8652	0.1728	-0.6508	0.3858	
87	-1.0452	-0.08	0.3702	0.1282	-0.4844	0.3045	
88	-0.8592	-0.0618	0.3988	0.1092	-0.3978	0.2441	
89	-0.4961	-0.058	0.2077	0.0718	-0.2743	0.1588	
90	-2.5547	-0.4613	0.6263	0.2544	-1.2446	0.282	
91	-2.0962	-0.4586	0.5245	0.2631	-1.2479	0.3307	
92	-1.4435	-0.254	0.5167	0.2107	-0.888	0.3781	
93	-0.8687	-0.0885	0.4548	0.1197	-0.4277	0.2907	
94	-0.6823	-0.033	0.3504	0.0894	-0.3013	0.2353	
95	-0.444	-0.0378	0.2559	0.0699	-0.2476	0.1719	

B/H=6		N=2		0 degree			
# of lap	Min	Mean	max	STDV	- peak	+ peak	
1	0.4172	1.0607	1.8671	0.248	0.3167	1.8048	
1	-3.6164	-0.884	0.0772	0.4333	-2.1839	0.4159	
2	-4.1316	-0.8521	0.0997	0.426	-2.13	0.4259	
3	-3.4322	-0.7966	0.0889	0.3746	-1.9205	0.3272	
4	-3.7302	-0.734	0.1345	0.3537	-1.7952	0.3271	
5	-3.4478	-0.7177	0.1599	0.3595	-1.7981	0.3507	
6	-3.8025	-0.738	0.242	0.3553	-1.8048	0.3288	
7	-3.3233	-0.7914	0.0708	0.3869	-1.9519	0.3692	
8	-2.6877	-0.5573	0.2864	0.2816	-1.4022	0.2875	
9	-3.0532	-0.5555	0.1671	0.3271	-1.6369	0.3259	
10	-3.1324	-0.6786	0.4723	0.3368	-1.689	0.3319	
11	-3.2937	-0.6859	0.274	0.3373	-1.6719	0.346	
12	-2.6104	-0.6554	0.3434	0.2367	-1.6356	0.3248	
13	-2.1266	-0.4879	0.1438	0.2508	-1.2395	0.2538	
14	-2.9263	-0.387	0.3031	0.22	-1.027	0.293	
15	-1.8943	-0.467	0.4743	0.2655	-1.2634	0.3284	
16	-2.4968	-0.5171	0.4598	0.2693	-1.3851	0.3509	
17	-2.6825	-0.1858	0.4235	0.1689	-0.8866	0.3149	
18	-1.4774	-0.1936	0.3983	0.1629	-0.6823	0.2951	
19	-1.3645	-0.2357	0.5548	0.1851	-0.7909	0.3195	
20	-1.9774	-0.1669	0.412	0.1715	-0.6814	0.3477	
21	-1.7494	-0.1312	0.5125	0.1376	-0.544	0.2817	
22	-1.0597	-0.1648	0.5675	0.1564	-0.534	0.3043	
23	-1.1179	-0.1794	0.5035	0.1659	-0.6771	0.3184	
24	-1.2723	-0.1703	0.4834	0.1528	-0.6265	0.2879	
25	-1.5363	-0.2033	0.3682	0.1725	-0.7177	0.3172	
26	-1.4477	-0.086	0.512	0.1284	-0.4712	0.2992	
27	-1.8016	-0.0643	0.3531	0.1171	-0.4158	0.287	
28	-0.5086	-0.0471	0.4434	0.0943	-0.3451	0.2509	
29	-0.7328	-0.0522	0.4327	0.1013	-0.3582	0.2518	
30	-0.6441	-0.0518	0.4882	0.0992	-0.3494	0.2458	
31	-1.4477	-0.086	0.512	0.1284	-0.4712	0.2992	
32	-1.2548	-0.0553	0.3489	0.1088	-0.3755	0.265	
33	-1.2517	-0.0313	0.4351	0.1012	-0.335	0.2724	
34	-0.8568	-0.063	0.3925	0.0915	-0.251	0.2399	
35	-0.7885	-0.0209	0.3399	0.0823	-0.2679	0.2261	
36	-0.5101	-0.0258	0.349	0.0823	-0.2727	0.2212	
37	-1.0229	-0.0563	0.3339	0.1043	-0.3693	0.2567	
38	-1.1898	-0.0283	0.3639	0.0927	-0.3063	0.2497	
39	-1.1616	-0.024	0.3548	0.0898	-0.2933	0.2453	
40	-0.5562	-0.0235	0.3541	0.0735	-0.244	0.1971	
41	-0.4744	-0.0115	0.334	0.0719	-0.2273	0.2043	
42	-0.4293	-0.0076	0.3363	0.0721	-0.2239	0.2087	
43	-1.1459	-0.0436	0.267	0.0903	-0.3143	0.2272	
44	-1.2472	-0.0334	0.2591	0.0708	-0.2459	0.179	
45	-0.4769	-0.0356	0.2451	0.0673	-0.2375	0.1663	
46	-0.3901	-0.0405	0.2199	0.0631	-0.2298	0.1488	
47	-0.3762	-0.0361	0.2215	0.0603	-0.217	0.1447	
48	-0.3863	-0.0616	0.1819	0.0671	-0.2628	0.1396	
49	-0.6667	-0.0639	0.2241	0.076	-0.2919	0.1641	
50	-0.8653	0.4101	2.0218	0.3181	-0.5442	1.3644	
51	-0.2725	0.4401	2.1892	0.2853	-0.4457	1.3259	
52	-0.2247	0.4253	2.2				

B/H=6 N=3 0 degree						
# of tap	Min	Mean	max	STDV	- peak	+ peak
1	0.4287	1.0498	1.9091	0.2392	0.3322	1.7673
2	-3.7218	-0.8936	0.3621	0.4391	-2.2108	0.4236
3	-3.9075	-0.8594	0.3697	0.4176	-2.112	0.3933
4	-3.4111	-0.8032	0.2876	0.3741	-1.9254	0.3191
5	-4.6553	-0.7431	0.2791	0.3556	-1.8099	0.3238
6	-5.1383	-0.7274	0.1184	0.3717	-1.8426	0.3876
7	-3.4931	-0.7444	0.0898	0.3659	-1.8422	0.3534
8	-3.9537	-0.7984	0.1654	0.3647	-1.9526	0.3557
9	-2.9427	-0.5618	0.2022	0.2942	-1.4445	0.3209
10	-2.5978	-0.6704	0.3137	0.3381	-1.6845	0.3438
11	-2.4787	-0.6853	0.2852	0.3407	-1.7073	0.3367
12	-2.9011	-0.6656	0.3178	0.3461	-1.7038	0.3727
13	-3.1757	-0.6547	0.2893	0.3317	-1.8498	0.3404
14	-2.2834	-0.494	0.182	0.2589	-1.2707	0.2826
15	-2.5458	-0.3694	0.4084	0.2269	-1.059	0.3202
16	-2.1481	-0.4694	0.4039	0.2742	-1.2919	0.353
17	-2.4502	-0.5179	0.4377	0.2979	-1.4117	0.3759
18	-1.7552	-0.1828	0.5406	0.17	-0.6926	0.3271
19	-1.3713	-0.1866	0.4614	0.1639	-0.8782	0.3051
20	-1.6032	-0.2318	0.7433	0.1915	-0.8062	0.3426
21	-1.7736	-0.166	0.396	0.1803	-0.707	0.3749
22	-1.6085	-0.1279	0.5731	0.1393	-0.5458	0.2901
23	-1.7209	-0.1605	0.6961	0.1611	-0.6438	0.3228
24	-1.1858	-0.1786	0.7301	0.1693	-0.6846	0.3314
25	-1.2234	-0.1577	0.5888	0.1558	-0.6351	0.2997
26	-1.5782	-0.1682	0.5946	0.1741	-0.7206	0.3242
27	-1.2028	-0.0811	0.3431	0.1319	-0.4766	0.3145
28	-1.2966	-0.0597	0.3973	0.1228	-0.428	0.3086
29	-0.8106	-0.0372	0.4597	0.1003	-0.3381	0.2637
30	-0.6189	-0.0466	0.4212	0.1032	-0.3564	0.2831
31	-0.7416	-0.0457	0.4237	0.1008	-0.3482	0.2588
32	-1.2028	-0.0911	0.3431	0.1319	-0.4766	0.3145
33	-0.9222	-0.0481	0.3284	0.109	-0.3751	0.2789
34	-0.9642	-0.0262	0.4881	0.1065	-0.3456	0.2833
35	-0.5587	-0.0004	0.4305	0.0833	-0.2502	0.2495
36	-0.8463	-0.013	0.43	0.0845	-0.2665	0.2408
37	-0.9543	-0.0182	0.3665	0.0836	-0.2601	0.2327
38	-1.215	-0.0488	0.322	0.1066	-0.3887	0.271
39	-0.8379	-0.0239	0.3427	0.0929	-0.3025	0.2547
40	-0.7014	-0.0188	0.3783	0.0912	-0.2925	0.2549
41	-0.5212	-0.0116	0.3041	0.0747	-0.2356	0.2125
42	-0.4913	-0.0052	0.2844	0.073	-0.2241	0.2138
43	-0.5423	-0.0029	0.3161	0.0737	-0.2239	0.2182
44	-0.8714	-0.0364	0.2793	0.0809	-0.3091	0.2382
45	-0.5952	-0.0267	0.2822	0.0724	-0.2439	0.1964
46	-0.697	-0.0285	0.2266	0.0693	-0.2363	0.1782
47	-0.3707	-0.0316	0.2417	0.0641	-0.224	0.1609
48	-0.4036	-0.0297	0.2179	0.0608	-0.2122	0.1527
49	-0.4234	-0.0571	0.2102	0.0657	-0.2542	0.1399
50	-0.5166	-0.0583	0.331	0.0748	-0.2827	0.1661
51	-0.7331	0.4234	1.9871	0.3265	-0.556	1.4029
52	-0.4114	0.4523	2.355	0.3018	-0.453	1.3576
53	-0.3097	0.4418	2.134	0.2895	-0.4589	1.3404
54	-0.3714	0.4285	2.5149	0.2972	-0.4051	1.318
55	-0.8898	0.3668	1.8721	0.3175	-0.5861	1.3192
56	-0.7383	0.41	2.1494	0.3181	-0.5444	1.3843
57	-0.3184	0.5363	2.2598	0.2919	-0.3393	1.4119
58	-0.1721	0.5064	2.316	0.28	-0.3336	1.4644
59	-0.2996	0.502	2.2067	0.2761	-0.3263	1.3304
60	-0.7056	0.3454	1.9759	0.285	-0.5396	1.2303
61	-0.6649	0.3015	1.8082	0.2801	-0.5388	1.1417
62	-0.2854	0.4735	1.8603	0.251	-0.2797	1.2266
63	-0.1909	0.4823	2.0753	0.232	-0.2338	1.1584
64	-0.1806	0.4187	2.0642	0.2287	-0.2674	1.1047
65	-0.7164	0.208	1.8155	0.252	-0.5479	0.9639
66	-0.5527	-0.0754	0.1677	0.0708	-0.2878	0.1369
67	-0.3958	-0.0821	0.1504	0.0667	-0.2823	0.118
68	-0.4321	-0.0918	0.1632	0.0685	-0.2972	0.1137
69	-0.4933	-0.0834	0.1947	0.0713	-0.2971	0.1304
70	-0.6099	-0.0811	0.1411	0.071	-0.2942	0.1319
71	-0.4515	-0.0847	0.1543	0.0676	-0.2876	0.1181
72	-0.4405	-0.0898	0.1778	0.0693	-0.2978	0.1185
73	-0.4406	-0.0861	0.1549	0.0717	-0.3112	0.119
74	-0.6214	-0.0984	0.1488	0.0746	-0.3121	0.1353
75	-0.4867	-0.0945	0.1393	0.0709	-0.3071	0.1181
76	-0.4867	-0.0946	0.1662	0.0723	-0.3114	0.1222
77	-0.5108	-0.0918	0.1915	0.0744	-0.315	0.1314
78	-3.2279	-0.601	0.3578	0.2978	-1.4945	0.2925
79	-2.8056	-0.5123	0.4343	0.2999	-1.412	0.3873
80	-2.2153	-0.2853	0.3727	0.2591	-1.0397	0.5091
81	-1.4029	-0.1104	0.3314	0.1487	-0.5584	0.3358
82	-1.431	-0.0635	0.3292	0.1021	-0.3688	0.2429
83	-1.1835	-0.0551	0.2402	0.0788	-0.2915	0.1813
84	-2.5959	-0.5626	0.5199	0.2824	-1.4097	0.2846
85	-2.6243	-0.5122	0.4763	0.289	-1.4003	0.3759
86	-1.8672	-0.2592	0.4055	0.2478	-1.002	0.4837
87	-1.3202	-0.129	0.3883	0.1799	-0.6688	0.4100
88	-1.0776	-0.0837	0.4016	0.1323	-0.4807	0.3132
89	-0.7731	-0.0681	0.3086	0.1043	-0.3791	0.2499
90	-0.8317	-0.0595	0.2285	0.0753	-0.2855	0.1884
91	-2.9389	-0.481	0.4685	0.254	-1.2729	0.311
92	-2.0402	-0.4634	0.5889	0.2761	-1.2916	0.3649
93	-1.563	-0.2611	0.3732	0.2164	-0.9103	0.388
94	-1.0386	-0.0643	0.4179	0.124	-0.4382	0.3076
95	-0.8945	-0.03	0.3692	0.0927	-0.311	0.245

B/H=6 N=8 0 degree						
# of tap	Min	Mean	max	STDV	- peak	+ peak
1	0.4	1.0443	1.8777	0.2367	0.3344	1.7543
2	-4.1165	-0.8761	0.1012	0.4496	-2.2248	0.4727
3	-5.9973	-0.8456	0.0288	0.4413	-2.1696	0.4784
4	-4.5602	-0.7906	0.14	0.3809	-1.9331	0.352
5	-3.3213	-0.73	0.1563	0.3532	-1.7926	0.3266
6	-3.0229	-0.7135	0.134	0.3494	-1.7618	0.3348
7	-2.9805	-0.727	0.1898	0.3523	-1.7839	0.3289
8	-4.2185	-0.7847	0.1069	0.386	-1.9428	0.3734
9	-2.5742	-0.5421	0.1636	0.2809	-1.3949	0.3007
10	-2.7835	-0.6555	0.3743	0.3348	-1.6599	0.3489
11	-3.6011	-0.6712	0.1993	0.3389	-1.6878	0.3454
12	-2.5326	-0.658	0.3586	0.3373	-1.67	0.3539
13	-3.1834	-0.6488	0.2923	0.3319	-1.6425	0.3488
14	-2.459	-0.4856	0.2932	0.2566	-1.2556	0.2843
15	-1.8916	-0.3603	0.3346	0.2224	-1.0276	0.3088
16	-2.1758	-0.459	0.5177	0.269	-1.2661	0.3481
17	-2.5745	-0.5168	0.3999	0.3004	-1.4719	0.3847
18	-1.9678	-0.1747	0.4518	0.166	-0.6727	0.3232
19	-1.3716	-0.1798	0.4784	0.1622	-0.6665	0.3069
20	-1.6463	-0.2255	0.5466	0.19	-0.7955	0.3444
21	-1.5338	-0.1591	0.4512	0.1753	-0.6852	0.3689
22	-1.2177	-0.1217	0.5938	0.1366	-0.5316	0.2881
23	-1.0542	-0.1544	0.5602	0.1598	-0.6338	0.325
24	-1.554	-0.1767	0.5448	0.1719	-0.6924	0.399
25	-1.5189	-0.1575	0.5708	0.1589	-0.6342	0.3192
26	-2.2203	-0.1874	0.4376	0.1692	-0.595	0.3201
27	-1.4258	-0.0709	0.4127	0.131	-0.4636	0.322
28	-1.265	-0.0478	0.4684	0.1171	-0.3991	0.3035
29	-0.8117	-0.0312	0.4284	0.0985	-0.3266	0.2642
30	-0.6643	-0.0414	0.5489	0.1048	-0.3557	0.2728
31	-0.8616	-0.0422	0.4098	0.1011	-0.3456	0.2612
32	-1.4258	-0.0709	0.4127	0.131	-0.4638	0.322
33	-1.2276	-0.0368	0.3222	0.1075	-0.3594	0.2857
34	-1.0219	-0.0206	0.3355	0.1046	-0.3344	0.2931
35	-0.4733	-0.0009	0.3698	0.0817	-0.248	0.2443
36	-0.5034	-0.0058	0.3689	0.0935	-0.2582	0.2446
37	-0.4653	-0.0103	0.4097	0.0832	-0.2588	0.2393
38	-0.9168	-0.0413	0.4017	0.1032	-0.351	0.2683
39	-0.8275	-0.0239	0.2731	0.0914	-0.2982	0.2504
40	-0.8625	-0.0168	0.3543	0.0907	-0.2887	0.2555
41	-0.4712	0.0015	0.3291	0.0728	-0.2189	0.2189
42	-0.5082	0.0009	0.3232	0.0727	-0.2171	0.2189
43	-0.6588	0.0008	0.3611	0.0744	-0.2225	0.2241
44	-0.698	0.0021	0.3159	0.0698	-0.2075	0.2412
45	-0.8038	-0.0191	0.2881	0.0712	-0.2326	0.1944
46	-0.4339	-0.0231	0.2379	0.0669	-0.2239	0.1776
47	-0.4443	-0.0229	0.215	0.0626	-0.2108	0.165
48	-0.35	-0.0233	0.2152	0.0603	-0.204	0.1575
49	-0.4812	-0.0545	0.2011	0.0662	-0.2531	0.144
50	-0.824	-0.0504	0.2688	0.0742	-0.273	0.1721
51	-0.6616	0.4179	2.076	0.3263	-0.5611	1.3969
52	-0.536	0.4492	2.4167	0.2933	-0.4306	1.329
53	-0.3945	0.4276	2.2235	0.285	-0.4273	1.2825
54	-0.4693	0.4251	1.9808	0.2885	-0.4404	1.2906
55	-0.6671	0.3611	1.9798	0.3124	-0.576	1.2882
56	-0.6258	0.4042	2.1162	0.3126	-0.5336	1.2821
57	-0.2207	0.5233	2.4834	0.2796	-0.3154	1.3619
58	-0.2685	0.4993	2.0492	0.2702	-0.3114	1.3099
59	-0.2518	0.4879	2.1598	0.2717	-0.3271	1.3028
60	-0.6399	0.3295	1.929	0.2921	-0.5467	1.2057
61	-0.6011	0.3048	1.8768	0.2761	-0.5238	1.1332
62	-0.1746	0.4661	1.8922	0.2455	-0.2703	1.20

Appendix D

Concentration

This appendix presents the values of mean relative concentration for 45 concentration taps on the surface of testing building.

C0=1000000								
B/H=0.5					B/H=1			
Tap #	N=1	N=2	N=3	N=8	N=1	N=2	N=3	N=8
1	0.00024	0.000176	0.000053	0	2.09E-05	0.000052	6.36E-05	7.47E-05
2	0.001366	0.001235	0.001187	0.001003	0.00139	0.001373	0.001326	0.002026
3	0.001655	0.001493	0.001425	0.00128	0.001759	0.001703	0.001619	0.002495
5	0.002738	0.002405	0.002106	0.001732	0.002893	0.002738	0.002483	0.003766
6	0.004432	0.003962	0.003375	0.002804	0.004268	0.003807	0.003487	0.005143
7	0.001255	0.001491	0.001379	0.00152	0.001642	0.001684	0.00197	0.003335
8	0.00142	0.001623	0.001547	0.001675	0.001945	0.002113	0.002659	0.004701
9	0.001572	0.001684	0.00164	0.001753	0.002189	0.002327	0.002953	0.005432
10	0.001029	0.000802	0.000761	0.000862	0.001631	0.001394	0.001365	0.002223
11	0.001227	0.000859	0.000877	0.000966	0.00201	0.001745	0.001704	0.002756
12	0.001403	0.001059	0.001042	0.00115	0.002236	0.002015	0.001895	0.003278
13	0.000591	0.000546	0.000544	0.00053	0.000307	0.000341	0.000349	0.000539
14	0.000851	0.00073	0.000747	0.000701	0.000308	0.000338	0.000333	0.000538
15	0.001355	0.001063	0.00114	0.001046	0.000312	0.000332	0.00034	0.000575
16	0.002555	0.001944	0.001906	0.001705	0.000285	0.00019	0.000288	0.000477
17	0.000558	0.00057	0.000555	0.00058	0.000292	0.00033	0.00035	0.000578
18	0.000913	0.000915	0.000927	0.000932	0.000334	0.000374	0.000397	0.000688
19	0	0	0	0	0.000288	0.000306	0.000321	0.000535
20	0.000468	0.000578	0.000551	0.000581	0.000408	0.000427	0.000545	0.001041
21	0.000607	0.000766	0.00076	0.000769	0.00041	0.000448	0.000577	0.001103
22	0.000892	0.001141	0.001135	0.001149	0.00032	0.000357	0.000434	0.00076
23	0.000297	0.000287	0.000275	0.00026	0.000229	0.000257	0.000267	0.000421
24	0.000158	0.000161	0.000162	0.000167	0.000166	0.000185	0.000187	0.000306
25	0.000109	0.000113	0.000111	0.000119	0.000137	0.000146	0.000151	0.00024
26	0.000083	0.000082	0.000086	0.000087	0.00012	0.000123	0.000128	0.00021
27	0.000068	0.000065	0.000068	0.000069	0.000107	0.000105	0.000109	0.000179
28	0.000057	0.000054	0.000056	0.000055	0.000098	0.000094	9.66E-05	0.00016
29	0.000298	0.000337	0.000325	0.000385	0.000262	0.000289	0.00031	0.00052
30	0.000163	0.000195	0.00019	0.000204	0.000189	0.000213	0.00023	0.000383
31	0.000159	0.000134	0.000162	0.000175	0.000151	0.000167	0.000179	0.000301
32	0.000306	0.000365	0.000346	0.000369	0.000353	0.000379	0.000469	0.000844
33	0.00017	0.000209	0.000196	0.000201	0.000236	0.000258	0.000303	0.000558
34	0.00012	0.000148	0.000138	0.000145	0.00018	0.000196	0.00023	0.000411
35	0.000092	0.000113	0.000107	0.000115	0.000143	0.000155	0.000184	0.000322
36	0.000074	0.000092	0.00009	0.000092	0.000121	0.000131	0.000147	0.00027
37	0.000064	0.00008	0.000078	0.000086	0.000104	0.000111	0.000132	0.000236
38	0.000254	0.000204	0.000174	0.000175	0.000381	0.000325	0.000325	0.000579
39	0.000143	0.000115	0.000101	0.000105	0.000255	0.000217	0.000221	0.000382
40	0.000223	0.000354	0.00034	0.000356	0.000287	0.000353	0.000479	0.000981
41	0.000164	0.000277	0.00026	0.000264	0.000212	0.000256	0.000348	0.000753
42	0.000142	0.000232	0.000218	0.000235	0.000166	0.000199	0.000272	0.000575
43	0.000289	0.000454	0.000458	0.000498	0.000267	0.000329	0.00043	0.000871
44	0.000217	0.000355	0.000357	0.00039	0.000203	0.000248	0.00032	0.000661
45	0.000186	0.000303	0.000305	0.000315	0.000171	0.000198	0.000258	0.000547
46	0.000214	0.000209	0.000255	0.000278	0.000253	0.000308	0.00039	0.000801
47	0.000169	0.000198	0.000236	0.000249	0.000205	0.000238	0.000314	0.000644

Tap #	B/H=2				B/H=4			
	N=1	N=2	N=3	N=8	N=1	N=2	N=3	N=8
1	0	0	0	0	0.000004	0.000018	0.000025	0
2	0.001445	0.001395	0.001246	0.001241	0.001087	0.001192	0.001323	0.001401
3	0.001613	0.001554	0.0014	0.001411	0.001139	0.001246	0.001367	0.00149
5	0.001931	0.001725	0.001555	0.001604	0.001183	0.001317	0.00142	0.001611
6	0.002129	0.002032	0.001821	0.001795	0.001284	0.00144	0.001551	0.001836
7	0.001097	0.00102	0.001022	0.000959	0.000986	0.00114	0.001255	0.00143
8	0.001177	0.001112	0.001139	0.001049	0.001045	0.001217	0.001357	0.001511
9	0.001209	0.001123	0.001234	0.001112	0.001096	0.001281	0.001436	0.001685
10	0.001069	0.001046	0.000991	0.000941	0.001032	0.00113	0.001248	0.001436
11	0.001117	0.001043	0.001055	0.00101	0.001105	0.001224	0.001345	0.001501
12	0.001198	0.00106	0.00101	0.000996	0.001087	0.001192	0.001313	0.001489
13	0.000153	0.000125	0.000123	0.00011	0.000099	0.000098	0.000109	0.000112
14	0.000126	0.000125	0.000121	0.00011	0.000102	0.0001	0.000111	0.000124
15	0.000121	0.000121	0.00011	0.000104	0.000103	0.000104	0.000115	0.00013
16	0.000119	0.000115	0.000106	0.000103	0.000107	0.000109	0.000121	0.000141
17	0.000133	0.000129	0.000123	0.000112	0.000096	0.000097	0.000108	0.000116
18	0.00013	0.000126	0.000118	0.000108	0.000102	0.000102	0.000113	0.000125
19	0.000124	0	0	0	0	0	0	0
20	0.000149	0.000158	0	0.000134	0.00009	0.000092	0.000103	0.000113
21	0.000146	0.000145	0.000138	0.000127	0.000095	0.000099	0.000107	0.000121
22	0.000128	0.000129	0.000116	0.000102	0.000104	0.000107	0.000119	0.00013
23	0.000129	0.000131	0.000117	0.000115	0.000098	0.000098	0.00011	0.000125
24	0.00011	0.000108	9.85E-05	0.000096	0.000086	0.000087	0.000097	0.000113
25	9.75E-05	0.000097	8.65E-05	8.25E-05	0.000078	0.000076	0.000085	0.000097
26	8.75E-05	8.35E-05	0.000076	0.000073	0.000068	0.000067	0.000076	0.000087
27	7.75E-05	0.000075	6.65E-05	6.45E-05	0.000061	0.000059	0.000068	0.000079
28	0.00007	0.000067	0.00006	0.000058	0.000056	0.000054	0.000061	0.000068
29	0.000147	0.000151	0.000136	0.000127	0.000094	0.000097	0.000109	0.000112
30	0.000119	0.000118	0.00011	0.000101	0.000083	0.000085	0.000095	0.000102
31	0.000102	0.000101	9.25E-05	8.45E-05	0.000074	0.000076	0.000087	0.000096
32	0.000153	0.000157	0.000149	0.000137	0.000087	0.000092	0.000101	0.00012
33	0.00012	0.000126	0.000117	0.000106	0.000075	0.000079	0.000088	0.000099
34	0.000102	0.0001	0.000067	8.85E-05	0.000067	0.00007	0.000078	0.000089
35	0.000089	0.000089	0.000083	7.55E-05	0.00006	0.000063	0.000071	0.000089
36	0.000078	7.65E-05	7.35E-05	0.000066	0.000055	0.000057	0.000065	0.000071
37	7.05E-05	7.05E-05	6.55E-05	0.00006	0.00005	0.000056	0.000059	0.000065
38	0.000115	0.000123	0.000113	0.000123	0.000087	0.000085	0.000099	0.000109
39	0.000093	0.000089	0.000087	9.55E-05	0.000075	0.000072	0.000084	0.000098
40	0.000128	0.000139	0.000132	0.000124	0.000084	0.000091	0.000098	0.00011
41	0.000105	0.000112	0.000108	0.000102	0.000073	0.000079	0.000086	0.000098
42	0.000089	0.000096	0.000091	8.35E-05	0.000066	0.000071	0.000077	0.000086
43	0.00013	0.00014	0.000135	0.000125	0.000093	0.000099	0.000107	0.000119
44	0.000108	0.000115	0.000114	0.000103	0.000081	0.000087	0.000094	0.000108
45	9.15E-05	9.75E-05	0.000097	8.65E-05	0.000073	0.000078	0.000085	0.000096
46	0.000077	0.000077	7.35E-05	6.75E-05	0.000102	0.000106	0.000115	0.000129
47	7.25E-05	0.00009	9.15E-05	0.000087	0.000091	0.000096	0.000104	0.000116